U.S. DEPARTMENT OF COMMERCE
National Technical Information Service

PB-295 609

Geothermal Environmental Impact Assessment: Baseline Data for Four Geothermal Areas in the United States

Geonomics, Inc, Berkeley, CA

Prepared for

Environmental Monitoring and Support Lab, Las Vegas, NV

Sep 78

TECHNICAL REPORT DATA

(Please read Instructions on the reverse before completing)

1. REPORT NO.
EPA-600/7-78-188

2.

3. RECIPIENT'S ACCESSION NO.
PB295609

4. TITLE AND SUBTITLE
GEOTHERMAL ENVIRONMENTAL IMPACT ASSESSMENT
Baseline Data for Four Geothermal Areas in the United States

5. REPORT DATE
September 1978

6. PERFORMING ORGANIZATION CODE

7. AUTHOR(S)
Subir Sanyal
Richard Weiss

8. PERFORMING ORGANIZATION REPORT NO.

9. PERFORMING ORGANIZATION NAME AND ADDRESS
Geonomics, Inc.
3165 Adeline Avenue
Berkeley, CA 94703

10. PROGRAM ELEMENT NO.
1NE624

11. CONTRACT/GRANT NO.
68-03-2468

12. SPONSORING AGENCY NAME AND ADDRESS
U.S. Environmental Protection Agency-Las Vegas, NV
Office Research and Development
Environmental Monitoring and Support Laboratory
Las Vegas, NV 89114

13. TYPE OF REPORT AND PERIOD COVERED
Interim

14. SPONSORING AGENCY CODE
EPA/600/07

15. SUPPLEMENTARY NOTES This is the first in a series of five reports prepared toward developing a groundwater monitoring strategy in a geothermal resource area. Contact Donald B. Gilmore, Project Officer, FTS 595-2969, x241, for additional information.

16. ABSTRACT

This report describes the existing data on climatology, hydrology, water chemistry, seismicity, and subsidence in the Rio Grande Rift Zone, New Mexico; The Geysers, California; the Klamath Falls, Oregon; and, with special emphasis, The Imperial Valley, California.

COLOR ILLUSTRATIONS REPRODUCED
IN BLACK AND WHITE

REPRODUCED BY
NATIONAL TECHNICAL
INFORMATION SERVICE
U.S. DEPARTMENT OF COMMERCE
SPRINGFIELD, VA. 22161

17. KEY WORDS AND DOCUMENT ANALYSIS

a. DESCRIPTORS	b. IDENTIFIERS/OPEN ENDED TERMS	c. COSATI Field/Group
Geothermal energy Environmental studies	Geothermal groundwater Monitoring	97P, R

18. DISTRIBUTION STATEMENT RELEASE TO PUBLIC	19. SECURITY CLASS *(This Report)* UNCLASSIFIED	21. NO. OF PAGES 505
	20. SECURITY CLASS *(This page)* UNCLASSIFIED	22. PRICE A22-A01

EPA Form 2220-1 (Rev. 4-77) PREVIOUS EDITION IS OBSOLETE

NOTICE

THIS DOCUMENT HAS BEEN REPRODUCED FROM THE BEST COPY FURNISHED US BY THE SPONSORING AGENCY. ALTHOUGH IT IS RECOGNIZED THAT CERTAIN PORTIONS ARE ILLEGIBLE, IT IS BEING RELEASED IN THE INTEREST OF MAKING AVAILABLE AS MUCH INFORMATION AS POSSIBLE.

United States
Environmental Protection
Agency

Environmental Monitoring
and Support Laboratory
P.O. Box 15027
Las Vegas NV 89114

EPA-600/7-78-188
September 1978

PB 295609

Research and Development

EPA

Geothermal Environmental Impact Assessment:

Baseline Data for Four Geothermal Areas in the United States

Interagency Energy-Environment Research and Development Program Report

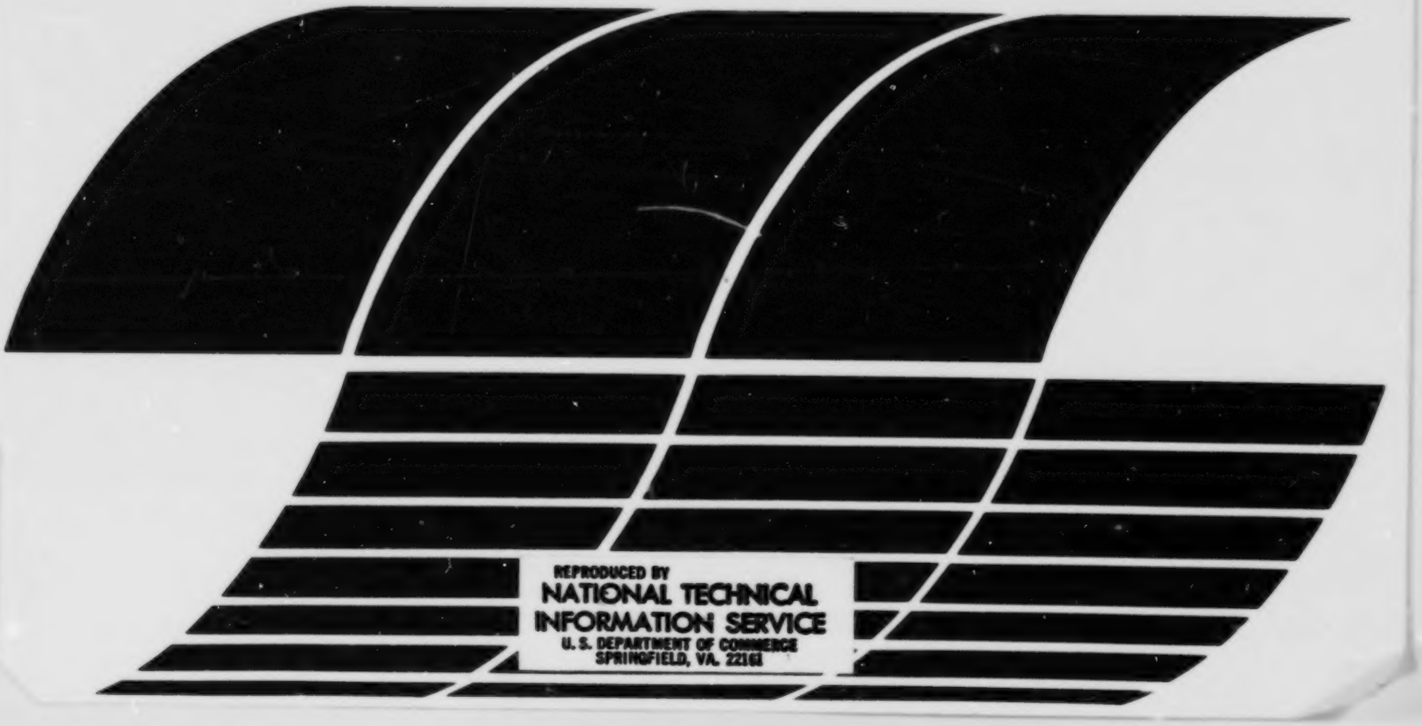

REPRODUCED BY
NATIONAL TECHNICAL
INFORMATION SERVICE
U.S. DEPARTMENT OF COMMERCE
SPRINGFIELD, VA. 22161

RESEARCH REPORTING SERIES

Research reports of the Office of Research and Development, U.S. Environmental Protection Agency, have been grouped into nine series. These nine broad categories were established to facilitate further development and application of environmental technology. Elimination of traditional grouping was consciously planned to foster technology transfer and a maximum interface in related fields. The nine series are:

1. Environmental Health Effects Research
2. Environmental Protection Technology
3. Ecological Research
4. Environmental Monitoring
5. Socioeconomic Environmental Studies
6. Scientific and Technical Assessment Reports (STAR)
7. Interagency Energy-Environment Research and Development
8. "Special" Reports
9. Miscellaneous Reports

This report has been assigned to the INTERAGENCY ENERGY—ENVIRONMENT RESEARCH AND DEVELOPMENT series. Reports in this series result from the effort funded under the 17-agency Federal Energy/Environment Research and Development Program. These studies relate to EPA'S mission to protect the public health and welfare from adverse effects of pollutants associated with energy systems. The goal of the Program is to assure the rapid development of domestic energy supplies in an environmentally-compatible manner by providing the necessary environmental data and control technology. Investigations include analyses of the transport of energy-related pollutants and their health and ecological effects; assessments of, and development of, control technologies for energy systems; and integrated assessments of a wide range of energy-related environmental issues.

This document is available to the public through the National Technical Information Service, Springfield, Virginia 22161.

EPA-600/7-78-188
September 1978

GEOTHERMAL ENVIRONMENTAL IMPACT ASSESSMENT
Baseline Data for Four Geothermal Areas in the United States

by

Geonomics, Inc.
Berkeley, California 94703

Contract No. 68-03-2468

Project Officer
Donald B. Gilmore
Monitoring Systems Research and Development Division
Environmental Monitoring and Support Laboratory
Las Vegas, Nevada 89114

ENVIRONMENTAL MONITORING AND SUPPORT LABORATORY
OFFICE OF RESEARCH AND DEVELOPMENT
U.S. ENVIRONMENTAL PROTECTION AGENCY
LAS VEGAS, NEVADA 89114

DISCLAIMER

This report has been reviewed by the Environmental Monitoring and Support Laboratory, Las Vegas, U.S. Environmental Protection Agency, and approved for publication. Approval does not signify that the contents necessarily reflect the views and policies of the U.S. Environmental Protection Agency, nor does mention of trade names or commercial products constitute endorsement or recommendation for use.

FOREWORD

Protection of the environment requires effective regulatory actions which are based on sound technical and scientific information. This information must include the quantitative description and linking of pollutant sources, transport mechanisms, interactions, and resulting effects on man and his environment. Because of the complexities involved, assessment of specific pollutants in the environment requires a total systems approach which transcends the media of air, water, and land. The Environmental Monitoring and Support Laboratory-Las Vegas contributes to the formation and enhancement of a sound monitoring data base for exposure assessment through programs designed to:

- develop and optimize systems and strategies for monitoring pollutants and their impact on the environment
- demonstrate new monitoring systems and technologies by applying them to fulfill special monitoring needs of the Agency's operating programs.

This report is the first in a series of five reports covering the following subjects:

- baseline geotechnical data for four geothermal areas in the United States
- subsurface environmental assessment of geothermal development
- a guide for decision-makers
- a pollution control technology guidance manual, and
- a groundwater monitoring methodology for geothermal developments.

The first two reports cover the baseline data necessary for the development of the last report. It will contain the strategy for monitoring change in groundwater quality as a result of any geothermal resource development, conversion and waste disposal.

The third report will be a guideline for those persons charged with responsibility for issuing permits for geothermal exploration, development, conversion and waste disposal.

Report 4 will cover justification of the need, by way of regulatory or anticipated regulatory requirements, for control of constituents of raw wastes and a description of waste control technology alternatives.

For further information on these reports, contact the Monitoring Systems Research and Development Division at the Environmental Monitoring and Support Laboratory, Las Vegas, Nevada.

George B. Morgan

George B. Morgan
Director
Environmental Monitoring and Support Laboratory
Las Vegas, Nevada

ABSTRACT

This report presents a compilation and technical assessment of the existing data on climate, geology, hydrology, water chemistry and seismicity for four geothermal areas in the United States: Imperial Valley and The Geysers, California; Klamath Falls, Oregon; and the Rio Grande Rift Zone, New Mexico. It is the culmination of the first step--namely, baseline data assessment--towards the goal of developing an environmental monitoring methodology with primary emphasis on groundwater degradation for geothermal areas.

The Imperial Valley displays high regional heat flow and contains six Known Geothermal Resource Areas (KGRAs), where geothermal water ranges approximately from 150° to 300°C (300° to 570°F) in temperature and from 15,000 to 300,000 mg/l in total dissolved solids (TDS). The valley is a sediment-filled structural trough undergoing intensive crustal deformation, active faulting, very high seismicity and significant subsidence. An extensive data compilation has resulted in a new comprehensive fault map of the valley. Groundwater quality varies from potable water to geothermal brines. Irrigation water considerably affects the natural groundwater system in the valley. Modified Stiff diagrams, Langelier-Ludwig diagrams and computer-generated chemical parameter surface plots have been useful in depicting the geohydrologic and chemical characteristics of groundwater in the valley.

The Geysers geothermal field produces steam of about 230°C (445°F) from a fractured greywacke formation. Numerous faults and notable seismic activity occur in this mountainous region. Compared to the surrounding area, an anomalously high level of microearthquake activity is concentrated at The Geysers geothermal field. Hydrology and water quality are discussed for nine drainage basins in The Geysers region. Much of the groundwater has a naturally high boron content.

Geothermal water is being utilized in Klamath Falls, Oregon, for space heating. Other geothermal waters occur in the northwest trending Klamath Basin structural depression. The thermal waters appear to be associated with faults and are located in rubbly, fractured basalt aquifers. The dissolved salts in these surface waters consist mainly of calcium and magnesium bicarbonates while deeper thermal waters contain principally sodium and calcium sulfates, chlorides, and bicarbonates. Four main aquifers, which include regional, intermediate and local flow systems, are identified. Historically, the area has displayed a very low level of seismicity.

The Rio Grande Rift Zone contains seven areas of potential goethermal interest. Complex folding in the mountins and discontinuous faulting throughout the rift zone make the geologic structure difficult to interpret. Several drainage basins occur which contain much saline water (> 1,000 mg/l TDS), and the available volume of freshwater varies widely. The highest seismicity occurs near Socorro, but is of considerably lower level than in Imperial Valley.

CONTENTS

Page

Foreword iii
Abstract v
Figures xi
Tables xvii
Plates xix

1. INTRODUCTION 1

    1.1 Objectives 1
    1.2 Scope of Investigation 3
    1.3 Baseline Assessment Report 3
    1.4 Report Organization 4

2. IMPERIAL VALLEY 7

    2.1 Introduction 7
        2.1.1 Summary 7
        2.1.2 Background 12
        2.1.3 Climatology 12

    2.2 Geothermal Characteristics 13
        2.2.1 Salton Sea Geothermal Area 15
        2.2.2 Heber Geothermal Area 16
        2.2.3 East Mesa Geothermal Area 16
        2.2.4 Brawley Geothermal Area 17
        2.2.5 Dunes Geothermal Area 18
        2.2.6 Glamis Geothermal Area 19
        2.2.7 Cerro Prieto Geothermal Area 19

    2.3 Geology 20
        2.3.1 Physiography of the Salton Trough 20
        2.3.2 Tectonic Evolution of the Salton Trough 22
        2.3.3 Structure of Imperial Valley 31
        2.3.4 Stratigraphy and Lithology of Salton Trough Rocks 46

    2.4 Hydrology 54
        2.4.1 Surface Water 54
        2.4.2 Ground Water 62
        2.4.3 Hydrologic Budget 103

Page

2.5 Chemical Characteristics of Ground Water 109
- 2.5.1 Types and Distribution of Ground Water 122
- 2.5.2 Single-Chemical Parameter Contoured Surface Plots 128
- 2.5.3 Trace Elements in Geothermal Waters 136

2.6 Seismicity 140
- 2.6.1 Historical Seismicity 140
- 2.6.2 Microseismicity 142
- 2.6.3 Seismic Risk 143
- 2.6.4 Relation of Earthquakes to Geothermal Activity 147

References 150

3. THE GEYSERS 163

3.1 Introduction 163
- 3.1.1 Summary 163
- 3.1.2 Background 164
- 3.1.3 Climatology 164

3.2 Geothermal Characteristics of The Geysers 169

3.3 Geology 172
- 3.3.1 Physiography 172
- 3.3.2 Regional Geologic Setting and Tectonic History 173
- 3.3.3 Structure 175
- 3.3.4 Stratigraphy and Lithology 175

3.4 Hydrology 181
- 3.4.1 Surface Water 182
- 3.4.2 Ground Water 182
- 3.4.3 Hydrologic Budget 190

3.5 Chemical Characteristics of Ground Water 191

3.6 Seismicity 193
- 3.6.1 Historical Seismicity 193
- 3.6.2 Microseismicity 196
- 3.6.3 Seismic Risk 198

References 208

4. KLAMATH FALLS 211

Page

4.1 Introduction 211
4.1.1 Summary 211
4.1.2 Background 211
4.1.3 Climatology 213

4.2 Geothermal Characteristics 221
4.2.1 History of Geothermal Exploration and Development 221
4.2.2 Temperature Gradients 223
4.2.3 Geothermal Potential 224

4.3 Geology 225
4.3.1 Physiography 225
4.3.2 Regional Geologic Setting and Tectonic History 227
4.3.3 Structure 230
4.3.4 Stratigraphy and Lithology 233

4.4 Hydrology 240
4.4.1 Surface Water 240
4.4.2 Ground Water 247
4.4.3 Hydrologic Budget 254

4.5 Chemical Characteristics of Ground Water 254
4.5.1 Chemistry of Thermal Waters 258

4.6 Seismicity 261
4.6.1 Historical Seismicity 261
4.6.2 Seismic Risk 261
4.6.3 Seismicity and Tectonism 263

References 266

5. RIO GRANDE RIFT ZONE 269

5.1 Introduction 269
5.1.1 Summary 269
5.1.2 Background 270
5.1.3 Climatology 272

5.2 Geothermal Characteristics 281

5.3 Geology 286

5.4 Hydrology 289

5.5 Chemical Characteristics of Ground Water 301

Page

5.6 Seismicity 310
5.6.1 Seismicity Along the Rio Grande Rift 310
5.6.2 Seismicity of the Valles Caldera Region 315

References 317

Appendices

A Geologic Time Scale 320
B U.S. - Metric Conversion Table 321
C Basic Concepts and Semantics of Hydrology 323
D Glossary 329
E List of Abbreviations 337

FIGURES

Number		Page
1.1	Location of study areas	2
2.1	Physiographic setting and location of Imperial Valley, California	8
2.2	Temperature gradient map showing locations of KGRAs in Imperial Valley, California	9
2.3	Mean annual precipitation, 1931-1960, Imperial Valley, California	14
2.4	A and B. Simplified diagram of "rhomb graben" formation C. Multiple "rhomb graben" formation	25
2.5	Tectonic setting of the Gulf of California	26
2.6	Schematic model for the evolutionary development of the Salton Trough	27
2.7	Structural interpretation of a ground magnetometer survey by Kelly and Soske (1936)	29
2.8	Map of possible faults and discontinuities in the Salton Sea area	42
2.9	Depth to basement complex, Imperial Valley, California	45
2.10	Location of sections, porosity profile sites and wells referenced in this report	48
2.11	Cross section of average percent volume of sand bodies in sedimentary section	49
2.12	Composite column of Salton Trough showing inferred time-stratigraphic relations, estimated maximum thickness and lithology	50
2.13	Salton Sea drainage basin	55

Number		Page
2.14	Total thickness of deposits with water containing less than 35,000 mg/l dissolved solids	67
2.15	Total thickness of deposits with water containing less than 35,000 mg/l dissolved solids in zone 4	68
2.16	Total thickness of deposits with water containing less than 35,000 mg/l dissolved solids in zone 3	69
2.17	Total thickness of deposits with water containing less than 35,000 mg/l dissolved solids in zone 2	70
2.18	Total thickness of deposits with water containing less than 35,000 mg/l dissolved solids in zone 1	71
2.19	Hydrologic section A-A'	72
2.20	Hydrologic section B-B'	73
2.21	Hydrologic section C-C'	74
2.22	Perforated intervals for wells in Imperial Valley, California	77
2.23	Ground water level contours of shallow aquifer system, 1962 and 1964, in Imperial and Mexicali Valleys	79
2.24	Inferred direction of movement in the deep water-bearing strata to generalized areas of known geothermal anomalies in Imperial and Mexicali Valleys	80
2.25	Change in ground water levels in East Mesa, 1939-1960	85
2.26	Average ground water level contours in 1939 in the Colorado River Delta region	86
2.27	Correlation between horizontal and vertical permeabilities, East Mesa KGRA, Imperial Valley, California	93

Number		Page
2.28	Porosity versus depth for two wells in southeast Imperial Valley	95
2.29	Porosity versus depth for two wells in central and northern Imperial Valley	96
2.30	Correlation between core permeability and core porosity, East Mesa KGRA, Imperial Valley, California	97
2.31	A. Basic model of a geothermal system	101
	B. Modified model for Salton Sea geothermal system, showing source of recharge and water quality changes	101
2.32	Complete Bouguer anomaly map of the Imperial Valley	104
2.33	Static temperature profiles in geothermal wells from the Salton Trough	105
2.34	Modified Stiff diagrams for characteristic Imperial Valley ground waters	113
2.35	Three-dimensional perspective of a Langelier-Ludwig diagram showing surfaces of salinity sections	115
2.36	Langelier-Ludwig diagram for ground water data in Imperial Valley, California	116
2.37	Salinity section A-B from Langelier-Ludwig diagram for ground water data in Imperial Valley, California	117
2.38	Salinity sections A-C and A-D from Langelier-Ludwig diagram for ground water data in Imperial Valley, California	118
2.39	Modified Stiff diagrams representing hypothetical analyses of ground water resulting from specified chemical changes in Colorado River water	120
2.40	Schematic surface of specific conductance values in Imperial Valley ground water	129
2.41	Schematic surface of sulfate values in Imperial Valley ground water	130

Number		Page
2.42	Schematic surface of bicarbonate values in Imperial Valley ground water	131
2.43	Schematic surface of chloride values in Imperial Valley ground water	132
2.44	Schematic surface of calcium values in Imperial Valley ground water	133
2.45	Recurrence curve for earthquakes in the Imperial Valley region, 1932-1972	145
2.46	Ranges of maximum acceleration in rock	146
2.47	Comparison of maximum acceleration in rock and stiff soil deposits for earthquake magnitude 7	146
2.48	Epicenters of injection-induced earthquakes at Rangely, Colorado	149
3.1	Location map of The Geysers study area	165
3.2	Precipitation in The Geysers-Clear Lake area	168
3.3	Earthquake epicenters located by the University of California, Berkeley, 1910-1976	194
3.4	Frequency of occurrence of earthquake intensities, Santa Rosa Valley region	199
3.5	Magnitude versus frequency of occurrence for earthquakes in the central Coast Range	201
4.1	Location map of the Klamath Basin study area	212
4.2	Normal monthly temperature and precipitation at Klamath Falls	215
4.3	Annual precipitation at Chiloquin and Klamath Falls, 1902-1972	217
4.4	Diagrammatic section of east side of Klamath graben	235
4.5	Salient features of local, intermediate and regional ground water flow systems	252

Number		Page
4.6	Earthquake epicenters in Oregon, 1841-1970	262
4.7	Magnitude versus frequency of occurrence for earthquakes in the Basin and Range Physiographic Province of southern Oregon	264
5.1	Map of Rio Grande Valley and area of direct surface runoff	271
5.2	Rio Grande drainage basin in New Mexico	273
5.3	Major topographic subdivisions of Rio Grande Rift	274
5.4	"Narrow" interpretation of Rio Grande Rift Zone	275
5.5	Average annual precipitation and lake surface evaporation	277
5.6	Normal annual precipitation in New Mexico	278
5.7	Life and crop zones in New Mexico	279
5.8	Vegetative-type map of New Mexico	280
5.9	Heat flow in New Mexico	282
5.10	Subdivisions of the Rio Grande Rift	284
5.11	Average monthly and annual discharges at selected gaging stations, Rio Grande Valley and area of direct surface runoff	292
5.12	Mean discharge of principal streams and annual runoff in New Mexico for periods of record	293
5.13	Decline of ground water level in Estancia Basin, Santa Fe and Torrance Counties, New Mexico, 1848-1960	302
5.14	Depth to ground water in New Mexico	303
5.15	Ground water reservoir in the Rio Grande Depression, New Mexico	304
5.16	Average annual suspended sediment discharge of streams and suspended sediment discharge by years at selected stations in New Mexico	305

Number		Page
5.17	Average annual dissolved solids discharge in years at selected stations in New Mexico	306
5.18	General occurrence of saline ground water in New Mexico	307
5.19	Thickness of fresh water unit (less than one gram per liter dissolved solids)	308
5.20	General availability of relatively fresh ground water in New Mexico	309
5.21	Principal sources of waste water in New Mexico	311
5.22	Seismic risk map by Richter (1958)	313
5.23	Seismic risk map by Algermissen (1969)	314

TABLES

Number		Page
1.1	List of principal project participants	6
2.1	Fault map reference	33
2.2	Chemical analyses of water from the Salton Sea	59
2.3	Selected chemical analyses of surface water in the Salton Sea Basin	61
2.4	Summary of "usable" and recoverable water in storage derived from the Colorado River and local sources	89
2.5	Results of USGS pumping tests in Imperial Valley, California	91
2.6	Trace element composition of Salton Trough geothermal waters	137
3.1	Average monthly and annual temperatures and precipitation at selected stations	167
3.2	Average annual stream discharge and depth of runoff	183
3.3	Modified Mercalli intensity scale	195
3.4	Earthquake recurrence data for the central Coast Range region	202
4.1	Mean monthly and annual temperatures and precipitation, and mean extremes of temperature, Klamath Basin, 1931-1960	216
4.2	Prevailing winds at Klamath Falls airport: percentage frequency of occurrence of calms and modal directions, with average speeds	219
4.3	Summary of stream flow data at selected points in the Klamath Basin	243

Number		Page
4.4	Chemical analyses of surface waters, 1959-1963 averages	248
4.5	Aquifer units of Klamath Basin	249
4.6	Chemical analyses of waters from springs and wells	255
5.1	Mean temperature and precipitation at places in the Rio Grande Basin, New Mexico	276
5.2	Generalized stratigraphic section in the Rio Grande Basin, New Mexico	288
5.3	Average Class A land pan evaporation, Rio Grande Basin in New Mexico	290
5.4	Annual discharge of the Rio Grande near Lobatos, Colorado	295
5.5	Annual discharge of the Rio Grande at San Marcial, New Mexico	297
5.6	Annual discharge of the Rio Grande at Fort Quitman, Texas	299

PLATES

Number	All plates in pocket
2.1	Geologic map, Imperial Valley, California
2.2	Fault map, Imperial Valley, California
2.3	Well location map, Imperial Valley, California
2.4	Chemical characteristics of shallow depth groundwater, Imperial Valley, California
2.5	Total dissolved solids in shallow depth groundwater, Imperial Valley, California
2.6	Chemical characteristics of intermediate depth groundwater, Imperial Valley, California
2.7	Total dissolved solids in intermediate depth groundwater, Imperial Valley, California
2.8	Chemical characteristics of deep groundwater, Imperial Valley, California
2.9	Total dissolved solids in geothermal water, Imperial Valley, California
2.10	Historic seismicity map, Imperial Valley, California
3.1	Preliminary field compilation of in-progress geologic mapping in The Geysers geothermal area, California (2 sheets)
3.2	Map showing preliminary hypocenters of earthquakes in the Healdsburg Quadrangle, Lake Berryessa to Clear Lake, California
4.1	Geologic map of the southern Klamath Basin and adjacent areas
5.1	Rio Grande Rift in New Mexico

SECTION 1

INTRODUCTION

This is the first in a series of reports concerning the environmental assessment of effluent extraction, energy conversion, and waste disposal in geothermal systems. The primary objective of the study is to provide the United States Environmental Protection Agency (EPA) with a monitoring approach to detect any ground water pollution, induced seismicity and/or induced subsidence caused by geothermal resource development. This approach is expected to serve as a model for monitoring any geothermal area. An important part of this study involves environmental assessment of four geothermal areas: Imperial Valley and The Geysers, California; Klamath Falls, Oregon; and the Rio Grande Rift Zone, New Mexico (Fig. 1.1). Each of these areas is representative of a distinct type of geothermal system. The Imperial Valley is representative of an intermediate to high temperature liquid-dominated system; The Geysers, of a vapor-dominated system; Klamath Falls, of a low temperature hot water system; and Rio Grande Rift, of a hot, dry rock system, and a high temperature liquid-dominated system.

This assessment requires evaluation of the geologic, hydrologic, climatic and seismic conditions, and definition of potential pollutants and environmental effects. From the data base provided by this assessment, a monitoring system will be designed, implemented and evaluated at one of the four areas.

1.1 OBJECTIVES

The objective of this study is to acquire and analyze data for the purpose of:

1) identifying pollutants as a result of geothermal development,

2) identifying pathways into the underground water environment,

3) identifying ecological hazards involved with long-term operating facilities,

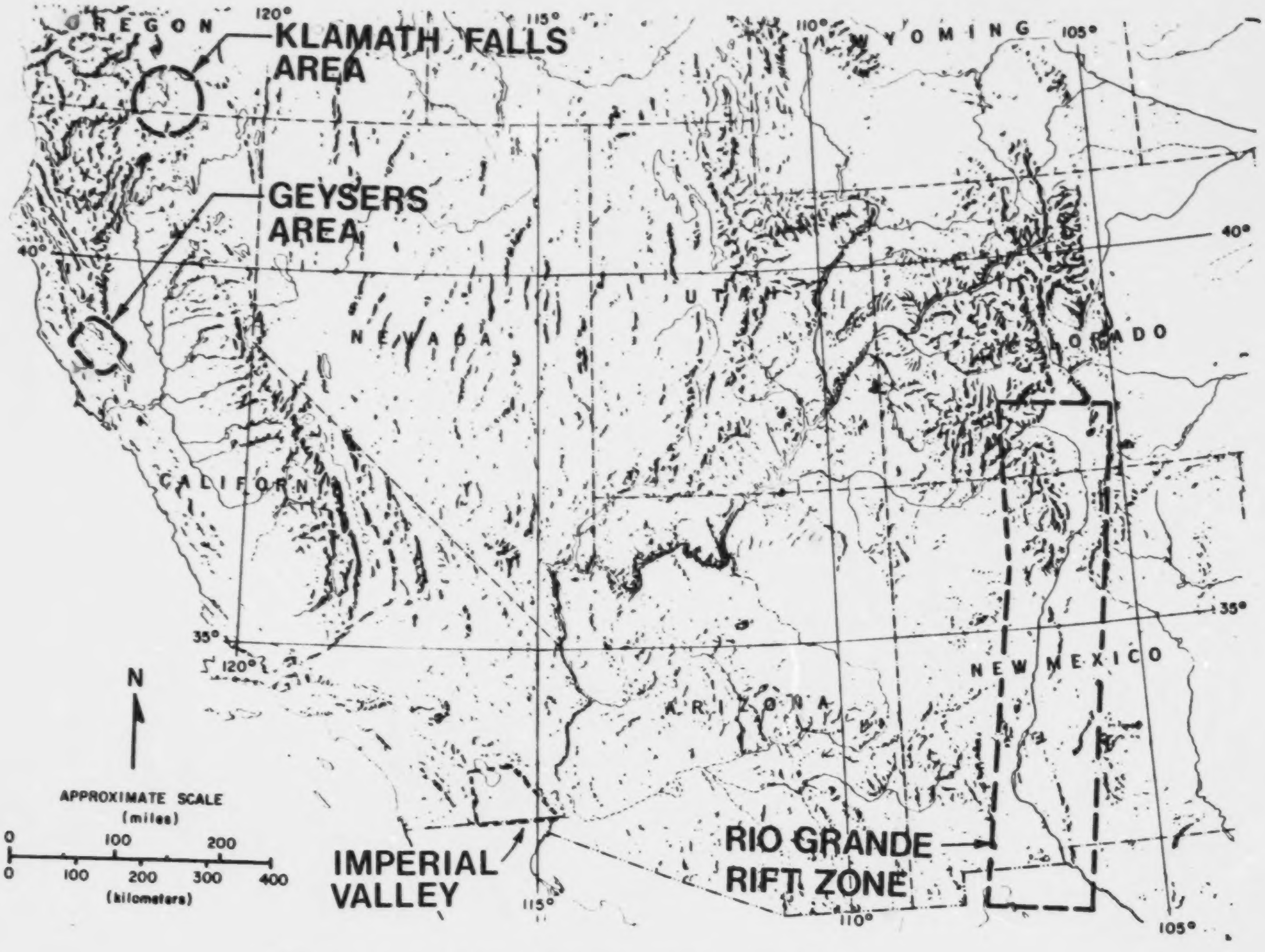
OREGON
120°
115°
110°
WYOMING
105°
KLAMATH FALLS AREA
GEYSERS AREA
40°
NEVADA
UTAH
COLORADO
CALIFORNIA
35°
120°
N
APPROXIMATE SCALE (miles)
0
100
200
0
100
200
300
400
(kilometers)
ARIZONA
NEW MEXICO
IMPERIAL VALLEY
115°
RIO GRANDE RIFT ZONE
110°
105°

Figure 1.1 Location of study areas.

4) designing a monitoring approach that will be applicable to any geothermal resource development and conversion facility, and

5) applying the methodology to a selected site and operating the system to verify its applicability.

The primary emphasis is on the environmental effects of changes in the ground water regime, both chemical and hydraulic, as a result of geothermal resource utilization. The primary effects are potential ground water pollution, subsidence, and induced seismic events which in turn may affect the ecology and socioeconomic conditions of the areas.

1.2 SCOPE OF INVESTIGATION

The scope of work is outlined in five tasks to be accomplished in three stages. Stage I is an assessment stage that includes Tasks 1 and 2. Task 1 will define the geology, hydrology, climatology and seismicity of the four geothermal areas and identify the aquifers in each area. Task 2 will define the various geothermal systems; quantify the pollutants from geothermal resources development, including phase of the produced fluids, subsidence possibilities, seismic effects, fluid disposal methods and thermal losses; and discuss their possible effects on the ground water of each area.

Stage II is a design and research stage that includes Task 3, resulting in the design of a monitoring system for one of the four areas.

Stage III includes Tasks 4 and 5 and is a monitoring, analysis and evaluation stage. Task 4 involves implementation and operation of the monitoring program under the direction of the project officer. Recommendations for improvement in the monitoring plan will be incorporated into Task 5. As a result of the experience in designing and operating a monitoring system, recommendations for a general monitoring methodology that will be most apt to meet the requirements of any geothermal resource development will be the culmination of Task 5.

1.3 BASELINE ASSESSMENT REPORT

This report, the result of the Task 1 investigation, summarizes, evaluates and synthesizes all available, relevant data on climatology, geology, hydrology and seismicity for the four geothermal areas previously mentioned. No original field work, laboratory research or chemical analyses were conducted, although some novel and valuable syntheses and representations of existing data were accomplished.

The goal of this report is to establish baseline and background data on each of the four areas. This will define what is known about the existing physical conditions so decisions on development of a monitoring system can be made.

The level of information necessary for subject evaluation in geology, hydrology, climatology and seismicity for each type of geothermal system will be established. Different levels of subject information will exist for each geothermal area, and it will be necessary to define a minimum number and quality of parameters to establish a viable and meaningful monitoring program that would be particularly responsive to each specific type of geothermal environment.

To describe potential effects on a ground water system, information is necessary describing physical properties and lithology of subsurface materials, permeability and hydraulic gradient, geometry of aquifers and aquitards, recharge and discharge areas and areal distribution of the chemical quality of the ground water. The physical properties and lithology of subsurface materials will determine what basic role each unit will play. For example, with this information deductions can be made about the underground flow system: will the unit conduct or resist water flow; is the flow intergranular or along fractures; will anisotropy preferentially induce more flow in one direction; what chemical changes due to underground flow can be expected from the solubility of the mineral constituents in geologic units; etc. Knowledge of the permeability, hydraulic gradient and geometry of aquifers and aquitards combined with lithologic information will allow estimates of the rate and direction of flow. Recharge and discharge areas must be known to trace the flow patterns and to predict the effects of man-induced recharge or discharge. Areal distribution of the chemical quality of ground water, including isotope data, will aid in identifying the sources of the water and provide some indication about flow patterns and interconnection of aquifers.

The seismicity portion of the study requires an understanding of the tectonic framework of the area being monitored. A record of historic, predevelopment seismic activity and an instrumentation network to monitor current activity would be necessary. For example, knowledge of the tectonic history and structural framework of the Salton Trough plays an integral part in understanding the causes of existing seismicity patterns and will aid in distinguishing between natural seismicity and seismicity which may result from geothermal development.

1.4 REPORT ORGANIZATION

This report was prepared by an interdisciplinary team of scientists from Geonomics, Inc., GeothermEx, and W. K. Summers and Associates. Section 1 (Introduction) and Section 2 (Imperial Valley) were prepared by Geonomics, Inc. The major portions of Sections 3 and 4 were prepared by GeothermEx and the major portion of Section 5 by W. K. Summers and Associates. Table 1.1 is a list of individuals who participated in the preparation of this report.

This report is arranged in five sections and five appendices. Each of the baseline studies follows a general outline, consisting of subsections on geothermal characteristics, geology, hydrology, chemical characteristics of ground water and seismicity. Each baseline study also includes an introductory section containing a summary, as well as information on background and climatology. References are cited at the end of each section. The format for the studies of each region was kept as consistent as possible, and most of the subsections are consistent between regions down to third-order headings. Variations in the micro-organization are due to different amounts of available data and different geologic, hydrologic and seismic conditions in each region.

Several topics discussed under individual regions are worthy of particular attention. The "Chemical Characteristics of Ground Water" section in the Imperial Valley study contains a number of standard and some novel approaches to establishment of baseline ground water conditions. The "Relation of Earthquakes to Geothermal Activity" section in the Imperial Valley study and the "Seismic Risk" discussion in The Geysers study both contain much information of general interest that could relate to any geothermal area.

The five appendices at the end of this report contain additional background information to aid in understanding some of the more technical material. The first appendix is a geologic time scale to accompany the geologic discussions. The second appendix contains U.S.-to-metric conversion factors used in this report. The third appendix is a discussion of concepts and semantics of hydrology. The fourth appendix is a glossary containing important technical terms used in this report. The fifth appendix is a list of abbreviations used in this report.

TABLE 1.1 LIST OF PRINCIPAL PROJECT PARTICIPANTS

GEONOMICS, INC.	
Project Management:	H. Tsvi Meidav, Project Manager Subir K. Sanyal, Deputy Project Manager and Scientific Coordinator
	Imperial Valley Area
Geology and Hydrology:	Richard B. Weiss Theodora Oldknow Maren Teilman
Seismology:	Maren Teilman Richard B. Weiss
Chemistry:	Felix Tsai
Geochemistry:	Franco B. Tonani Richard B. Weiss Theodora Oldknow
Computer Graphics:	Sirisak Juprasert
Research, Administration:	Gio' M. Morse
Editing:	Evelyn Bless
GEOTHERMEX	
	The Geysers Area
	James B. Koenig Roger Greensfelder
	Klamath Falls Area
	Murray Gardner
W. K. SUMMERS & ASSOCIATES	
	The Rio Grand Rift Area and Hydrology Appendix
	W. K. Summers

SECTION 2

IMPERIAL VALLEY

2.1 INTRODUCTION

This section presents baseline data on climatology, geology, hydrology and seismology to aid in assessment of environmental impacts of potential geothermal development in Imperial Valley, California. The major emphasis is on ground water contamination, with detailed descriptions of aspects of climatology, geothermal characteristics, tectonics, faults, stratigraphy, lithology and surface water that are related to and influence the ground water regime. A section on baseline seismicity of Imperial Valley, microseismicity and seismic risk is also included.

2.1.1 Summary

The Salton Trough (Fig. 2.1) is an area of high regional heat flow and contains numerous geothermal anomalies (Combs, 1971) (Fig. 2.2). It is one of the most seismically active areas in the United States,and significant subsidence rates have been measured. Geologic evidence shows that the trough has experienced intensive crustal deformations, active faulting (Richter, 1958; Allen, et al., 1965; Brune and Allen, 1967) and subsidence (Elders, et al.,1972) and that this intensive deformation is continuing.

The Imperial Valley (Figs. 2.1 and 2.2) is a hot, naturally arid area with less than 76.2 mm (3 in) of mean annual precipitation. It is a relatively flat alluvial valley with the central portion heavily irrigated. It is a broad structural and topographic depression that has been filled with over 6,000 m (20,000 ft) of later Tertiary deltaic and lacustrine sands, silts and gravels overlain by alluvium and lake sediments. The underlying pre-Tertiary granitic and metamorphic complex is intensely step-faulted down from the mountains surrounding both sides of the valley.

The combination of graphic chemical analytic representations presented in this report provides an effective basis for establishing baseline water quality parameters in Imperial Valley and other geothermal areas. These representations include modified Stiff diagrams, salinity circles, Langelier-Ludwig diagrams and single-chemical parameter plots.

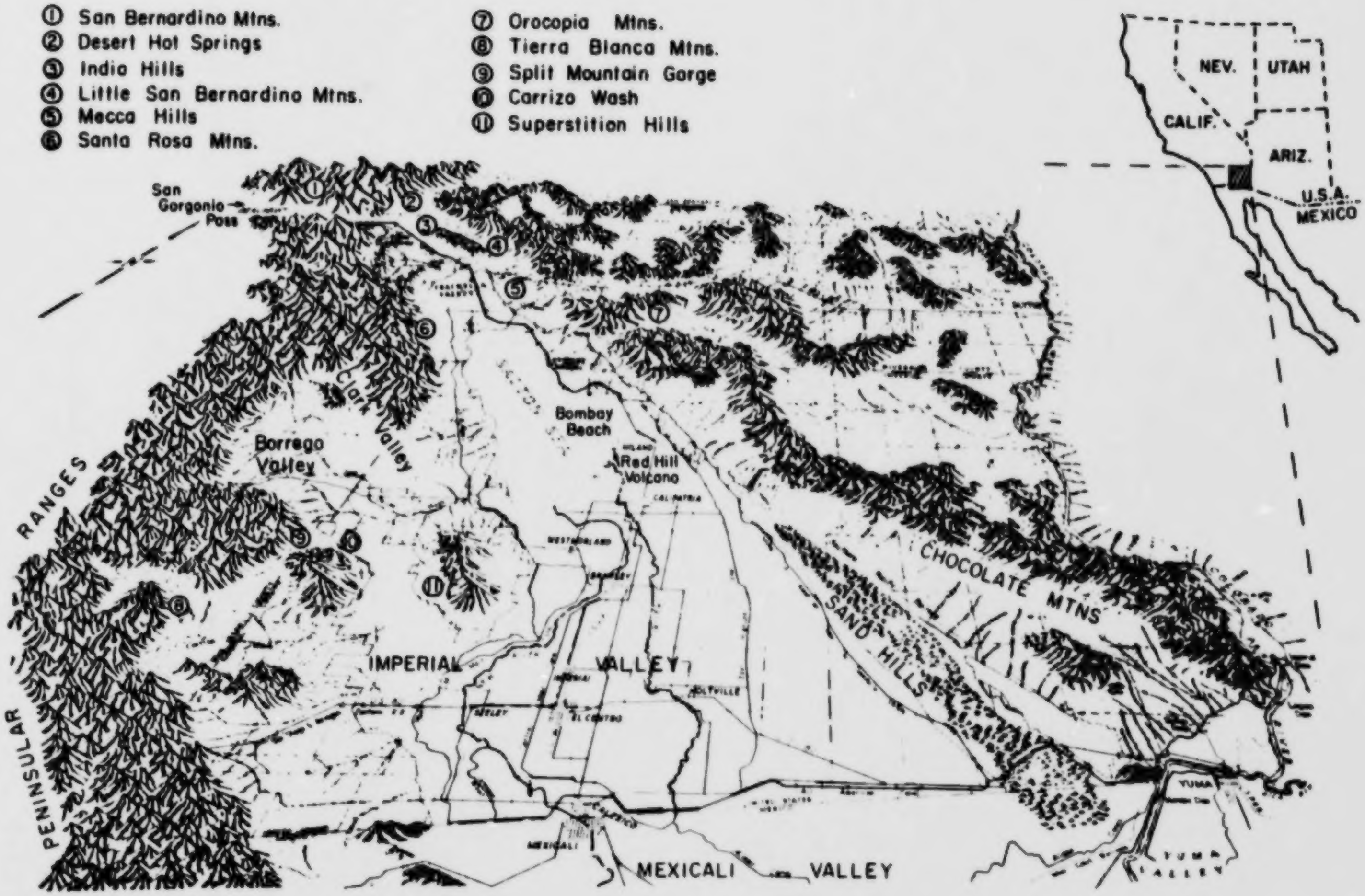
① San Bernardino Mtns.
② Desert Hot Springs
③ Indio Hills
④ Little San Bernardino Mtns.
⑤ Mecca Hills
⑥ Santa Rosa Mtns.
⑦ Orocopia Mtns.
⑧ Tierra Blanca Mtns.
⑨ Split Mountain Gorge
⑩ Carrizo Wash
⑪ Superstition Hills
San Gorgonio Pass
NEV.
UTAH
CALIF.
ARIZ.
U.S.A.
MEXICO
Clark Valley
Borrego Valley
Bombay Beach
Red Hill Volcano
RANGES
PENINSULAR
IMPERIAL
VALLEY
CHOCOLATE MTNS
SAND HILLS
MEXICALI
VALLEY
YUMA VALLEY

Figure 2.1 Physiographic setting and location of Imperial Valley, California. (Coplen, 1976)

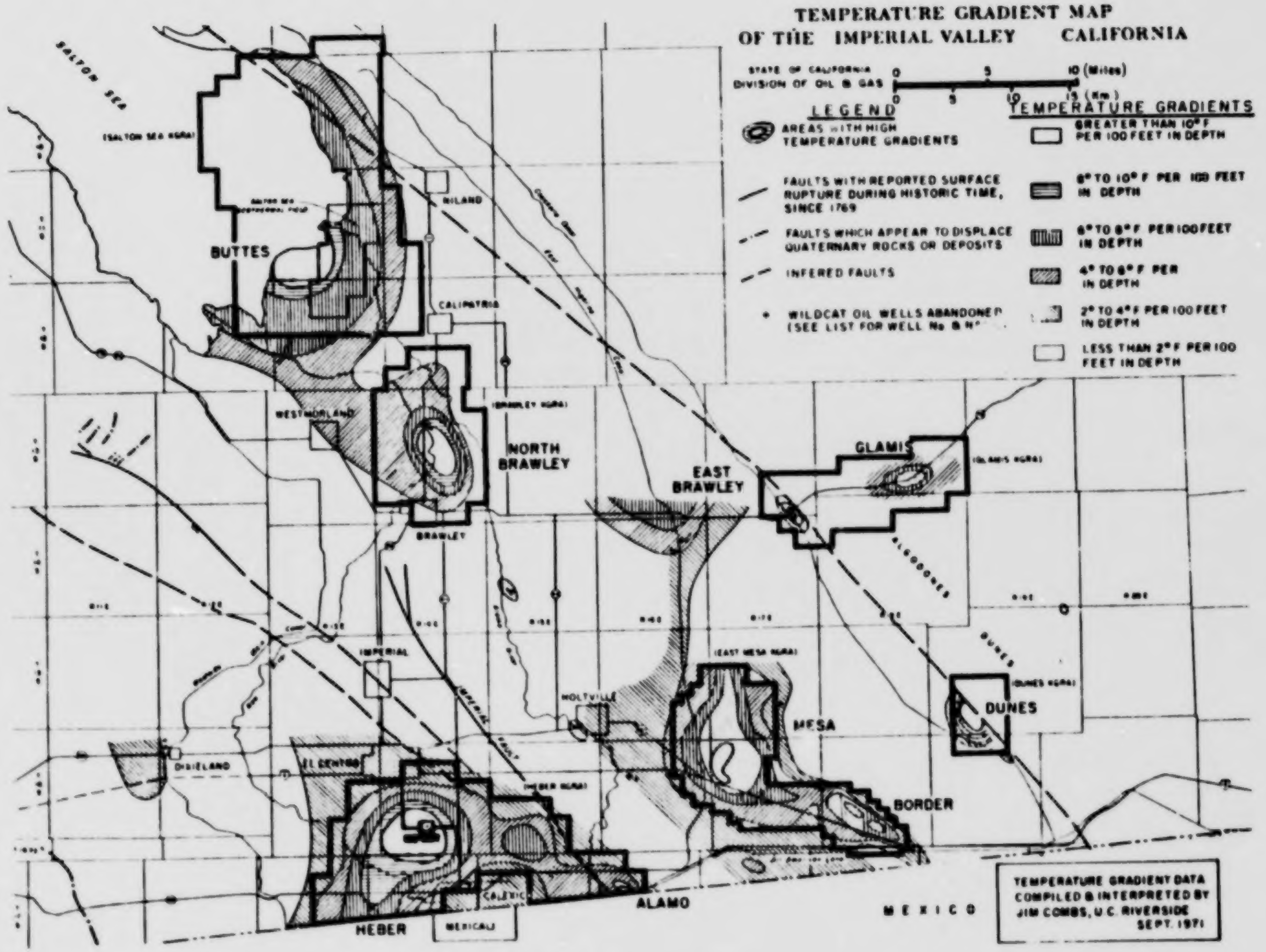
TEMPERATURE GRADIENT MAP
OF THE IMPERIAL VALLEY CALIFORNIA
STATE OF CALIFORNIA
DIVISION OF OIL & GAS
0 5 10 (Miles)
0 5 10 15 (Km)
LEGEND
AREAS WITH HIGH TEMPERATURE GRADIENTS
FAULTS WITH REPORTED SURFACE RUPTURE DURING HISTORIC TIME, SINCE 1769
FAULTS WHICH APPEAR TO DISPLACE QUATERNARY ROCKS OR DEPOSITS
INFERED FAULTS
WILDCAT OIL WELLS ABANDONED (SEE LIST FOR WELL No & N°
TEMPERATURE GRADIENTS
GREATER THAN 10° F PER 100 FEET IN DEPTH
8° TO 10° F PER 100 FEET IN DEPTH
6° TO 8° F PER 100 FEET IN DEPTH
4° TO 6° F PER IN DEPTH
2° TO 4° F PER 100 FEET IN DEPTH
LESS THAN 2° F PER 100 FEET IN DEPTH
SALTON SEA
(SALTON SEA KGRA)
BUTTES
NILAND
CALIPATRIA
WESTMORLAND
(BRAWLEY KGRA)
NORTH BRAWLEY
BRAWLEY
EAST BRAWLEY
GLAMIS
(GLAMIS KGRA)
ALGODONES
DUNES
(DUNES KGRA)
DUNES
IMPERIAL
IMPERIAL FAULT
HOLTVILLE
(EAST MESA KGRA)
MESA
BORDER
DIXIELAND
EL CENTRO
(HEBER KGRA)
HEBER
CALEXICO
MEXICALI
ALAMO
MEXICO
TEMPERATURE GRADIENT DATA COMPILED & INTERPRETED BY JIM COMBS, U.C. RIVERSIDE SEPT. 1971

Figure 2.2 Temperature gradient map showing locations of KGRAs in Imperial Valley, California. (Palmer, et al., 1975)

Modified Stiff diagrams, prepared for this report, depict the areal distribution of the chemical characteristics of waters in each of three depth zones (Plates 2.4, 2.6 and 2.8). The three depth zones, based on perforated well intervals, defined for this study (Fig. 2.22) are shallow, from 24 to 91 m (80 to 300 ft); intermediate, from 91 to 457 m (300 to 1,500 ft); and deep, more than 457 m (1,500 ft).

The modified Stiff diagrams aided in defining the areal and depth distribution of five water types in Imperial Valley. These are a sodium chloride water, a high sulfate water, a sodium chloride with high sulfate and/or magnesium water, a sodium chloride with high calcium water and a sodium bicarbonate water (Fig. 2.34). The Stiff diagrams depict the great variation in the chemical characteristics of ground water throughout the valley, from the purest waters coming off the Peninsular Range to the hypersaline brines occurring in the Salton Sea geothermal area. The salinity circles (Plates 2.5, 2.7 and 2.9) and the schematic surface of specific conductance values (Fig. 2.40) define variations of ground water salinity and depict a salinity gradient, with salinity increasing from the southeastern valley to the west and north as well as with depth.

Langelier-Ludwig diagrams (Figs. 2.36, 2.37 and 2.38) show chemical changes and groupings of waters. Single-chemical parameter contoured surfaces provide a graphic method for correlating chemical changes in ground water with geologic or structural features and for recognizing chemical correlations.

The geology of the Imperial Valley (Plate 2.1) is complicated with myriad fault traces (Plate 2.2) and thousands of meters of discontinuous, folded and layered sediments. The San Andreas, San Jacinto, Elsinore and Salton Trough Fault Zones are all components of the San Andreas Fault System that fractures the sediments and basement of the valley. A detailed compilation of these faults has been prepared for this report (Plate 2.2) and many fault traces have been located in each of these fault zones. Many other concealed traces in alluvial areas remain to be discovered with further detailed investigation. The Salton Trough Fault Zone has been defined in this report as a unique zone, containing parallel and subparallel fault traces between the San Andreas and San Jacinto Fault Zones. Most of the faults in this zone are concealed and have been inferred from geophysical evidence.

Rocks in the Salton Trough range in age from Precambrian basement complex to Recent alluvium and dune sands and ,correspondingly,from dense, competent hard rocks to totally unconsolidated sedimentary deposits to young volcanics (Plate 2.1, Fig. 2.12). Most of the central valley is Pliocene and younger. One deep well near Brawley intercepted over 4,000 m (13,000 ft) of interbedded fine-grained sandstone and siltstone. The main source of the thick section of Eocene to Holocene nonmarine sediments has been Colorado Plateau debris transported by the Colorado River, with some contribution from local sources. Tertiary volcanic and intrusive rocks occur within the sedimentary section.

Imperial Valley ground water generally flows northward and westward as underflow from the Colorado River, canal leakage and irrigation discharge (Fig. 2.23). This flow is generally distributed into a shallow and a deep aquifer. Flow pattern complications arise from fault and stratigraphic aquitards which channel and restrict water flow. It is conjectured that local convective patterns tend to cause regional waters to flow radially inward towards the geothermal anomalies (Fig. 2.24). All water is discharged from the closed Salton Sea Drainage Basin through evaporation and evapotranspiration.

The flow rate of wells is quite variable throughout the valley (Table 2.5), from over 3,800 lpm (1,000 gpm) in a shallow well in the southeastern valley to essentially nil in some shallow wells in the central portion of the valley. However, deep wells in the central portion of the valley flow as well or better than wells at the valley margins.

The total volume of water in storage has been estimated between 0.20 and 0.59 billion ha-m (1.6 and 4.8 billion acre-ft), with another estimate of 0.14 billion ha-m (1.2 billion acre-ft) of usable and recoverable water in storage.

Artificially induced recharge of Imperial Valley ground water from irrigation has had a notable effect on ground water levels, especially in the southeastern portion of the valley.

Seismic activity is widespread and abundant in Imperial Valley (Plate 2.10). Nine earthquakes of magnitude 6.7 or greater have occurred in the Salton Trough since 1850. The Imperial Valley earthquake of 1940 was the most significant event in terms of human disturbance. Although it has been difficult to correlate much of the historic seismicity with active faults, correlation of microseismicity with active faults has been more fruitful.

Microearthquake activity is associated with geothermal anomalies, and their occurrence may increase with geothermal development or reinjection of geothermal fluids. A number of microseismic monitoring networks have been installed in Imperial Valley by the U.S. Geological Survey (USGS), California Institute of Technology (Cal Tech) and Chevron Oil Company. Changes in earthquake recurrence statistics and/or in the depth and location of events from preproduction activity can be used to determine production-induced seismicity.

2.1.2 Background

The Imperial Valley is located in Imperial County in the southeasternmost corner of California (Fig. 1.1). It contains six Known Geothermal Resource Areas (KGRAs). They are the Salton Sea, Brawley, Glamis, East Mesa, Dunes, and Heber KGRAs. The Cerro Prieto field in northern Mexico, also part of the Salton Trough, is already in production. Ongoing commercial geothermal activity will involve production from and probable reinjection into specific reservoir formations.

The Imperial Valley could be divided environmentally into two segments: 1) the central portion of the valley west of the East Highline Canal which is heavily irrigated, and 2) the area east of the canal which is largely barren. Based upon the difference in land use, we would rank the potential environmental impacts in the agricultural portion of the valley differently from those in the sandy regions which are uninhabited.

The Imperial Valley is one of the richest farming areas of the United States with a total agricultural productive capacity of about $500 million per year. The valley, a flat alluvial plain, is laced with more than 6,400 km (4,000 mi) of precisely aligned canals and drains. Any land subsidence due to massive withdrawal of fluid would create havoc with the hydraulic gradients of these canals and drains. Potentially negative environmental impacts in the agricultural area addressed in this section include induced earthquake activity, induced rise in ground water levels and ground water degradation.

Previous studies on ground water in Imperial Valley were conducted by Dutcher, et al.,(1972) and Loeltz, et al.,(1975). Water quality data has been published by Hardt and French (1976), Reed (1975), Cosner and Apps (1977), Loeltz, et al., (1975) and Geonomics (1976). Many investigators have conducted geologic and seismologic studies in Imperial Valley, and the major ones are mentioned in the respective subject sections.

The geothermal anomalies in Imperial Valley were initially discovered through research programs conducted by the Institute of Geophysics and Planetary Physics at the University of California, Riverside (U.C.R.). These researchers have published many studies on the geothermal occurrences in Imperial Valley, particularly Rex, et al. (1971) and Rex, et al.,(1972).

2.1.3 Climatology

The Imperial Valley is a naturally arid area. It is a relatively flat alluvial valley. The central portion west of the East Highline Canal is heavily irrigated and the area east of the canal is largely barren. The irrigated portion of the valley is a rich farmland.

In the summer months temperatures as high as 52°C (125°F) have been recorded and the average daily maximum in July is about 42°C (108°F) (based on recordings made at Indio, California,from 1877 to 1960). While subfreezing temperatures have been recorded, the lowest average daily minimum, occurring in January, is 3°C (38°F). The mean annual temperature for 1931-1960 was 23°C (73°F).

The mean annual precipitation (Fig. 2.3) ranges from less than 80 mm (3 in) near the Salton Sea to over 1,020 mm (40 in) on Mount San Gorgonio, the highest peak in the San Bernardino Mountains (Fig. 2.1). The mean precipitation over most of the area, including the irrigable tracts, is less than 200 mm (8 in). A large part of the runoff generated by precipitation is absorbed in the alluvium of the valleys and plains. There is an annual cyclic precipitation pattern. Most rainfall occurs between October and April, with the major part occurring from November through March (Hely and Peck, 1964). Precipitation is virtually nil from May to September, although there have been occasional years with a significant percentage of the annual rainfall during this period.

Natural water loss occurs by evaporation from water and land surfaces and transpiration from vegetated areas. The combination of these two components of water loss is called evapotranspiration. Evapotranspiration in humid regions is generally computed by subtracting mean annual runoff from mean annual precipitation. This method is valid for the mountainous regions to the west of Imperial Valley. However, when runoff is absorbed by alluvial deposits, like those in Imperial Valley, the method must be modified to include transpiration of absorbed runoff. Evapotranspiration in the Peninsular Range to the west of Imperial Valley ranges from about 100 mm (4 in) at the valley margin to over 410 mm (16 in). In the Chocolate Mountains to the east it is about 100 mm (4 in) and in the nonirrigated areas of the valley it is 80 mm (3 in) or less.

Rates of evapotranspiration in the irrigated parts of the valley vary considerably with vegetative type and irrigation practices. They greatly exceed precipitation and are over 910 mm (36 in) annually over all of the irrigated region; in some areas the rate may exceed 1,520 mm (60 in) (Hely and Peck, 1964). This high rate of evapotranspiration results in high humidity in the irrigated areas.

2.2 GEOTHERMAL CHARACTERISTICS

The Imperial Valley region is potentially one of the most important geothermal areas in the United States. High heat flow from the hot, shallow mantle beneath the northern extension of the East Pacific Rise (Fig. 2.5), together with the faulting

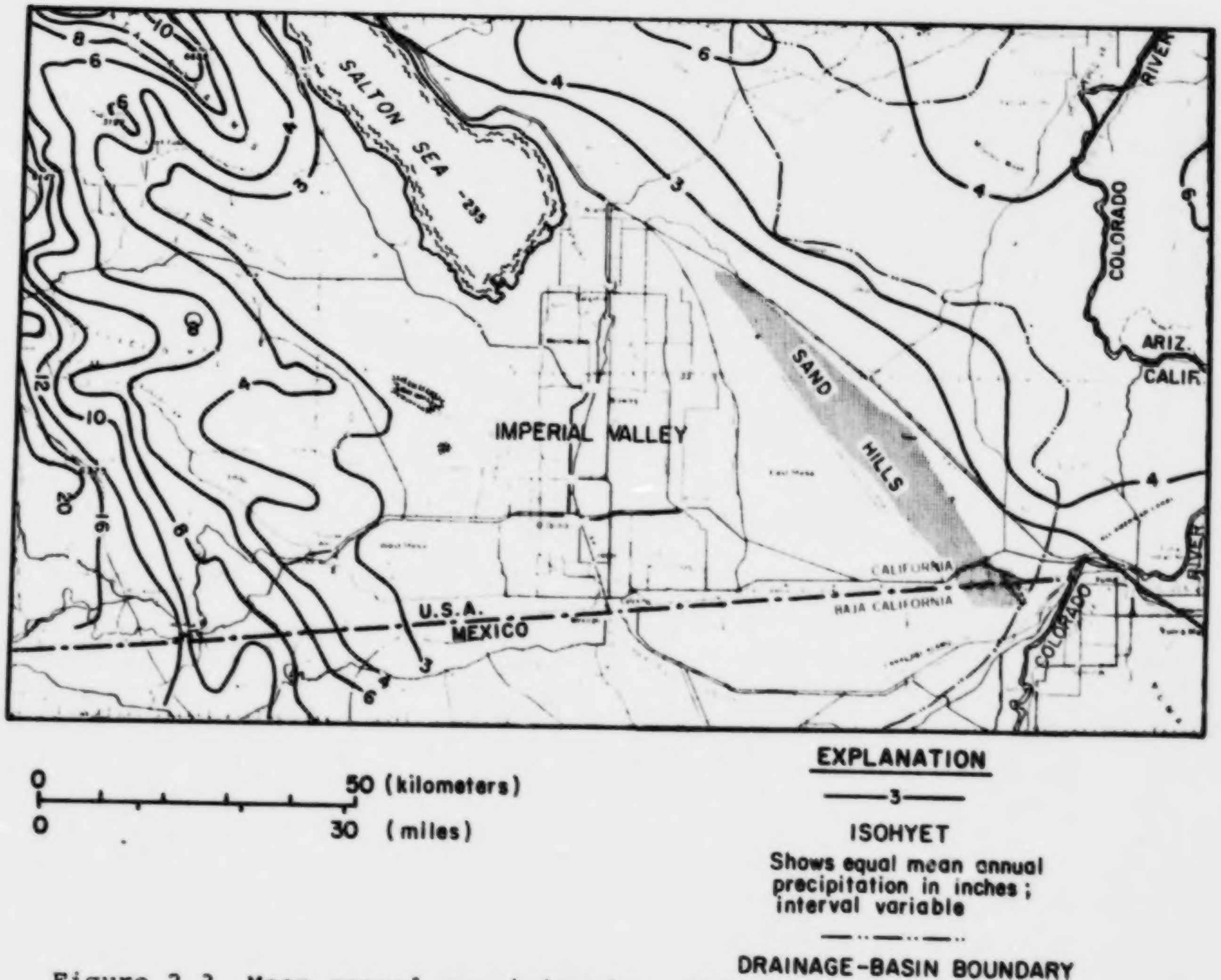
SALTON SEA -235
IMPERIAL VALLEY
SAND HILLS
COLORADO RIVER
ARIZ.
CALIF.
CALIFORNIA
BAJA CALIFORNIA
U.S.A.
MEXICO
COLORADO
RIVER
3
4
6
8
10
12
16
20
0
50 (kilometers)
0
30 (miles)
EXPLANATION
3
ISOHYET
Shows equal mean annual precipitation in inches; interval variable
DRAINAGE-BASIN BOUNDARY

Figure 2.3 Mean annual precipitation, 1931-1960, Imperial Valley, California (Hely and Peck, 1964)

and fracturing due to rifting, have combined to generate silicic volcanism and high geothermal gradients in the region.

Within these six Imperial Valley KGRAs (Fig. 2.2) there are four known geothermal reservoirs, each containing hot brines of different character: a high-temperature (300°C [572°F]), high-enthalpy (1,046 kilojoules/kg [450 BTU/lb], high-salinity (250,000 ppm total dissolved solids [TDS]) brine, at Niland in the Salton Sea KGRA; and three other reservoirs with fluids of lower temperature (up to 200°C [392°F]), enthalpy (around 800 kilojoules/kg [350 BTU/lb] for East Mesa), and salinity (15,000 to 25,000 ppm TDS) at Brawley, Heber and East Mesa. Each of these reservoirs is in fractured sandstones of youthful geologic age. Within the Salton Trough, Cerro Prieto, Mexico, 32 km (20 mi) south of the border, is a part of this same geothermal province which is characterized by fluids with high temperature and enthalpy, and lower salinity of 15,000 to 20,000 ppm.

The East Mesa field is under development by the U. S. Bureau of Reclamation (USBR); the Heber field is under development by a number of private companies, including Chevron, Magma Power and Republic Geothermal; and the Brawley field is under development by the Union Oil Company. The Salton Sea field, which is no doubt one of the largest geothermal fields in the world, has defied development so far because of the very high salinity and corrosive characteristics of the geothermal fluids produced in that area. A joint effort of the Electric Power Research Institute (EPRI) and San Diego Gas & Electric Company (SDG&E) to develop a geothermal test facility at Niland is under way. A number of companies are presently engaged in active exploration activities in the valley, and considerable drilling activity is expected to take place in that area in the near future.

More detailed descriptions of each of the individual geothermal areas, are outlined below.

2.2.1 Salton Sea Geothermal Area

The Salton Sea KGRA, also known as the Buttes or Niland geothermal area, is located along the southern shore of the Salton Sea (Fig. 2.2).

Five Quaternary rhyolite domes are located within the Salton Sea KGRA (Robinson and Elders, 1971). Elders, et al., (1972) have proposed that this geothermal area is the northernmost landward extension of the East Pacific Rise. Unaltered deltaic sediments reach a depth of at least 1,500 m (5,000 ft). No steam is present as a discrete phase in the geothermal reservoir, and thermal brines are highly corrosive.

Thermal springs first attracted commercial interest in 1927 when three exploratory wells were drilled for steam. In the 1930s, more than 50 shallow wells were drilled for carbon dioxide production. It was not until 1957, when the first deep hole was drilled, that large amounts of thermal brines were encountered. Twelve additional wells have been completed in the last decade. Testing to estimate power generation potential is concentrated in several wells near Obsidian Butte. Although the Salton Sea KGRA probably contains the greatest volume and highest temperature fluids in the Salton Trough, development of this resource has been hampered by the high salinity and corrosiveness of the fluid.

SDG&E and the U.S. Energy Research and Development Administration (ERDA) have installed a 10 MW geothermal test facility. Lawrence Livermore Laboratory (LLL) is experimenting with scale corrosion and efficient conversion of geothermal energy for electric power. Both of these programs are trying to resolve the technological problems involved in utilizing the high temperature, high-salinity geothermal fluid characteristic of the Salton Sea KGRA.

2.2.2 Heber Geothermal Area

The Heber geothermal area is south of El Centro (Fig. 2.2), within an extensive array of cultivated fields. It is a flat region, near sea level, and has no rock outcrops.

The geothermal anomaly was discovered by a wildcat well drilled by Amerada Hess Corporation in 1945. The Chevron Oil Company confirmed this discovery with a shallow test hole in 1963. Since then, various companies have drilled wells. The Chevron Oil Company and Magma Thermal Power Company wells have both produced thermal waters (Palmer, et al., 1975). Heber is one of several water-dominated geothermal fields in the Salton Basin physiographic province.

The Heber geothermal anomaly is in the moderate temperature range. Salinity is much lower in Heber than in the Salton Sea (Palmer, et al., 1975). The lithology of the geothermal reservoir includes sands, silts and shales. An 18 m (60 ft) thick layer of gabbro at 1,340 m (4,400 ft) depth has been reported from one well in the area (Butler, pers. comm., 1976).

2.2.3 East Mesa Geothermal Area

The East Mesa KGRA is located east of the town of Holtville (Fig. 2.2). It is on the eastern flank of the Salton Trough. Wildcat wells in the area indicate deltaic sediments reach a depth greater than 3,200 m (10,600 ft). Bedrock is about 3,700 m (12,000 ft) deep (Bureau of Reclamation, 1974). These deltaic sediments are predominantly quartz and calcite, with some dolomite, plagioclase, potassium feldspars, mica and clay; gypsum occurs sporadically throughout the sediments (Muffler and Doe, 1968).

USBR in cooperation with the USGS, the National Science Foundation (NSF) and others is evaluating the East Mesa KGRA to determine the full extent of the field and its capability for production of desalted water from geothermal fluids. USBR located five deep well sites on the basis of geophysical surveys. Wells have been drilled at these sites and are being tested for productivity and to estimate reservoir conditions. Geothermal production well Mesa 6-1 was drilled to a total depth of 2,450 m (8,030 ft). This well has been used to supply geothermal liquid for desalting equipment shakedown operations and tests, and for other purposes. Mesa 6-1 has produced primarily from the upper zone, to a lesser extent from the next two lower zones and probably not at all from the bottom zones. Test well Mesa 6-2 was drilled to a total depth of 1,830 m (6,005 ft). Temperature at the bottom of the hole was measured at 187°C (369°F) and maximum flow was 890 kg/min (1,962 lb/min). A series of additional flow tests has been conducted since then. Test well Mesa 5-1 was drilled to a total depth of 1,834 m (6,016 ft). Bottom hole temperature was 149°C (300°F), and the final flow pressure was 87.5 kg/sq cm (1,245 psi). Mesa 5-1 is an injection well. Mesa 31-1 was drilled to a total depth of 1,899 m (6,231 ft). Bottom hole temperature was 157°C (315°F), and final flow pressure was 167 kg/sq cm (2,376 psi). Two desalting test units have been installed at the East Mesa test site. Operations have produced high quality water (Bureau of Reclamation, 1974).

2.2.4 Brawley Geothermal Area

The Brawley KGRA, also known as the North Brawley geothermal area is located southeast of the Salton Sea, near the town of Brawley (Fig. 2.2). Meidav and Furgerson (1972) identified the North Brawley thermal anomaly by the very low resistivity of 0.35 to 0.76 ohm-m at depths greater than 180 m (600 ft). This is a four-fold decrease in resistivity compared to surrounding rocks. It would require an eight-fold increase in temperature gradient were salinity and stratigraphic factors to be ignored. There is evidence of at least one and perhaps two hydrologic discontinuities from the Sand Hills to a few kilometers northwest of the town of Brawley which would signify faults and would account for salinity and/or stratigraphic changes along the line. These discontinuities are the Brawley and the Calipatria Faults. These faults (Plate 2.2) first appeared in the literature on maps by Rex (1970). Later, gravity surveys confirmed the presence of large vertical displacements beneath the valley alluvium.

The sedimentary section from 0 to 305 m (0 to 1,000 ft) in the Brawley area contains a lower percent volume of sand bodies than some other fields in Imperial Valley. In Brawley, well Amerada Veysey 1 penetrates sediments containing 61% sand. The deposits of usable and recoverable water in storage have been estimated to be about 4,000 m (13,000 ft) thick in Brawley (Dutcher, et al., 1972). A study by U.C.R. has estimated the depth to basement in this area to be about 6,100 m (20,000 ft).

2.2.5 Dunes Geothermal Area

The Dunes KGRA is located in southeastern Imperial Valley, east of Holtville and adjacent to the Sand Hills (Fig. 2.2). Numerous shallow wells have been drilled in the area and many have geophysical logs. Randall (1971) described upper portions of the Cenozoic section in terms of percent volume of sand bodies per 150 m (490 ft) and observed that major parts of the section contain as much as 90% unconsolidated, highly porous sand bodies, with minor amounts of shale. Elders and Bird (1974) noted the importance of these shale layers in confining the hydrothermal system, thereby preventing surface expression. After closely examining cuttings and recoverable core from CDWR Dunes No. 1 and U.C.R. No. 15, they observed that impermeable shale layers served as sites for silica deposition by the upward-circulating hydrothermal waters. This continuing deposition eventually formed a mushroom-shaped cap rock that sealed the hydrothermal system.

Coplen (1972) suggests that local waters are almost totally derived from the Colorado River. These waters are notably low in salts and therefore are vastly different from the waters in northern parts of the valley (Rex, 1972).

Much of what is known about regional structure of the Dunes area has been deduced from geophysical studies. Kovach, et al. (1962) and Biehler, et al. (1964), on the basis of seismic refraction data, observed that basement depth increases from 700 m (2,300 ft) to 3,500 m (11,500 ft) as the Sand Hills are crossed from east to west. Numerous workers have postulated that a southeastern extension of the San Andreas Fault System traverses the axis of the Sand Hills (Biehler, et al., 1964; Garfunkel, 1972a). Combs (1972) and Elders and Bird (1974) have speculated that this fault and related faults might be responsible in part for the formation of the Dunes hydrothermal system.

Combs (1971) discovered the Dunes anomaly on the basis of shallow thermal-gradient boreholes. Combs (1972) suggested the anomaly is an oval-shaped feature, 2.6 sq km (1 sq mi) in area, with the hottest regions near the center, and further suggested the importance of the self-sealing mechanism. In the hottest holes, U.C.R. No. 115 and CDWR Dunes No. 1 (estimated heat flow, 25 HFU [Combs, 1972]), a silica-cemented sandstone was encountered between 60 and 115 m (197 and 377 ft) depths. Biehler (1971) completed a detailed gravity survey over the Dunes anomaly and obtained a 2 milligal (mgal) positive closure that corresponds in shape with the thermal anomaly, although the gravity closure is centered almost 1.9 km (1.2 mi) to the northeast of the thermal anomaly. Biehler (1971) attributed this closure to the existence of the higher density silicified sand body as encountered at U.C.R. No. 115. Black, et al., (1973) measured two orthogonal, 3 km (1.9 mi) long, resistivity profiles over the center of the Dunes anomaly, indicating that resistivity drops by 50% over the geothermal anomaly, at least to a depth of 200 m (660 ft). Van De Verg (pers. comm., 1975) did seismic refraction profiling over the Dunes anomaly and noted that basement depths do not change greatly at or near the anomaly. In summary, the Dunes anomaly can be characterized as a 2.6 sq km (1 sq mi) region of high heat flow, local positive gravity and depressed electrical resistivity. However, reversal of the temperature gradient at about 100°C (212°F) and 305 m (1,000 ft) depth (Coplen, et al.,1973) reduces hopes of developing this area at this time.

2.2.6 Glamis Geothermal Area

The Glamis KGRA is about 32 km (20 mi) east of the town of Brawley, astride the Sand Hills and the trace of the San Andreas Fault (Fig. 2.2). Interest in this area was precipitated by a temperature gradient reported to be greater than 2.2°C/100 m (36°F/300 ft) (Rex, 1970). However, this gradient was based on one shallow drill, and further exploration in this area has been disappointing. The initial drill hole probably intersected an isolated hot spring. Basement is shallow here, and a gravity anomaly, which is often typical of geothermal reservoirs, is not present.

2.2.7 Cerro Prieto Geothermal Area

The Cerro Prieto geothermal area is 35 km (22 mi) south-southeast of Mexicali, Baja California. This geothermal field is located along the projection of the Elsinore and San Jacinto Faults into the Salton Trough. A number of subparallel faults strike northwest in this area (Reed, 1972).

The local area is topographically dominated by a rhyo-dacitic, Holocene volcano, Cerro Prieto, located 4 km (2.5 mi) west of the geothermal field. Hydrothermal activity extends for approximately 40 sq km (15 sq mi) and is expressed by northwest trending, linear zones of mud volcanos and hot springs (Mercado, 1968).

Reed (1972) describes the sediments penetrated by wells at Cerro Prieto as representative of a marginal area of the late Cenozoic Colorado River Delta, of which the bulk of sediment is sandstone and shale similar in mineralogy to the central Colorado Delta deposits of Imperial Valley described by Muffler and Doe (1968). Interfingering with these sediments are fanglomerates and alluvial sands derived from the local mountains.

At Cerro Prieto, a 75 MW geothermal power plant has been in operation since 1973. A second 75 MW plant is currently under construction. Of the many geothermal areas in western North America, the Cerro Prieto geothermal area is the only producing field with a two-phase (steam and water) flow. Other fields of this two-phase type now in the exploration stage will be able to benefit from information gained by development at Cerro Prieto.

2.3 GEOLOGY

The geology of the Imperial Valley area is quite complex and is described in the following four sections. The first section describes the physiography of the Salton Trough in general, with emphasis on Imperial Valley. The second section, "Tectonic Evolution of the Salton Trough," explains background information on past and present tectonic mechanisms in the Salton Trough. It presents a context in which to view the areal occurrence of geothermal anomalies and the areal and temporal patterns of faulting, sedimentation and seismicity of Imperial Valley. The third section provides the structural geology of Imperial Valley and extensively refers to a complete fault map (Plate 2.2) specially prepared for this report. The last section describes the stratigraphy and lithology of Salton Trough rocks. This description is augmented by Plate 2.1, which shows the geology of Imperial Valley, and by Fig. 2.12, a composite column of the Salton Trough showing inferred time-stratigraphic relations, estimated maximum thickness and lithology.

2.3.1 Physiography of the Salton Trough

The Imperial Valley geothermal areas are located in the Salton Trough geologic province of the western United States and Mexico (Figs. 2.1 and 2.2). The Salton Trough is the northern landward extension of the Gulf of California (Dibblee, 1954), separated from the gulf by the Colorado River Delta. It extends southward to the gulf and is protected from inundation by the crest of the Colorado River Delta. The delta crest, in Mexicali Valley, south of the international border, rises to over 30 m (100 ft) west of the Yuma Valley (Fig. 2.1).

The Salton Trough is roughly a triangular area, about 210 km (130 mi) long north to south and widening to 110 km (70 mi) in the southern portion. Mesozoic mountains, consisting of older metasedimentary and granite basement rocks with some Tertiary volcanics, border three sides of the steeply step-faulted basement complex of the Salton Trough. This complex structural and topographic depression is bounded on the north by San Gorgonio Pass, which is between the San Jacinto and San Bernardino Mountains. It is bounded on the east by the Little San Bernardino and Chocolate Mountains and on the west by the San Jacinto, Santa Rosa and Coyote Mountains of the Peninsular Range.

Topographically, the Salton Trough is a broad, flat area covered by alluvium. It is commonly divided into four distinct physiographic units from north to south (Fig. 2.1). They are the Coachella Valley, the Salton Sink, the Imperial Valley and the Mexicali Valley. The trend of the entire trough as well as each of its parts is northwest-southeast. The Coachella Valley is about 71 km (44 mi) long and 13 to 23 km (8 to 14 mi) wide. The Salton Sink is the lowest part of the valley and is currently inundated by the Salton Sea. The Salton Sea also trends northwest-southeast and is about 42 by 14 to 23 km (26 by 9 to 14 mi).

Flooding of the Colorado River in 1904-1907 created the present-day Salton Sea. The sea had a surface elevation of 71 m (232 ft) below sea level in 1968; however, the lowest land elevation beneath the sea is about 84 m (275 ft) below sea level (Littlefield, 1966). Constant high evaporation losses, as well as solutions of salt in sediments underlying the sea (California Department of Water Resources, 1970), are major factors in producing the very high salinity of Salton Sea waters.

Imperial Valley is immediately south of the Salton Sea. It trends north-northwest, about 56 km (35 mi) in length, about 64 km (40 mi) wide at the north, spreading to about 113 km (70 mi) at the international boundary.

The major part of Imperial Valley is below sea level. Streams flow from the Chocolate Mountains on the east and the Peninsular Range on the west toward the center of the valley. Natural surface drainage in the central portion of the valley is carried mainly by the New and Alamo Rivers, which have incised channels to 12 m (40 ft). Most of the myriad irrigation canals in the valley eventually discharge into these two rivers.

The Imperial Valley consists of four subareas. They are, from east to west, the Sand Hills area, the East Mesa area, the main valley area and the West Mesa area (Fig. 2.18). Most of the Sand Hills area consists of transverse dune ridges, with up to 90 m (300 ft) of relief, and smaller barchan or barchan-like sand dunes. The East Mesa is a triangular area southwest of the Sand Hills and is a sloping surface that merges gradually with the main valley area. The main valley area is bounded essentially by the shorelines of prehistoric Lake Cahuilla and contains the soft, silty lacustrine deposits of this lake. It is a large area of cultivated and irrigated land. The soils here contain a larger proportion of clay and silt than the sandier soils of the adjacent East and West Mesa areas. The land surface is extremely flat, with an average gradient of 0.32 m/km (1.7 ft/mi) from the international boundary to the lowest part of the valley in the Salton Sea. The volcanic features of Obsidian Butte and other rhyolite obsidian buttes outcrop near the southern shore of the Salton Sea.

The West Mesa area is topographically complex and lies between the main valley area and the Peninsular Range to the west. Altitudes range from more than 30 m (100 ft) below sea level in the northwestern part of the area to over 600 m (2,000 ft) at the foot of the Peninsular Range in the southwestern part. Spurs and inliers of the Peninsular Range consisting mainly of basement-complex rocks appear on the West Mesa as the Fish Creek, Coyote and Jacumba Mountains and the Superstition Mountain. Western Imperial Valley is drained by San Felipe Creek.

The Mexicali Valley is the part of the Colorado River Delta which is above sea level and is largely south of the international boundary. It is 113 km (70 mi) wide at the international boundary and continues for 97 km (60 mi) southward to the Gulf of California. This report will focus on the Imperial Valley section of the Salton Trough.

2.3.2 Tectonic Evolution of the Salton Trough

Hypotheses concerning the tectonic evolution of the Salton Trough are still being developed and improved. A simplified outline of the most currently accepted hypothesis, proposed by Elders, et al. (1972), is presented below. This hypothesis is based on a crustal spreading model, and while broad features and processes are explained, some details still remain enigmatic. The authors note that any theory must reconcile the following observations:

1) right lateral strike-slip motion in the trough,

2) sinking of the center of the trough relative to the sides,

3) areas with enormously high temperature gradients,

4) volcanism suggestive of localized melting,

5) geophysical evidence of rapid lateral changes in the crust from north to south,

6) crustal thinning from 32 km (20 mi) in the north to 22 km (14 mi) in the south, and

7) widespread seismicity.

The development of the Salton Trough according to the crustal spreading model will be traced from the Mesozoic era to the present. Two main events relevant to the evolution of the trough were occurring during the Mesozoic. The first was the formation of the core of the Peninsular Range by intrusion of a Cretaceous batholith into Mesozoic metasediments and metavolcanics (Jahns, 1954; Allison, 1964) and minor Paleozoic rocks (McEldowney, 1968). In the second relevant Mesozoic event, Paleozoic and Precambrian cratonic rocks of the Basin and Range Province were undergoing Mesozoic orogeny, deformation and metamorphism and were being invaded by Mesozoic to early Tertiary granitic plutons (Burchfiel and Davis, 1972; Silver, 1971; Suppe and Armstrong, 1971).

Since the source of the clasts in the Cretaceous and Eocene sediments on the eastern slope of the Peninsular Range was to the east of the present-day Gulf of California (Minch, 1972), the Peninsular Range must have been opposite the state of Sonora, Mexico, at least during Cretaceous to Eocene time. Movement on the ancestral San Andreas Fault brought the Peninsular Range northward.

Correlation of basement terrains in the Orocopia Mountains, San Gabriel Mountains and the Fort Tejon Pass region indicates about 300 km (190 mi) of fault displacement since the Oligocene epoch on the active trace of the San Andreas Fault (Crowell, 1962). Inactive faults east of Orocopia show additional slip which would bring the total displacement to about 600 km (375 mi) since the late Cretaceous or early Tertiary (Garfunkel, 1972 a). This displacement is consistent with the Peninsular Range sediment source,being to the east of the present Gulf of California.

During the early or mid-Tertiary, as the Peninsular Range was progressing northward, movement was accelerating on the San Andreas Fault while motion between the Pacific Plate and North American Plate was gradually decreasing. By post-Miocene time all the motion was transferred to the numerous en-echelon right-lateral faults of the San Andreas System,and it became the plate boundary. The continental sliver including Baja,California, and part of southern California to the west of the San Andreas then became part of the Pacific Plate (Garfunkel, 1972a). Although this general conceptual model is understood, the details of this plate boundary migration still remain unclear (Elders, et al., 1972).

The gaps produced by tensional forces offsetting the en-echelon, right-stepped, right-lateral, strike-slip faults of the San Andreas System formed the depressions of the Gulf of California and the Salton Trough. These gaps are called "rhomb grabens" by Garfunkel (1972a). Figures 2.4A and 2.4B are simplified diagrams of "rhomb graben" formation; Fig. 2.4C depicts multiple "rhomb graben" formation.

The northern part of the gulf was formed by this mechanism by late Miocene time, and Baja California was transferred from the Mexican mainland within the last 4 million years (Larson, et al.,1968).

The crustal thinning from north to south noted by Elders, et al. (1972), and the formation of the Salton Trough structural low and consequent sedimentary deposition, support the "rhomb graben" formation theory.

A map of the Gulf of California and Salton Trough showing the actual "rhomb grabens" based on geophysical evidence is shown in Fig. 2.5. Elders, et al. (1972) also suggest that magma generated at depth tends to rise towards the surface where these deepening and widening rifts are formed as successive sections of the crust are slid off along strike-slip faults.

Figure 2.6 is a schematic model, oriented parallel to the strike-slip faults, depicting four stages of evolutionary development of the Salton Trough. The beginning stage (Fig. 2.6A) shows two crustal layers, a lighter one over a denser one, experiencing heating from a hot zone in the mantle. In the second stage (Fig. 2.6B) the lower crust undergoes ductile thinning while the upper crust is brittle and fractures under the tensional forces caused by both the upwelling mantle and the strike-slip motion of the faults. This process causes down-faulting of the less dense crust and consequent accumulation of low density sediments in the trough. The sedimentation and rifting are contemporaneous so that older sediments are deformed and faulted as the depression forms and the fill thickens towards the center of the trough. In the third stage (Fig. 2.6C) basaltic magma, produced by rising upper mantle temperatures, breaks through the Mohorovicic Discontinuity (Moho) and denser crust. Considerable heat is thereby transferred towards the surface which produces sediment metamorphism and deformation, crustal thinning and gravity downfaulting around the tilted margins of the trough. In the final stage (Fig. 2.6D) a new, thinner crust of basaltic magma forms closer to the surface. Where the 700°C (1,300°F) isotherm rises into the crust, granitic basement rocks begin to melt and rhyolite volcanoes bring up bits of basalt, granite and metamorphosed sediments. Temperatures sufficient to produce green schist metamorphism are produced from plumes of hot brine.

The San Andreas Fault System is currently active ,and its motion continues to produce and expand the "rhomb graben" depressions. As these depressions are formed and continue to

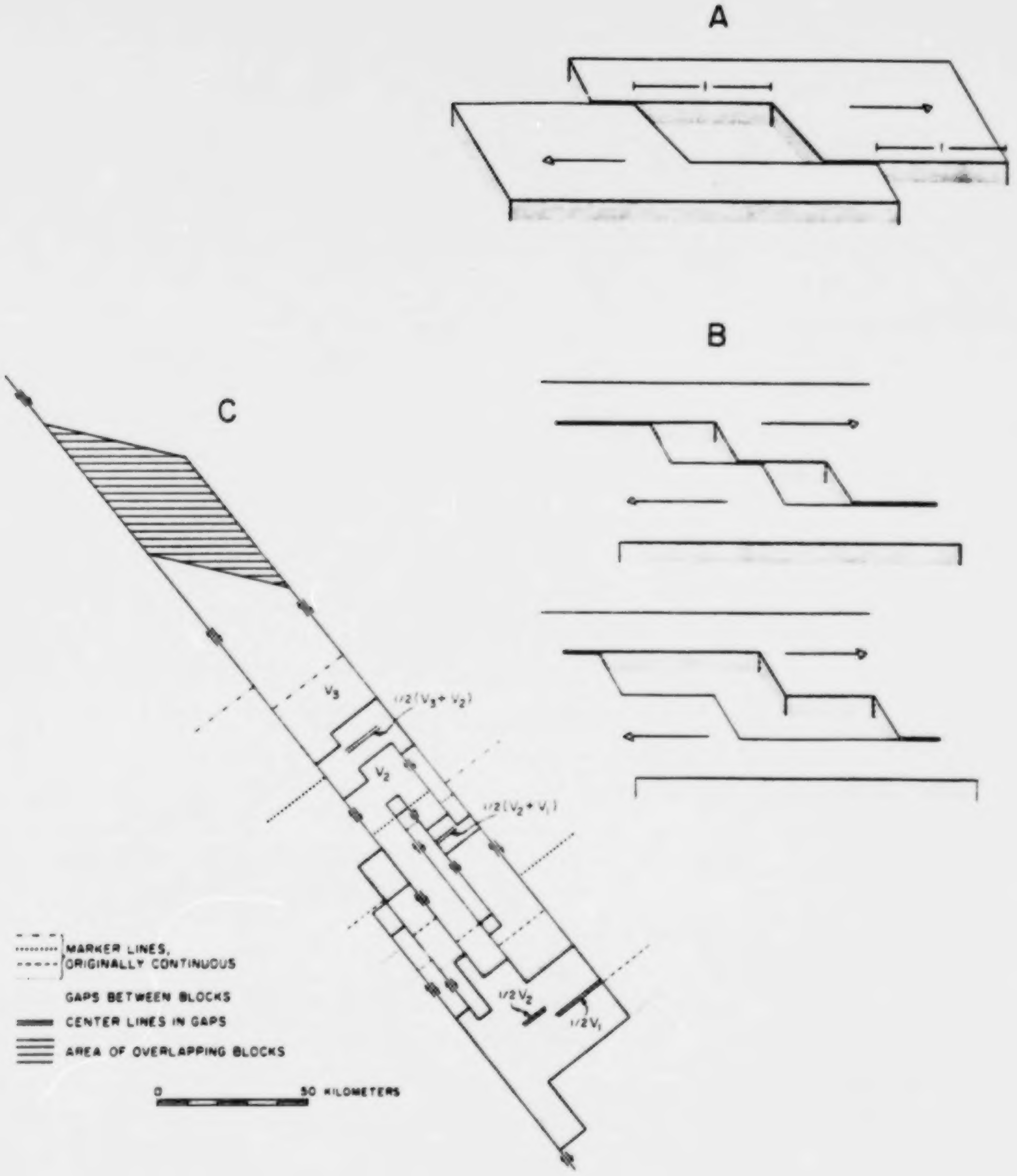
A
l
l
B
C
V3
1/2(V3+V2)
V2
1/2(V2+V1)
1/2V2
1/2V1
MARKER LINES, ORIGINALLY CONTINUOUS
GAPS BETWEEN BLOCKS
CENTER LINES IN GAPS
AREA OF OVERLAPPING BLOCKS
0
50 KILOMETERS

Figure 2.4 A and B. Simplified diagram of "rhomb graben" formation. C. Multiple "rhomb graben" formation. (Garfunkel, 1972a)

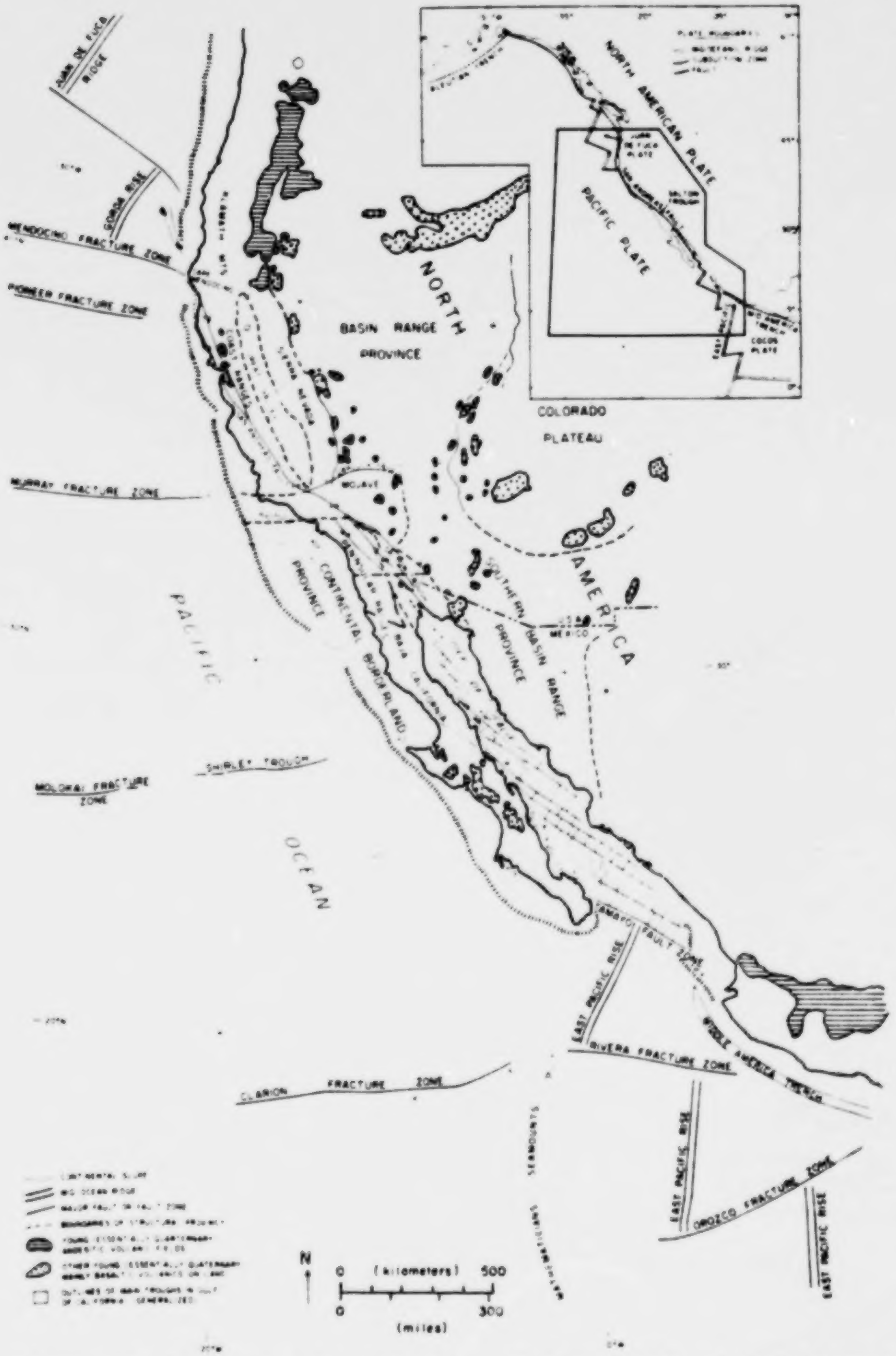
JUAN DE FUCA RIDGE
GORDA RISE
MENDOCINO FRACTURE ZONE
PIONEER FRACTURE ZONE
KLAMATH MTS
SIERRA NEVADA
NORTH
BASIN RANGE PROVINCE
COLORADO PLATEAU
MOJAVE
MURRAY FRACTURE ZONE
CONTINENTAL BORDERLAND PROVINCE
PACIFIC
SOUTHERN BASIN RANGE PROVINCE
MEXICO
AMERICA
BAJA CALIFORNIA
SHIRLEY TROUGH
MOLOKAI FRACTURE ZONE
OCEAN
TAMAYO FAULT ZONE
EAST PACIFIC RISE
RIVERA FRACTURE ZONE
MIDDLE AMERICA TRENCH
CLARION FRACTURE ZONE
SEAMOUNTS
OROZCO FRACTURE ZONE
NORTH AMERICAN PLATE
PACIFIC PLATE
JUAN DE FUCA PLATE
SALTON TROUGH
ALEUTIAN TRENCH
COCOS PLATE
PLATE BOUNDARIES
N
0 (kilometers) 500
0 300
(miles)

Figure 2.5 Tectonic setting of the Gulf of California. (Garfunkel, 1972a)

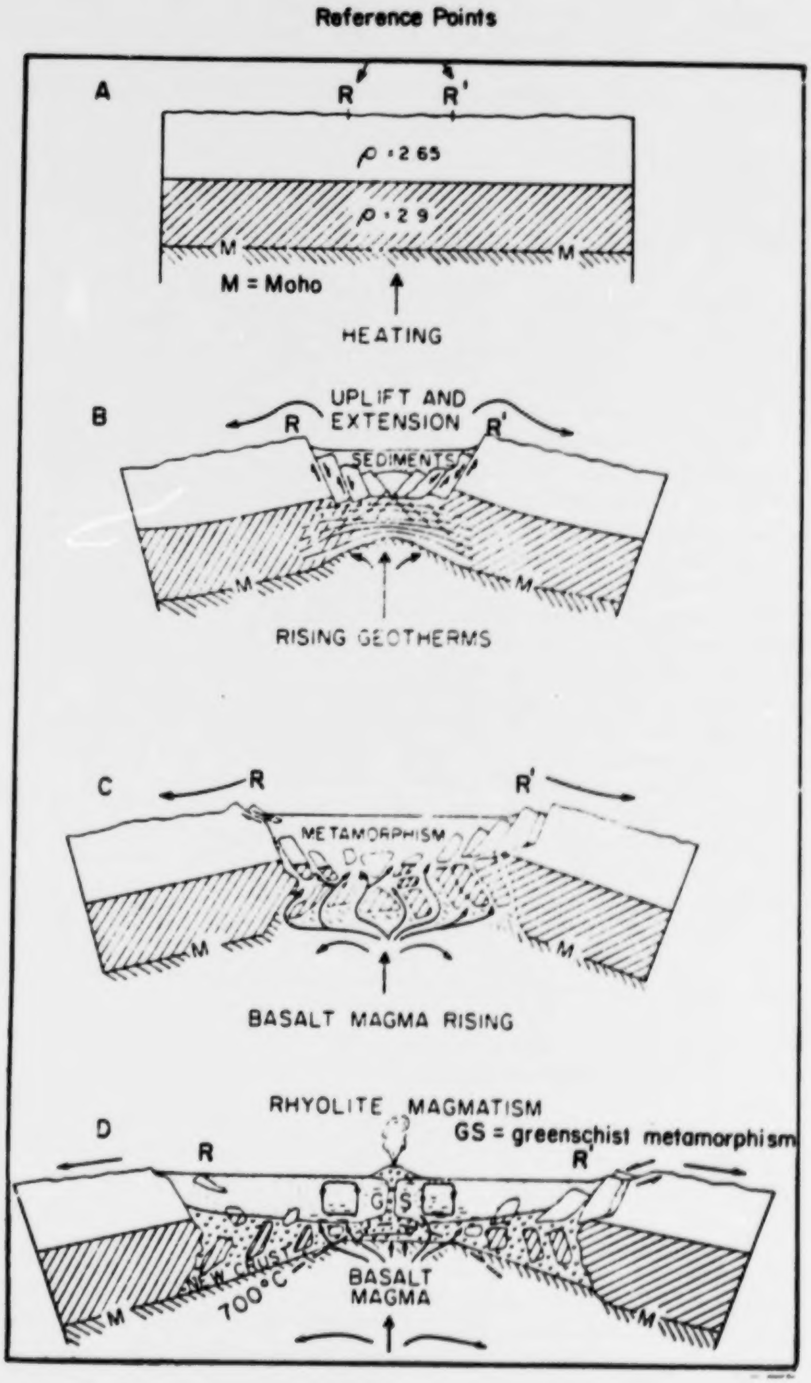
Reference Points
A
R
R'
ρ = 2.65
ρ = 2.9
M
M
M = Moho
HEATING
B
UPLIFT AND EXTENSION
R
R'
SEDIMENTS
M
M
RISING GEOTHERMS
C
R
R'
METAMORPHISM
M
M
BASALT MAGMA RISING
RHYOLITE MAGMATISM
GS = greenschist metamorphism
D
R
R'
G S
NEW CRUST
700°C
BASALT MAGMA
M
M

Figure 2.6 Schematic model for the evolutionary development of the Salton Trough. (Elders, et al., 1972)

expand, they receive sediments from the Colorado River, local lakes and streams or the marine environment, depending on their location and geologic conditions at the time of deposition. Some areas in the central part of the Salton Trough have accumulated over 6,100 m (20,000 ft) of sediments (Biehler, 1964).

Current Tectonic Activity--

Widespread active faulting, seismicity, volcanism, subsidence and anomalous geothermal gradients throughout Imperial Valley attest to the ongoing tectonism of the area.

First, there is the fumarolic-solfataric activity in the Obsidian Buttes area near the Salton Sea, which is a common characteristic for most active geothermal areas in the world. Second, rapid subsidence, on the order of 1.5 cm/yr (0.6 in /yr), of the entire Imperial Valley is indicative of ongoing tectonism. The subsidence rates and directions are somewhat different in different parts of the valley. Geodetic dates by Lofgren (1974) illustrate this with indications of northward tilting which reaches a maximum somewhere in the southern half of the Salton Sea. Third, evidence from trilateration surveys and Lofgren's geodetic data show that active faulting does exist in the Salton Sea Buttes area and can be extended backwards in time by examination of Kelley and Soske's (1936) ground magnetometer survey of the area (Fig. 2.7). Unlike the aeromagnetic data of the area (Griscom and Muffler, 1971), which loses some resolution due to the filtering effect of airplane height, the ground magnetometer survey provides rich detail of the shallow subsurface. Examination of that map (Fig. 2.7) shows clear evidence of faulting and right-lateral displacement through the Red Hill volcano, named as the Red Hill Fault on the map. There is clear evidence for a displacement of about 0.5 to 0.8 km (0.3 to 0.5 mi) along the Red Hill Fault at conjugate points A-A' and less certain evidence for right-lateral displacement of conjugate points B-B' of about 2.3 km (1.4 mi). Such offsets are explained in terms of transcurrent faulting of a geologic structure subsequent to its formation. If we assume a constant rate of displacement on the Red Hill Fault, then these two offsets represent two epochs of volcanism. The reported age of one of the volcanoes, at 16,000 to 55,000 years (Muffler and White, 1968) provides a means for assessing the date of movement on the Red Hill Fault. Assuming a mean age for the Red Hill volcano of 36,000 ± 20,000 years and that the displacement of 0.5 km (0.3 mi) occurred subsequent to the formation of the Red Hill Fault, movement would be on the order of 1.4 ± 0.4 cm/yr (0.55 ± 0.16 in /yr). This value is within the same order of magnitude as the present-day movement of 0.5 cm/yr (0.2 in /yr) determined by Lofgren (1974). Lofgren (1974) ascribes the displacement to movement on the Brawley Fault, which was the only known fault at the time. We tend to believe that the movement might have occurred along the Red Hill Fault. A much tighter trilateration network is needed to resolve that

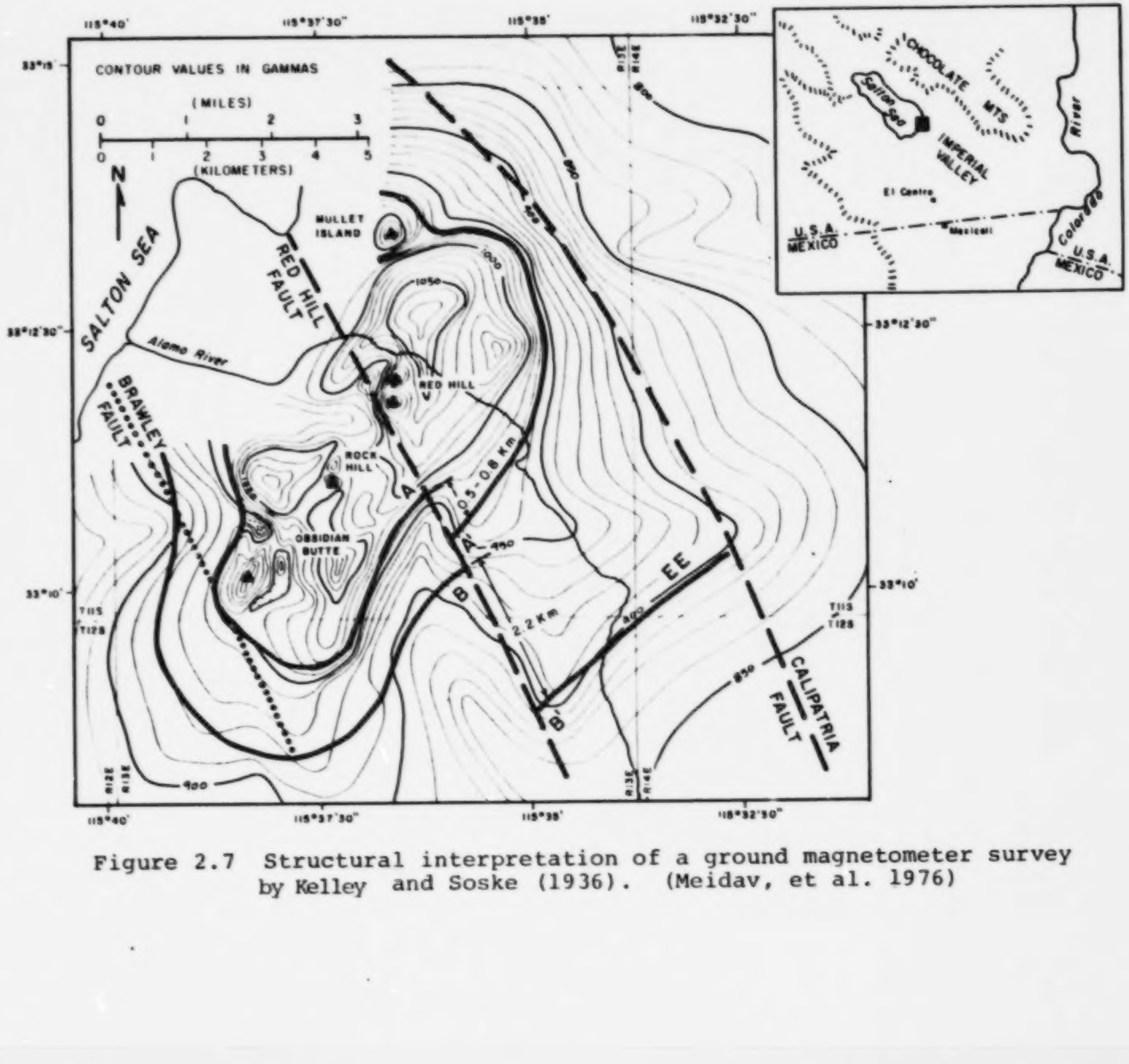
CONTOUR VALUES IN GAMMAS
(MILES)
0 1 2 3
0 1 2 3 4 5
(KILOMETERS)
N
SALTON SEA
MULLET ISLAND
RED HILL FAULT
Alamo River
BRAWLEY FAULT
RED HILL
ROCK HILL
OBSIDIAN BUTTE
A
A'
B
B'
0.5-0.8 Km
2.2 Km
EE
CALIPATRIA FAULT
1000
1050
950
900
850
800
115°40'
115°37'30"
115°35'
115°32'30"
33°15'
33°12'30"
33°10'
T11S
T12S
R13E
R14E
CHOCOLATE MTS
Salton Sea
IMPERIAL VALLEY
El Centro
Mexicali
River
Colorado
U.S.A.
MEXICO

Figure 2.7 Structural interpretation of a ground magnetometer survey by Kelley and Soske (1936). (Meidav, et al. 1976)

question. Likewise, the larger postulated displacement of 2.3 km (1.4 mi) along conjugate points B-B' is likely to represent an older event of plutonism in the area. Assuming an average movement of 1.4 ± 0.4 cm/yr (0.55 ± 0.16 in /yr), the earlier plutonism in the Red Hill region (possibly one that gave rise to the entire Salton Buttes stock) took place 170,000 ± 50,000 years ago. Robinson, et al. (1976) have presented mineralogical evidence supporting the theory of more than one cycle of volcanism.

Randall (1974) supports the hypothesis of at least two epochs of heat flow activity in the region, based upon analysis of the isothermal contour maps of the Salton Sea geothermal field. According to Randall, the shape of the isothermal patterns and its evident relationship to the most recent cycle of volcanism (about 16,000 years ago) suggest that the presently known Salton Sea geothermal field is defined by the spatial position and location of the intrusive mass, rather than by the presence or absence of a cap rock or any convective circulation. Randall further theorizes that the geologic event that resulted in the formation of the Salton Sea geothermal anomaly and the volcanic domes happened so recently, geologically speaking, that insufficient time has elapsed for the local lithologic and structural variation to significantly affect the shape of the isotherms that define the thermal anomaly. These conclusions were based on the limited areal and depth extent of the drill hole data available for analysis. Data from Meidav, et al. (1976), while not in disagreement with Randall's data as regards the shallow, very high temperature regime of the Salton Sea volcanic domes area, suggests that broader geothermal anomalies may extend into the area well beyond the high temperature, elliptically shaped Salton Sea anomaly. From the analysis of electric log data, Randall has constructed a map of depth to the top of a metamorphic zone which has been encountered in most of the wells drilled in the area. Shales in the sedimentary strata change into low-grade metamorphic rocks as a result of the application of high temperatures. The metamorphosed surface conforms in shape to many of the isothermal surfaces, and it probably serves as a cap rock for the higher temperature reservoir in the area.

The inability to correlate individual beds from well to well Randall attributed to the presence of a large number of faults in the area. This finding is supported by the previously reported marine acoustic survey in the Salton Sea (Meidav, 1968) and further corroborated by Meidav, et al. (1976). Randall's evidence is also discussed in Section 2.3.3, "Structure of the Imperial Valley."

2.3.3 Structure of the Imperial Valley

The Imperial Valley is a broad structural and topographic depression. It has steep step-faulted basement margins and prominent mountain ranges on both the east and west. The broad, relatively flat basement floor is 6 to 7 km (3.7 to 4.3 mi) deep (Elders, et al.,1972), and according to Biehler (1964) it lies beneath more than 6,100 m (20,000 ft) of marine and nonmarine sediments. The areal distribution of the rocks on the mountainous margins and the sediments within the valley are shown on the geologic map (Plate 2.1). Numerous right-lateral strike-slip faults extend through the valley; the great majority are components of the San Andreas Fault System and most of them trend northwest (Dibblee, 1954). Three major fault zones of the San Andreas Fault System in Imperial Valley are, from northeast to southwest, the San Andreas Fault Zone (Plate 2.2, No. 28 through 36a) located on the northeast side of Imperial Valley, the San Jacinto Fault Zone (Plate 2.2, No. 2 through 11) in the southwestern portion of Imperial Valley and the Elsinore Fault Zone (Plate 2.2, 12 through 15) in the southwestern portion of Imperial Valley. In addition, this study refers to another fracture zone, herein called the Salton Trough Fault Zone (Plate 2.2, No. 17 through 27), lying between the San Andreas and San Jacinto Fault Zones. All of these faults and the sediment structure in Imperial Valley are discussed in more detail below.

Faults--

The major structural trends in Imperial Valley are the San Andreas, the San Jacinto and the Elsinore Fault Zones, and a number of newly discovered and inferred faults which occur in the alluvial areas in the central part of the valley. This latter area, between the mapped traces of the San Jacinto Fault Zone and the San Andreas Fault Zone, will be referred to as the "Salton Trough Fault Zone" in this report.

All of the faults in these four zones are components of the San Andreas Fault System, which generally trends north-northwest and exhibits right-lateral displacement. Numerous smaller east-northeast trending faults have been mapped in the Peninsular Range to the west (Dibblee, 1954), in the mountains to the northeast (Jennings, 1975; Sylvester and Smith, 1976) and recently within the valley itself (Meidav, et al., 1976). Left-lateral displacement has been noted on some of these east-northeast trending faults.

There are different representations of the number, amount and length of fault traces proposed in Imperial Valley (Loeltz et al., 1975; Rogers, 1965; Strand, 1962; Jennings, 1967; Jennings, 1975; Dutcher, et al.,1972; many proprietary reports and other publications). Most of the published fault maps of Imperial Valley represent a generalized picture of fault traces; in reality the picture may be considerably more complex than presented on these maps. Many of the fault locations are based on geophysical evidence, some on field mapping, and some on remote sensing techniques. The trend to date has been that as more detailed work is done in an area, more complex fault structures become apparent. For example, after detailed resistivity studies were conducted just south of the Salton Sea, many more faults were discovered than had been previously identified (Fig. 2.8) (Meidav, et al., 1976). It is felt that with sufficiently detailed investigation similar fault occurrences may be discovered throughout the Salton Trough Fault Zone and in other parts of the valley. Dibblee (1954) considers the San Jacinto Fault Zone more complex than the San Andreas, and the Elsinore Fault Zone more complex than the San Jacinto. The concealed faults of the Salton Trough Fault Zone may turn out to be as complicated as any of these other zones, but it would have been impossible for Dibblee to detect the myriad occurrence of concealed faults in the Salton Trough Fault Zone in his field mapping and to compare its complexity with the others.

The occurrence of faults plays an extremely important role in geothermal development. For example, faults may provide structural control for the location of geothermal fields, they may provide conduits for the lateral and vertical flow of geothermal fluids and fresh ground water, and they can act as aquitards or aquicludes in the hydrologic system. Since the occurrence of faults can play an important role in the total geothermal and hydrologic system, it is important to clarify and update the existing knowledge about occurrence of faults in Imperial Valley. To do this, a comprehensive fault map was prepared for this study (Plate 2.2). This map is a compilation of fault traces shown in various published maps and includes the most recent data. A table keyed to the map (Table 2.1) provides references for fault locations, discrepant fault locations, most recent fault movement and evidence of faulting. This map and table provide one of the more comprehensive reviews of faults in the Imperial Valley that has been published to date.

The San Andreas Fault Zone--

The San Andreas Fault (Plate 2.2, No. 28 and 28a) is traced from the Durmid area (Plate 2.1), on the northeast shore of the Salton Sea, southeastward to the international boundary. North of the study area the San Andreas splays into two segments called the Banning and Mission Creek Faults. Some faults terminating at the Mission Creek Fault show evidence of left-lateral displacement (Jennings, 1975). Just north of the study area, the Banning and Mission Creek segments come together into one zone called the Banning-Mission Creek Fault (Plate 2.2, No. 36 and 36a). A complex of subparallel branches of the San Andreas Fault occurs in a zone 8 to 16 km (5 to 10 mi) wide extending from the Durmid Hills area to the north end of the Coachella Valley. Right-lateral separation of drainage and vertical separation (northeast side upthrown) of approximately 1,000 m (3,300 ft) are observable along the fault in this area (Babcock, 1969).

TABLE 2.1 FAULT MAP REFERENCE

NO.	FAULT NAME	FAULT ZONE	REFERENCE	EVIDENCE	MOST RECENT MOVEMENT	REMARKS
1	Unnamed - along northwest edge of Salton Sea	Indeterminate	Jennings, 1975	Abrupt rise in topography	Pre-Quaternary	
1a	Unnamed - short segment on eastern edge of Santa Rosa Mountains	Indeterminate	Jennings, 1975		Quaternary	
1b	Unnamed - short segments in various locations	Indeterminate, unless obvious alignment with specific fault or zone	Jennings, 1975		Quaternary	
2	Clark Fault	San Jacinto	Jennings, 1975		Quaternary	
3	San Felipe Hills Fault	San Jacinto	Jennings, 1975		Pre-Quaternary	
4	Unnamed - near San Felipe Hills Fault	San Jacinto	Jennings, 1975		Quaternary	
5	Unnamed - approx. same trace as 3	San Jacinto	Loeltz, et al., 1975			
6	Coyote Creek Fault	San Jacinto	Jennings, 1975	Surface rupture	1968	Breaks probably occurred during Borrego Mtn. Earthquake of 1968.
7	Superstition Mtn. Fault	San Jacinto	Jennings, 1967 Jennings, 1975		Quaternary	
7a	San Jacinto Fault	San Jacinto	Loeltz, et al., 1975			Mapped along Jennings, 1975, Superstition Mtn. Fault. Blends with Coyote Creek Fault to northwest.
8	Superstition Hills Fault	San Jacinto	Jennings, 1967 Jennings, 1975	Surface rupture	Quaternary, 1951, 1965, 1968, 1969	
8a	Superstition Hills Fault	San Jacinto	Loeltz, et al., 1975			Less southern extension than 9, slightly more northern extension.
9	Unnamed - approx. 86 km length on map	San Jacinto	Jennings, 1975		Pre-Quaternary, Quaternary (?)	Agrees with 10, Dutcher, et al., 1972, except Jennings, 1975, considers trace concealed.
10	San Jacinto Fault	San Jacinto	Dutcher, et al., 1972		Quaternary	This reference considers trace above international border as approximately located though queried.

(continued)

TABLE 2.1 (continued)

NO.	FAULT NAME	FAULT ZONE	REFERENCE	EVIDENCE	MOST RECENT MOVEMENT	REMARKS
11	Unnamed - approx. 32 km length on map	San Jacinto	Jennings, 1975	Short segment had creep triggered by earthquake with epicenter along Imperial Fault 69	Pre-Quaternary, 1969	Originally mapped by Dibblee, 1954.
12	Elsinore	Elsinore	Jennings, 1975	Surface rupture	Quaternary	Westernmost fault zone of San Andreas System.
13	Laguna Salada	Elsinore	Strand, 1962 Jennings, 1975		Quaternary	Extends into Elsinore (14) Fault in northern Mexico.
13a	Elsinore	Elsinore	Lomnitz, et al., 1970			Same trace as 13, different in name only.
14	Elsinore	Elsinore	Dutcher, et al., 1972		Some microseismic activity	Merges into Laguna Salada Fault as trace mapped northward.
15	Unnamed - queried segment between Laguna Salada (13,13a) and Elsinore (12) Faults	Elsinore	Jennings, 1975		Pre-Quaternary	
16	Imperial Fault	San Jacinto or transition between SJ & Salton Trough	Jennings, 1975	Surface ruptures, microseismic activity	1940, 1966, 1968, 1971	Also associated earthquake swarm along 15 km just north of border in June 1973 (Hill, et al., 1975).
16a	Imperial Fault	same as above	Strand, 1962 Jennings, 1967 Loeltz, et al., 1975		1940, 1966, 1968, 1971	Approximate agreement with 16.
17	Brawley Fault segment	Salton Trough	Sharp, 1976	Tectonic fracture and displacement, strike N3°W	January & February 1975	Newly recognized segment from rupture during earthquake swarm in 1975 (Sharp, 1976), may be different fault than earlier recognized 17d.
17a	Northward extension of 17 and two inferred short transform segments	Salton Trough	Johnson & Hadley, 1976	Epicenter defined location during earthquake swarm	January & February 1975	

(continued)

TABLE 2.1 (continued)

NO.	FAULT NAME	FAULT ZONE	REFERENCE	EVIDENCE	MOST RECENT MOVEMENT	REMARKS
17b	Probable Brawley Fault - Salton Sea Area	Salton Trough	Hill, et al., 1975a Meidav, et al., 1976	1. Microearthquake epicenter location 2. Electrical resistivity data		
17c	Brawley Fault - Salton Sea Area	Salton Trough	Randall, 1974	Stratigraphic correlation between wells		
17d	Brawley - trace through Imperial Valley	Salton Trough	Jennings, 1975		Quaternary	
18	Unnamed - between Brawley & Calipatria	Salton Trough	Jennings, 1975		Quaternary	Approximate agreement with Red Hill Fault of Meidav, et al., 1976.
18a	Red Hill	Salton Trough	Meidav, et al., 1976	Electrical resistivity data, possible surface displacement at Red Hill Volcano	Quaternary	Also supported by structural interpretation of ground magnetometer survey by Kelley & Soske, 1936.
18b	Unnamed - very close to Red Hill	Salton Trough	Randall, 1974	Borehole stratigraphic correlation		
19	Calipatria	Salton Trough	Meidav, et al., 1976	Electrical resistivity data, also alignment of thermal springs through Mullet Island		
19a	Calipatria	Salton Trough	Jennings, 1975		Quaternary	Main trace runs north from international border, secondary splay occurs north of Calipatria, both traces end in Salton Sea.
19b	Unnamed - close to Calipatria traces	Salton Trough	Randall, 1974	Borehole stratigraphic correlation		Four probable traces in approximate area of 18, 19, and 19a.
20	Wister	Salton Trough	Meidav, et al., 1976	Electrical resistivity data		
21	Westmorland	Salton Trough	Meidav, et al., 1976	Electrical resistivity data		
22	Fondo	Salton Trough	Meidav, et al., 1976	Electrical resistivity data		

(continued)

TABLE 2.1 (continued)

NO.	FAULT NAME	FAULT ZONE	REFERENCE	EVIDENCE	MOST RECENT MOVEMENT	REMARKS
23	Transform Faults, AA through GG	Salton Trough	Meidav, et al., 1976	Electrical resistivity data		
24	Salton Sea Faults or discontinuities	Salton Trough	Meidav, 1968	Sparker Survey		Dashed lines probable fault or discontinuity.
25	Mesa Fault	Salton Trough	Combs & Hadley, 1977	Geophysical Study		
26	Holtville and short parallel trace to east	Salton Trough	Babcock, 1971	Infra-red aerial photography, possible surface displacement		
27	Unnamed in East Mesa Area, 27 km long	Salton Trough	Rex, 1970	Geophysical		Roughly parallel, but slightly west of 19a.
28	San Andreas	San Andreas	Strand, 1962 Jennings, 1967			
28a	San Andreas	San Andreas	Loeltz, et al., 1975			
29	Unnamed - of 30 km length through Dunes KGRA	San Andreas	Loeltz, et al., 1975			
30	Algodones Fault	San Andreas	Jennings, 1975	Possible surface rupture in West Yuma Mesa area, to southwest		
30a	Algodones Fault	San Andreas	Loeltz, et al., 1975			
30b	Unnamed - between Algodones Fault (30a) and Sand Hills Fault (30d)	San Andreas	Jennings, 1967			
30c	Algodones Fault	San Andreas	Olmsted, et al., 1973	Gravity, aeromagnetic, electrical resistivity and seismic surveys, also borehole stratigraphic correlation		Based on work done in West Yuma area.
30d	Sand Hills Fault	San Andreas	Jennings, 1975			

(continued)

TABLE 2.1 (continued)

NO.	FAULT NAME	FAULT ZONE	REFERENCE	EVIDENCE	MOST RECENT MOVEMENT	REMARKS
31	San Andreas and associated splays along NE shore of Salton Sea	San Andreas	Jennings, 1975		Quaternary, creep-triggered by earthquakes along other faults	
32	Hidden Springs Fault	San Andreas	Hays, 1957, Jennings, 1967 Jennings, 1975		Quaternary?	
33	Powerline Fault	San Andreas	Babcock, 1969 Jennings, 1975		Quaternary?	
34	Unnamed - parallel and northeast of Powerline Fault	San Andreas	Babcock, 1969 Jennings, 1975	Gravity Survey		No surface expression except one location of seeps.
35	Hot Springs Fault	San Andreas	Babcock, 1969 Jennings, 1975		Quaternary?	
36	Banning-Mission Creek Fault	San Andreas	Loeltz, et al., 1975	Observed creep, surface displacement	Quaternary	
36a	Banning-Mission Creek and associated splays	San Andreas	Jennings, 1967			

Vertical separation on the Hidden Springs and Powerline Faults created a horst between each of these faults and the San Andreas Fault (Babcock, 1974).

The Hidden Springs Fault (Plate 2.2, No. 32) was mapped in the Mecca Hills (Fig. 2.1), north of the Durmid Hills, by Hays (1957). This fault in the Durmid Hills area is marked by a scarp near the Coachella Canal and by alignment of springs. The Hot Springs Fault (Plate 2.2, No. 35) location is indicated by alignment of hot springs. The trace of the Powerline Fault (Plate 2.2, No. 33) is marked by permeable sandy beds, uplifted on the southwest side of the fault, and by lake silt on the downthrown, northeast side. Springs are also found along this trace. Two gravity profiles run by Babcock (1969) revealed a buried fault east of the Powerline Fault and roughly parallel with it. Ground water seeps are found in one area of this inferred fault.

The southern segment of the San Andreas Fault has a fairly low rate of seismic activity (Allen, et al. 1972). Brune and Allen (1967) conducted a regional survey to measure microearthquake frequency and distribution in the Salton Trough. Virtually no microearthquakes occurred between Desert Hot Springs (Fig. 2.1) and the Mexican border. However, the fault traces along the northeastern margin of the Salton Sea are so distinct in the field that displacement must have occurred in very recent time (Sharp, 1972). Allen, et al. (1972) report slightly eroded small scarplets as much as 50 cm (20 in high along this segment. The Borrego Mountain earthquake of April 9, 1968, the epicenter of which was about 50 km (31 mi) to the west, is also known to have triggered fault creep in this segment of the San Andreas Fault.

Surface expression of the San Andreas Fault dies out southeast of the Durmid area. The main fault trace itself is not evident south of Bombay Beach and is believed to splay to the west and south into numerous parallel and subparallel segments. Geomorphic expression of the fault is hidden by Pleistocene Lake Cahuilla sediments and Quaternary alluvium. It is also possible that the San Andreas Fault has transferred its locus of energy release to traces to the west. This possible mechanism is discussed in more detail in the Salton Trough Fault Zone subsection below. The existence of the San Andreas on the northeast side of the Imperial Valley is inferred from gravity data (Biehler, 1964),and the location of its trace south of the Salton Sea is not precisely known (Sylvester and Smith, 1976). Seismic refraction profiles at the northeast margin of the Sand Hills reveal the probable trace of the Algodones Fault (part of the San Andreas Fault Zone) (Plate 2.2, No. 30, 30a and 30c) which extends southeast to the Yuma area (Olmsted, et al.,1973). Various geophysical studies (Kovach, et al.,1962; Meidav, 1968; Wilt, 1975) suggest the continuity of the fault in the southeast Imperial Valley. Some of these inferred traces are mapped along the Sand Hills and are named the Sand Hills Fault (Plate 2.2, No. 30d).

San Jacinto Fault Zone--

A number of locally active discontinuous traces of the San Jacinto Fault Zone (Plate 2.2, No. 2 through 11) enter the valley from the northwest, paralleling the trend of the San Andreas Fault System. The fault zone enters the trough as two main strands and is about 10 km (6 mi) wide. The Clark Fault (Plate 2.2, No. 2) is on the north and extends through Clark Valley and along the southern tip of the Santa Rosa Mountains. A small trace (Plate 2.2, No. 5) lies along the western part of Clark Valley and extends southward from the Clark Fault into the Borrego Badlands, where it disappears under alluvium or dies out. The second strand, the Coyote Creek Fault (Plate 2.2, No. 6), is the southernmost trace. The Superstition Mountain Fault (Plate 2.2, No. 7) and Superstition Hills Fault (Plate 2.2, No. 8) are southeastward projections of these two strands. The Imperial Fault (Plate 2.2, No. 16 and 16a), as represented by fracturing during the 1940 Imperial Valley earthquake (M = 7.0), may also belong to the San Jacinto Fault Zone. This fault, if projected northwest, aligns with the Clark Fault and the two could join at depth (Sharp, 1967). The San Felipe Hills Fault (Plate 2.2, No. 3) lies approximately along this trend, too. Twenty-four kilometers (15 mi) of right-lateral separation have been noted on the San Jacinto Fault (Plate 2.2, No. 7a) in the Peninsular Range northwest of the Salton Trough (Sharp, 1967). Five kilometers (3 mi) of this slip has been along the Coyote Creek Fault. This fault has breaks with vertical components which show separations in excess of 1 km (0.6 mi).

On April 9, 1968, a magnitude 6.4 shock occurred near Borrego Mountain, in northwestern Imperial Valley (Allen, et al., 1968). Right-lateral surface displacement accompanied the earthquake along several strands within the complex San Jacinto Fault Zone. The Coyote Creek Fault moved a maximum of 38 cm (15 in). Smaller surficial offsets occurred along the Superstition Hills Fault and Imperial Fault. Previous to this movement, offset gullies, displaced alluvium and fault scarps gave evidence of the relatively recent activity in this zone. Minor, vertical northeast trending cross faults occur in the Borrego Badlands and Superstition Hills. Drag folds associated with these cross faults suggest left-lateral displacement (Dibblee, 1954).

Elsinore Fault Zone--

The most southwesterly fault zone in Imperial Valley is the Elsinore Fault Zone (Plate 2.2, No. 12 through 15). It extends southeastward from the Peninsular Range into the Salton Trough near the Tierra Blanca Mountains (Fig. 2.1) and continues into Mexico as the Laguna Salada Fault. Continuity of the Elsinore Fault (Plate 2.2, No. 12, 13a and 14) to the Laguna Salada Fault (Plate 2.2, No. 13) can be established by the steep gravity gradient traced northwest to the Elsinore Fault along the west side of the Cucapas Mountains in northern Mexico. It is a distinct, but discontinuous, zone of surficial fractures. Continuity between these strands cannot always be demonstrated because they may be hidden by overlying, recent alluvial deposits. The strike-slip offset along this zone is small compared with displacement estimated on the San Jacinto and San Andreas Fault Zones (Sharp, 1967). Local vertical displacement along the Elsinore Fault is significant. Over 900 m (2,950 ft) of dip-slip movement has been observed on this fault northwest of the valley (Jahns, 1954). However, Dibblee (1954) points out that the fault movement has been twice reversed so the displacement may be more apparent than real. Right-lateral movement is indicated by drag folds in Cenozoic sediments (Dibblee, 1954), but the actual amount of displacement is unknown. It could be several times that of the dip-slip displacement.

Historic movement in the Elsinore Fault Zone has not been documented,and within the Salton Trough only the segment south of the international boundary has demonstrated appreciable seismicity in recent times (Sharp, 1972).

Lateral shear or torsion between the Elsinore and San Jacinto Faults is probably responsible for the many fault blocks and shattered plutonic rocks in the Vallecito and Fish Creek Mountains, on the western border of Imperial Valley. These mountains contain many northeast trending,steeply dipping normal faults (Plate 2.2, No. 16), most with the northwest sides up. The Coyote Mountains consist of northward tilted, upended metasediments elevated along the Elsinore Fault.

Salton Trough Fault Zone--

The Salton Trough Fault Zone includes the faults numbered 17 through 27 on Plate 2.2. The great majority of these faults show no surficial expression and have been located by geophysical methods.

A regional resistivity survey in Imperial Valley resulted in the discovery of two major faults which run from south of Brawley to the Salton Sea area (Meidav and Rex, 1970). These faults first appeared in the literature on maps by Rex (1970) and were named the Brawley and Calipatria Faults (Plate 2.2, No.17b, 17c and 17d and 19 and 19a, respectively). Later gravity surveys confirmed the presence of large vertical displacements beneath the valley alluvium. However, both surveys were inconclusive in demonstrating the continuity of major fault zones in the southern part of the trough.

Four additional faults striking about N45°W are inferred from a resistivity survey of the Salton Sea geothermal field. They are the Westmorland, Fondo, Red Hill and Wister Faults

(Plate 2.2, No. 21, 22, 18a and 20 respectively) (Meidav, et al., 1976) (Figure 2.8). Transverse discontinuities (Plate 2.2, No. 23) occur between the six faults, trending northeast into the Salton Sea, but they could also have more of an east-west sense than a northeast-southwest sense. It is felt that the discovery of these faults is typical of the complex structure that may be found with additional detailed resistivity surveys in other parts of Imperial Valley. The Westmorland and Red Hill Faults are major aquicludes in the Salton Sea geothermal field. However, all of the faults along the southeastern shore of the sea may behave as aquitards separating the hypersaline brines indicative of the Salton Sea geothermal area from the less saline water outside the volcanic field. The Red Hill Fault, confirmed by a ground magnetometer survey (Kelley and Soske, 1936), also shows evidence of right-lateral displacement through the Red Hill Volcano.

Five volcanic domes, extruded onto valley floor sediments between 16,000 and 55,000 years ago (Muffler and White, 1968a), lie along a northeast trending line on the southern edge of the Salton Sea. If the Salton Sea area is the northernmost spreading center of the landward extension of the East Pacific Rise, then the volcanism, high heat flows, symmetrical magnetic anomalies and transform faults are logical expressions of this activity. The discovery of the six aforementioned faults just south of the Salton Sea (Fig. 2.8) and the absence of seismicity or gravitational expressions of the San Andreas Fault south of Bombay Beach tend to support the hypothesis implied by Elders, et al. (1972) that the Salton Sea volcanic field is the locus of transfer of energy release and fault activity from the San Andreas Fault southwestward to the Salton Trough Fault Zone.

The Brawley earthquake swarm of 1975 (Sharp, 1976; Johnson and Hadley, 1976) produced displacement along a 10.5 km (6.5 mi) fault segment (Plate 2.2, No. 17) that branches northward from the Imperial Fault, about 8 km (5 mi) east-northeast of El Centro. Movement at the surface was apparently vertical and reached a maximum of more than 0.2 m (0.7 ft) at one road in the area. En-echelon cracking implied a developing right-lateral component, but no major structures were laterally offset by the faulting. This trace was called the Brawley Fault, but it has a distinctly different location than the Brawley Fault traces (Plate 2.2, No. 17a through 17d) previously identified by geophysical methods. However, the original fault location by electrical and gravity surveys had no control in the southern portion of Imperial Valley, so this newer trace may define the actual trace of the Brawley Fault or perhaps represents the trace of a different fault.

The general trend of the rupture zone, as well as the trace of the older movements along the Brawley Fault (No. 17), is

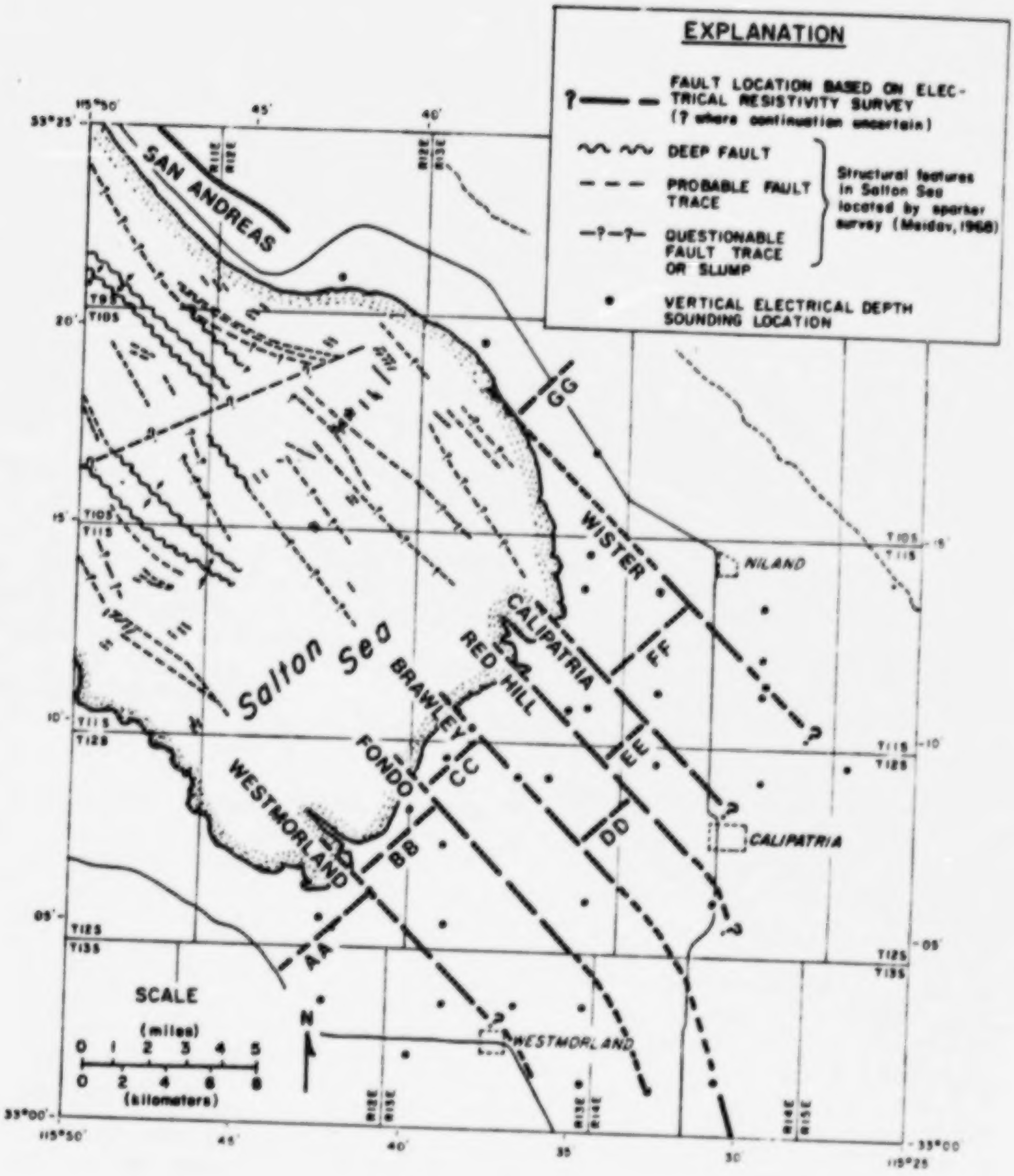
EXPLANATION
FAULT LOCATION BASED ON ELECTRICAL RESISTIVITY SURVEY (? where continuation uncertain)
DEEP FAULT
PROBABLE FAULT TRACE
QUESTIONABLE FAULT TRACE OR SLUMP
Structural features in Salton Sea located by sparker survey (Meidav, 1968)
VERTICAL ELECTRICAL DEPTH SOUNDING LOCATION
SAN ANDREAS
Salton Sea
WISTER
CALIPATRIA
RED HILL
BRAWLEY
FONDO
WESTMORLAND
AA
BB
CC
DD
EE
FF
GG
NILAND
CALIPATRIA
WESTMORLAND
SCALE
(miles)
0 1 2 3 4 5
0 2 4 6 8
(kilometers)
N
33°25'
33°00'
115°50'
115°25'
45'
40'
35
30'
20'
15'
10'
05'
T9S
T10S
T11S
T12S
T13S
R11E
R12E
R13E
R14E
R15E
R16E

Figure 2.8 Map of possible faults and discontinuities in the Salton Sea area. (Meidav, et al.,1976)

about N3°W. The strike of the long axis of the swarm's epicenter pattern was N8°W. Two short northeast trending normal faults, showing left-lateral rotational cracking at the surface, were inferred by epicentral location. Savage, et al. (1974) report that fault slip has possibly occurred since 1934 on the Brawley Fault (No. 17d), near the southeast end of the Salton Sea, about 24 km (15 mi) north of the town of Brawley. But it has not been conclusively demonstrated whether faulting there is directly contiguous with the zone of movement to the south reported by Sharp (1976).

The Holtville Fault (Plate 2.2, No. 26) (Babcock, 1971) trends southeast and is approximately 11 km (6.8 mi) long. Its location is inferred from low angle infrared aerial photography and offset in man-made structures, notably 2 m (7 ft) of shortening of the concrete runway at the Holtville airport. Babcock specifies that without ground evidence the infrared photos do not conclusively prove faulting because trends in the area can also be shorelines of ancient Lake Cahuilla. It is also possible that shortening in the Holtville airport runway may be due to compressional buckling caused by near surface subsidence.

During a five-week period, in the summer of 1973, locations were determined for 36 microearthquakes having epicenters within the 155 sq km (60 sq mi) areal extent of the Mesa geothermal anomaly (Combs and Hadley, 1977). Epicenter and focal depth determinations defined a newly located right-lateral strike-slip fault, the Mesa Fault (Plate 2.2, No. 25). First motion studies indicated strike-slip faulting although there is no surface expression of this fault. The northwest-southeast trending Mesa Fault (Plate 2.2, No. 25) probably acts as a conduit for rising geothermal fluids of the Mesa geothermal anomaly.

Six right-lateral strike-slip faults (Plate 2.2, No. 17c, 18b, 19d, 17b, 18a and 19) were inferred southeast of the Salton Sea through studies of borehole cuttings and electric log data from 16 holes (Randall, 1974). Randall (1974) made approximate subsurface stratigraphic correlations from borehole to borehole using a characteristic shale and sandstone marker horizon. He states that he drew these inferred faults parallel to the San Andreas Fault trend. Using the southwesternmost well as a pivot point, these structures have been redrawn on the fault map (Plate 2.2) generally parallel to the Jennings (1975) trend of the San Andreas along the northeast shore of the Salton Sea. These replotted traces of Randall's inferred faults correspond fairly well to the Brawley, Red Hill, and Calipatria traces of Meidav, et al. (1976).

Sediment Structure--

Sediment structure in Imperial Valley is relatively complicated. The basement complex is composed of both the plutonic rocks of early and late Mesozoic age and the Precambrian to Mesozoic metamorphic rocks which they intrude (Bushee, et al., 1963). Overlying this pre-Tertiary basement complex is a thick sequence of dominantly nonmarine sedimentary rocks which range in age from Eocene to Holocene. The depth-to-bedrock map (Fig. 2.9) shows the areal distribution of sediment thickness. The contours show the greatest thickness of over 6,100 m (20,000 ft) in the central part of the valley south of the Salton Sea. The bedrock surface generally defines a roughly ellipsoid-shaped surface with a northwest-southeast trending major axis. Sharp discontinuities of the bedrock surface occur where it is offset by major faults. Generally the sediments lower in the section show more deformation since they have been exposed to the continuing tectonic movements of the Salton Trough for a longer period of time.

The development of the Salton Trough in the late Cenozoic has involved folding and warping in addition to faulting. Most of the folding is related to major fault activity and indicates right-lateral drag. Some folding is unrelated or indirectly related to the faulting,and these folds are not as tight as those near faults (Loeltz, et al., 1975). Dibblee (1954) noted much tight right-lateral drag folding near and related to faulting and that the folds become broader further from the fault.

Folding of sediments in Imperial Valley is more intense than the mild deformation, mainly warping, seen in upper Tertiary and Quaternary nonmarine deposits along the Colorado River immediately to the east (Metzger, et al., 1974). The sediments throughout the trough display a number of intermediate and small-scale folds, as well as homoclinal dips over large areas.

The pattern of modern sedimentary accumulation and the beginning of anticlinal hills on the southwest side of the valley reflect continuing diastrophism in the trough. The basement floor probably once showed much relief,but progressive diastrophism and erosion have allowed youngest to oldest sediments to lie directly upon the basement floor. Localized intraformational unconformities are also fairly common. There is little lateral continuity, especially as evidenced along the margins of the trough within the coarser detritus and lacustrine beds. However, in the axial parts of the trough, sediments are almost uniformly fine grained. Flanks of the trough show widespread instability, marked by erosional truncation of thick sections of sediment that probably accumulated since Pleistocene time (Sharp, 1972). This detritus has perhaps been redeposited beneath the Salton Sea, or elsewhere in the axial part of the basin, suggesting continuous subsidence within the axial part of the trough.

The only completely exposed Cenozoic sequence is a southwest dipping homocline in the southwestern portion of Imperial

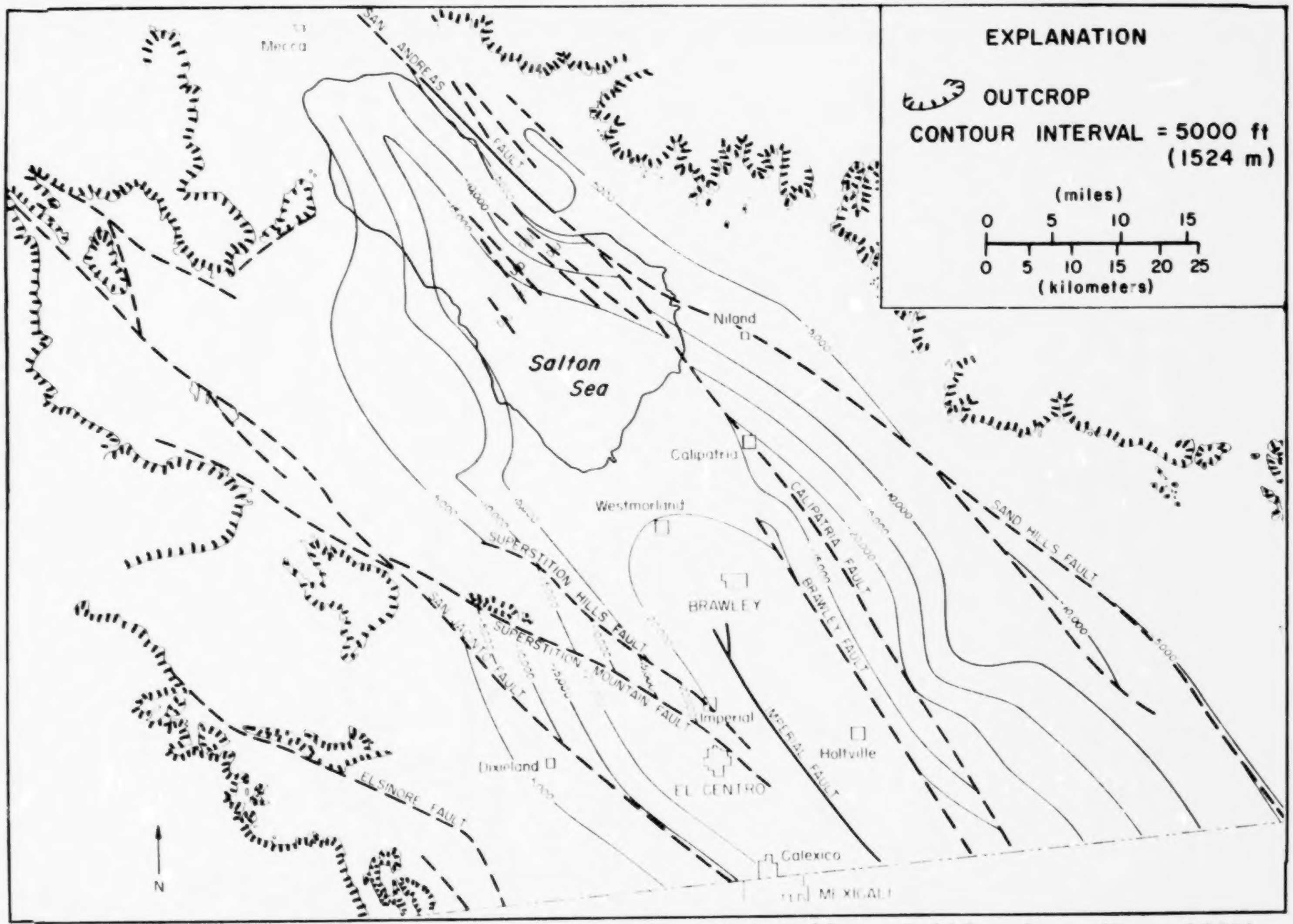
EXPLANATION
OUTCROP
CONTOUR INTERVAL = 5000 ft
(1524 m)
(miles)
0
5
10
15
0
5
10
15
20
25
(kilometers)
Mecca
SAN ANDREAS FAULT
Salton Sea
Niland
Calipatria
Westmorland
BRAWLEY
CALIPATRIA FAULT
BRAWLEY FAULT
SAND HILLS FAULT
SUPERSTITION HILLS FAULT
SUPERSTITION MOUNTAIN FAULT
SAN JACINTO FAULT
IMPERIAL FAULT
Imperial
Holtville
EL CENTRO
Dixieland
ELSINORE FAULT
Calexico
MEXICALI
N
5000
10,000
15,000
20,000

Figure 2.9 Depth to basement complex, Imperial Valley, California. (Rex, 1970)

Valley on the north side of Carrizo Valley. The Tertiary sediments on the south side of the Elsinore Fault are upended and show intense folding (Dibblee, 1954). Further details of anticlinal and synclinal structures, faults and folds associated with specific physiographic features in the mountains to the west of and on the west side of the valley are detailed by Dibblee (1954). In the northwest part of the valley these features can be observed in Cenozoic exposures in the Superstition Hills and Santa Rosa Mountains. Prominant folding, including overturning and isoclinal folding, occurs in linear belts adjacent to fault zones, as seen in the Mecca Hills and Ocotillo Badlands (Sharp and Clark, 1972).

Historic seismicity within the valley would suggest continuing deformations within the trough sediments. Meidav (1969) reported that the upper water-bearing deposits in the valley dip slightly southward. Furthermore, warping is suggested on the west side of the trough by the Lake Cahuilla shorelines which are tilted southeast, and by one strand on the east side which is tilted northwest.

2.3.4 Stratigraphy and Lithology of Salton Trough Rocks

The Salton Trough has been filled with late Tertiary deltaic and lacustrine sands, silts and gravels overlain by Quaternary alluvium and lake sediments. These deposits have a maximum measured depth of 6,100 m (20,000 ft) (Biehler, et al., 1964; Babcock, 1969) to the pre-Tertiary granite and metamorphic basement complex (Fig. 2.9).

Rocks of the Salton Trough range in age from Precambrian basement complex to Recent alluvium and dune sands, and correspondingly from dense, competent, hard rocks to totally unconsolidated sedimentary deposits. Most of the central Imperial Valley fill is Pliocene and younger; none is older than mid-Miocene, and rocks as old as Eocene only occur in the bordering mountains (Durham, 1954, p. 27). One deep well, near Brawley, was drilled through more than 4,000 km (13,000 ft) of interbedded, fine-grained sandstone and siltstone (Muffler and Doe, 1968). The most complete stratigraphic section, consisting of more than 5,500 m (18,000 ft) of sediments, is exposed from Split Mountain Gorge to Carrizo Wash (Garfunkel, 1972b). Hydrologically, the younger and nearer-surface sedimentary units play a much more important role in the ground water flow system and will therefore be emphasized.

The Cenozoic sedimentary rocks in Imperial Valley have been divided into three major categories by the California Department of Water Resources (1970). The lower (oldest) unit consists of early to mid-Tertiary, mainly nonmarine sedimentary rocks with some volcanic and marine sediments. The middle unit is the late Tertiary Imperial Formation claystone and sandstone of marine origin. The upper (youngest) unit is the Pliocene or Quaternary nonmarine clastic, deltaic and lacustrine deposits derived from Colorado River detritus. The heterogenous deposits of this upper unit are thousands of meters thick.

The main source of the thick section of Eocene to Holocene nonmarine sediments in Imperial Valley has been Colorado Plateau debris transported and deposited by the Colorado River. Some of these sediments are also from local sources deposited in alluvial fans, barrier beaches, lacustrine beds and braided beaches (Coplen, 1976).

An illustration of the interfingering and lensing nature of the alternating sand, silt and shale layers is shown on cross section D-D' (Fig. 2.10) of average percent volume of sand bodies in the sedimentary section (Fig. 2.11).

Source areas for each type of sediment can be clearly identified by their distinctive mineralogies (Van De Kamp, 1973; Muffler and Doe, 1968). Both types of sediment contain small amounts of clay and heavy minerals but those from the Colorado Plateau source area contain 60% to 70% quartz, 20% feldspar, 2% chert and calcite; while those from local tributary valleys and basin margins contain 40% to 50% quartz, 30% feldspar, 1% chert and no calcite. The local deposits exhibit sharp lateral facies changes (Van De Kamp, 1973) which are attributed to the meandering course of the Colorado River and its tributaries (Coplen, 1976).

Undifferentiated Tertiary volcanic and intrusive rocks of various ages consisting of local andesite, rhyolite and basaltic lava flows and tuffs occur within the sedimentary section. Recent volcanic activity has deposited the Niland Obsidian (Dibblee, 1954). They are among the youngest rocks in the valley. Changes in lithology occur at depths greater than 900 m (3,000 ft), and greenschist facies minerals form at temperatures above 300°C (597°F) (Muffler and White, 1968b).

Stratigraphic and Lithologic Description of Units--
A brief lithologic description of individual units is presented below in chronological order, from oldest to youngest. The areal distribution of these units is shown on the geologic map of Imperial Valley (Plate 2.1). Figure 2.12 presents a composite column of the Salton Trough showing inferred time-stratigraphic relations, estimated maximum thickness and lithology. In the Mecca Hills area (Fig. 2.1) correlative age relations and stratigraphic thicknesses across faults and along strike are uncertain due to sharp facies changes, absence of marker beds or fossils and numerous diastems (Sylvester and Smith, 1976). This cautionary note should be extended to our study area in Imperial Valley.

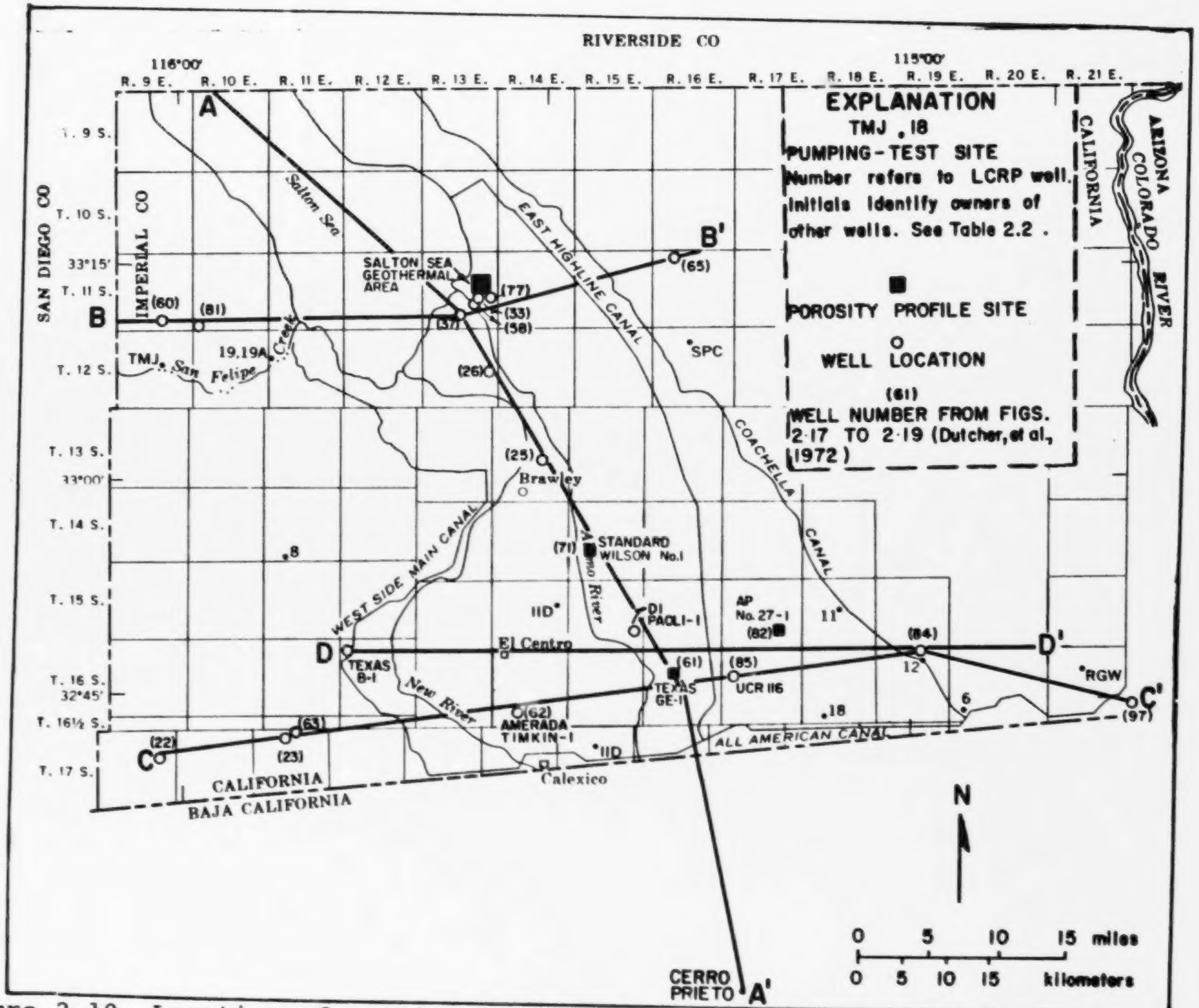
RIVERSIDE CO
116°00'
115°00'
R. 9 E.
R. 10 E.
R. 11 E.
R. 12 E.
R. 13 E.
R. 14 E.
R. 15 E.
R. 16 E.
R. 17 E.
R. 18 E.
R. 19 E.
R. 20 E.
R. 21 E.
T. 9 S.
T. 10 S.
33°15'
T. 11 S.
T. 12 S.
T. 13 S.
33°00'
T. 14 S.
T. 15 S.
T. 16 S.
32°45'
T. 16½ S.
T. 17 S.
SAN DIEGO CO
IMPERIAL CO
ARIZONA
COLORADO RIVER
CALIFORNIA
EXPLANATION
TMJ .18
PUMPING-TEST SITE
Number refers to LCRP well. Initials identify owners of other wells. See Table 2.2 .
POROSITY PROFILE SITE
WELL LOCATION
(61)
WELL NUMBER FROM FIGS. 2·17 TO 2·19 (Dutcher, et al, 1972)
A
A'
B
B'
C
C'
D
D'
Salton Sea
SALTON SEA GEOTHERMAL AREA
EAST HIGHLINE CANAL
COACHELLA CANAL
WEST SIDE MAIN CANAL
ALL AMERICAN CANAL
San Felipe Creek
Alamo River
New River
Brawley
El Centro
Calexico
(60)
(81)
(37)
(33)
(58)
(77)
(65)
(26)
(25)
(71)
STANDARD WILSON No.1
DI PAOLI-1
AP No. 27-1
(82)
(61)
TEXAS GE-1
(85)
UCR 116
(84)
12
11
18
6
RGW
(97)
TEXAS B-1
(62)
AMERADA TIMKIN-1
(22)
(23)
(63)
IID
IID
SPC
TMJ
19,19A
8
CALIFORNIA
BAJA CALIFORNIA
CERRO PRIETO
N
0 5 10 15 miles
0 5 10 15 kilometers

Figure 2.10 Location of sections, porosity profile sites and wells referenced in this report.

LOCATION OF SECTION SHOWN ON FIG. 2.10

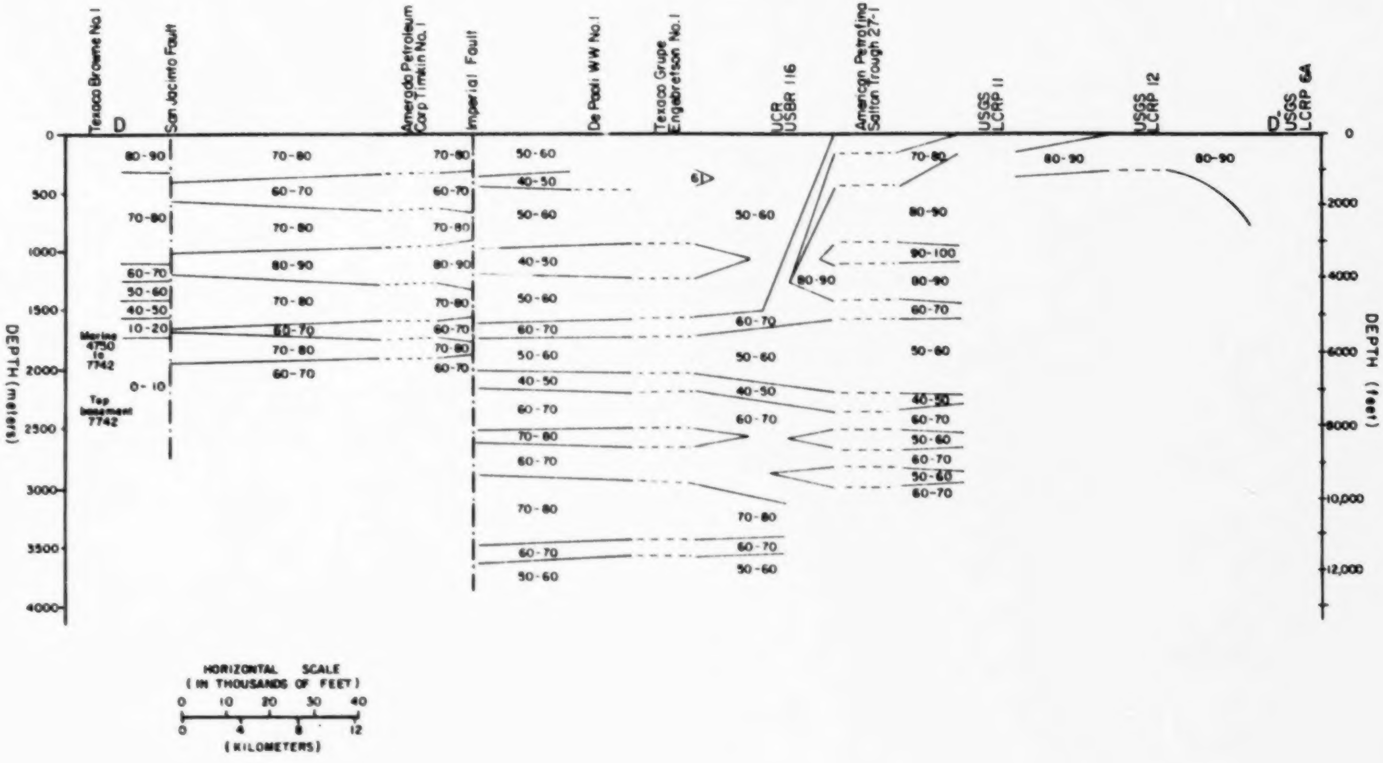
Texaco Browne No.1
D
San Jacinto Fault
Amerada Petroleum Corp Timkin No.1
Imperial Fault
De Paoli WW No.1
Texaco Grupe Engebretson No.1
UCR USBR 116
American Petrofina Salton Trough 27-1
USGS LCRP 11
USGS LCRP 12
D'
USGS LCRP 6A
DEPTH (meters)
0
500
1000
1500
2000
2500
3000
3500
4000
DEPTH (feet)
2000
4000
6000
8000
10,000
12,000
Marine 4750 to 7742
Top basement 7742
80-90
70-80
60-70
50-60
40-50
10-20
0-10
90-100
HORIZONTAL SCALE (IN THOUSANDS OF FEET)
10
20
30
40
4
8
12
(KILOMETERS)

Figure 2.11 Cross section of average percent volume of sand bodies in sedimentary section. (Randall, 1971)

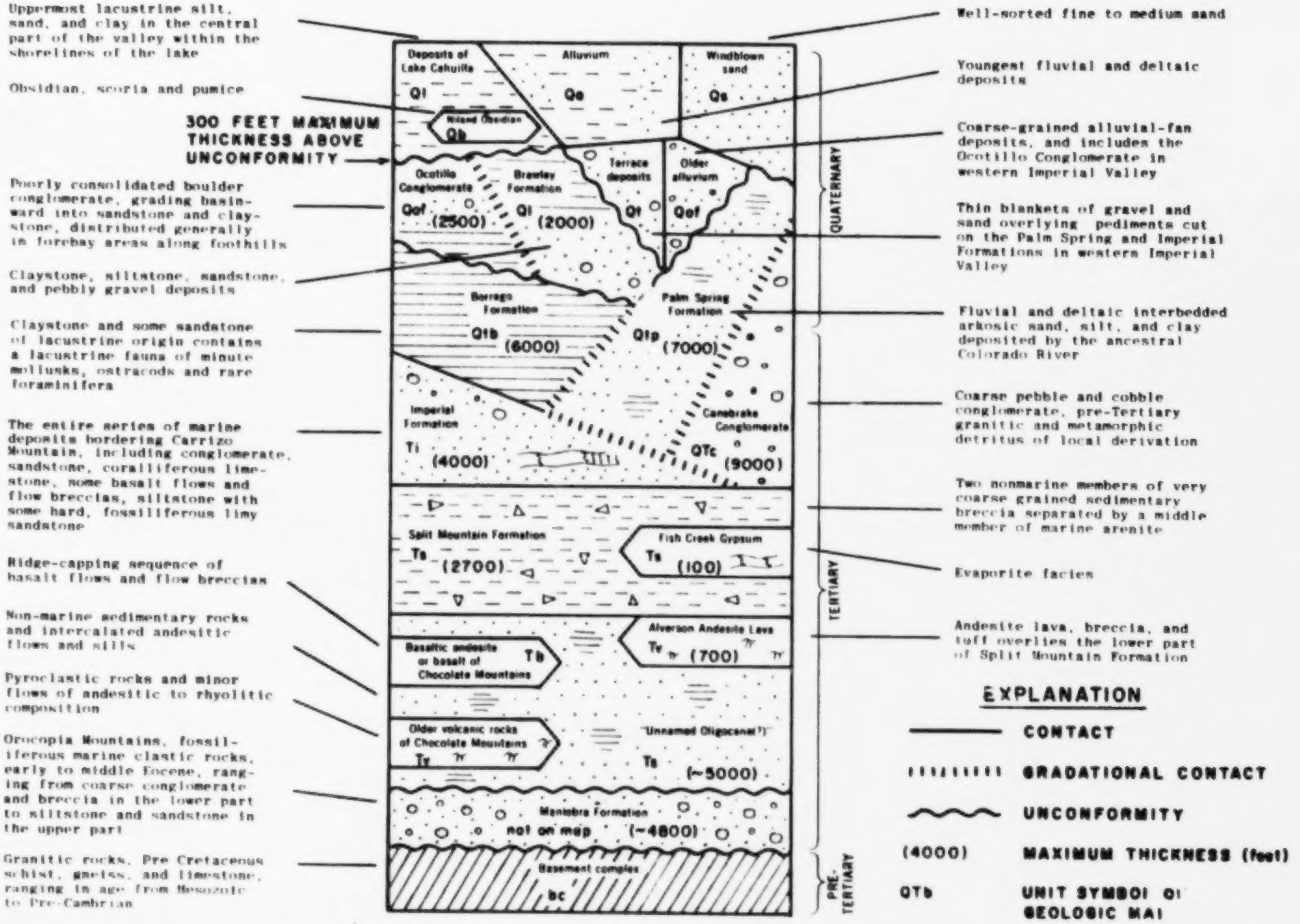
Uppermost lacustrine silt, sand, and clay in the central part of the valley within the shorelines of the lake
Obsidian, scoria and pumice
300 FEET MAXIMUM THICKNESS ABOVE UNCONFORMITY
Poorly consolidated boulder conglomerate, grading basinward into sandstone and claystone, distributed generally in forebay areas along foothills
Claystone, siltstone, sandstone, and pebbly gravel deposits
Claystone and some sandstone of lacustrine origin contains a lacustrine fauna of minute mollusks, ostracods and rare foraminifera
The entire series of marine deposits bordering Carrizo Mountain, including conglomerate, sandstone, coralliferous limestone, some basalt flows and flow breccias, siltstone with some hard, fossiliferous limy sandstone
Ridge-capping sequence of basalt flows and flow breccias
Non-marine sedimentary rocks and intercalated andesitic flows and sills
Pyroclastic rocks and minor flows of andesitic to rhyolitic composition
Orocopia Mountains, fossiliferous marine clastic rocks, early to middle Eocene, ranging from coarse conglomerate and breccia in the lower part to siltstone and sandstone in the upper part
Granitic rocks, Pre Cretaceous schist, gneiss, and limestone, ranging in age from Mesozoic to Pre-Cambrian
Deposits of Lake Cahuilla
Ql
Alluvium
Qa
Windblown sand
Qs
Niland Obsidian
Qb
Ocotillo Conglomerate
Qof
(2500)
Brawley Formation
Ql
(2000)
Terrace deposits
Qt
Older alluvium
Qof
Borrego Formation
Qtb
(6000)
Palm Spring Formation
Qtp
(7000)
Imperial Formation
Ti
(4000)
Canebrake Conglomerate
QTc
(9000)
Split Mountain Formation
Ts
(2700)
Fish Creek Gypsum
Ts
(100)
Alverson Andesite Lava
Tv
(700)
Basaltic andesite or basalt of Chocolate Mountains
Tb
Older volcanic rocks of Chocolate Mountains
Tv
"Unnamed Oligocene(?)"
Ts
(~5000)
Maniobra Formation
not on map
(~4800)
Basement complex
bc
QUATERNARY
TERTIARY
PRE-TERTIARY
Well-sorted fine to medium sand
Youngest fluvial and deltaic deposits
Coarse-grained alluvial-fan deposits, and includes the Ocotillo Conglomerate in western Imperial Valley
Thin blankets of gravel and sand overlying pediments cut on the Palm Spring and Imperial Formations in western Imperial Valley
Fluvial and deltaic interbedded arkosic sand, silt, and clay deposited by the ancestral Colorado River
Coarse pebble and cobble conglomerate, pre-Tertiary granitic and metamorphic detritus of local derivation
Two nonmarine members of very coarse grained sedimentary breccia separated by a middle member of marine arenite
Evaporite facies
Andesite lava, breccia, and tuff overlies the lower part of Split Mountain Formation
EXPLANATION
CONTACT
GRADATIONAL CONTACT
UNCONFORMITY
(4000)
MAXIMUM THICKNESS (feet)
QTb
UNIT SYMBOL OF GEOLOGIC MAP

Figure 2.12 Composite column of Salton Trough showing inferred time-stratigraphic relations, estimated maximum thickness and lithology. (adapted from Loeltz, et al.,1975)

Pre-Tertiary granitic and metamorphic rocks of the basement complex lie below an unconformity and are divided into the following three main units:

1) Pre-Cenozoic granitic and metamorphic rocks consisting of gneiss, limestone, schist and granite, ranging in age from Precambrian to Mesozoic.

2) Orocopia Schist, a Precambrian dark grey micaschist, named by Miller (1944), exposed for many thousands of meters in the Orocopia Mountains and extending west.

3) Undifferentiated Mesozoic granitic rocks.

The remaining rocks in the section are Cenozoic, with the greatest thickness being of Pliocene age and younger.

The lower and mid-Eocene Maniobra Formation of Crowell and Suzuki (1959) consists of about 1,500 m (4,900 ft) of fossiliferous marine clastic rocks, ranging from coarse conglomerate and breccia in the lower section to siltstone and sandstone in the upper part. It is exposed northwest of the Salton Sea in the Orocopia Mountains (Fig. 2.1).

The Maniobra Formation is unconformably overlain by about 1,500 m (5,000 ft) of unnamed Oligocene nonmarine sedimentary rocks (Crowell, 1962, p. 28) in the Orocopia Mountains. These rocks are part of the "Unnamed Oligocene" of Crowell and Suzuki (1959) and Durham and Allison (1961) which consists of nonmarine conglomerate, sandstone, breccia, mudstone and evaporite deposits. Rocks of similar composition, which are probably correlative, are also exposed in the Chocolate Mountains northeast of the valley and in parts of the Peninsular Range, just west of the valley (Durham and Allison, 1961).

The following three igneous formations have been placed stratigraphically within the "Unnamed Oligocene" (Loeltz, et al., 1975) (Fig. 2.12): the older volcanic rocks of the Chocolate Mountains consisting of pyroclastics and flows of andesitic to rhyolitic composition; the basaltic andesite or basalt of the Chocolate Mountains which forms a "ridge capping sequence of dark grey to dark brown flows and flow breccias" (Loeltz, et al., 1975); and the Alverson Andesite consisting of upper Miocene basic andesite lava, breccia and tuff, up to 210 m (700 ft) thick (Dibblee, 1954). The Alverson Andesite lies above the lower part of the Split Mountain Formation as defined by Tarbet and Holman (1944) but below the Split Mountain Formation as redefined by Woodard (1961) (Loeltz, et al.,1975, p. 9). Nearby contemporaneous rocks in the Yuma area, and their associated nonmarine sedimentary formations, are mid-Tertiary in age while their intruding volcanics are late mid-Tertiary and have been dated at 23 to 26 million years (Olmsted, et al.,1973).

The Split Mountain Formation, approximately 800 m (2,700 ft) thick, has been defined by Tarbet and Holman (1944) and redefined by Woodard (1961). It is composed of two very coarse-grained nonmarine sedimentary breccia members separated by a middle marine arenite member (Loeltz, et al., 1975). The middle member includes the bedded white playa deposit of gypsum and anhydrite up to 30 m (100 ft) thick (Dibblee, 1954). In contrast, the California Department of Water Resources (1970) identifies the upper member as marine and the lower and middle members as nonmarine. However, they do not cite descriptive or stratigraphic references in their bibliography.

The Imperial Formation is estimated to be early Miocene to early Pleistocene, although the exact age still remains controversial (Loeltz, et al. ,1975). It is up to 1,200 m (4,000 ft) thick, of shallow marine origin, and represents the last marine invasion of Imperial Valley. It is a light grey claystone and lesser interbedded arkosic sandstone with calcareous oyster "shell reefs." For a more detailed description, see Christensen (1957), who describes a complete section in the Coyote Mountains type area.

The Mecca Formation, up to 300 m (1,000 ft) thick, (located off the geologic map) is exposed in the Mecca Hills in northeastern Coachella Valley. It is a reddish arkosic claystone conglomerate with the basal strata containing chiefly metamorphic debris (Sylvester and Smith, 1976). It is of continental origin , lies upon the basement complex and is overlain by the Palm Springs Formation (Dibblee, 1954). It would be difficult to accurately depict this formation in its proper place on Fig. 2.12, "Composite Column of the Salton Trough," so it has, therefore, been omitted.

The Borrego Formation has been defined by Tarbet and Holman (1944) and Babcock (1974). It is up to 1,800 m (6,000 ft) thick and grades laterally into the Palm Springs Formation. Arnal (1961, p. 473) reported a late Pliocene to early Pleistocene age, while Babcock (1974, p. 323) reports a Pleistocene age for this formation. It is a light gray claystone with minor amounts of buff lacustrine sandstone containing lacustrine fauna of minute mollusks, ostracods and rare foraminifera. Mineralogical analyses of the Borrego Formation in the Durmid area indicate much detritus of local origin (Muffler and Doe, 1968) while the Borrego Formation occurring in the rest of the Salton Trough is of Colorado River origin (Merriam and Bandy, 1965). Subsidence of the Salton Trough at approximately the same rate as deposition of the Borrego Formation is suggested by the presence along strike for more than 1,800 m (6,000 ft) of uniformly thin evaporate layers interbedded with clay and silt (Babcock, 1974).

The Palm Springs Formation of Woodring (1932) attains a maximum thickness of about 2,100 m (7,000 ft) and is considered to be Plio-Pleistocene in age (Loeltz, et al., 1975). It consists of interbedded light gray arkosic sandstones and reddish clays of terrestrial origin and grades westward into the Canebrake Conglomerate. It contains Pliocene and/ or Pleistocene vertebrate fossils west of the Salton Sea (California Department of Water Resources, 1970).

The Canebrake Conglomerate of Dibblee (1954) is an unsorted and poorly consolidated gray, coarse pebble and cobble conglomerate and fanglomerate containing pre-Tertiary granitic and metamorphic debris of local origin. It is up to 2,700 m (9,000 ft) thick and of continental origin. It occurs in western Imperial Valley and grades basinward into the Palm Springs and Imperial Formations.

Dibblee's (1954) Ocotillo Conglomerate, probably of upper Pliocene or lower Pleistocene age, has unconformable contacts both in the northeast and northwest Imperial Valley. In the northeast it overlies the Borrego Formation with a local unconformity. In the northwest the San Andreas Fault lies between it and the underlying Palm Springs Formation (Dibblee, 1954). It is up to 760 m (2,500 ft) thick, consisting of gray, poorly consolidated boulder conglomerate, composed mainly of granitic and Orocopia Schist detritus, grading basinward into pink sandstone and claystone. It is generally distributed in forebay areas along the Indio and Mecca Hills; to the east it grades into the Brawley Formation.

The upper Pliocene Brawley Formation of Dibblee (1954) is about 600 m (2,000 ft) thick. It is composed of light gray lacustrine claystone, siltstones, minor buff sandstones, and pebbly gravel deposits (Dibblee, 1954; California Department of Water Resources, 1970). The Brawley Formation is lithologically very similar to the underlying Borrego Formation,and they cannot be distinguished from each other where they are not in unconformable contact (Loeltz, et al.,1975).

All of the remaining units lie unconformably over the older formations previously described. They all are Quaternary to Recent deposits and have a total thickness up to 90 m (300 ft) (California Department of Water Resources, 1970). These units are terrace deposits, older alluvium, lake deposits, windblown sand and the Niland Obsidian. The first two are contemporaneous and apparently predate the following four (Loeltz, et al., 1975). The terrace deposits occur to the southwest of the Salton Sea and are a "thin pediment gravel and sand, formed mostly on the Palm Springs Formation. It may grade into fans of older alluvium" (Loeltz, et al., 1975).

The older alluvium has major outcrops on the piedmont slopes of the Chocolate Mountains, although it may be only a thin veneer here, and minor outcrops in Borrego Valley and western Imperial Valley. It consists largely of coarse-grained alluvial fan deposits and includes the Ocotillo conglomerate, in western Imperial Valley, as defined by Loeltz, et al (1975). It grades into the Brawley Formation towards the center of the valley.

The lake deposits consist of sand and clay and include the deposits of Lake Cahuilla, exposed in the middle of the trough, and the deposits of the Brawley Formation, from which they cannot be differentiated in the subsurface (Loeltz, et al., 1975).

The unit designated "alluvium" occurs largely on East Mesa, between the Sand Hills and Chocolate Mountains piedmont slope and northward, and on West Mesa, Lower Borrego Valley, and the southwestern Imperial Valley. It consists of the youngest fluvial and deltaic sand, gravel and silt and some dune sand, where the sand is less than 3 m (10 ft) thick (Loeltz, et al., 1975).

The windblown sand unit is restricted to the Sand Hills, although well-sorted fine to medium windblown sand is extensive on the sides of the valley (Loeltz, et al.,1975).

The Niland Obsidian occurs near the southeast shore of the Salton Sea, as small dome-shaped outcrops of obsidian, scoria and pumice, and is associated with hot springs.

2.4 HYDROLOGY

The hydrology of Imperial Valley is described in this section, with particular emphasis on ground water. An overview of surface water flow and quality in the internally drained Salton Sea drainage basin (Fig. 2.13) is presented. Water-bearing units and their physical properties, recoverable water in storage, ground water flow, recharge and discharge, origin of ground water and a ground water model of a geothermal system are discussed. The section concludes with a brief discussion of the hydrologic budget of Imperial Valley, including inflow and outflow of the Salton Sea drainage basin.

2.4.1 Surface Water

The Imperial Valley lies within the Salton Sea drainage basin (Fig. 2.13). All streams in the basin flow from the surrounding mountains, internally, towards the Salton Sea, and all water leaving the basin is discharged through evaporation or evapotranspiration. The Salton Sea drainage basin includes 21,640 sq km (8,360 sq mi) of drainage area (Fig. 2.13) with about 3,600 m (11,700 ft) of relief. In the San Bernardino

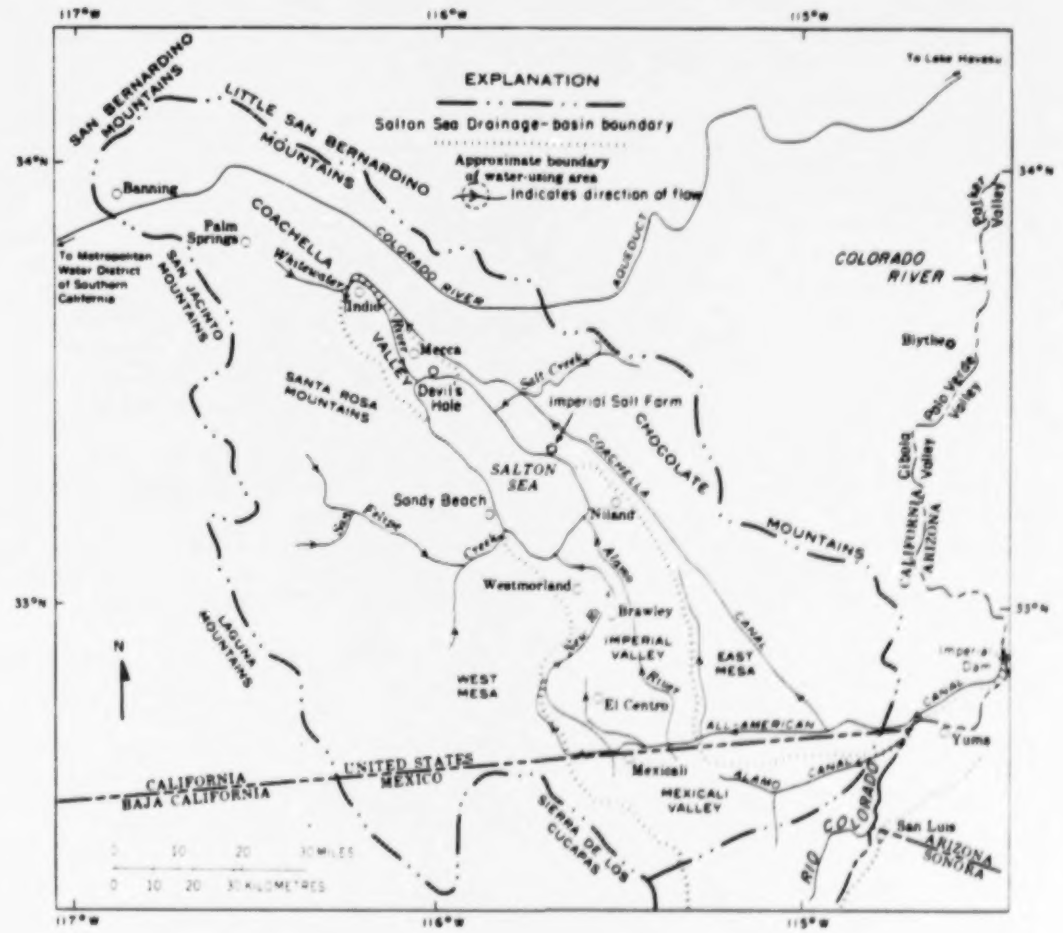
117°W
116°W
115°W
34°N
33°N
EXPLANATION
Salton Sea Drainage-basin boundary
Approximate boundary of water-using area
Indicates direction of flow
To Lake Havasu
SAN BERNARDINO MOUNTAINS
LITTLE SAN BERNARDINO MOUNTAINS
Banning
Palm Springs
To Metropolitan Water District of Southern California
SAN JACINTO MOUNTAINS
COACHELLA VALLEY
COLORADO RIVER
AQUEDUCT
Whitewater River
Indio
Mecca
Devil's Hole
SANTA ROSA MOUNTAINS
Salt Creek
Imperial Salt Farm
SALTON SEA
COACHELLA
CHOCOLATE MOUNTAINS
Sandy Beach
San Felipe Creek
Niland
Alamo
Westmorland
Brawley
IMPERIAL VALLEY
River
New
EAST MESA
WEST MESA
El Centro
CANAL
ALL-AMERICAN
LAGUNA MOUNTAINS
N
COLORADO RIVER
Palo Verde Valley
Blythe
Cibola Valley
CALIFORNIA
ARIZONA
Imperial Dam
CANAL
Yuma
UNITED STATES
MEXICO
CALIFORNIA
BAJA CALIFORNIA
Mexicali
MEXICALI VALLEY
ALAMO CANAL
SIERRA DE LOS CUCAPAS
RIO COLORADO
San Luis
ARIZONA
SONORA
0 10 20 30 MILES
0 10 20 30 KILOMETRES

Figure 2.13 Salton Sea drainage basin. (McDonald and Loeltz, 1976)

Mountains, along the west and northeast rims of the basin, elevations range from less than 900 m (3,000 ft) to more than 3,500 m (11,500 ft). About one fifth of the area of the basin is below or just slightly above mean sea level (msl). The surface drainage pattern is indicated by the flow direction arrows on Figure 2.13.

Historically, the Colorado River has discharged water and sediment via the many distributaries in its delta, and in the past, some of these distributaries have flowed northward into the Salton Sea basin. Currently, the Colorado River flows southward to the Gulf of California; thus,the natural drainage area of the Salton Sea is now topographically distinct from the delta region of the Colorado River. This separation was augmented early in this century by construction of levees on the delta to prevent overflow to the north. Permanent separation of the two drainage basins was ensured by later construction of numerous flood-control reservoirs in the Colorado River basin.

The Salton Sink, the lowest area in the Salton Trough, is currently occupied by the Salton Sea. The sink also contained water during at least eight years of the nineteenth century (MacDougal, 1914), and in the past few centuries it has occasionally contained water as a result of unusual runoff from the bordering mountains or overflow from the Colorado River.

Irrigation began in Imperial Valley in 1901. Additional diversion channels for irrigation and flood protection were constructed after 1901, but before they could be properly protected a series of floods eroded them. This flooding diverted nearly the entire flow of the Colorado River into the Salton Sea basin. Flood water began to collect in the sea in November 1904 and continued until February 1907. The depth of the Salton Sea was more than 25 m (80 ft) and it covered over 1,300 sq km (500 sq mi) by 1907. The water level receded 17 m (55 ft) in the next 12 years. However, increasing drainage from irrigation reversed this trend around 1925. In 1970 the elevation of the Salton Sea shore was -71 m (-234 ft) and the maximum depth was about 12 m (40 ft).

Runoff--

The Imperial Valley depends mostly on irrigation canals and deep wells for its water, although runoff from the surrounding mountains contributes some water to perennial streams. Runoff in arid regions is dependent on drainage by ephemeral streams which flow only briefly during and after some storms. The water table is far below most of the local stream channels, which often traverse deposits of alluvium. These deposits absorb a part or all of the flow that originates in relatively impermeable areas in the mountains surrounding Imperial Valley, where there are no extensive alluvial deposits. The average flow in a channel of this type tends to increase as the drainage area increases. However, when flow reaches permeable alluvium in the valley, more runoff is absorbed than in the impermeable mountainous areas. This results in either a change in the rate of increase of flow, or conversely, a decrease in average flow as the drainage area increases. Therefore, the residual flow in channels, below the point where absorption of flow begins, does not represent the total runoff.

Under natural conditions the soils in irrigated areas should contribute some runoff. However, the preparation of fields for irrigation by flooding prevents any local runoff and therefore the contribution to runoff from irrigated areas is negligible.

Inflow and outflow in the Salton Sea drainage basin is discussed in Section 2.4.3,"Hydrologic Budget."

Surface Water Quality--
Salinity of surface water in the Salton Sea drainage basin has ranged from less than 500 ppm TDS in the Colorado River at Yuma to over 213,000 ppm TDS in the Salton Sea in 1936. Currently, Colorado River water contains 700 to 800 ppm TDS around Yuma and 30,000 to 35,000 ppm TDS in the Salton Sea. The chemical characteristics of surface water in the Salton Sea, in its major inflow sources and tributaries and in the lower Colorado River are discussed below.

Salton Sea--The Salton Sea contains over 740,000 ha-m (6 million acre-ft) of sodium chloride water. In June 1967 it contained an average TDS of about 36,000 ppm, which is slightly more saline than ocean water.

The composition of the water varies with time and with location in the sea. Changes with time are due to variations in sea volume, mineral content of inflowing waters and precipitation of ions from the water when concentrations reach solubility limits. This temporal variation is shown on Table 2.2. Changes of composition with location and depth are due to slight circulation of Salton Sea water, to locations of inflow channels and to surface evaporation.

The first chemical analysis of the Salton Sea, in June 1907, reported the mineral content of the sea as approximately 85 million metric tons (77 million tons) and 3,600 ppm TDS. The salinity of the sea rose from 3,600 ppm in 1907 to 40,000 ppm in 1925, mainly due to the continued solution of minerals from the sea bed and the rapid decline in sea volume by evaporation. As the quantity of soluble minerals on the sea floor decreased, the rate of increase in mineral content gradually slowed. The highest salinity was measured in 1936, as 213,000 ppm, after a shortage of irrigation water in 1931-35.

The Salton Sink, as a topographic low, has been subjected to inundation, sedimentation and subsequent evaporative cycles over many thousands of years. When the waters evaporated, large salt deposits formed which were then covered during the next inundation-sedimentation cycle; thus many wells in Imperial Valley show increasing salinity with depth.

A 1927-28 study of the Colorado River at Yuma, Arizona, reported the weighted-average concentration of dissolved solids in the river as less than 513 ppm (Howard, 1955). Based on this figure, the amount of minerals contributed to the Salton Sea by the Colorado River between November 1904 and June 1907 was less than one-seventh of the mineral content measured on June 3, 1907. Therefore the sea bed itself must have supplied the remaining mineral content.

Sodium and chloride have been the major dissolved constituents in the Salton Sea and will remain so because of their high solubility. Sulfate has been the next most abundant ion. The ratio of sulfate to chloride in the sea has increased and is still increasing (Table 2.2). Some other constituents in the sea are calcium, magnesium and bicarbonate.

Comparison of the Salton Sea inflow with Colorado River water indicates a large increase in the concentration of all ions except bicarbonate (Table 2.2). Carbonate was apparently deposited in the soils or removed by biological activity. This increase in sodium plus potassium and in chloride (Table 2.2) is partly accounted for by concentration due to evapotranspiration, but a greater amount of these constitutents has probably been leached from soils irrigated with Colorado River water.

Concentrations of calcium and sulfate are apparently at or near levels which will form a gypsum ($CaSO_4\ 2H_2O$) precipitate. As the salinity of the sea increases, calcium and sulfate concentrations will be partly controlled by the precipitation of gypsum. When the sea becomes saturated with gypsum ,a nearly constant sulfate concentration may result.

Major Inflow Sources and Tributaries--The natural saline-mineral content of soils in most of the Imperial and Coachella Valleys was high before irrigation began. Some soils that were initially too saline for agricultural production had to be leached. The first irrigation attempts in Imperial Valley were carried out on level farmland without provision for drainage except through natural channels. Water logging and salt accumulation soon occurred. To alleviate this problem and create a favorable salt balance --that is, to have the quantity of dissolved mineral salts delivered in irrigation water be less than the quantity removed from the area by drainage --an extensive tile drainage network was installed throughout the irrigated areas of Imperial Valley. Imperial Irrigation District (IID)

TABLE 2.2 CHEMICAL ANALYSES OF WATER FROM THE SALTON SEA (Hely, et al., 1966)

[Concentrations in parts per million]

	Agency [1]	Calcium (Ca)	Magnesium (Mg)	Sodium and potassium (Na+K)	Bicarbonate (HCO$_3$)	Sulfate (SO$_4$)	Chloride (Cl)	Salinity (calculated)[2]	Volume of water (millions of acre-ft)	Mineral content (millions of tons)
June 3, 1907	CI	100	64	1,140	134	476	1,700	3,550	16	77
Nov. 12, 1907	USGS	107	68	1,260	165	529	1,860	3,910	15	80
Feb. 28, 1908	USGS	142	77	1,280	182	562	1,920	4,070	15	83
May 25, 1908	CI	119	76	1,370	156	567	2,040	4,250	14	81
June 8, 1909	CI	127	90	1,620	149	659	2,410	4,980	13	88
May 22, 1910	CI	137	98	1,900	129	764	2,810	5,770	12	94
June 3, 1911	CI	156	117	2,290	117	917	3,390	6,920	10	94
June 10, 1912	CI	173	136	2,710	246	1,070	3,950	8,160	9.2	100
June 18, 1913	CI	198	162	3,220	229	1,250	4,740	9,680	8.2	110
June 12, 1914	CI	222	190	3,810	223	1,480	5,600	11,400	7.2	110
June 8, 1915	CI	253	226	4,430	242	1,740	6,510	13,300	6.3	110
June 10, 1916	CI	299	272	5,330	232	2,080	7,880	16,000	5.3	120
June 10, 1923	CI	684	659	12,500	169	5,380	18,300	37,600	2.5	130
Mar. 21, 1929	Cal							33,200	3.1	140
Dec. 22, 1945	IID	766	880	11,100	207	6,780	16,000	35,600	4.05	196
Dec. 20, 1946	IID	831	921	11,000	207	6,900	15,900	35,700	4.07	197
Dec. 17, 1947	IID	742	942	11,100	210	6,990	16,000	35,900	4.01	196
Sept. 20, 1948	IID	780	1,050	12,100	198	7,490	17,400	38,900	3.94	208
Dec. 15, 1948	IID	869	986	11,300	213	7,150	16,500	36,900	3.97	199
Sept. 19, 1949	IID	918	1,020	11,900	206	7,500	17,200	38,700	4.02	211
Dec. 15, 1949	IID	970	973	11,200	217	7,160	16,400	36,800	4.08	204
Sept. 20, 1950	IID	869	1,120	11,700	202	7,350	17,100	38,200	4.11	214
Dec. 20, 1950	IID	782	983	11,200	221	7,120	16,200	36,400	4.20	208
May 19, 1951	IID	870	980	10,800	204	6,950	15,800	35,500	4.40	212
Sept. 25, 1951	IID	839	985	12,100	209	7,210	17,600	38,800	4.34	229
June 4, 1952	IID	818	909	10,400	213	6,820	14,900	34,000	4.72	218
Nov. 19, 1952	IID	812	939	10,600	192	7,120	15,200	34,800	4.67	221
May 18, 1953	IID	808	899	10,200	212	6,780	14,600	33,400	4.94	224
Nov. 23, 1953	IID	964	891	10,000	212	6,780	14,700	33,400	4.92	223
May 24, 1954	IID	912	878	9,830	226	6,500	14,400	32,600	5.24	232
Nov. 15, 1954	IID	872	822	9,940	215	6,560	14,300	32,600	5.16	228
June 13, 1955	IID	742	936	9,620	208	6,220	13,900	31,500	5.35	229
Nov. 21, 1955	IID	721	889	10,000	204	6,810	14,200	32,700	5.24	233
May 21, 1956	IID	708	889	9,980	204	6,840	14,100	32,600	5.42	240
Dec. 10, 1956	IID	736	905	10,200	206	7,160	14,300	33,400	5.20	236
May 27, 1957	IID	738	910	9,980	200	7,050	14,100	32,900	5.40	241
Nov. 25, 1957	IID	774	946	10,200	200	7,300	14,300	33,600	5.23	239
May 12, 1958	IID	779	939	10,100	189	7,170	14,300	33,400	5.43	247
Nov. 10, 1958	IID	762	951	10,300	179	7,330	14,500	33,900	5.23	241
May 25, 1959	IID	803	886	10,100	208	7,190	14,300	33,300	5.40	245
Nov. 9, 1959	IID	840	893	10,800	204	7,360	15,200	35,200	5.26	252
May 27, 1960	IID	807	877	10,400	191	7,130	14,600	33,900	5.48	253
Nov. 14, 1960	IID	813	950	10,400	199	7,290	14,800	34,400	5.40	253
Apr. 4, 1961	USGS	821	929	9,830	182	7,060	14,000	32,700	5.60	249
May 22, 1961	IID	813	967	10,100	197	7,230	14,400	33,600	5.60	256
Sept. 22, 1961	USGS	850	1,020	10,100	174	7,260	14,600	33,900	5.48	253
Nov. 20, 1961	IID	811	991	10,100	188	7,260	14,400	33,700	5.47	251
Jan. 29, 1962	USGS	889	905	10,000	183	7,250	14,200	33,300	5.58	253
Mar. 19, 1962	USGS	831	938	9,910	174	7,140	14,100	33,000	5.67	254
May 21, 1962	IID	796	957	10,100	196	7,280	14,300	33,500	5.72	261
Sept. 10, 1962	USGS	801	985	10,100	177	7,320	14,400	33,700	5.63	258
Nov. 12, 1962	IID	802	1,010	10,100	192	7,260	14,400	33,700	5.65	259
May 8, 1963	USGS	775	928	9,590	167	6,980	13,600	32,000	5.92	258
Oct. 10, 1963	USGS	792	964	9,740	178	7,210	13,800	32,600	5.91	262
Nov. 4, 1963	IID	820	968	9,380	198	6,900	13,400	31,600	5.97	257
May 18, 1964	IID	905	1,010	9,700	175	7,110	13,900	33,000	6.15	276
May 28, 1964	USGS	776	926	9,540	180	7,010	13,500	31,800	6.13	265

[1] Agencies responsible for publication or file data: CI, Carnegie Institution of Washington; Cal, state of California; IID, Imperial Irrigation District; USGS, U.S. Geological survey. Data were obtained from the following publications or files:

Years	*Symbol*	*Source*
1907-16	CI	Sykes (1937).
1907-08	USGS	Van Winkle and Eaton (1910).
1923	CI	Carnegie Institution of Washington (1924).
1929	Cal	Coleman (1929).
1945-64	IID	Files of the Imperial Irrigation District.
1961-64	USGS	Files of the U.S. Geological survey.

[2] Calculated as the sum of constituents shown using half the bicarbonate concentration, except that for 1929, which was determined by evaporation.

sample analyses indicate that mineral salts accumulated in the valley through 1948, but since then the quantities of dissolved mineral salts leaving the valley in drain water are greater than the quantities entering canal waters.

Selected chemical analyses of surface water in the Salton Sea basin are presented in Table 2.3 and are discussed below.

The salinity of the Alamo and New Rivers (Fig. 2.13) flowing into the Salton Sea varies according to the proportions of canal water and drainage water in each. Usually the New River is considerably more saline than the Alamo River. A small flow source to the Alamo River and a much larger source to the New River is drain water from the Mexicali Valley. Irelan (1971) reports that more frequent drain samples are necessary before a mineral budget for Imperial Valley can be established.

The Alamo River, sampled near Calipatria in 1967, has an annual flow of 62,000 ha-m (500,000 acre-ft). TDS content is about 2,500 ppm. The water has a sodium chloride sulfate character and a fluoride concentration of about 1 ppm.

The New River near Westmorland has a sodium chloride character with almost 1 ppm fluoride concentration and a TDS of around 3,500 ppm. Its annual flow is less than 62,000 ha-m (500,000 acre-ft).

The Coachella Valley, unlike Imperial Valley, is underlain by productive aquifers of fairly low salinity. Colorado River water has replaced much of the ground water previously pumped for irrigation. Based on rough computations for 1962-65, it appears that more chloride left the valley than entered it through canal water and that sulfate concentrations entering and leaving were nearly equal.

At Mecca (Fig. 2.13), the Whitewater River, flowing annually at less than 12,300 ha-m (100,000 acre-ft), has a TDS of about 2,000 to 2,500 ppm. The water shows a fairly high fluoride concentration of 3.5 ppm and has a sodium sulfate chloride nature.

San Felipe Creek (Fig. 2.13) runoff is mostly flood water and varies from 12 to 1,100 ha-m (100 to 8,700 acre-ft) per year. Chemical analysis from 1955 to 1957 showed a range of 7,000 to 9,000 ppm TDS, a sodium chloride character and notable sulfate concentrations.

Salt Creek (Fig. 2.13), measured in 1967, was sodium chloride in character, showed a high fluoride concentration and contained about 4,500 ppm TDS. It has a constant flow derived mostly from Coachella Canal seepage of approximately 490 ha-m (4,000 acre-ft) per year.

TABLE 2.3 SELECTED CHEMICAL ANALYSES OF SURFACE WATER IN THE SALTON SEA BASIN (Irelan, 1971)

[Results in milligrams per liter unless otherwise indicated]

No.	Source	Date	Discharge (Cfs)	Silica (SiO2)	Calcium (Ca)	Magnesium (Mg)	Sodium (Na)	Potassium (K)	Bicarbonate (HCO3)	Sulfate (SO4)	Chloride (Cl)	Dissolved solids (sum)	Specific conductance (micromhos at 25°C)
1.	Alamo River at international boundary	Feb. 5, 1962	2.0	13	199	108	611		311	1,000	690	2,490	4,150
2.	Alamo River at international boundary	May 2, 1962	4.2	14	172	76	380		288	675	455	1,910	3,200
3.	Alamo River near Niland	Dec. 30, 1964	639	13	250	160	726		254	975	1,160	3,410	5,530
4.	Alamo River near Niland	Mar. 26, 1965	786	10	230	108	550		224	825	833	2,670	4,180
5.	New River at international boundary	Jan. 12, 1965	124	25	281	93	1,580		260	675	2,560	5,350	9,000
6.	New River at international boundary	June 15, 1965	122	22	266	126	1,330		240	750	2,190	4,800	7,940
7.	New River near Westmoreland	Dec. 30, 1964	386	20	250	123	1,120		268	850	1,750	4,250	7,010
8.	New River near Westmoreland	Mar. 26, 1965	543	14	238	108	827		256	750	1,310	3,380	5,430
9.	Whitewater River near Mecca	Nov. 17, 1964	82	18	166	51	600		336	950	472	2,420	3,670
10.	Whitewater River near Mecca	June 7, 1965	139	18	170	44	530		336	825	435	2,190	3,410

Lower Colorado River--Approximately 740,000 ha-m (6 million acre-ft) of Colorado River water flows annually to Imperial Dam. The major portion is allocated to the All-American Canal, a lesser amount to the Gila Gravity Main Canal, and the remainder is released down the river channel.

All the irrigation water for Imperial Valley is derived from the All-American Canal. The Colorado River water entering the canal at Imperial Dam has contained from 637 to 912 mg/l TDS during the 25-year period from 1941 through 1965 (Irelan, 1971, p. E-12). There have been fluctuations in the general trend,but the mineral content of this water has generally increased from less than 800 mg/l through 1954 to a 800 to 900 mg/l range during 1955-65. This increase in salinity is due to increased irrigation and water diversion above the dam.

In Cibola Valley, above Imperial Dam (Fig. 2.13), much irrigated acreage has been added in the last two decades but no surface drains have been constructed. Leaching of soluble salts from this land has added substantially to the Colorado River's mineral burden at Imperial Dam. Irelan (1971) reports that Palo Verde and Parker Valleys (Fig. 2.13) exchange some sodium in the soils for calcium. Common salt (sodium chloride) is also leached from these valley soils. The combined water budgets for the Colorado River between Parker and Imperial Dams (1961-65 data) indicated deposition of calcite and gypsum, some base-exchange replacement of calcium by sodium and removal of sodium chloride.

The ever-increasing diversion of water to the Colorado River Aqueduct has resulted in an increase in ionic concentration at Imperial Dam. The amount of water available for diluting the more concentrated inflows is reduced by the quantity of water diverted from the river.

2.4.2 Groundwater

Local geology plays an important role in determining groundwater quality and distribution in Imperial Valley. The hydrologic and chemical characteristics of Imperial Valley waters are highly dependent on sedimentary stratigraphy and the waters' location with respect to prominent faults. Hydrothermal processes may also play an important role in altering water quality and flow characteristics.

Sedimentary deposits are heterogenous and range from impermeable clays to very permeable coarse sands and gravels. The areal and vertical distribution of sediments in the valley are strongly related to contributions from the Colorado River, which has been the dominant source of valley sediments since the Miocene (Muffler and Doe, 1968). In general, the grain size of valley sediments is inversely proportional to the distance from the present-day Colorado River Delta (Merriam and Bandy, 1965), so that sediments of the southern and eastern Imperial Valley are much coarser than northern and central valley deposits. This relationship generally holds to a depth of at least 2,000 m (6,600 ft) (Randall, 1971) and holds best for central and eastern valley deposits. West valley deposits are less affected by contributions from the Colorado River than by deposition from local sources. Other processes tend to concentrate coarse deposits (sands) on the flanks and fine deposits (clays) in the central valley. The action of northwest prevailing winds concentrates sands in southern and easterly dune belts; deposition in the several post-Miocene lakes has concentrated clays and evaporites in the central Imperial Valley. The net effects of these sedimentary processes are: 1) they tend to form natural stratigraphic cap rocks for central valley geothermal systems, 2) they separate shallow and deep ground water systems, and 3) they make central valley waters saltier and more stagnant than eastern or western waters.

All of the deposits of hydrologic interest are deltaic, lacustrine, fluvial or alluvial sediments of nonmarine origin. The most recent nonmarine unit is the Imperial Formation which lies deeper than 4,097 m (13,443 ft) in the central Imperial Valley (Muffler and Doe, 1968). The sedimentary sequence thickens towards the center of the valley, and individual beds and layers are difficult to trace or delineate due to the nonuniform, lensing nature of the deposits. The valley is crossed by numerous known, inferred and yet to be located faults, most trending northwest-southeast (Plate 2.2). These faults act as ground water barriers and conduits introducing local alterations in water table levels and flow patterns. Meidav and Furgerson (1972) have shown that many faults of the San Andreas System act as aquitards for valley waters. They postulate that high salinity gradients existing across northwest trending faults further increase salinities of central valley ground water by forming barriers to fluid mixing. It was noted, for instance, that artesian waters exist only east of the Alamo River, suggesting that this river marks one of the proposed aquitards. Meidav and Furgerson (1972) have also observed salinity increasing from the southeast to the northwest. This could be accounted for by assuming a single recharge source at the Colorado River. Waters northward and westward would be further along the flow path from the Colorado River towards the Salton Sea, implying that these waters could become more saline due to longer contact with reservoir rocks.

The regional water flow pattern is complicated, but in general ground water flows northward and westward towards the Salton Sea as underflow from the Colorado River. This regional flow is generally separated into a shallower and a deeper hydrologic unit. Ground water in both units flows in the same direction, but faults and lithologic discontinuities complicate the basic pattern. These geologic features may channel or obstruct water flow, and local convection patterns from hydrothermal systems may cause regional waters to flow towards geothermal anomalies. Separation of deep and shallow aquifers also tends to complicate flow patterns, especially when shallow and deep waters can communicate by fault-induced permeability. In some cases careful analyses have allowed local flow patterns to be deduced (Bird, 1975).

The major ground water flow, in addition to underflow from the Colorado River, comes from canal leakage and irrigation discharge. The original source of all of this water is the Colorado River. These Colorado River waters flow towards the central and northern portions of the valley and finally into the Salton Sea. Minor contributions to the ground water system come from northward underflow from the Mexicali Valley and local runoff flowing towards the center of the valley from the mountains on the eastern and western margins. Ground water flow in aquifers deeper than 900 m (3,000 ft) is probably downward from the shallower aquifers and then radially towards heat anomaly convection cells (Dutcher, et al.,1972). Once in the convection cells, the water recirculates as convection currents.

The flow rate of Imperial Valley wells is variable and depends on the location and depth of the well. Many shallow wells at eastern and western valley margins have flows greater than 3,800 lpm (1,000 gpm), whereas central valley shallow wells have produced only a fraction of this. This is partly why the extensive irrigation system was needed in Imperial Valley. Deep wells in the central valley, however, flow as well or better than deep wells at the valley margins. Adequate sampling of these wells is not yet available to establish a clear pattern.

The total volume of water in storage has been estimated between 2.0 and 5.9 x 10^8 ha-m (1.6 and 4.8 billion acre-ft) depending on the porosity depth function used (Rex, 1970, p. 14). Combs (1971, p. 11) estimated a total of 2.6 x 10^8 ha-m (2.1 billion acre-ft) total water in storage between 900 and 3,000 m (3,000 and 10,000 ft) depth. Dutcher, et al., (1972) estimated 2.0 x 10^8 ha-m (1.6 billion acre-ft) of water with less than 35,000 mg/l TDS in Imperial Valley.

Previous Investigations--

Three major sources for hydrology and ground water quality data in Imperial Valley are "Preliminary Appraisal of Ground water in Storage with Reference to Geothermal Resources in the Imperial Valley Area, California" (Dutcher, et al., 1972); "Geohydrologic Reconnaissance of the Imperial Valley, California (Loeltz, et al., 1975); and "Selected Data on Water Wells, Geothermal Wells and Oil Tests in the Imperial Valley, California (Hardt and French, 1976). These references were used extensively and many other site-specific sources were utilized for additional detail.

Dutcher, et al.,(1972) present a general conceptual hydrologic model on which they based estimates of ground water in storage. They divide the ground water regime into four depth zones from the surface to the basement complex and further subdivide the nearest surface zone into four ground water storage units. They then estimate the quantity of recoverable water in each unit based on estimates of porosity, specific yield, thickness and areal extent of each unit.

The data presented in Dutcher, et al. (1972) is based on an insufficient amount of control data and an unproven conceptual model. Estimates are based on huge extrapolations of meager data and even though they may be the best estimates attainable with available data, they may be subject to extreme modifications. Therefore these limitations should be recognized in the following discussions which refer to the work of Dutcher, et al.,(1972).

Loeltz, et al.,(1975) address only the upper few hundred meters of heterogenous nonmarine deposits. They include transmissivities derived from pump tests, specific yield derived from soil moisture studies, ground water movement, discussions of recharge and discharge and ground water quality. Although this was published in 1975, the study and report was completed by 1966 (Olmsted, pers. comm., 1977) and therefore does not include any information collected since 1966.

Hardt and French (1976) is strictly a data compilation of over 430 wells in Imperial Valley. It includes complete water quality and sample depth interval data for 74 wells. These data were used extensively in the water quality section in preparation of modified Stiff and Langelier-Ludwig diagrams and in contouring of water parameters. Reed (1975) and Cosner (1977) provided additional water quality data for the artesian aquifer and geothermal wells, respectively.

Limitations of Data--

We have made no attempt at original data generation in this phase of the study and have utilized data available from previous studies, assuming it to be correct unless discrepancies became apparent. This is particularly relevant with respect to the water quality data. It was beyond the scope of this report to reconcile differing sample procedures and analytic techniques used by different workers. The available data were compiled, interpreted and described using standard hydrologic and geochemical techniques. If the results seemed reasonable, the raw data was considered sufficient.

It is important to note again the great extrapolations used by Dutcher, et al., (1972). Their conclusions are based on conceptual modeling of the mechanism and elements of the hydrothermal system. The accuracy of their estimates is only proportional to the reliability of their conceptual model and their raw data, collected up to June 1971.

Water-Bearing Units--

Hydrologic investigations of Imperial Valley have generally referred to about a thousand meters of upper water-bearing strata and a confined aquifer below separated by a relatively impermeable clay layer (e.g., Loeltz, et al., 1975; Geonomics, 1976). To date, no one has attempted to correlate aquifers with individual geologic formations (described above in Section 2.3.4, "Stratigraphy and Lithology of Salton Trough Rocks"). Due to "intermittent and interfingering alluvial fan, flood-plain and lacustrine" sedimentation (Sylvester and Smith, 1976) and active tectonics of Imperial Valley, it is impossible to project the spatial distribution of these units over any considerable area. Sylvester and Smith (1976) further note "stratigraphic thickness, age relations, and correlation of various lithologic units along strike and across faults are tenuous because of numerous diastems, abrupt facies changes, the lack of fossils, and distinctive marker beds."

Dutcher, et al.,(1972) have taken the upper-lower classification further by dividing the lower and deeper water-bearing strata into three essentially horizontal units, one on top of another, and by dividing the upper water-bearing strata into four areal hydrologic units. Their objective in establishing this classification was to enable estimation of the total quantity of usable and recoverable water in storage in Imperial Valley. These classifications are based on each unit having similar estimated porosity and/or specific yield. They define the thickness and areal extent of each unit in Figures 2.14, 2.15, 2.16, 2.17 and 2.18. All of the units have their thickest sections in the center of the valley parallel to the north-northwest axis of the valley. The total thickness of deposits with usable water attains a maximum of 4,600 m (15,000 ft) in the south central valley (Fig. 2.14). These units can be considered aquifers, originally defined by Meinzer (1923) as any water-bearing formation; however, they should be considered only in a general classification sense, not as continuous units with distinct confining boundary layers.

Hydrologic section A-A' (Fig. 2.19) crosses the valley along its axis,and hydrologic sections B-B' and C-C' (Figs. 2.20 and 2.21) cross the valley perpendicular to the valley axis. These show schematic cross sections of the hydrologic units, including their respective specific yields, isothermal contours, areas of ground water with more than 35,000 mg/l TDS, a sketch of the configuration of the basement-complex surface, locations of selected data wells and fault locations. The four depth zones depicted in these hydrologic sections, and mentioned previously, are described below as defined by Dutcher, et al. (1972).

Zone 4 is the deepest zone and is defined as containing all reservoir rocks with recoverable water containing less than

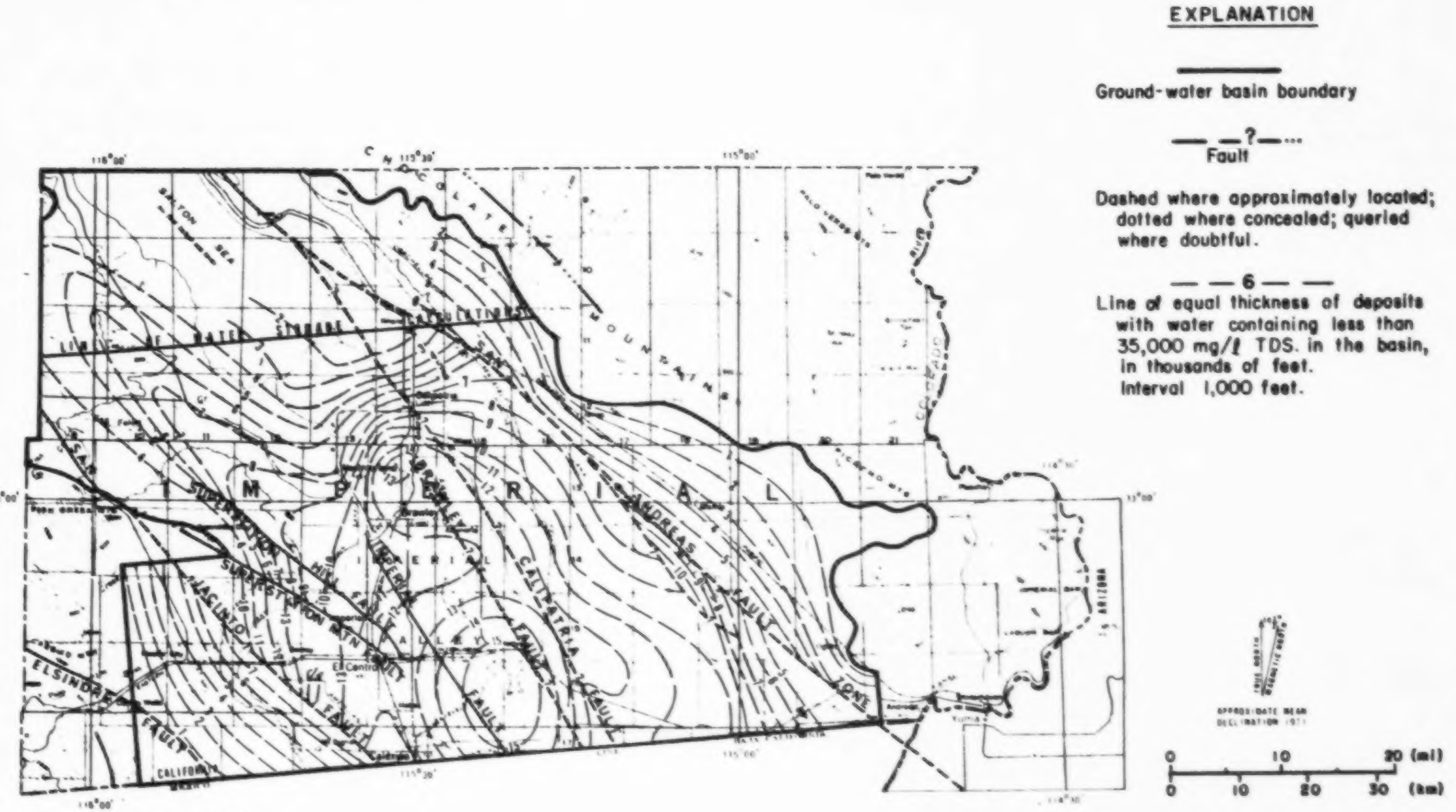
EXPLANATION
Ground-water basin boundary
Fault
Dashed where approximately located; dotted where concealed; queried where doubtful.
6
Line of equal thickness of deposits with water containing less than 35,000 mg/ℓ TDS. in the basin, in thousands of feet. Interval 1,000 feet.
I M P E R I A L
SAN ANDREAS FAULT
CALIPATRIA FAULT
IMPERIAL FAULT
BRAWLEY FAULT
SUPERSTITION HILLS FAULT
SUPERSTITION MTN FAULT
SAN JACINTO FAULT
ELSINORE FAULT
SALTON SEA
CHOCOLATE MOUNTAINS
ARIZONA
CALIFORNIA
El Centro
APPROXIMATE MEAN DECLINATION 1971
0 10 20 (mi)
0 10 20 30 (km)
116°00'
115°30'
115°00'
114°30'
33°00'

Base from U.S. Geological Survey State of California (south half) 1:500 000 1970

Figure 2.14 Total thickness of deposits with water containing less than 35,000 mg/l dissolved solids. (Dutcher, et al., 1972)

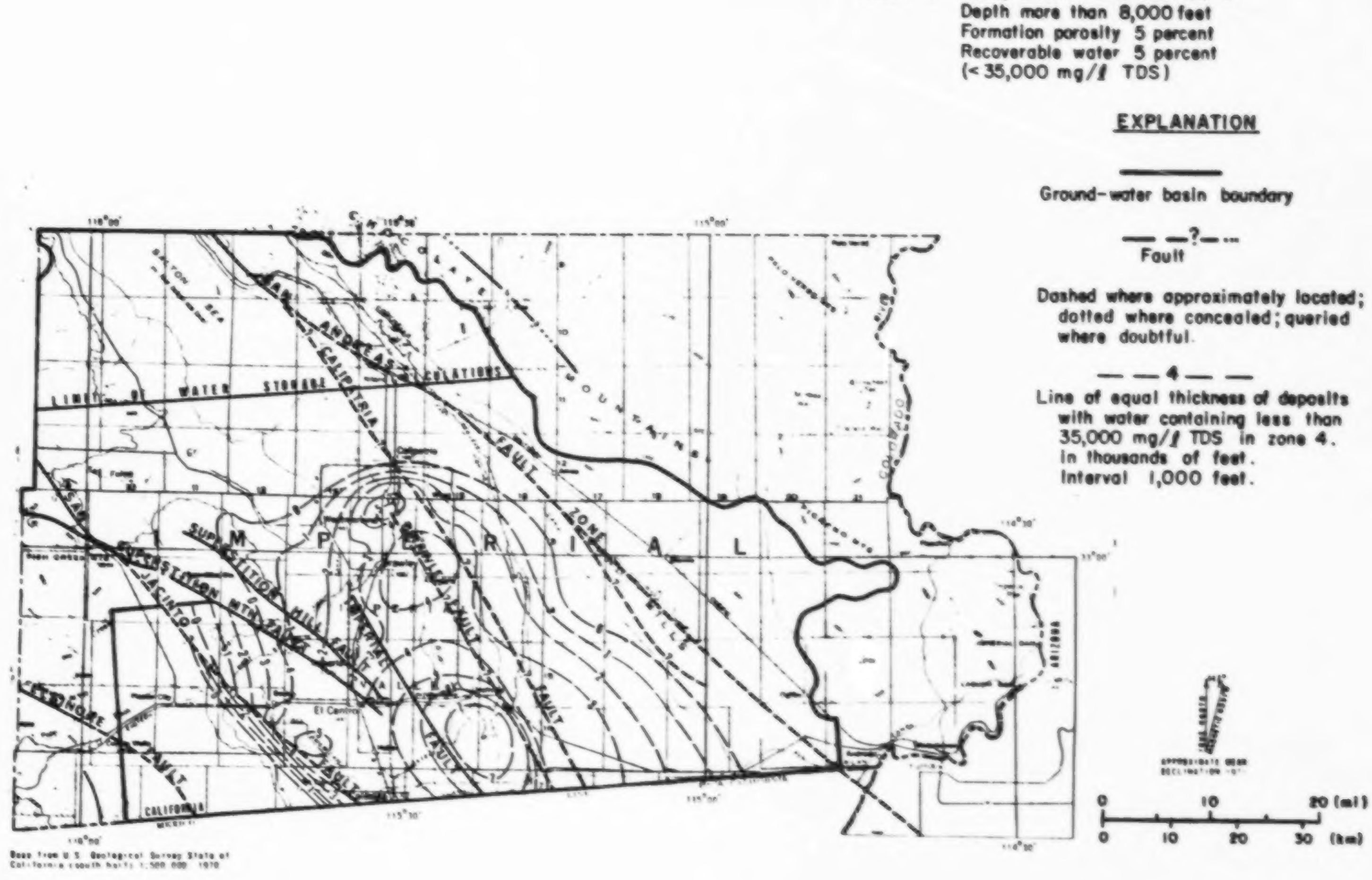

ZONE - 4 Temperature more than 100°C
Depth more than 8,000 feet
Formation porosity 5 percent
Recoverable water 5 percent
(< 35,000 mg/ℓ TDS)
EXPLANATION
Ground-water basin boundary
Fault
Dashed where approximately located; dotted where concealed; queried where doubtful.
4
Line of equal thickness of deposits with water containing less than 35,000 mg/ℓ TDS in zone 4. In thousands of feet. Interval 1,000 feet.
SALTON SEA
SAN ANDREAS FAULT
CALIPATRIA FAULT
LIMIT OF WATER STORAGE
FAULT ZONE
IMPERIAL
SUPERSTITION HILL FAULT
SUPERSTITION MTN FAULT
SAN JACINTO FAULT
ELSINORE FAULT
SAND HILLS
COLORADO
ARIZONA
CALIFORNIA
El Centro
0 10 20 (mi)
0 10 20 30 (km)
Base from U.S. Geological Survey State of California (south half) 1:500 000 1970

Figure 2.15 Total thickness of deposits with water containing less than 35,000 mg/l dissolved solids in zone 4. (Dutcher, et al., 1972)

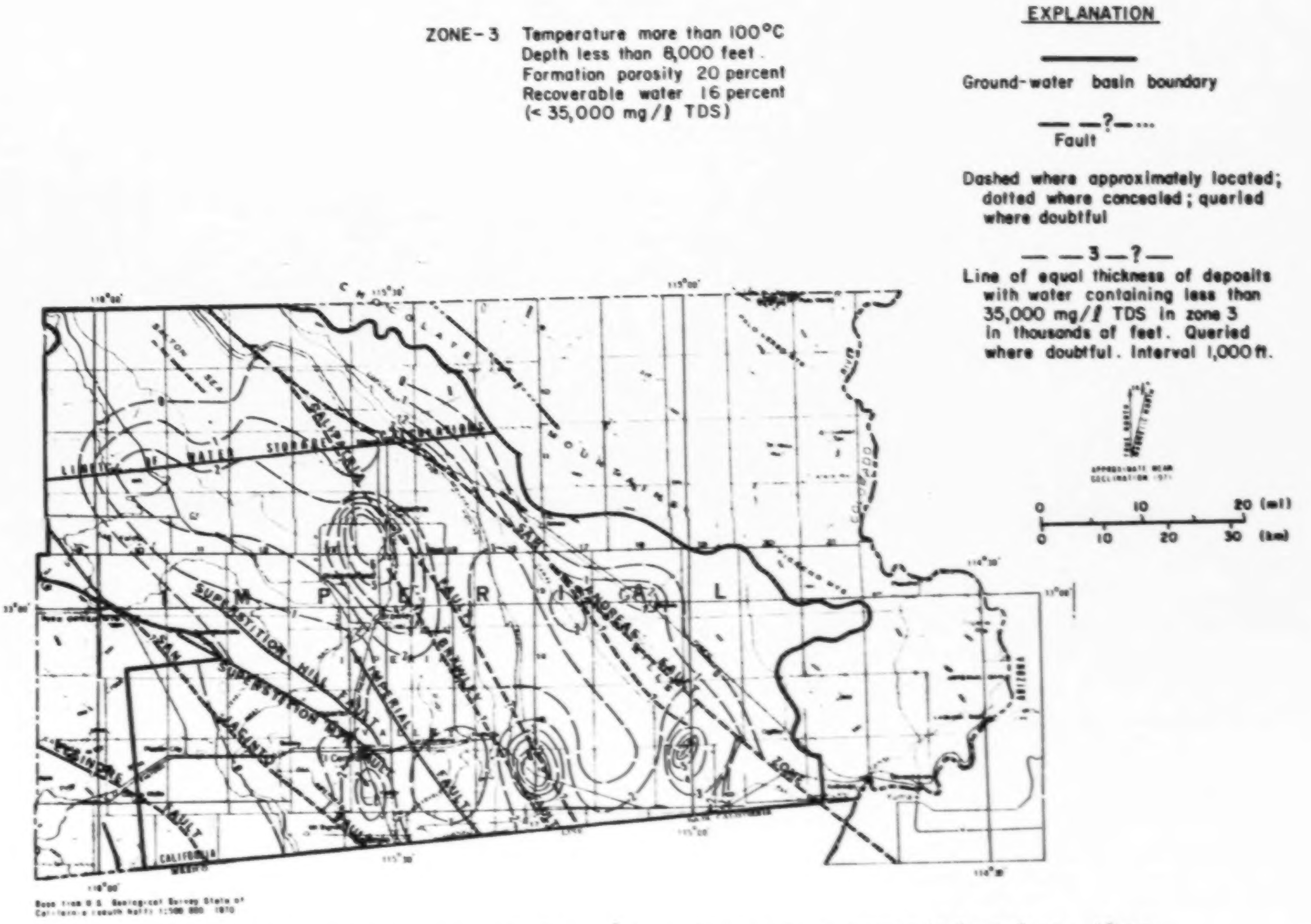
ZONE-3 Temperature more than 100°C
Depth less than 8,000 feet.
Formation porosity 20 percent
Recoverable water 16 percent
(< 35,000 mg/l TDS)
EXPLANATION
Ground-water basin boundary
— —?—···
Fault
Dashed where approximately located; dotted where concealed; queried where doubtful
— —3—?—
Line of equal thickness of deposits with water containing less than 35,000 mg/l TDS in zone 3 in thousands of feet. Queried where doubtful. Interval 1,000 ft.
APPROXIMATE MEAN DECLINATION 1971
0
10
20 (mi)
0
10
20
30 (km)
IMPERIAL
SALTON SEA
SAN ANDREAS FAULT
SUPERSTITION HILL FAULT
SUPERSTITION MT. FAULT
SAN JACINTO FAULT
IMPERIAL FAULT
BRAWLEY FAULT
ELSINORE FAULT
LIMIT OF WATER STORAGE UNIT
CHOCOLATE MOUNTAINS
ARIZONA
CALIFORNIA
MEXICO
Base from U.S. Geological Survey State of California (south half) 1:500 000 1970

Figure 2.16 Total thickness of deposits with water containing less than 35,000 mg/l dissolved solids in zone 3. (Dutcher, et al., 1972)

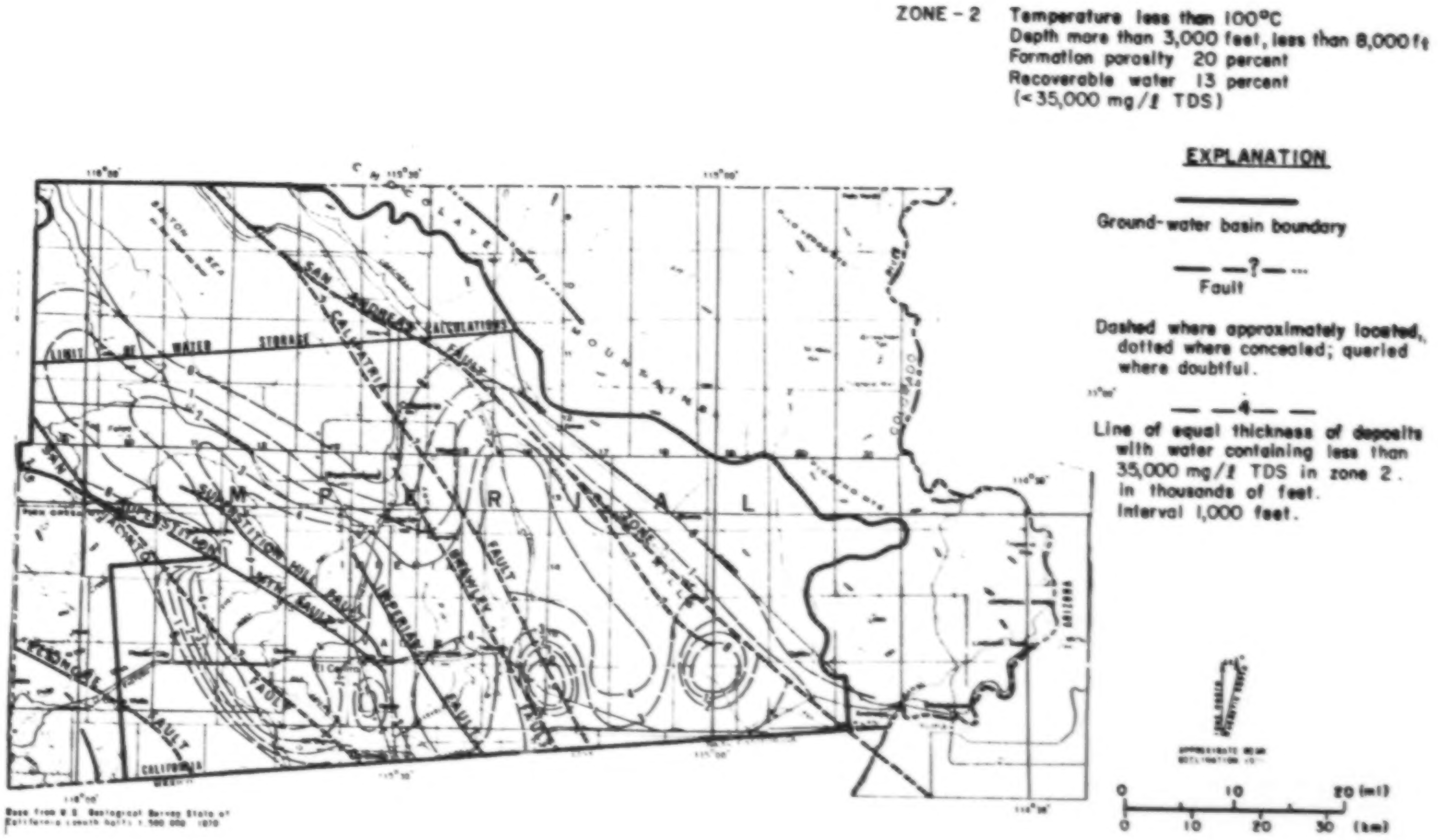

ZONE - 2
Temperature less than 100°C
Depth more than 3,000 feet, less than 8,000 ft
Formation porosity 20 percent
Recoverable water 13 percent
(<35,000 mg/l TDS)
EXPLANATION
Ground-water basin boundary
Fault
Dashed where approximately located, dotted where concealed; queried where doubtful.
Line of equal thickness of deposits with water containing less than 35,000 mg/l TDS in zone 2. in thousands of feet. Interval 1,000 feet.
0
10
20 (mi)
0
10
20
30 (km)
SALTON SEA
SAN ANDREAS
CALIPATRIA
FAULT
LIMIT OF WATER STORAGE CALCULATIONS
CHOCOLATE
MOUNTAINS
I M P E R I A L
SAN JACINTO
SUPERSTITION
SUPERSTITION HILLS FAULT
IMPERIAL
BRAWLEY
FAULT
ELSINORE
CALIFORNIA
ARIZONA
COLORADO
Base from U.S. Geological Survey State of California (south half) 1:500,000 1970

Figure 2.17 Total thickness of deposits with water containing less than 35,000 mg/l dissolved solids in zone 2. (Dutcher, et al., 1972)

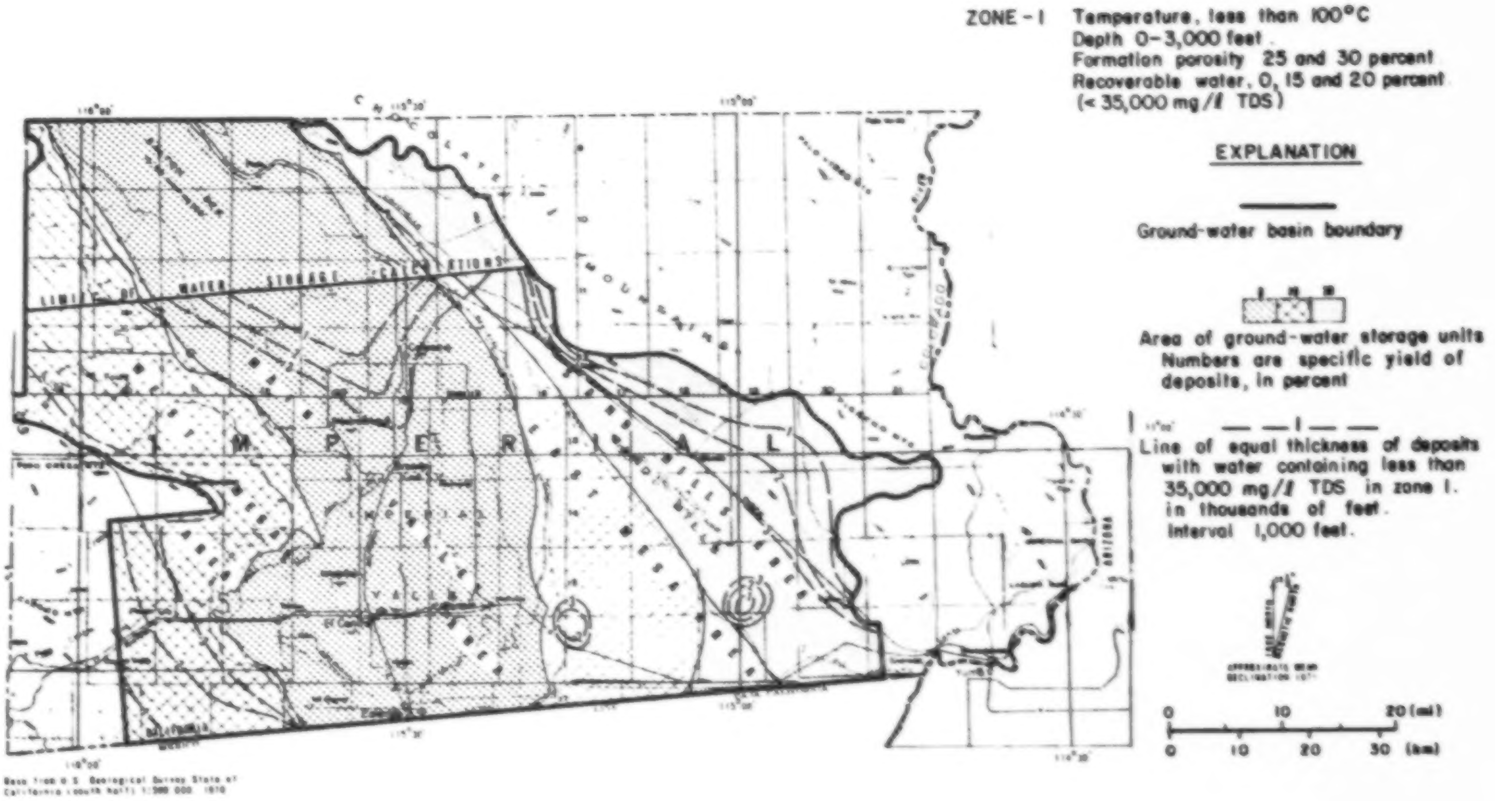
ZONE - I
Temperature, less than 100°C
Depth 0-3,000 feet
Formation porosity 25 and 30 percent
Recoverable water, 0, 15 and 20 percent
(< 35,000 mg/l TDS)
EXPLANATION
Ground-water basin boundary
Area of ground-water storage units
Numbers are specific yield of deposits, in percent
Line of equal thickness of deposits with water containing less than 35,000 mg/l TDS in zone 1. in thousands of feet. Interval 1,000 feet.
0
10
20 (mi)
0
10
20
30 (km)
IMPERIAL
LIMIT OF WATER STORAGE CALCULATIONS
ARIZONA
COLORADO
116°00'
115°30'
115°00'
114°30'

Figure 2.18 . Total thickness of deposits with water containing less than 35,000 mg/l dissolved solids in zone 1. (Dutcher, et al., 1972)

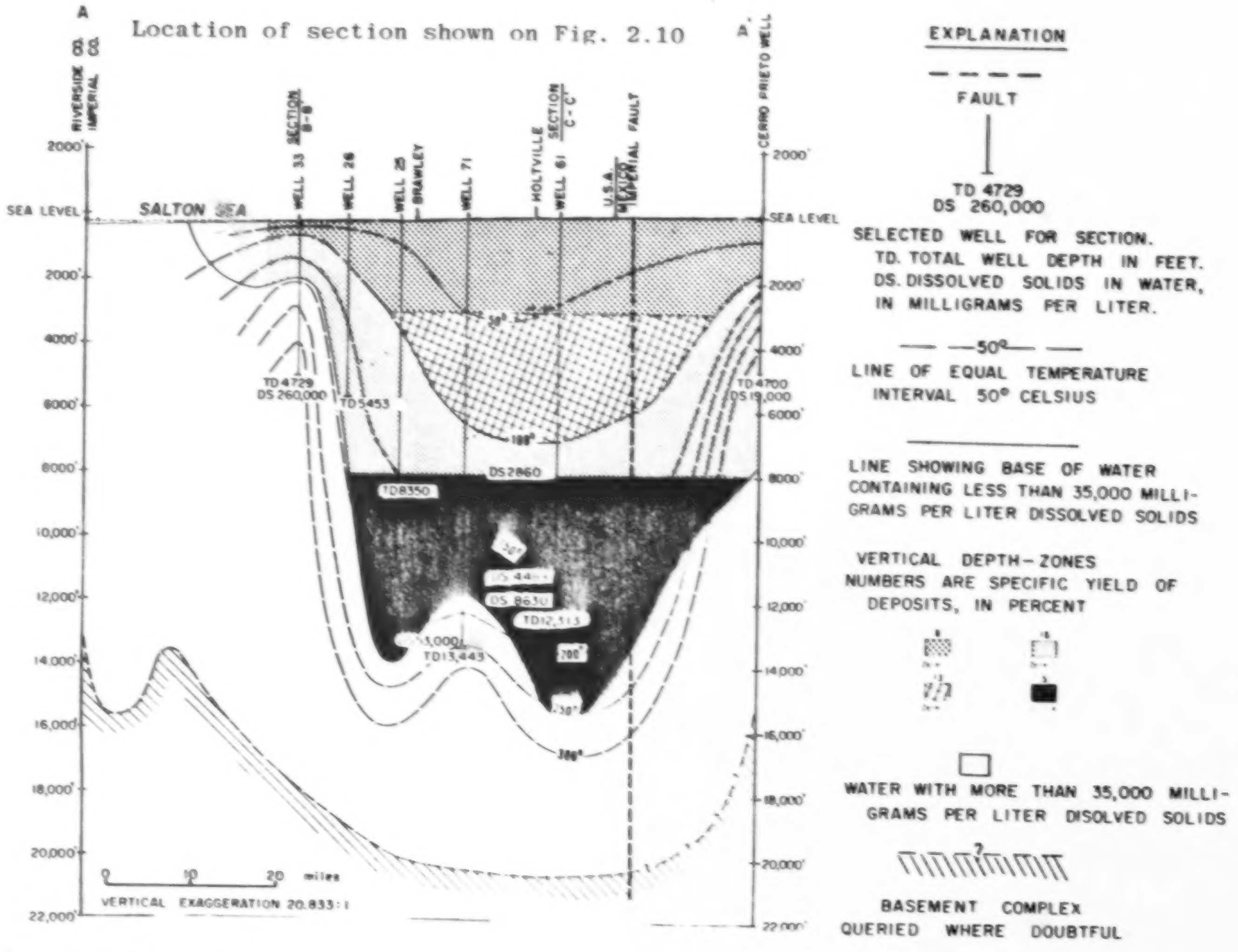
Location of section shown on Fig. 2.10

A
88
RIVERSIDE
IMPERIAL
A'
CERRO PRIETO WELL
SALTON SEA
WELL 33
SECTION B-B'
WELL 26
WELL 25
BRAWLEY
WELL 71
HOLTVILLE
WELL 61
SECTION C-C'
U.S.A.
MEXICO
IMPERIAL FAULT
2000'
SEA LEVEL
2000'
4000'
6000'
8000'
10,000'
12,000'
14,000'
16,000'
18,000'
20,000'
22,000'
TD 4729
DS 260,000
TD5453
TD8350
DS2860
TD 4700
DS 19,000
50°
100°
150°
200°
250°
300°
DS 44
DS 8630
TD12,313
3,000
TD13,443
0
10
20 miles
VERTICAL EXAGGERATION 20.833:1
EXPLANATION
FAULT
TD 4729
DS 260,000
SELECTED WELL FOR SECTION.
TD. TOTAL WELL DEPTH IN FEET.
DS. DISSOLVED SOLIDS IN WATER, IN MILLIGRAMS PER LITER.
50°
LINE OF EQUAL TEMPERATURE INTERVAL 50° CELSIUS
LINE SHOWING BASE OF WATER CONTAINING LESS THAN 35,000 MILLIGRAMS PER LITER DISSOLVED SOLIDS
VERTICAL DEPTH-ZONES
NUMBERS ARE SPECIFIC YIELD OF DEPOSITS, IN PERCENT
WATER WITH MORE THAN 35,000 MILLIGRAMS PER LITER DISOLVED SOLIDS
?
BASEMENT COMPLEX
QUERIED WHERE DOUBTFUL

Figure 2.19 Hydrologic section A-A'. (Dutcher, et al., 1972)

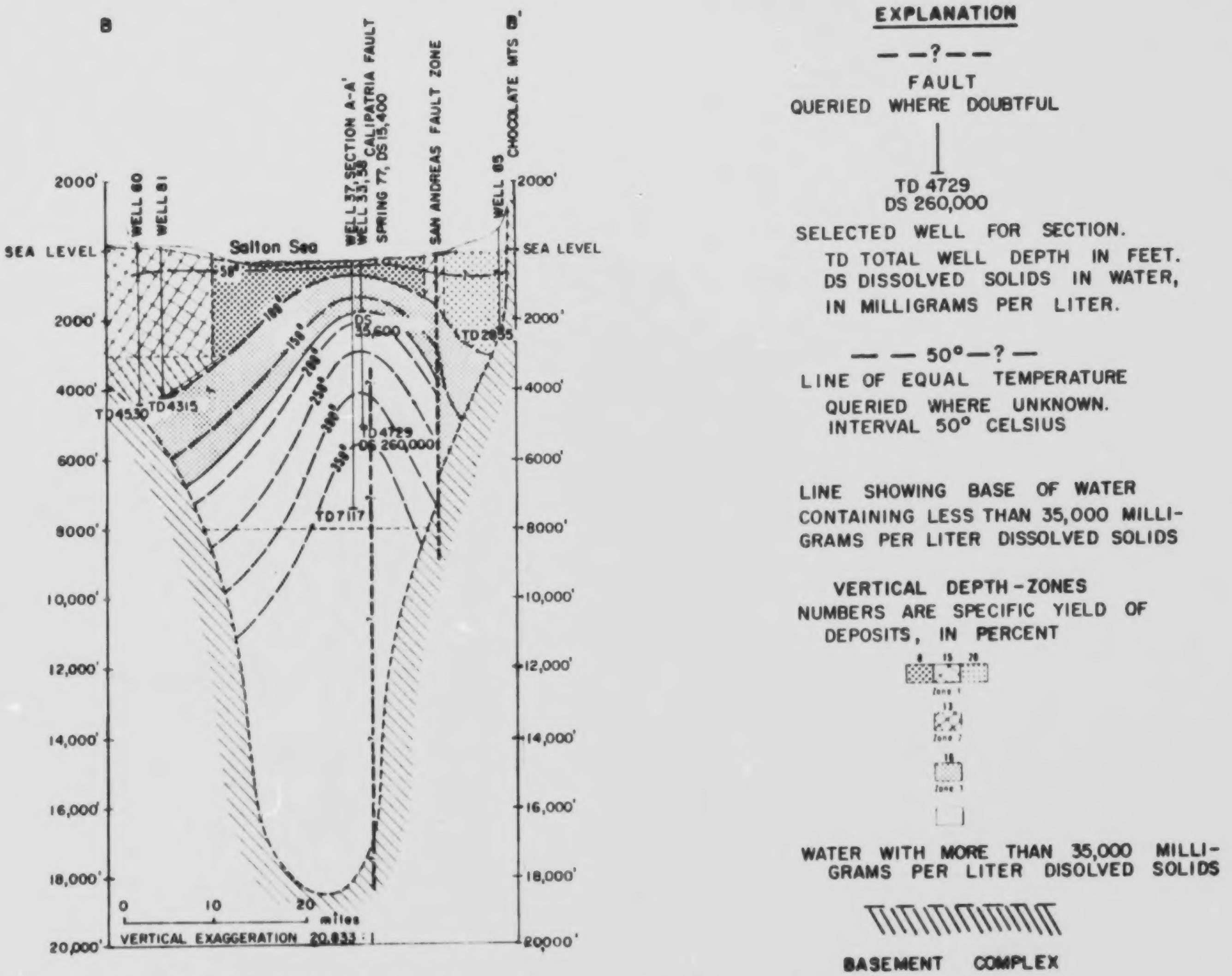
B
B'
WELL 60
WELL 81
Salton Sea
WELL 37, SECTION A-A'
WELL 53, 58
CALIPATRIA FAULT
SPRING 77, DS 15,400
SAN ANDREAS FAULT ZONE
WELL 65
CHOCOLATE MTS
2000'
SEA LEVEL
2000'
4000'
6000'
8000'
10,000'
12,000'
14,000'
16,000'
18,000'
20,000'
TD 4530
TD 4315
DS 35,600
TD 4729
DS 260,000
TD 7117
TD 2835
50°
100°
150°
200°
250°
300°
350°
0
10
20
miles
VERTICAL EXAGGERATION 20.833
EXPLANATION
— —?— —
FAULT
QUERIED WHERE DOUBTFUL
TD 4729
DS 260,000
SELECTED WELL FOR SECTION.
TD TOTAL WELL DEPTH IN FEET.
DS DISSOLVED SOLIDS IN WATER, IN MILLIGRAMS PER LITER.
— — 50° —? —
LINE OF EQUAL TEMPERATURE
QUERIED WHERE UNKNOWN.
INTERVAL 50° CELSIUS
LINE SHOWING BASE OF WATER CONTAINING LESS THAN 35,000 MILLIGRAMS PER LITER DISSOLVED SOLIDS
VERTICAL DEPTH-ZONES
NUMBERS ARE SPECIFIC YIELD OF DEPOSITS, IN PERCENT
8
15
20
Zone 1
13
Zone 2
18
Zone 3
WATER WITH MORE THAN 35,000 MILLIGRAMS PER LITER DISOLVED SOLIDS
BASEMENT COMPLEX

Figure 2.20 Hydrologic section B-B'. (Dutcher, et al.,1972)

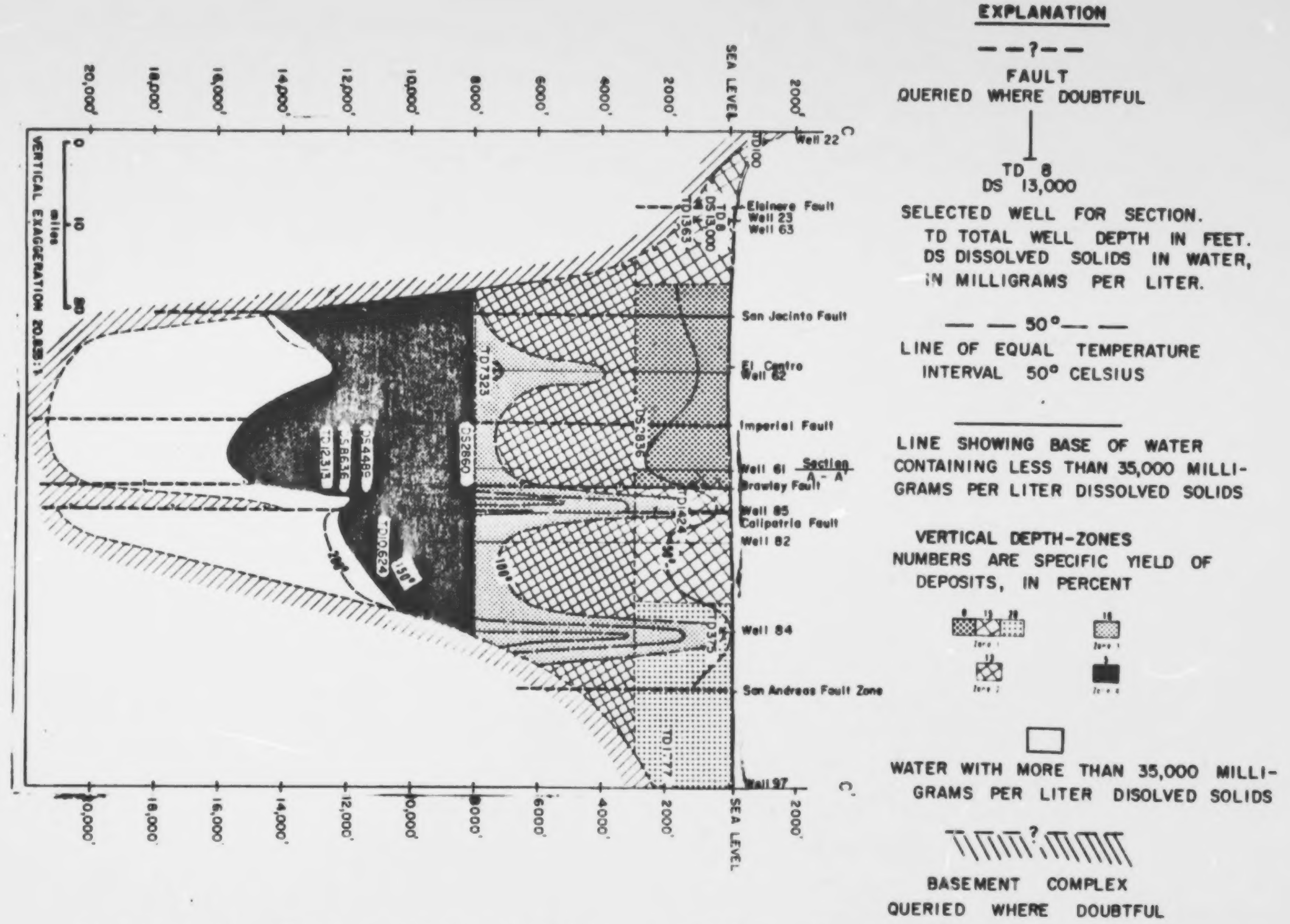
EXPLANATION
FAULT
QUERIED WHERE DOUBTFUL
TD 8
DS 13,000
SELECTED WELL FOR SECTION.
TD TOTAL WELL DEPTH IN FEET.
DS DISSOLVED SOLIDS IN WATER, IN MILLIGRAMS PER LITER.
50°
LINE OF EQUAL TEMPERATURE INTERVAL 50° CELSIUS
LINE SHOWING BASE OF WATER CONTAINING LESS THAN 35,000 MILLIGRAMS PER LITER DISSOLVED SOLIDS
VERTICAL DEPTH-ZONES
NUMBERS ARE SPECIFIC YIELD OF DEPOSITS, IN PERCENT
WATER WITH MORE THAN 35,000 MILLIGRAMS PER LITER DISOLVED SOLIDS
BASEMENT COMPLEX
QUERIED WHERE DOUBTFUL
C
C'
Well 22
Elsinore Fault
Well 23
Well 63
San Jacinto Fault
El Centro
Well 62
Imperial Fault
Well 61
Section A - A'
Brawley Fault
Well 85
Calipatria Fault
Well 82
Well 84
San Andreas Fault Zone
Well 97
TD100
TD 8
DS 13,000
TD1363
DS2836
TD1424
TD375
TD1777
TD7323
DS2860
DS4489
DS8636
TD12,313
TD10,624
50°
100°
150°
200°
2000'
SEA LEVEL
2000'
4000'
6000'
8000'
10,000'
12,000'
14,000'
16,000'
18,000'
20,000'
0
10
20
miles
VERTICAL EXAGGERATION 20.835:1

Figure 2.21 Hydrologic section C-C'. (Dutcher, et al.,1972)

35,000 mg/l TDS at depths greater than 2,438 m (8,000 ft). The 2,438 m (8,000 ft) boundary was chosen somewhat arbitrarily due to decreasing porosity and permeability and increasing temperature and metamorphism below such depths. In general the rocks below 2,438 m (8,000 ft) are fractured, have very low intergranular permeability and have an average estimated porosity of about 5%. The areal extent and thickness of zone 4 deposits—that is, the thickness of deposits between the basement-complex contours (Rex, et al., 1971) and the 2,400 m depth plane--is shown in Figure 2.15. The maximum thickness is about 2,100 m (7,000 feet) south of Holtville and occurs between mapped traces of the Imperial and Brawley Faults.

Zone 3 is areally much larger and not as thick as underlying zone 4. Zone 3 is defined as that volume of sediments between the 100°C (212°F) isothermal surface and the 2,438 m (8,000 ft) boundary of zone 4. The thickness and areal extent of this zone are shown in Figure 2.16. It reaches a maximum thickness of approximately 2,100 m (7,000 ft) about 32 km (20 mi) east of Holtville. It thickens to over 1,800 m (6,000 ft) in two other areas, one centered about 11 km (7 mi) southeast of Holtville and another centered about 10 km (6 mi) northeast of Westmorland. Both of these areas are essentially between the mapped traces of the Calipatria and Brawley Faults.

Zone 2 includes all deposits below 914 m (3,000 ft) to the top of the 100°C (212°F) isothermal surface (top of zone 3); hence all the water contained in zone 2 will have temperatures less than 100°C (212°F). The thickness and areal extent of zone 2 is shown in Figure 2.17. It attains a maximum thickness of about 1,200 m (4,000 ft) in three large areas. The area east of the Calipatria Fault is over 40 km (25 mi) long and 5 to 11 km (3 to 7 mi) wide; another area centered about 6 km (4 mi) south-southeast of Holtville is about 13 km (8 mi) in diameter; and the third area of zone 2 maximum thickness is irregularly shaped, from 18 to 27 km (11 to 17 mi) wide in the southwest portion of the valley. The porosity for this zone is estimated to be about 20%.

Zone 1 is defined as deposits below the water table to either 914 m (3,000 ft) depth, the bedrock surface or the 100°C (212°F) isotherm, whichever is shallowest. It attains its maximum thickness of 914 m (3,000 ft) over most of the central part of the valley (Fig. 2.18). This zone is further divided areally into four sections, called the Sand Hills area, the East Mesa area, the Main Valley area and the West Mesa area (Fig. 2.18). These areas have specific yields assigned for the water storage computations, of 20%, 15%, 0% and 15% respectively. The Main Valley specific yield is considered 0% because any water derived from the ground in this highly irrigated area would be imported from the Colorado River through the irrigation system and not from a naturally recharged ground water reservoir.

Depth Classifications Used in This Study--The extent and depth continuity of the nearer-surface ground water units are not well-defined in the Imperial Valley area. A division of the shallower water-bearing strata into a general framework of geometric distribution of water flow and occurrence is necessary to enable correlation of water quality parameters and water chemistry changes. Correlation of geologic units is extremely difficult in Imperial Valley,so an empirical approach was tried as a first attempt to define aquifer depth zones. This was accomplished by plotting perforated depth intervals for 143 wells throughout the valley (Fig. 2.22). The hypothesis was that the drillers would drill to the first good water-bearing strata and perforate the well casing there. We could then deduce "preferred" perforated intervals and assume the best aquifers occur at those depths. Admittedly, this is a simplistic approach, and others interpreting these data may choose different intervals than were chosen here. Many important factors were not considered, for example, areal location of well with respect to depth interval perforated, altitude of the perforated interval, aquifers occurring below the first good aquifer intercepted by the driller, etc. However, this is considered to be a first attempt, within the scope of this report, and is expected to be modified with further investigation and analysis.

Shallow, intermediate and deep depth intervals were chosen from the well perforation interval plot. The shallow water bearing strata is defined as the depth interval between 24 to 91 m (80 to 300 ft). This corresponds to elevations from 82 m (270 ft) above sea level to 114 m (374 ft) below sea level for the perforated interval of the wells in our shallow water-bearing strata category. The intermediate water-bearing strata is defined as the depth interval between 91 to 457 m (300 to 1,500 ft). This corresponds to a perforated interval elevation range from 59 m (195 ft) above sea level to about 457 m (1,500 ft) below sea level for the wells in our sample. The deep water bearing strata is defined as the depth interval below 457 m (1,500 ft). This represents strata from about 520 to 4,300 m (1,700 to 14,000 ft) below sea level for the wells in our sample. All wells with perforated intervals that overlapped the interval boundaries were deleted from our sample.

The upper limit of 24 m (80 ft) for the shallow water bearing strata was chosen to minimize effects of irrigation water that has passed the tile drain and has become quite saline by downward percolation through the nearer surface sediments, which are rich in soluble salts derived in part from fertilizer and pesticide residues.

There appears to be some justification for these depth intervals. In plotting the chemical quality data (Section 2.5)

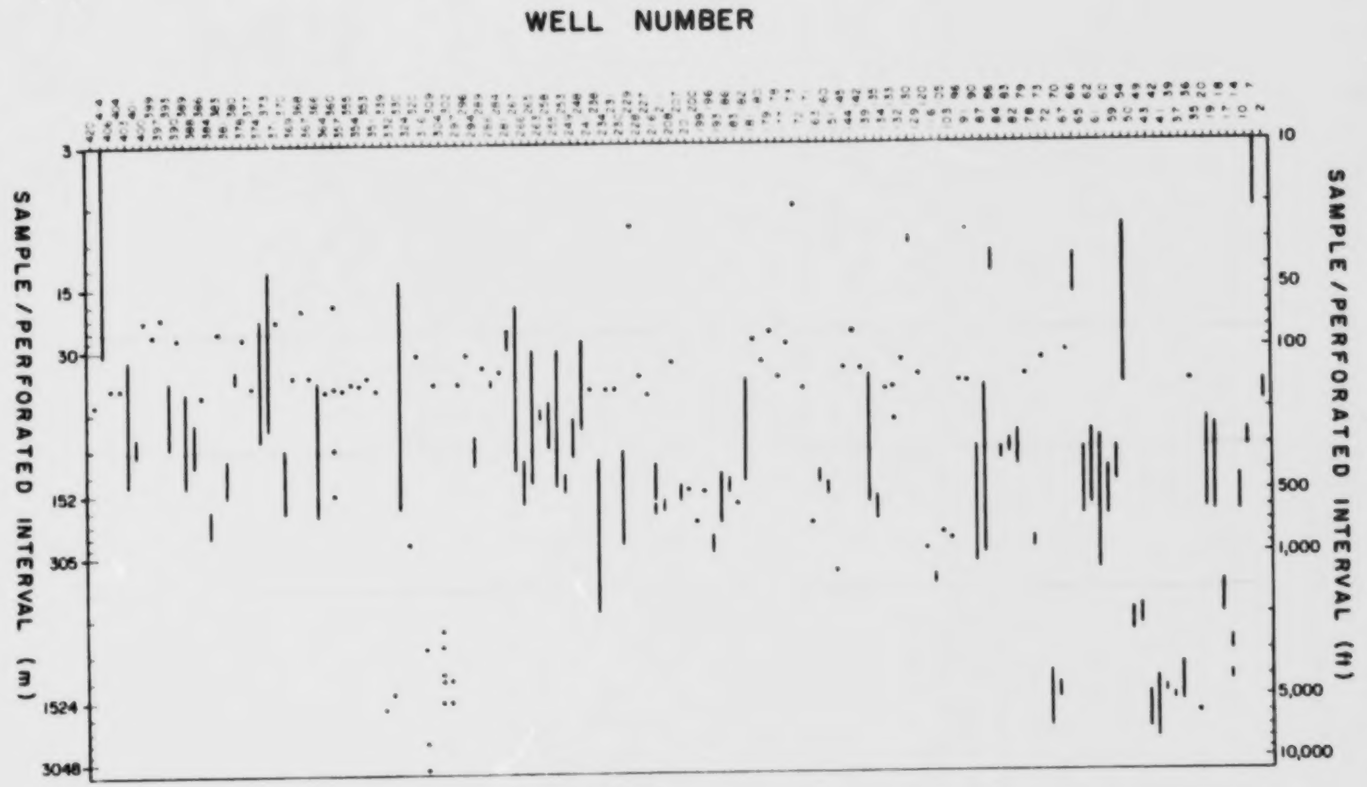

EXPLANATION

EACH HORIZONTAL LINE OR POINT REPRESENTS THE SAMPLE/PERFORATED INTERVAL FOR ONE WELL. (DATA FROM HARDT AND FRENCH, 1972)

DEPTH INTERVAL BOUNDARY
24-91m (80-300 ft) — SHALLOW INTERVAL
91-457m (300-1500 ft) — INTERMEDIATE INTERVAL
DEEPER THAN 457m (1500 ft) — DEEP INTERVAL

Figure 2.22 Perforated intervals for wells in Imperial Valley, California.

definite groupings appear to distinguish the shallow and intermediate depth zones. This is particularly evident in the Langelier-Ludwig diagram (Fig. 2.36), where most of the intermediate waters are grouped along Section AD and the shallow waters are grouped along Section AB.

Ground Water Flow--
Discussion of ground water flow in Imperial Valley will be divided into two sections--one on the shallow water-bearing strata and one on the deeper water-bearing strata. Although we do refer to shallow (upper) and deep (lower) water-bearing strata, it is important to note that these classifications must be used in a very general sense. Their thickness, upper and lower boundaries and areal extent are not well-defined. Although Dutcher, et al., (1972) suggested four vertical depth zones for Imperial Valley (Section 2.4.2, "Water Bearing Units," above), insufficient data is available to discuss flow patterns in these four depth zones or even to determine how and whether these zones are confined.

The general direction of flow in the upper and lower water bearing strata is from the Colorado River, near the southeast corner of Imperial Valley, northwestward towards the center of the valley and the Salton Sea. Minor amounts of locally derived water flow from the mountains on the western and eastern sides of the valley towards the center of the valley and the Salton Sea. The limits of water derived from local sources for the shallow and deep water-bearing units are shown in Figures 2.23 and 2.24, respectively. In the deeper water-bearing strata interruptions in the general pattern are implied with radial flow towards geothermal areas since geothermal recharge is assumed from the deeper aquifer (Fig. 2.24) (Dutcher, et al., 1972) and from percolation down fault zones.

Water entering the valley's ground water system eventually flows into the Salton Sea, is transpired or evaporated on its way there, or percolates downward to deeper strata.

Direction of Flow in Upper Water-Bearing Strata--Groundwater flow patterns in the upper aquifer are described by the water level contours in Figure 2.23 and on Plate 2.1. The ground water level contours for 1962 and 1964 shown in Figure 2.23 and those for 1965 shown in Plate 2.1 generally agree very well with each other, but Figure 2.23 covers a somewhat larger area and shows slightly more detail and will therefore be referred to in the following discussion.

Flow occurs in a direction perpendicular to the ground water level contours at a rate proportional to the steepness of the hydraulic gradient and permeability; assuming homogenous isotropic media and in conjunction with topographic relief, the

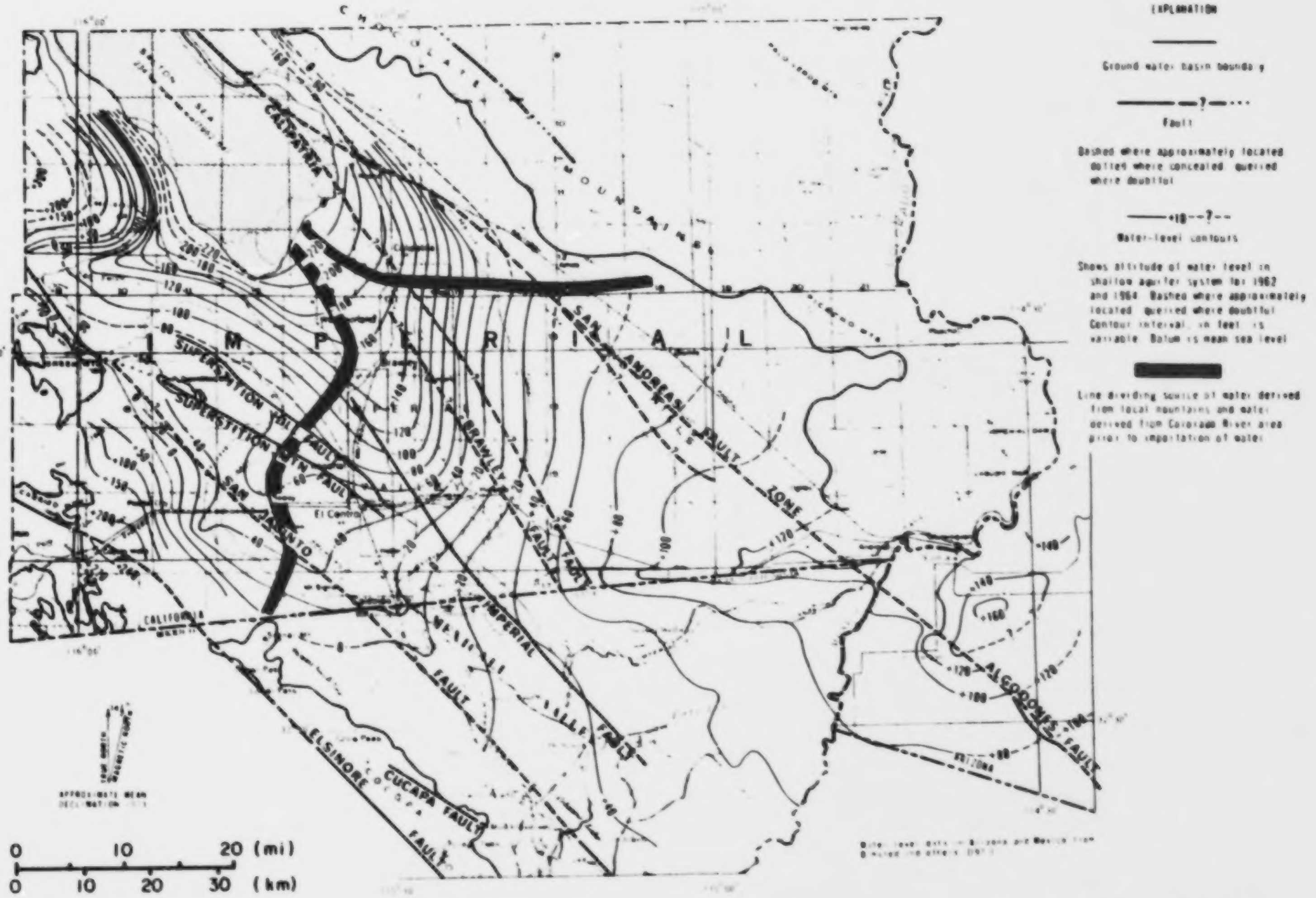
EXPLANATION
Ground water basin boundary
Fault
Dashed where approximately located dotted where concealed queried where doubtful
—+10--?--
Water-level contours
Shows altitude of water level in shallow aquifer system for 1962 and 1964 Dashed where approximately located queried where doubtful Contour interval, in feet, is variable Datum is mean sea level
Line dividing source of water derived from local mountains and water derived from Colorado River area prior to importation of water
IMPERIAL
CALIPATRIA
SAN ANDREAS FAULT ZONE
BRAWLEY FAULT
SUPERSTITION HILLS FAULT
SUPERSTITION MTN FAULT
SAN JACINTO
IMPERIAL
FAULT
ELSINORE FAULT
CUCAPA FAULT
ALGODONES FAULT
CALIFORNIA
El Centro
0 10 20 (mi)
0 10 20 30 (km)
APPROXIMATE MEAN DECLINATION

Figure 2.23 Ground water level contours of shallow aquifer system, 1962 and 1964, in Imperial and Mexicali Valleys (Dutcher, et al.,1972)

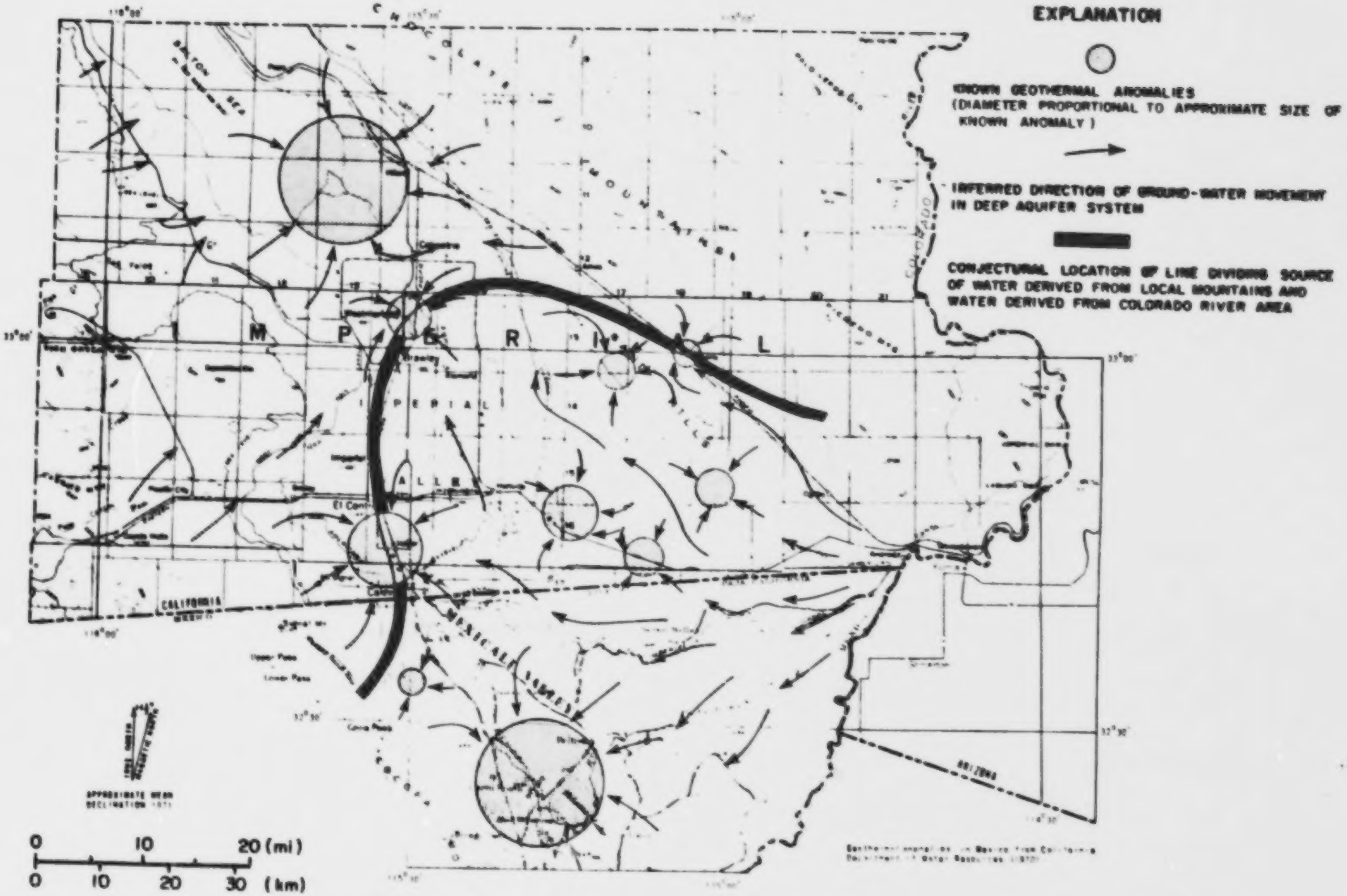
EXPLANATION
KNOWN GEOTHERMAL ANOMALIES (DIAMETER PROPORTIONAL TO APPROXIMATE SIZE OF KNOWN ANOMALY)
INFERRED DIRECTION OF GROUND-WATER MOVEMENT IN DEEP AQUIFER SYSTEM
CONJECTURAL LOCATION OF LINE DIVIDING SOURCE OF WATER DERIVED FROM LOCAL MOUNTAINS AND WATER DERIVED FROM COLORADO RIVER AREA
I M P E R I A L
IMPERIAL VALLEY
MEXICALI VALLEY
SALTON SEA
CHOCOLATE MOUNTAINS
COLORADO
CALIFORNIA
El Centro
APPROXIMATE MEAN DECLINATION 1971
0 10 20 (mi)
0 10 20 30 (km)

Figure 2.24 Inferred direction of movement in the deep water-bearing strata to generalized areas of known geothermal anomalies in Imperial and Mexicali Valleys. (Dutcher, et al.,1972)

hydraulic gradient can give an indication of aquifer properties. In areas of low relief, steep hydraulic gradients may indicate a low permeability aquifer (or higher velocity flow rate), while a low hydraulic gradient may indicate a more permeable aquifer (or a lower velocity flow rate). This trend can be generally seen by referring to the ground water level contours in the southeast corner of Imperial Valley and comparing them to the contours in the north-central part of the valley. The contours in the southeast are spaced further apart than those in the north central part, indicating that the sediments in the north-central part may be less permeable than those in the southeastern part. Lithologic evidence shows that the sediments of Imperial Valley are, in fact, coarsest near the crest of the Colorado River Delta in the southeastern part of the valley and finer towards the center of the valley (Merriam and Bandy, 1965). Since coarse sediments are generally more permeable than finer sediments, this lithologic evidence corroborates the water level contour implication. The water level contour implication is further supported by pump tests resulting in the highest measured permeabilities in the southeastern part of the valley and low yields in the central valley (Loeltz, et al., 1975, p. 15).

From the Yuma area, ground water flows westward. Before irrigation began, the ground water divide between waters flowing to the Salton Sea and waters flowing to the Gulf of California was apparently around the axis of the Colorado River Delta. This axis runs from the Yuma-Pilot Knob area southwest, about midway between the international boundary and the present course of the Colorado River. Ground water south of the axis flowed towards the Gulf of California and that to the north of the axis flowed towards the Salton Sea. After the influence of irrigation the ground water divide appears to have migrated northward to the All-American Canal. This is apparent from the ground water level contours on Figure 2.23, which indicates most of the ground water in the shallow aquifer south of the All-American Canal will flow towards the Gulf of California, and water north of the canal will flow towards the Salton Sea. Some of the shallow aquifer water will also flow southwest and then northwest west of the mapped trace of the Imperial Fault.

It can also be seen that the hydraulic gradient increases towards the center of the valley from essentially zero near the apex of the Colorado River Delta between Yuma and Pilot Knob to about 3.4 m per km (18 ft per mi) in the east central portion of the valley, then down to about 1.1 m per km (6 ft per mi) just south of the Salton Sea.

In the southwestern part of the valley all the ground water is derived from local sources and flows towards the northeast (Fig. 2.23). The highest water elevation in the southwestern part of the valley is 85 m (280 ft) above sea level near the base of the Peninsular Range.

The highest groundwater elevation contour on the map appears in the Santa Rosa Mountains in the northwestern portion of the valley and is 91 m (300 ft) above sea level. From this high, water flows east or south and then east. This part of the map also shows the steepest hydraulic gradients of 11 to 4.5 m per km (60 to 24 ft per mi).

Evidence of groundwater barrier effects in the shallow water-bearing strata are apparent only on the Algodones and perhaps Elsinore Faults (Fig. 2.23). The section of the Elsinore Fault in the southwestern portion of the valley shows about a 12 m (40 ft) elevation difference across the fault. On the west side of the fault the groundwater level elevation is about 70 m (240 ft) and there are locally derived very low salinity waters, while east of the fault the groundwater level elevation is about 60 m (200 ft) and the water is markedly more saline. The Algodones Fault section in the southwest of Yuma shows groundwater level elevation differences of about 6 m (20 ft) across the fault.

Direction of Flow in the Deeper Water-Bearing Strata--Insufficient data is available to construct a piezometric surface map for the deeper water-bearing strata. Therefore, the direction of flow is inferred from a conceptual model of the groundwater system and its relation to the geothermal convection cells (Fig. 2.31) (see "Groundwater Model of Imperial Valley Geothermal Systems" below).

The trend of the flow direction in the deeper water-bearing strata is similar to that in the shallower strata. That is, north of the international boundary, groundwater generally flows towards the Salton Sea from the Colorado River and from the mountains on the eastern and western margins of the valley (Fig. 2.24). In the Mexicali Valley, south of the international boundary, deeper groundwater flows towards the Cerro Prieto geothermal field. The difference in flow patterns between the shallow and deep strata appears in the larger area recharged from local meteoric water and in the suggested flow patterns around the geothermal anomalies in the deep strata (Fig. 2.24). Ground water flow in deeper water-bearing strata is thought to be radial inward toward each of the geothermal fields. The larger the field, the more area this radial flow pattern will affect. Some groundwater in the deeper strata is also thought to flow upwards to shallower depths.

Recharge--

The Colorado River is the most important source of recharge in Imperial Valley (Dutcher, et al., 1972) with minor contributions from local precipitation, runoff and tributary underflow. Only a small part of this recharge reaches the Salton Sea as continuous flow through aquifers, with a large part flowing downward to the deep geothermal convection cells and the remainder evaporated or transpired from the surface.

Colorado River water enters the groundwater system as underflow, canal leakage and irrigation water. In the past, the Colorado River has flowed into the Salton Trough. In these times the river provided water to the Imperial Valley, as it did during the canal breaks from 1904 to 1907, when the present-day Salton Sea was formed by filling of the Salton Trough. When the Colorado River is flowing into the Gulf of California, the two main areas where groundwater enters the valley as underflow are beneath the alluvial section between the Cargo Muchacho Mountains and Pilot Knob, and beneath the Mexicali Valley.

Irrigation recharge to the shallow aquifer started in 1901. More than 174 x 10^3 ha (430,000 acres) are irrigated in Imperial Valley, and leakage from the irrigation canals as well as water applied in excess of crop requirements contributes to the natural recharge. However, much of the excess water applied to crops is intercepted and removed from the groundwater system by the tile drain network underlying the irrigated areas.

Use of the All-American and Coachella Canals significantly increased groundwater recharge. The All-American Canal became the sole conveyance for Colorado River water to the valley in 1942, and in 1948 the Coachella Canal was added to service the lower Coachella Valley. These canals, as well as their many tributary canals throughout the irrigated areas of the valley, supply much recharge. These canals are unlined and flow across much permeable, sandy ground, especially in the eastern part of the valley (see "Recharge by Imported Water," below). The exact rate of canal leakage cannot be determined. Loeltz, et al. (1975) estimated the recharge to East Mesa at about 8.6 x 10^5 ha-m (7 million acre-ft) through 1967. They also estimated that the Coachella Canal contributed about 3.3 x 10^5 ha-m (2.7 million acre-ft) from 1950 through 1967 and the All-American Canal contributed about 5.5 x 10^5 ha-m (4.5 million acre-ft) through 1967. The water imported in this manner is eventually discharged to the tile drains and through natural discharge areas.

Tributary underflow plays a very minor role compared to recharge by imported water. Tributary recharge receives its greatest contribution from the Mexicali Valley and Carrizo and San Felipe Creeks, with much less from Pinto and Coyote Washes. This all totals to less than 2.5 x 10^3 ha-m/yr (20,000 acre-ft/yr).

Precipitation and runoff provide a very minor source of recharge in Imperial Valley. Direct infiltration occurs only on the higher alluvial slopes of the mountains bordering the southwestern part of the valley. Some infiltration along washes and stream beds discharges to the central valley or Salton Sea. The total contribution of recharge due to precipitation and runoff is less than 1.2 x 10^3 ha-m/yr (10,000 acre-ft/yr).

Recharge by Imported Water--The groundwater level contours in Imperial Valley as represented in 1962 and 1964 (Fig. 2.23) or 1965 (Plate 2.1) do not represent a natural groundwater system but rather one showing marked effects of artificial recharge due to irrigation. The recharge due to irrigation originates from the Colorado River and flows throughout the valley in many miles of unlined irrigation canals. Some of the canals are up to 60 m (200 ft) wide, and the groundwater levels beneath them show great rises due to infiltration of water from the canals. The network of canals is dense enough in Imperial Valley to raise the regional water table significantly, as well as the water level just beneath and around the canals. Figure 2.25 shows the change in water levels in East Mesa during the period 1939-60. This figure illustrates the marked water level increases of over 21 m (70 ft) along the Coachella Canal and over 12 m (40 ft) along the All-American Canal since they started operating in 1948 and 1942, respectively. The change in groundwater level elevation has been small along the East Highline Canal (Loeltz, et al., 1975), which runs north-south along the boundary of the lakebed deposits of the main valley area. This contrast in groundwater level change between the East Highline, All-American and Coachella Canals may be due to the tile drain system of the irrigated main valley area directly conducting the leaked, imported water to outlet channels.

The highest groundwater level elevations to the east of Imperial Valley are shown in the groundwater mound under the Yuma Mesa area, south of Yuma. The elevation of this mound was over 49 m (160 ft) in 1962-64. It is interesting to note the contrast between this mound and the groundwater level contours for 1939 in this area (Fig. 2.26) which shows a southerly sloping surface going from 38 m (125 ft) at the Colorado River to about 27 m (90 ft) south of Upper Mesa and east of the Algodones Fault. This mound is a result of a combination of two factors. First, irrigation of citrus groves in this area causes extensive recharge, and second, the recharge area happens to coincide with a subsurface silty aquitard layer that keeps the groundwater table elevated in the form of a mound (Olmsted, pers. comm., 1977).

Evidence of the groundwater barrier effect of the Algodones Fault is apparent from the groundwater level contours of both periods; however, the elevation difference before irrigation commenced was only 1.5 to 3 m (5 to 10 ft), while it rose to about 6 m (20 ft) by 1964.

The rising groundwater levels in Imperial Valley have lowered the hydraulic gradient westward from the Colorado River (Olmsted, et al., 1973, p. H84). This effect can be seen by comparing average water level contours in 1939 for the Colorado River Delta region (Fig. 2.26) with the 1962 and 1964 water level contours for Imperial Valley (Fig. 2.23). For example,

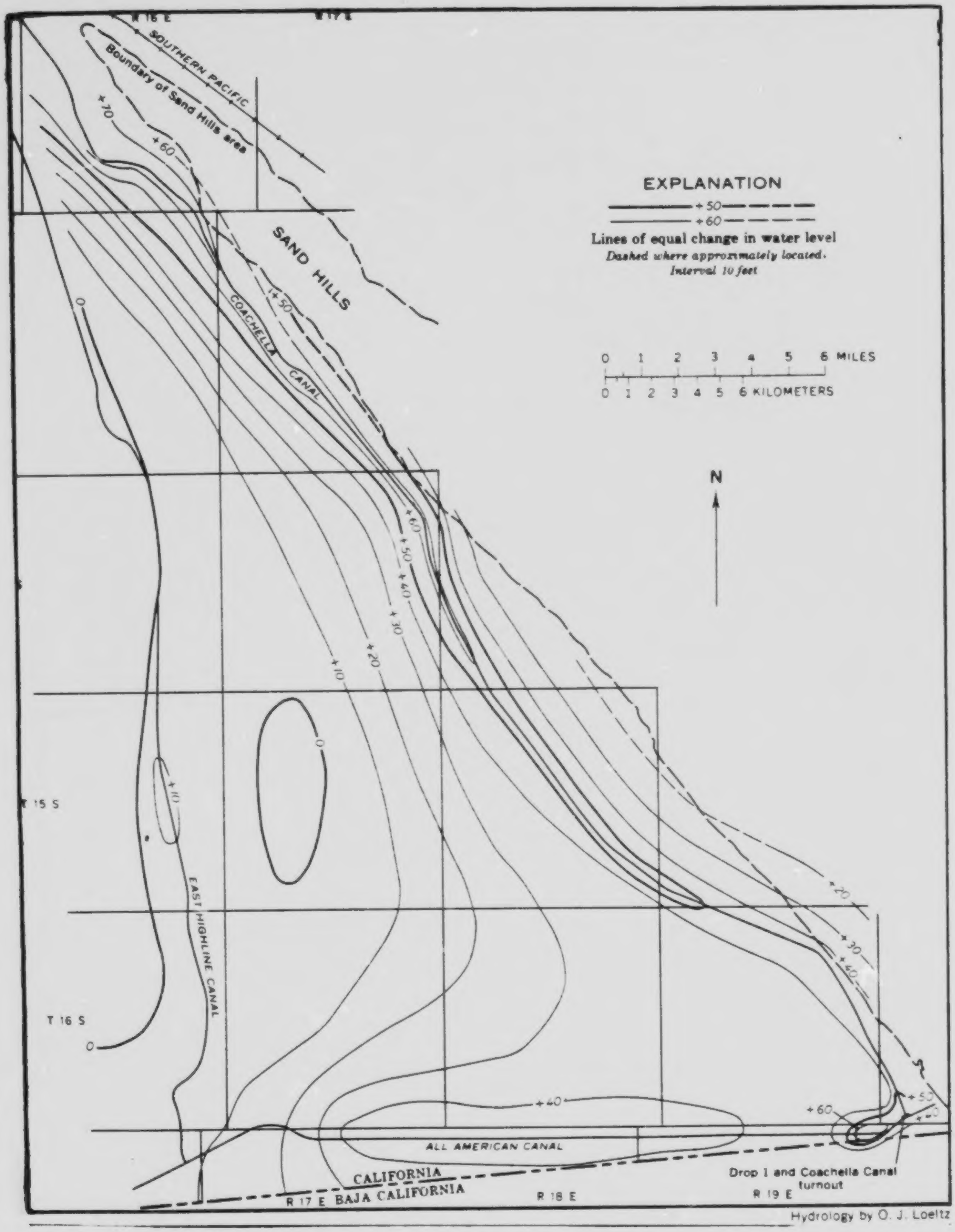
R 16 E
R 17 E
SOUTHERN PACIFIC
Boundary of Sand Hills area
SAND HILLS
COACHELLA CANAL
EAST HIGHLINE CANAL
ALL AMERICAN CANAL
CALIFORNIA
BAJA CALIFORNIA
R 17 E
R 18 E
R 19 E
T 15 S
T 16 S
Drop 1 and Coachella Canal turnout
+70
+60
+50
+40
+30
+20
+10
0
EXPLANATION
+50
+60
Lines of equal change in water level
Dashed where approximately located.
Interval 10 feet
0 1 2 3 4 5 6 MILES
0 1 2 3 4 5 6 KILOMETERS
N
Hydrology by O. J. Loeltz

Figure 2.25 Change in groundwater levels in East Mesa, 1939-60. (Loeltz, et al.,1975)

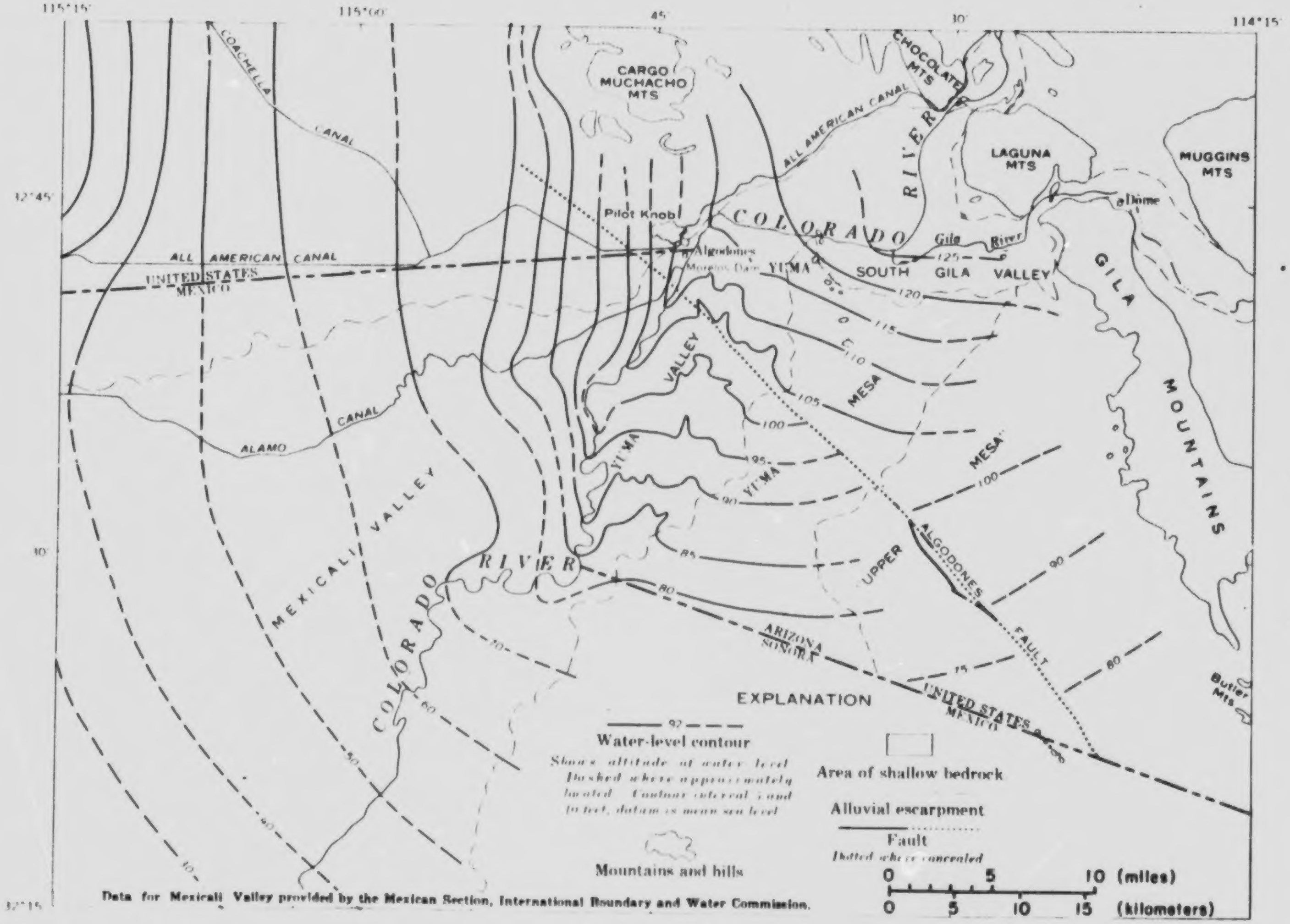
115°15'
115°00'
45'
30'
114°15'
32°45'
30'
32°15'
COACHELLA CANAL
CARGO MUCHACHO MTS
CHOCOLATE MTS
ALL AMERICAN CANAL
LAGUNA MTS
MUGGINS MTS
Dome
Pilot Knob
Algodones
Morelos Dam
COLORADO RIVER
YUMA
Gila River
SOUTH GILA VALLEY
GILA MOUNTAINS
UNITED STATES
MEXICO
ALAMO CANAL
YUMA VALLEY
YUMA MESA
MEXICALI VALLEY
UPPER MESA
ALGODONES FAULT
ARIZONA
SONORA
Butler Mts
125
120
115
110
105
100
95
90
85
80
75
70
60
50
40
10
EXPLANATION
92
Water-level contour
Shows altitude of water level. Dashed where approximately located. Contour interval 5 and 10 feet, datum is mean sea level
Mountains and hills
Area of shallow bedrock
Alluvial escarpment
Fault
Dotted where concealed
0 5 10 (miles)
0 5 10 15 (kilometers)

Data for Mexicali Valley provided by the Mexican Section, International Boundary and Water Commission.

Figure 2.26 Average groundwater level contours in 1939 in the Colorado River Delta region. (Olmsted, et al.,1973)

the hydraulic gradient in 1939 from the Colorado River near Yuma westward to the north facing apex of the 130° bend in the All-American Canal, between Pilot Knob and the Coachella Canal, was about 0.59 m per km (3.1 ft per mi). The hydraulic gradient for the same area using the 1962 and 1964 data is essentially zero. The gradient in an area midway between the All-American and Coachella Canals, an area that would be somewhat less influenced by the rising water table directly under a canal, was about 0.51 m per km (2.7 ft per mile) for 1939 and about 0.28 m per km (1.5 ft per mile) for 1962 and 1964.

Lowering of the hydraulic gradient in this manner reduces the velocity and amount of underflow from the Colorado River into Imperial Valley. At the same time the groundwater supply and water table elevations are being increased through addition of irrigation waters at the surface. So in essence the natural system of groundwater recharge for the shallow aquifer is being drastically altered by the man-induced effects of the irrigation system. It is transferring the recharge paths from Colorado River underflow to infiltration from the surface downward and then north and westward. Suggestions of this change in recharge source areas can also be seen by comparing the groundwater level contours for 1939 (Fig. 2.26) with those for 1962 and 1964 (Fig. 2.23). In 1939 the V-shaped contours around the Colorado River are much more pronounced than those on the later map. These downstream pointing V's represent a high elevation groundwater front. In the later map the V-shape contours have formed around the All-American Canal, and to some extent the Coachella Canal, indicating that the high fronts have migrated from the Colorado River to the irrigation canals.

Groundwater Discharge--

Although much Imperial Valley groundwater discharges into the Salton Sea, all water that actually leaves the Salton Sea Drainage Basin must leave through evaporation or evapotranspiration. (These processes are discussed in Section 2.1.3 and the subsection "Outflow" in Section 2.4.3 below).

Groundwater discharge to the Salton Sea occurs mainly through an extensive tile drain system which lies several feet below the surface of the irrigated areas. This network discharges about 1.2 x 10^5 ha-m/yr (1 million acre-ft/yr) of groundwater and surface waste-water into the Salton Sea. Some of the discharge from the drains has moved upward from deeper aquifers, especially near the east edge of the irrigated area.

A similar mechanism occurs under the New and Alamo Rivers near the Salton Sea. The groundwater level contours approaching the elevation of the topographic contours on Plate 2.1 indicate an upward flow of groundwater here. This upward leakage from the shallow aquifer averages a few thousand ha-m/yr (few tens of thousands of acre-ft/yr).

Minor discharge is provided from springs, seeps and wells. Many springs and seeps are found to the northeast of the Salton Sea, paralleling the San Andreas Fault Zone. A few, with smaller flows, are found southwest of the Salton Sea. Some are found downstream from the Coachella Canal and are fed by water from the canal. The total discharge from springs and seeps, not counting that due to seepage from the Coachella Canal, is estimated to be only a few hundred ha-m/yr (few thousand acre-ft/yr).

Origin of Groundwater--The quantity of groundwater derived from the Colorado River is much greater than the quantity derived from local sources for all areas and depth zones in Imperial Valley except West Mesa (Dutcher, et al., 1972). Lines dividing the source of water derived from local mountains and those derived from the Colorado River are shown in Figures 2.23 and 2.24 for the shallow and deeper water-bearing strata, respectively. Comparison of these lines shows a larger area of local recharge for the deeper aquifer. However, the quantity of recharge from local sources into the deep water-bearing strata under the Sand Hills, East Mesa and main valley areas is still much less than the quantity derived from the Colorado River.

Dutcher, et al. (1972) have estimated the percentage of recharge by local precipitation and Colorado River water for their four depth zones and four areal subunits (Table 2.4). They estimate 38% of total groundwater in Imperial Valley is from local sources and 62% is from the Colorado River. Nineteen percent of the total groundwater in storage in Imperial Valley underlies West Mesa. All of this water is derived from local meteoric sources. The Sand Hills area contains 17% of the total groundwater in storage in the valley and 13% of this is locally derived. For the East Mesa area, which contains 25% of the total groundwater in storage, only 6% is of local origin. In the main valley area, with 38% of the total water in storage, 39% is from local sources.

In the Sand Hills area, the percentage of locally derived groundwater varies with depth, between 11% and 15% down to about 2,400 m (8,000 ft). Essentially no recoverable groundwater occurs below 2,400 m (8,000 ft) in the Sand Hills area. For the East Mesa area, 5% to 7% of groundwater is from local sources to depths of about 2,400 m (8,000 ft). But, below 2,400 m (8,000 ft) there is no contribution from local sources. In the main valley area the percentage of locally derived groundwater goes from 41% to 31% from depth zone 2 down to the basement complex.

Geothermal fluid in most hot water and vapor-dominated systems is derived from meteoric water (Craig, et al., 1956; Craig, 1963; Craig, 1966). Isotopic evidence shows that this is probably the case for Salton Sea geothermal fluid (Craig, 1966). However, south central Imperial Valley and central Mexicali Valley geothermal fluids are derived from Colorado River water

TABLE 2.4 SUMMARY OF "USABLE" AND RECOVERABLE WATER IN STORAGE DERIVED FROM THE COLORADO RIVER AND LOCAL SOURCES

[Estimates in millions of acre-feet]

Vertical depth zone	Storage in areal subunits				Total	Percentage in each depth zone
	Sand Hills	East Mesa	Main valley	West Mesa		
Zone 1:						31
Local	16	6	0	119	141	
Colorado River	110	97	0	.9	208	
Zone 2:						32
Local	2.6	4.7	75	63	145	
Colorado River	25	84	106	0	215	
Zone 3:						28
Local	5.3	4.8	68	29	107	
Colorado River	32	63	102	0	197	
Zone 4:						9
Local	0	0	24	2.4	26	
Colorado River	.1	19	53	0	72	
Totals:	191	279	428	214	1,112	—
Local	24	16	167	213	420	38
Colorado River	167	263	261	0.9	692	62
Percentage of total:						
Local	13	6	39	100	38	
Colorado River	87	94	61	0	62	

Note:

1. Usable water defined as having less than 35,000 mg/l TDS.
2. Basis for estimating local sources not explained in original reference.

(Coplen, 1972). Specifically, the geothermal fluids of the Dunes and East Mesa anomalies (Coplen, et al., 1973) as well as the Heber anomaly (Coplen, 1976) have been shown to originate from the Colorado River.

Major studies of groundwater origin in Imperial Valley have utilized isotope analyses. In order to determine the origin of the subsurface water by isotope analysis, it is necessary to isotopically characterize all of the possible sources and then compare these with spring water, well water and geothermal fluid samples. For Imperial Valley five possible sources are recognized (Coplen, 1972). They are local meteoric water, ancient or recent Colorado River water, ancestral sea water from the Gulf of California, water derived from snow melt in the mountains to the west and north of Imperial Valley and juvenile water. Juvenile water does not appear to be necessary to satisfy observed chemical and isotopic relations in geothermal waters (White, 1968 and 1970; Craig, 1966) and is not considered further as a source for Imperial Valley geothermal waters. There is also no evidence of ocean water in the groundwater or geothermal systems in Imperial Valley (Coplen, 1972). Comparison of well waters and geothermal waters with the remaining sample source waters shows different origins for groundwater in different parts of Imperial Valley. Coplen (1972) concluded that local precipitation plays an insignificant part in central southern Imperial Valley groundwater system, but much water from the hot springs to the south and east of the Salton Sea is derived from local precipitation. Coplen (1972) further states that the observed decrease in δO^{18} ratios with depth may indicate downward seepage of partially evaporated Colorado River water from a large lake in recent times; that groundwater in the south-central part of the valley, the major groundwater reservoir, is derived from the Colorado River; and the salt in the Salton Sea water is also derived from the Colorado River. This last conclusion can be reconciled with the Hely, et al. (1966) statement that the salinity of Salton Sea water is a result of solution of evaporite deposits on the floor of the Salton Sink, if we consider the evaporite deposits formed by evaporation of Colorado River water.

Permeability--

A number of pump tests were conducted, and permeability data is available for the upper 300 m (1,000 ft) of sediments in Imperial Valley. Pump test sites are shown in Fig. 2.10, and pump test data is presented in Table 2.5.

The results of these pump tests show a moderate to high yield in the eastern and western parts of the valley in locations where wells penetrate from less than one hundred to a few hundred meters of Colorado River or marginal alluvial deposits. These wells commonly have transmissivities of several million liters per day per meter with specific capacity of up to 620

TABLE 2.5 RESULTS OF USGS PUMPING TESTS IN IMPERIAL VALLEY, CALIFORNIA (Loeltz, et al., 1975)

Well (fig 2.20)	Owner or name	Date of test	Type of test[1]	Interval tested (ft below land surface)	Yield (gpm)	Draw-down (ft)	Specific capacity in gpm per foot of drawdown	Transmissivity computed from tests (gpd per ft)[2]	Conformance of test data to theoretical values	Reliability of computed transmissivity[3]	Indicated average field hydraulic conductivity (gpd per sq ft)[4]
Western Imperial Valley											
12S/ 9E-22A2	T. M. Jacobs	7-29-63	R	286- 667	1,450	14	100	290,000	Excellent	Good	780
13S/11E-18J1	LCRP 19	8-20-64	R	310- 650	150	4	38	100,000	Fair	Fair	300
18J2	LCRP 19A	8-20-64	R	35- 55	45	8.5	5	37,000	do	do	1,800
14S/11E-32R	LCRP 8	8-11-62	R	136- 165 218- 258 310- 354 380- 416 430- 560	250	13	19	130,000	Good	Good	480
Central Imperial Valley											
15S/14E-18C	Imperial Irrigation District.	8-9-58	R	140- 440	180	86	2	2,200	Good	Good	7
17S/15E-10N	do	8-18-58	R	110- 450	90	68	1.3	1,700	do	do	5
Eastern Imperial Valley											
15S/16E-9A	Southern Pacific Co.	7-9-63	R	150-1,000	975	43	23	62,000	Excellent	Good	73
		7-9-63	D	150-1,000	675	27	25	47,000	Good	do	55
16S/18E-15M	LCRP 11	8-10-63	R	309- 894	1,000	20	50	220,000	do	do	380
		8-10-63	D	309- 894	1,000	20	50	220,000	Excellent	do	380
16S/18E-32R	LCRP 18	6-29-64	R	140- 630	900	21	43	140,000	do	do	240
16S/19E-11D	LCRP 12	8-14-63	R	300- 610	990	24	41	240,000	Good	do	770
16S/20E-31K	LCRP 6	8-2-62	R	340- 410 510- 520	1,035	12	85	850,000	Excellent	do	10,000
		8-2-62	D	340- 410 510- 520	1,035	12	85	880,000	Good	do	10,000
16S/21E-16B	R. G. Winder	12-4-62	R	598- 806	1,550	38	43	[5] 630,000	Poor	Poor	3,000
		12-4-62	D	598- 806	1,550	38	43	[5] 580,000	do	do	2,800

1. Type of test; D:drawdown, R:recovery
   All wells completed in Quaternary alluvium. LCRP, Lower Colorado River Project of the USGS

2. Most values significant to only one figure

3.

Reliability	Difference between computed transmissivity and considered true transmissivity
good	<25%
fair	25% to 50%
poor	>50%

4. Indicated average field hydraulic conductivity=Test Interval

5. May be too high by a factor of 2

lpm/m (50 gpm/ft) of drawdown in favorable areas.

The central part of the valley has low yields and transmissivity. These range from about 12,000 to 120,000 lpd/m (1,000 to 10,000 gpd/ft) down to depths of 150 m (500 ft). Lower transmissivities at lower depths are suggested by the geology and generally decreasing porosity with depth (see following subsection,"Porosity").

The very permeable Colorado River deposits in the southeast corner of the valley have extremely high yields and transmissivities. Well LCRP 6 (Fig. 2.10) has a yield of over 3,800 lpm (1,000 gpm) and a transmissivity well over 10,000,000 lpd/m (800,000 gpd/ft). Yields in this area are comparable to those of wells in the Yuma and Mexicali Valleys. It is not known how far eastward this zone of high transmissivity extends, but traces of former Colorado River channels indicate it may go for several miles. From this area the transmissivity decreases to the northwest, although the yields still remain high. For example, wells LCRP 11, 12 and 18 (Fig. 2.10) have yields up to 3,800 lpm (1,000 gpm) and their transmissivities range from 1.7 to 3.5 million lpd/m (140,000 to 240,000 gpd/ft).

One well in the West Mesa area, LCRP 8 (Fig. 2.10), has a yield of 950 lpm (250 gpm) and a transmissivity of 1,600,000 lpd/m (130,000 gpd/ft). Two wells in the central part of the valley have yields of 340 to 600 lpm (90 and 160 gpm) with transmissivities of 21,000 and 28,000 lpd/m (1,700 and 2,200 gpd/ft).

Imperial Valley geothermal reservoirs show mostly intergranular type permeability, except the Salton Sea field, where fracture permeability is also present. However, fracture permeability may also be encountered at as yet undrilled deeper levels of the other geothermal fields in the valley. Pressure buildup and drawdown analyses from the geothermal wells in the valley give effective permeability values of the order of up to a few liters per day per square meter (a few millidarcies to a few hundred millidarcies).Figure 2.27 shows the correlation between horizontal and vertical permeabilities measured on core samples from the East Mesa geothermal field. This plot shows a variable relation between the horizontal and vertical permeabilities, ranging from 5:1 at low permeabilities to less than 1:1 at higher permeabilities. Correlations such as this, and that shown in Figure 2.30 between porosity and permeability, are not accurate because of the difficulty in obtaining reliable core samples for such measurement; however, these correlations do reflect general trends.

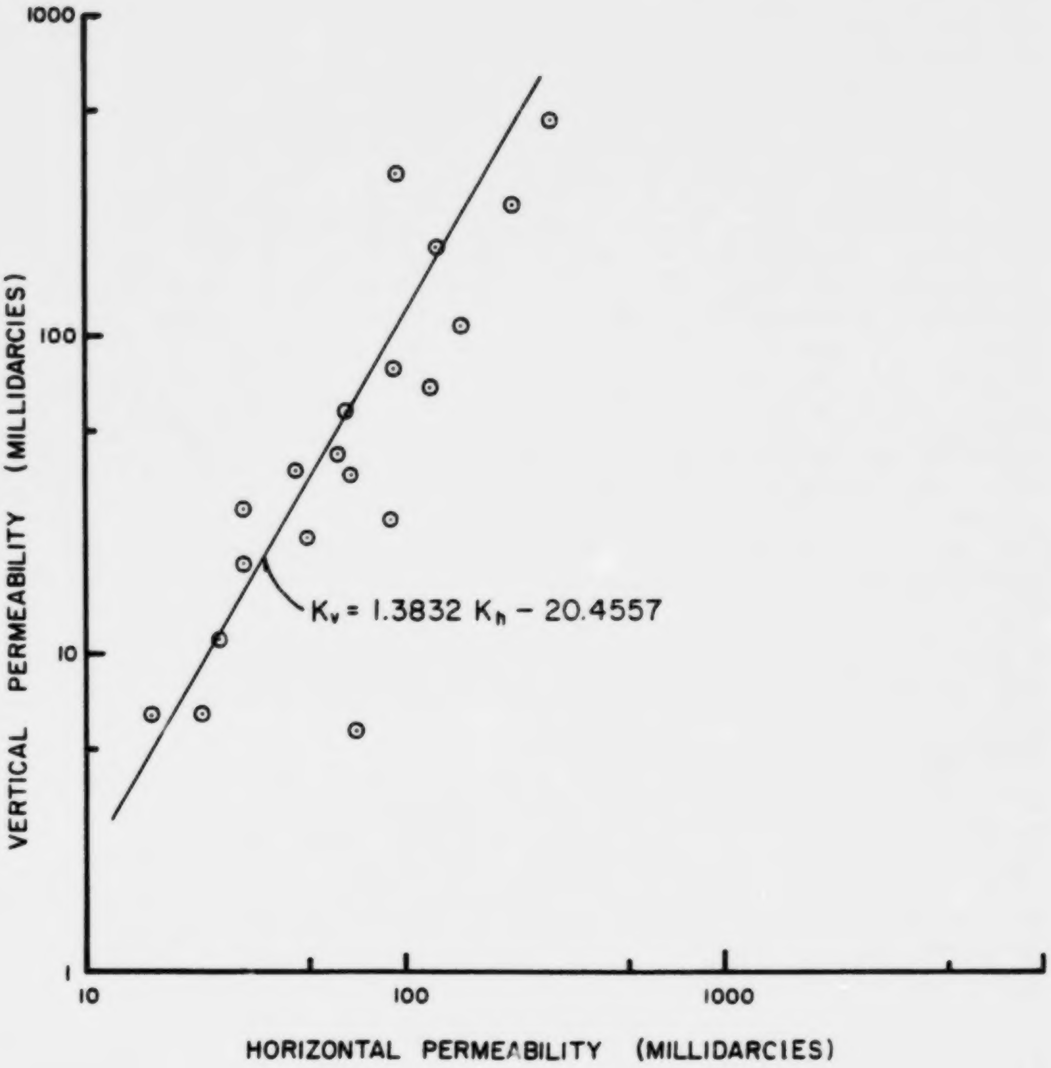

Figure 2.27 Correlation between horizontal and vertical permeabilities, East Mesa KGRA, Imperial Valley, California.

Porosity--

Plots of porosity versus depth determined from well logs from the Imperial Valley are shown in Figures 2.28 and 2.29. The locations of these wells are shown in Figure 2.10. All of these plots reflect the alternating shale and sandstone layers of the valley through the step-like increase and decrease of porosity with depth. Superimposed on these small scale step-like increases and decreases, three of the plots show a distinct trend of decrease in porosity with depth. This trend is especially well illustrated by Wilson No. 1 well plot (Fig. 2.29). The well is located in the central part of the valley, and the porosity decreases from about 60% at 600 m (2,000 ft) depth to less than 20% at 2,100 m (7,000 ft) depth. The trend is somewhat more gradual for American Petrofina well 27-1 (Fig. 2.28), in the East Mesa area, which generally goes from about 50% porosity at 600 m (2,000 ft) to about 15% at 3,000 m (10,000 ft). The composite log from the Salton Sea geothermal area shows large, somewhat inconsistent variations of porosity with depth (Fig. 2.29). A marked sudden decrease of porosity in these wells around the 900 and 1,200 m (3,000 and 4,000 ft) depth may indicate the location of the geothermal reservoir capping layer. The porosity shown on the plot for the Grupe-Engebretson No. 1 well in the south-central part of the valley is more generalized than the others. The porosity goes from about 35% at 600 m (2,000 ft) to 10% to 20% around 3,700 m (12,000 ft). In general, the porosity present in Imperial Valley reservoirs is of intergranular type. However, in the Salton Sea geothermal reservoir, fracture porosity is present. Fracture porosity may also be present in deeper parts of the other geothermal fields in the valley. Figure 2.30 shows the correlation between the porosity and permeability measured from cores from the East Mesa field.

Recoverable Water in Storage--

Rex (1970, p. 14) estimated 2.0 to 5.9 x 10^8 ha-m (1.6 to 4.8 billion acre-ft) of total water in storage in Imperial Valley. Combs (1971, p. 11) revised this estimate to include only economically exploitable reserves, those between 900 m (3,000 ft) and 3,000 m (10,000 ft) depth. He used a porosity depth function from the American Petrofina Salton Trough Prospect No. 27-1 well to calculate total water in storage in this depth interval at 2.6 x 10^8 ha-m (2.1 billion acre-ft).

A more detailed, although still extremely rough, estimate of 1.4 x 10^8 ha-m (1.1 billion acre-ft) total "usable" and recoverable water in storage was made by Dutcher, et al. (1972). They defined "usable" water as that containing less than 35,000 mg/l TDS regardless of any specific ion concentration. Table 2.4 summarizes the Dutcher, et al. (1972) estimate of "usable" and recoverable water in Imperial Valley. They divided Imperial Valley into four vertical depth zones and four areal units which are defined in the subsection on "Water-Bearing Units" above. As can be seen from Table 2.4, almost 40% of the total water in

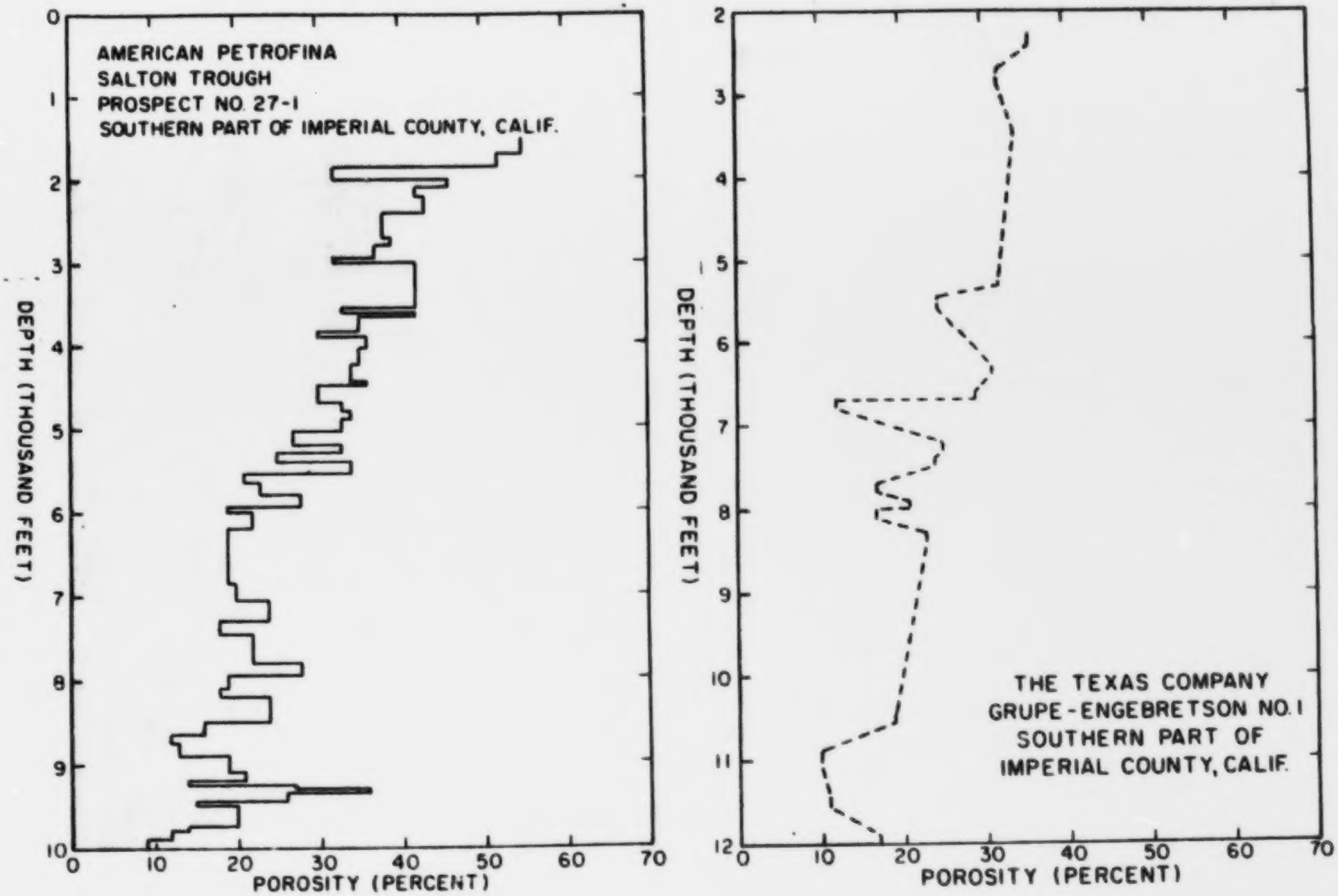

Figure 2.28 Porosity versus depth for two wells in southeast Imperial Valley. (Combs, 1971)

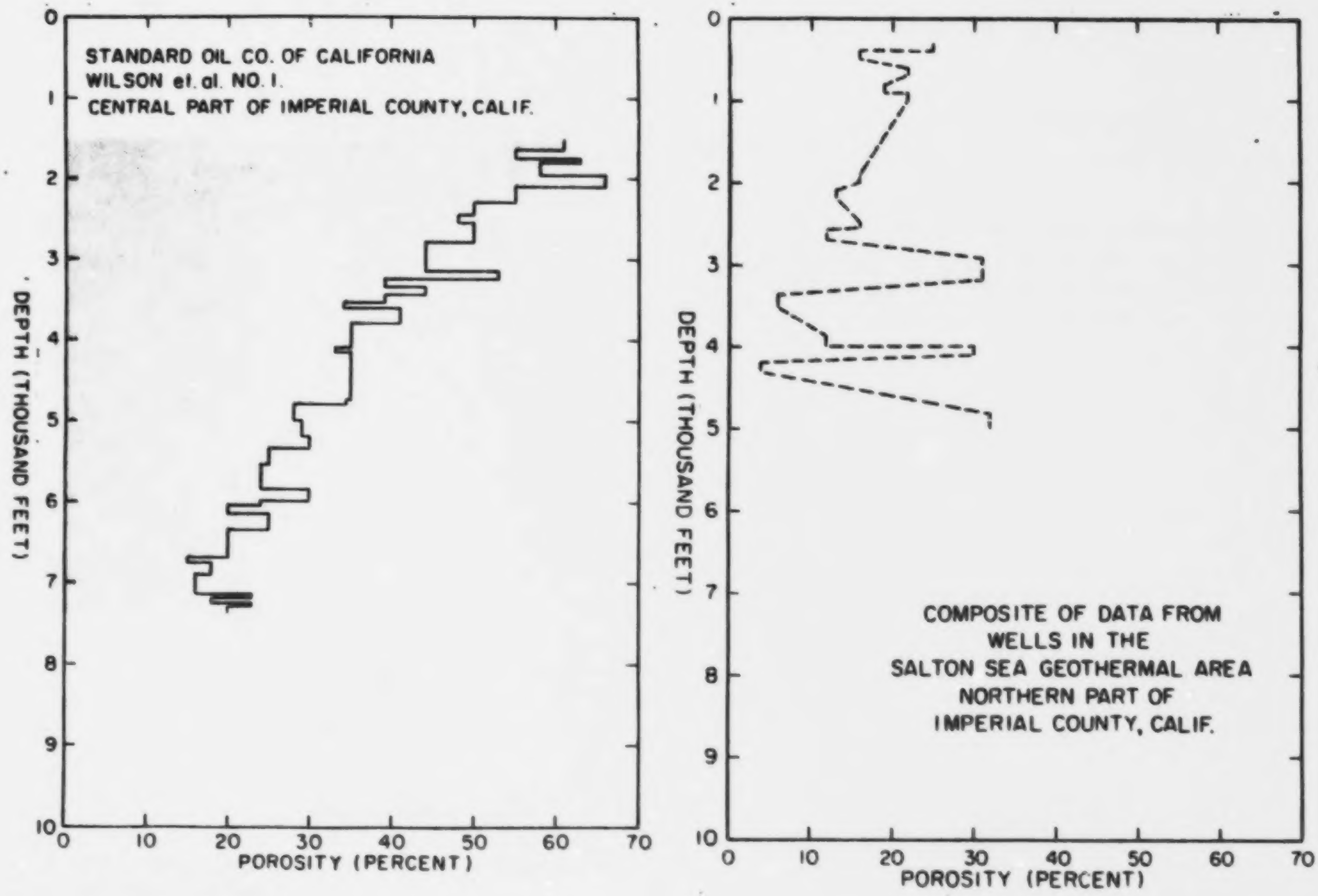

Figure 2.29 Porosity versus depth for two wells in central and northern Imperial Valley. (Combs, 1971)

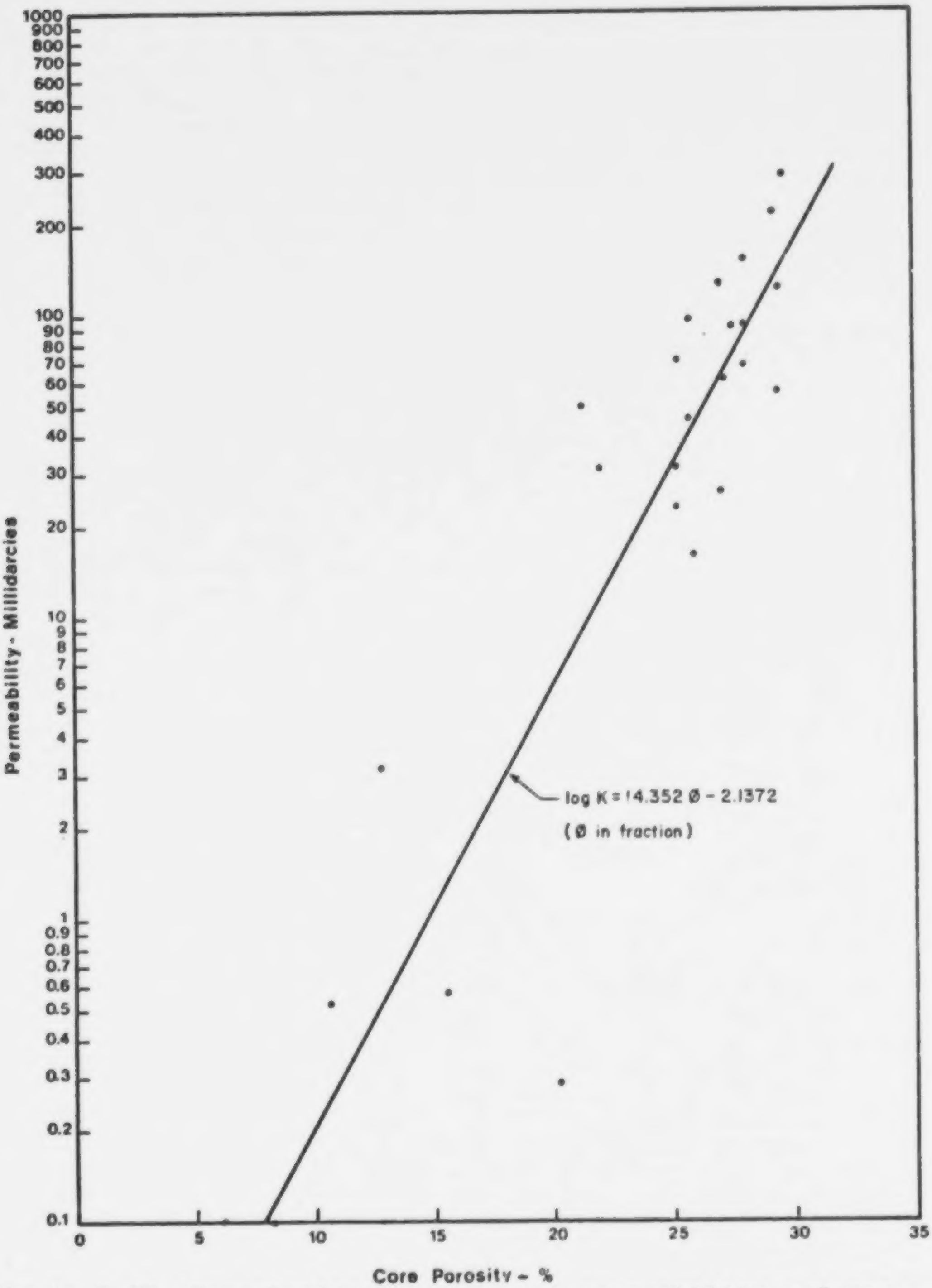

Figure 2.30 Correlation between core permeability and core porosity, East Mesa KGRA, Imperial Valley, California.

storage is contained in the thicker sediments of the main valley area, 25% under the East Mesa area, and less than 20% each in the thinner sedimentary accumulations of the east and west margin areas. Dutcher, et al. (1972) estimate that about 2.5 x 10^7 ha-m (200 million acre-ft) of the total, or about 18%, is at temperatures greater than 150°C (302°F). Of these hot waters 65% of the total is in storage beneath the main valley area. This may be due to the thicker sedimentary accumulations of the main valley area providing better hydraulic communication with deeper waters which have possibly been heated at depths closer to the heat sources. Details of the assumptions, methods and estimates used by Dutcher, et al. (1972) are outlined below.

Dutcher's Water Storage Estimates--Dutcher, et al. (1972) made water in storage estimates for water that would be "usable" and recoverable. The term "usable" water, as defined in the previous paragraph, was based upon the consideration that it is presently uneconomic to utilize water with more than 35,000 mg/l TDS. Also, the lower the TDS the greater proportion of water that can be blended with desalted water. The criteria of recoverability were based on the assumptions that it is possible, using sound engineering practice, to withdraw water from the ground over a long period of time; that the physical state of the fluid and the physical character of the rock are principal factors in recovery; that no water would be available from shallow aquifers in the main valley area due to the tile drain system and that whatever was recovered would only be imported irrigation water. However, no consideration was given to the economic feasibility of recovery.

An estimate of the amount of "usable," recoverable water in storage is computed by multiplying the area of the storage unit by the thickness of the deposit by the specific yield or total porosity of the deposit. All of these values are estimates and approximations based on representative or extrapolated data; hence the product is even less reliable than the individual components.

The total thickness of these water-bearing rocks and deposits was estimated by Rex (1970) who utilized gravity data collected by Biehler (1964) and additional seismic data (Fig. 2.8). Well logs confirm Rex's (1970) interpretation. The distribution of rocks containing more than 35,000 mg/l TDS was plotted and contoured areally and superimposed onto the depth to basement-complex contours resulting in a contoured plot of total thickness of deposits with usable water (Fig. 2.14). Naturally, the thickest deposits are in the center of the valley, and they thin to zero thickness along the east, west and northern margins of the Imperial Valley sedimentary basin. The contours were not evaluated southward into Mexicali Valley. One section south of Holtville has more than 4,600 m (15,000 ft) of sediments containing "usable" and recoverable water in storage, and another section north of Brawley has more than 4,000 m (13,000 ft).

Parameters relevant to the amount and properties of recoverable water in storage in each depth zone are discussed below.

Water in Storage in Each Depth Zone--(Classification and characteristics of the four depth zones are described in the subsection on "Water-Bearing Units," above).

The contour of zero thickness for the deepest zone, zone 4, encloses an area of about 2,600 sq km (1,000 sq mi) (Fig. 2.15) and is up to 2,100 m (7,000 ft) thick. It is estimated to contain 2.3 x 10^8 ha-m (1.9 billion acre-ft) of rock with 5% porosity. It was felt by Dutcher, et al. (1972) that most of the water in this rock would be recoverable since it is hotter than 149°C (300°F). This amounts to about 1.2 x 10^7 ha-m (100 million acre-ft) of recoverable water in zone 4. However, this specific yield estimate may be somewhat high.

Zone 3, above zone 4, has much more water in storage than zone 4 since it is much larger and has higher porosity. The porosity of the rock is about 20%, but due to low permeability only about 16% of the water in storage is estimated to be recoverable. About 2.3 x 10^8 ha-m (1.9 billion acre-ft) of rock are included in the 4,400 sq km (1,700 sq mi) area of this zone (Fig. 2.16). Hence, there should be about 3.7 x 10^7 ha-m (300 million acre-ft) of recoverable water, all at temperatures greater than 100°C (212°F), in zone 3.

The deposits of zone 2 enclose an area of 4,270 sq km (1,650 sq mi) (Figure 2.17), and the estimated volume of rock contained in the zone is 3.5 x 10^8 ha-m (2.8 billion acre-ft). It was estimated that the amount of recoverable water or specific yield of this zone would be about two-thirds of the porosity or 13%. This multiplied by the rock volume gives 4.4 x 10^7 ha-m (360 million acre-ft) of recoverable water in zone 2.

For the shallowest zone, zone 1, water in storage is estimated from the area, depth and specific yield of each of the four areal units. The Sand Hills area has an estimated specific yield of 20% and area of about 1,170 sq km (450 sq mi). The East and West Mesa areas have an estimated specific yield of 15% each and areas of 910 and 1,200 sq km (350 and 465 sq mi), respectively. No water will be recovered from the main valley area since essentially all the ground water in that area is from irrigation input. Dutcher, et al. (1972) compute a total of about 4.3 x 10^7 ha-m (350 million acre-ft) of "usable" and recoverable water in storage in zone 1. This total is comprised of 1.67 x 10^7 ha-m (126 million acre-ft) in the Sand Hills area,

1.28×10^7 ha-m (103 million acre-ft) in the East Mesa area and 1.5 $\times 10^7$ ha-m (120 million acre-ft) in the West Mesa area.

Again, it is important to emphasize that these estimates are based on a conceptual model with very limited estimates and extrapolations. Although the computations and logic may be sound, the approximations used will certainly be altered in the future when more detailed data becomes available. These estimates will only serve as a "best guess" until more reliable computations can be made.

Groundwater Model of Imperial Valley Geothermal Systems--
The relationship between shallow ground water, deep ground water and geothermal water must be known in order to assess environmental effects of geothermal development. This includes knowledge of the mechanisms of recharge and discharge, heat transfer, fluid flow direction and rate, water chemistry, geometry of ground water reservoirs and aquifers, field boundaries and the rate and location of fluid extraction and injection. This knowledge is still being developed, and presently insufficient data is available for detailed definition of the deep and geothermal ground water systems in Imperial Valley. Therefore, it is necessary to utilize a representative model of the geothermal system that is consistent with the data we have observed. Development of this model is traced below from basic characteristics to specific Imperial Valley geothermal fields. In the future, as more data is collected and analyzed, these models will be altered and improved.

A basic model of geothermal systems contains four basic features. They are: a natural heat source, a water supply, a ground water reservoir and a cap rock (Facca, 1973, p. 62). The heat source in most cases would be of magmatic origin, the water supply would have to be sufficient to saturate and replenish the permeable rock or aquifer of the ground water reservoir, and the cap rock would seal the system to continue convective currents in the aquifer or at least trap the water long enough for it to be heated (Fig. 2.31). In this general geothermal convection system model, ground water in the permeable aquifer is heated by conductive heat flow through the bedrock from the magmatic heat source. Since heated water rises, it starts convective currents within the aquifer beneath the capping and confining formation above. This heated water may escape through fractures in the cap rock or through a well piercing the cap rock. Replacement of water in the aquifer may occur through downward percolation, from deeper aquifers through fractures or from more distant parts of the aquifer.

Specific models for Imperial Valley must also consider the fault systems in the valley, the great variation in salt concentration in geothermal brines, two different meteoric water sources, up to 6,000 m (20,000 ft) of sands, silts and clays

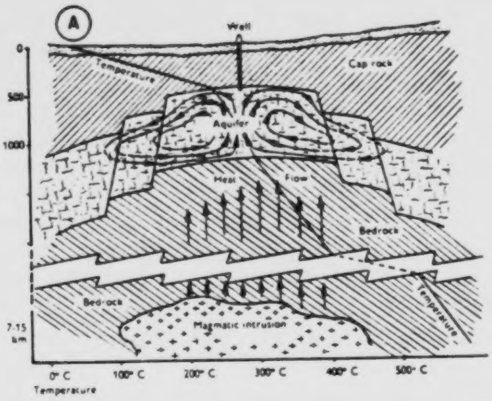
A
Well
Cap rock
Temperature
Aquifer
Heat
Flow
Bedrock
Bedrock
Temperature
Magmatic intrusion
Depth (m)
0
500
1000
7-15 km
0° C
100° C
200° C
300° C
400° C
500° C
Temperature

Figure 2.31 A. Basic model of a geothermal system. (Facca, 1973)

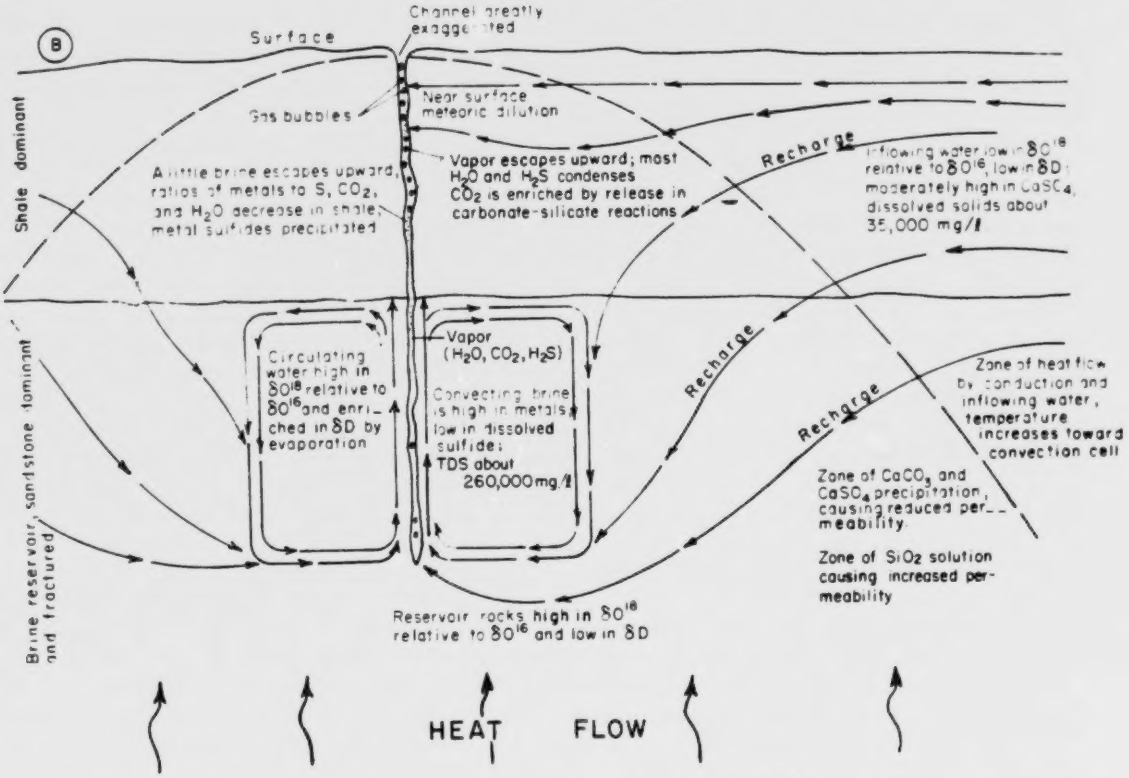
B
Surface
Channel greatly exaggerated
Shale dominant
Gas bubbles
Near surface meteoric dilution
A little brine escapes upward; ratios of metals to S, CO_2, and H_2O decrease in shale; metal sulfides precipitated
Vapor escapes upward; most H_2O and H_2S condenses CO_2 is enriched by release in carbonate-silicate reactions
Recharge
Inflowing water low in δO^{18} relative to δO^{16}, low in δD; moderately high in $CaSO_4$, dissolved solids about 35,000 mg/l
Brine reservoir, sandstone dominant and fractured
Circulating water high in δO^{18} relative to δO^{16} and enriched in δD by evaporation
Vapor (H_2O, CO_2, H_2S)
Convecting brine is high in metals, low in dissolved sulfide; TDS about 260,000 mg/l
Recharge
Recharge
Zone of heat flow by conduction and inflowing water, temperature increases toward convection cell
Zone of $CaCO_3$ and $CaSO_4$ precipitation, causing reduced permeability
Zone of SiO_2 solution causing increased permeability
Reservoir rocks high in δO^{18} relative to δO^{16} and low in δD
HEAT FLOW

Figure 2.31 B. Modified model for Salton Sea geothermal system, showing source of recharge and water quality changes. (Dutcher, et al., 1972)

overlying an igneous and metamorphic basement complex and an apparently random distribution of geothermal anomalies (Rex, 1970). Conceptual models for genesis of Salton Sea geothermal fluids have been proposed by Craig (1966), Berry (1966), Helgeson (1968), White (1968) and Dutcher, et al.,(1972). Craig (1968) proposed that the Salton Sea geothermal brine is formed by local precipitation leaching down through sediments and concentrating in the geothermal convection cell. Berry's (1966) model attributes the concentration of the brines to filtration of Colorado River source water. Helgeson (1968) believes that the Colorado River water had been concentrated by evaporation before the last few hundred meters of sediments were deposited. White (1968) suggests that rock-water interaction between evaporites and ground water produces the hypersaline brines. Recharge to the deep geothermal aquifer is from downward percolation of shallow ground water, and this water circulates in convective heat cells below a shale dominant cap rock. Further concentration is permitted by fluids and gases escaping through fractures to the surface. Dutcher, et al. (1972) basically accept White's (1968) model with slight modifications. They do not require the evaporite deposits for hypersaline brine production (Fig. 2.31B).

The Dutcher, et al. (1972) model (Fig. 2.31B) shows a shale dominant upper layer overlying a sandstone-dominant fractured brine reservoir. The interface between these two layers in Imperial Valley generally appears to be between 600 and 900 m (2,000 and 3,000 ft) (Dutcher, et al., 1972, p. 31; Meidav and Sanyal, 1976; Coplen, 1976, p. 25), although it might be only about 300 m (1,000 ft) at Heber (Meidav, et al., 1975). Recharge is through downward percolation from shallower aquifers above the brine reservoir. This inflowing water has low δO^{18} and δD isotope ratios suggesting that the water has not yet been heated. This model suggests high calcium sulfate and TDS of about 35,000 mg/l for the recharge water of the Salton Sea geothermal field. The downward percolating water is heated, and its temperature increases as it flows towards the convection cell. The reservoir rock this recharge fluid enters is high in δO^{18} and low in δD. This fluid-rock interaction reduces the δO^{18} ratio of the rock, and evaporation increases the δD ratio of the water in the convection cell. The convecting brine becomes concentrated by escape of water, carbon dioxide, hydrogen sulfide and other vapors through fractures in the dominantly sandstone brine reservoir. Most of the water and hydrogen sulfide vapor condenses in the upward escaping-vapor, and carbon dioxide is enriched by release in carbonate-silicate reactions with the surrounding rock. This sublimination enriches the water in δD, and the convecting brine becomes high in metals and low in dissolved sulfide and may attain a maximum TDS content up to 385,000 mg/l. Within and around the convection cell hydrothermal fluids are precipitating calcium carbonate and calcium sulfate, which causes reduced permeability in the reservoir while the same fluid is dissolving silica, causing increased permeability.

Brine that escapes upward reacts with the shale, resulting in lower ratios of metals to sulphur, carbon dioxide and water. Metal sulfides are also precipitated. It is a dynamic system, and all these processes and chemical reactions occur continuously and simultaneously.

Meidav, et al., (1975) proposed a conceptual model of the East Mesa geothermal anomaly which explains the occurrence of high residual gravity anomalies over this field. Similar gravity anomalies have been noted over other geothermal fields in the valley (Fig. 2.32). According to Meidav, et al. (1975) this gravity high may be explained by densification of porous rocks due to precipitation of minerals in the cooler parts of a convecting geothermal system. The top of such a convection system is shown by the sharp decrease in the temperature gradient in wells (Fig. 2.33). In the convection cell, the vertical temperature gradient is very small. In this figure, the static temperature profiles in wells from Salton Sea, Heber, East Mesa and Cerro Prieto geothermal fields are compared. It is interesting to note that the top of the convection zone at Heber appears to be much shallower than that at East Mesa. Also, the Salton Sea and Cerro Prieto wells do not show any sign of the onset of convection within the limits of Figure 2.33. Figure 2.2 shows the temperature gradient anomalies observed over the geothermal fields in Imperial Valley. Geothermal fields in the valley are characterized by gravity, electrical resistivity and temperature gradient anomalies.

Dutcher, et al., (1972) suggest that the difference in brine concentration between the Salton Sea geothermal field and other geothermal fields to the south is due to a lower concentration of salts in the recharge water. That is, the recharge water for the Heber area, for example, may contain 1,500 to 2,000 mg/l TDS. If this is concentrated about ten times by the convection cell, it would result in a brine with about 20,000 mg/l concentration. A similar mechanism for the Salton Sea geothermal field, assuming a recharge with 25,000 to 35,000 mg/l TDS, will result in a brine concentrated to hundreds of thousands of milligrams per liter TDS.

2.4.3 Hydrologic Budget

The hydrologic budget of an area relates the total amount of water entering a drainage basin to water use and the total amount of water leaving the drainage basin. A general hydrologic budget for Imperial Valley is presented below, followed by more detailed discussions of Salton Sea drainage basin inflow and outflow.

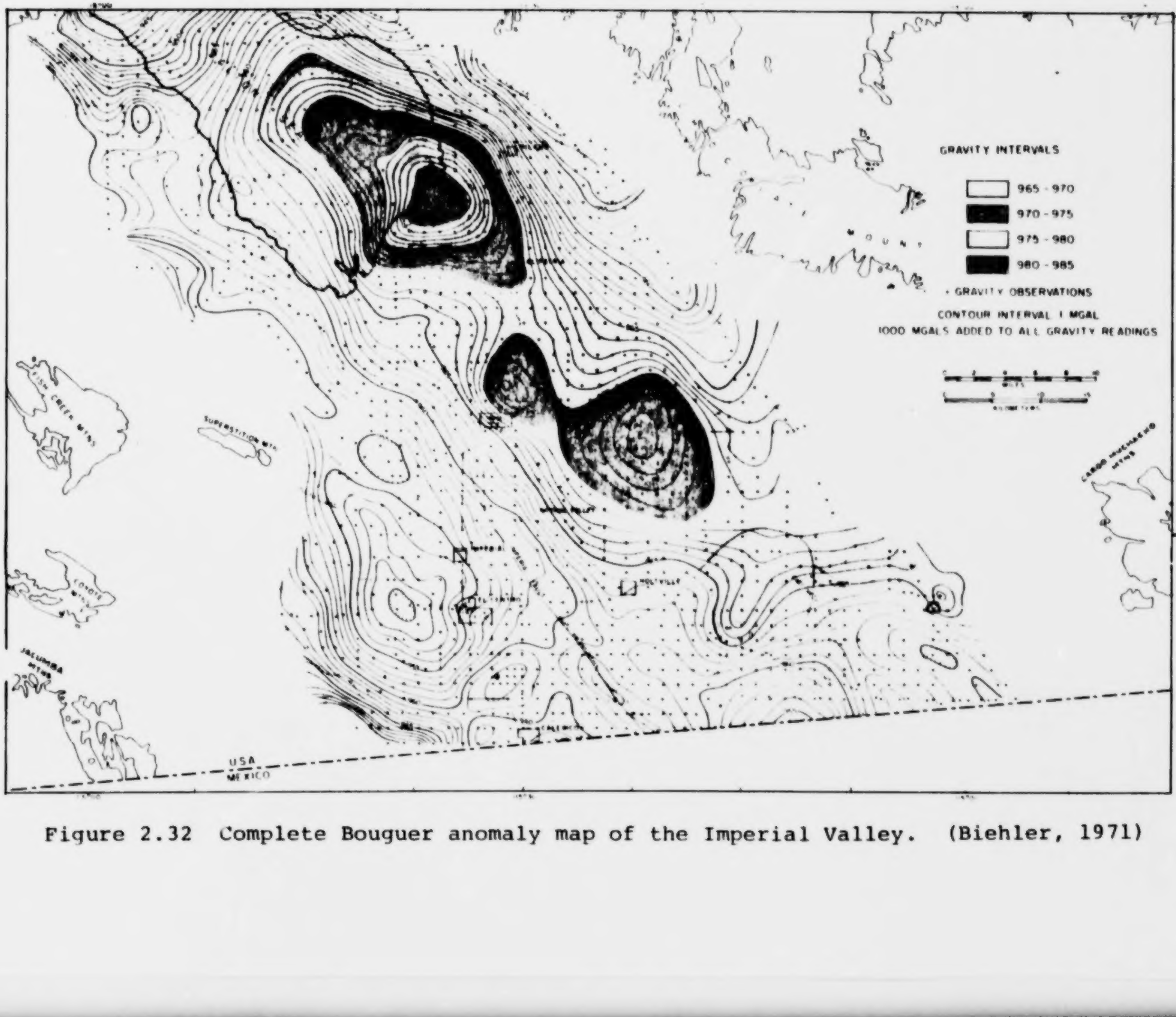
GRAVITY INTERVALS
965 - 970
970 - 975
975 - 980
980 - 985
· GRAVITY OBSERVATIONS
CONTOUR INTERVAL 1 MGAL
1000 MGALS ADDED TO ALL GRAVITY READINGS
FISH CREEK MTNS
SUPERSTITION MTN
COYOTE MTNS
JACUMBA MTNS
CARGO MUCHACHO MTNS
HOLTVILLE
USA
MEXICO

Figure 2.32 Complete Bouguer anomaly map of the Imperial Valley. (Biehler, 1971)

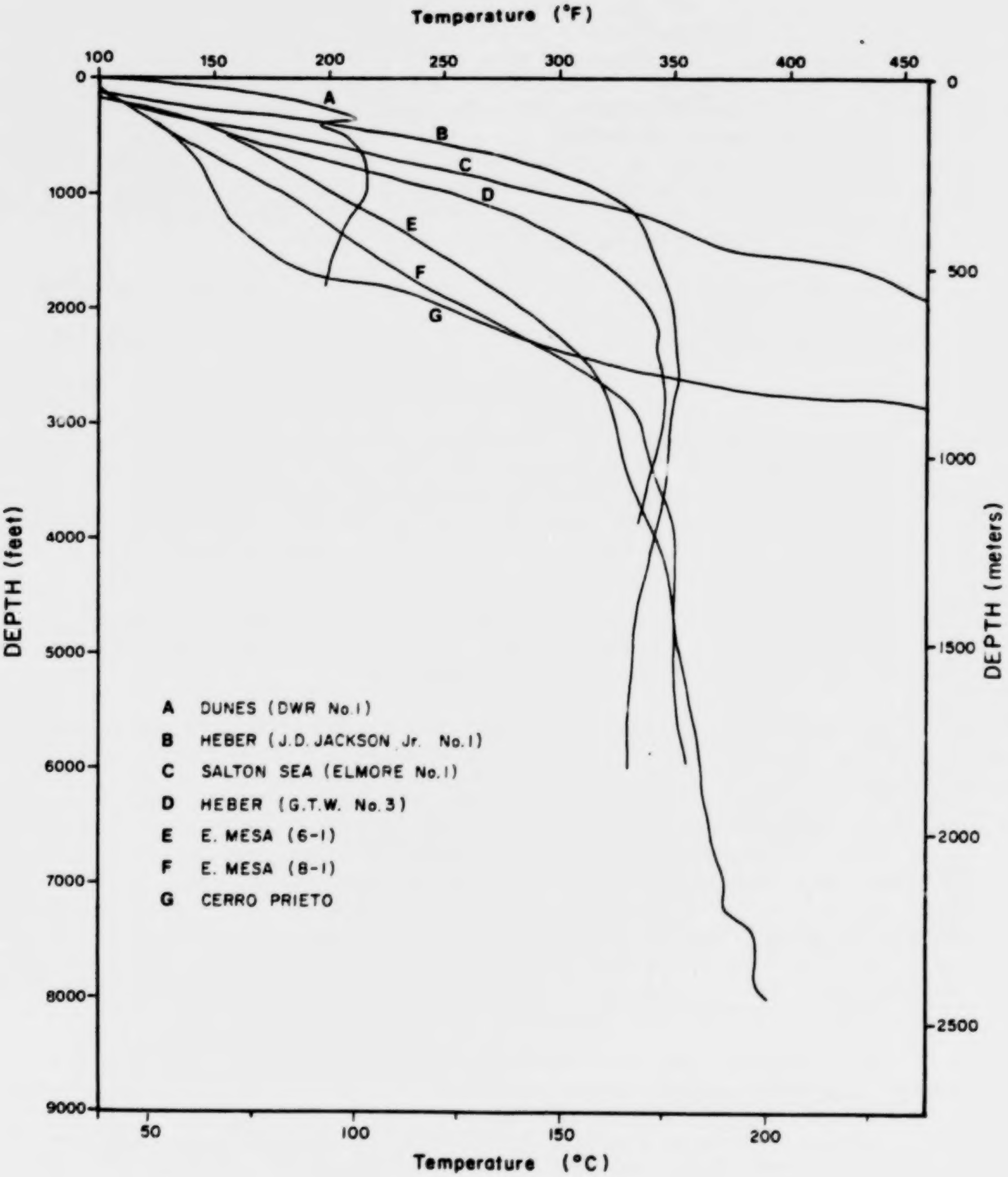

Figure 2.33 Static temperature profiles in geothermal wells from the Salton Trough.

The Imperial Valley Irrigation and Coachella Valley Consolidated Water Districts usually import about 370,000 ha-m (3 million acre-ft) of Colorado River water per year for their domestic and agricultural needs. During 1961-1963 the gross annual diversion to nearly 200,000 ha (500,000 acres) in the Imperial and Coachella Valleys was 444,000 ha-m (3,603,000 acre-ft), or 2.19 ha-m per ha (7.2 acre-ft per acre) irrigated. This rate of use, however, is affected by conveyance losses averaging 36,000 ha-m (290,000 acre-ft) annually below Pilot Knob and by discharge of all unconsumed water to the Salton Sea. These large losses are not included in the following water budget for irrigated land in Imperial Valley:

Measured inflow	377,000 ha-m (3,056,000 acre-ft)
Measured outflow	157,000 ha-m (1,270,000 acre-ft)
Residual	220,000 ha-m (1,786,000 acre-ft)

The residual represents an average consumptive use on 174,000 ha (432,000 acres) of 1.25 ha-m per ha (4.1 acre-ft per acre), including uses in unplanted areas within the irrigated tract. A similar computation for the Coachella Valley indicates consumptive use of 1.16 ha-m per ha (3.8 acre-ft per acre).

Inflow--

Most surface water is derived from the Colorado River through irrigation runoff. It amounts to 123,000 to 154,000 ha-m (1 to 1¼ million acre-ft) annually.

Inflow to the Salton Sea consists of discharge from surface channels, ground water seepage directly to the Salton Sea and precipitation on the water surface. This water flows perennially to the Salton Sea via the Alamo, New and Whitewater Rivers and many drains and ditches. Ninety percent of the inflow comes from the Imperial Valley, primarily via the Alamo and New Rivers, and 10% comes from the Whitewater River and minor channels in the Coachella Valley. Average annual inflow for 1961-63 from the Alamo and New Rivers and 30 other channels was 156,700 ha-m (1,270,000 acre-ft). Average annual inflow for the same period was 13,600 ha-m (110,000 acre-ft) from the Whitewater River and 18 drains in the Coachella Valley.

Salt Creek, on the eastern side of the Salton Sea, has a small perennial base flow into the Salton Sea. The Coachella Canal crosses the lower part of the Salt Creek Basin and several other small drainage basins southeast of Salt Creek. Only a few percent of the flow in Salt Creek comes from runoff; the majority is from canal seepage.

San Felipe Creek, which flows to the southwest shore of the Salton Sea, drains an area of more than 2,600 sq km (1,000 sq mi), including much mountainous area and some small tracts irrigated with local water supplies. A small base flow persists only during the winter months and storm runoff usually accounts for 90% of this flow.

Surface inflow to the Salton Sea from areas not irrigated is quite small during most years but will increase during periods of heavy storm intensity. The Alamo and New Rivers have average annual flows of over and less than 62,000 ha-m (500,000 acre-ft), respectively. The Whitewater River annually contributes less than 12,300 ha-m (100,000 acre-ft) of water to the Salton Sea.

Outflow--

Evaporation, at a rate of approximately 1.8 m (5.8 ft) per year, is the only outflow from the Salton Sea. This figure is from a detailed study of the hydrology of the Salton Sea drainage basin in 1961-62 by USGS in conjunction with other agencies (Hely, et al. 1966). In this study water budget, energy budget, mass transfer and evaporation pan methods were used to determine evaporation rates from the Salton Sea. The water budget method utilizes a relationship between evaporation, precipitation, runoff and change in water storage for a hydrologic unit. The equation is:

$$\Delta V = I_s + I_g + P - E$$

where ΔV = change in volume

I_s = inflow in surface channels

I_g = inflow as ground water seepage

P = precipitation on the water surface

E = evaporation

The energy budget method accounts for all heat energy reaching, stored in and leaving a water body. The objective is to determine the amount of energy utilized in the evaporation process and the quantity of water evaporated. The energy budget for a body of water is expressed as a function of incident and reflected solar radiation, incident, reflected and emitted long wave radiation, energy in the water body, energy used and advected by evaporation and conducted energy.

The mass transfer method relates evaporation from a water surface to the product of windspeed multiplied by the humidity gradient of the air; the equation is:

$$E = N\mu \, (e_o - e_a)$$

where E = evaporation, in inches per day

N = an empirical coefficient

μ = average windspeed, in miles per hour, at a selected height above the water surface

e_o = vapor pressure, in millibars, of saturated air at the temperature of the water surface

e_a = vapor pressure of the air, in millibars, at a selected height above the water

The evaporation pan method uses actual measured rates of evaporation. Evaporation pan data is recorded at three stations around the Salton Sea; each is equipped with a recording rain gauge, an anemometer with a cumulative wind-movement indicator and a 0.6 m (2 ft) sunken and screened evaporation pan. The three stations, at Sandia Beach, Devil's Hole and Imperial Salt Farm (Fig. 2.13) were established in 1947 by the U.S. Soil Conservation Service.

Annual evaporation from the Salton Sea for 1961-62 determined by the water budget and energy budget methods corresponded well. Evaporation pan data coefficients vary somewhat erratically from month to month and for corresponding months in different years. On an annual basis, however, data from the three sunken pans is considered reliable. Average annual evaporation from the Salton Sea for 1948-62 was 1.76 m (5.78 ft). This number corresponds to La Rue's (1916) estimate of 1.8 m (5.8 ft) and Blaney's (1955) average annual evaporation figure of 1.8 m (6.0 ft).

The U.S. Weather Bureau evaporation map of the United States (Kohler, et al., 1959) indicates 2.1 m (6.8 ft) of annual evaporation for the Salton Sea. However, this map is based on scant data and is highly generalized (Hely, et al.,1966). Additionally, it does not take into account the fact that the salinity of the Salton Sea will depress the evaporation rate relative to a fresh water body by about 2% (Harbeck, 1955).

Future Hydrologic Regimen--

Irrigation has been, and will continue to be, by far the greatest influence of man on the hydrologic regimen of the Salton Sea. Increasing recreational development of the Salton Sea will necessitate more concern in the future about the effects of industrial and agricultural development on its water level and salt content.

The development of geothermal wells near the Salton Sea could result in brine disposal problems. Establishment of evaporation basins for geothermal brine disposal, at altitudes above the Salton Sea surface, might result in saline residue contaminating usable ground water. Geothermal brines could not be pumped into the Salton Sea since this would raise the salinity of Salton Sea water. Therefore, geothermal power utilization must include a satisfactory waste disposal system.

Use of Colorado River water in the Salton Sea Basin involves substantial losses during transport. Seepage from the Coachella and All-American Canals averages 40,000 ha-m (330,000 acre-ft) annually. Canal lining or sealants may be necessary to prevent these losses in the future. However, part of the seepage recharges aquifers, and irrigation tract runoff maintains the water level in the Salton Sea. Considerable excess discharge is also necessary to maintain low soil salinity and thereby high agricultural productivity. A decrease in inflow to the Salton Sea would gradually increase salinity and recede the shoreline thus reducing the recreational value of the area.

Given present irrigation and drainage arrangements, no harmful salt quantities are accumulating in parts of Imperial and Coachella Valleys irrigated by the imported Colorado River water (Irelan, 1971). However, the imported water's mineral load must be carefully monitored so the current salt balance can be maintained.

2.5 CHEMICAL CHARACTERISTICS OF GROUND WATER

Knowledge of currently existing chemical characteristics of ground water is essential to define a baseline for future comparison. An integral part of any monitoring methodology developed will be an accurate definition of the starting, or baseline, conditions. The following results of the ground water quality investigation describe the occurrence and distribution of ground water types in Imperial Valley. The methods explored in this study will greatly assist in evaluating their applicability in establishing a baseline condition in any geothermal area.

Water quality data for 145 wells in Imperial Valley were compiled and plotted in three depth intervals using modified Stiff diagrams, Langelier-Ludwig diagrams and three-dimensional surface plots of the single-chemical parameter contours. The depth intervals, chosen from a plot of well perforation intervals (Fig. 2.22), are shallow, from 24 to 91 m (80 to 300 ft), intermediate, from 91 to 457 m (300 to 1,500 ft) and deep, depths greater than 457 m (1,500 ft).

The modified Stiff diagrams show the areal distribution of five distinct water types: a sodium chloride water, a high sulfate water, a sodium chloride with high sulfate and/or magnesium water, a sodium chloride with high calcium water, and a sodium bicarbonate water. The Langlier-Ludwig plot shows two distinct chemical groups of water. One group, essentially along the Na+K axis, contains a high proportion of shallow depth interval points, and the other group, essentially along the SO_4+Cl axis, contains a high proportion of intermediate depth interval points. Several structural features, such as the Elsinore Fault trace, the trend of the Calipatria Fault and several geothermal anomalies, can be deciphered from the single parameter contour plots.

Objectives and Limitations--

The objective of these representations of water quality is twofold. First, it is intended to represent baseline chemical characteristics of Imperial Valley waters, and second, it is anticipated that some insight into aquifer geometry and distribution of ground water might be derived from the graphic displays.

This phase of the study is largely descriptive and data presented in this report provides a useful vehicle for synthesis, analysis and interpretation of baseline ground water conditions and some aquifer relations in Imperial Valley.

Within the scope of the project the limitations of this approach appear in two main areas: first, data availability limitations, and second, limitations of the interpretive techniques. These limitations are detailed below.

Data acquisition was terminated when a point of diminishing return was reached. That is, the water quality data search was extensive, but not exhaustive. The sources used include:

"Selected Data on Water Wells, Geothermal Wells and Oil Tests in Imperial Valley, California," by W. F. Hardt and J. J. French (1976), a compilation of ground water quality data for 436 wells; this source contains analyses that have previously appeared in many separate publications. The data published in this report was also available in digitized format on magnetic tape which was used for the three-dimensional surface plots of single-chemical parameter contours.

"Chemistry of Thermal Water in Selected Geothermal Areas of California," by M. J. Reed (1975), a report that includes chemical analysis of ground water from 48 wells, mostly from the artesian aquifer in Imperial Valley.

"Lawrence Berkeley Laboratory Brine Data File," by S. Cosner and J. Apps, (1977), a compilation including 27 chemical analyses of geothermal well waters in Imperial Valley.

"Geotechnical Aspects of The Environmental Impact of Geothermal Power Generation at Heber, Imperial Valley, California," by Geonomics (1976), which includes analyses of a number of geothermal wells in the Heber and Cerro Prieto geothermal areas.

The chemical analyses used in this report are not reproduced here since they are available in the above-mentioned publications. The sample numbering system employed in this report allows easy reference to original sources and is shown on Plates 2.3 and 2.8.

The criteria used to select the ground water quality data for inclusion in this study were:

1) sample depth interval must be specified, and

2) sample depth interval must fall completely within one of the preliminary water — bearing strata depth intervals.

Wells with no specified sample depth interval were excluded because it would make correlations of chemical quality with water bearing strata more difficult, if not impossible. Analyses of ground water samples which overlapped water-bearing strata depth intervals were excluded for the same reason.

As a result of these limiting criteria the total number of analyses included in this survey is 145. This consists of 55 wells in the shallow water-bearing strata, 64 wells in the intermediate water-bearing strata, and 26 wells in the deep water-bearing strata.

The quality of the chemical analyses was not evaluated. This would have proven to be an extremely difficult, time-consuming and often arbitrary task. The work was conducted on the assumption that the chemical analyses were reliable, unless discrepancies became apparent. It is felt that this was the best way to approach this task, within the scope of the project.

The Stiff and Langelier-Ludwig graphical techniques are commonly used in ground water quality studies. Each of these methods has limitations with respect to interpretation and aquifer correlations. Stiff diagrams permit representation of the areal distribution of waters, but it is difficult to delineate chemical groupings and mixing relationships from them. They would be most useful when comparing only a few characteristic water types within a limited concentration range. Because the waters in Imperial Valley have such a wide range of concentrations, from a few hundred to over a quarter of a million milligrams per liter TDS, it was necessary to modify the Stiff diagrams to represent percent reactance instead of milliequivalents per liter. This limited the usefulness of the diagrams since relative concentrations would not be seen, but the salinity circle overlay plots somewhat overcome this deficiency.

The Langelier-Ludwig plots depict chemical groupings of waters and can represent, with their salinity cross sections, mixing and rock-water interactions, as well as concentration and dilution.

The approach taken in this report is an assessment of baseline data which is largely descriptive in nature. The methods used provide strong suggestions of aquifer-water correlations and a useful basis for comparison with future water chemistry surveys to determine changes from a baseline condition. From this point intensive study of the data by sophisticated statistical, computer and critical analytic techniques will be necessary to further define the relationships of different waters and aquifers.

Description of Methods--

Three basic graphical display techniques were utilized to establish baseline water quality conditions in Imperial Valley and to define the areal and vertical distribution of distinctive ground water types and aquifers. These techniques are modified Stiff diagrams, Langelier-Ludwig plots and single-chemical parameter plots. Details of these methods are described below.

Modified Stiff Diagrams--Stiff diagrams (Stiff, 1951) are closed polygons which show relative concentrations of major ionic constituents of water (Fig. 2.34; Plates 2.4, 2.6 and 2.8). Water with similar chemical characteristics will have Stiff diagrams with similar shapes. The modified Stiff diagrams used for this study are plotted with ionic concentrations in percent reactance in order to accommodate the great range in salt concentrations, from about 700 mg/l to over 360,000 mg/l. For each diagram the well number, sample depth interval and TDS in ppm are shown by adjacent numbers. The Stiff patterns themselves are plotted on a base map to show the areal distribution of different types of waters.

For this study the Stiff diagram is constructed with a vertical line bisecting three horizontal axes (Fig. 2.34; Plates 2.4, 2.6 and 2.8). The axes to the left of the vertical line represent the major cations—from top to bottom, calcium, magnesium and sodium plus potassium--in percent reactance from zero to one hundred. Similarly, the major anions--bicarbonate plus carbonate, sulfate and chloride--are represented from top to bottom on the right side of the diagram. The percent reactance

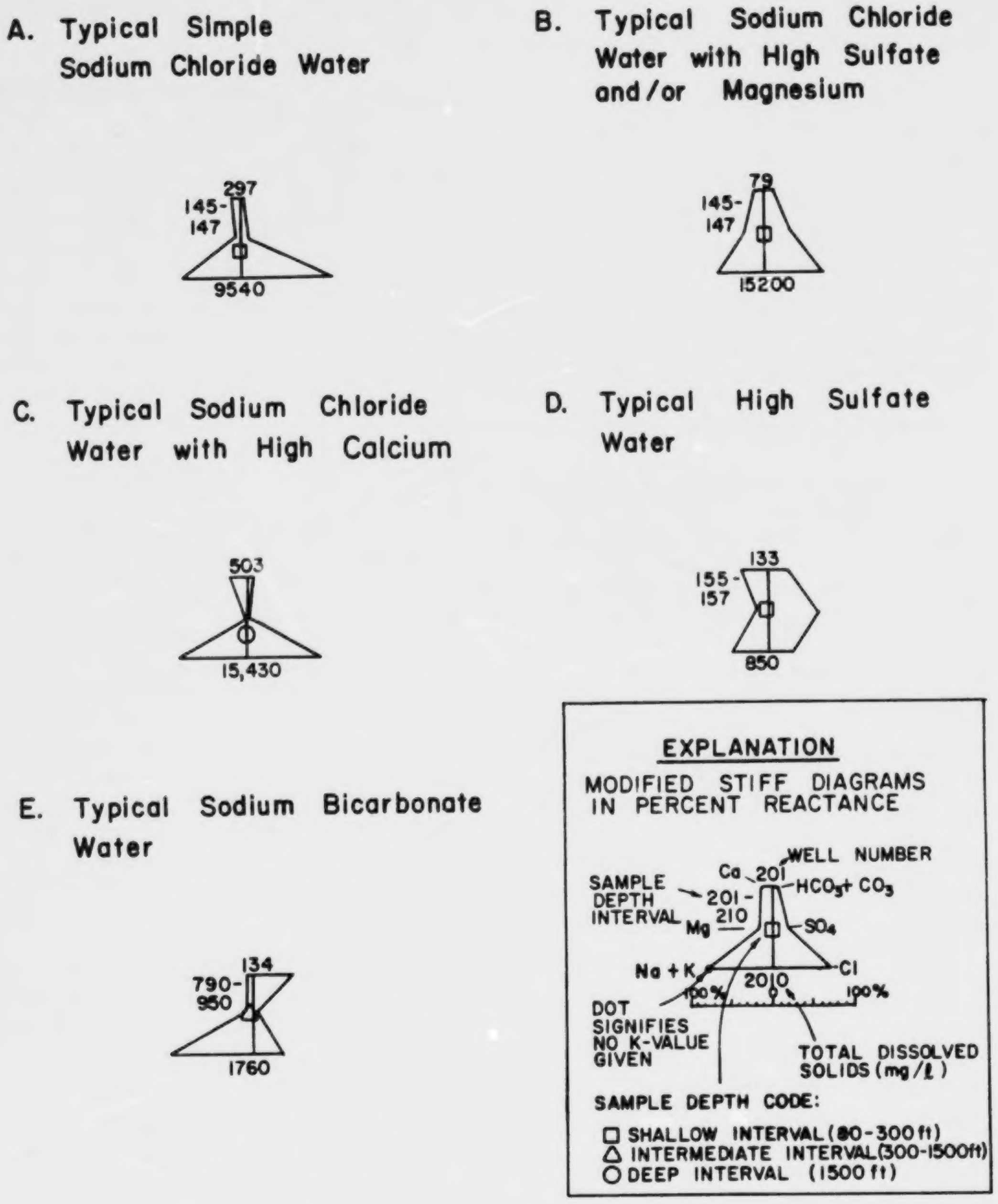
A. Typical Simple Sodium Chloride Water
297
145-
147
9540
B. Typical Sodium Chloride Water with High Sulfate and/or Magnesium
79
145-
147
15200
C. Typical Sodium Chloride Water with High Calcium
503
15,430
D. Typical High Sulfate Water
133
155-
157
850
E. Typical Sodium Bicarbonate Water
134
790-
950
1760
EXPLANATION
MODIFIED STIFF DIAGRAMS IN PERCENT REACTANCE
WELL NUMBER
Ca
201
HCO3+ CO3
SAMPLE DEPTH INTERVAL
201-
210
Mg
SO4
Na + K
Cl
2010
100%
100%
DOT SIGNIFIES NO K-VALUE GIVEN
TOTAL DISSOLVED SOLIDS (mg/ℓ)
SAMPLE DEPTH CODE:
□ SHALLOW INTERVAL (80-300 ft)
△ INTERMEDIATE INTERVAL (300-1500 ft)
○ DEEP INTERVAL (1500 ft)

Figure 2.34 Modified Stiff diagrams for characteristic Imperial Valley groundwaters.

values are calculated separately for cations and anions as the individual ion concentration expressed in milliequivalents per liter divided by the respective total anion or cation concentration expressed in milliequivalents per liter.

These diagrams differ from those originated by Stiff (1951) in that he used milliequivalents per liter for the scale and had the ions represented in a different order. To accommodate for the loss of expression of concentration, salinity circles were plotted as an overlay to the modified Stiff diagrams (Plates 2.5, 2.7 and 2.9). These circles are drawn to represent the TDS concentration, with the salinity circle's diameter proportional to the logarithm of the TDS concentration. That is, a circle that has twice the diameter of another will have a TDS concentration ten times as great. The logarithmic scale was necessary to include the great range of TDS values in the Imperial Valley ground water. Average sample interval elevations are plotted with the salinity circles for added information.

Langelier-Ludwig Diagrams--The Langelier-Ludwig (L-L) diagram (Langelier and Ludwig, 1942) (Figs. 2.35 and 2.36) is similar to the rhombohedral section of the Piper diagram (Piper, 1944). It is a square plot of percent reactance of alkalic cations (Na+K) ascending from 0 to 100 on the left-hand vertical axis and hardness cations (Ca+Mg) descending from 100 to 0 on the right—hand vertical axis (Fig. 2.36). The horizontal axes plot percent reactance of carbonate anions (HCO_3+CO_3) and non-carbonate anions (SO_4+Cl), with each axis reciprocating the scale of the opposite axis. This diagram provides a method for "segregating analytic data for critical study with respect to sources of the dissolved constituents in waters, modifications in the character of a water as it passes through an area and related geochemical problems" (Piper, 1944). It allows for investigation of compositional relations among samples and statistical populations of samples in the form of clusters of points.

Salinity sections (Figs. 2.37 and 2.38) can be drawn at any orientation on the Langelier-Ludwig diagram to depict changes in concentration. These sections are constructed by projecting all the data points desired to be included in the section onto a straight line extending from one L-L diagram axis to an opposite axis. A triangle is formed by extending two lines from above at an angle of about 90° to intersect the ends of the L-L diagram section line. This section can be visualized as one side of a four-sided pyramid with the L-L diagram as the base (Fig. 2.35). The apex of the pyramid would represent zero salinity. Lines of constant chemical constituent ratio and decreasing salinity would connect points on the L-L diagram, at the pyramid base, to the pyramid's apex. Then an appropriate milliequivalents per liter scale is chosen as planes parallel to the base of the pyramid. The data point is plotted on the salinity section

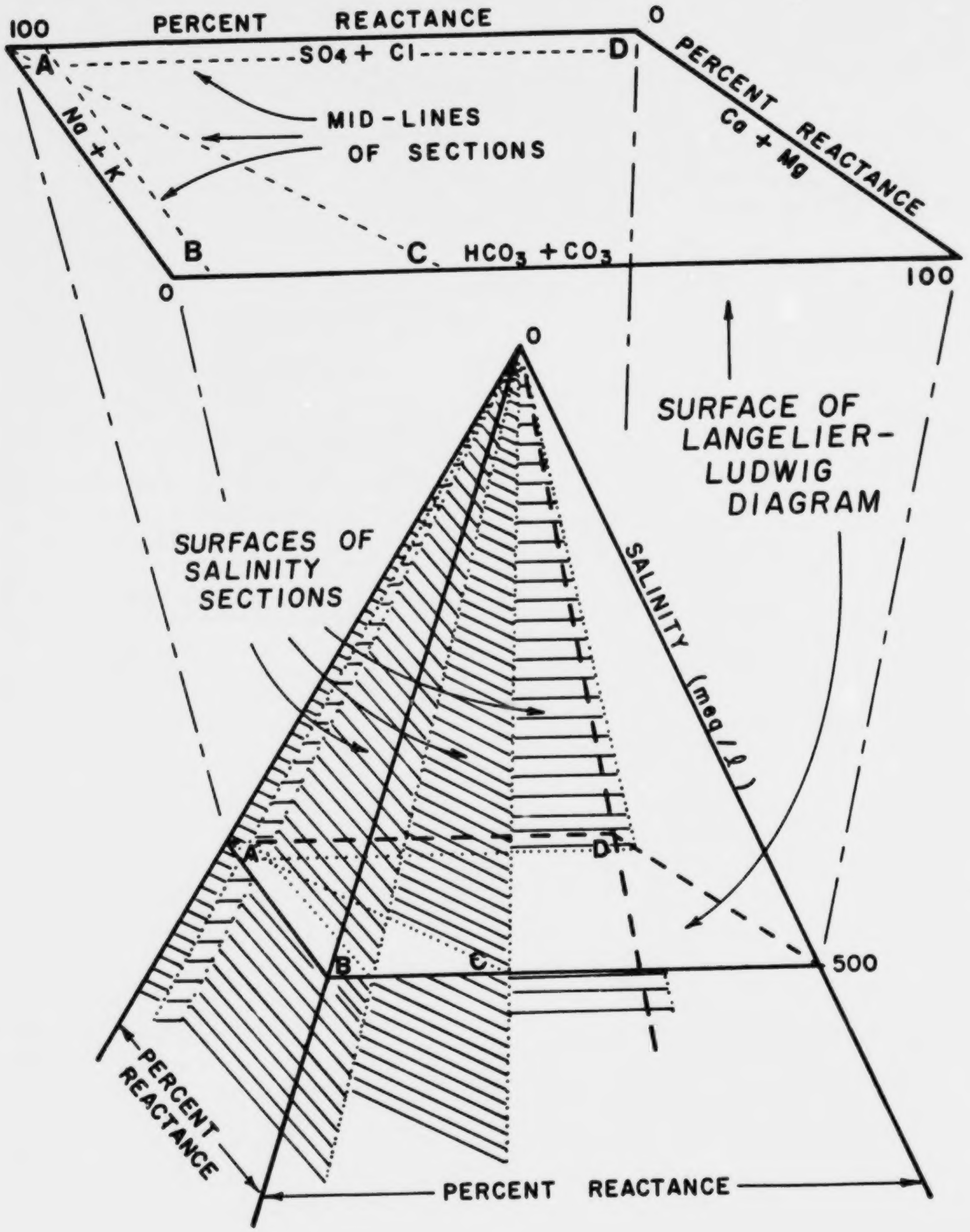
100
PERCENT REACTANCE
0
A
SO4 + Cl
D
PERCENT REACTANCE
Ca + Mg
Na + K
MID-LINES OF SECTIONS
B
C
HCO3 + CO3
0
100
0
SURFACE OF LANGELIER-LUDWIG DIAGRAM
SURFACES OF SALINITY SECTIONS
SALINITY (meq/ℓ)
A
D
B
C
500
PERCENT REACTANCE
PERCENT REACTANCE

Figure 2.35 Three-dimensional perspective of a Langelier-Ludwig diagram showing surfaces of salinity sections.

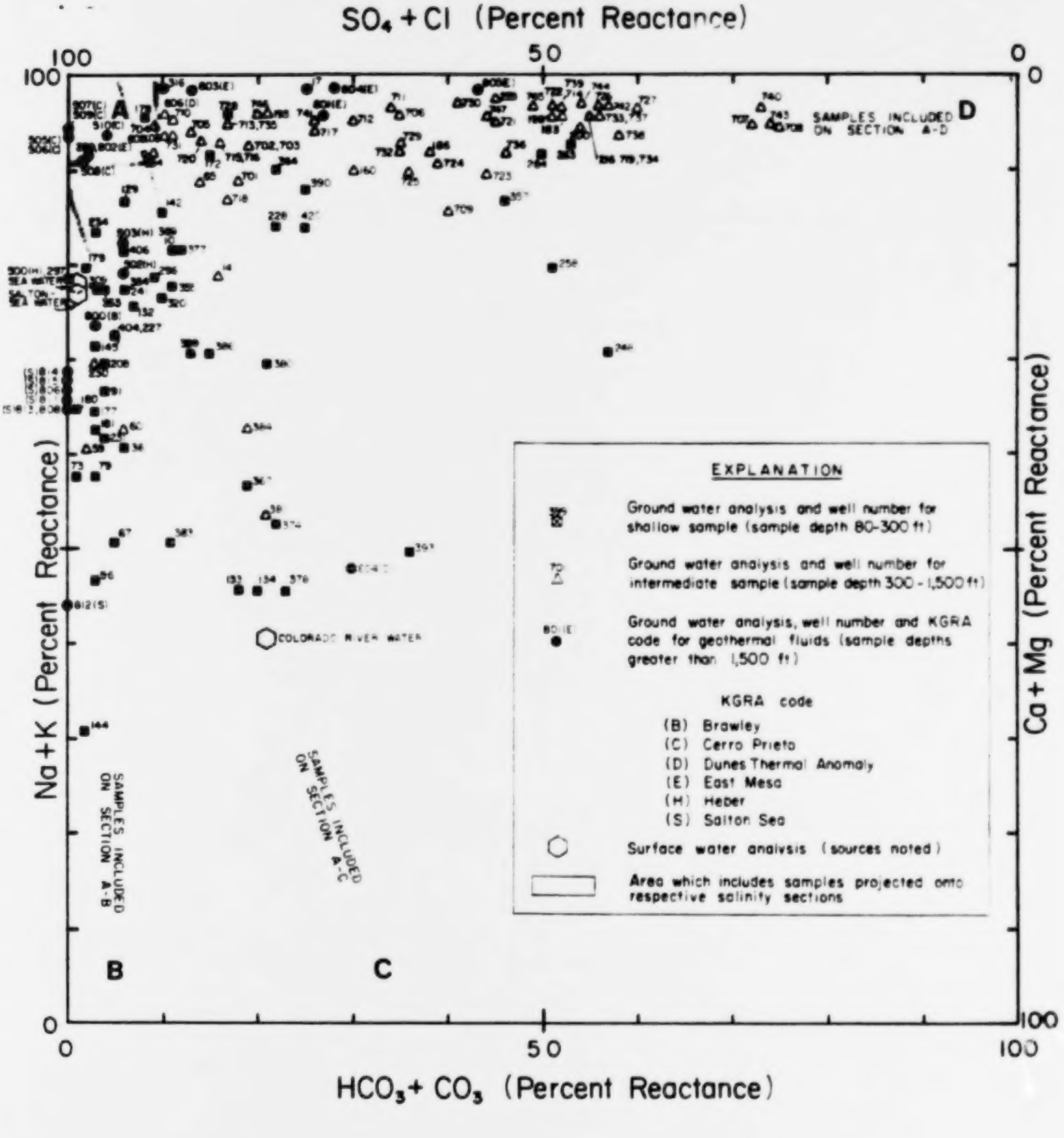

Figure 2.36 Langelier-Ludwig diagram for groundwater data in Imperial Valley, California.

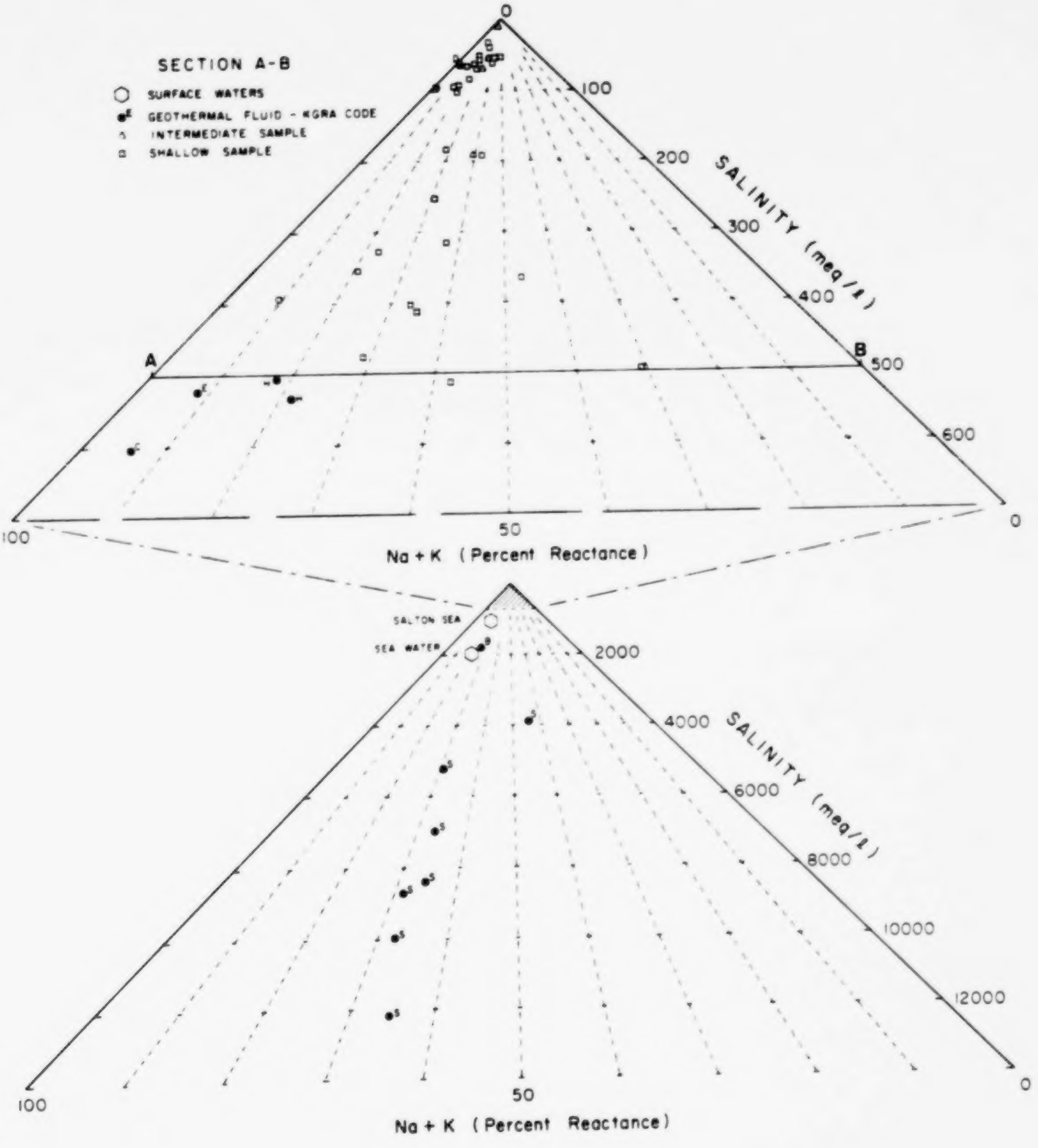

Figure 2.37 Salinity section A-B from Langelier-Ludwig diagram for groundwater data in Imperial Valley, California.

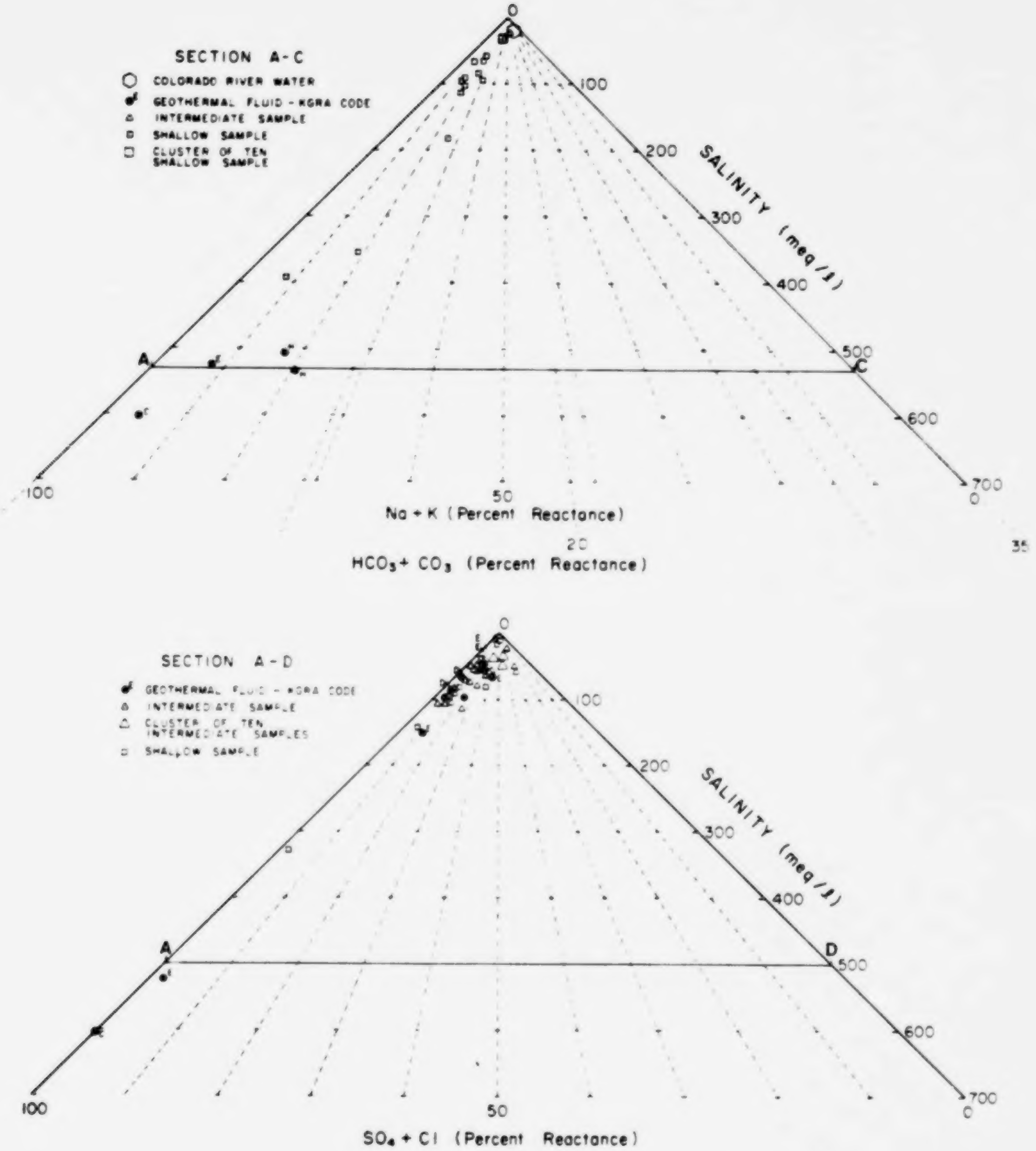

Figure 2.38 Salinity sections A-C and A-D from Langelier-Ludwig diagram for groundwater data in Imperial Valley, California.

where the salinity value plane intersects the chemical constituent ratio line. Similar to the L-L diagram, the salinity sections also allow for investigation of compositional relations and statistical populations of samples.

Single Chemical Parameter Plots--Three-dimensional surface plots of single chemical parameter contours (Figs. 2.40 to 2.44) were used as an additional technique for possible correlation of ground water chemistry with aquifers, geologic structure or geothermal anomalies. Since a good portion of the ground water quality data was already digitized, and computer contouring and surface drawing routines were available, the capability to do computer contouring and plotting of specific chemical parameters existed. This technique could eventually allow generation of many vertical and horizontal cross sections and surfaces, as well as trials with different depth interval categories, with minimal effort and cost. The essence of the idea is to define the extremely complicated, contorted subsurface structure and lithology of Imperial Valley, as well as changes in chemical parameters in the ground water system, that would be shown in the appropriate combination of contoured cross sections and three-dimensional surface plots of these contoured cross sections.

Contoured surfaces for some chemical parameters are illustrated in this report and one can delineate specific structural trends and anomalies on them. It is anticipated that further interpretation and data manipulation will be possible in later phases of this study.

Guide to Changes in Water Characteristics--

To aid in tracing the possible genesis of a ground water in Imperial Valley, chemical reactions that could alter Colorado River source water were defined and considered (Olmsted, et al., 1973). In this approach recent Colorado River water is assumed to undergo certain common geochemical reactions in combination with various degrees of evaporative concentration. The results of these reactions are computed, providing a set of known chemical causes and effects on Colorado River water. By comparing these known changes with analyses of actual waters, it is possible to get a suggestion of the processes the water has undergone in the ground. A sample of some of these changes, as shown by modified Stiff patterns, is presented in Figure 2.39. Since many people may be accustomed to seeing Stiff patterns plotted in milliequivalents per liter, this figure also compares modified Stiff patterns plotted in percent reactance with those in plotted milliequivalents per liter to illustrate the characteristics of these different representations.

The first chemical change shown, that of simple evaporation, shows the percent reactance modified Stiff pattern remaining the same size and shape with increasing concentrations due

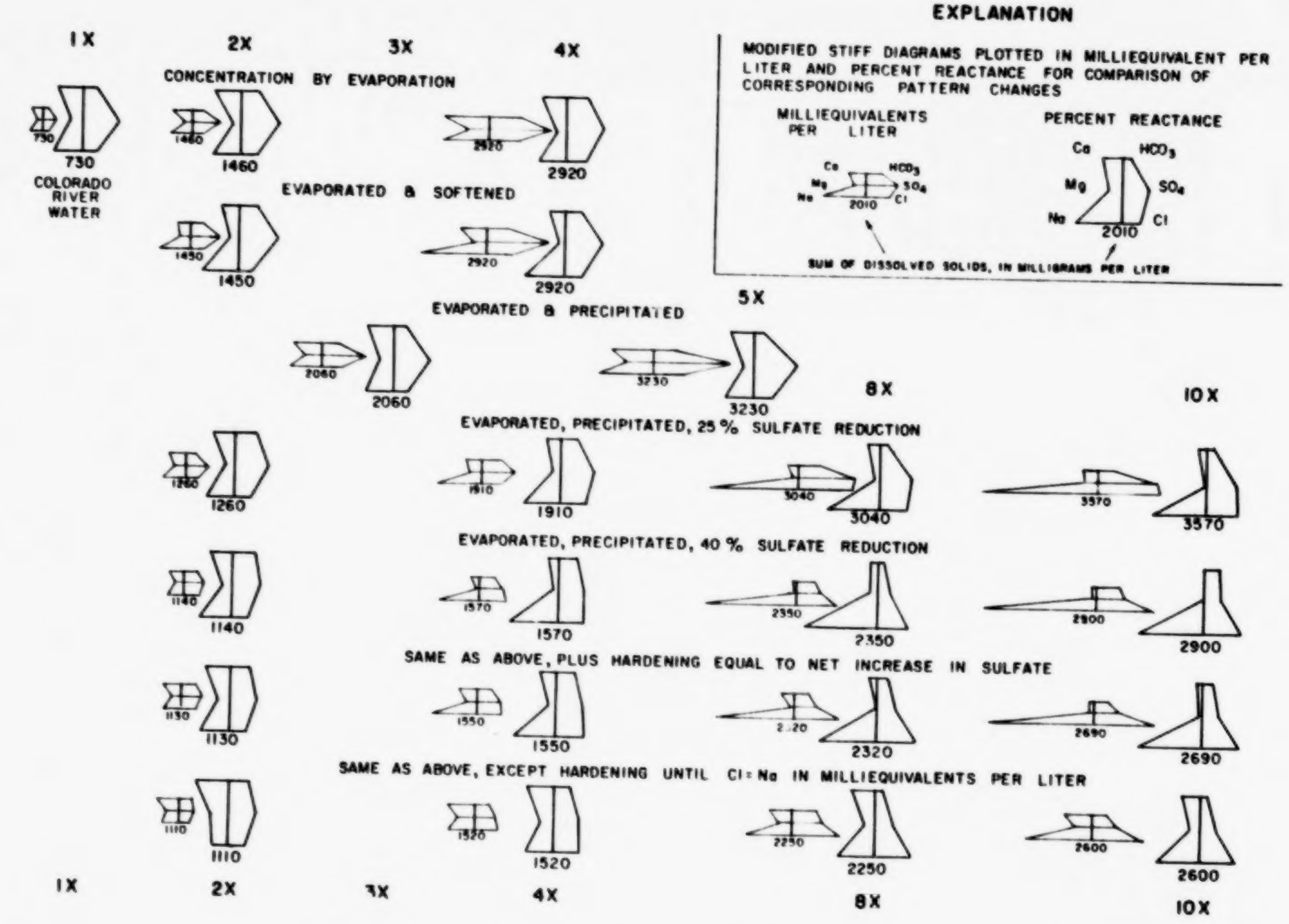
EXPLANATION
MODIFIED STIFF DIAGRAMS PLOTTED IN MILLIEQUIVALENT PER LITER AND PERCENT REACTANCE FOR COMPARISON OF CORRESPONDING PATTERN CHANGES
MILLIEQUIVALENTS PER LITER
PERCENT REACTANCE
Ca
Mg
Na
HCO3
SO4
Cl
2010
SUM OF DISSOLVED SOLIDS, IN MILLIGRAMS PER LITER
1X
2X
3X
4X
5X
8X
10X
CONCENTRATION BY EVAPORATION
730
COLORADO RIVER WATER
1460
2920
EVAPORATED & SOFTENED
1450
2920
EVAPORATED & PRECIPITATED
2060
3230
EVAPORATED, PRECIPITATED, 25% SULFATE REDUCTION
1260
1910
3040
3570
EVAPORATED, PRECIPITATED, 40% SULFATE REDUCTION
1140
1570
2350
2900
SAME AS ABOVE, PLUS HARDENING EQUAL TO NET INCREASE IN SULFATE
1130
1550
2320
2690
SAME AS ABOVE, EXCEPT HARDENING UNTIL Cl=Na IN MILLIEQUIVALENTS PER LITER
1110
1520
2250
2600

Figure 2.39 Modified Stiff diagrams representing hypothetical analyses of groundwater resulting from specified chemical changes in Colorado River water. (modified from Olmsted, et al., 1973)

to evaporation (Fig. 2.39). The modified Stiff pattern plotted in milliequivalents per liter maintains a similar shape but elongates markedly with increasing concentration due to evaporation.

Other chemical changes that may be expected in groundwater in this area are softening, carbonate precipitation, sulfate reduction, hardening, re-solution of precipitated salts, oxidation of dissolved organic substances and mixing of waters of different chemical composition (Olmsted, et al., 1973). The last three processes would be difficult to represent and calculate meaningfully,so they are not presented in Figure 2.39, as are the other five.

Softening is the replacement of calcium or magnesium, the hardness-causing constituents, by sodium. This generally occurs by cation exchange with clay minerals. This change is illustrated in the second line of diagrams in Figure 2.39.

Carbonate precipitation occurs when water with high bicarbonate and calcium or magnesium content is sufficiently evaporated, resulting in concentration and precipitation of calcium or magnesium bicarbonate. To distinguish between loss of calcium and magnesium from softening and loss from carbonate precipitation,one can look for a reduction in bicarbonate, which occurs with carbonate precipitation but not with softening. This process is labeled "evaporated and precipitated" on the third line of diagrams in Figure 2.39.

Sulfate reduction is believed to be a major process occurring in Yuma area groundwater (Olmsted, et al., 1973), an area very similar to Imperial Valley. Exactly how sulfate reduction occurs is poorly understood but it is known to be an organic process. The last four lines of diagrams in Figure 2.39 involve sulfate reduction.

Hardening, the reverse of softening, is a base-exchange process where sodium is replaced by calcium or magnesium. Like softening, however, hardening is the result of reactions with clay minerals. The last two lines of diagrams in Figure 2.39 involve hardening.

One conclusion that may be drawn by comparing the different chemical reactions shown in Figure 2.39 is that the TDS content is a poor measure of the amount of evaporative concentration of the sample. The chemical reactions the sample has undergone also significantly influence the TDS. This can be seen in Fig. 2.39 by comparing the 2,920 mg/l TDS content of the 4X "concentration by evaporation" example with the 2,900 mg/l TDS content of the 10X concentration by "evaporated, precipitated, 40% sulfate reduction" example.

2.5.1 Types and Distribution of Groundwater

The classification, analysis and discussion presented is mainly descriptive, and it is felt that the charts prepared for this report will serve as a vehicle for future analysis and interpretation. Investigators with different backgrounds, hypotheses and knowledge of Imperial Valley may see different relations and correlations from the same basic representation of data. For example, detailed statistical or computer plots of additional parameters and sections may prove extremely revealing and useful. At the very least, the data presented here will serve as an adequate reference for baseline geochemical relationships, which will be elaborated in subsequent reports.

One limitation of the data used in this report regards the areal and vertical distribution of samples (Plate 2.3). Since the great majority of wells in the valley were drilled for water, their objective was to find the best producing layer at the shallowest depth. This objective leads to a very biased sample. That is, we will have samples from the shallowest, best producing aquifers. This means that there will be no wells in areas that are less populated, or less useful, or where usable water is too deep to be economically extracted. Samples in areas that are drilled will mostly have representation in the first good producing aquifer they penetrate, with all aquifers below not being represented. This situation is illustrated by comparing the areal distribution of wells in the shallow and intermediate depth zones (Plate 2.3). The intermediate depth zone has samples mainly from the artesian aquifer beneath the area between the East Highline Canal and the Alamo River, while many samples from the shallow depth zone occur around this area. Any well drilled between the East Highline Canal and the Alamo River will most likely penetrate the artesian aquifer while any well outside of this area will be perforated above the depth of the intermediate zone, and we get no information about the water below the shallow depth zone in these areas.

Our sample was additionally limited by the lack of perforated interval data for the majority of wells for which we had chemical data. This resulted in a great concentration of well samples in an area east of the Alamo River to the southeastern Imperial Valley and a lower sample density in the western and southwestern portions of the valley. Northwestern Imperial Valley, the West Mesa area, the area east of the Coachella Canal (except for the southeastern part of the valley) and the area east of the Salton Sea are essentially unrepresented in our sample.

The following discussion on the types and distribution of groundwater in Imperial Valley is largely based on the representations of groundwater characteristics shown in the modified Stiff diagrams for the shallow, intermediate and deep depth zones (Plates 2.4, 2.6 and 2.8). Frequent reference to these plates and to Figure 2.34, showing modified Stiff diagrams for typical waters, will aid in the following discussion.

Identification and Classification of Characteristic Waters--

Modified Stiff diagrams plotted for the shallow, intermediate and deep depth intervals show the distribution of five distinct water types in Imperial Valley: a sodium chloride water, a sodium chloride with high sulfate and/or magnesium water, a sodium chloride with high calcium water, a high sulfate water and a sodium bicarbonate water (Fig. 2.34). Definition of these categories was largely based on distinguishable changes in the shape of the modified Stiff diagrams. Since the modified Stiff diagrams are plotted in percent reactance, this means that this classification is based solely on the proportion of ionic constituents to each other and not at all on the concentration of the solution. This is a very important factor to keep in mind for the following discussion.

Points are plotted for all the sample wells on one Langelier-Ludwig diagram (Fig. 2.36) and three accompanying salinity cross sections (Figs. 2.37 and 2.38). Points from the three different depth zones are plotted with three different symbols to enable possible correlation of composition with depth. Classifications derived from these plots would be different from those derived from the modified Stiff diagrams because of the way the anions and cations are grouped in the plot. It was anticipated that distinctive clusters of points would represent distinctive groups of origin waters or mixing paths on the L-L diagram and salinity cross sections; and, in fact, there is a marked correlation between depth interval and sample composition. Although there is some scatter, a definite concentration of shallow interval samples occurs in a zone with greater than 90 percent reactance (SO_4+Cl) and between approximately 55 and 85 percent reactance (Na+K) (Fig. 2.36). A distinct concentration of intermediate depth samples occurs in a zone with greater than 90 percent reactance (Na+K) and between approximately 25 to 95 percent reactance (SO_4+Cl). Distinct clusters in this zone occur between 25 and 30 and between 40 and 52 percent reactance (SO_4+Cl).

Most of the geothermal waters plot above 98 percent reactance (SO_4+Cl) or (Na+K) (Fig. 2.36). The Salton Sea wells occur at 100 percent reactance (SO_4+Cl) and between 64 and 69 percent reactance (Na+K). Three of the East Mesa wells plot at 98 percent reactance (Na+K) and between 57 and 87 percent reactance (SO_4+Cl).

Salinity section A-D (Fig. 2.38) shows a very dense cluster of points in a triangular pattern. This is suggestive of complete mixing of the three waters having compositions represented by the apexes of the triangular patterns. The composition of these waters appears to be a fairly pure water of low salinity, a sodium bicarbonate water having a salinity of approximately 60 meq/l, and a sodium chloride water having a salinity of approximately 110 meq/l. A line of points for the Salton Sea geothermal wells in section A-B of Figure 2.37 shows a relatively constant ratio of chemical constituents becoming more and more concentrated by evaporation.

Sodium Chloride Waters--The three sodium chloride waters mentioned in the previous section will be described below. The first water is the simple sodium chloride water which contains a very high proportion of sodium and chloride and a small percent reactance of other anions and cations (Fig. 2.34). This water is typified by sample number 297, 320 or 145 in the shallow aquifer (Plate 2.4). It will be referred to as the simple sodium chloride water in the following discussion.

The sodium chloride with high sulfate or magnesium is a water with a high proportion of sodium and chloride, but this water also contains appreciable amounts of sulfate or magnesium, generally about 20 to 30 percent reactance, and significantly lesser amounts of calcium and bicarbonate (Fig. 2.34). Salton Sea surface waters are typical of this water type. This water will be referred to as the NaCl-SO_4-Mg water in the following discussion.

The sodium chloride water with high calcium also has a very high proportion of sodium and chloride to the other anions and cations, but the amount of calcium is noticeably larger than the percent reactance of any other remaining ion (Fig. 2.34). This water would be typified by samples in the Salton Sea geothermal area (Plate 2.8). This water will be referred to as the NaCl-Ca water in the following discussion.

The simple sodium chloride water occurs in all three depth zones, but there is a statistically significant correlation of this water with the shallow depth zone (Plate 2.4). Water of this type is fairly well distributed throughout the area east of the New River within the shallow depth zone. The sodium chloride water occurs very sparsely in the intermediate and deep aquifers (Plates 2.6 and 2.8).

The NaCl-SO_4-Mg water is present in only the shallow and intermediate depth zones for our sample. In the shallow zone it occurs near inlets in the southern portion of the Salton Sea and is typical of Salton Sea water. Similar type waters with high sodium chloride and notable sulfate occur in the shallow and intermediate depth zones in southeastern Imperial Valley. A few samples of other similar waters of this type in the shallow depth zone occur to the west and northwest of El Centro. A few more samples of this type occur in the northernmost area of the intermediate depth zone samples.

The NaCl-Ca water only occurs in the deep aquifer and shows a statistically significant correlation with this aquifer. It occurs in the Cerro Prieto, Heber and Salton Sea geothermal fields and there appears to be a distinct north-south trend between these occurrences. It is possible that there may be some conduit providing a hydraulic connection between these waters or they may all be undergoing a similar chemical reaction.

It is possible that the distinctions between these three sodium chloride waters may obscure more general ground water relations. Simpler distribution patterns may possibly be recognized if all the sodium chloride waters were considered as one group.

Sulfate Water--The high sulfate waters are typified by average Colorado River water (Plate 2.4; Fig. 2.34). This water has higher percent reactance sulfate than any other anion, often 50 percent reactance or greater. Most of these waters have calcium and sodium percent reactance greater than magnesium with the calcium and sodium often greater than 30 percent reactance each. This water occurs mainly in the shallow aquifer (Plate 2.4) and has a statistically significant correlation with it. It occurs mainly beneath and very close to canals in the southeastern portion of Imperial Valley, obviously due to leakage of Colorado River water from the canals. One sample of this water occurs in the intermediate depth zone directly beneath the All-American Canal and one occurs in the deep depth zone, in the Dunes geothermal field, just to the northwest of the Coachella Canal.

Sodium Bicarbonate Waters--The sodium bicarbonate waters in Imperial Valley have higher percent reactance of sodium and bicarbonate than any other ion (Fig. 2.34). Most of these waters also have significant chloride. Although samples of this water occur in all three depth zones there is a marked statistically significant correlation of this type of water with the intermediate depth zone (Plate 2.6). Almost 80% of the samples of this type of water occur in the intermediate depth zone. This is largely confined to the artesian aquifer area, between the Alamo River and the East Highline Canal. Four of the samples of this water type occurring in the shallow depth zone are located just west of the Elsinore Fault trace in the southwestern corner of Imperial Valley. These waters have the lowest salinities of all our samples, even lower than Colorado River water. A sample in the intermediate depth zone, located directly below these four samples, has exactly the same chemical characteristics. Another sample of this water type in the shallow aquifer occurs in the southern part of the East Mesa area, areally to the southeast of this water's occurrence in the intermediate depth zone. In the deep depth zone, these waters occur in the East Mesa KGRA and about 6.4 km (4 mi) to the southeast of Holtville.

Discussion of Characteristic Waters by Depth Zone--

Modified Stiff diagrams for the shallow depth interval (Plate 2.4) show the occurrence of four of the characteristic water types. The sodium chloride water occurs throughout the southeastern Imperial Valley, approximately up to the New River. The high sulfate water appears to be characteristically Colorado River water and occurs in southeastern Imperial Valley, but is generally restricted to the Coachella and All-American Canal areas. This would lead one to believe that the Colorado River water reacts quite quickly with the sediments and changes character, picking up significant amounts of sodium and chloride with very small flow distances in the ground. Salton Sea water is included in the NaCl-SO_4-Mg groundwater group. It also occurs near inlets to the Salton Sea and in an area up to 24 km (15 mi) west-northwest of El Centro. The sodium bicarbonate water in the shallow depth interval mainly occurs in four wells in the extreme southwest corner of the valley.

Most wells in the intermediate zone (Plate 2.6) tap the artesian aquifer beneath the area between the Alamo River and the East Highline Canal. The sodium bicarbonate water is very typical of the intermediate depth interval. Other waters occurring in the intermediate depth zone are a few sporadic simple sodium chloride waters and some NaCl-SO_4-Mg water in the Dunes geothermal area and in the north part of East Mesa; one intermediate depth high sulfate water also occurs under the All-American Canal.

In the deep geothermal depth interval (Plate 2.8), the NaCl-SO_4-Ca water is characteristic of the Salton Sea, Heber and Cerro Prieto geothermal fields. However, the concentration of the fluids of the Salton Sea field is about ten to twenty times that of Heber and Cerro Prieto. The sodium bicarbonate water occurs in the deeper zones just west of East Mesa. East Mesa has a sodium chloride water with some samples high in bicarbonate. An oil test well about 10 km (6 mi) southeast of Brawley has a sodium chloride water at 4,097 m (13,442 ft) depth containing 52,852 mg/l TDS. A sample from the Dunes geothermal field shows the high sulfate water characteristic of the Colorado River.

Four analyses are available for deep well No. 316 at depths from 834 to 3,752 m (2,737 to 12,310 ft). These analyses show a change in the character of the water with depth, from essentially a simple sodium chloride water at around 850 m (2,800 ft) gradually developing into a sodium bicarbonate water at about 3,700 m (12,000 ft). Also, TDS content increases fairly linearly from 850 m (2,800 ft) to 3,400 m (11,200 ft) with salinity going from 3,227 to 8,843 mg/l. But, between 3,400 m (11,200 ft) and 3,700 m (12,000 ft) a marked discontinuity occurs in the linear salinity increase and TDS increase from 8,843 to 18,215 mg/l in the 143 m (470 ft) between these two sample intervals. This marked increase suggests some kind of impermeable boundary, or perhaps fault, separating these intervals. A more saline zone is also noted in the 1,202 to 1,227 m (3,945 to 4,026 ft) depth interval in well No. 304 where a TDS content of 19,000 mg/l is bounded above by a 13,000 mg/l water and below by a 11,800 mg/l water.

Changes in Water Characteristics With Time--
An attempt was made to delineate changes of water characteristics with time. Unfortunately data distribution with location and time was not adequate for a detailed analysis of these chemical changes. Regular or consistent patterns were not observed; however, observations that were noted are discussed below.

Eighteen sample wells had complete chemical analyses over periods of 1 to 19 years. Six of these analyses were over only one- or two-year periods. Some wells showed changes and others did not. Well Nos. 60, 230, 253, 364, 381, 384, 420, 713, 714, 720, 738, 742 and 743 (Plate 2.3) exhibit very little or no significant changes in water character or concentration over sample intervals which run from 1 to 11 years. These shallow and intermediate depth samples are areally distributed throughout the valley ,and the composition of these waters varies from very low salinity sodium bicarbonate water to sodium chloride sulfate waters with over 2,760 mg/l TDS.

Well No. 10 (Plate 2.4), near the Coachella Canal, to the north of Imperial Valley, has the most complete set of analyses with time. There are ten analyses for the 19-year period between 1948 and 1967. The character of this sodium chloride water with notable carbonate, sulfate and calcium remains basically the same throughout the analysis period. The TDS content decreases from 3,850 mg/l in 1948 to 3,000 mg/l in the 1962 sample, then starts increasing to 3,475 mg/l for the most recent sample which was taken in 1967.

The 1962 and 1970 analyses of well No. 160 (Plate 2.6), penetrating the intermediate depth artesian aquifer east of the Alamo River, are quite similar. Both are sodium bicarbonate waters with very high chloride content. There was an increase in TDS from 1,640 mg/l in 1962 to 1,780 mg/l in 1970 and a small increase in sulfate. Marked increases in TDS, to 1,910 mg/l, and in sulfate, from 250 to 450 mg/l, appeared in an analysis done in 1963. Almost three-quarters of the 270 mg/l increase in the TDS content is attributed to the increased sulfate. If this analysis between 1962 and 1970 were not available, the increase in sulfate would never have been known in this location. This serves as an example of one of the problems involved in deciding on sample intervals when developing a monitoring methodology.

There are three complete analyses available for well No. 248 (Plate 2.4), in the southwestern Imperial Valley, just southwest of the Elsinore Fault trace. These analyses took place in 1959, 1962 and 1972. Basically, the water is very low in TDS, on the order of a few hundred milligrams per liter, but a noticeable change in the character of the water occurred between 1959 and 1962, when it changed from a sodium magnesium bicarbonate chloride water to a sodium bicarbonate chloride water. That is, a marked reduction in magnesium, from 67 to 3.2 mg/l, occurred in this period. In the period from 1962 to 1972 there was a significant increase in sulfate, from 25 to 46 mg/l, and TDS from 262 to 390 mg/l.

Well No. 393, a shallow well in the extreme southwestern Imperial Valley (Plate 2.4), shows a change in character in between the end points of a sample period, as did well No. 160. The samples for 1967 and November 1972 are quite similar sodium carbonate chloride waters with a somewhat smaller calcium content in November 1972 than in 1967. The TDS content was 360 mg/l in 1967 and 341 mg/l in November 1972. However, a sample taken in July 1972 exhibits distinctly higher sulfate and a TDS content of 455 mg/l. This example again points out the necessity to remain aware of possible undetected changes in water characteristics between sampling periods.

Well No. 731, in the intermediate depth artesian aquifer west of the East Highline Canal (Plate 2.6), shows a slight reduction in TDS, from 2,510 mg/l in 1961 to 2,440 mg/l in 1970, accompanied by an increase in sulfate from 88 to 130 mg/l.

2.5.2 Single-Chemical Parameter Contoured Surface Plots

The areal distribution of the concentration of five representative chemical parameters is schematically shown by the three-dimensional surfaces plotted on Figures 2.40 through 2.44. The five chemical parameters contoured in this manner are specific conductance, sulfate, bicarbonate, chloride and calcium. Interpretation and comparison of the patterns of each of these surfaces will aid in determination of chemical and/or structural trends, areas of high correlation between parameters and areas of low or no correlation between others.

This technique depicts the areal variation of the concentration of any single parameter or combination of parameters. This is accomplished by inputting into the computer the parameter values and their corresponding geographic coordinates. Computer routines then generate a contour map of these values. Once the contour map is completed another routine generates an "orthogonal projection" of the contour map, resulting in the three-dimensional perspective of the contoured surface.

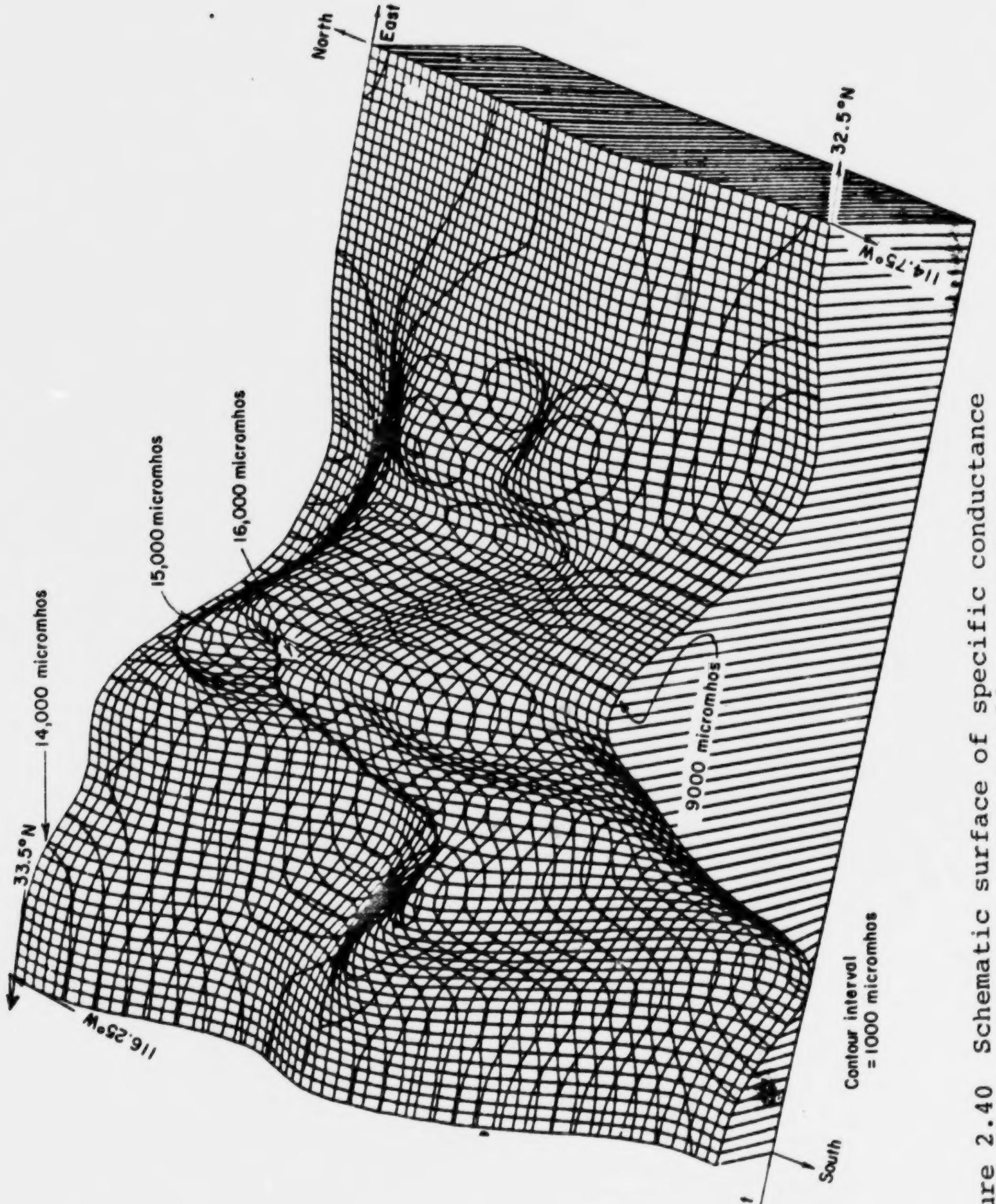

Figure 2.40 Schematic surface of specific conductance values in Imperial Valley groundwater.

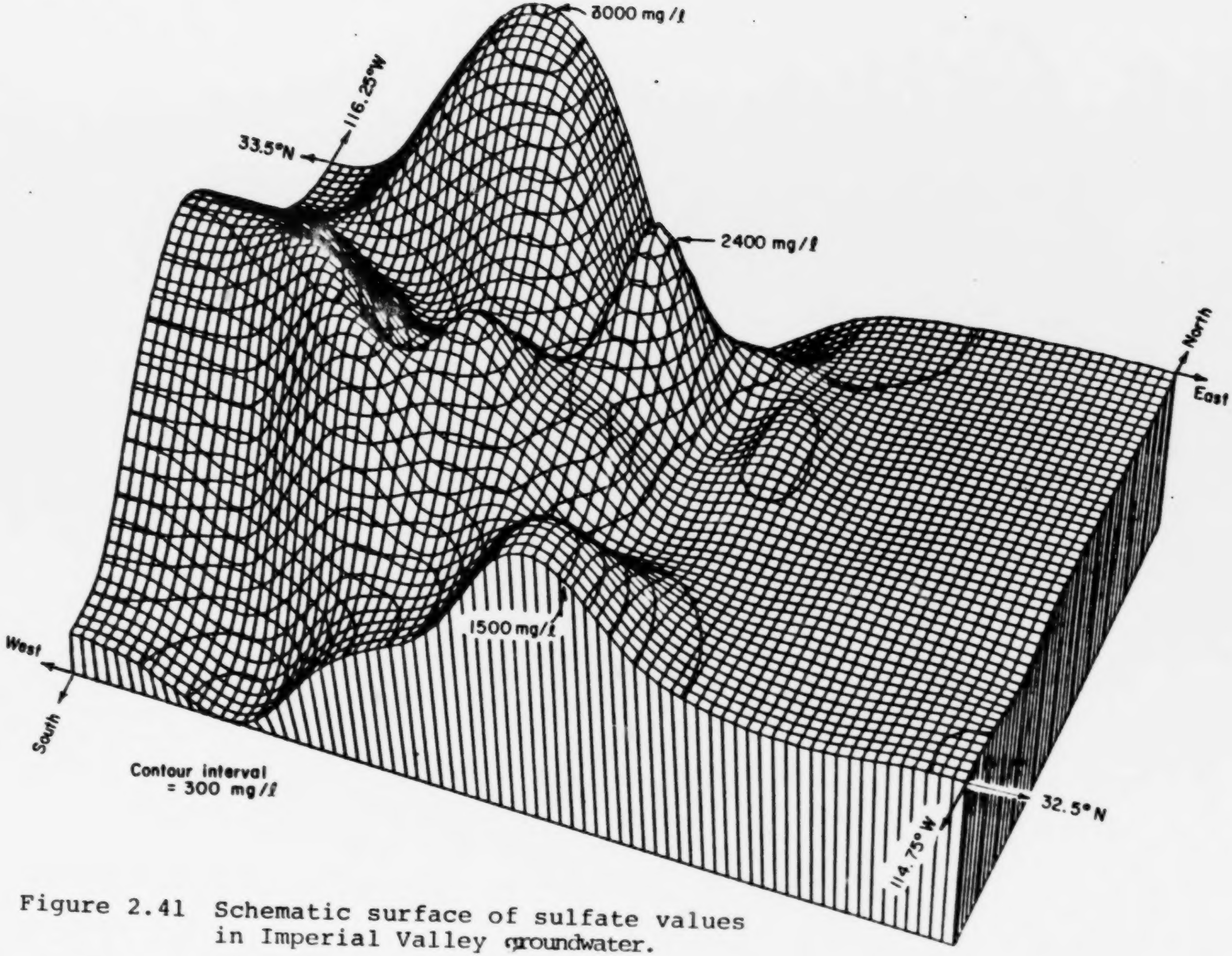

Figure 2.41 Schematic surface of sulfate values in Imperial Valley groundwater.

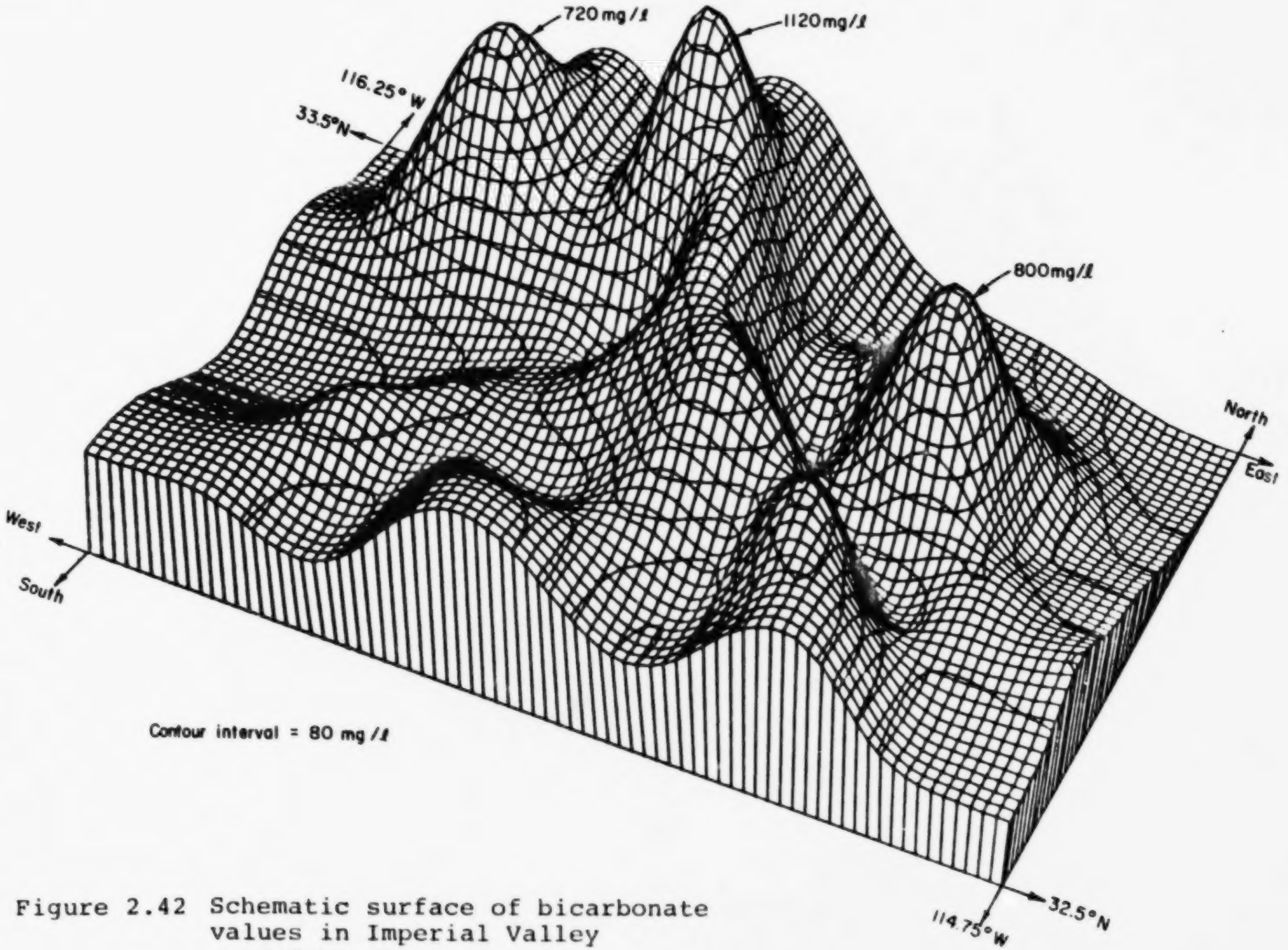

Figure 2.42 Schematic surface of bicarbonate values in Imperial Valley groundwater.

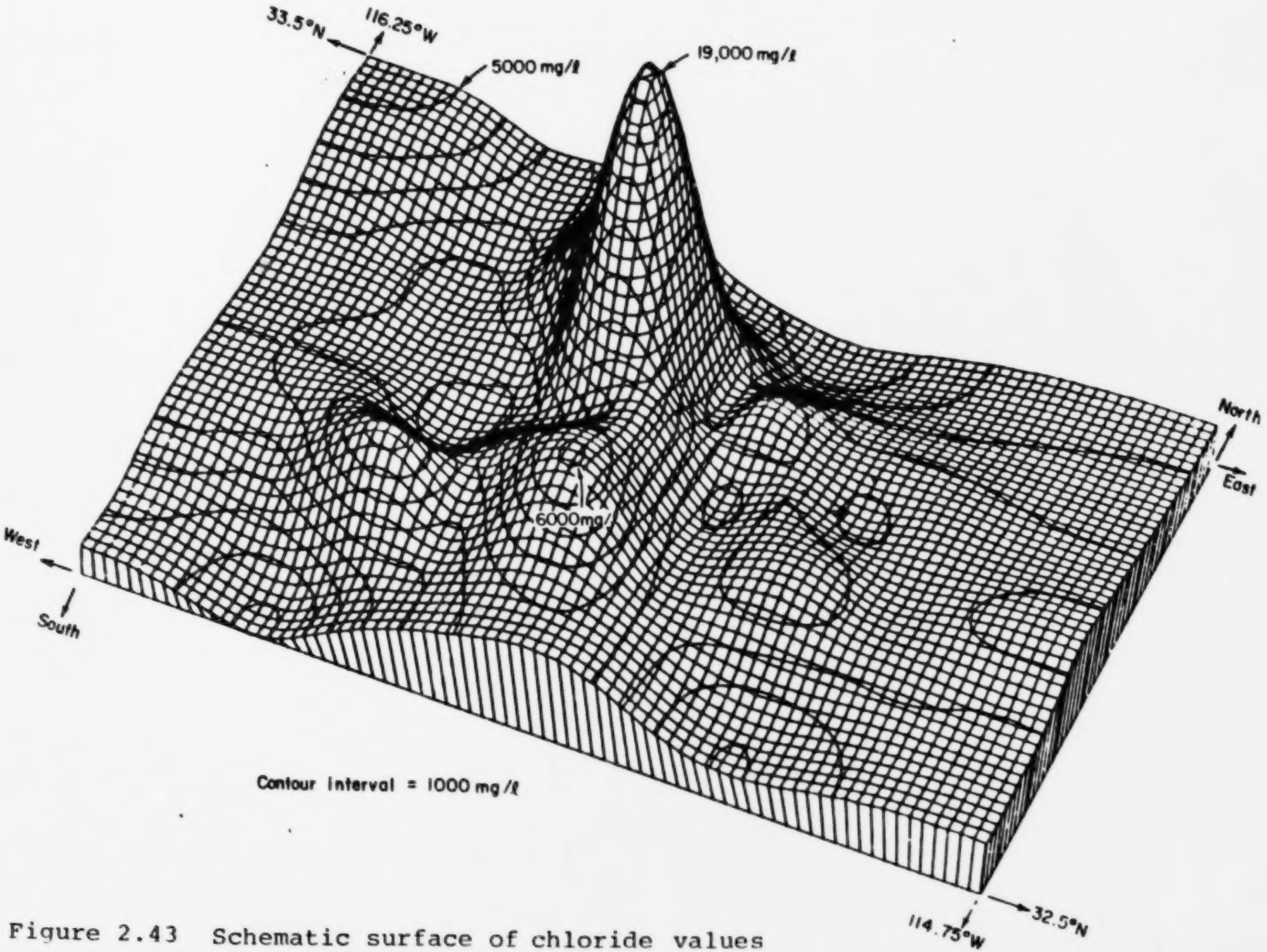

Figure 2.43 Schematic surface of chloride values in Imperial Valley groundwater.

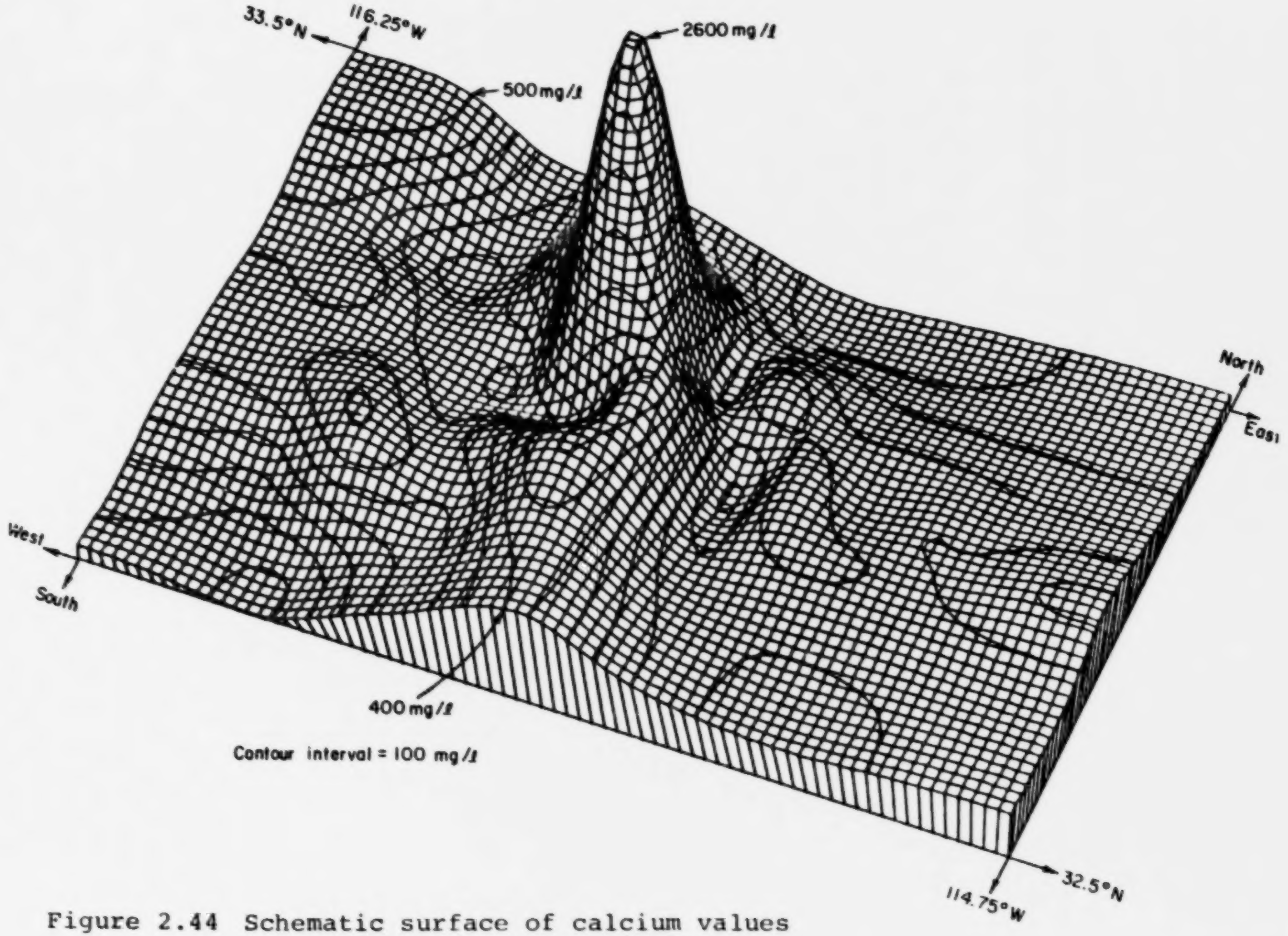

Figure 2.44 Schematic surface of calcium values in Imperial Valley groundwater.

Limitations--

These chemical parameter surfaces were plotted using an available digitized water quality data base and available computer library graphic routines. Limitations in the digitized data base and limitations in the capabilities of the computer library graphic routines necessitated certain compromises in the resulting plots.

The rationale behind this approach was to determine, with minimum development cost, the feasibility of utilizing this methodology in hydrologic and water quality studies. These limitations and compromises are outlined below and should be kept in mind when perusing the plots.

The structure and content of the data base did not allow separation of the plotted surfaces by aquifer depth interval because there was an insufficient number of water quality analyses with the information necessary for this separation. That is, the minimum areal distribution of data points necessary to produce a reasonable contour map was not available. Therefore, the resulting plots represent essentially all perforated depth intervals except those in our sample which explicitly stated a perforated depth interval that included a depth less than 24 m (80 ft) or any well whose depth was less than 24 m (80 ft).

The remaining limitations involve the computer routines. The available contouring routine requires the input data values to be arranged in a regular rectangular grid. Since our data had a somewhat random areal distribution, it was necessary to generate a surface through the data points with a bicubic spline subroutine which then overlaid a rectangular grid on this surface. The intersection points of the generated surface and this rectangular grid were then fed into the contouring program. This technique resulted in a generalization and averaging of the original data that could not be monitored or controlled. Therefore the surface that is contoured and plotted does not precisely represent the actual input data. Some particularly high or low values were averaged; a maximum value cutoff had to be established for some plots so the lesser variations would not be masked by a very large contour interval; some unrepresentative wells received undue emphasis; and so on. Therefore these surfaces are currently only a schematic representation of the true data and actual values cannot be read from the plots. Despite these difficulties, the plots demonstrate that they may potentially be a valuable technique to rapidly appraise chemical changes and correlations in the ground water system, as well as geologic and structural relations.

The five chemical parameters shown in Figures 2.40 through 2.44 were chosen largely for demonstration purposes; however, the modified Stiff diagrams on Plates 2.4, 2.6 and 2.8 were studied in an attempt to choose parameters that would show some distinguishing areal distributions. It appears that the parameters chosen do demonstrate the potential utility of the technique.

Discussion of the Contoured Surfaces--

A preliminary description of some features of the computer contoured surfaces follows. Much more information could be derived from these plots with further study and correlation with specific geothermal, lithologic and structural locations as well as with improvements in the graphical techniques.

The schematic surface of specific conductance values in Imperial Valley ground water (Fig. 2.40) shows an extremely distinct northerly trending discontinuity going up in a significant, sharp rise to the west. Since specific conductance is proportional to salinity, it is readily apparent from this plot that there is a distinct high salinity trend running northerly through the central part of the valley, and it drops off to both the east and west, albeit more steeply to the east. The drop in specific conductance near the southwest corner of the plot may be correlated with the ground water barrier effect of the Elsinore Fault zone separating the very pure water entering the valley from the Peninsular Range, to the southwest of the fault, from the more saline central valley waters.

The schematic surface of sulfate values in Imperial Valley ground water (Fig. 2.41) shows much higher sulfate in the western side of the valley. The sulfate values on the eastern side of the valley are surprisingly consistent. This trend is different from what one would expect from looking at the modified Stiff diagrams, which show the characteristic Colorado River waters in the southern valley with high percent reactance sulfate. Upon further study the sulfate highs on the plot may be correlated with geothermal fields or other structures.

The schematic surface of bicarbonate values (Fig. 2.42) is quite erratic, with high peaks distributed throughout the central and eastern parts of the valley. A distinct north-south or northwest-southeast discontinuity appears in the east-central part of the valley, probably at the boundary of the artesian aquifer (i.e., at the Alamo River). Values of this discontinuity rise to the west and then the schematic surface of bicarbonate values gradually decreases to the west. One very high peak occurs at the location of the artesian aquifer, which contains predominantly sodium bicarbonate water.

The schematic surface of chloride values in Imperial Valley ground water (Fig. 2.43) was expected to have a high correlation with the schematic specific conductance value surface, but it correlates very poorly, if at all. The chloride surface shows one extreme peak in the location of the Salton Sea geothermal field. Values are generally higher in the western and northwestern parts of the valley.

One very interesting correlation is that between the schematic chloride surface and the schematic surface of calcium values (Fig. 2.44). These two plots are essentially congruous, despite the fact that the actual concentrations plotted for chloride are about five to ten times those plotted for calcium. This illustrates one more potential use of this technique. That is, one can see the areal distribution of ratios between different ions. For example, if one compiled cross plots and tables of all data for an area to determine constituent ratios, the areal distribution of these constituents would not be considered in the calculation. With plots such as those represented here one could easily determine which areas have high correlations between which constituents and which areas do not. The separate correlation calculation could be made for separate geographic areas.

A useful adjunct to utilization of this technique would be accompanying plots of residual surfaces, the residuals being the difference between the actual data value and the smoothed, computed surface value at each actual data point. This would aid in determining which trends are based on field data and which are more the result of the computer smoothing routines.

2.5.3 Trace Elements in Geothermal Waters

Geothermal waters contain an unusually high concentration of trace elements compared to meteoric and sea water. Table 2.6 presents trace element analyses of geothermal wells located on Plate 2.8 and analyses for Salton Sea water and standard ocean water for comparison. Note the relatively high concentration of trace elements in Salton Sea geothermal waters as compared to waters from Heber and Cerro Prieto.

Geothermal waters in most instances cannot be used as a domestic or irrigation water resource, due to high salinity and high concentrations of trace elements, especially arsenic, boron, barium, fluoride, manganese and zinc. These waters also contain significant quantities of lithium, an element so unusual in ordinary water that it is used as a tracer in groundwater studies (Phelps and Anspaugh, 1976).

Because the trace element concentrations in water from various geothermal fields and even from individual geothermal wells in the same field substantially differ, hazards due to trace element concentrations must be individually evaluated.

A good background discussion of water quality with respect to potential use appears in the section titled "Relationship of Quality of Water to Use" in Hem (1970) and in Appendix A, "Identification Systems and Criteria Used in this Report," in California Department of Water Resources (1970). Therefore, this topic will not be addressed here.

TABLE 2.6 TRACE ELEMENT COMPOSITION OF SALTON TROUGH GEOTHERMAL WATERS

WELL NAME	NOWLIN #1	HOLTZ #1	HOLTZ #2	C.B. JACKSON #1	J.D. JACKSON #1	WILSON #1	MESA 6-1	MESA 6-2
SOURCE	GEONOMICS '76					COSNER '77		
MAP #	500	501	502	503	504	800	802	803
LOCATION	Heber	Heber	Heber	Heber	Heber	Brawley	E. Mesa	E. Mesa
DATE							6-9-76	10-23-73
	(ppm)	(ppm)	(ppm)	(ppm)	(ppm)	(mg/l)	(mg/l)	(mg/l)
Ag							<0.013	<0.004
Al	0.4	15	12	0.5	18		0.04	
Ar								
As							0.26	0.045
B	4.8	4.1	8	4.8	5.2		9.75	
Ba		6	3	3	3			
Br								
Cd							0.010	0.002
Cs								1.82
Co							0.06	
Cu	0.2	0.5	0.4	0.4	0.4			
CO_2								
F	1.6	1.7	1.5	0.9	0.6		0.99	3.2
Fe	0.9	15	5	20	10	0.4	8.8	0.06
Ge							<0.1	
Hg							0.002	0.007
Li	6.6	4	4.1	2.8	3.4		40	4
Mo							0.005	
Mn		0.9	0.9	1.3	1.9		0.95	0.01
Ni							0.1	0.02
NO_3							trace	<0.1
NH_4						165	40.75	17
PO_4							0.02	0.8
Rb								0.6
SiO_2	120	268	187	267	268		320	250
Sr		37	42	32	36			0.17
Zn	0.68	0.3	0.1	0.4	0.5			0.08
Zr								
H_2S								

TABLE 2.6 (continued)

WELL NAME	MESA 8-1	MESA 31-1	ELMORE #1	IID #1	MAGMAMAX #1	PIONEER #3	RIVER RANCH #1	SINCLAIR #3
SOURCE	COSNER '77							
MAP #	804	805	806	808	811	812	813	814
LOCATION	E. Mesa	E. Mesa	Salton Sea	Salton Sea	Salton Sea	Salton Sea	Salton Sea	Salton Sea
DATE	6-22-76	6-18-76						4-19-62
	(mg/l)	(mg/l)	(mg/l)	(mg/l)	(mg/l)	(mg/l)	(mg/l)	(ppm)
Ag	<0.01	<0.01		<1	0.43			0
Al	0.02	0.02	<15				94	
Ar								10
As	0.053	0.025						
B	1.6	2.5	350	390			470	210
Ba			480	250	55.3		199	540
Br								
Cd	trace	0.02			1.12		137	
Cs				20	250			
Co	0.01	0.02						
Cu			12	3			6.5	0
CO_2				500				
F	1.6	1.42			12			2.4
Fe	<0.1	<0.1	2,500	2,000	172	50	1,305	166
Ge	<0.1	<0.1						
Hg	0.014	0.008			0.014			
Li	1.1	0.6	270	210	75.6		259	49
Mo	0.005	0.005						
Mn	0.01	0.01	570	1,370			1,375	410
Ni	<0.1	<0.1			1.05		6.5	
NO_3	0.34					1,050	26	
NH_4	4.95	2.45			570		496	340
PO_4	<0.1	<0.01			<0.8			
Rb				70	50.4			
SiO_2	389	274		400	435		760	350
Sr	2.1	1.4	1,050	440	102.4		470	360
Zn				500	283		724	
Zr	<0.01	<0.01						
H_2S								

TABLE 2.6 (continued)

WELL NAME	SINCLAIR #4	I-A	M-5	M-8	SALTON SEA	SEA WATER
SOURCE	COSNER '77	REED '72	REED '72	REED '72	DWR '70	GOLDBERG '63
MAP #	815	505	507	510		
LOCATION	Salton Sea	Cerro Prieto	Cerro Prieto	Cerro Prieto	11S/11E-21P	
DATE	7-5-67					
	(ppm)	(mg/l)	(mg/l)	(mg/l)	(mg/l)	(mg/l)
Ag						0.0003
Al						0.01
Ar						
As	10				0	0.003
B	332	7	9.9	11	9.2	4.6
Ba					1	0.03
Br	25					65
Cd					<0.005	0.00011
Cs						0.005
Co					<0.0005	0.005
Cu					0.005	0.003
CO_2						
F	14				3.2	1.3
Fe	1,148				0.01	0.01
Ge						0.00007
Hg					<0.2	0.00003
Li	287				3.2	0.17
Mo						0.01
Mn	1,025				0.01	0.002
Ni					.003	0.002
NO_3	5				14	
NH_4	442					
PO_4						
Rb						0.12
SiO_2	90	220	1,060	942		6.4
Sr	434				11	8
Zn					0.062	0.01
H_2S		109	1,270	1,159		

2.6 SEISMICITY

Imperial Valley is one of the most seismically active areas in the United States. Geothermal production and reinjection may induce seismicity in and around geothermal areas in Imperial Valley. It is necessary to distinguish between naturally occurring seismicity and induced seismicity to assess this potential environmental impact. The following section discusses historical seismicity, microseismicity, seismic risk and the relation between earthquakes and geothermal activity in Imperial Valley area in order to define a baseline level of seismicity and seismic risk.

2.6.1 Historical Seismicity

The Salton Trough in general, and Imperial Valley in particular, is characterized by a high level of seismic activity and a large amount of strain release. Richter (1958) reports that twelve earthquakes of magnitude (M) 6 or greater have occurred in the Salton Trough since 1900, and nine earthquakes greater than magnitude 6.7 have occurred since 1850.

Plate 2.10 is an historical seismicity map for earthquakes reported by the National Oceanic and Atmospheric Administration (NOAA) Earthquake Data File, through June 1976. (Meyers and von Hake, 1976). This map shows the geographic distribution of instrumentally recorded epicenters in Imperial Valley from 1932 to 1975, with a few additional epicenters located from 1927 to 1931. The density of epicenters is much greater in the western part of the valley, especially along the San Jacinto Fault Zone. The minimal number of epicenter locations along the San Andreas Fault Zone in the eastern part of the valley supports the hypothesis of a shift to the west of the locus of energy release in the San Andreas Fault south of Bombay Beach (see "Salton Trough Fault Zone" subsection, Section 2.3.3).Until additional stations were added in 1973, this eastern portion of the map was near the boundary of coverage for the Cal Tech seismographic network. Allen, et al., (1965) are confident that this low level of activity is representative of the actual seismicity of this eastern area.

Although earthquakes are generally correlated with faults, this correlation is not apparent in the Imperial Valley seismicity map. This scatter in the epicenter locations is probably due to:

1) inaccurate locations of epicenters, especially earlier locations,

2) high density of fault traces, many of which have not been identified yet,

3) seismicity at depth, which may not be directly correlated with surface geology,

4) earthquakes not always occurring on preexisting breaks, and

5) the fact that much strain may be released through fault creep.

A 20-year average of cumulative shear taken from the Peninsular Range to the Chocolate Mountains (Whitten, 1956) suggests that the entire San Andreas Fault System in the Imperial Valley area is moving right-laterally at an average rate of approximately 80 mm/yr (3.1 in/yr). The actual movement is by no means constant but has varied greatly with time (Garfunkel, 1972a) and location in the valley (Scholz and Fitch, 1969). Earthquakes occurring along the San Andreas Fault System typically have focal depths of 5 to 8 km (3 to 5 mi), which is approximately the basement-sediment interface. Events generally occur on nearly vertical fault planes and are often associated with Quaternary fault scarps. A limiting depth for hypocenters in the valley is about 12 to 15 km (8 to 9 mi) because at depths greater than this the high thermal gradients generate temperatures sufficient to cause the rocks to move plastically in response to stress; in the geothermal areas of the valley this limiting depth is about 8 km (5 mi) lower (Johnson and Hadley, 1976).

The Imperial Valley Earthquake of 1940--

In terms of human disturbance the Imperial Valley earthquake of May 18, 1940,was the most significant earthquake in the Salton Trough. Damage caused by the earthquake extended into Baja California (Mexico), the adjacent Yuma Valley and the Salton Sea area to the north. The shock had a magnitude of 7.0 (Richter, 1958) and could be felt for a radius of about 180 km (112 mi). Casualty reports show that nine persons died due to the earthquake. Damage was estimated at 5 to 6 million dollars, including loss of crops due to interruption of water services, and serious damage occurred in towns of the central and southern Imperial Valley.

The focal depth was shallow and the dominant motion was right-lateral displacement along the Imperial Fault (Plate 2.2, Nos. 16 and 16a). Surface faulting could be traced for several kilometers northwest and southeast of the epicenter but the character of the traces was variable. Northwestward, the fault displacement gradually diminished from 1.5 m (4.9 ft) offsets near El Centro to 150 mm (5.9 in) near Brawley. The fault trace curved and splayed northwestward until no evidence of surface faulting could be found north of Brawley. Southeastward, the trace was nearly straight and offsets gradually diminished until none could be found 25 km (15.5 mi) south of the border.

2.6.2 Microseismicity

High levels of microearthquake activity are associated with the Salton Sea, North Brawley and East Mesa geothermal areas (Combs and Hadley, 1977; Hill, et al., 1975a; Johnson and Hadley, 1976).

Earthquake Swarms--
Earthquake swarm activity has been documented on several occasions in the valley; in some cases, swarms occur on the same faults as major shocks (Hill, et al. 1975b; Sharp, 1976; Johnson and Hadley, 1977; Combs and Hadley, 1977). A number of swarms that have occurred since 1969 have been studied carefully and these studies have yielded a wealth of data on the structure and tectonics of the area.

Seismic events in Imperial and Mexicali Valleys during April and May 1969 were recorded after an extensive seismic net in the Salton Trough region was established by Cal Tech. From these as well as from previous recordings, and other geological data, scientists were able to support the "rhomb graben" theory for the tectonic evolution of the Salton Trough (see Section 2.3.2). The mechanism for local crustal spreading, suggested from fault plane solutions, involves en-echelon normal and strike-slip faults trending oblique to the regional transform faults. Motion along these faults could account for the observed crustal rifting.

In 1973, operation of the USGS-Cal Tech seismic net commenced in the valley. Several swarms were recorded near Brawley, Salton Buttes and El Centro on the Imperial Fault. This earthquake data tends to verify earlier observations on regional seismicity and establishes definite fault traces for the Brawley and Imperial Faults.

During late January 1975, the Brawley area was the site of a major earthquake swarm. Analyses of focal depths, temporal migration and first motions of earthquakes yielded the following observations:

1) Earthquake focal depths were shallower inside the Brawley thermal area than outside, probably because higher subsurface temperatures cause deeply buried rocks to move plastically in response to stress. Most earthquakes in this swarm occurred between 4 and 8 km (2.5 and 5 mi) depths,

2) In the Brawley field many earthquakes occurred along northeastward trending left-lateral and normal faults (east-northeast faults 17a, on Plate 2.2, for example).

This left-lateral fault motion is assumed to be responsible for the observed crustal spreading at Brawley. Some researchers have included Heber as another region of crustal spreading, but its position relative to transform fault segments makes this assertion doubtful. Earthquake activity at Heber is also noticeably less than at North Brawley or Salton Buttes.

Microseismic Monitoring Networks--
In 1973 the USGS, in cooperation with Cal Tech, established a 16 station telemetered seismograph network in Imperial Valley to record and interpret earthquakes related to geothermal phenomena (Hill, et al. 1975a). In the Heber area Chevron Oil Company has established a closely spaced seismic net to gather information on background seismicity and the relationship the proposed geothermal production might have on seismic activity.

In conjunction with the LLL Imperial Valley Environmental Project, the USGS has completed installation, in October 1976, of six seismometers in the Salton Sea geothermal field region (Phelps and Anspaugh, 1976). These instruments will be incorporated with the USGS regional telemetered network.

2.6.3 Seismic Risk

Earthquake-associated damage in Imperial Valley could result from fault displacement, strong ground motion (shaking), ground failure or any combination of these effects. The great majority of earthquake damage is caused by vibratory ground motion, not surface rupture. Surface rupture often does not occur. Based on intensity and duration of shaking and near-surface soil and geologic conditions, vibratory ground motion often triggers significant ground failure. Man-made structures can undergo vibration damage and natural landforms can experience liquefaction, landsliding and settlement.

The extent of this damage would depend on many variables: earthquake magnitude, epicentral location, depth of focus, duration of shaking, intensity of shaking, near-surface soil foundation and geologic conditions, and structural design. These factors influence the effect of a particular earthquake on a particular structure.

Fault traces are widespread throughout the valley and even though earthquakes will occur on faults, these faults may be located virtually anywhere in the valley. However, experience has shown that the intensity of an earthquake is not necessarily highest at the surface trace of an earthquake-generating fault.

Unless a structure is astride an active fault and can be directly affected by fault displacement, proximity to an active fault need not be given undue consideration. In most cases, ground condition and structural design are more influential parameters in determining damage due to strong ground motion and ground failure. Important input in evaluating potential damage due to ground motion and ground failure is the level of historic seismicity and expected or estimated rock accelerations.

In Figure 2.45, a frequency-magnitude relation (recurrence curve) is plotted for earthquakes in Imperial Valley during the period 1932 to 1972. Recurrence curves are useful in establishing seismic risk. This is a probablistic approach and does not mean that specific earthquake occurrences or locations can be predicted. The seismic activity used for constructing the recurrence curve is representative of the sum of all recorded earthquakes in the valley.

Maximum Ground Acceleration--

Relationships between maximum acceleration in rock, magnitude of earthquake and the distance of the rock site from the zone of energy release have been proposed by a number of investigators and summarized by Seed, et al. (1969). This work has been updated utilizing additional rock acceleration data recorded from the San Fernando earthquake of 1971 and new analytical techniques.

Figure 2.46 shows ranges of maximum rock acceleration as a function of distance from the causative fault estimated by Schnabel and Seed (1972). These rock accelerations would generally be higher for higher magnitude earthquakes. Also, as the distance from the causative fault increases, the maximum acceleration decreases. Figure 2.46 shows, for example, that an earthquake of magnitude 5.6 occurring at a distance of 20 km (12.5 m) from a given structure will most likely generate a rock acceleration of about 0.09 to 0.23 times the acceleration of gravity (g). This difference in the estimate of maximum acceleration is due to the effects of different source mechanisms, travel paths, topography and rock types.

It must be emphasized that a considerable degree of judgment should be exercised in applying these estimates to any particular site, especially if the site is not on bedrock. Local site conditions-- that is, the type of deposits that lie above bedrock and beneath a particular site--have a great influence on the amplification or attenuation of the rock acceleration. It may be noted that, except for locations very near the causative fault on earthquakes with magnitude 8 or greater, the maximum rock accelerations in Figure 2.46 are substantially lower than the maximum ground accelerations proposed by Housner (1965) (Fig. 2.47), which reflect the amplifying influence of soil deposits. The acceleration record of the 1940 Imperial Valley earthquake

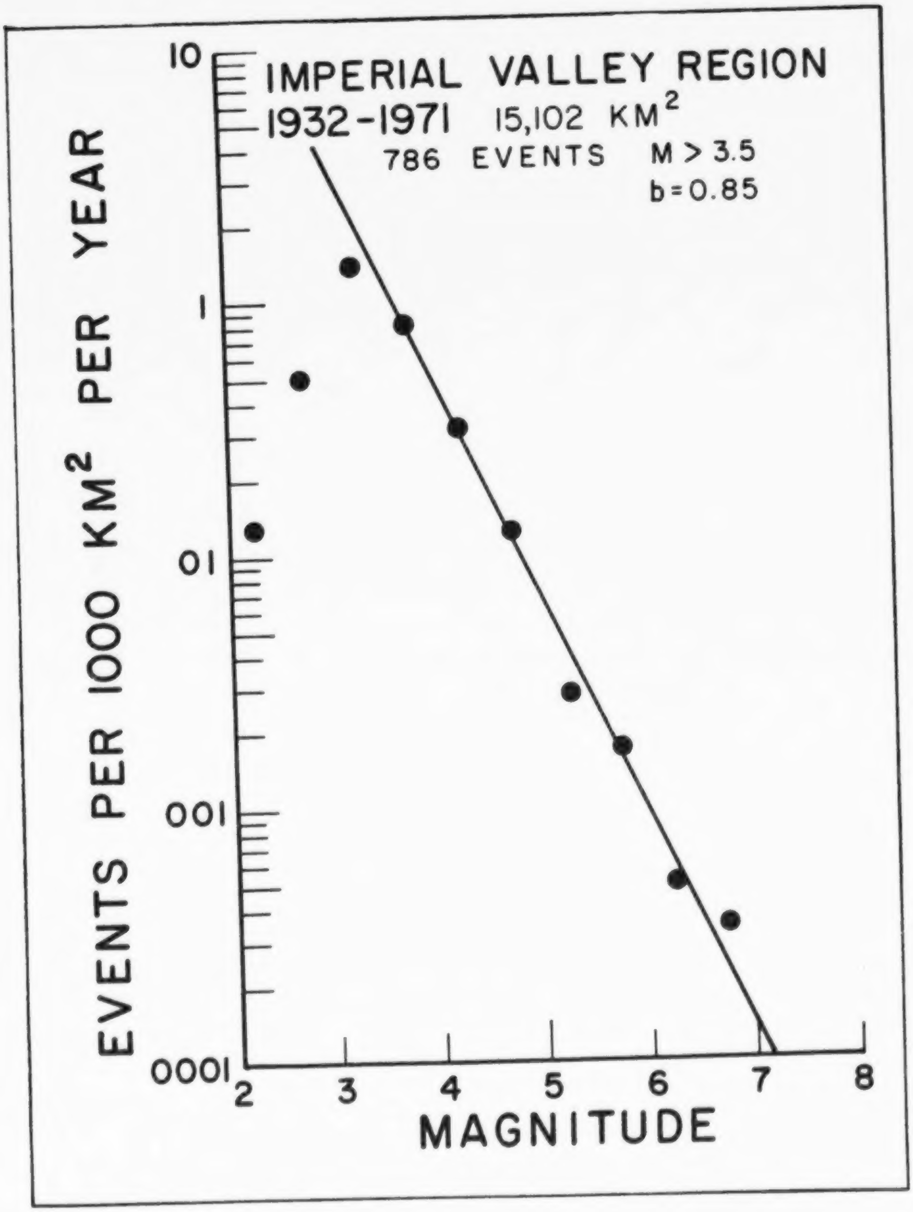

Figure 2.45 Recurrence curve for earthquakes in Imperial Valley region,1932-72. (Hileman, et al.,1973)

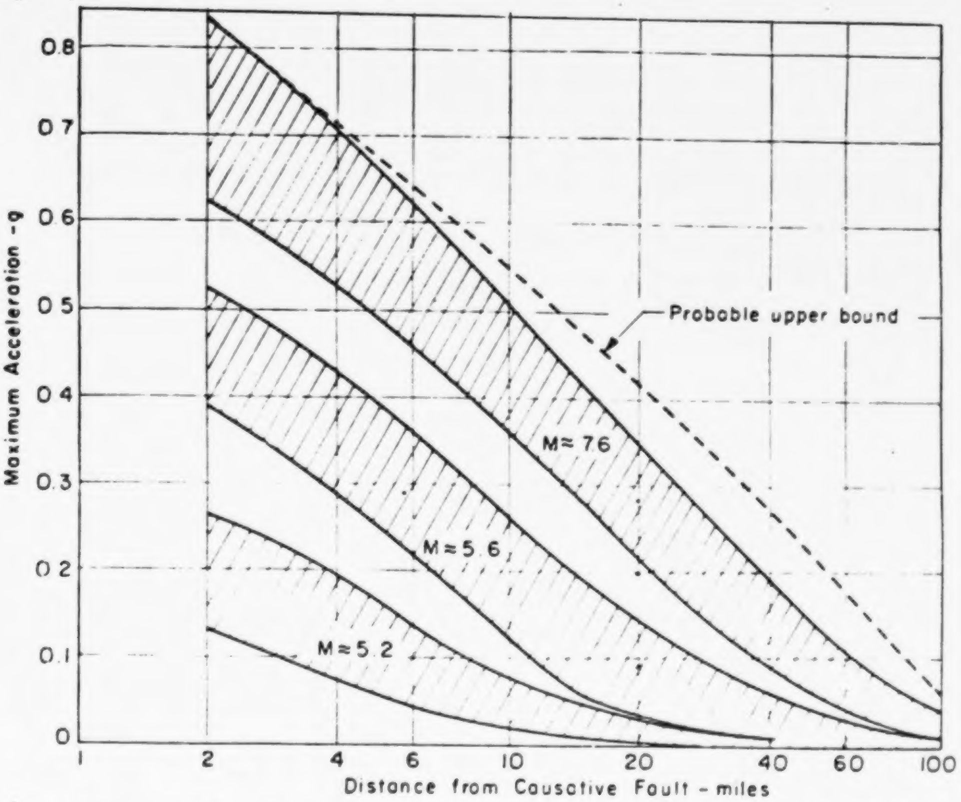

Figure 2.46 Ranges of maximum acceleration in rock. (Schnabel and Seed, 1972)

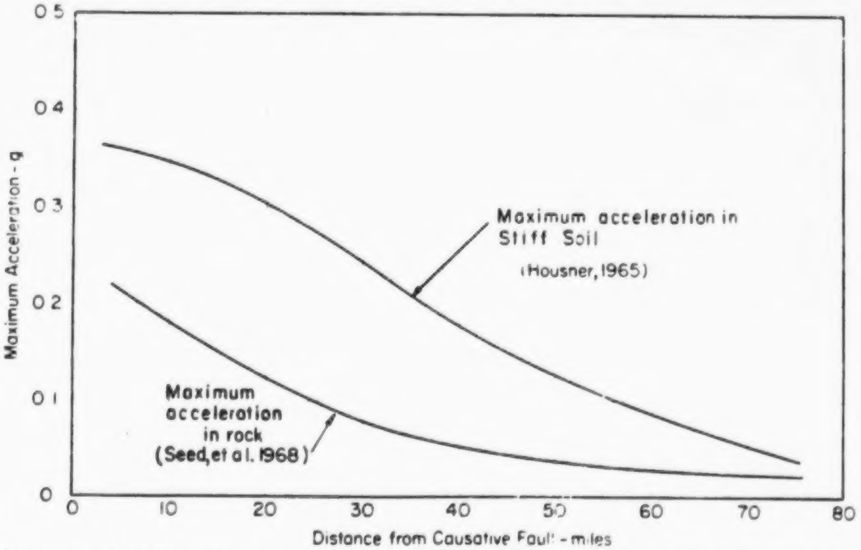

Figure 2.47 Comparison of maximum acceleration in rock and stiff soil deposits for earthquake magitude 7. (Seed, et al., 1969)

showed a maximum acceleration of 0.32 g. This value is in good agreement with the maximum anticipated acceleration on soil deposits shown in Figure 2.47. However, it is possible that if the El Centro recording station had been located on a rock outcrop, the maximum recorded acceleration would have been only about 0.20 g. In addition, Housner (1965) has claimed that the upper boundary for the maximum acceleration recorded at El Centro during the May 1940 earthquake is still higher (about 0.50 g). These differences in the motions developed at the ground surface can be attributed to the modifying influence of the soil deposits underlying the recording station.

Data presented by Duke and Leeds (1962) shows that the soil deposits at the recording station at El Centro consist of about 30 m (99 ft) of stiff clay underlain by several hundred meters of sediments. The maximum accelerations recorded over such sites would tend to be higher than anticipated for sites on rock outcrop. Hence, Housner's curve for stiff soil conditions (Fig. 2.47) is more applicable for the El Centro site.

The preceding discussion points out the wide variations in recorded accelerations that can be caused by local site conditions. Still greater scatter may be caused by other factors, such as earthquake source mechanisms and seismic wave travel paths. For this reason, site specific ground acceleration studies must be completed for each prospective plant site to determine the actual earthquake risk at that site.

2.6.4 Relation of Earthquakes to Geothermal Activity

Two relationships between earthquakes and geothermal activity have been noted. The first one is a correlation of microearthquake activity and geothermal anomalies which may be useful in the discovery of geothermal resource areas. The second is fluid withdrawal, with or without reinjection, which may trigger local seismic activity.

With respect to the first correlation, high levels of microearthquake activity are associated with the Salton Sea, North Brawley and East Mesa geothermal areas (Combs and Hadley, 1977; Hill, et al.,1975a,Johnson and Hadley, 1976). Ward (1972) suggests that shocks are generally more frequent and of smaller magnitude in geothermal areas than in other areas of the same tectonic setting. Faults related to these microearthquakes may serve as conduits for circulating brines. In fact, faults in Imperial Valley may be the "plumbing" for some of the geothermal areas. For example, at the Salton Sea geothermal area it was observed that carbon dioxide wells began emitting large quantities of gas just after earthquakes in the 1930's. Also, earthquake focal depths are usually shallower in geothermal areas than in other seismic areas, implying that microearthquakes are related to geothermal processes.

The possibility of triggering earthquakes by geothermal production and reinjection is of some concern. Although existing producing fields at The Geysers, California, and Wairakei, New Zealand, have long been associated with preexisting earthquake activity, neither production areas nor the surrounding communities have been hampered by earthquakes and no associations have been drawn between geothermal production and earthquake activity.

Existing oil field and waste well data have yielded clues to the effect of fluid injection on triggering earthquakes. Of the thousands of existing oil field and waste injection wells, only a few instances of earthquakes triggered by fluid injection have been cited in the literature. One of them is at the Rocky Mountain Arsenal waste disposal well near Denver, Colorado, and another is at the Rangely Oil Field in northwestern Colorado (Raleigh, et al., 1976). Epicenters of injection-induced earthquakes at Rangely are shown in Figure 2.48. The largest event registered here was a magnitude 6 earthquake. Earthquakes are inferred to be caused by an increase in pore pressure that results in shear failure, therefore reducing the normal stress across fracture surfaces. However, regional tectonics, the stress field and rock properties in Imperial Valley are different from Rangely, so the Rangely experience may not be applied to Imperial Valley.

Withdrawal of geothermal fluids may alter deep ground water flow patterns, and perhaps even the surface flow rate. The effect of these alterations on the tectonic stress regime is unknown. Any attempt to assess these effects now, and the effect of fluid reinjection, is speculative. It will require several years of continuous monitoring activity, superimposed on the known background seismicity, to understand the possible withdrawal and reinjection effects.

Two criteria can be considered useful in detecting induced earthquakes: frequency-magnitude (recurrence) statistic changes in the area of the geothermal field, and changes in depth and location of events from pre-production activity (Phelps and Anspaugh, 1976).

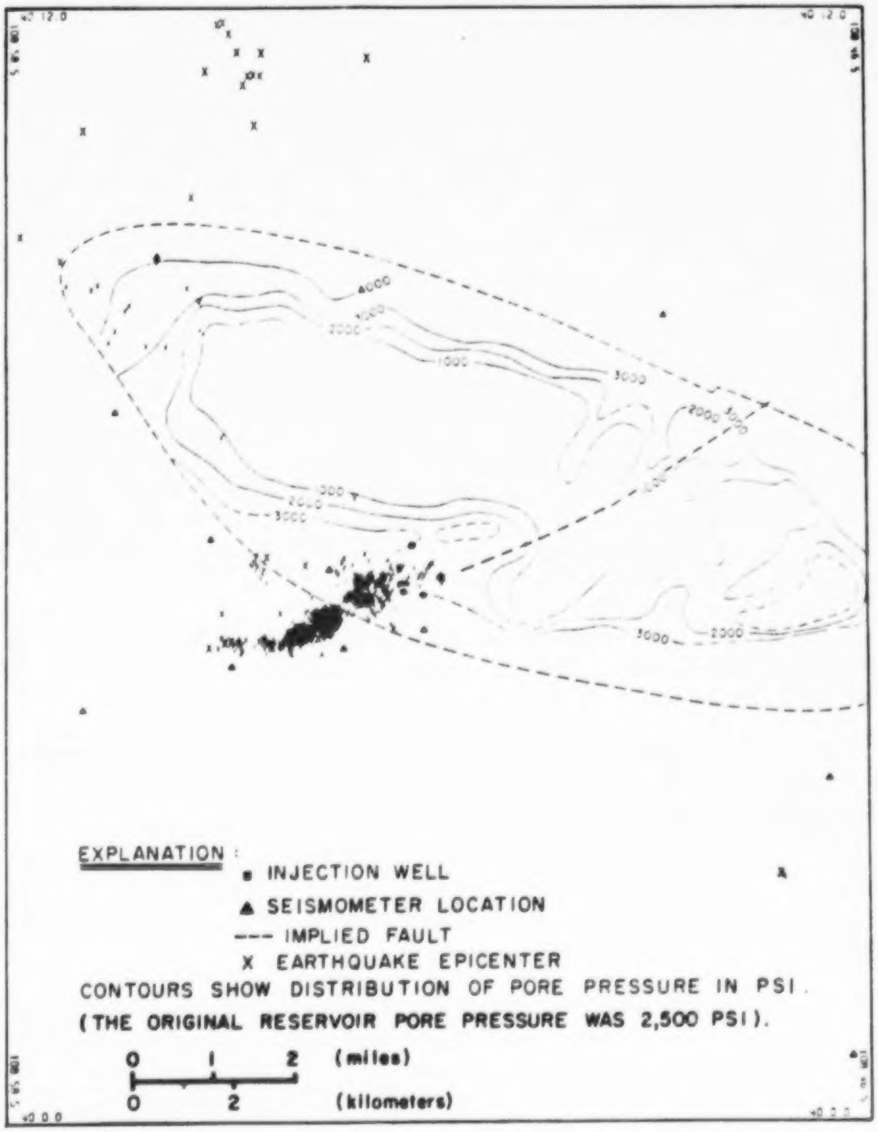
40 12.0
4000
3000
2000
1000
EXPLANATION :
■ INJECTION WELL
▲ SEISMOMETER LOCATION
--- IMPLIED FAULT
X EARTHQUAKE EPICENTER
CONTOURS SHOW DISTRIBUTION OF PORE PRESSURE IN PSI.
(THE ORIGINAL RESERVOIR PORE PRESSURE WAS 2,500 PSI).
0 1 2 (miles)
0 2 (kilometers)
40 0.0

Figure 2.48 Epicenters of injection-induced earthquakes at Rangely, Colorado. (Raleigh, et al., 1972)

REFERENCES

Allen, C. R., A. Grantz, J. N. Brune, M. M. Clark, R. V. Sharp, E. W. Theodore, E. W. Wolfe and M. Wyss. The Borrego Mountain, California Earthquake of 9 April 1968: A Preliminary Report. Bull. Seism. Soc. Am., v. 58, p. 1183-1186, 1968.

Allen, C. R., P. St. Amand, C. F. Richter and J. M. Nordquist. Relationship Between Seismicity and Geologic Structure in the Southern California Region. Bull. Seis. Soc. Am., v. 55, p. 753-787, 1965.

Allen, C. R., M. Wyss, J. M. Brune, A. Grantz and R. E. Wallace. Displacements on the Imperial, Superstition Hills, and San Andreas Faults triggered by the Borrego Mountain Earthquake. USGS Prof. Paper 787, 207 p., 1972.

Allison, E. C. Geology of Areas Bordering Gulf of California--A Symposium. Am. Assoc. Pet. Geol. Mem., v. 3, p. 3-29, 1964.

Arnal, R. E. Limnology, Sedimentation, and Microorganisms of the Salton Sea, California. Bull. Geol. Soc. Am., v. 72, p. 427-478, 1961.

Babcock, E. A. Structural Geology and Geophysics of the Durmid Area, Imperial Valley, California. Institute of Geophysics and Planetary Physics, University of California, Riverside, 145 p., November, 1969.

__________. Detection of Active Faulting Using Oblique Infrared Aerial Photography in the Imperial Valley, California; in Cooperative Geological-Geophysical-Geochemical Investigations of Geothermal Resources in the Imperial Valley Area of California, R. W. Rex, Principal Investigator, University of California, Riverside, p. 143-150, 1971.

__________. Geology of the Northeast Margin of the Salton Trough, Salton Sea, California. Bull. Geol. Soc. Am., v. 35, p. 321-332, March 1974.

Berry, F. A. F. Proposed Origin of Subsurface Thermal Brines, Imperial Valley, California (abs.). Bull. Am. Assoc. Pet. Geol., v. 50, No. 3, p. 644-645, 1966.

Biehler, S. Geophysical Study of the Salton Trough of Southern California. Ph. D. diss., California Institute of Technology, unpub., 139 p., 1964.

__________. Gravity Studies in the Imperial Valley; in Cooperative Geological-Geophysical-Geochemical Investigations of Geothermal Resources in the Imperial Valley Area of California, R. W. Rex, Principal Investigator, University of California, Riverside, p. 29-43, 1971.

Biehler, S., R. L. Kovach and C. R. Allen. Geophysical Framework of Northern End of Gulf of California Structural Province; in Marine Geology of the Gulf of California, Am. Assoc. Pet. Geol. Mem., v. 3, p. 126-143, 1964.

Bird, D. K. Geology and Geochemistry of the Dunes Hydrothermal System, Imperial Valley of California. M.S. thesis, University of California, Riverside, unpub., 132 p., 1975.

Black, W. E., J. S. Nelson and J. Combs. Thermal and Electrical Resistivity Investigations of the Dunes Geothermal Anomaly, Imperial Valley, California. EOS Trans. Am. Geophys. Un. 54, No. 11, p. 1214, 1973.

Blaney, H. F. Evaporation from and Stabilization of Salton Sea Water Surface. Trans. Am. Geophys. Union, v. 36, No. 4, p. 633-640, 1955.

Brune, J.N.,and C. R. Allen. A Microearthquake Survey of the San Andreas Fault System in Southern California. Bull. Seism. Soc. Am., v. 57, p. 277-296, 1967.

Burchfiel, B. C.,and G. A. Davis. Structural Framework and Evolution of the Southern Part of the Cordilleran Orogen, Western United States. Am. J. Sci., v. 272, p. 97-118, 1972.

Bureau of Reclamation. Geothermal Resource Investigations, East Mesa Test Site, Imperial Valley, California, A Status Report. U. S. Dept. of the Interior, 64 p., November 1974.

Bushee, J., J. Holden, B. Geyer and G. Gastil. Lead-alpha Dates for some Basement Rocks of Southwestern California. Bull. Geol. Soc. Am., v. 74, p. 803-806, 1963.

California Department of Water Resources. Geothermal Wastes and the Water Resources of the Salton Sea Area. Bull. 143-7, 123 p., 1970.

Carnegie Institute of Washington. Yearbook 22. Washington, D.C., p. 66, 1924.

Christensen, A. D. Part of the Geology of the Coyote Mountain Area, Imperial County, California. M.A. thesis, University of California, Los Angeles, unpub., 188 p., 1957.

Combs, J., Heat Flow and Geothermal Resources for the Imperial Valley; in Cooperative Geological-Geophysical-Geochemical Investigations of Geothermal Resources in the Imperial Valley Area of California, R. W. Rex, Principal Investigator, University of California, Riverside, p. 5-28, 1971.

__________. Thermal Studies; in Cooperative Investigation of Geothermal Resources in the Imperial Valley and Their Potential Value for Desalting of Water and Other Purposes, R. W. Rex, Principal Investigator, University of California, Riverside, p. B1-B23, 1972.

Combs, J., and D. Hadley. Microearthquake Investigation of the Mesa Geothermal Anomaly, Imperial Valley, California. Geophysics, v. 42, No. 1, p. 17-33, 1977.

Coleman, G. A. A Biological Survey of the Salton Sea. Cal. Dept. of Fish and Game, v. 15, No. 3, p. 218-227, 1929.

Coplen, T. B. Origin of the Geothermal Waters in the Imperial Valley of Southern California; in Cooperative Investigations of Geothermal Resources in the Imperial Valley Area and Their Potential Value for Desalting of Water and Other Purposes, R. W. Rex, Principal Investigator, University of California, Riverside, p. E1-E33, 1972.

__________. Cooperative Geochemical Resource Assessment of the Mesa Geothermal System. Institute of Geophysics and Planetary Physics, University of California, Riverside, Final Report to U.S. Department of the Interior, Bureau of Reclamation, Contract No. 14-06-300-2479, 97 p., 1976.

Coplen, T. B., J. Combs, W. A. Elders, W. R. Robert, G. Burckhalter and R. Laird. Preliminary Findings of an Investigation of the Dunes Thermal Anomaly, Imperial Valley, California. Department of Water Resources, State of California, and the Institute of Geophysics and Planetary Physics, University of California, Riverside, 48 p., 1973.

Coplen, T. B., P. Kolesar, R. E. Taylor, C. Kendall and C. Mooser. Investigations of the Dunes Geothermal Anomaly, Imperial Valley, California, Part IV. Institute of Geophysics and Planetary Physics, University of California, Riverside, 42 p., 1975.

Cosner, S., and J. Apps. Lawrence Berkeley Laboratory Brine Data File. Revision February 3, 1977.

Craig, H. The Isotopic Geochemistry of Water and Carbon in Geothermal Areas. Proc. Spoleto Conf. on Nuclear Geology; in Nuclear Geology in Geothermal Areas, ed. E. Tongiorgi, Consiglio Nazionale delle Ricerche, Pisa, p. 17-35, 1963.

__________. Isotopic Composition and Origin of the Red Sea and Salton Sea Geothermal Brines. Science, v. 154, p. 1544-1548, 1966.

Craig, H., G. Boato and D. E. White. Isotopic Geochemistry of Thermal Waters. Pub. Nat. Acad. Sci. Nat. Res. Counc. Wash., v. 400, p. 29-38, 1956.

Crowell, J. C., Displacement Along the San Andreas Fault, California. Geol. Soc. Am. Special Paper 71, 61 p., 1962.

Crowell, J. C. and T. Suzuki. Eocene Stratigraphy and Paleontology, Orocopia Mountains, Southeastern California. Bull. Geol. Soc. Am., v. 70, p. 581-592, 1959.

Dibblee, T. W. Geology of the Imperial Valley Region, Geology of Southern California. Cal. Div. of Mines and Geol., Bull. 170, Ch. 2, p. 21-28, 1954.

Duke, C.M., and D. J. Leeds. Site Characteristics of Southern California Strong-motion Earthquake Stations. Cal. Div. of Mines and Geol. Special Publication 38, 28 p., 1962.

Durham, J. W., The Marine Cenozoic of Southern California; in Geology of Southern California, R. H. Jahns, ed., Cal. Div. of Mines and Geol., Bull. 170, Ch. 3, p. 23-31, 1954.

Durham, J. W. and E. C. Allison. Stratigraphic Position of the Fish Creek Gypsum at Split Mountain Gorge, Imperial County, California. Geol. Soc. Am. Special Paper No. 68, 22 p., 19 .

Dutcher, L. C., W. F. Hardt and W. R. Moyle, Jr. Preliminary Appraisal of Ground Water in Storage with Reference to Geothermal Resources in the Imperial Valley Area. USGS Circ. 649, 57 p., 1972.

Elders, W. A., and D. K. Bird. Petrological Studies; in Investigations of the Dunes Geothermal Anomaly, Imperial Valley, California. Institute of Geophysics and Planetary Physics, University of California, Riverside, California, No. 74-13, 14 p., 1974.

Elders, W. A., R. W. Rex, T. Meidav, P. T. Robinson and S. Biehler. Crustal Spreading in Southern California. Science, v. 178, p. 15-24, 1972.

Facca, G. The Structure and Behavior of Geothermal Fields; in Geothermal Energy (Earth Sciences, 12), Paris, The UNESCO Press, p. 61-72, 1973.

Garfunkel, Z. The Tectonics of the Salton Trough of California; in Cooperative Investigations of Geothermal Resources in the Imperial Valley Area and their Potential Value for Desalting of Water and Other Purposes, R. W. Rex, Principal Investigator, University of California, Riverside, p. H1-H33, 1972a.

__________. The Structure of the Salton Trough in Southern California; in Cooperative Investigation of Geothermal Resources in the Imperial Valley Area and Their Potential Value for Desalting of Water and Other Purposes, R. W. Rex, Principal Investigator, University of California, Riverside, p. I1-I57, 1972b.

Geonomics, Inc. A Report on Some Geotechnical Aspects of the Environmental Impact of Geothermal Power Generation at Heber, Imperial Valley, California. Electric Power Research Institute, Res. Proj. 580, ER-299, Report No. 1, 79 p., 1976.

Goldberg, E. D. Chemistry - the Oceans as a Chemical System; in Composition of Sea Water, Comparative and Descriptive Oceanography, Vol. 2 of The Sea, M. N. Hill, New York Interscience Publishers, p. 3-25, 1963.

Griscom, A. and L. J. P. Muffler. Aeromagnetic Map and Interpretation of the Salton Sea Geothermal Area, California. USGS Geophys. Inv. Map No. GP-754, 1971.

Harbeck, G. E., Jr. The Effect of Salinity on Evaporation. USGS Prof. Paper 272-A, p. 1-6, 1955.

Hardt, W. F. and J. J. French. Selected Data on Water Wells, Geothermal Wells and Oil Tests in Imperial Valley, California. USGS Water Resources Division, Menlo Park, Open File Report, 1976.

Hays, W. H. Geology of the Central Mecca Hills, Riverside County, California. Ph. D. diss., Yale University, unpub., 324 p., 1957.

Helgeson, H. C. Geologic and Thermodynamic Characteristics of the Salton Sea Geothermal System. Am. J. Sci., v. 266, p. 129-166, 1968.

Hely, A. G., and E. L. Peck. Precipitation, Runoff and Water Loss in the Lower Colorado River-Salton Sea Area. USGS Prof. Paper 486-B, 16 p., 1964.

Hely, A. G., G. H. Hughes and B. Irelan. Hydrologic Regimen of the Salton Sea. USGS Prof. Paper 486-C, 32 p., 1966.

Hem, J. D. Study and Interpretation of the Chemical Characteristics of Natural Water. USGS Water Supply Paper 1473, 363 p., 1970.

Hileman, J. A., C. R. Allen and J. M. Nordquist. Seismicity of the Southern California Region, 1 January, 1932 to 31 December, 1972. Bull. Seis. Lab., California Institute of Technology, Pasadena, California, 1973.

Hill, D. P., P. Mowinckel and K. M. Lahr. Catalog of Earthquakes in the Imperial Valley, California, June 1973 to May 1974. USGS, Menlo Park, California, Open File Report No. 75-101, 25 p., 1975a.

Hill, D. P., P. Mowinckel and L. G. Peake. Earthquakes, Active Faults, and Geothermal Areas in the Imperial Valley, California. Science, v. 188, p. 1306-1308, 1975b.

Housner, G. W. Intensity of Earthquake Ground Shaking near the Causative Fault. Proceedings, Third World Conference on Earthquake Engineering, New Zealand, v. 1, 1965.

Howard, C. S. Quality of Water of Colorado River, 1925-1940. USGS Open File Report, 103 p., 1955.

Irelan, B. Salinity of Surface Water in the Lower Colorado River-Salton Sea Area. USGS Prof. Paper 486-E, 39 p., 1971.

Jahns, R. H. Investigations and Problems of Southern California Geology. Cal. Div. of Mines and Geol., Bull. 170, Ch. 1, p. 5-29, 1954.

Jennings, C. W. Geological Map of California, Salton Sea Sheet. Calif. Div. Mines and Geol., 1967.

__________. Fault Map of California. Cal. Div. Mines and Geol., Calif. Geol. Data Map Series, Map No. 1, Faults, Volcanoes, Thermal Springs, and Wells, 1975.

Johnson, C. E., and D. M. Hadley. Tectonic Implications of the Brawley Earthquake Swarm, Imperial Valley, California. Bull. Seis. Soc. Am., v. 66, No. 4, p. 1133-1144, 1976.

Kelley, V. C., and J. L. Soske. Origin of the Salton Volcanic Domes, Salton Sea, California. J. Geol., v. 44, p. 496-509, 1936.

Kohler, M. A., T. J. Nordenson and D. R. Baker. Evaporation Maps for the United States. U. S. Weather Bur. Tech. Paper 37, 13 p., 1959.

Kovach, R. L., C. R. Allen and F. Press. Geophysical Investigations in the Colorado Delta Region. J. Geophys. Res., v. 67, p. 2847-2871, 1962.

Langelier, W. F., and H. F. Ludwig. Graphical Methods for Indicating the Mineral Character of Natural Waters. J. Am. Water-Works Assoc., v. 34, p. 335-352, 1942.

Larson, R. L., H. W. Menard and S. M. Smith. Gulf of California: Result of Ocean Floor Spreading and Transform Faulting. Science, v. 161, p. 781-784, 1968.

La Rue, E. C. Colorado River and Its Utilization. USGS Water Supply, Paper 395, 231 p., 1916.

Littlefield, W. M. Hydrology and Physiography of the Salton Sea, California. USGS Hydrol. Inv. Atlas, HA-222, 1966.

Loeltz, O. J., B. Irelan, J. H. Robinson and F. H. Olmsted. Geohydrologic Reconnaissance of the Imperial Valley, California. USGS Prof. Paper 486-K, 54 p., 1975.

Lofgren, B. E. Measuring Ground Movement in Geothermal Areas of Imperial Valley, California. Proc. of Conference on Research for the Development of Geothermal Energy Resources, Pasadena, California, p. 128-133, 1974.

Lomnitz, C., F. Mooser, C. R. Allen, J. N. Brune and W. Thatcher. Seismicity and Tectonics of the Northern Gulf of California Region, Mexico--Preliminary Results. Instituto Geofisico Internacional Anales, v. 10, No. 2, p. 37-48, 1970.

MacDougal, D. T., et al. The Salton Sea. Carnegie Inst., Wash., Pub. 193, 182 p., 1914.

McDonald, C. C., and O. J. Loeltz. Water Resources of Lower Colorado River-Salton Sea Area as of 1971, Summary Report. USGS Prof. Paper 486A, 34 p., 1976.

McEldowney, R. C. An Occurrence of Paleozoic Fossils in Baja California, Mexico. Geol. Soc. Am. Abs. with Program, v. 2, No. 2, p. 117, 1968.

Meidav, T. Report on a Marine Seismic Survey, Salton Sea, Southern Part. Submitted to California Department of Water Resources, 1968a. [Also in Geothermal Wastes and the Water Resources of the Salton Sea Area. Calif. Dept. Water Res. Bull. 143-7, Sacramento, California, 1972.]

__________. Structural Characteristics of the Salton Sea, California (abs.). Trans. Am. Geophys. Un., v. 49, No. 3, presented at Western National Meeting of the AGU in San Francisco, December 2-5, 1968.

__________. Geoelectrical Exploration of a Geothermal Area in Southern California (abs.). Trans. Am. Geophys. Un., v. 50, No. 4, p. 348, 1969.

Meidav, T., and R. Furgerson. Resistivity Studies of the Imperial Valley Geothermal Area, California. Geothermics, v. 1, No. 2, p. 47-62, 1972.

Meidav, T., R. James and S. Sanyal. Utilization of Gravimetric Data for Estimation of Hydrothermal Reservoir Characteristics in the East Mesa Field, Imperial Valley, California. Stanford Geothermal Program Workshop on Geothermal Reservoir Engineering and Well Simulation, Stanford University, 1975.

Meidav, H. T., and R. W. Rex. Investigation of Geothermal Resources in the Imperial Valley and Their Potential Value for Desalination of Water and Electricity Production. University of California, Riverside, 54 p., 1970.

Meidav, H. T., and S. Sanyal. A Comparison of Hydrothermal Reservoirs of the Western United States. Electric Power Research Institute, Res. Proj. No. 580, 170 p., 1976.

Meidav, H. T., R. West, A. Katzenstein and Y. Rotstein. An Electrical Survey of the Salton Sea Geothermal Field, Imperial Valley, California. Lawrence Livermore Laboratory Res. Proj. No. 8432305, 132 p., 1976.

Meinzer, O. E. Outline of Ground Water Hydrology, with Definitions. USGS Water Supply Paper No. 494, 71 p., 1923.

Mercado, G. S. Localizacion de Zonas de Maxima Actividad Hidrotermal por Medio de Proporciones Quimicas, Campo Geotermico Cerro Prieto, Baja California, Mexico. Tercio Cong. Mex. Quimica, Guadalajara, 32 p., 1968.

Merriam, R.,and O. L. Bandy. Source of Upper Cenozoic Sediments in Colorado River Delta Region. Sed. Petrol., v. 35, No. 4, p. 911-916, 1965.

Metzger, D. G., O. J. Loeltz and B. Irelan. Geohydrology of the Parker-Blythe-Cibola Area, Arizona and California. USGS Prof. Paper, 486-G, 130 p., 1974.

Meyers, H., and C. A. von Hake. Earthquake Data File Summary. U. S. Department of Commerce, National Oceanic and Atmospheric Administration, Environmental Data Service, National Geophysical and Solar-Terrestrial Data Center, Boulder, Colorado, 53 p., 1976.

Miller, W. J. Geology of the Palm Springs-Blythe Strip, Riverside County, California. Calif. J. Mines and Geol., v. 40, p. 11-72, 1944.

Minch, J. A. The Late Mesozoic-Early Tertiary Framework of Continental Sedimentation, Northern Peninsular Range, Baja California, Mexico. Ph. D. diss., University of California, Riverside, unpub., 192 p., 1972.

Muffler, L. J. P., and B. R. Doe. Composition and Mean Age of Detritus of the Colorado River Delta in the Salton Trough, Southeastern California. J. of Sed. Petrol., v. 35, p. 384-399, 1968.

Muffler, L. J. P., and D. E. White. Active Metamorphism of Upper Cenozoic Sediments in the Salton Sea Geothermal Field and Salton Trough, Southeastern California. J. of Sed. Petrol., v. 35, p. 384-399, 1968a.

__________. Origin of CO_2 in the Salton Sea Geothermal Field, Southeastern California, U.S.A. XXIII International Geol. Congress, Prague, 1968, v. 17, Symposium II, Proc., Genesis of Mineral and Thermal Waters, p. 185-194, 1968b.

Olmsted, F. H., O. J. Loeltz and B. Irelan. Geohydrology of the Yuma Area, Arizona and California. USGS Prof. Paper No. 486-H, 227 p., 1973.

Palmer, T. D., J. H. Howard and D. P. Lande. Geothermal Development of the Salton Trough, California and Mexico. Lawrence Livermore Laboratory, 45 p., 1975.

Phelps, P. L., and L. R. Anspaugh. Imperial Valley Environmental Project: Progress Report. Lawrence Livermore Laboratory, UCRL-50044-76-1, 214 p., 1976.

Piper, A. M. A Graphic Procedure in the Geochemical Interpretation of Water Analyses. Trans. Am. Geophys. Un., Hydrology Papers, p. 914-923, 1944.

Raleigh, C. B., J. H. Healy and J. D. Bredehoeft. Faulting and Crustal Stress at Rangely, Colorado; in Flow and Fracture of Rocks, Geophys. Monogr. 16, Am. Geophys. Un., p. 275-284, 1972.

__________. An Experiment in Earthquake Control at Rangeley, Colorado. Science, v. 191, p. 1230-1236, 1976.

Randall, W. Percent Volume Sand Bodies in the Imperial Valley (Preliminary Report); in Cooperative Geological-Geophysical-Geochemical Investigations of Geothermal Resources in the Imperial Valley Area of California, R. W. Rex, Principal Investigator, University of California, Riverside, p. 119-124, 1971.

__________. An Analysis of the Subsurface Structure and Stratigraphy of the Salton Sea Geothermal Anomaly, Imperial Valley, California. Ph. D. diss., University of California, Riverside, unpub., December 1974.

Reed, M. J. Preliminary Report on the Geology and Geochemistry of the Cerro Prieto Field; in Cooperative Investigations of Geothermal Resources in the Imperial Valley Area and their Potential Value for Desalting of Water and Other Purposes, R. W. Rex, Principal Investigator, University of California, Riverside, 1972.

__________. Chemistry of Thermal Water in Selected Geothermal Areas of California. Calif. Div. Oil and Gas, Report No. TR15, 1975.

Rex, R. W. Investigation of Geothermal Resources in the Imperial Valley and Their Potential Value for Desalination of Water and Electricity Production. University of California, Riverside, 14 p., 1970.

__________. Origin of the Salt in the Imperial Valley and Surrounding Watershed Areas; in Cooperative Investigations of Geothermal Resources in the Imperial Valley Area and their Potential Value for Desalting of Water and Other Purposes, R. W. Rex, Principal Investigator, University of California, Riverside, Section F, 1972.

Rex, R. W., E. A. Babcock, S. Biehler, J. Combs, T. B. Copen, W. A. Elders, R. B. Furgerson, Z. Garfunkel, T. Meidav and P. T. Robinson. Cooperative Geological-Geophysical-Geochemical Investigations of Geothermal Resources in the Imperial Valley Area of California, University of California, Riverside, 153 p., 1971.

Rex, R. W., S. Biehler, J. Combs, T. B. Coplen, R. B. Furgerson, Z. Garfunkel, T. R. Getts, J. P. Maas and M. Reed. Cooperative Investigations of Geothermal Resources in the Imperial Valley Area and their Potential Value for Desalting of Water and Other Purposes, University of California, Riverside, 268 p., 1972.

Richter, C. F. Elementary Seismology. W. H. Freeman and Company, Inc., 768 p., 1958.

Robinson, P. T., and W. A. Elders. Late Cenozoic Volcanism in the Imperial Valley, California; in Cooperative Geological-Geophysical-Geochemical Investigations of Geothermal Resources in the Imperial Valley Area of California, R. W. Rex, Principal Investigator, University of California, Riverside, p. 151-153, 1971.

Robinson, P. T., W. A. Elders and L. J. P. Muffler. Quaternary Volcanism in the Salton Sea Geothermal Field, Imperial Valley, California. Bull. Geol. Soc. Am., v. 87, No. 3, p. 347-360, 1976.

Rogers, T. H. Geologic Map of California, Santa Ana Sheet. Cal. Div. Mines and Geol., 1965.

Savage, J. C., D. Goodreau and W. H. Prescott. Possible Fault Slip on the Brawley Fault, Imperial Valley, California. Bull. Seism. Soc. Am., v. 64, p. 713-715, 1974.

Schnabel, P. B., and H. B. Seed. Accelerations in Rock for Earthquakes in the Western United States. Earthquake Engineering Research Center, College of Engineering, University of California, Berkeley, Rept. No. EERC 72-2, 15 p., July 1972.

Scholz, C. H., and T. J. Fitch. Strain Accumulation Along the San Andreas Fault. J. Geophys. Res., v. 74, No. 27, 1969.

Seed, H. B., I. M. Idriss and F. W. Kiefer. Characteristics of Rock Motions During Earthquakes. J. Soil Mech. and Fndns. Div. ASCE, v. 95, p. 1199-1218, 1969.

Sharp, R. V. San Jacinto Fault Zone in the Peninsular Ranges of Southern California. Bull. Geol. Soc. Am., v. 78, p. 705-730, 1967.

__________. The Borrego Mountain Earthquake of April 9, 1968. Tectonic Setting of the Salton Trough. USGS Prof. Paper 787, p. 3-15, 1972.

__________. Surface Faulting in Imperial Valley During the Earthquake Swarm of January-February, 1975. Bull. Seism. Soc. Am., v. 66, No. 4, p. 1145-1154, 1976.

Sharp, R. V., and M. M. Clark. Geologic Evidence of Previous Faulting Near the 1968 Rupture on the Coyote Creek Fault In The Borrego Mountain Earthquake of April 9, 1968, USGS Prof. Paper No. 787, p. 131-140, 1972.

Silver, L. T. Problems of Crystalline Rocks of the Transverse Ranges. Geol. Soc. Am. Abs. with Program, v. 3, p. 193-194, 1971.

Stiff, H. A. Jr. The Interpretation of Chemical Water Analysis by Means of Patterns. J. Pet. Tech., v. 3, No. 10, p. 15ff, 1951.

Strand, R. G. Geologic Map of California, San Diego-El Centro Sheet. Cal. Div. Mines and Geol., 1962.

Suppe, J., and R. L. Armstrong. K-Ar Reconnaissance of Mesozoic Basement Rocks of Southern California. Geol. Soc. Am. Abs. with Program, v. 3, p. 205, 1971.

Sykes, G. The Colorado Delta. Carnegie Inst., Wash., Pub. 460, 193 p., 1937.

Sylvester, A. G., and R. R. Smith. Tectonic Transpression in San Andreas Fault Zone. Bull. Am. Assoc. Petrol. Geol., v. 1.60, No. 12, p. 2081-2102, 1976.

Tarbet, L. A., and W. H. Holman. Stratigraphy and Micropaleontology of the West Side of Imperial Valley, California (abs.). Bull. Am. Assoc. of Petrol. Geol., v. 28, p. 1781-1782, 1944.

Van De Kamp, P. C. Holocene Continental Sedimentation in the Salton Basin, California, A Reconnaissance. Bull. Geol. Soc. Am., v. 84, p. 827-848, 1973.

Van Winkle, W., and F. M. Eaton. The Quality of Surface Waters of California. USGS Water Supply Paper 237, 142 p., 1910.

Ward, P. L. Microearthquakes: Prospecting Tool and Possible Hazard in the Development of Geothermal Resources. Geothermics, v. 1, No. 1, p. 3-13, 1972.

Whitten, C. A. Crustal Movement in California and Nevada. Trans. Am. Geophys. Un., v. 37, No. 4, p. 393-398, 1956.

White, D. E. Saline Waters of Sedimentary Rocks; in Fluids in Subsurface Environments. Am. Assoc. Pet. Geol. Mem. 4, p. 342-366, 1965.

__________. Environments of Generation of Some Base-metal Ore Deposits. Econ. Geol., v. 63, No. 4, p. 301-335, 1968.

__________. Geochemistry Applied to the Discovery, Evaluation and Exploitation of Geothermal Energy Resources; in United Nations Symposium on the Development and Utilization of Geothermal Resources, Pisa, v. 2, Part I, Geothermics, Special Issue 2, 1970.

Wilt, M. J. An Electrical Survey of the Dunes Geothermal Anomaly and Surrounding Region, Imperial Valley, California. M.S. thesis, University of California, Riverside, unpub., 128 p., 1975.

Woodard, G. D. Stratigraphic Succession of the West Colorado Desert, San Diego and Imperial Counties, Southern California. Geol. Soc. Am. Abs. with Program, Cordilleran Section, San Diego, California, p. 73-74, 1961.

Woodring, W. P. Distribution and Age of the Marine Tertiary Deposits of the Colorado Desert. Carnegie Inst., Wash., Pub. No. 18, p. 1-25, 1932.

SECTION 3

THE GEYSERS

3.1 INTRODUCTION

This section presents baseline data on climatology, geology, hydrology and seismology to aid in assessment of environmental impacts of geothermal development in The Geysers geothermal area, California. Descriptions of aspects of climatology, geothermal characteristics, tectonics, faults, stratigraphy, lithology and surface water that are related to and influence the ground water regime are discussed. A comprehensive discussion of seismic risk in general, and The Geysers area in particular, is included.

3.1.1 Summary

The Geysers geothermal field produces 99% pure steam from fractured Mesozoic greywacke of the Franciscan Formation. Near the original fumaroles, wells were drilled to less than 600 m (2,000 ft), producing from a fractured reservoir at average shut-in pressures of 14 to 17.5 kg/sq cm (200 to 250 psig), and with several degrees of superheat. Wells drilled at distances of up to 11 km (7 mi) from the original site go to depths of 2,100 to 2,700 m (7,000 to 9,000 ft), encountering a reservoir at about 230°C (446°F), with markedly subhydrostatic pressures (32 to 35 kg/sq cm [450 to 500 psig]). Approximately 50 sq km (20 sq mi), capable of sustaining production of at least 2,000 MW, has been proven by drilling.

Steam from The Geysers carries notable quantities of hydrogen sulfide, ammonia and boron as part of the average 1% of noncondensible gases (principally carbon dioxide). Because of potential pollution problems, all condensed steam is reinjected into the geothermal reservoir. Evaporated steam liberates hydrogen sulfide to the environment.

Elsewhere in the region, ground water anomalies in boron, ammonia, chloride and magnesium are noted. The wide extent of these anomalies suggests that additional thermal resources (perhaps in the form of saline hot water) exist beneath areas north and northeast of The Geysers field.

3.1.2 Background

The Geysers geothermal field is located in Lake and Sonoma Counties, of the northern Coast Ranges, California, some 130 km (80 mi) north of San Francisco (Fig. 3.1). Exploration for geothermal steam began in this area of fumaroles in the 1920s. However, first commercial production of electricity from the steam was achieved only in 1960. Exploration has continued over an ever-widening area in four counties (Lake, Sonoma, Napa and Mendocino). This has entailed geologic mapping, hydrologic and hydrochemical surveys, gravimetry, aeromagnetometry, geoelectrical and seismic surveys and the drilling of hundreds of shallow holes for temperature gradients, by private companies, government agencies and institutional researchers. The work has accelerated greatly since the inception of the Federal Geothermal Leasing Program in 1973. Over 120 deep exploratory wells have been drilled to date. For this study, published and unpublished data files were canvassed and compiled into text, illustrations and tables. Additionally, interviews were held with persons active in exploration or research into the geothermal system. Finally, field checks were made into areas of inadequate or inconsistent data.

Principal published sources include geologic mapping by Hearn, et al. (1975) and McLaughlin (1974), seismic studies by Bufe, et al. (1976) and Iyer (1975) and hydrologic surveys by the California Department of Water Resources (1957) and by Upson and Kunkel (1955).

3.1.3 Climatology

The Coast Range in this region is subject to a Mediterranean climate, characterized by mild winters and warm summers, with nearly all precipitation falling as winter rain. Prevailing winds are westerly, with average speeds in the neighborhood of 16 km/hr (10 mph), being rather faster in summer than winter. As a consequence of low wind speeds and summer fog which occurs mainly in the immediate vicinity of the coastline, the temperature moderating influence of the ocean decreases markedly with distance from the coast. Therefore, summers become hotter and winters cooler going east from Healdsburg to Clear Lake. Similarly, diurnal extremes become greater to the east.

Temperature--

Average annual temperature at Healdsburg is nearly 16°C (60°F) in the Healdsburg-Cloverdale area, and about 14°C (57°F) at Lakeport. Across the area, representative mean minimum and maximum temperatures are 2°C (36°F) and 13°C (56°F) in January, and 12°C (54°F) and 33°C (92°F) in July. At Clear Lake, average extreme values are more divergent, with a low of 0°C (32°F) in

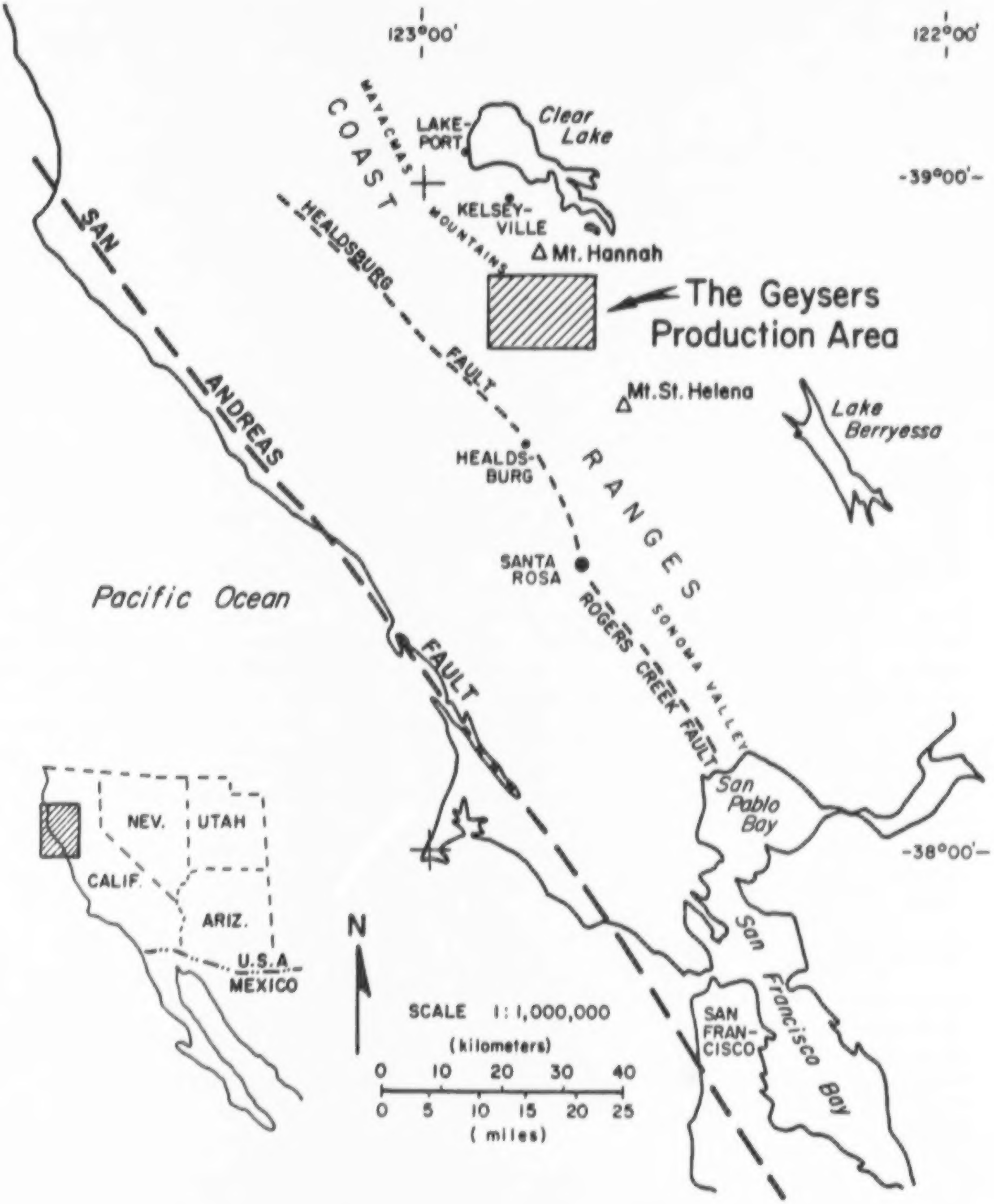
123°00'
122°00'
-39°00'-
-38°00'-
COAST
MAYACMAS MOUNTAINS
LAKEPORT
Clear Lake
KELSEYVILLE
Δ Mt. Hannah
HEALDSBURG FAULT
The Geysers Production Area
Mt. St. Helena
Lake Berryessa
HEALDSBURG
RANGES
SANTA ROSA
ROGERS CREEK FAULT
SONOMA VALLEY
SAN ANDREAS FAULT
Pacific Ocean
San Pablo Bay
San Francisco Bay
SAN FRANCISCO
NEV.
UTAH
CALIF.
ARIZ.
U.S.A.
MEXICO
N
SCALE 1:1,000,000
(kilometers)
0 10 20 30 40
0 5 10 15 20 25
(miles)

Figure 3.1 Location map of The Geysers study area.

January and high of 36°C (96°F) in July. The freeze-free period averages approximately 200 days but is only about 150 days at Clear Lake. Table 3.1 summarizes temperature data for the region.

Precipitation--

Average annual precipitation ranges from a low of 635 mm (25 in) at Clear Lake to a maximum of 2,030+ mm (80+ in) at the Helen Mine, in the Mayacmas Mountains. Practically all precipitation falls as rain, although in some years a few inches of snow falls at elevations over about 300 m (1,000 ft). About 95% of rainfall occurs during the months October through April; rainfall is heaviest from December to February. Precipitation data is summarized in Table 3.1 and Figure 3.2.

Wind--

Wind data has been collected on Cloverdale Peak and near The Geysers by Pacific Gas and Electric Company (PG & E) (Mooney, 1975). The Geysers station is located on a ridge crest about 3 km (2 mi) north of The Geysers, at an elevation of 974 m (3,195 ft); Cloverdale Peak station is at an elevation of 891 m (2,924 ft) and is approximately 31 km (19 mi) northwest of The Geysers. The data is given in terms of frequency of occurrence for winds in 16 azimuthal sectors and in 9 speed intervals, for the period November 1, 1972, to October 31, 1974. It is seen that at Cloverdale Peak winds are predominantly from the north at an average speed of 13 km/hr (8 mph); winds from the south to southwest are also frequent, at average speeds from 13 to 19 km/hr (8 to 12 mph). Near The Geysers, wind distribution is bimodal, being most frequent from the north-northeast at 23 km/hr (14 mph) and southwest at 14 km/hr (9 mph). At both stations southwesterly winds characterize winterstorm (cyclonic) weather, while northerly winds accompany prevailing good weather (anticyclonic) conditions. Winds rarely have speeds below 6 km/hr (4 mph) or above 29 km/hr (18 mph); occurrences beyond these limits are some 15% of the total.

Evaporation and Transpiration--

Pan evaporation averages nearly 1,370 mm (54 in) annually in the study region, and measurement points have been located at Geyserville, Knights Valley, Lower Lake and Lakeport. Because pan evaporation data is not readily interpretable, it is not detailed here. However, details are available from California Department of Water Resources Bulletins 73-1 (1974) and 113-3 (1975).

Data on evaporation and transpiration for native vegetation are very sparse; practically all studies on evapotranspiration have concerned irrigated crops. However, one detailed study of evapotranspiration in native vegetation is available. This concerns a 17.5 ha (43 acre) area located 16 km (10 mi) northeast of Lincoln, in Placer County, California (Lewis and Burgy,

TABLE 3.1 AVERAGE MONTHLY AND ANNUAL TEMPERATURES AND PRECIPITATION AT SELECTED STATIONS[1]

STATION		JAN.	FEB.	MAR.	APR.	MAY	JUNE	JULY	AUG.	SEPT.	OCT.	NOV.	DEC.
HEALDSBURG	(T)	46.9	50.4	53.8	57.4	62.3	67.2	69.4	68.9	68.0	62.1	53.9	48.3
	(P)	8.5	7.3	4.9	2.9	1.2	0.5	0	0.1	0.4	2.2	3.9	7.9
ST. HELENA	(T)	45.8	49.0	52.4	56.7	61.8	67.1	70.7	69.7	67.5	60.8	53.2	47.4
	(P)	7.0	6.3	4.3	2.4	1.0	0.3	0	0.1	0.2	1.7	3.1	6.6
LAKEPORT	(T)	[2] 42.6	46.2	49.6	52.1	61.8	68.9	75.7	74.8	68.5	57.6	49.2	41.5
	(P)	6.1	4.9	3.4	2.0	0.9	0.5	0.1	0.1	0.2	1.7	2.9	5.9

AVERAGE ANNUAL TEMPERATURE AND PRECIPITATION

STATION	TEMP.	PRECIP.	
CLOVERDALE	60.4	40.5	
HEALDSBURG	59.1	39.8	
THE GEYSERS	NA	51.7[3]	(estimated)
LAKEPORT	56.9[3]	28.5	
LOWER LAKE	NA	29[5]	
MIDDLETOWN	NA	46.8[3]	
CALISTOGA	NA	37.8[3]	
ST. HELENA	58.5	33.1	
HELEN MINE	NA	88.0[4]	
MT. ST. HELENA	NA	60.5[5]	

---

1) Temperature (T) in °F and precipitation (P) in inches. Data source is Water Information Center, 1974, unless otherwise noted in the following footnotes.

2) U.S. Dept. of Interior, 1973.

3) NOAA, 1975 (Climatological Data, Annual Summary).

4) Kunkel and upson, 1960 (Water Supply Paper 1495).

5) Upson and Kunkel, 1955 (Water Supply Paper 1297).

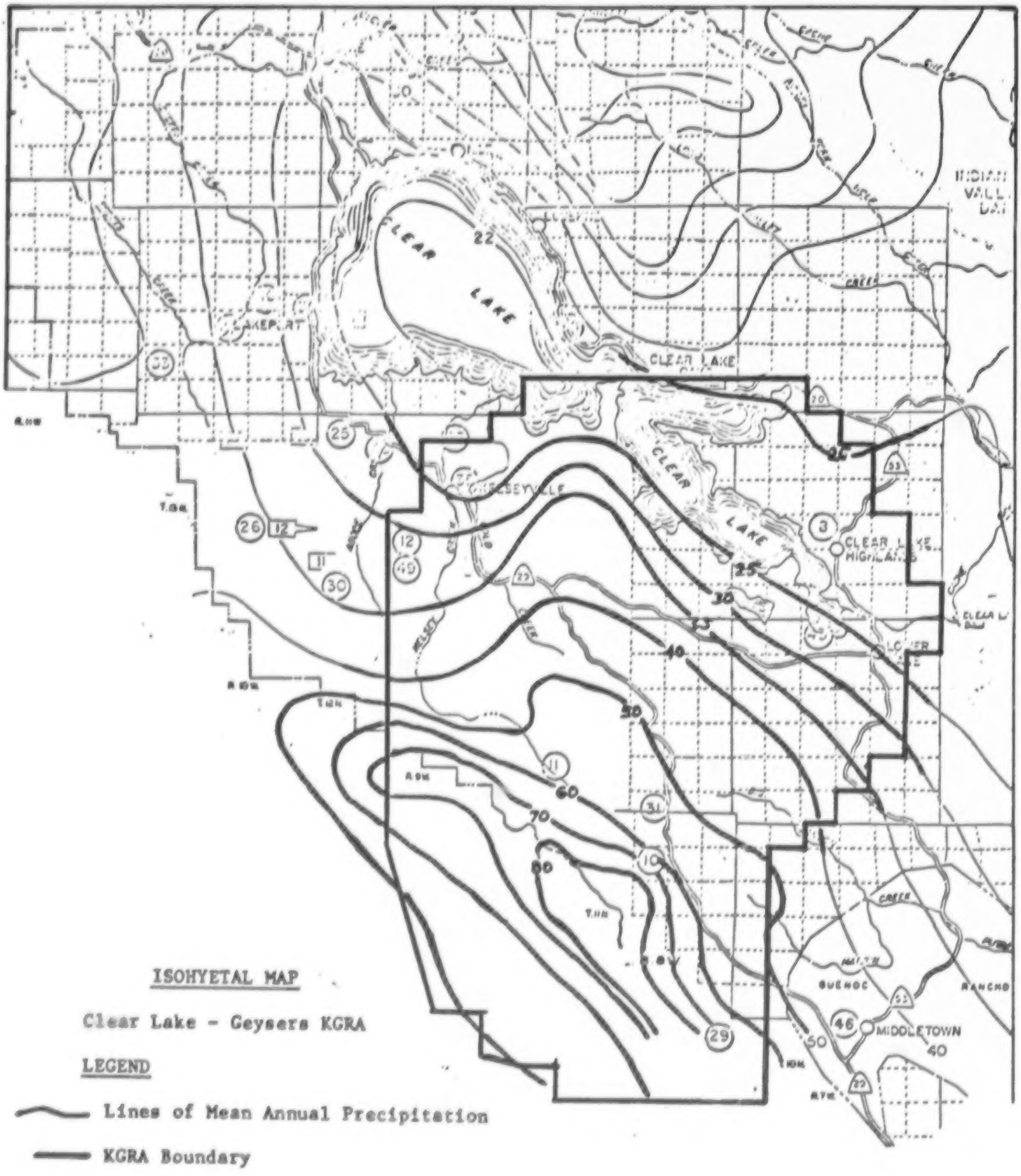
ISOHYETAL MAP
Clear Lake - Geysers KGRA
LEGEND
Lines of Mean Annual Precipitation
KGRA Boundary
CLEAR LAKE
22
LAKEPORT
35
CLEAR LAKE
INDIAN VALLEY DAM
25
26
30
12
49
KELSEYVILLE
3
CLEAR LAKE HIGHLANDS
25
30
35
40
50
60
70
80
11
31
10
29
GUENOC
RANCHO
46
MIDDLETOWN
40
50

Figure 3.2 Precipitation in The Geysers-Clear Lake area, (mean annual, in inches)

1961-67); this is in the foothills of the Sierra Nevada Mountains, at an elevation of about 180 m (600 ft) above sea level. Vegetation is chaparral, comprising chiefly buckbrush, poison oak, several species of oak, and yellow pine. Rainfall there averages 635 mm (25 in) annually. Comprehensive monitoring of climatic and hydrologic conditions, including soil moisture and ground water storage, was carried out during the seven-year study.

The study showed that evapotranspiration (ET) ranged from 510 to 685 mm (20 to 27 in) per year, depending on rainfall. Minimum ET (510 mm [20 in]) occurred when rainfall was 810 mm (32 in), and maximum ET (685 mm [27 in]) when rainfall was 865 mm (34 in); significant decreases in soil moisture and ground water storage accompanied the period of minimum rainfall and ET. It was concluded that, up to a maximum of about 685 mm (27 in), ET used essentially all available rainfall in any given year; for rainfall greater than 685 mm (27 in), ET increased only slightly, to a maximum of 710 mm (28 in).

Vegetation over much of the present study region is somewhat comparable in makeup with that of the Placer County area, being largely mixed chaparral in nature; however, mixed broadleaf woodland (chiefly oak, with madrone, laurel and toyon), and conifer woodland at higher elevations, are present in the Mayacmas Mountains. Because rainfall in the study area is greater than in the reference area, it can be reasonably assumed that the established plant community has a minimum ET equal to or greater than that of the reference area, i.e., some 560 mm (22 in) annually. More specifically, it is reasonable to assume that: (1) the Mayacmas Mountains area has ET near or perhaps greater than the maximum ET observed in the reference area, (2) the drier, scrubbier area to the east has ET very close to that of the reference area. On this basis, it is thought that ET has an average annual depth of some 685 to 760 mm (27 to 30 in) in the Mayacmas Mountains, and about 560 mm (22 in) in the drier area to the east.

Irrigated crops generally use more water than chaparral. In the study area, vineyards and orchards are the main crop types. During the irrigation season (April 1 to September 30), orchards with cover crops consume some 760 mm (30 in) of water; vineyards (wine grapes) use only about 400 mm (16 in); alfalfa and pasture grass use 760 to 1,015 mm (30 to 40 in) (California Dept. of Water Resources, 1975).

3.2 GEOTHERMAL CHARACTERISTICS OF THE GEYSERS

Geothermal steam at The Geysers is stored in fractured greywacke sandstone of the Franciscan Formation. Although in its unfractured state greywacke has limited capacity to store or transmit water to wells, when fractured it becomes the principal geothermal aquifer. Other rocks of the Franciscan Formation, principally serpentine, serve as aquicludes, impairing the flow of fluid from aquifers.

Although the geothermal wells yield essentially dry steam, there is evidence that both steam and water coexist within the fractured rock reservoir. It may be possible that steam is boiling off of a deeper seated hot water body; conversely, water may be injected under pressure into the heated rocks and there flashed to steam. The question of possible recharge to the reservoir is moot. Answers to the question of natural recharge will await better data on the rates at which pressure and flow decline in deep wells across many parts of the field. To date, data have been released that show declines in pressure and mass flow primarily from a shallow, older part of the geothermal field.

Well yields, shut-in pressures and calculated enthalpies are sufficiently constant across a 9.5 km (6 mi) zone of the geothermal field to suggest that there is relatively free communication through the rock reservoir. As the outer boundaries of the field are not clearly known, and as it is surely greater than 47 sq km (18 sq mi) in area, the total of fluid in storage, even ignoring recharge, is vast.

Development began in the late 1950's with the drilling of wells to several tens of meters in depth along the northern bank of Big Sulphur Creek. This was the area from which fumaroles (natural steam vents) had discharged since prehistoric times. Well yields were moderate to small, shut-in pressures were low, and declines in pressure and flow were noticed after only a few years of production. Careful measurements were thwarted by the presence of a blowout in the midst of this part of the field. This well still discharges to the atmosphere under only partial control.

It has since been recognized that this shallow part of The Geysers field is supported principally by upward leakage of steam along faults that penetrate into the deeper field. At least one of the older, shallow wells has been deepened and now produces at greater pressure and rate of flow from this deeper pool.

Wells have been drilled to increasingly greater depths since the mid-1950's, and over an ever-widening area. Maximum depth is over 2,700 m (9,000 ft), and average depth is about 2,100 m (7,000 ft). Rates of flow average between 68,000 and 90,700 kg (150,000 and 200,000 lbs) of steam per hour. Shut-in pressures are on the order of 35 to 32 kg/sq cm (500 to 450 lbs/sq in.). Enthalpies often calculate to about the maximum obtainable for saturated steam conditions. This suggests that liquid water and steam are in some form of coexistence within the reservoir rocks.

Rates of satisfactory completion are high, averaging four out of every five holes drilled. Unsuccessful holes usually are characterized by high temperatures, although steam flow or absence of steam may occur.

Holes are drilled by rotary drilling method, using mud as the circulating medium to depths below that of known fresh water aquifers. Drilling thereupon switches to air. The hole usually is cased to depths of about 900 to 1,200 m (3,000 to 4,000 ft), and continued open thereafter. Formation strength is great enough to support open holes, except in rare cases where caving or bridging deep within the hole has been noted.

Well spacing has been at 16 ha (40 acre) intervals across the parts of the field under recent development. It is assumed that a similar policy will be carried out for the remainder of the field. Given average well conditions, a single section (260 ha [640 acres]) appears capable of supporting a 110 MW electric generating station. No interference is reported between wells at a 16 ha (40 acre) spacing. It may even be possible to construct additional wells on a 8 ha (20 acre) spacing if individual wells suffer declines in pressure or total flow.

True field life is unknown. Even individual well life is uncertain and subject to site-specific characteristics. As individual power generation stations are to be amortized over a 30- to 35-year period, it is assumed that data is available to the field operators to assure the viability of such investments. As an analogy, it is known that geothermal pools at Larderello, Italy, have continued to supply steam to wells for over half a century.

Even ignoring the question of recharge, it has been shown that over 85% of the heat is contained in the rock masses, and less than 15% is present in the fluid phase. Therefore, the question of depletion of heat is really a question of rate of transfer of heat from rock to water. As conductive transfer of heat is slow, it may be possible to chill individual fracture surfaces, but it is unlikely that the entire field can be cooled significantly because of the great quantity of heat stored in these rocks.

At present some 20% of the geothermal fluid is condensed and returned to the reservoir via reinjection wells. These usually are unsuccessful holes drilled for steam and disused steam wells, as well as specially drilled shallow holes. The condensed, heat-depleted geothermal fluid is fed by gravity into wells, where it reenters the formation under hydrostatic head. The rates and paths by which it recirculates within the reservoir are unknown. It is possible that this action will chill the reservoir rock very locally; however, in reality, reinjection may serve as a form of secondary recovery of heat from the rock.

The withdrawal of fluid from a rock reservoir may result in ground subsidence. This has been true in ground water basins, as well as in reservoirs of oil, gas and geothermal fluid. Geothermal subsidence is noted at Wairakei, New Zealand.

At The Geysers, the reservoir rocks are hard, locally metamorphosed sedimentary and igneous rocks. Reservoir fluid is steam rather than hot water. Therefore, these rocks would not be affected by a reduction in hydrostatic pressures as much as would the softer sedimentary and volcaniclastic rocks at Wairakei. To date, compaction and subsidence has not manifested itself as a problem at The Geysers, even though pressure has been reduced in certain shallow parts of the geothermal field. Further, reinjection of condensates from the geothermal power plants may prevent significant development of this problem by partially maintaining mass and pressure within the deep reservoir.

3.3 GEOLOGY

The geology of The Geysers-Clear Lake region is discussed in this section under the topics of physiography, regional geologic setting and tectonic history, structure, stratigraphy and lithology. In general, geology is poorly exposed in this rugged, heavily vegetated area and numerous generations of geologists and geophysicists have slowly unravelled an even more complex pattern of sedimentation, basin deformation, igneous intrusions and volcanism. Plate 3.1 A and B present a geologic map and cross sections (McLaughlin, 1974) of The Geysers area.

3.3.1 Physiography

The study region comprises approximately 1,044 sq km (400 sq mi), located in the northern Coast Ranges, within Sonoma, Lake, Mendocino and Napa Counties, California. This area is described crudely by a triangle with verticles at Cloverdale, Calistoga and the northeast side of Clear Lake.

Topography is dominated by northwest trending linear ridges separated by narrow, V-shaped valleys. Major streams, probably antecedent, have cut trenches across this northwest-oriented grain. However, the great preponderance of stream mileage runs parallel to grain. The Mayacmas Range and southern Clear Lake basin occupy most of the study region; Napa Valley and northern Putah Creek Basin occupy its southernmost part.

The Mayacmas Range forms the highest range in this region, with ridge crests commonly above 900 m (3,000 ft) in elevation and highest peaks above 1,200 m (4,000 ft) (Mount St. Helena, Cobb Mountain). Maximum relief, therefore, is 900 m (3,000 ft) with 600 m (2,000 ft) of relief common. Slopes are steep and often unstable and landslide-prone. Ridge crests often are flat to gently rolling, reflecting an erosion surface cut late in Tertiary time. Geomorphically, therefore, the Mayacmas Range exhibits an uplifted submature landscape, incised by youthful, still downcutting streams.

Clear Lake Basin has considerably lower average elevation and relief than the Mayacmas Range. Clear Lake has an altitude of 404 m (1,326 ft), and major tributary valleys rise to some 460 m (1,500 ft). Except for Mount Konocti, which rises to 1,280 m (4,200 ft),maximum elevations on ridges within the basin are in the neighborhood of 700 m (2,300 ft). Generally, these are rolling and flat-topped, and, furthermore, a number of small, flat-floored valleys are present. Therefore, the geomorphology of this basin is essentially submature. However, uplift locally has caused some rejuvenation of erosion, as evidenced by incised stream channels. Evidently, Quaternary uplift has been much less here than in the adjoining Mayacmas Mountains; subsidence accompanying volcanism (described below) may be the reason.

Putah Creek Basin in the study region is much like Clear Lake Basin, in terms of overall geomorphic appearance and elevation. The two basins are separated by a sinuous low divide, which trends southeasterly from Swigler Mountain. Average elevation in Putah Creek Basin is somewhat lower, with flat-floored valleys at about 300 m (1,000 ft).

Napa Valley, which heads on the south flank of Mount St. Helena, is flat-floored and has an altitude of 110 m (361 ft) near Calistoga. In overall aspect, it is similar to Alexander Valley, which flanks the study region on the west.

3.3.2 Regional Geologic Setting and Tectonic History

The history of faulting in this region can be divided into three periods. The first period entailed chiefly thrust faulting, as the result of compressional forces accompanying subduction of the Pacific tectonic plate beneath the North American plate. This occurred from late Jurassic into Eocene time. Thrust faults separating Franciscan and Great Valley rocks, and within the Great Valley Sequence, formed at this time, during the deformation and final obliteration of the Franciscan and Great Valley depositional basins. These faults tend to have shallower dips than the other types and have no predominant trend direction. Serpentine has frequently flowed into these zones.

The second period involves chiefly right-lateral strike-slip on northwest trending faults; the San Andreas Fault System is its most well-known expression. This mode of deformation began in Oligocene time, when the East Pacific Rise collided with the trench (subduction zone) at the continental margin, and has continued until the present time. Practically all Coast Range seismicity originates on northwest trending right-lateral strike-slip faults.

In the past period, beginning in late Pliocene time, uplift of the Coast Ranges and volcanic activity of the Clear Lake-Sonoma Valley region has been accompanied by normal faulting; this has also continued to the present. Normal faults are abundant in the Clear Lake Volcanic Field, and are probably the result of both continued range uplift and basin subsidence. Most of these faults trend northwesterly, but a number also trend north-northeasterly. The latter probably formed in response to volcanic subsidence of the Clear Lake Basin.

Individual faults in the study area rarely are simple fractures, but rather are zones of varying width and complexity, along which there has been intense shearing and fracturing of rock materials. The complexity and intensity of fracturing in the several episodes of deformation have resulted in intricate patterns of faulting and highly complex surface geology. Locally, Franciscan rocks have been sheared and subsequently altered to a fine-grained, montmorillonite-rich clay matrix, within which are found coherent boulders and blocks of unaltered, unsheared rock. This is known as mélange structure.

Beginning in Pliocene epoch, and continuing locally to the present, there has been differential doming and downwarping of large portions of the northern Coast Ranges. The Mayacmas Range has been uplifted sharply, with uplift apparently reaching 900 to 1,200 m (3,000 to 4,000 ft) in places, by evidence from deformed and offset surfaces. Areas exposing Sonoma Volcanics appear to have subsided, at least in part, with the upper surface of Franciscan rocks depressed by several tens to a few hundred meters. The area around Clear Lake, northeast of the Mayacmas Range, appears also to have subsided (or collapsed, depending upon interpretation) tectonically. Both of these downwarped areas may have moved in response to withdrawal of magma from large underground chambers. The uplift of the Mayacmas appears in part to have originated with magmatic doming, although other tectonic stresses undoubtedly were involved.

This differential vertical movement seems to have occurred principally along the northwest trending faults previously active in strike-slip movement. Accompanying vertical (or near-vertical offset) has been rotation of blocks, such that for a large area west from the Mayacmas crest, blocks have rotated to the northeast or east. Northeast of the Mayacmas Range, blocks have subsided (Clear Lake), but the component of rotation along vertical faults is unknown.

3.3.3 Structure

The Coast Ranges are cut by numerous linear, steeply dipping, predominantly northwest trending faults. Most of these are strike-slip (lateral displacement) faults, but some are of the normal or reverse type (essentially vertical displacement). A few of these are recognized as being seismically active. The best known active fault is the San Andreas, 71 km (44 mi) west of the study area at its closest point of approach, which extends for about 1,130 km (700 mi) from Imperial Valley to near Cape Mendocino, and has been the source of many strong to great earthquakes in historic time. Although certain additional faults are considered active, most faults are believed to have ceased activity in earlier geologic epochs, based upon the available geologic data. A number of minor faults displace units of the Clear Lake Volcanic Series, and some of these should be considered potentially active.

Regional dips at The Geysers are northeasterly. Farther to the south and west a reversal in dip to the southwest is noted (McLaughlin, 1974). Therefore, an anticlinal structure may be recognized (commonly called an antiform), cut by numerous faults along which rotation of individual blocks has occurred. It is the sense of rotation that gives rise to the antiform. This structure is believed to plunge to the southeast. Therefore, the greatest structural relief is noted at the northwest end of the structure, near The Geysers.

Other plunging blocks may exist parallel to The Geysers antiform. A regionally downdropped block is northeast of the Collayomi Fault and is here called the Clear Lake-Middletown Lowland. It consists of Great Valley Sequence rocks, atop imbricated, serpentinite-soled thrust sheets, and probably in turn atop Franciscan rocks. Nowhere is Franciscan rock exposed in this lowland block.

3.3.4. Stratigraphy and Lithology

Franciscan Formation--

Basement in the region consists of the Franciscan Formation and associated rocks of late Mesozoic age. Franciscan sedimentary rocks, in approximate order of abundance, are greywacke, shale, conglomerate, chert and very minor lenses of limestone. Interbedded and intruded into these sediments are basalt, diabase, gabbro and related mafic crystalline rocks, as well as masses of serpentinized peridotite and pyroxenite, and exotic boulders of eclogite.

It is believed that Franciscan sediments accumulated in a deep water oceanic trench, perhaps similar to that off of present-day Chile or Japan. Sorting of sediment is poor and bedding features are weakly developed to nonexistent.

Greywacke, which comprises about 60% of the entire sequence, is massive, poorly bedded, poorly sorted and,as a result, nonporous. (This rock forms the geothermal reservoir). Greywacke consists of approximately equal amounts of quartz, feldspar and lithic fragments (preexisting chert and quartz porphyry, and cannibalized Franciscan greywacke and shale) in a matrix of the same materials ground very fine. Unsheared Franciscan greywacke contains very little clay mineral in its matrix.

Shale is, in reality, a microgreywacke, consisting of the same materials as greywacke matrix, in finer grain size. Shale crops out irregularly, but often is identified in well cuttings and in deep road cuts. Therefore, it may be more abundant than recognized.

Undersea eruptions and intrusions of mafic lavas resulted in formation of igneous sheets, necks, dike complexes and stocks within Franciscan sediment. Volcanically induced changes in composition and temperature of sea water are believed to have resulted in the episodic precipitation of chert. Chert is well but thinly bedded, and interleaved with very thin partings of shale. Soft-sediment crumpling within the trench resulted in extreme contortions of bedding. The resistant chert appears more abundant on the surface than in cross section.

Igneous rocks are all mafic to ultramafic in composition. Tuffs and other ejecta are rare. Ultramafic rocks are believed to be portions of the Mesozoic subcrust which intruded and/or were tectonically crumpled into the complex of sediment and mafic lava. Mafic igneous rocks may form 15% to 20% of the entire Franciscan assemblage. Ultramafic rocks, although very recognizable and widespread at the surface today, are believed to be less abundant overall.

Fossils are rare in this deep-water assemblage. However, rare fossils and radiometric age-dates suggest that deposition began in late Jurassic time and continued probably to late Cretaceous time and possibly into Paleocene epoch.

Subduction of trench sediment and igneous rocks is believed to have occurred rapidly. This is invoked to account for (1) extreme shearing, (2) low-temperature, high-pressure metamorphism, (3) complex deformation and juxtaposition of the Franciscan materials, as well as (4) intrusion of eclogite masses and (5) present-day distribution of the Franciscan with regard to other formations.

Metamorphism has resulted in widespread development of zeolite facies in Franciscan greywacke and shale; and in localized development of blueschist facies (characterized principally by lawsonite and glaucophane). Mafic igneous rocks have been converted to greenstone, with common soda metasomatism, perhaps as a result of reaction with contained seawater. Serpentinization of ultramafic rocks may have occurred then or at a later time under near-surface conditions. Very local, and anomalous, development of greenschist facies (epidote-albite-tremolite-quartz) in sedimentary and igenous rocks also may date from the period of subduction, as relatively small masses were heated to higher than normal temperatures, or were intruded from greater depths.

Deformation during this cycle is believed by many to have destroyed stratigraphic continuity or identity and to have created "tectonic" units. These consist of broken slabs of various size and stratigraphic position, rotated, sheared intensively, juxtaposed irregularly and set in a fine-grained matrix. These tectonic units are referred to as mélange. An important consideration is the development of chlorite and clay minerals within the mélange matrix. Coherent slabs may range from fist-size to hundreds of square meters in extent, set in highly sheared matrix. The resultant mélange is highly unstable and tends to fail in steep slopes or when cut.

Franciscan and equivalent rocks are exposed across an area of 104,000 sq km (40,000 sq mi) or more, extending from southwestern Oregon to the Los Angeles basin and perhaps beyond. Franciscan rocks are believed to underlie an equivalent area, onshore and offshore, having a total area of perhaps 207,000 sq km (80,000 sq mi). Nothing has ever been observed to underlie Franciscan rocks. Seismic profiles run across northern California in the early 1960's suggested that materials of mantle or near-mantle densities (perhaps mafic intrusions or ultramafic sheets) underlie rock of Franciscan densities at depths of 14 to 21 km (9 to 13 mi). Observed and calculated thicknesses of Franciscan rocks are on the order of 1,500 m (5,000 ft), which agrees closely with the seismic profiles.

Great Valley Sequence--

While the Franciscan Formation was being accumulated in a deep water trench, another sequence of rock was deposited in a near-shore marine environment east of the trench, perhaps similar to the present continental shelf and slope. This group of sandstone, shale, siltstone and conglomerate is also of late Jurassic to late Cretaceous age and is known collectively as the Great Valley Sequence, from its principal areas of exposure along the western margin of the Great Valley. This sequence of rocks may be up to 10,700 m (35,000 ft) thick. Relatively minor amounts of basalt, diabase, and chert are present in its lowest portion.

Formation names have been applied locally. The Knoxville Formation, of upper Jurassic age, is recognized widely and often is found in tectonic contact with equivalent-age Franciscan rocks. The Knoxville rocks consist of dark shale and light colored siltstone, rhythmically interbedded and having a distinctive outcrop pattern. Higher in the Great Valley Sequence, massive sandstone and conglomerate beds are abundant, along with lenses of fossiliferous limestone. Units of all lithologies often are lensing, and some are time-transgressive. This has resulted in development of two distinctive systems of nomenclature: one based on fossil content, independent of lithology, and another based upon lithology, independent of stratigraphic continuity.

Mafic volcanic and ultramafic rocks, often serpentinites, are present near the base of the Great Valley Sequence, in the Knoxville Formation. These crystalline rocks are indistinguishable from those in the Franciscan and may have identical sources. In proximity to these mafic and ultramafic rocks, Knoxville sediments are deformed and sheared to a degree comparable to the Franciscan.

The Knoxville Formation may reach 6,100 m (20,000 ft) in thickness, and the total Great Valley Sequence may be 9,100 m to 12,200 m (30,000 to 40,000 ft) thick. The best exposures of the sequence are at the east end of the Coast Ranges, where the sequence dips homoclinally beneath the Central Valley.

It is believed that destruction of the Mesozoic trench at the beginning of Tertiary time was accompanied by shearing, compressive folding, and imbricated thrust faulting, in which Great Valley and Franciscan rocks were intricately deformed together. Commonly, the Franciscan is described as having been underthrust beneath Great Valley rocks. Serpentinized peridotite is believed to have served as the lubricated sole of the thrusts. Indeed, serpentinite or a sheared mixture of serpentinite, greenstone and fault gouge usually is present between Franciscan and Great Valley rocks wherever they are observed in close proximity.

Thrusting of Franciscan beneath Great Valley rocks is a concept required by the finding that these rocks are in part contemporaneous and by the fact that depositional contact between the two formations has never been demonstrated. Wherever they are in contact, a fault or serpentinite body intervenes. Swe and Dickinson (1970) adopted and refined this concept and described the Great Valley Sequence, as exposed in the Lower Lake 15-minute quadrangle, as a series of four main stratigraphic units which has been complexly folded and broken into three or more thrust slices. Although there is no evidence within the area to indicate when regional thrusting began, it is believed to have begun by late Cretaceous time. Field relationships at Round Valley, 120 km (75 mi) to the northwest, suggest that regional thrusting persisted into early Oligocene time (perhaps 35 to 38 million years ago).

Tertiary Sedimentation--

Local basins of marine sedimentation persisted after the destruction of the regional basins that began in late Cretaceous time. Marine sediments of Paleocene and Eocene age (38 to 65 million years in age) are found scattered across parts of the northern Coast Ranges. Within 6 km (4 mi) south and east of Lower Lake, these are represented by the Martinez and Tejon Formations, of Paleocene and Eocene age, respectively. According to Brice (1953), who mapped the Lower Lake quadrangle in the late 1940's, the Martinez Formation is composed of massive sandstone beds, with some conglomerate and shale in its upper portion; its maximum thickness is 1,300 m (4,250 ft). The Tejon Formation is a white, conglomeratic sandstone, with a maximum thickness of 370 m (1,200 ft). Depositional environment for both formations apparently varied from shallow marine to continental, indicating that uplift of the region had begun.

The entire region must have been raised above sea level by the close of Eocene time (38 million years ago), because, other than limited deposits of Miocene and Pliocene age near the present coast line, no marine sediments younger than Eocene are known in the northern Coast Ranges. In late Pliocene or early Pleistocene time, probably no more than 4 million years ago, a basin larger than and including the present Clear Lake Basin began to accumulate freshwater sediments now called the Cache Formation. This is composed predominantly of gravel, silt, and sand, but water-lain tuffs (volcanic ash) and tuffaceous sands become dominant near the top of the formation; these are intercalated with clay, marl, pebbly limestone and diatomite.

Apparently the Cache Formation was deposited by streams entering one or more tectonic or structural basins, and whose surface was covered from time to time by lakes and swamps (Brice, 1953). The fine-grained rocks at the top of the unit are lake deposits. The maximum thickness of the Cache beds was calculated (Brice, 1953) to be 1,980 m (6,500 ft), which is unusually great for a freshwater deposit. Work in progress by geologists of the USGS suggests a downward revision in thickness of the Cache Formation.

Pliocene and Quaternary Volcanism--

Volcanic activity in the region began with the eruption of the Sonoma Volcanics in Pliocene time, during the period from 6 to 3 million years ago. These deposits covered an elliptical area extending from just north of San Pablo Bay to the vicinity of Healdsburg and Calistoga. They consist of basalt, andesite and rhyolite lava flows and ash, interbedded with volcanically derived sediment. The northern part of the Sonoma Volcanics, in the vicinity of Mount St. Helena, is principally rhyolite tuffs and dacite tuffs and flows, cut by small intrusions of similar composition.

Thickness of Sonoma rocks varies greatly, from a few tens of meters to hundreds of meters. The greatest thicknesses are believed to be located north of Calistoga, and to reach 900 to 1,500 m (3,000 to 5,000 ft) at a maximum. This may have been the central vent area for late-stage Sonoma eruptions.

Paleobotanical and vertebrate evidence, as well as potassium-argon (K-Ar) age-dates, suggest that Sonoma Volcanism has migrated northward during the Pliocene epoch. Inception was about 8 million years before present (mybp) at the south end of Napa Valley. The youngest dated Sonoma rocks are 2.9 million years, from the slopes of Mount St. Helena at the northern edge of the Sonoma Volcanics. Rocks of intermediate ages are known from locations between these points.

In early Pleistocene time, a period of largely silicic volcanism began south of Clear Lake, forming the Clear Lake Volcanic Series. Clear Lake Volcanism appears to have begun with the eruption of unique, low-viscosity, quartz-bearing olivine basalts. Its age is given as early Pleistocene. These flowed into and onto Sonoma terrain. A period of dacitic-andesitic volcanism followed, succeeded about 500,000 years ago by a major period of silicic volcanism. This included eruption of rhyolite glass flows and tuffs and dacite flows and tuffs and extrusion of rhyodacite domes. Still more recent are obsidian flows, of approximately 100,000 years of age. Youngest of all are well-preserved cinder cones and maars, perhaps in the age range of 10,000 to 40,000 years, located at the southern and eastern edges of Clear Lake.

Evidence suggests northward migration of magmatism in Pleistocene time. For example, Cobb Mountain (K-Ar age-date of 1 mybp) and the quartz-bearing olivine basalts are at the southern end of the Clear Lake Volcanic Series. Northward are the one-half million year old silicic lavas and domes. Still farther north and northeast are the youngest mafic and silicic cones and flows. This appears to extend the northward progression that began near San Francisco Bay at the end of Miocene time.

Clear Lake Volcanic Series rocks are not as widespread or thick as the Sonoma Volcanics. In many places, thickness is but a few tens of meters except around vent sources. The greatest recorded thickness is 730 m (2,400 ft) in the Kettenhofen No. 1 well near Mount Konocti. Total thickness in that area may be 900 m (3,000 ft), with greater thickness for plugs and volcanic necks.

Several discrete centers of rhyolite, dacite and andesite volcanism are recognized, including Cobb Mountain, Mounts Hannah, Siegler and Konocti and Boggs Mountain. In addition, there are numerous smaller basaltic cinder cones. Widely differing degrees of erosion of these ancient volcanoes attest to a span of activity covering much of the Pleistocene epoch. Mount Konocti is deeply eroded, Cobb Mountain is somewhat less eroded, and Mounts Hannah and Siegler are only somewhat eroded. However, morphology does not correlate very closely with time of youngest volcanic activity: radiometric age-dates for rocks of the Clear Lake Volcanic Series range from 0.03 to 2.5 mybp. The rhyolite of Borax Lake is dated at 0.08 mybp (Hearn, et al., 1975).

Although maximum thickness of extruded lava and ash is probably less than 760 m (2,500 ft), intrusive necks and stocks may extend downward to great depth and may be fingers rising away from a much larger, possibly molten, igneous body at depth. The minimum depth of this hypothetical body (often referred to as the Clear Lake Batholith) may be 5 to 8 km (3 to 5 mi), based on nonconclusive evidence. This hypothetical intrusive mass, and the stocks of the several extrusive centers mentioned above, may form the heat source for the geothermal field.

Quaternary Sediments--

Lacustrine deposits in Clear Lake and the adjacent closed depression may be the oldest Quaternary sediments in the region. More recent deposits are sand, gravel and silt deposited in stream channels, as fans abutting the mountains and as valley fill.

3.4 HYDROLOGY

The study area comprises portions of four drainage basins: that of the Russian River on the west, which empties into the Pacific Ocean; Cache Creek and Putah Creek Basins, which drain the east flank of the Mayacmas Mountains and flow easterly into the Sacramento River; and the Napa River, which heads on the flanks of Mount St. Helena and flows southeasterly into San Pablo Bay.

Practically all precipitation either becomes stream runoff or is stored temporarily in soil zones, from which it is evaporated and transpired. A very small amount percolates downward to join ground water reservoirs in permeable rocks and alluvium. Most shallow ground water is stored in shallow alluvium which occurs in valleys flanking the Mayacmas Mountains.

3.4.1 Surface Water

Stream Flow--

Numerous stream-gaging stations have been operated for 20 to 30 years in the study region. Table 3.2 presents average annual discharge data for eleven streams draining the Mayacmas Mountains.

Depth of runoff (see Table 3.2) amounts to some 635 mm (25 in) on the east side of the Mayacmas Mountains, and 785 mm (31 in) on the west side. Roughly, this amounts to about one-half of total precipitation. In the drier region extending between Lower Lake and Middletown, runoff depth is about 355 mm (14 in) annually, occurring as about 40% precipitation. Runoff depth of 300 mm (11.8 in) was computed for the land surface of Clear Lake Basin, by correcting the discharge of Cache Creek for evaporation from and precipitation on the lake surface (evaporation from the lake is estimated at 914 mm [36 in] annually).

3.4.2 Groundwater

Groundwater data for the study region is quite limited, both geographically and temporally. Water wells are located almost entirely within the narrow alluviated valleys that flank the Mayacmas Mountains, and published records for them cover only a few years. Generally, these wells penetrate only alluvium, which rarely is deeper than about 75 m (250 ft). Therefore, information concerning groundwater in bedrock, which is more widely exposed than alluvium, is nearly nonexistent.

In the following, groundwater in each of the major alluviated valleys is discussed on an individual basis. Finally, groundwater conditions in bedrock areas of the Mayacmas Mountains are treated in a necessarily speculative manner. Valleys treated are listed here by county: in Lake County, Big Valley, High Valley, Excelsior Valley, Burns Valley, Borax Lake Basin, Collayomi Valley and several small flats southeast of Mount Konocti; in Sonoma County, Alexander Valley; in Napa County, upper Napa Valley (near Calistoga).

Big Valley--

Big Valley is a gently rolling plain, sloping northward into Clear Lake and encompassing some 8,100 ha (20,000 acres). Elevations range from 400 to 460 m (1,320 to about 1,500 ft). Kelsey, Highland, and Adobe Creeks are the major drainages, but there are a number of other minor creeks as well. All manifest seasonal--that is, not perennial--flow.

Principal geologic units in this valley are the Mesozoic basement rocks of the Franciscan Formation, the Plio-Pleistocene sedimentary Cache Formation, the Pleistocene Clear Lake Volcanic Series and Quaternary unconsolidated sediments, including lake, terrace and stream deposits. The young, mostly permeable un-

TABLE 3.2 AVERAGE ANNUAL STREAM DISCHARGE[1] AND DEPTH OF RUNOFF

STREAM	DRAINAGE AREA (sq mi)	DISCHARGE (acre-ft)	DEPTH OF RUNOFF (in
Russian River Basin			
Big Sulphur Creek	82	147,000	33.6
Russian River (Healdsburg)	793	1,043,000	24.7
Maacama Creek	43.4	67,740	29.3
Putah Creek Basin			
Putah Creek	112	148,000	24.8
Dry Creek	8.4	21,230	47.4
Cache Creek Basin			
Cache Creek	528	251,400	11.8[2]
Highland Creek	12.7	15,570	23.0
Kelsey Creek	37.2	54,270	27.3
Adobe Creek	6.4	9,060	26.5
Seigler Creek	12.5	9,420	14.1
Copsey Creek	13.2	9,830	14.0
Burns Valley Creek	4.4	1,110	4.7
Napa River Basin			
Napa River (2.5 mi east St. Helena)	81.4	68,390	15.8

1) Data from USGS (1976)
2) Computed for land surface adjacent to Clear Lake, by correcting for evaporation and precipitation on the lake.

consolidated sediments reach a maximum thickness of 65 m (213 ft) north of Kelseyville; older Quaternary and Cache deposits are about 150 m (500 ft) thick. Thickness of the underlying volcanic rocks is unknown but is probably less than 460 m (1,500 ft).

Principal occurrence of ground water is in the younger, coarser-grained Quaternary sediments. Much of the ground water is unconfined, but confined areas exist locally where extensive layers of clay are present near the land surface. Within the older Quaternary sediments (largely terrace gravels, lake and floodplain deposits of fine sand, silt and clay), perched ground water occurs in the more permeable materials. Within the older lake deposits, a thin bed of lithic tuff, 0.6 m (2 ft) thick, forms a permeable and widespread aquifer. Only two wells are known to tap water from the volcanic rocks on Cameback Ridge. These rocks are highly fractured and yield significant quantities of water; however, on account of their depth, they are not encountered by any of the wells in Big Valley. While Franciscan basement is fractured and therefore probably has significant permeablity, no data on its hydraulic properties is available.

Although not stated explicitly in the documents consulted (California Department of Water Resources, [1957]; Soil Mechanics and Foundation Engineers, Inc., [1967]), the ground water reservoir as known and utilized extends from the land surface to a depth of some 30 m (100 ft). To this depth, total storage capacity is 14,260 ha-m (118,500 acre-ft), and average specific yield is 8% (California Department of Water Resources, 1957).

Water levels, and hence water in storage, vary seasonally, being highest in the spring and lowest in the fall. Average seasonal lowering of the water table varies from 3 to 7.5 m (10 to 25 ft), depending on location. No long-term decline in water level has been observed. Therefore, for the period of record (1949-60), recharge has equaled discharge. Average depth to the water table is near zero in the spring and 6 m (20 ft) in the autumn.

Recharge to the Big Valley ground water reservoir occurs principally by infiltration of water in the channels of Kelsey and Adobe Creeks. Mean annual surface water inflow from these and three other, minor creeks is about 7,400 ha-m (60,000 acre-ft). Direct precipitation contributes about 3,700 ha-m (30,000 acre-ft). A certain amount of recharge must occur as underflow from bedrock in the flanking uplands, but no quantitative estimates of this are available.

As mentioned previously, average annual discharge and recharge are equivalent. Although explicit figures for these factors are not available, a lower limit may be deduced from the mean seasonal fluctuation of water in storage. This has been estimated as 1,700 ha-m (14,000 acre-ft), based on water-level changes, specific yield, and reservoir area (Soil Mechanics and Foundation Engineers, Inc., 1967). Of course, this figure does not include annual water throughout, which moves through the basin into Clear Lake as underflow. Since total well pumpage is unknown, it is not possible to say what fraction of the 1,700 ha-m (14,000 acre-ft) is man-induced and what is naturally-occurring discharge within the basin. Movement of ground water is essentially northward toward Clear Lake.

High Valley--

High Valley is a nearly closed basin lying just north of Clearlake Oaks. It is a flat to gently sloping alluvial plain of about 810 ha (2,000 acres), with a total drainage area of some 31 sq km (12 sq mi); its average elevation is about 120 m (400 ft) above that of Clear Lake. Several short, intermittent creeks drain the surrounding hills; only in the wettest periods does surface water flow out of the valley into Clear Lake, through Schindler Creek.

Geologically, the valley consists of a thin deposit of stream alluvium and lake sediments resting on Franciscan basement; maximum depth to basement is about 30 m (100 ft), or a little more. Much of the alluvium is fine-grained and nearly impermeable; permeable lenses of gravel are located along the valley margin.

Nearly all ground water used is pumped from wells in the alluvium. Water levels near the valley center have seasonal fluctuation of some 6 to 15 m (20 to 50 ft). Because there is little artificial draft on the ground water body, there must be considerable natural summer discharge by underflow (Upson and Kunkel, 1955); probably this occurs mainly through the volcanics to the east rather than as underflow in Schindler Creek.

Valley East of Clearlake Oaks--

Immediately east of Clearlake Oaks lies a small unnamed valley, which is actually part of Clear Lake Basin, with a total drainage area of about 1,600 ha (4,000 acres); 400 ha (1,000 acres) is alluvial plain.

The entire drainage area is underlain by Franciscan Formation, which is considered non-water-bearing in this region (Upson and Kunkel, 1955). Therefore, alluvium is the only significant water-bearing unit. Little information on its thickness or lithology is available, but it is probably some tens of meters thick. Depth to ground water is less than 8 m (25 ft) at most places, and the water is unconfined.

Borax Lake Basin--

Borax Lake lies in a closed basin from 1.5 to 3 km (1 to 2 mi) north of Clearlake Park. Total drainage area is some 5 to 6.5 sq km (2 to 2.5 sq mi), and most of the basin floor is occupied by Borax Lake. The alluvium is underlain by Franciscan rocks at a maximum depth of perhaps 23 m (75 ft). Borax Lake and Burns Valley are separated by a low rise comprised of late Quaternary flows of rhyolite and obsidian. Young cinder deposits and historic solfataric activity in this area indicate that these volcanics were vented very locally. Before eruption of these rocks, Borax Lake Basin and Burns Valley were connected and both part of Clear Lake Basin. Now, however, Borax Lake Basin is a closed depression.

Burns Valley--

This is a long, narrow valley traversed by intermittent unnamed creeks that flow into Clear Lake. The tributary drainage area is about 31 to 32.5 sq km (12 to 12.5 sq mi), about 400 ha (1,000 acres of which are covered by alluvium). The name "Burns Valley Creek" in Table 3.2 refers to the collector stream flowing into Clear Lake.

The drainage area of Burns Valley is underlain by the Franciscan Group, the Cache Formation and some basaltic rocks. At most places, alluvium rests directly upon the Cache Formation, and these are the chief water-bearing units here. The alluvium is nowhere more than 15 m (50 ft) thick. Although more permeable than the Cache beds, the alluvium has such a small saturated thickness that water storage in it is quite limited; small to moderate yields are available from the Cache Formation, which is at least 60 m (200 ft) thick and probably stores more water.

Well records (Upson and Kunkel, 1955) show that water levels average from 1.5 to 4.5 m (5 to 15 ft) below land surface and have a seasonal fluctuation of 1.5 to 2.5 m (5 to 8 ft). Total volume of water in storage is estimated at 6,200 to 9,300 ha-m (50,000 to 75,000 acre-ft). Well pumpage was only about 4 ha-m (30 acre-ft) per year in 1949 and may not be much more than that today. No net depletion of the reservoir should occur at withdrawal rates several times larger, since surface runoff is some 135 ha-m (1,100 acre-ft) annually.

Excelsior Valley--

This irregularly shaped valley lies from one to two miles south of Lower Lake. It is drained by Copsey Creek, a small intermittent tributary to Cache Creek. The valley comprises north and south portions, separated by a low bedrock ridge through which Copsey Creek has cut a channel. The alluviated area of the valley comprises some 570 ha (1,400 acres); the total drainage area is about 36 sq km (14 sq mi).

The drainage area of the valley is underlain by sandstone and shales of the Cretaceous Great Valley Sequence and the Eocene Martinez Formation. Drilling reports indicate that these rocks are "dry" (Upson and Kunkel, 1955). The lava plateaus at the southeast end of the valley have not been tapped by wells. However, the lavas absorb precipitation and store it in joints; in a few places this water discharges as springs. Maximum thickness of alluvium in the valley is estimated at less than 7.5 m (25 ft), and it is the only significant water-bearing material. However, as it is predominantly a fine-grained flood plain deposit, producing wells are nearly all near the valley's edge, where coarser sediments are present.

Ground water in the valley is unconfined and stands at levels 3 to 5 m (10 to 17 ft) below the land surface. Storage capacity is quite small in the thin alluvial cover, probably less than 250 ha-m (2,000 acre-ft). All ground water comes from rainfall in the drainage area, which enters storage largely by direct infiltration on the alluvium and seepage from hillslopes. Water does not come from other basins by underflow, nor does much enter by percolation in the bed of Copsey Creek.

Only one well pumps significant water, but this amounts to only a few tenths of a hectare-meter per year.

Small Flats South of Mount Konocti--

Bonfield, Hesse, Ely and Manning flats are south of Mount Konocti. Manning Flat is a small alluvial plain located about 8 km (5 mi) west of Lower Lake, with a drainage area of about 5 sq km (2 sq mi); the plain covers 80 ha (200 acres). It was a closed basin containing an intermittent lake until about 100 years ago, when a tunnel was constructed to drain it into nearby Thurston Lake. This flat comprises a less than 6 m (20 ft) thick silt layer resting upon rhyodacite of the Clear Lake Volcanics. No significant amount of ground water is stored in either of these materials (Upson and Kunkel, 1955); one 60 m (200 ft) deep well was dry.

Bonfield, Hesse and Ely Flats, west of Manning Flat, are a series of shallow basins along the channel of Thurston Creek, which flows into Thurston Lake. Total drainage area is about 31 sq km (12 sq mi). The flats are underlain by alluvium which is less than 6 m (20 ft) thick and generally poorly sorted or fine-grained. Except for one well in Hesse Flat, wells that penetrate the alluvium have small yields. The alluvium rests upon either rhyodacite or rhyolite obsidian of the Clear Lake Volcanic Series. Only the obsidian yields significant water, and this underlies Hesse and Bonfield, but not Ely, Flats.

Ground water occurs in the alluvium of all three basins, in the obsidian bordering Bonfield and Hesse Flats, and presumably in rhyodacite at depths greater than 60 m (200 ft). In most wells, water levels are 3 to 6 m (10 to 20 ft) below the surface and water is unconfined. The water table in the obsidian seems to be shallow but may be perched. Insufficient data exists to make a satisfactory estimate of water in storage or depth of the main water body.

Collayomi Valley--

Collayomi and Long Valleys are arms of the same depression in the headward part of the Putah Creek drainage. Collayomi Valley, the larger of the two, extends from approximately 5 km (3 mi) west to 6.5 km (4 mi) south of Middletown. It has a drainage area of 140 sq km (54 sq mi); of this, the alluvial plain covers about 10 sq km (4 sq mi). Major streams in the valley are St. Helena and Dry Creeks, which head south of Middletown and are tributaries of Putah Creek; Putah Creek flows through the west arm of the valley and heads about 11 km (7 mi) northwest of Middletown.

The drainage area is underlain by non-water bearing sandstone, shales and serpentinites of the Knoxville (Great Valley Sequence) and Franciscan Formations. Alluvium reaches a maximum depth of perhaps 75 m (250 ft) and is the only significant water-bearing unit. However, fine-grained materials (silts and clays) seem to predominate near the valley axis, and so nearly all ground water is stored near the valley margins and along the channels of Putah and St. Helena Creeks, where sands and gravels are predominant.

The ground water table is shallow, averaging 4.5 m (15 ft) deep in midsummer, and seasonal fluctuations are generally about 1.5 m (5 ft). Most developed ground water is pumped from sumps dug in along the channels of St. Helena and Putah Creeks; these yield from 760 to 1,900 lpm (200 to 500 gpm). Gross storage capacity may be some 3,700 ha-m (30,000 acre-ft), but usable capacity would be considerably less. Considering minimum natural ground water discharge in stream channels, in the driest month (July), Upson and Kunkel (1955) estimated that at least 135 ha-m (1,100 acre-ft) per year could be discharged artificially, without long-term depletion. This is much more than was being utilized in 1955.

Alexander Valley--

This valley lies along the west base of the Mayacmas Mountains. It is about 32 km (20 mi) long, with an average breadth of 1.5 to 2.5 km (1 to 1.5 mi), and the Russian River flows through its entire length. Numerous streams enter the valley from both sides; Big Sulphur Creek is the largest drainage from the Mayacmas Mountains; Maacama Creek is also significant.

Geologic formations underlying the valley include the Franciscan and Knoxville Formations, massive conglomerates of

Cretaceous (?) age, the Sonoma Volcanics, the Glen Ellen Formation and various stream alluvium deposits. The alluvium bears the most water, and wells near the river, where deposits are coarsest, yield from 760 to 1,900 lpm (200 to 500 gpm); its maximum thickness exceeds 18 m (60 ft).

Ground water occurs under water table conditions (unconfined) over most of the valley but may be locally semi-confined by overlying deposits of silt and clay (Cardwell, 1965). At most places, water levels are 1.5 to 4.5 m (5 to 15 ft) below the land surface in the spring and about 1.5 m (5 ft) deeper in the summer.

Water also occurs in limited quantities in older formations. Most important is the Glen Ellen, encountered at depths of 18 to 120+ m (60 to 400+ ft), which yields up to 1,500 lpm (400 gpm). Many wells in the southern part of the valley produce from this formation. The Cretaceous (?) conglomerate yields moderate flows; no data on the hydrologic characteristics of older formations is available, as they have not been drilled.

Storage in alluvium has been estimated as some 6,200 ha-m (50,000 acre-ft). Discharge by natural means (discharge to the river, underflow at the south end of the valley and evapotranspiration) probably exceeds artificial discharge (principally by irrigation wells) by a sizeable amount (Cardwell, 1965). Well pumpage in 1964 was roughly 370 ha-m (3,000 acre-ft); clearly, recharge by rainfall, infiltration in stream beds and underflow is considerably greater than this amount.

Upper Napa Valley--

As discussed here, upper Napa Valley comprises the area extending from Calistoga to the uppermost end of the valley, and has an area of about 13 sq km (5 sq mi). Average elevation on the valley floor is nearly 120 m (400 ft) and rises to between 600 and 1,300 m (2,000 and 4,300 ft) on flanking mountains. The area is drained by the Napa River, which flows throughout the length of Napa Valley.

The Pliocene-age Sonoma Volcanics cover most of the uplands, while the valley is covered by Quaternary alluvium. The alluvium is underlain by volcanics, and the volcanics are underlain by the Franciscan Formation throughout the drainage area.

The most important water-bearing units are within alluvium and the Sonoma Volcanics. Permeable horizons in the Pliocene sedimentary section (in the Huichica and Glen Ellen Formations) form rather low-yield aquifers in the southern part of the valley but are not present near Calistoga. The Franciscan and Knoxville Formations are virtually non-water-bearing in this area (Kunkel and Upson, 1960). In the Calistoga area, many of the wells produce from the Sonoma Volcanics, particularly from welded tuffs of the St. Helena rhyolite member; the St. Helena rhyolite is several tens of meters thick in the vicinity of Calistoga. In general, pumice and tuff are the main aquifers in the Sonoma Volcanics, while flows are poor yielders.

Ground water storage and recharge/discharge data specific to the Calistoga area are not available; parameters covering the entire valley are available (Kunkel and Upson, 1960) but really are not helpful here. Generally, however, water levels have an average depth of 7.5 m (25 ft).

Mayacmas Mountains--

Rocks of the Franciscan Formation form the preponderance of outcrops in the Mayacmas Mountains, particularly in the vicinity of The Geysers geothermal field. Lithology in this formation includes sedimentary, metamorphic and igneous types: greywacke sandstone, basalt and serpentinite are the three most abundant. None of them has primary porosity; water is stored in small quantities in joints and fractures induced by late Cenozoic tectonism.

Numerous springs in the Mayacmas Mountains indicated that ground water is present; these meet most domestic and stock-watering needs in the mountains. Few water wells have been drilled into Franciscan rocks, but those have yields in the order of 3.8 lpm (1 gpm). This is in the order of 1% of that of wells producing from unconsolidated materials, with specific yields in the neighborhood of 8%. Therefore, an order-of-magnitude specific yield for Franciscan rocks is estimated to be some 0.1%.

3.4.3 Hydrologic Budget

By comparing precipitation (P), depth of runoff (RO) and depth of evapotranspiration (ET), it may readily be seen that, across the study area,

$$P \cong RO + ET$$

This equation does not take into account variations in soil moisture and ground water storage, or ground water discharge. The complete hydrologic balance is expressed by the equation

$$P = ET + RO + \Delta SMS + \Delta GWS + GWD$$

where Δ SMS = change in soil moisture storage
Δ GWS = change in ground water storage
GWD = ground water discharge

Complete solution of the equation requires much more detailed and complete data than is available to this study.

The Placer County study (Lewis and Burgy, 1961-670, sited on this soil overlying moderately fractured metamorphic rock, showed that maximum changes in ground water storage were about 25 mm (1 in) in any two consecutive years of observation; maximum changes in ground water discharge amounted to no more than 130 mm (5 in). The magnitude of these changes was strongly dependent on variations in rainfall from one year to the next. These relationships probably apply to bedrock areas of the study region in an approximate way. In alluviated valley areas, however, it is expected that ΔSMS and ΔGWS are significantly greater, because infiltration rates and soil thickness are considerably greater than in bedrock areas.

3.5 CHEMICAL CHARACTERISTICS OF GROUNDWATER

The quality of ground and surface waters in this region is generally quite good, except that certain ground and surface waters in Clear Lake (Cache Creek) Basin are high in boron as a result of recent volcanic activity. Boron in concentrations greater than about 1 ppm is injurious to many plant species. In Clear Lake, boron is 1.4 ppm, and in Borax Lake about about 590 ppm. The chemical characteristics of ground water and water quality are discussed below by individual drainage basin.

Big Valley--

Quality of both ground and surface waters in Big Valley is generally very good. TDS average about 4 ppm in surface waters and 500 ppm in ground waters. Boron in ground waters generally is under 0.3 ppm, but reaches concentrations between 0.7 and 2.5 ppm in several wells.

High Valley--

Water quality data is not available for High Valley; however, the water is suitable for domestic and agricultural purposes.

Valley East of Clearlake Oaks--

A few wells in the western part of the valley supply adequate water for domestic use; no irrigation wells exist.

The quality of the ground water is poor, and several wells in the western portion of the valley were destroyed because the water had a very unpleasant taste. One well in the eastern part is reported to have high soda and iron content.

At the south edge of the valley east of Clearlake Oaks lies the Sulphur Bank Mine, where sulphur and great quantitites of quicksilver were mined. Thermal spring waters in this area are highly charged with minerals and gases. As reported by Roberson and Whitehead (1961), these waters are rich in ammonia and nitrogen (up to 485 ppm, as NH_4^+), nitrate (up to 470 ppm), bicarbonate (up to 4,000 ppm), sulfate (up to 4,900 ppm) and chloride (up to 869 ppm); hydrogen sulfide reaches about 10 ppm in two springs. Their analyses did not include cations. Ecoview Environmental Consultants (1976) reported the chemistry of one spring above Sulphur Bank Mine, which showed the following cation concentrations (in ppm): calcium = 235; magnesium = 200; sodium = 780; potassium = 26; boron = 50. Anion and gases were of the order reported by Roberson and Whitehead (1961).

In view of this highly charged thermal water at Sulphur Bank, it is not surprising that cool ground waters in the adjacent valley are also heavily mineralized; probably this occurs by leakage along faults and subsequent mixing with shallow, relatively pure water.

Borax Lake Basin--

Several wells are located on the low volcanic hill between Borax Lake and Burns Valley. Apparently this ground water is of acceptable quality for domestic and orchard irrigation use.

No wells are located in the alluvium bordering Borax Lake. However, it can be predicted that ground water there is highly mineralized, especially in boron. The waters and muds of Borax Lake are extremely alkaline, saline and borated and were once mined for borax. It appears that the source of the borax was borated solfataras or springs that issued from the bottom of the lake. Probably, these had the same volcanic source as springs at Sulphur Bank, about 1.5 km (1 mi) to the north.

Burns Valley--

Except for a narrow strip along the lakeshore, the ground water of Burns Valley is of good quality. Chloride and hardness and conductance were determined as 7 and 63 ppm and 263 micromhos, respectively, in a well about 0.8 km (0.5 mi) from the lake.

Small Flats South of Mount Konocti--

No water quality data is available for the four small flats south of Mount Konocti.

Collayomi Valley--

Partial analyses of water show that chloride and hardness are about 4 and 150 ppm, respectively. All water in the valley appears suitable for domestic and agricultural use (Upson and Kunkel, 1955).

Alexander Valley--

Chemically, ground water in Alexander Valley generally is of the hard, bicarbonate type. Hardness (as calcium carbonate [$CaCO_3$]) ranges from 80 to 1,300 ppm; TDS range up to 1,300 ppm; boron varies from 0 to 40 ppm (Cardwell, 1965) but is usually under 0.5 ppm. Overall, the water is adequate for irrigation but requires softening for domestic use.

Upper Napa Valley--

Water quality data is limited for the Calistoga area. TDS throughout Napa Valley average about 200 to 700 ppm. TDS are not given by Kunkel and Upson (1960) for the Calistoga area, but chloride there is given as 190 ppm; this suggests that TDS may range to nearly 1,000 ppm.

Mayacmas Mountains--

Ground water quality information is unavailable for the Mayacmas Mountains.

Excelsior Valley--

Ground water quality data is very sparse for this basin. TDS in ground water occurring in the Excelsior Valley may average 150 to 300 ppm.

3.6 SEISMICITY

This section presents, in general terms, the historical seismicity, microseismicity and seismic risk in The Geysers-Clear Lake region.

3.6.1 Historical Seismicity

Figure 3.3 shows earthquake epicenters as located by the Seismograph Station at the University of California, Berkeley (U.C.B.), for the period 1910-76. Currently the accuracy of U.C. epicenters in this area is probably better than ± 5 km (3 mi) for magnitude 3.5 or greater shocks; however, before 1963, when the U.C. seismograph network was greatly improved, accuracy probably improved from about ±20 km (12 mi) in 1910 to ±10 km (6 mi) in 1962 (McEvilly, pers. comm., 1974). For this reason, one cannot see distinct clustering of U.C. epicenters along the active Rodgers Creek-Healdsburg Fault System, nor along any other faults.

Historical Seismicity and Earthquake Damage--

Since 1855, more than 140 earthquakes have been felt in the Santa Rosa-Sonoma Valley-Clear Lake region. While some ten of these did significant damage in Santa Rosa and Sonoma Valleys, only one was destructive in the study region itself. This was the great 1906 (M = 8.25 earthquake, caused by rupture along the San Andreas Fault; the break extended from San Juan Bautista on the south to Point Arena, or perhaps Shelter Cover, on the north, a distance of at least 300 km (190 mi); along its reach through Sonoma and Mendocino Counties, strike-slip displacement averaged about 4.5 m (15 ft). Damage to buildings in Santa Rosa Valley varied from nil to major. In the following, it is important to keep in mind that intensity values are qualitative in nature and combine effects of both vibratory and permanent ground motions. Modified Mercalli (MM) intensity (Table 3.3)

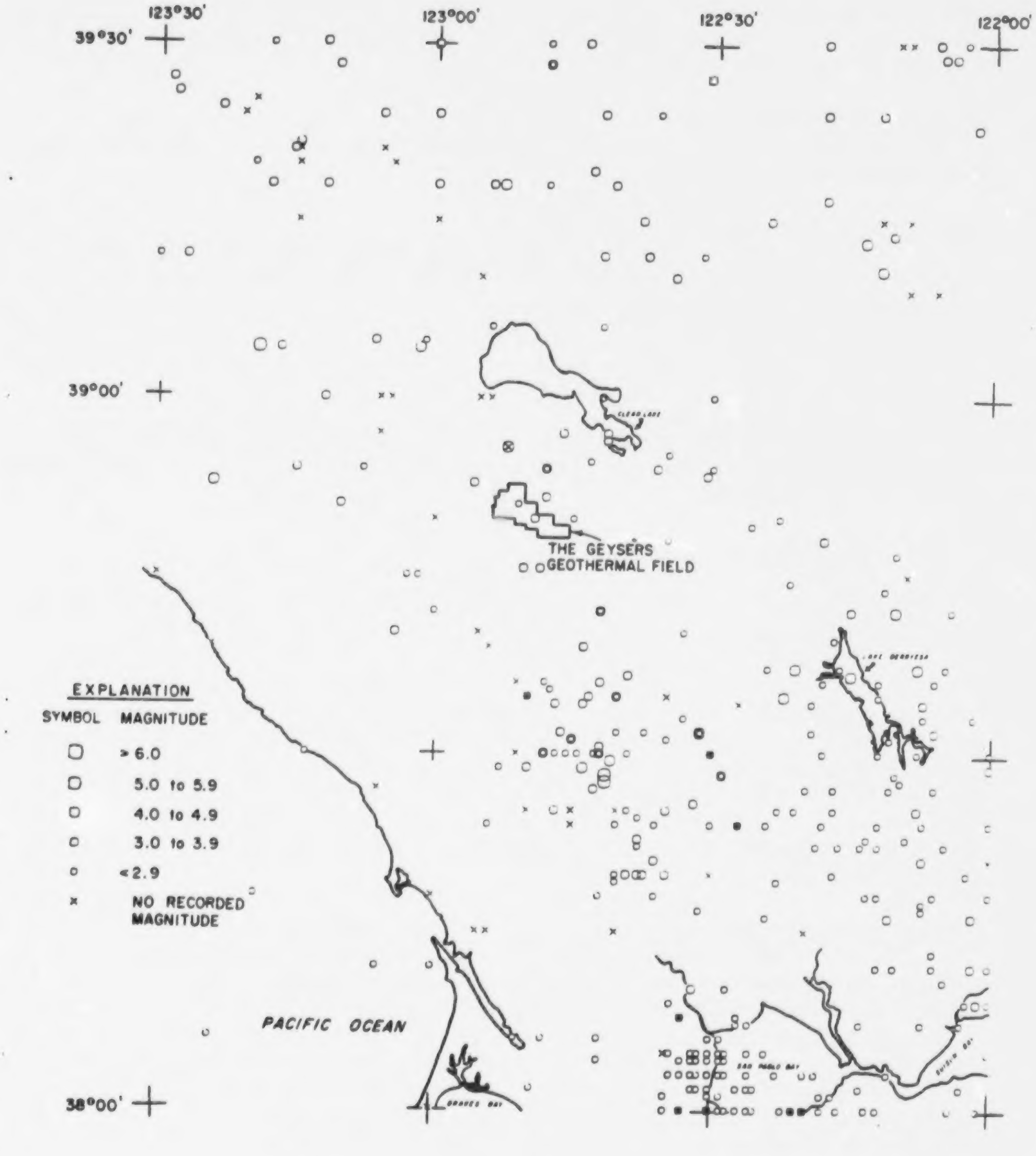
123°30'
123°00'
122°30'
122°00'
39°30'
39°00'
38°00'
CLEAR LAKE
THE GEYSERS GEOTHERMAL FIELD
LAKE BERRYESSA
EXPLANATION
SYMBOL MAGNITUDE
> 6.0
5.0 to 5.9
4.0 to 4.9
3.0 to 3.9
<2.9
NO RECORDED MAGNITUDE
PACIFIC OCEAN
DRAKES BAY
SAN PABLO BAY
SUISUN BAY

Figure 3.3 Earthquake epicenters located by the University of California, Berkeley, 1910-76.

TABLE 3.3 MODIFIED MERCALLI INTENSITY SCALE

(ABRIDGED)

I. Not felt except by a very few under specially favorable circumstances. (I Rossi-Forel scale.)

II. Felt only by a few persons at rest, especially on upper floors of buildings. Delicately suspended objects may swing. (I to II Rossi-Forel scale.)

III. Felt quite noticeably indoors, especially on upper floors of buildings, but many people do not recognize it as an earthquake. Standing motorcars may rock slightly. Vibration like passing of truck. Duration estimated. (III Rossi-Forel scale.)

IV. During the day felt indoors by many, outdoors by few. At night some awakened. Dishes, windows, doors disturbed; walls make creaking sound. Sensation like heavy truck striking building. Standing motorcars rocked noticeably. (IV to V Rossi-Forel scale.)

V. Felt by nearly everyone, many awakened. Some dishes, windows, etc., broken; a few instances of cracked plaster; unstable objects overturned. Disturbances of trees, poles, and other tall objects sometimes noticed. Pendulum clocks may stop. (V to VI Rossi-Forel scale.)

VI. Felt by all, many frightened and run outdoors. Some heavy furniture moved; a few instances of fallen plaster or damaged chimneys. Damage slight. (VI to VII Rossi-Forel scale.)

VII. Everybody runs outdoors. Damage **negligible** in buildings of good design and construction; **slight** to moderate in well-built ordinary structures; **considerable** in poorly built or badly designed structures; some chimneys broken. Noticed by persons driving motorcars. (VIII Rossi-Forel scale.)

VIII. Damage **slight** in specially designed structures; **considerable** in ordinary substantial buildings with partial collapse; **great** in poorly built structures. Panel walls thrown out of frame structures. Fall of chimneys, factory stacks, columns, monuments, walls. Heavy furniture overturned. Sand and mud ejected in small amounts. Changes in well water. Persons driving motorcars disturbed. (VIII+ to IX— Rossi-Forel scale.)

IX. Damage **considerable** in specially designed structures; well-designed frame structures thrown out of plumb; **great** in substantial buildings, with partial collapse. Buildings shifted off foundations. Ground cracked conspicuously. Underground pipes broken. (IX+ Rossi-Forel scale.)

X. Some well-built wooden structures destroyed; most masonry and frame structures destroyed with foundations; ground badly cracked. Rails bent. Landslides considerable from riverbanks and steep slopes. Shifted sand and mud. Water splashed (slopped) over banks. (X Rossi-Forel scale.)

XI. Few, if any, (masonry) structures remain standing. Bridges destroyed. Broad fissures in ground. Underground pipelines, completely out of service. Earth slumps and land slips in soft ground. Rails bent greatly.

XII. Damage total. Waves seen on ground surfaces. Lines of sight and level distorted. Objects thrown upward into air.

ranged from about VII to IX in the valley, reaching IX in the city of Santa Rosa due to soft, saturated ground conditions there. The ground was extensively fissured in Santa Rosa, probably as a result of lurching and differential settlement; some liquefaction may have occurred. In the Mayacmas Mountains, MM intensity was about VI to VII, with very minor damage reported from The Geysers; intensity VII characterized Sonoma Valley. Around Clear Lake, damage was confined to alluviated areas along the north and west shores: MM intensity VII prevailed in the area from Kelseyville to Upper Lake, as evidenced by fallen chimneys; fissures were reported in alluvial ground south of Kelseyville. Detailed information on damage caused by the 1906 earthquake may be found in Lawson, et al. (1908).

Two of the three most important factors controlling earthquake damage versus magnitude, fault distance and ground consolidation were well-exemplified in the 1906 earthquake. For constant distance from the fault rupture, damage to a given type of structure was controlled by shallow ground conditions, being minimal on bedrock and maximal on water-saturated unconsolidated alluvium; for given ground conditions, damage varied inversely with epicentral distance.

Other than the 1906 event, no shock in the region has been of sufficient magnitude to cause significant damage in the study area. The largest had magnitudes estimated to have been near 5, and produced MM intensity VII (fallen chimneys) at Upper Lake and along the Russian River from Healdsburg to Ukiah; these places are located near the margins of the study area and on alluvium. However, maximum MM intensity within the study area probably did not exceed VI on alluvium and V on bedrock.

In 1969 two earthquakes, with magnitudes 5.6 and 5.7, occurred on the southern end of the Healdsburg Fault, on the north side of Santa Rosa. They caused substantial damage to buildings in Santa Rosa but not within the study area.

3.6.2 Microseismicity

The Geysers geothermal field is characterized by high microseismicity (Bufe, et al., 1976). Most microearthquakes there have had magnitudes less than 2 and focal depths in the range of 2.6 to 6.0 km (1.6 to 3.75 mi). It is widely accepted that this prolific, shallow microseismicity is caused by increased temperature and pore pressure of water within the geothermal reservoir. This condition weakens the rocks to such an extent that regional strain is released continuously by small-displacement fault-rupture events in the geothermal field. Such activity serves to help maintain the system of open fractures necessary to create most geothermal reservoirs.

Teleseismic residuals in the area have been analyzed by Iyer (1975). He found that positive residuals of about 0.5 second characterize ray paths near the margin of the gravity anomaly; these increase to 1.5 second for rays penetrating the anomaly's center. This is believed to be strong evidence for the existence of a magma chamber.

Immediately following the Santa Rosa earthquakes in 1969, the National Center for Earthquake Research (NCER) of the USGS extended its dense Bay Area seismograph network into the Santa Rosa Valley area. Plate 3.2 shows NCER epicenters and stations in the area from 38°30' to 39° N latitude and 122° to 123° W longitude for the period 1969-76 (Bufe, et al., 1976) and a correlation between epicenters and the mapped traces of the Rodgers Creek-Healdsburg Fault Systems. This correlation appears because of the relatively high accuracy and precision of the NCER data: most epicenters are accurate to better than ±1 km (0.6 mi). An updated version of this map, with more accurate epicenter locations, will be released by the USGS by the end of 1977. Most of the epicenters at the southern end of the Healdsburg Fault are aftershocks of the 1969 Santa Rosa earthquakes.

Both the USGS and U.C.B. data indicate a lack of seismicity along the San Andreas Fault; this is characteristic of the fault northward from the Santa Cruz Mountains to Point Arena. It may also be seen that there is very little seismicity west of the Rodgers Creek-Healdsburg Fault but a great deal to the east. This could be a result of the 1906 earthquake, which probably released most of the stored crustal strain energy in the western part of the map area. Crustal strain apparently is still low there, but geodetic measurements at Fort Ross and Point Reyes (Greensfelder, 1972, p. 9) indicate that strain is now accumulating along the San Andreas Fault.

The NCER data show high microseismicity in The Geysers geothermal field, but epicenter locations do not resolve specific active faults. It seems safe to say that seismicity there is produced by microfracturing throughout the geothermal field. This is probably the result of low-level strain release which is localized by high temperature and pore pressure in the geothermal system. To the east, in the Clear Lake area, microseismicity is much lower than in The Geysers area. Nearly one-half of all microearthquakes in this area occurred in a two-day-long swarm located under the south flank of Mount Konocti, and one mile west of the trace of the Konocti Bay Fault. All of these shocks had a similar focal mechanism, with modal planes paralleling the fault, and the shocks may have occurred on the fault (Bufe, pers. comm., 1976). Therefore, we conclude that the Konocti Bay Fault is seismically active. Otherwise, epicentral data do not delineate faults in the Clear Lake area.

3.6.3 Seismic Risk

Seismic risk is the likelihood of damage from an earthquake. This hazard is comprised of two distinct classes of ground movement--vibrational and permanent. The degree of these hazards varies geographically as a function of seismic potential and near-surface geologic conditions. Seismic risk, i.e., the probability of property loss or human injury, is a function of naturally occurring seismic hazards and the earthquake resistance of the works of man. Where there are no man-made structures, seismic risk is small. Evaluation of seismic risk means estimation of all of the following: the location, magnitude and frequency of earthquakes; vibratory motion in rock; the response of unconsolidated earth materials to these rock motions; and the response of man-made structures to resultant ground surface motions. The disciplines of seismology, geology, soils and structural engineering must all be used, and expert practitioners in each of these fields will admit to significant uncertainties in prediction of the phenomena with which they deal.

Seismic risk elements discussed in this section are intensity, occurrence, vibratory rock and ground motion, and permanent ground motions including faulting, liquefaction, landsliding, differential settlement and lurch-cracking. These elements are not specified in sufficient detail for aseismic engineering of structures at specific sites. However, all important risk factors are presented and should form adequate guidelines for detailed, site-specific analyses.

Intensity Recurrence--

Figure 3.4 is a graph showing the historic frequency of occurrence of earthquake intensities (MM) in the Santa Rosa Valley area, as well as for the entire San Francisco Bay region. Due to their historically sparse populations, the Mayacmas Mountains and Lower Lake-Middletown areas do not afford adequate reporting of intensities. However, the distribution of epicenters and the predominance of bedrock as foundation materials in the study region assured that the curves of Figure 3.4 represent upper bounds for intensity recurrence there.

The data used to construct the curves covers the period 1810-1966 for the entire Bay region, and 1855-1966 in Santa Rosa Valley (Algermissen, et al., 1969, p. 37-42). It can be seen that the frequency of occurrence of strong ground shaking (intensities VI, VII, and VIII) has been nearly as great in Santa Rosa Valley as in the entire San Francisco Bay region. Note that extending the data base up to the present; thus, including the 1969 Santa Rosa earthquakes of intensity VII-VIII would bring the two curves even closer together.

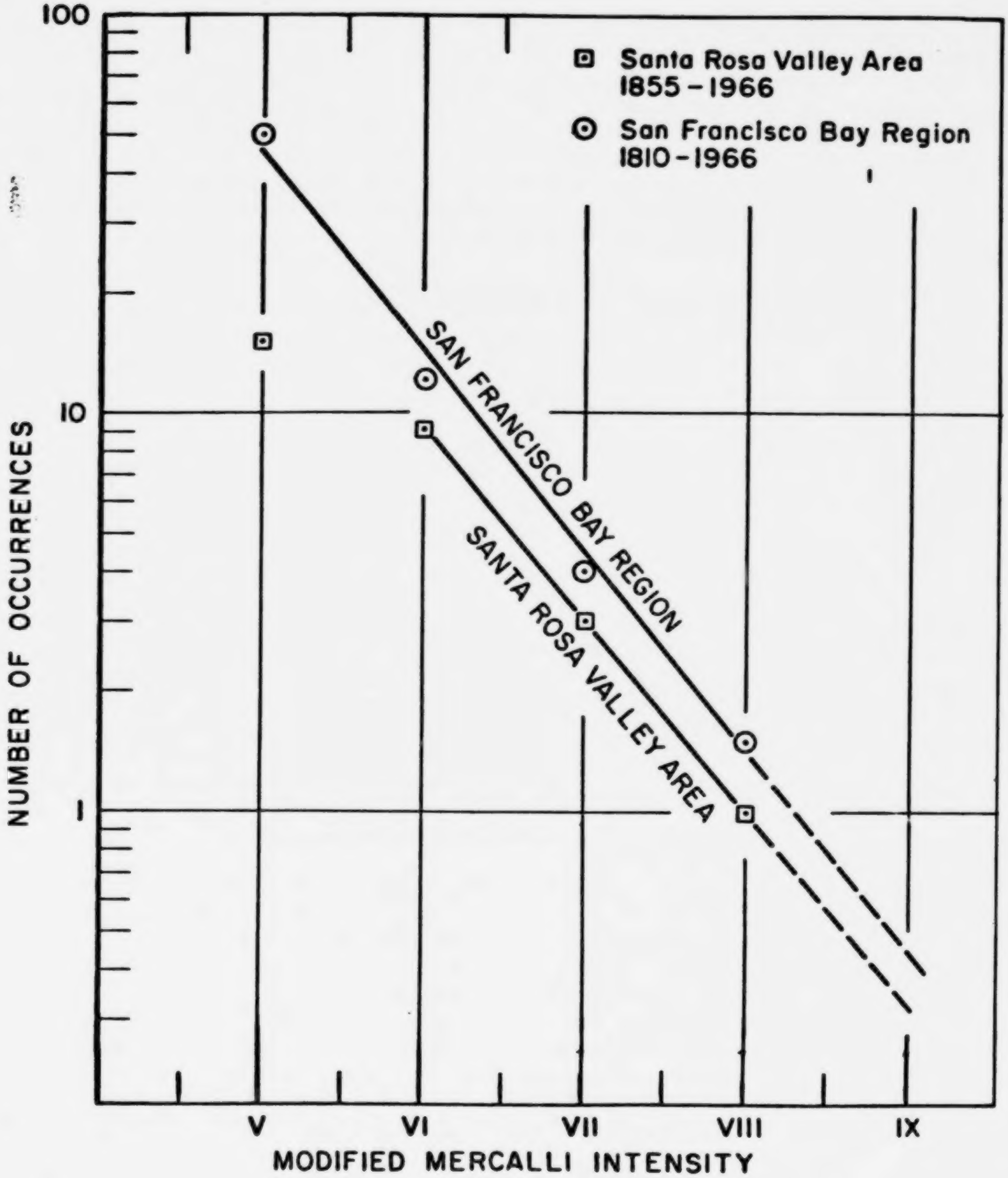

Figure 3.4 Frequency of occurrence of earthquake intensities, Santa Rosa Valley region.
(data from Algermissen, et al., 1969)

If the last 160 years are fairly representative of long-term seismicity of the Bay region, then it seems we should expect potentially damaging ground shaking (intensity VII or greater) about once every 30 years, on the average, in alluviated portions of the study region. On bedrock within the study region, the "30-year intensity" is probably about VI; intensity VII or greater may be expected about once every century; and intensity VIII, which may be damaging to modern structures, no more than about once in 3 centuries.

Magnitude versus Frequency of Occurrence--

In order to make a more refined, quantitative assessment of maximum probable ground shaking, it is necessary to analyze magnitude versus frequency of occurrence of earthquakes. As described below, definition of the true or long-term average magnitude equal frequency characteristic of this region is not a simple matter. This is because the historic seismicity record is short relative to long-term variations of regional crustal strain, and because instrumental magnitudes are available only since 1932.

The greater San Francisco Bay region, extending from Monterey Bay on the south to Ukiah on the north, and east to Vacaville, is one of the most seismically active areas of California. Seismicity was much higher in this region during the nineteenth century than it has been in the twentieth: since the great 1906 earthquake, a few moderate (magnitude less than 6.0) and no major shocks have occurred; however, between 1836 and 1906 there were 5 major (magnitude probably greater than 7.0), and a number of moderate shocks. The following analysis of magnitude versus frequency of occurrence demonstrates and interprets this temporal change in seismicity.

Figure 3.5 shows relationships between earthquake magnitude and frequency of occurrence for two regions: the entire central California Coast Range area, and the area covered by the Santa Rosa Sheet (Koenig, 1963) bounded by 38° to 39° N latitude and 122° and 124° W longitude, including all of Sonoma and Napa Counties and portions of five others. Two curves are shown for the central Coast Range area, one for the period 1810 to 1931, and another for the period 1932 to 1961. These curves are based on the work of Ryall, et al. (1966, p. 1124), who estimated magnitudes of most pre-1932 earthquakes from intensity data. The seismicity of this region is stated in terms of a 19,000 sq km (7,500 sq mi) area of the Santa Rosa Sheet. For the Santa Rosa Sheet, there is one curve covering the period 1944 to 1971, as magnitude data for pre-1944 earthquakes is unavailable. Data for the area covered by the Santa Rosa Sheet (Koenig, 1963) is from the University of California (1977), whose earthquake records begin in 1910; Figure 3.5 is a plot of U.C.B. epicenter data for the area from 38° to 39° 30' N latitude and 122° to 123° 30' W longitude for the interval 1910 to 1976. Table 3.4

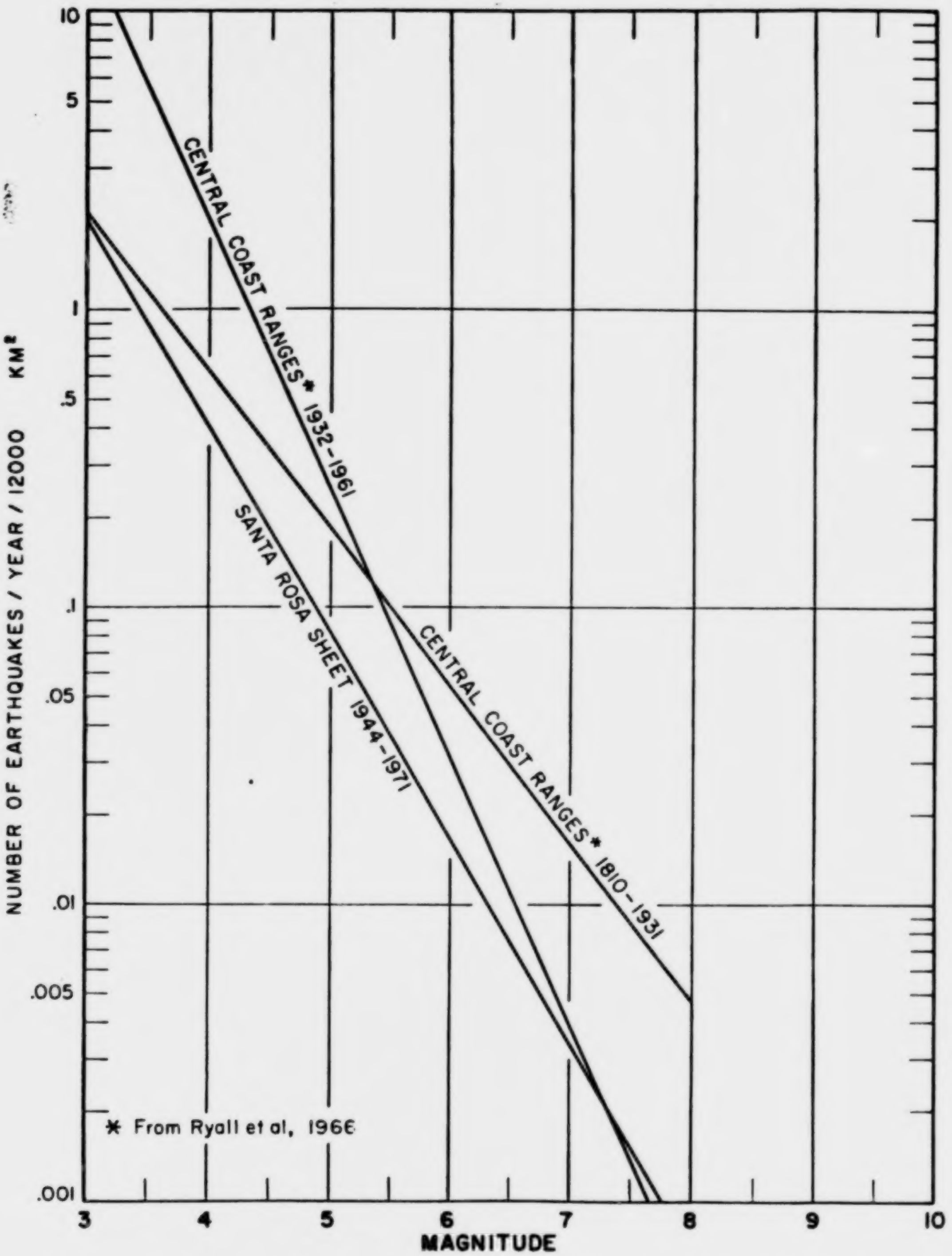

Figure 3.5 Magnitude versus frequency of occurrence for earthquakes in the central Coast Range.

TABLE 3.4 EARTHQUAKE RECURRENCE DATA FOR THE CENTRAL COAST RANGE REGION

Earthquake Data Set			Recurrence Parameters*		Average Recurrence Intervals (yrs)				
					1,000 km^2		12,000 km^2		
Region	Area (km^2)	Period (years)	a	b	M: 6	7	6	7	8
Santa Rosa Sheet	12,000	1944-1971	1.42	0.72	720	3600	60	300	1500
Central Coast Ranges	33,000	1932-1961	2.83	0.90	370	2960	32	250	2000
Central Coast Ranges	37,000	1810-1931	0.84	0.53	216	735	18	62	210

*Parameters of the equation $\log N = a - b\,M$;
'a' is normalized on an annual and per 1000 km^2 basis.
For the Central Coast Ranges, 'a' and 'b' are from Ryall et al, 1966, p. 1124.

presents the data of Figure 3.5 in numerical form, as well as average recurrence intervals for magnitudes 6, 7, and 8.

The region covered by the Santa Rosa Sheet was chosen for analysis because it is both convenient and large enough to afford a fair sample of seismicity important to the study area. The reliability of magnitude-frequency curves as indicators of future seismicity is proportional to the time-area sample of past seismicity used to prepare them. There is good reason to believe that the 28-year record (1944-71) of the Santa Rosa Sheet area, as well as the 30-year record (1932-61) of the central Coast Range, is a poor index of future seismicity. This is because the 1906 earthquake released nearly all the accumulated strain in the central Coast Range area; thus seismicity has been abnormally low since 1906. On the other hand, it could be argued that seismicity was abnormally high in the 100-year period immediately preceding the 1906 event due to an unusually high level of strain. Long-term average seismicity for the region probably falls in between that of the pre- and post-1906 periods.

Table 3.4 and Figure 3.5 show that, for the period 1932 to 1971, seismicity (per unit area) of the Santa Rosa Sheet is similar to that of the larger central Coast Range zone for magnitudes 6 and greater. Therefore, the long-term unit-area seismicity of the two regions should be similar, and we believe that the recurrence intervals for the central Coast Range for 1810-1931 are a reasonably good indicator of future seismicity affecting the study region. Geodetic and geologic data bearing on the long-term displacement rate along the San Andreas Fault suggest a recurrence interval of from 100 to 400 years for magnitude 8 or greater earthquakes at any place along the fault (Wallace, 1970). This is in satisfactory agreement with the seismicity data.

Vibratory Ground Motion--
Previously, it was concluded that potentially damaging ground shaking may recur at an average rate of about once every 30 years on alluvial ground. This is a very crude estimate of the frequency of occurrence of damaging ground motions. Although there is insufficient data to define the character of future ground shaking in alluviated areas, we are able to describe with some confidence the characterisitcs of seismic ground motion on bedrock.

In addition, we can predict the gross geographic distribution of permanent (not vibrational) ground movements: liquefaction, lurch-cracks and differential settlement occur only in alluvial areas, and landsliding only in hilly areas.

Maximum Bedrock Acceleration--

Maximum shaking in rock is commonly specified in terms of maximum credible and maximum probable accelerations. Maximum credible acceleration at any given place is defined as the maximum acceleration that could reasonably be expected to occur, given the known geologic framework. Thus it is based entirely on the location, length and relative recency of faults in the region surrounding a site under consideration. Maximum probable acceleration at a site is derived from statistical analysis of the recorded seismicity of the surrounding region.

Shaking is not completely described by maximum acceleration, above, one also needs to know its duration and spectral character, i.e., the distribution of amplitude relative to vibrational period. Spectral shapes appropriate for rock can be computed and scaled to fit maximum acceleration values from existing accelerograms. As an additional matter, rock accelerations may be modified by topography, but this is not well understood; in the 1971 San Fernando earthquake, shattered overturned soil was frequently noted on ridge tops.

For most engineering work, it is both realistic and practical to use maximum probable acceleration in regions where the spatial and temporal distribution of destructive earthquakes is not well understood. Of course, most areas fall into this category, the present one included. In other words, where seismicity is largely known in a statistical (not deterministic) way, it is sensible to predict ground motion in a probablistic manner.

Maximum Credible Acceleration--

Only three major (more than a few kilometers in length) active faults are known to lie within 50 km (31 mi) of the study region; faulting beyond this distance is not capable of producing significant damage. The three faults are, from west to east, the San Andreas, Healdsburg-Rodgers Creek and Maacmas Faults. The first two are proven seismically active; the Maacmas Fault appears to creep (aseismic slippage), but no earthquakes are known to have occurred on it. In addition, there is speculation that the Collayomi Fault may be active, but there is little evidence for this. Other, shorter faults may be active or potentially active, particularly some in The Geysers-Clear Lake region. However, except for the Konocti Bay Fault, there is no clear evidence for their activity. At an arbitrary location, accelerations induced by earthquakes on shorter faults, many of which are unknown, may exceed those from events on major faults.

Maximum credible bedrock acceleration may be estimated from the length of and distance from a given fault. Empirical data (Bonilla, 1970) relates rupture length and magnitude. Assuming that the entire mapped length of an active fault may rupture during a single event, one can estimate the maximum credible magnitude of earthquakes on particular faults. In this way, we estimate 8.5 on the San Andreas, 7.5 on the Healdsburg-Rodgers Creek and 6.5 on the Maacmas Fault. From empirical curves relating peak rock acceleration, earthquake magnitude and distance from the causative fault (Schnabel and Seed, 1973), we find that maximum credible bedrock acceleration in the study region varies from about 0.7 g adjacent to active faults down to about 0.2 g south of Lower Lake.

Duration of strong shaking for these maximum credible events varies from about 20 seconds for M = 6.5 to 40 seconds for M = 8.5.

Maximum Probable Acceleration--

Maximum probable acceration may be derived using seismicity models of varying sophistication. The most sophisticated type involves both known fault sources and random sources of earthquakes. It requires that regional seismicity be apportioned among known active faults and unknown or unmapped faults which must be assumed to have a random distribution. Such an analysis would be useful for the study area; however, it is beyond the scope of this report.

A much simpler technique simply assumes that all earthquakes are randomly distributed, implicitly on unknown faults. According to the method of Cornell (1968), and using magnitude-frequency parameters for 1810-1930 in the central Coast Range (see Table 3.4), maximum probable bedrock acceleration per 100 years is about 0.26 g in this area. This has a 63% chance of being exceeded in any 100-year interval, or 30% in 50 years. Design to this value would not be "conservative," in the engineering sense of the term.

A more conservative design might use the 200-year maximum probable bedrock acceleration, with a 30% chance of being exceeded in any 100-year interval (or 15% in 50 years); this is 0.42 g.

However, we expect most of the larger earthquakes to be associated with the Healdsburg or San Andreas Faults, located beyond the region of expected geothermal development. Therefore, the accelerations given above are really too high for the given time periods, but by an unknown amount. A more sophisticated analysis, as outlined above, would certainly give smaller values of acceleration in the area of concern.

Permanent Ground Deformation--

Liquefaction, differential settlement, lurch-cracking, surface faulting and landsliding comprise the various types of permanent ground deformation, or ground failure. All but faulting result from ground shaking; faulting is the proximate cause of ground shaking. Strictly speaking, liquefaction is a cause, rather than a manifestation, of ground failure.

Although permanent ground deformations may locally do serious damage to building foundations, ground shaking will cause more widespread and greater total depth of deformation.

Liquefaction and its Effects--

Liquefaction is defined as the transformation of a granular material from a solid into a liquefied state as a consequence of increased pore-water pressures. It is a common occurrence in water-saturated sandy deposits subjected to strong earthquake shaking, and is the proximate cause of low angle flow and lateral spreading landslides, lurch-cracking and "quick condition" failures. Liquefaction may be an important problem where the ground water table in alluvial areas is generally not more than 3 to 6 m (10 to 20 ft) deep. It may also occur in water-saturated fills, such as are often constructed for drilling pads and power plant facilities in the Mayacmas Mountains. During the 1906 earthquake, liquefaction apparently occurred near the Santa Rosa cemetery and at Altruria where water ejection (reported formation of springs) was noted in connection with ground disturbances; in Santa Rosa itself, liquefaction apparently did not take place. During the 1969 earthquakes, liquefaction may have been involved in the ground failures that damaged pipes, streets and curbs. Youd (1973) has described the mechanics and effects of liquefaction in some detail, which we need not repeat here. However, a brief description of effects is given below.

Flow Landslides--

These result when mobilized soil is unrestrained, and large masses of earth materials may travel long distances in the form of liquefied flows or blocks of intact materials riding on liquefied materials. In the 1906 earthquake, one such slide occurred at the base of San Bruno Mountain on the San Francisco Peninsula, flowing several hundred yards on a slope of about 18%.

Lateral Spreading Landslides--

These are probably much more common than the above type and involve smaller displacements. Youd (1973) uses the term to denote all limited-displacement ground failures associated with liquefaction, including lurch-cracks. Repeated episodes of limited flow may occur during a strong earthquake, resulting in a large total displacement; they are most probable on gentle slopes, having angles of the order of 1% to 2%. Such landslides are common in moderate and strong earthquakes and were the cause of extensive damage in the San Fernando earthquake of 1971.

Quick Condition Failure--

Seeping forces, caused by upward percolating pore water, often reduce the strength of granular soils to a point of instability, which is termed a "quick condition." This condition is usually limited to thick sand layers extending from below the water table to the surface. Loss of bearing capacity is the most common effect of a quick condition; buoyant rise of buried tanks is also common. In the 1964 Niigata, Japan, earthquake, several high-rise apartment buildings rotated and sank into liquefied soil.

Differential Settlement--

This can be quite severe in man-made fills but may also occur in natural ground. Liquefaction may be a factor in causing differential settlement.

Landsliding and Faulting--

Landslides and land slumps are frequently triggered by strong ground shaking. In the Mayacmas Mountains extensive areas are underlain by mélange deposits of the Franciscan Formation which are particularly prone to landsliding, even without earthquake shaking.

The Study Area--

Much of the Franciscan Formation, particularly the mélange deposits, is subject to landsliding under aseismic conditions. Of course, these same areas are subject to additional landslide potential under earthquake loading. Therefore, slope stability studies for siting geothermal facilities should include analysis of the effect of earthquake shaking.

Failure by liquefaction may be a problem in saturated alluvium or fills which contain much silt- to sand-sized material. Good drainage may practically eliminate potential problems in such fills.

REFERENCES

Algermissen, S. T., J. C. Stepp, W. A. Rinehart and E. P. Arnold. Studies in Seismicity and Damage Statistics, Appendix B. U.S. Department of Commerce, Environmental Science Services Administration, Coast and Geodetic Survey, 68 p., 1969.

Bonilla, M. G. Surface Faulting and Related Effects; in Earthquake Engineering, R. L. Wiegel, Principal Investigator, Prentice Hall, New Jersey, p. 4774, 1970.

Brice, J. E. Geology of the Lower Lake Quadrangle, California. Cal. Div. Mines and Geol. Bull. 166, 1953.

Bufe, C. G., J. H. Pfluke, F. W. Lester and S. M. Marks. Map Showing Preliminary Hypocenters of Earthquakes in the Healdsburg Quadrangle, Lake Berryessa to Clear Lake, California, January 1969-June 1976. USGS, Open File Report 76-8021, 1976.

California Department of Water Resources. Lake County Investigation. Bull. 14, 1957.

__________. Evaporation from Water Surfaces in California. Bull. 73-1, 1974.

__________. Vegetative Water Use in California, 1974. Bull. 113-3, 1975.

Cardwell, G. T. Geology and Ground Water in Russian River Valley and in Round, Laytonville and Little Lake Valleys, Sonoma and Mendocino Counties, California. USGS Water Supply Paper 1548, 154 p., 1965.

Cornell, C. A. Engineering Seismic Risk Analysis. Bull. Seism. Soc. Am., v. 58, p. 1583-1606, 1968.

Ecoview Environmental Consultants. Borax Lake Study Area, Lake County, California Consulting Report for Philips Petroleum Company, 1976.

Greensfelder, R. W. Crustal Movement Investigation in California. Cal. Div. Mines and Geol., Special Publication 37, 1972.

Hearn, B. C., Jr., J. M. Donnelly and F. E. Goff. Preliminary Geologic Map of the Clear Lake Volcanic Field, Lake County, California. USGS Open File Report 75-391, 1975.

Iyer, H. M. Teleseismic Residuals at The Geysers Geothermal Area. Trans. Am. Geophys. Un., v. 56, p. 1020, 1975.

Koenig, J. Geologic Map of California, Santa Rosa Sheet. Cal. Div. of Mines and Geol., 1963.

Kunkel, F., and J. E. Upson. Geology and Ground Water in Napa and Sonoma Valley, Napa and Sonoma Counties, California. USGS Water Supply Paper 1495, 1960.

Lawson, A. C., et al. Report of the State Earthquake Investigation Commission. Carnegie Inst., Wash., 1908.

Lewis, D. C., and R. H. Burgy. Water Use by Native Vegetation and Hydrologic Studies. Dept. of Water Science and Engineering, University of California, Davis, Annual Reports No. 2-7, 1961-67.

McLaughlin, R. J. Preliminary Geologic Map of The Geysers Steam Field and Vicinity, Sonoma County, California. USGS Open File Map 74-238, 1974.

Mooney, M. L. Mendocino Transmission Line Study, Cloverdale Peak, The Geysers, and Mt. Vaca. Pacific Gas and Electric Co., Meteorological Office, 1975.

National Oceanic and Atmospheric Administration. Climatological Data, Annual Summary, California. v. 79, No. 13, 1975.

Roberson, C. E., and H. C. Whitehead. Ammoniated Thermal Waters of Lake and Colusa Counties, California. USGS Water Supply Paper 1535-A, 1961.

Ryall, A., D. B. Slemmons and L. D. Gedney. Seismicity, Tectonism, and Surface Faulting in the Western United States. Bull. Seis. Soc. Am., v. 63, p. 1105-1135, 1966.

Schnabel, P. B., and H. B. Seed. Accelerations in Rock for Earthquakes in the Western United States. Bull. Seis. Soc. Am., v. 63, p. 501-516, 1973.

Soil Mechanics and Foundation Engineers, Inc. Big Valley Ground Water Recharge Investigation. Consulting Report for Lake County Flood Control and Water Conservation District, 1967.

Swe, W., and W. R. Dickinson. Sedimentation and Thrusting of Late Mesozoic Rocks in the Coast Ranges near Clear Lake, California, Bull. Geol. Soc. Am., v. 81, p. 165-188, 1970.

University of California. Bull. of Seismographic Stations (Geonomics plot from magnetic tape), 1977.

Upson, J. E., and F. Kunkel. Ground Water of the Lower Lake-Middletown Area, Lake County, California. USGS Water Supply Paper 1297, 1955.

U. S. Department of the Interior. Final Environmental Statement for the Geothermal Leasing Program, Vol. II of IV, 1973.

U. S. Geological Survey. Surface Water Supply of the United States, 1966-1970, Part II, Pacific Slope Basins in California. USGS Water Supply Papers 2129 and 2131, 1976.

Wallace, R. E. Earthquake Recurrence Intervals on the San Andreas Fault. Bull. Geol. Soc. Am. v. 81, p. 2875-2890, 1970.

Youd, L. T. Liquefaction, Flow and Associated Ground Failure. USGS Circular 688, 1973.

SECTION 4

KLAMATH FALLS

4.1 INTRODUCTION

This section presents baseline data on climatology, geology, hydrology and seismology to aid in assessment of environmental impacts of potential geothermal development in Klamath Falls, Oregon. Descriptions of aspects of climatology, geothermal characteristics, tectonic history, faults, stratigraphy, lithology and surface water that are related to and influence the ground water regime are discussed, as well as ground water systems and the chemical characteristics of ground water. A brief section on the extremely low seismicity of the area is included.

4.1.1 Summary

Klamath Falls, in south-central Oregon, is within a long, northwest trending structural depression, the Klamath Basin (Fig. 4.1). At Klamath Falls City, some 300 shallow wells, generally less than 150 m (500 ft) in depth, tap thermal aquifers at temperatures to more than 104°C (220°F). Water from these wells is used for space heating in homes, schools and numerous commercial buildings. Other, presumably smaller, thermal anomalies are present at Klamath Hills, Olene and elsewhere in the Klamath Basin. All appear to be fault-controlled, and to store hot water in rubbly, fractured basalt aquifers.

Surface waters are dominated chemically by calcium, magnesium and bicarbonate; deeper thermal waters are principally sodium chloride and sulfate chloride in composition. As there is no data from wells deeper than 600 m (2,000 ft) the nature of a deep circulation system is problematic.

4.1.2 Background

Location--
The area under discussion here covers the central and southern parts of the Klamath Basin topographic and geologic area, located in Klamath County, southwestern Oregon (Fig. 4.1). Most geothermal anomalies and all of those likely to undergo development lie between latitudes 42° 30'N and 42° 00'N. Westward the area extends to the foothills of the Cascade Range, and eastward, to a line of ridges extending through Naylox Mountain,

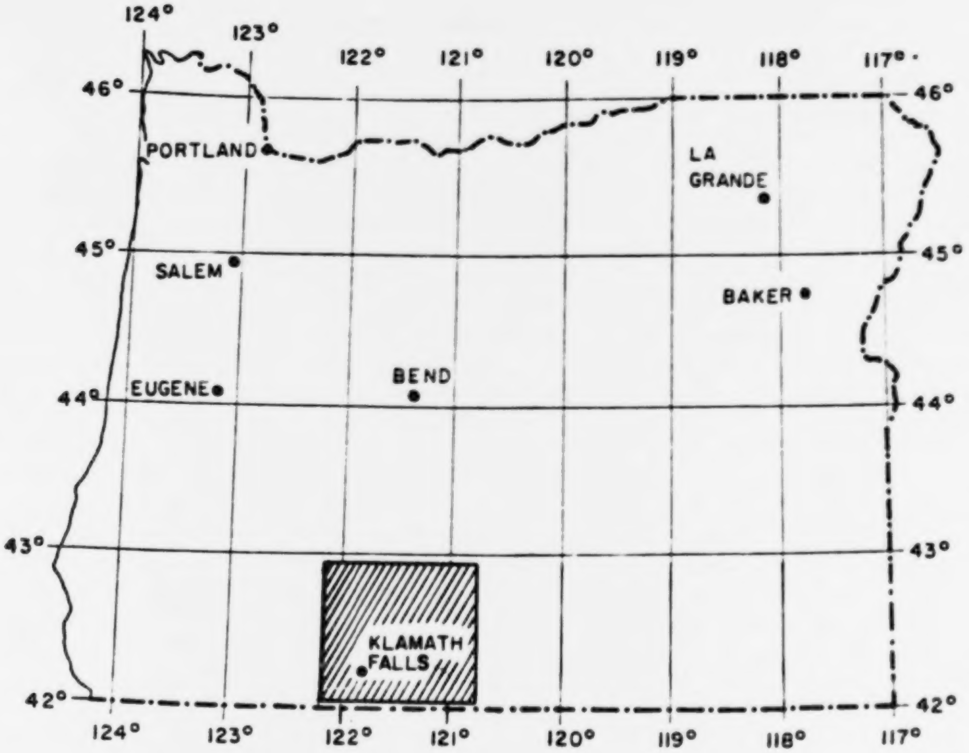
124°
123°
122°
121°
120°
119°
118°
117°
46°
45°
44°
43°
42°
PORTLAND
LA GRANDE
SALEM
BAKER
EUGENE
BEND
KLAMATH FALLS

Figure 4.1 Location map of the Klamath Basin study area.

Hogback Mountain and Stukel Mountain. While most of the following discussion focuses on this area, data from the surrounding region is presented whenever it is necessary for an understanding of the geothermal resource.

The Klamath Basin region is covered by U.S. Army Map Service sheets at a scale of 1:250,000. The area of study is also covered by recent USGS topographic quadrangle maps at a scale of 1:62,500.

Method of Study--
This study is based on a compilation of published and unpublished data. Much of the information contained in this report has been obtained from unpublished materials. The chief sources of this type of data have been the Oregon State Engineer (ground water records), State of Oregon Department of Geology and Mineral Industries (geologic mapping and geothermal development data), Oregon Institute of Technology (OIT) at Klamath Falls (local geothermal development data) and the Weyerhaeuser Corporation (detailed geologic mapping).

Previous Work--
Several reconnaissance and detailed studies of various aspects of the geology, hydrology and geothermal resource development have been made during the past twenty years. Among those sources accessible for this study are the reconnaissance geologic mapping of Peterson and McIntyre (1970) and the detailed geologic studies by Hardyman, et al. (1972). The basic hydrology of the region has been covered by Newcomb and Hart (1958), Illian (1970) and Leonard and Harris (1974). The geothermal resource as a whole, including reconnaissance geophysics and geochemistry, is covered by Sammel (1976). Many other geological, geophysical and geochemical studies have been carried out on the resource by private companies interested in geothermal exploration, but most of this data was not available for use here.

4.1.3 Climatology

The Klamath and Cascade Mountains impede the easterly flow of moist, temperate air from the Pacific Ocean into the Klamath Basin region. The climate of this region is characterized by warm, dry summers and cool to cold, more humid winters. Because elevations vary from 1,200 m (4,000 ft) on valley floors to over 2,400 m (8,000 ft) in the mountains, there is a considerable variation in local climatic conditions.

All weather stations in the Klamath Basin region are in the lowlands. Klamath Falls and Klamath Falls airport (elevation 1,245 m [4,085 ft]) are the most important data-gathering points. Supplemental data from Fort Klamath and Chiloquin in the north, from Keno in the west, and from Merrill and Malin in the south part of the basin is also available.

The chief source of data presented here is the Columbia Basin Climatological Handbook, compiled by the Meteorological Committee of the Pacific Northwest River Basins Commission (1968-69). Unless otherwise noted, information given below is from this source.

Temperature--

Maximum recorded temperatures range from 41°C (105°F) at Klamath Falls (in 1911) to -32°C (-25°F) in Malin (in 1937). The Klamath Basin has a short growing season. The first killing frost (-2°C [28°F]) occurs on October 18, and the last on May 4, on the average. However, temperatures of -2°C (28°F) or below have been recorded each month of the year in Klamath Falls. Figure 4.2 shows normal monthly temperature at Klamath Falls. More detailed temperature data is given in Table 4.1. Mean annual temperature at several stations for the period 1931 to 1960 is as follows: Chiloquin, 6.8°C (44.3°F); Klamath Falls, 9.1°C (48.3°F); Klamath Falls airport, 8.2°C (46.8°F). By contrast the mean annual temperature at Crater Lake, at an elevation of about 2,400 m (7,900 ft) in the Cascade Mountains, is 3.8°C (38.9°F).

Precipitation--

Average annual precipitation in the region varies with altitude. Lowland-station figures range from 477 mm (18.79 in) at Keno and 450 mm (17.72 in) at Chiloquin to 357 mm (14.06 in) at Klamath Falls and 338 mm (13.34 in) at Klamath Falls airport. Precipitation at Crater Lake, on the crest of the Cascade Range, is 1,235 mm (48.61 in), and amounts of 1,525 mm (60 in) or more are common along the crest. Figure 4.3 is a histogram of annual precipitation for the period 1931 to 1972 at Klamath Falls and Chiloquin.

Average monthly precipitation is shown in Figure 4.2 and Table 4.1. Greatest amounts fall in December and January, and least fall in the summer. In all, 70% of annual precipitation falls between October and March. This precipitation generally occurs as mixed rain and snow in the lowlands and as snow in the mountains.

Wind--

Wind data is available only for Klamath Falls airport. Average wind speed is about 10 km/hr (6 mph), varying from a low of 7.1 km/hr (4.4 mph) in September to a maximum of 11.8 km/hr (7.3 mph) in March. Peak wind speeds range from 32 to 40 km/hr (20 to 25 mph) in summer to 72.5 km/hr (45 mph) in January. Calm periods are least frequent during March through June (averaging about 17%) and most frequent in October (33%). Predominant wind directions have a trimodal distribution in all months but May through August, when they are bimodal. The three chief directions are south-southeast, west, and north to north-northwest, and together they account for some 40% of all winds.

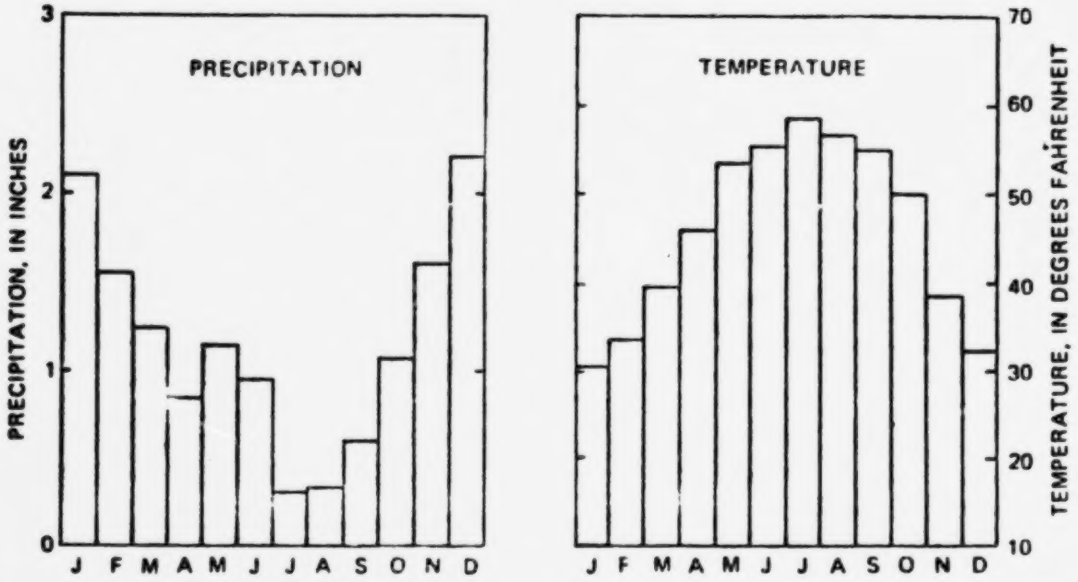

Figure 4.2 Normal monthly temperature and precipitation at Klamath Falls.

TABLE 4.1 MEAN MONTHLY AND ANNUAL TEMPERATURES AND PRECIPITATION, AND MEAN EXTREMES OF TEMPERATURE, KLAMATH BASIN, 1931-60

Means

Klamath Falls Airport

	Jan.	Feb.	Mar.	Apr.	May	June	July	Aug.	Sept.	Oct.	Nov.	Dec.	Ann.
T	28.8	33.8	37.1	44.7	51.1	57.4	67.2	64.5	59.5	48.2	38.2	31.6	46.8
P	1.62	1.06	0.85	0.61	1.19	0.98	0.12	0.21	0.53	0.99	1.37	1.81	11.34

Chiloquin

	Jan.	Feb.	Mar.	Apr.	May	June	July	Aug.	Sept.	Oct.	Nov.	Dec.	Ann.
T	27.3	31.2	36.4	42.9	49.4	55.2	62.3	60.6	54.6	45.6	35.7	30.6	44.3
P	2.79	1.99	1.62	1.03	1.46	1.09	0.32	0.28	0.65	1.43	2.75	2.76	17.72

Mean Extremes of Temperature

	Mean Minimum	Mean Maximum
Klamath Falls Airport		
January	20.4	37.2
July	50.6	83.9
Chiloquin		
January	14.7	38.8
July	37.4	84.3

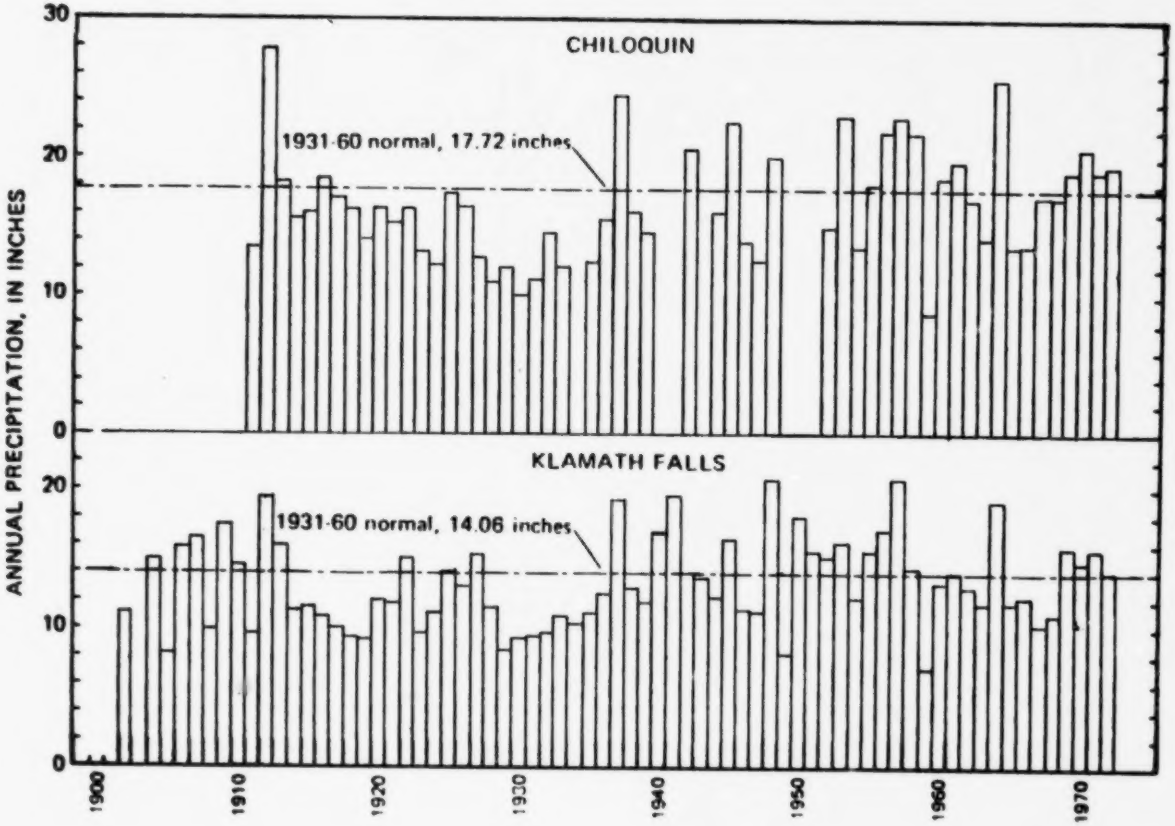

Figure 4.3 Annual precipitation at Chiloquin and Klamath Falls, 1902-72. (Leonard and Harris, 1974)

Other winds are rather evenly distributed among the remaining twelve points of the compass. South-southeasterly winds predominate during the winter, west winds in the spring, and northerly winds during the summer and fall. This data is summarized in Table 4.2.

The extent to which winds at Klamath Falls airport characterize those throughout Klamath Basin is unknown. However, it may be guessed that the percentage calm and average speeds are representative of much of the basin.

Humidity--
Relative humidity is reported only from Klamath Falls airport. This is maximum when temperatures are lowest, in the early morning hours. Seasonally, the diurnal maxima do not vary much, ranging from 74% to 83%. Minima occur in late afternoon and show large seasonal change, from 26% in July to 74% in December.

Dew point is an indicator of absolute humidity. At Klamath Falls airport, it shows slight diurnal change (about -17°C [2°F]). Seasonal variation is large, from about -7°C (20°F) in January to 8°C (47°F) in July. Presumably, the increase is related to local evapotranspiration from irrigated fields and lake surfaces.

Evaporation in Klamath Basin is not precisely known. Average annual pan evaporation (class A) is estimated at 1,400 mm (55 in), and lake evaporation at 1,020 mm (40 in). This high rate of evaporation reflects the low relative humidity of the region.

Ground Fog--
During the months of November through February, ground fog occurs rather frequently in southern Klamath Basin. At Klamath Falls airport, fog is reported 9.3% of the time in November, decreasing rather steadily to 2.6% in June. It averages about 0.5% in summer months (July to September) and 3.4% in October.

The detailed distribution of such fogs about the basin is unknown, but the data from Klamath Falls airport may be considered characteristic of Lower Klamath Lake Basin.

Significant quantities of water vapor are released from evaporative cooling towers of major power plants. Therefore, geothermal electric power development, should it occur, could cause significant local increases in ground fog in Lower Klamath Lake Basin, particularly during the months of November through February, when natural fogs are most frequent. For this reason, the siting of such facilities may need to be considered in relation to land uses adversely affected by such fog.

TABLE 4.2 PREVAILING WINDS AT KLAMATH FALLS AIRPORT: PERCENTAGE FREQUENCY OF OCCURRFNCE OF CALMS AND MODAL DIRECTIONS, WITH AVERAGE SPEEDS

Month	Calm %	Modal Dir.	Directions %	Average Speed (mph)
January	20.8	SSE	15.5	11.2
		W	8.9	8.0
		N	7.7	6.6
February	20.6	SSE	13.2	10.7
		N	10.9	5.5
		W	9.7	8.4
March	16.7	W	14.8	9.6
		SSE	12.0	11.5
		NNW	8.3	7.3
		N	7.4	6.5
April	18.6	W	14.5	8.7
		NNW	11.6	8.7
		SSE	8.2	11.4
		N	7.7	5.9
May	16.6	W	18.8	7.9
		NNW	13.9	9.1
		N	9.6	6.4
June	17.5	W	18.0	7.5
		NNW	16.1	8.7
		N	9.8	6.9
July	25.0	NNW	18.0	8.3
		W	13.4	6.9
		N	10.8	6.1
August	27.3	NNW	15.0	8.1
		W	11.9	6.2
		N	7.2	5.4
September	27.9	NNW	15.8	7.1
		N	12.6	5.3
		W	8.7	6.9

TABLE 4.2 (continued)

Month	Calm %	Model Dir.	Directions %	Average Speed (mph)
October	33.2	N	11.3	5.4
		NNW	9.8	6.8
		W	8.4	7.4
November	26.2	SSE	14.5	11.3
		N	10.3	4.3
		NNW	9.2	5.4
		W	7.3	7.8
December	29.2	SSE	12.9	10.7
		W	8.8	8.7
		N	6.8	3.7
		NNW	6.7	5.2

4.2 GEOTHERMAL CHARACTERISTICS

Thermal springs and wells occur in areas of upwelling ground water. Circulation to 3,100 m (10,000 ft) is believed likely. Warming of circulating ground water to more than 120°C (250°F) may occur at those depths without a magmatic component of heat. Data available at this time indicates that the most intense zones of upwelling are along faults forming the east side of the main graben trend. However, this conclusion must be tempered by the observations that almost no drilling has been done in the lake- and marsh-covered central graben area.

4.2.1 History of Geothermal Exploration and Development

There are several thermal springs in the Klamath Basin. These include the now defunct hot springs at Klamath Falls, the hot springs in Lost River at Olene Gap (sec. 14, T. 39 S., R. 10 E.) and the hot spring on the west shore of Upper Klamath Lake at Eagle Point (sec. 23, T. 36 S., R. 7-1/2 E.). Additional thermal anomalies have been discovered in the course of water well drilling. The most notable areas are in the eastern part of the town of Klamath Falls, along the southwest side of the Klamath Hills and at the north end of Stukel Mountain.

Klamath Falls--
Hot ground water at Klamath Falls has been utilized for the space heating of homes, schools, and public buildings for more than 70 years. The thermal water there is found in fractured basalts and silicified lacustrine sediments (probably the Sedimentary and Lower Basalt Aquifer units described in Section 4.4.2, below), along one or more faults in the graben complex. The water is produced from depths ranging from less than 30 m (100 ft) to a maximum of 550 m (1,800 ft) in a zone as much as 3 km (2 mi) wide northeast-southwest and extending for at least 8 km (5 mi) northwest-southeast. Temperatures in this zone range from about 60°C (140°F) to 113°C (235°F). No holes have been drilled beyond 550 m (1,800 ft). The deepest holes are on the campus of OIT, at the north end of Klamath Falls. Development of this zone is continuing and progressing southward. A KGRA has been established here.

The average power derived from this resource is estimated to be only about 5.6 MW and is used principally for space heating some 500 structures in the city. These include homes, businesses and public buildings (Lund, et al., 1974). Hot well water has been used directly in heating and drinking water systems in older installations. The water is then discharged to the sewers and ultimately into the Klamath River. However, present practice is to use downhole heat exchangers, with municipal water as the circulating fluid, minimizing the discharge of either the slightly mineralized water or the spent warm water had been drilled. This data is not yet available. Ground noise and electrical resistivity surveys had been carried out previously by Gulf Oil Company, from whom Thermal Power acquired the greater part of its lease position.

The deep hole appears to have been drilled within the complexly faulted Klamath Hills horst, northeast of the topographic and Bouguer gravity gradient which indicates a major fault zone. The reversal of temperature gradient below 140 m (450 ft) suggests that an unmapped fault was crossed near this point and that the lower part of the hole was drilled in a different and older block than was the upper part.

Results of this drilling discourage further prospecting in the Klamath Hills horst itself, but it is possible that the source of the greater than 93°C (200°F) water is at depth to the west, toward the central basin. Temperatures at depth are likely to reach or even exceed 150°C (300°F).

Other exploration companies hold leases in the Klamath Basin and have conducted exploration programs here, but there are no known plans for further deep testing of the basin at this time.

4.2.2 Temperature Gradients

Several water wells provide temperature gradient data. From these it can be seen that regional gradients are about 36°C/km (2°F/100 ft). This is roughly average for crystalline rock in the western United States. Gradient varies with heat flow and thermal conductivity of rock, according to the relation

$$\frac{dQ}{dt} = K\frac{dT}{dz}$$

Thus, for given heat flow, temperature gradient is higher in poorly consolidated sediment (low conductivity) and lower in crystalline rock (higher conductivity). For example, gradients of 36° to 53°C per km (3° to 4°F per 100 ft) may be encountered in unconsolidated sediments, under average western U.S. heat flow conditions of about 1.5 to 2 heat flow units (HFU). Gradients are altered by convective circulation of water along faults or communication between aquifer systems.

Recharge along range fronts commonly is associated with depressed gradients, with near-isothermal conditions often extending downward for several tens of meters. Upwelling thermal water often is characterized by very high gradients (occasionally to 80° to 180°C per km [5.5° to 11°F per ft]) in shallow zones, and especially in alluvium.

Several companies and government agencies have drilled shallow temperature gradient holes in the Klamath Basin: Gulf Oil Company, Natomas Company, Hunt Oil Company, Thermal Power Company, Weyerhaeuser Company and the USGS, among others. Proprietary information from the private companies is not available, but the USGS results were published recently (Sass and Sammel, 1976; Sammel, 1976).

Two 180 m (590 ft) holes were drilled and logged by the USGS during 1973 in the Lower Klamath Lake area, and temperature gradients in many existing water wells were accurately logged. It was concluded that local stratigraphic and hydrologic conditions determine the temperature regime in most places (Sass and Sammel, 1976; Sammel, 1976). Interfaces between basin sediments and basalt flows, as well as lateral convective flow in permeable zones within the basalt sequences, influence temperature gradients. Sammel (1976) concluded that observed heat fluxes in shallow wells, some lower than 0.5 HFU, do not accurately relate to temperatures at depth. Downward movement of cold water is considered to cause such perturbation. Sass and Sammel (1976) think that low thermal conductivity in fine-grained sediments produces unrepresentative, high temperature gradients in many basins.

4.2.3 Geothermal Potential

Geochemical data and temperature gradients indicate a moderate temperature hot water reservoir, circulation and heating of meteoric water along major faults and mildly saline water at depth.

Another possibility, although less likely, is that these same factors indicate a high temperature vapor-dominated reservoir, whose fluids are diluted and cooled by mixing with meteoric ground water as they rise toward the surface. Hydrochemical data from formations underlying Pliocene basalts (described in Section 4.3, below) is not available to help answer this question. Only deep drilling can determine deeper conditions of temperature and water quality. Appreciable amounts of hot water may exist in the deep central Klamath Basin, perhaps at 3,000 to 4,000 m (10,000 to 13,000 ft). It is likely that abundant thermal water occurs at drillable depths, principally in fault zones, where isotherms are bowed upward. The availability of this water in extensive areas in the eastern part of the Lower Klamath Lake sub-basin suggests that continued development for domestic and commercial space heating will take place. However, the total thermal fluid in storage along these fault zones may be trivial in comparison with commercial needs for electric power generation. It is unknown whether deeper, as yet unsampled thermal fluids exist in quantities sufficient for commercial power production.

4.3 GEOLOGY

The physiography, regional geologic setting, tectonic history and structure of the Klamath Basin region are discussed in this section. The lithology, stratigraphy and more important structural features of the two prominent geothermal areas in the Upper and Lower Klamath Lake sub-basins are emphasized.

4.3.1 Physiography

The Klamath Basin is essentially coincident with the drainage basins of the Lost River and Klamath River, with its tributaries, Sycan River, Williamson River and Sprague River. The basin extends for a distance of about 110 km (70 mi) east from the crest of the Cascade Range to the Quartz Mountain-Gearhart Mountain area. The northern boundary of the basin is the low drainage divide located near Chemult. From here it extends for a distance of about 185 km (115 mi), to the edge of the Modoc Lava Beds, California.

Throughout this region, major trends in the Cascade Range are northerly. In general, valleys and ridges on the east side of the basin trend northerly; but immediately north of the Oregon border, they trend northwesterly. The structural significance of this trend change is discussed in Section 4.3.3, below.

Klamath Basin is a region of diverse topography. Its most typical features are the large, flat-bottomed lake- or marsh-covered depressions such as Klamath Marsh, Upper Klamath and Agency Lakes, Lower Klamath Lake, Swan Lake and Tule Lake. These sub-basins were covered by more extensive lakes during Pleistocene time. The south part of Lower Klamath Lake, Swan Lake and Tule Lake are basins of interior drainage, as are other smaller sub-basins. Generally, lake bottom flatlands have a surface relief of less than 30 m (100 ft), except where fault blocks or eruptive centers protrude through them. The elevation of the water surface in Upper Klamath Lake is approximately 1,260 m (4,140 ft). As the lake has a maximum depth of only about 11 m (35 ft), the lake bed is about 1,250 m (4,100 ft) in elevation. Elevations in the Tule Lake and Lower Klamath Lake flatlands range from about 1,220 to 1,250 m (4,000 to 4,100 ft).

The main basins of the region are separated by upland areas consisting of narrow, elongate, fault-block ridges, small, lava-capped plateaus and volcanic piles.

The most important of the fault-block ridges are Bryant Mountain (1915 m [6,280 ft]), Swan Lake Rim (2,210 m [7,260 ft]), Stuckel Mountain (1,990 m [6,525 ft]), and Naylox Mountain-Hogback Mountain (1,740 m [5,700 ft]). They have steep flanking slopes; relief between ridgetops and adjacent flatlands often exceeds 180 m/km (1,000 ft/mi). These ridges are geologically youthful and are only very slightly dissected by stream erosion. In some, such as Stuckel Mountain and Bryant Mountain, faulting is so recent that undrained, sag-pond depressions are still preserved. Uplift of these fault-block ridges during Pleistocene time was an important factor in development of impeded drainage and maintenance of extensive lakes. Only major rivers have managed to cut through these uplifted ridges since their formation, such as the Lost River at Olene Gap and the Klamath River as it leaves the basin in the west.

Volcanic landforms are also important parts of upland topography in the basin. On the west, apart from minor fault-block ridges, volcanic landforms dominate the Cascade Mountains. These comprise an upland plateau-like area, ranging from 1,200 to 1,500 m (4,000 to 5,000 ft) in elevation, made up of basalt flows on which numerous shield and stratovolcanoes have been built. Within the study area and vicinity, the largest eruptive centers are as follows: Pelican Butte (2,449 m [8,036 ft]), the Aspen Butte-Mount Harrison complex (2,502 m [8,208 ft]), Brown Mountain (2228 m [7,311 ft]), Mount McLaughlin (2,894 m [9,495 ft]), Mount Mazama-Crater Lake (present rim elevation 2,438 to 2,469 m [8,000 to 8,100 ft]) and the Medicine Lake Highland (2,134 to 2,225 m [7,000 to 7,300 ft]). Relief on the flanks of the major volcanoes is steep, ranging from a few meters to over 180 m/km (1,000 ft/mi). Many smaller lava and cinder cones are also present.

The various volcanic features present in this terrain include the large caldera at Crater Lake and a smaller caldera, now almost filled with resurgent lavas, at Medicine Lake. Several of the Cascade Range eruptive areas are so young that unvegetated aa and pahoehoe flow surfaces are still present, as at Brown Mountain, Modoc Lava Beds and Medicine Lake Highland.

East of the Cascade Range, low basalt-capped plateaus are present in several areas, notably north of Agency Lake and along the north side of the Sprague River Valley. Isolated large and small eruptive centers also occur in this region. The largest is Yamsay Mountain (2,498 m [8,196 ft]), and smaller ones occur closer to the geothermal area, such as at Hamaker Mountain (2,010 m [6,596 ft]), Moyina Hill (1,736 m [5,696 ft]), Hopper Hill (1,567 m [5,141 ft]) and Edgewood Mountain-Swan Lake Point (2,040 to 2,213 m [6,694 to 7,260 ft]).

The volcanic features of the Klamath Basin region were formed over a long period of time. Thus, the degree of erosional modification they have undergone varies greatly. The higher, older peaks, such as Yamsay Mountain, Pelican Butte and Mount Mazama-Crater Lake, were eroded by glaciers during the Pleistocene ice ages, and subsequently by streams. Other areas, such as the Modoc Lava Beds and Brown Mountain, are essentially unmodified by erosion.

The geothermal prospect areas of particular interest in this study are associated with buried fault zones parallel to the steep flanks of linear ridge-blocks in the Upper and Lower Klamath Lake sub-basins (Plate 4.1). The Klamath Hills Zone, Klamath Falls City Zone and the broad zone extending from Olene Gap around the northwest end of Stukel Mountain are all examples. Some geothermal anomalies also occur in areas of relatively low relief, such as around Miller Hill and near Midland. These are also believed to be associated with faulting, though of smaller displacement than the others. Outside of the study area, a few areas of warm water are reported in Poe, Yonna, Langell and Sprague River Valleys, outlined by wells located in the lowlands.

Mass-wasting processes such as landsliding or mud flow activity are not significant in geothermal prospect areas in particular, nor in the Klamath Basin as a whole. In addition, many years of water withdrawal from the aquifers of the region have not been reported to have caused ground subsidence. Extraction of geothermal fluids over a period of several decades in the Klamath Falls City geothermal field does not appear to have affected land surface stability.

4.3.2 Regional Geologic Setting and Tectonic History

Rocks exposed in the project area are of late Cenozoic volcanic and nonmarine sedimentary origin. In order to understand the nature of underlying rocks and the older history of the area, one must examine outcrops of older rocks located some distance beyond the margins of Klamath Basin.

The oldest rocks in the region are exposed in the Klamath Mountain, 56 to 80 km (35 to 50 mi) west of the basin. They consist of slate, phyllite, greywacke, metavolcanic rock (greenstone), and minor amounts of chert and marble, all assigned to the Applegate Group, of probable Triassic age. These rocks were strongly deformed and injected by serpentinite bodies along major zones of faulting in late Mesozoic time. During middle to late Cretaceous time, stocks of granitic to dioritic composition, such as that exposed at Mount Ashland, were intruded into this assemblage.

East and north of Klamath Basin, the pre-Cenozoic section is buried beneath younger rocks over a distance of several hundred kilometers, as far as the Blue Mountain of central Oregon. However, based on the regional distribution of late Paleozoic and Mesozoic eugeosynclinal metasediments and metavolcanics, it seems probable that the Klamath Basin area is also underlain by rocks of this type at some great but unknown depth.

Sedimentary rocks of late Cretaceous age overlie the older igneous and metamorphic assemblage along a major unconformity. These rocks, assigned to the Hornbrook Formation, dip eastward under the western Cascade Range between Medford, Oregon and Yreka, California. They consist of conglomerate, greywacke sandstone, siltstone and shale mostly of marine origin, ranging over 900 m (3,000 ft) thick. Partly correlative marine sediments reappear in the Blue Mountains uplift in central Oregon, to the northeast of the project area. However, a deep oil test well drilled near Lakeview, the Humble Oil and Refining Company Leavitt No. 1 (sec. 2, T. 40 S., R. 20 E.), is reported to have penetrated volcanic rocks of Cretaceous age without finding sediments equivalent to the Hornbrook Formation. Thus, the subsurface distribution of these rocks under the Klamath Basin is uncertain. If they are present and contain their original connate marine water, they could influence the composition of deeply circulating ground water.

A succession consisting of arkosic sandstone, conglomerate, rhyolite to andesite ash-flow tuffs, tuffaceous sediments and andesite and basalt flows overlies the Hornbrook Formation in the southwestern Cascade Mountain. The term Western Cascades Volcanic Series has been proposed for a partly equivalent assemblage farther north in the range, and the same term is loosely applied here (Callaghan and Buddington, 1938). Along the west side of the range and in the Klamath River Canyon, west of the project area, these rocks dip eastward under the more recent lavas of the so-called High Cascades Series. Several broad stratigraphic units were outlined by Wells (1956) in the Western Cascades section of the Medford quadrangle. These units were poorly understood and their stratigraphy is currently under revision. In Bear Creek Valley, the interval immediately above the Hornbrook Formation, strata consist of a thick, lenticular deposit of fluviatile tuffaceous, arkosic sandstone and conglomerate containing a few coal seams. These rocks are informally referred to as the Payne Cliff Formation, which ranges in thickness from about 60 to 1,800 m (200 to 6,000 ft) in a short distance. The age of this formation is uncertain, but it directly underlies the Upper Eocene Colestin Formation, consisting of andesite flows, mudflow breccia, tuff, conglomerate and tuffaceous sediments. The Colestin Formation is highly lenticular in character, and its lateral relationship to the Payne Cliff Formation is uncertain at this time. In view of the rapid thickness and lithologic changes occurring in the section immediately above the Hornbrook Formation, it is impossible to resolve its configuration under the Klamath Basin.

The Little Butte Volcanic Group overlies both the Payne Cliff and Colestin Formation. The thickness of this sequence in its type area east of Medford is about 900 m (3,000 ft) (Wells, 1956). Here it is made up of two recognizable units. The lower is predominantly andesite flows, flow breccias and agglomerates assigned to the Roxy Formation. This unit is about 580 m (1,900 ft) thick. The Wasson Formation, consisting of about 335 m (1,100 ft) of acidic ash-flow tuffs, flow breccias and local basalt flows forms the upper unit in the group. Recent unpublished studies to the south indicate that the section thickens dramatically in the vicinity of the Klamath River, where undifferentiated thicknesses of Colestin Formation and Little Butte Volcanics are reported to range from 3,700 m (12,000 ft) to possibly 6,100 m (20,000 ft) (Williams, 1949; Hammond, pers. comm.). Along the Klamath River, this thick section contains a wide variety of lithologic units, including andesite flows and breccias, basalt flows, thick acidic ash-flow tuffs, tuffaceous sediments and minor diatomite. The radiometric age of the lower part of the Roxy Formation is about 30 million years, or Oligocene, according to unpublished data from the USGS.

The uppermost formation of the Western Cascades sequence is the Heppsie Andesite. This unit consists of thickly bedded andesite flows of great but unknown thickness. Radiometric dating indicates that it is of Miocene age. This section appears to rest unconformably on the Little Butte Volcanics.

The Western Cascades sequence is separated from the overlying High Cascades Volcanics by an angular unconformity along which a great deal of erosion occurred. As a result, these younger volcanics may rest on a variety of older units, and the section beneath them is unpredictable in any specific location. Exposures of the Western Cascades sequence nearest the Klamath Basin are in the canyon of the Klamath River, about 40 km (25 mi) southwest of Klamath Falls. None of the fault-block ridges within the basin are known to contain rocks as old as this assemblage.

Sections of Oligocene and Miocene volcanic rocks are exposed in fault-block ridges lying 80 or more km (50+ mi) east of Klamath Falls (Peterson and McIntyre, 1970). Reconnaissance studies indicate that these rocks are partly equivalent in age and similar in lithology to the Western Cascades sequence. Therefore, it is probable that the entire Klamath Basin is underlain by these Miocene and older volcanics.

The nature of the Western Cascades volcanic rocks beneath the Klamath Basin is known only in a general way, and the depth at which they might be reached in deep geothermal exploration wells is unknown. However, they may be present, at least in local areas in and adjacent to horst blocks, at depths which could make them the desired reservoir rocks in geothermal prospects.

Only one well within the Klamath Basin has been drilled to a depth which is likely to have penetrated these rocks. This is the Thermal Power Company well in the Klamath Hills (SW 1/4, sec. 35, T. 40 S., R. 9 E.), drilled to a depth of 1,781 m (5,842 ft). Data from this well is not available at this time.

Following a period of tilting and erosion in late Miocene or early Pliocene time, eruption of the High Cascades Volcanic Assemblage began, accompanied by volcanism, faulting and lake formation in Klamath Basin. The High Cascades Assemblage has two main subdivisions. One of these contains extensive basalt flows. These form a plateau-like region which is particularly well exposed along both sides of the Klamath River Canyon southwest of the Klamath Basin. Some low, relatively small eruptive centers surrounded by similar basalts may be sources for these flows. The second main group of High Cascades rocks consists of lavas and pyroclastics which form the major shield volcanoes and stratovolcanoes that characterize the range. These rocks are typically andesites, but basalt and minor amounts of dacite are sometimes present. Medicine Lake Highland, Mount McLaughlin, the Aspen Butte-Mount Harriman complex, Pelican Butte and Mount Mazama-Crater Lake are examples of this assemblage.

Paleomagnetic dating of some High Cascade volcanoes to the north of the project area indicates that they were all built during the last 1.5 million years. If, as is likely, the similar volcanic rocks of Klamath Basin are contemporaneous, then widespread Quaternary magmatic activity is indicated. Therefore, still-cooling intrusions are probably the source of the geothermal anomaly in Klamath Basin.

There is no clearly defined boundary between the geologic conditions of the High Cascades and those of Klamath Basin. Rather, the entire basin is a zone of transition between the Cascade Range and the Basin and Range Province. The eruptive history of the basin contains many features like those of the High Cascades, although no radiometric or other dating is available to determine exact time relations. Basalt-capped tablelands are extensive in the basin, between the west flank of Winter Rim and Chiloquin and in other areas. Also present are small basalt eruptive centers, as well as a few large andesite stratovolcanoes. The largest of these is Yamsay Mountain, in the northeast part of the Klamath River drainage. Normal faulting, which characterizes the Klamath Basin, extends into the High Cascades and seems to be in some way related to the location of eruptive centers there.

While volcanism continued, a period of lacustrine deposition occurred in Klamath Basin as a result of the impedance of drainage by volcanic activity and faulting. In late Pliocene or early Pleistocene time, intensification of faulting created present topographic and hydrologic conditions.

4.3.3 Structure

Only the broadest aspects of pre-Pliocene structural evolution can be deduced from the available data. From Eocene or Oligocene to Pliocene time, the region now occupied by the southern Cascade Mountains, the Klamath Basin and a large area to the east was downwarped strongly and was the site of deposition of large quantities of volcanic rocks and volcaniclastic sediments. At present, these older Tertiary rocks dip east or northeast along the western Cascade front in the Medford-Ashland-Yreka area. Eighty or more kilometers (50+ mi) to the east of Klamath Falls, they dip generally southwest toward Klamath Basin. In the large area between these two outcrop belts, they are covered by younger materials, so that their structure is unknown. A major angular unconformity separates the older Tertiary volcanic rocks from the Pliocene and younger lavas of the High Cascades.

During later Pliocene and Quaternary time, a system of normal faults was superimposed on the regional downwarp. Evidence of oldest faulting in this period consists of alignments of small eruptive centers. Trends of these centers range from northwesterly in the southern to northerly in the central Klamath Basin, parallel to trends of later faults in the same areas (Peterson and McIntyre, 1970). Faulting reached a climax in Pleistocene time. Since the latest major movements, the Klamath and Lost Rivers have been able to establish exterior drainage across the faulted topography, but numerous areas of internal drainage remain.

Normal faulting in the Klamath Basin region occurs in a zone about 50 to 65 km (30 to 40 mi) wide, from Buck Mountain, Surveyor Mountain and Lake of the Woods, in the High Cascades on the west, to near Bly Mountain, the Sprague River Valley and Goodlow Rim on the east. Various segments of the trend extend from the Tule Lake area of northern California, through southern Oregon, to the Upper Klamath Lake Basin. Related structural features are present even farther northeast, near Chemult (Peterson and McIntyre, 1970). This broad zone is flanked on the west by relatively unfaulted rocks with an eastward to northeastward homoclinal dip and by recent volcanic rocks which are unfaulted. East of the fault zone, only a few minor faults are present.

Several generalizations can be made concerning normal faulting within the study area (Plate 4.1):

1) Fault trends are consistent in strike. In the southern two-thirds of the map area (Plate 4.1), the strike is almost exclusively northwesterly. In the northern third, fault strike becomes northerly. Gravity data indicates that short, buried, northeast trending faults segment the major northwest trending faultblocks.

2) Fault displacements diminish in magnitude both eastward and westward from the Klamath Lake area. Only a

few faults, with negligible offset, occur west of the Buck Mountain-Surveyor Mountain-Hayden Mountain trend. A similar decrease is seen eastward from Swan Lake Mountain. Within the Klamath Basin graben, displacement varies from tens of meters to several hundred meters.

3) Dips of fault planes range from about 55° to 60° at the surface but might decrease with depth. Many of the faults show "scissoring," wherein vertical displacement decreases to zero along strike and then increases but in a reversed sense.

4) The common sense of movement is stepwide downdropping of blocks, going from the east and west sides of Klamath Basin towards its axis. Within the graben complex, large subsidiary horst and graben blocks have developed.

The close relationship between geothermal anomalies and the fault pattern may be seen by a comparison of the surface geologic map (Plate 4.1) with temperatures of ground water (see Section 4.4, below). It is apparent that fault zones provide major conduits for the circulation of both cold and heated ground water and that they localize the known geothermal anomalies.

With one exception, geothermal anomalies within the study area occur along the faults bounding the east side of the inner part of the graben complex. The exception is the hot spring at Eagle Point, just west of the graben center.

Geologic structure in the main geothermal areas is summarized briefly below.

Klamath Falls Hot Water Field--

The best known geothermal anomaly in the region underlies part of the city of Klamath Falls. The area of highest temperatures occurs in a northwest trending zone parallel to nearby faults. The fault along the southwest side of Bald Hill Ridge appears to form the eastern boundary of this field (Plate 4.1). Minor faults within the productive area isolate reservoirs to some degree, as shown by differing depths of producing horizons in different fault-blocks. They also provide the main channels for upward circulation of hot water which then spreads laterally in permeable zones.

The faults in this geothermal field are not the most significant in the immediate vicinity, and reasons for the restriction of upward hot water movement to this particular area are not readily apparent.

Olene Gap-Nuss Lake-Stukel Mountain Zone--
This is a large, poorly defined thermal area including the hot spring at Olene Gap and warm water wells in the adjacent area on the west and southwest around the edge of the Stukel Mountain horst. The Olene Gap Hot Spring appears to be related to the north and northwest trending faults which bound both sides of the adjacent ridge to the north. These seem to converge and possibly intersect in the gap. Surface geology does not support the presence of a major north-northeast trending fault passing through the gap, as proposed by Peterson and Groh (1967). However, gravity data indicates that a northeasterly trending fault is probably present at the northwest end of Stukel Mountain, intersecting numerous north and northwest trending faults, some of which bound the horst block. The Nuss Lake warm water occurrences are located in this complex of fault intersections.

Occurrences of warm water continue along the southwest side of Stukel Mountain in the boundary fault zone.

Klamath Hills Hot Water Zone--
A narrow, northwest trending zone of hot water wells runs along the southwest side of the Klamath Hills horst, near the major fault or fault zone that bounds it. The precise location of this fault is unknown, but gravity data indicates a position within 1.6 km (1 mi) of the southwest side of the hills, beneath the valley alluvium. This appears to be one of the largest faults of the region in terms of its gravity expression, although it is not related to a topographically high horst block, in comparison with most other known major faults of the region. This may imply a greater age for this feature.

Other isolated minor thermal anomalies are present along the Klamath Hills Fault trend near Midland, and in the newly discovered Greensprings Drive subdivision, north of the Klamath River and Highway 66. A few warm water wells also occur in small northwest trending fault zones, such as at Miller Hill.

Eagle Springs Zone--
The isolated Eagle Springs warm water area lies on the shore of Upper Klamath Lake at Eagle Point (sec. 23, T. 36 S., R. 7 E.). This spring is located along a prominent fault bounding the ridge. The extent of the thermal anomaly is unknown. As noted above, this occurrence is unusual because of its location on the west side of the graben axis.

4.3.4 Stratigraphy and Lithology

Formal stratigraphic names have not been applied to most of the rock units occurring here. In the following, these units will be referred to by the symbols identifying them on the accompanying geologic map (Plate 4.1). As currently known from reconnaissance mapping, all rocks exposed in the study area are of middle or late Pliocene to Holocene age. Two broad stratigraphic successions are present: one is found in fault-block ridges along the east side of the central lowland; the other occurs in hills along the west side of the basin and in the adjacent High Cascades. Henceforth, they will be referred to as the west- and east-side sections.

The lack of recognizable horizons common to both sections, and of radiometric age-dates, precludes making any but the most tentative correlations between them. The east-side section contains prominent lacustrine rocks as well as basalt flows. This lacustrine facies thins toward the large eruptive centers of the High Cascades, where the section is made up almost entirely of flows, breccias, and cinders of basaltic and andesitic composition. In order to avoid confusion, the east- and west-side sections are described separately.

East-Side Section--

(Tb) - Basalt, dark flows and flow breccias; (Tbp) - coarse palagonitic tuffs; (Tbc) - basalt eruptive centers; (Tbcc) - basalt cinder cones--All rock types in this group are believed to be essentially contemporaneous with one another and to represent different phases of the same eruptive cycle. They are exposed in horst-blocks along the west side of the Upper and Lower Klamath Lake sub-basins, such as Naylox, Hogback, Stukel and Bryant Mountain. The base of the section has not been identified in any of these exposures (Fig. 4.4).

Two main facies comprise this lithologic group. One lies entirely outside of the map area, from Chiloquin to within about 1.5 km (1 mi) of the north edge of the map (Plate 4.1), and is made up of coarse palagonitic tuff containing basalt scoria and flow breccia. This material often exhibits high initial dips, suggesting that it was piled up around eruptive centers. Alteration of the glassy basalt cinders and tuff to a brown palagonitic clay-zeolite mixture suggests that these materials formed lake deposits. Passing southward into the map area, one finds a different facies, composed of numerous 3 to 6 m (10 to 20 ft) thick basalt flows and agglutinated flow breccias. These are mainly dark grey and fine-grained, containing a few plagioclase phenocrysts. A few thin basalt flows with diktytaxitic texture, water-laid cinder lenses and piles of palagonitic tuff are interbedded with the dominant flows.

Rapid local facies changes occur near the numerous small volcanic vents. For example, a tuff mound surrounded and overlapped by flows can be seen along the Plum Hills scarp (E 1/2, sec. 31, T. 37 S., R. 9 E.). To the south, at large quarries in the west face of the Stuckel Mountain fault-block, one finds coarse agglutinated basalt breccia, which is probably a near-vent deposit. Because known faults are the loci of both most rock exposures and ancient eruptive centers, it is believed that lithologic variations seen in outcrop are not representative of

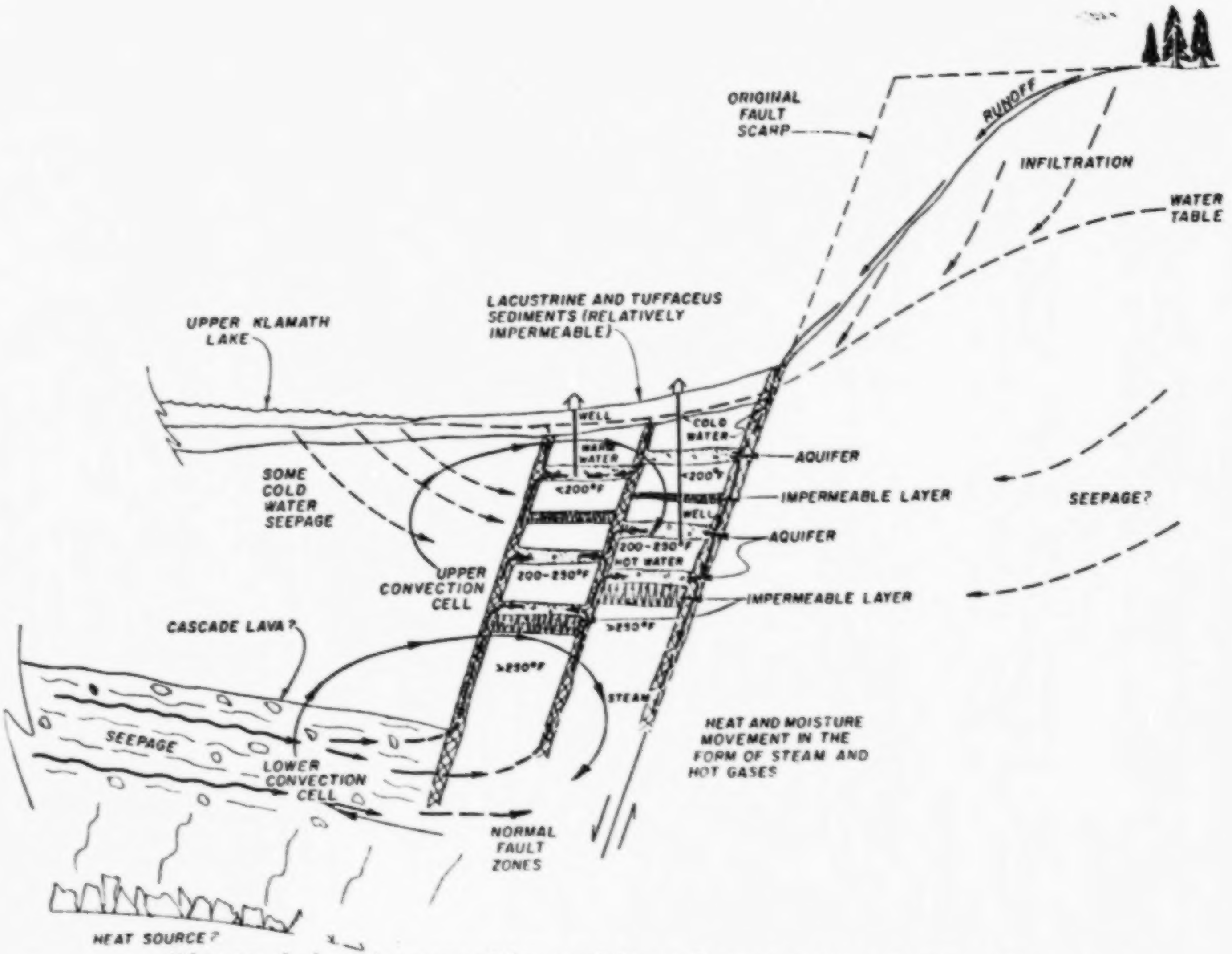
ORIGINAL FAULT SCARP
RUNOFF
INFILTRATION
WATER TABLE
LACUSTRINE AND TUFFACEUS SEDIMENTS (RELATIVELY IMPERMEABLE)
UPPER KLAMATH LAKE
WELL
COLD WATER
WARM WATER
<200°F
AQUIFER
IMPERMEABLE LAYER
SEEPAGE?
SOME COLD WATER SEEPAGE
WELL
200-250°F HOT WATER
AQUIFER
200-250°F
IMPERMEABLE LAYER
UPPER CONVECTION CELL
>250°F
CASCADE LAVA?
>250°F
STEAM
SEEPAGE
HEAT AND MOISTURE MOVEMENT IN THE FORM OF STEAM AND HOT GASES
LOWER CONVECTION CELL
NORMAL FAULT ZONES
HEAT SOURCE?

Figure 4.4 Diagrammatic section of east side of Klamath graben.

this rock group as a whole. That is, relatively homogeneous flows probably occupy most areas between faults.

The exposed section is at least 450 m (1,500 ft) thick at Naylox Mountain, more than 600 m (2,000 ft) thick at Stukel Mountain and of even greater probable thickness in Bryant Mountain.

This lithologic group has the greatest shallow reservoir potential for geothermal fluids. Therefore, abrupt facies changes and their effects on reservoir characteristics are likely to be an important factor in geothermal development in the region.

Water well data in the region indicates that the basalt flow and flow breccia parts of the (Tb) interval are highly porous and permeable; many high-yielding irrigation wells produce from it. Based on limited lithologic data contained in well drillers' reports, it appears that water comes from fractures in flows and from interflow rubble and cinder zones. Hot water in geothermal zones of the area is also obtained from this unit. The small amount of lithologic data available from geothermal wells indicates that the basalt aquifer is not severely altered by thermal fluids, even though the overlying diatomite has been converted to porcellanite and opal breccia.

Relationships between the (Tb) unit and lacustrine rocks of the (Tp) unit are complex. It is probable that the (Tb) eruptives impounded drainage, creating the lakes in which the predominantly sedimentary (Tp) unit was deposited. (Tp) sediments locally overlie (Tb) on ridges along the east side of the basin. However, it seems likely that the (Tb) phase was partly contemporaneous with the lacustrine (Tp) phase. Thus, the two units probably interfinger in some places.

The age of the (Tb) unit is not known directly. Overlying lacustrine sediments (Tp) have been dated as of middle or late Pliocene age; the youngest Western Cascades volcanic rocks believed to underlie the unit are of Miocene age. Thus, it is likely that the (Tb) basalts are of early to middle Pliocene age.

(Tp) - Diatomite and palagonite-tuff sandstone and siltstone; (Tpb) - basalt flows and shallow intrusives in the lacustrine sediments--This unit is widely exposed in the project area and beyond. Major outcrop areas occur in small fault-blocks in and around Klamath Falls; on the east slope of Hogback and Naylox Mountain, where it overlies the (Tb) basalts; in the Stukel Mountain block also overlying (Tb); in the Klamath Hills; and in the floor of Yonna Valley to the east (Peterson and McIntyre, 1970). Based on gravity studies, it is presumed to make up most of the thick low density section present in the Lower Klamath Lake sub-basin (Peterson and Groh, 1967).

The characteristic rock types in the unit are compact, massive-bedded white diatomite and moderately well-indurated grey-brown palagonitic tuff and tuffaceous sediments. These sediments are of lacustrine origin.

Other rock types are important locally. Among them are coarse palagonite tuff and basalt scoria and bombs, marking eruptive centers. These centers form ringshaped mounds which are particularly well exposed in Meadow Valley, along the west side of Swan Valley and in the north end of Yonna Valley.

Basalt flows, sills and dikes are also locally present in the lacustrine rocks. The basalt is dark grey to black, finely crystalline to glassy, often with scattered phenocrysts of olivine and plagioclase. Pillow structures sometimes seen in the flows indicate that they cooled under water. Examples of intrusive basalts can be seen in a quarry in NW 1/4 sec. 11, T. 39 S., R. 8 E. Flows interbedded within the section can be seen in highway cuts near the center of sec. 5, T. 35 S., T. 9 E., and in many other places. These basalts have been mapped as a separate unit (Tpb) where exposures are large enough to be seen on the scale of the map (Plate 4.1).

Thickness trends in the (Tp) unit are unknown. Partial sections a few tens of meters thick are exposed in fault-block uplifts around the edges of Upper and Lower Klamath Lake, and good exposures can be seen to the east in Yonna and Poe Valleys. Drillers' logs show thicknesses frequently exceeding 300 m (1,000 ft).

Gravity data indicates that a section of low density material as much as 1,800 m (6,000 ft) thick may occur under the Lower Klamath Lake sub-basin, southwest of the Klamath Hills Fault Zone (Peterson and Groh, 1967). Much of the low density material causing the anomaly is likely to consist of (Tp) sediments.

Lacustrine sediments (Tp) are present in all of the geothermal areas discussed here. They have been hydrothermally altered to hard, flinty opalite in the Klamath Falls geothermal field and also, to a minor extent, in the Klamath Hills area. Porosity and permeability in the (Tp) unit are generally low. Thus, it may serve as a cap rock over more porous basalts in the underlying (Tb) unit.

The assigned Pliocene age of the (Tp) unit is based on the presence of diatoms (Pliocene) in the section near Dorris, California, and on a few vertebrate fossils found near Stukel Mountain (middle Pliocene) and Merrill (late Pliocene) (Peterson and McIntyre, 1970; Hanna and Gester, 1963).

(Qtbf) Basalt flows--A tableland basalt sequence overlies (Tp) lake beds in the northwest corner of Swan Lake Valley, northeast of the geothermal areas. This unit consists of several light grey flow units with diktytaxitic texture. It reaches a maximum thickness of about 45 m (150 ft). These flows form the surface of an eroded plateau which is analogous to, if not correlative with, the similar plateau north of Sprague River and Chiloquin. This basalt unit also may be related to the plateau-forming basalts of the High Cascades Sequence, but no precise correlation has been established.

The (Qtbf) unit is younger than the upper Pliocene (Tp) lake beds on which it rests. It has been subjected to both faulting and considerable erosion and is thus probably of late Pliocene or early Pleistocene age. As yet, it has not been recognized in the downfaulted sections penetrated by water wells in the Lower Klamath Lake sub-basin.

(Qal) - Silt, sand, gravel, diatomite, peat and pumice--In many parts of the area, (Tp) is the youngest unit present. However, after the period of intense normal faulting had established the present topographic framework, sedimentation continued in the lowland areas. A variety of sediments is present in these young basins: coarse scree slopes and fans along the steep range-fronts; river-deposited silts and sands; clay and diatomite in the lakes; and extensive reed-sedge peat in marshes. Locally, thin pumice deposits are present, perhaps derived from sources to the southwest.

All of these materials have been mapped as undifferentiated Quaternary alluvium. Only a few feet of this section is exposed in any single location. Descriptions on water well logs are usually not sufficiently detailed to distinguish between sediments of the present lacustrine cycle and those of Pliocene age. Thus, the thickness of this material is not yet known. It is estimated to reach a maximum of only a few tens of meters in the central part of the present basin.

In general, these Quaternary deposits are poorly consolidated. As the bulk of the section is fine-grained, it does not contain important aquifers. Where the unit is thick enough to be of any significance to geothermal development, it probably comprises part of the overall cap rock interval, and it is not anticipated that any geothermal development would withdraw fluids from it.

West-Side Section--

The stratigraphic succession in this area can be tentatively divided into four major assemblages. Each of these has been subdivided into local volcanostratigraphic units during field mapping. However, only a summary of the larger intervals has any significance in the present study.

Unit 1--The oldest rock assemblage appears to consist of the basalt flows and small eruptive centers of Spence Mountain and Eagle Point Ridge, (QtbSpc), the basalt flows of Indian Springs Ridge (QtbISP and QtbISPc), and the basalt flows of Mount Harrison (QtbHC, QtbH). These rocks are dark grey, finely-crystalline basalts containing a few percent of small plagioclase phenocrysts. Near eruptive centers, large amounts of agglutinate and cinders are present. These rocks are grouped together on the basis of their similar macroscopic appearance, although their field relationships are not known. Their appearance also suggests that they are correlative with the (Tb) basalt unit on the east side of Klamath Lake. Eruption of these rocks predates the extensive normal faulting in the region. Field evidence indicates that they underlie flows of the next unit discussed below. The thickness of this assemblage is unknown, as the base is not exposed. The Weyerhaeuser Spence Mountain geothermal gradient hole, drilled on the flank of the Spence Mountain Eruptive Center (NE 1/4 sec. 15, T. 37 S., R. 7 E.), penetrated 611 m (2,006 ft) of rocks belonging to this section, apparently without reaching its base.

Unit 2--This assemblage consists mainly of extensive thin flows of light to medium grey, fine-grained holocrystalline basalt (Qtbha and Qtbhad). The abundance of plagioclase in this rock imparts both an unusually light color and a high alumina content. Texturally, the rock ranges from aphanitic, to slightly porphyritic and diktytaxitic. The diktytaxitic variety forms the plateau surface of Johnson Prairie and other upland areas bordering the Klamath River Canyon, where over 180 m (600 ft) of these lavas rest unconformably on the western Cascades Volcanics. It is present as the uppermost part of the flow sequence on ridges between Aspen Lake and Howard Bay, where it overlies the assemblage described above.

Basalt of a similar appearance (Qtbh) makes up several of the moderate-sized volcanoes of the High Cascades, such as Grizzly Mountain, Parker Mountain, Little Chinquapin Mountain and others. These may have been the sources for some or all of the extensive flows. The age and correlation of the (Qtbh) rocks is not precisely known. As noted above, they overlie the basalt assemblage believed to be correlative with (Tb) east of Klamath Lake. They are themselves similar in appearance to the flows of the (Qtbf) sequence east of the lake and are believed to be essentially contemporaneous with them. These flows have been faulted and deeply eroded by the Klamath River.

Unit 3--Following the eruption of the (Qtbh) suite and the climax of faulting, several closed topographic depressions were formed in the High Cascades. Diatomite, palogonite tuff, and other volcaniclastic materials were deposited locally in lakes that occupied these depressions. These have been mapped as (QTtr, Qol and Qold). The most extensive of these deposits occur in the graben complex northwest of Keno. The age of these rocks is not precisely known but they appear to be younger than the very similar materials east of Klamath Lake (Tp) and to overlie the (Qtbh) basalt flows.

Unit 4--A number of volcanic events occurred in the High Cascades during and after the later stages of faulting. The most notable one built the major stratovolcanoes of the range, whose peaks are believed to be younger than the (Qtbh) flows and are mostly unaffected by faulting. The highest peaks had reached their present elevation before the most recent stage of glaciation. However, eruptions at Brown Mountain, Crater Lake and the Medicine Lake Highland have all occurred in post-glacial time. As noted earlier, recent studies in the central Cascade Mountains indicate that this eruptive cycle began about 1.5 million years ago.

A number of local volcanic units can be recognized around specific eruptive centers, such as the basalt and andesite flows (QbWFPc, QbWFP, QbAB, and related rocks), shallow intrusives (Qbsip) and cinder cones (Qtbcc, Qbcc) shown on Plate 4.1. These are of local interest only and are not discussed further here.

4.4 HYDROLOGY

4.4.1 Surface Water

Topography and Drainage--

The Klamath physiographic basin, or greater Klamath drainage basin, includes the upper part of the Klamath River drainage basin, as well as part of the Lost River Basin, and several smaller closed basins, such as Swan Valley, Crater Lake, and Lower Klamath Lake. This area comprises some 14,800 sq km (5,700 sq mi). Of this, about 4,150 sq km (1,600 sq mi) contributes little or no surface water to the Klamath River System, except that which is artificially diverted to it from the Lost River (Phillips, 1969).

The greater Klamath drainage basin is bounded on the west by the crest of the Cascade Range, which separates it from the Rogue River Basin. On the north, the divide between the Klamath River Basin and that of the Deschutes-Columbia System occurs on a low plateau north of Klamath Marsh. On the northeast and east it is separated from the various interior drainage basins of the Basin and Range Physiographic Province by a divide extending southward from Winter Ridge to Barnes Rim.

In this area of youthful topography, as described by Newcomb and Hart (1958), the valley plains are imperfectly connected by a rudely integrated drainage system which collects downstream in the Klamath River proper. The Williamson River, the principal headwater stream, rises in a spring zone in the SE 1/3 sec. 4, T. 33 S., R. 11 E. While flowing northward for 26 km (16 mi), it receives the flow of several springs and of Deep and Jackson Creeks, which drain the west side of Yamsay Mountain, and of Jack Creek, which drains the northeastern part of the basin. It then turns westward and flows about 6 km (4 mi) across a pumice plain to the northeastern end of the Klamath Marsh. In Klamath Marsh it receives the flow of Big Spring Creek and other smaller creeks. Two of these, Scott and Band Creeks, drain from the east side of Mount Mazama-Crater Lake. From Klamath Marsh the Williamson River flows over a basalt rim near Kirk, descending about 90 m in 8 km (300 ft in 5 mi), and continues south where it discharges into Upper Klamath Lake after receiving the Spring Creek and Sprague River inflows.

The north and south forks of the Sprague River rise on the flanks of Gearhart Mountain, at the east side of the basin. About 6 km (4 mi) northwest of Bly, they join to form the main river. After flowing through Beatty Gap, the Sprague River is joined by the Sycan River from the north. Several creeks and springs enter the river as it flows an airline distance of 40 km (25 mi) westward, through the lowland known as the Sprague River Valley, to its confluence with the Williamson River near Chiloquin. Wood River and Sevenmile Creek separately drain southward into Agency Lake, which is a northern lobe of Upper Klamath Lake, now nearly separated by the encroachment of the delta of the Williamson River.

Along the western side of Upper Klamath Lake, several creeks, including Threemile, Cherry, Rock, Fourmile and Rocky Creeks, enter from the Cascade slope.

The surface of Upper Klamath Lake stands near 1,260 m (4,140 ft) in altitude but varies seasonally by several feet and is controlled, in part, for power generation and irrigation. This is the largest natural lake wholly in Oregon, covering approximately 40 sq km (15 sq mi). A low dam in the Link River at the south end of the lake regulates the lake level, and controls the release of about 54,300 ha-m (440,000 acre-ft) per year, between the 1,261 and 1,263 meter (4,137 and 4,143 ft) lake levels (Phillips, 1969).

Outflow from Upper Klamath Lake is through Link River, a short, narrow, rockbound trench which descends about 12 m (40 ft) to Lake Ewauna. Out of Lake Ewauna the main stem of the Klamath River flows along the northwest side of the extensive Klamath Valley lowland and the wide playa and marsh known as Lower Klamath Lake. It then passes through basalt ridges near Keno at an altitude of about 1,235 m (4,050 ft). The river descends through a deep youthful canyon below Keno and enters the State of California at an altitude of about 900 m (2,960 ft).

Lost River Basin is a separate river basin, but because use of its water for irrigation is so much integrated with that of the Klamath River, and because it partly occupies the same structural basin, it is included here as part of the Klamath Basin in Oregon. Headwaters of Lost River gather in the mountains and plateaus forming the youthful topography athwart the Oregon-California line east of Klamath Valley and Tule Lake Basin. There are storage reservoirs on the tributaries, the outflow of which is used mainly for irrigation. Through Olene Gap, Lost River enters Klamath Valley at an altitude of about 1,250 m (4,100 ft) and flows southward into Tule Lake, a lake-sump whose bed stands about 14 m (45 ft) below the floor of Lower Klamath Lake, from which it is separated by narrow ridges.

Natural drainage in the Lost River and Lower Klamath Lake areas has been considerably modified by irrigation and drainage works. Much of the flow of Lost River is diverted into the Klamath River drainage and other irrigation canals by a small dam in the SW 1/4, sec. 29, T. 35 S., R. 10 E.; at certain times, water from Klamath River is also diverted into Lost River. Lower Klamath Lake, formerly an extensive marshland, has been altered by construction of the Southern Pacific Railroad and Highway 97 embankment along the northwest side of the basin. Water is impounded on the west side of this embankment. To the east, the floor of the old lake is now drained by a series of canals and is under cultivation.

The KGRAs in the region treated herein are located in the southern part of the Klamath Basin drainage system. The hot spring at Eagle Point flows directly into Upper Klamath Lake. The original thermal springs at Klamath Falls and the present effluent water from hot water wells enter the system below Link River. The Olene Gap Hot Springs enter Lost River, and any effluent produced around the north and west ends of Stukel Mountain would also reach this system. Geothermal effluents from the development of the hot water zone along the south side of the Klamath Hills would flow naturally into Lower Klamath Lake. However, since that area is now drained by a series of canals and the old lake bottom is under cultivation, the effluent would enter the canal system and drain southward into the White Lake Sump, where it would evaporate.

Streamflow--

A summary of streamflow data in Klamath Basin is given in Table 4.3. Principal uses for surface water in the Oregon part of the drainage system are irrigation and industrial use by the forest product industry. A further important use is the preservation of the habitat for migratory water fowl. Wildlife refuges are established on Klamath Marsh, Upper Klamath Lake, downstream in the Klamath River proper. The Williamson River, the principal headwater stream, rises in a spring zone in the SE 1/3 sec. 4, T. 33 S., R. 11 E. While flowing northward for 26 km (16 mi), it receives the flow of several springs and of Deep and Jackson Creeks, which drain the west side of Yamsay Mountain, and of Jack Creek, which drains the northeastern part of the basin. It then turns westward and flows about 6 km (4 mi) across a pumice plain to the northeastern end of the Klamath Marsh. In Klamath Marsh it receives the flow of Big Spring Creek and other smaller creeks. Two of these, Scott and Band Creeks, drain from the east side of Mount Mazama-Crater Lake. From Klamath Marsh the Williamson River flows over a basalt rim near Kirk, descending about 90 m in 8 km (300 ft in 5 mi), and continues south where it discharges into Upper Klamath Lake after receiving the Spring Creek and Sprague River inflows.

The north and south forks of the Sprague River rise on the flanks of Gearhart Mountain, at the east side of the basin. About 6 km (4 mi) northwest of Bly, they join to form the main river. After flowing through Beatty Gap, the Sprague River is joined by the Sycan River from the north. Several creeks and springs enter the river as it flows an airline distance of 40 km (25 mi) westward, through the lowland known as the Sprague River Valley, to its confluence with the Williamson River near Chiloquin. Wood River and Sevenmile Creek separately drain southward into Agency Lake, which is a northern lobe of Upper Klamath Lake, now nearly separated by the encroachment of the delta of the Williamson River.

Along the western side of Upper Klamath Lake, several creeks, including Threemile, Cherry, Rock, Fourmile and Rocky Creeks, enter from the Cascade slope.

The surface of Upper Klamath Lake stands near 1,260 m (4,140 ft) in altitude but varies seasonally by several feet and is controlled, in part, for power generation and irrigation. This is the largest natural lake wholly in Oregon, covering approximately 40 sq km (15 sq mi). A low dam in the Link River at the south end of the lake regulates the lake level, and controls the release of about 54,300 ha-m (440,000 acre-ft) per year, between the 1,261 and 1,263 meter (4,137 and 4,143 ft) lake levels (Phillips, 1969).

Outflow from Upper Klamath Lake is through Link River, a short, narrow, rockbound trench which descends about 12 m (40 ft) to Lake Ewauna. Out of Lake Ewauna the main stem of the Klamath River flows along the northwest side of the extensive Klamath Valley lowland and the wide playa and marsh known as Lower Klamath Lake. It then passes through basalt ridges near Keno at an altitude of about 1,235 m (4,050 ft). The river descends through a deep youthful canyon below Keno and enters

TABLE 4.3 SUMMARY OF STREAM FLOW DATA AT SELECTED POINTS IN THE KLAMATH BASIN

(a) Summary of streamflow data at selected sites in the Klamath River Basin

Stream	Drainage area (square miles)	Years of record	Streamflow			
			Average		Cubic feet per second	
			Cubic feet per second	Acre-feet per year	Maximun	Minimum
Williamson River near Klamath Agency	1,290	12	236	170,900	1,590	0
Sprague River near Beatty	513	16	306	221,500	6,980	57
Sprague River near Chiloquin	1,580	45	555	401,800	14,900	50
Williamson River below Sprague River	3,000	49	1,013	733,400	16,100	320
Link River at Klamath Falls	3,810	62	1,603	1,161,000	9,400	17
Klamath River at Keno	3,920[a]	46	1,678	1,215,000	9,250	26
Klamath River below John C. Boyle powerplant	4,080[a]	7	1,767	1,279,000	8,830	311

[a] Excluding adjacent basins of Lost River and Lower Klamath Lake.

(b) Link River at Klamath Falls, Oregon

LOCATION: Lat 42°13'25", long 121°47'35", in SW 1/4 NW 1/4 sec. 32, T. 38 S., R. 9 E., Klamath County, on right bank 600 ft upstream from outlet of Keno Canal and 0.4 mile upstream from Main Street Bridge at Klamath Falls.

DRAINAGE AREA: 3,810 sq mi, approximately, including 26.2 sq mi in closed basin of Crater Lake.

PERIOD OF RECORD: May 1904 to September 1970.

GAGE: Water-stage recorder. Datum of gage is 4,083.71 ft above mean sea level; or 4,085.50 ft above mean sea level, datum of Bureau of Reclamation. See WSP 1929 for history of changes prior to Nov. 16, 1961.

AVERAGE DISCHARGE: 66 years, 1,538 cfs (1,151,000 acre-ft per year), not adjusted for "A" Canal.

EXTREMES: Maximum and minimum discharges, in cubic feet per second, for the water years 1966-70 are contained in the following table:

TABLE 4.3 (continued)

	Maximum		Minimum daily	
Wtr yr	Date	Discharge	Date	Discharge
1966	Nov. 5, 1965	4,250	July 17, 1966	99
1967	May 13, 1967	5,320	Mar. 17, 1967	120
1968	Mar. 25, 1968	3,360	Aug. 25, 1968	74
1969	Apr. 5, 1969	6,980	Dec. 15, 1968	104
1970	Jan. 31, 1970	7,270	May 7-9, 1970	108

Period of record: Maximum discharge 8,400 cfs May 12, 1904 (gage height at Main Street Bridge, 7.30 ft, datum then in use, from floodmarks); minimum daily, 17 cfs Dec. 13, 1937.

REMARKS: Records good. Flow regulated since 1919 by Upper Klamath Lake (see station 11507000). Large diurnal fluctuation caused by powerplant above station. Water diverted above station by main or "A" Canal of Klamath project (see station 11506000). Many other diversions above lake. All records presented herein include flow in Keno Canal which, since September 1908, has diverted from Upper Klamath Lake at Link River Dam for power generation, and returns flow to Link River below station.

(c) Diversion from Klamath River to Lost River near Olene, Oregon

LOCATION: Lat 42°08'25", long 121°41'20", in NE 1/4 NW 1/4 sec. 31, R. 39 S., R. 10 E., Klamath County, on south bank of Lost River diversion canal, 9.5 mile east of bridge on State Highway 39, 019 mile downstream from dam on Lost River, and 3.8 miles southwest of Olene.

PERIOD OF RECORD: April 1931 to September 1968 (discontinued). Published with records for Lost River diversion canal near Olene in 1931.

GAGE: Nonrecording gage. Altitude of gage is 4,080 ft (from topographic map).

AVERAGE DISCHAGE: 38 years, 35.1 cfs (25,430 acre-ft per year).

EXTREMES: Maximum and minimum discharges, in cubic feet per second, for the water years 1966-68 are contained in the following table:

	Maximum daily		Minimum	
Wtr yr	Date	Discharge	Date	Discharge
1966	Apr. 2, 1966	705	At times	0
1967	June 16, 1967	587	do.	0
1968	June 21, 1968	714	do.	0

Period of record: Maximum daily discharge, 710 cfs Apr. 15, 1951; no flow at times.

TABLE 4.3 (continued)

REMARKS: Records fair. Discharge computed from daily record of gate openings and gage readings at wasteway with coefficients applied based on discharge measurements. Canal was built to divert water from Lost River to Klamath River and thereby aid in reclamation of Tule Lake (see station 11486000). Beginning in April 1931, water has been diverted at times from Klamath River and released into Los River, from which it is rediverted for irrigation of lands near Tule Lake. Since 1949, records include water removed from the diversion canal by Miller Hill pumping plant (capacity, 105 cfs).

(d) Klamath River at Keno, Oregon

LOCATION: Lat 42°08'00", long 121°57'40", in NW 1/4 SE 1/4 sec. 35, T. 39 S., R. 7 E., Klamath County, on left bank 1.7 miles northwest of Keno and 4.5 miles upstream from Spencer Creek.

DRAINAGE AREA: 3,920 sq mi, approximately (not including Lost River or Lower Klamath Lake basins).

PERIOD OF RECORD: June 1904 to December 1913, October 1929 to September 1970. Monthly discharge only October to December 1929, published in WSP 1315-B.

GAGE: Water-stage recorder. Datum of gage is 3,961 ft above mean sea level (from river-profile survey). See WSP 1929 for history of changes prior to June 10, 1964.

AVERAGE DISCHARGE: 50 years, 1,665 cfs (1,206,000 acre-ft per year).

EXTREMES: Maximums and minimums (discharge in cubic feet per second, gage height in feet) for the water years 1966-70 are contained in the following table:

	Maximum			Minimum	
Wtr yr	Date	Discharge	G.H.	Date	Discharge
1966	Nov. 5, 1965	4,270	9.03	July 18, 1966	239
1967	May 14, 1967	6,070	10.34	July 20, 1967	188
1968	Dec. 19, 1967	2,900	7.82	June 1-2, July 22,23, 1968	248
1969	Apr. 4, 1969	7,880	11.47	July 13, 1969	207
1970	Jan. 29, 1970	8,920	12.08	June 30, July 1,2,4, 1970	234

Period of record: Maximum discharge, 8,920 cfs Jan. 29, 1970 (gage height, 12.08 ft); minimum, 26 cfs Sept. 23, 1956; minimum daily, 60 cfs May 19, 1934.

Maximum stage, 15.3 ft, from floodmark (original datum), about May 10, 1904 (discharge, 9,250 cfs).

TABLE 4.3 (continued)

REMARKS: Records good. Since 1919, flow regulated by Upper Klamath Lake (see station 11507000). Diversions for irrigation above station. Lost River diversion canal records and Lower Klamath Lake diversion canal and pumpage records, furnished by Bureau of Reclamation, were discontinued in 1968.

(a) from Phillips, 1969

(b), (c), (d) from U. S. Geol. Survey, 1976 and at southern Klamath Lake and Tule Lake, in California. Almost all public water supplies in the basin are obtained from ground water.

Surface Water Quality--
Water quality in the larger streams and springs of the basin is good to excellent, low in suspended sediment and dissolved solids. It is of calcium magnesium type. In general, the dissolved solids concentration and hardness increase from the Williamson River downstream to Keno, due to evaporation in excess of precipitation, to addition of municipal and industrual wastes, and to the return of drainage from irrigated lands and marshes. Water chemical analyses from several locations in the system are given in Table 4.4.

Sediment movement in streams is not great because much of the inflow is from springs and also because the streams have low gradients through most of the system. However, the water which passes through Klamath Marsh, Agency Lake, Upper Klamath Lake and other smaller marsh areas often has a brownish color and considerable suspended organic matter derived from decaying marsh vegetation and from algae and diatom blooms that occur annually in Upper Klamath Lake. In addition since Upper Klamath Lake is undergoing eutrophication, during late summer a strong odor of putrefaction is evident around the lake shore.

4.4.2 Ground Water

Water Bearing Units--
Four main aquifer units have been distinguished in the Klamath Basin (Illian, 1970) (Table 4.5). These units are accepted here, although Sammel (1976) has proposed some changes in nomenclature and has split some of Illian's units. Three of these units crop out within the project area. The fourth is present in the subsurface but is not known to have been penetrated by a well in the basin.

The sedimentary aquifer is distributed throughout the area but is of significant thickness only in the lowlands. It is composed of alluvium, terrace materials, Pleistocene-Holocene lake deposits, Pliocene-Pleistocene lake deposits and their locally lithified equivalents. Illian (1970) included some of the youngest basalt flows (Qb), as well as Holocene Mazama Ash, in this assemblage. Data on the productivity of water wells completed in this unit indicates that specific capacities range from 0.12 to 62 lpm/m (0.01 to 5 gpm/ft) of drawdown and average about 5.6 lpm/m (0.45 gpm/ft). A black sand or gravel layer encountered in this interval may yield from 25 to 125 lpm/m (2 to 10 gpm/ft). These values are low and suggest near-impermeability. However, these sedimentary beds often yield sufficient quantities of water for domestic purposes.

TABLE 4.4 CHEMICAL ANALYSES OF SURFACE WATERS, 1959-63 AVERAGES (Oregon State Sanitary Authority, 1964)

Station[1]	pH field	T., °C	D.O. mg/ℓ	B.O.D.	SO_4	Cl	PO_4	NH_3-N	NO_3-N	T S [2]	S S [3]	Alk.	Hard.	Na	K	F	Cond. UMHOS CM
K-1	7.7	11	9.8	1.1	4.7	3.0	0.13	0.51	0.09	121	23	44.5	35.8	8.4	2.4	0.12	98
K-2	7.5	8.8	10.3	1.3	7.1	3.6	0.18	0.33	0.12	107	11	34.6	25.4	9.1	2.1	0.21	75
K-3	7.5	10.0	9.5	1.7	6.4	3.6	0.17	0.42	0.10	114	15	38.2	30.7	9.0	2.1	0.17	82
K-4	8.1	11.3	9.7	5.4	8.5	4.2	0.11	0.61	0.17	141	27	47.2	34.9	9.8	2.3	0.24	96
K-5	7.9	11.5	7.5	4.4	18.5	5.4	0.22	0.99	0.18	162	25	57.7	42.5	9.3	2.8	0.31	136
K-6	7.9	11.7	7.8	4.5	35.1	7.9	0.29	0.97	0.25	221	32	74.2	71.9	20.5	3.9	0.30	231
K-7	7.7	11.1	9.6	3.0	29.3	6.0	0.24	0.50	0.39	194	27	71.8	67.0	18.2	3.4	0.24	214

[1] Station Locations

K-1 Sprague River bridge near Chiloquin
K-2 Williamson River bridge one mile north of Chiloquin
K-3 Williamson River at old Highway 97 bridge
K-4 Link River at Fremont Bridge in Klamath Falls
K-5 Klamath River at Highway 97 bridge in Klamath Falls
K-6 Klamath River bridge at Keno
K-7 Klamath River below Copco's Big Bend powerhouse

[2] T S = total solids

[3] S S = suspended solids (thus, T D S = T S - S S)

TABLE 4.5 AQUIFER UNITS OF KLAMATH BASIN

Unit Name	Corresponding geologic map-unit symbols (figure 1)	Lithologic Composition	Water-bearing Characteristics	Corresponding Units from Sammel (1976)
Sedimentary Aquifer	Ql, Qal, Qf, Tst, Tpt, Qtb	Sand, silt, clay, gravel and their lithified equivalents; basalt	Poor	1. Alluvial Terrace deposits 2. Pleistocene and Holocene lake deposits 3. Quaternary basalt 4. Older lake deposits 5. Yonna Formation
Volcanic Centers Aquifer	QTvcb	Lava flows and cinders (mostly basaltic)	Mod. to High	6. Quaternary/Late Tertiary eruptive centers
Lower Basalt Aquifer	QTvc	Basalt	High	7. Quaternary/Late Tertiary basalt
Volcanic Ash Aquifer	Ttf (deep subsurface; not present on figure 1)	Volcanic ash and sediments	Poor	

The Volcanic Centers Aquifer consists of basalt ash, cinders, breccia and flows, which accumulated around local vents. There are numerous exposures of these eruptive centers in mountain ridges, and many small ones probably are buried beneath the valleys. The water-yielding characteristics of this unit are generally excellent, reflecting the porous nature of the breccias and cinders. However, wells in this unit show a wide range of specific capacity, from less than 12 to over 1,240 lpm/m (1 to 100+ gpm/ft). Stratigraphically, this aquifer unit is discontinuous and local and may be overlain or truncated by the younger Sedimentary Aquifer. Locally, it may be in intrusive contact with older portions of the Sedimentary Aquifer.

The Lower Basalt Aquifer unit is composed of basalt flows and minor interflow cinder zones. It underlies the Pliocene-Pleistocene lacustrine sequence mapped as (Qts) on the geologic map, but it may grade laterally into the lavas of the Volcanic Centers Aquifer. It is the main aquifer unit in the Klamath Basin. It is usually buried by 300 m (1,000 ft) or more of sediments in the graben valleys and exposed in numerous low hills. High permeability in fractured lavas and interflow cinder zones gives the unit specific capacities which range from 400 to 6,200 lpm/m (33 to 500 gpm/ft) with an average of about 1,800 lpm/m (145 gpm/ft). Sammel (1976) estimated an average of only 460 lpm/m (37 gpm/ft), but he admits that his figure is based on rough estimates and sparse data. In this unit, average permeability and specific capacity figures may not be meaningful, because interflow cinder and scoria zones 3 to 14 m (10 to 45 ft) in thickness may provide nearly infinite permeability. Lost circulation zones in this unit make deep drilling expensive and hazardous.

Many water wells located near the edges of the major graben valleys are completed in the upper part of this unit, but none of them are known to have penetrated it completely. However, it is likely that the Thermal Power Company deep geothermal exploration well in the Klamath Hills (SW 1/4 sec. 35, T. 40 S., R. 9 E.), drilled to a total depth of 1,781 m (5,842 ft), did pass through this unit into the underlying Volcanic Ash Aquifer. No details concerning this well have yet been released.

The Volcanic Ash Aquifer is believed to be composed of thick acidic ash-flow tuffs, interbedded with minor flows, palagonite tuff lenses and some fine-grained tuffaceous sediments. The assemblage is not exposed in the fault-block ridges around the Klamath Basin, but it is projected under the basin from distant outcrops both to the east and west. No water wells are known to have penetrated this unit in the basin, but it is likely to have been encountered in the Thermal Power Company (Natomas Company) deep geothermal test in the Klamath Hills.

Ground Water Flow--

The Klamath Basin includes regional, intermediate and local ground water flow systems. Relationships among these systems are shown in Figure 4.5. The regional system receives recharge from the Cascade Range on the west and from highlands on the east, to the limits of the drainage basin in the Yamsay Mountain-Gearhart Mountain and Quartz Mountain areas. This water is believed to descend to depths greater than 3,000 m (10,000 ft) below land surface under some areas of the Klamath Basin. It is considered to discharge in wells and springs in the Lower Klamath region, based on the high temperature gradients encountered in this area and the relatively high ionic concentrations in these waters.

Water of local and intermediate flow systems also discharges within the regional discharge area, having shorter transit times and shallower depths of circulation. Therefore, mixing can be expected to cause appreciable variation in water temperatures and in chemical characteristics, reflecting differences in depth and time of circulation. This may be observed even in closely spaced wells. Waters of intermediate flow systems fall between those of regional and local systems in terms of temperature, flow pattern, chemical character and degree of seasonal water level fluctuation.

Intermediate depth ground water flow systems in this region are characterized by temperatures from 7°to 29°C (45° to 85°F), and TDS varying from 100 to 800 mg/l, but averaging less than 200 mg/l.

Low temperatures and low TDS are characteristic of the local flow systems. These waters have short, shallow circulation paths and are often recharged and discharged within the same aquifer or topographic feature.

Sammel (1976) has provided a fairly comprehensive listing of wells in the central part of Klamath Basin.

Permeability--

Numerous water wells produce from the Sedimentary Aquifer, the Volcanic Centers Aquifer and the Lower Basalt Aquifer. Wells in the Sedimentary Aquifer in the flatlands adjacent to the Klamath Hills typically yield less than 110 lpm (30 gpm). This contrasts with the Lower Basalt Aquifer, reached at depths of more than 210 m (680 ft), with yields up to 13,000 lpm (3,500 gpm) with 25 m (83 ft) of drawdown (530 lpm/m [43 gpm/ft]). Basalt and cinders are encountered in the Keno area at depths of 3 to 45 m (10 to 150 ft). Production from this unit varies from 27 lpm (7 gpm) with 18 m (60 ft) of drawdown, to 75 lpm (20 gpm) with no observable drawdown. A well area near Henley, close to the center of the basin, produces up to

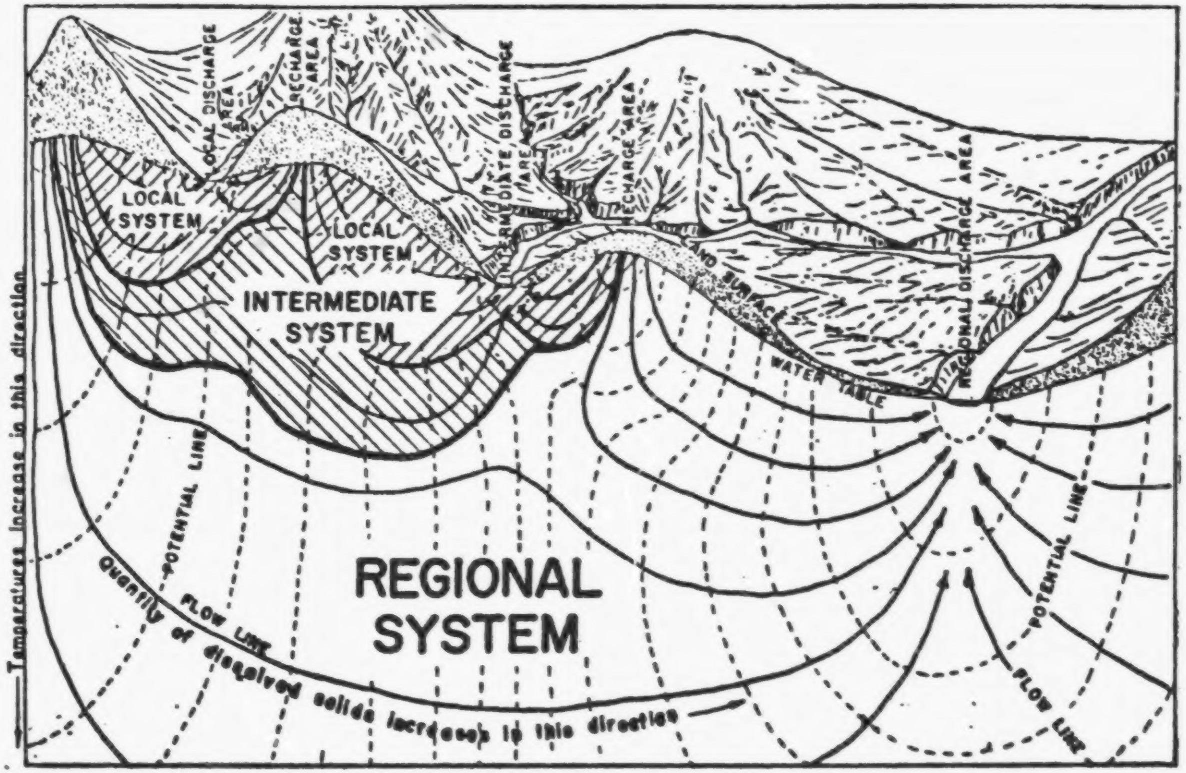
LOCAL DISCHARGE AREA
RECHARGE AREA
INTERMEDIATE DISCHARGE AREA
RECHARGE AREA
REGIONAL DISCHARGE AREA
LOCAL SYSTEM
LOCAL SYSTEM
INTERMEDIATE SYSTEM
LAND SURFACE
WATER TABLE
REGIONAL SYSTEM
POTENTIAL LINE
FLOW LINE
POTENTIAL LINE
FLOW LINE
Temperatures increase in this direction
Quantity of dissolved solids increases in this direction

Figure 4.5 Salient features of local, intermediate and regional groundwater flow systems. (Illian, 1970)

3,800 lpm (1,000 gpm) from water-bearing gravels of the Sedimentary Aquifer, which here is over 380 m (1,250 ft) thick. Closer to the hills, the Volcanic Centers and Lower Basalt Aquifers are intercepted at from 90 to 180 m (300 to 600 ft).

Recharge and Discharge--
Ground water recharge occurs in the Cascade Mountains west of the basin and in upland areas to the east and north of the basin, where heavy precipitation occurs over areas of permeable soil or fractured volcanic rocks. Few water wells have been drilled in the recharge areas. Those that exist produce water of low TDS and low temperature.

The Klamath Basin has been divided into four sub-basins (Illian, 1970). Of these, only the southwestern corner of the Upper Klamath Lake and the Lost River sub-basins are of concern here.

The Upper Klamath Lake sub-basin is bounded on the west by the crest of the Cascade Mountains and on the east by Chiloquin Ridge and Naylox Mountain. It extends southward approximately to Link River and Klamath Falls.

Based on climatological, soils and evapotranspiration data, it is estimated that about 99,000 ha-m (800,000 acre-ft) of water per year is recharged to the ground water system in this sub-basin. Water wells in the area are not abundant; water levels are generally shallow. Some artesian wells report pressures to .67 kg/sq cm (9.6 psi) indicating a piezometric level 6.7 m (22 ft) above land surface. The highest reported production is from the Lower Basalt Aquifer, which yields 4,500 lpm (1,200 gpm) with 28 m (92 ft) of drawdown 137 lpm/m (11 gpm/ft). Water temperatures range from 8° to 11°C (47° to 51°F).

The Lost River sub-basin covers 7,820 sq km (3,019 sq mi) in the southern portion of the Klamath Basin. Of the total, 3,405 sq km (1,315 sq mi) are in Oregon and 4,410 sq km (1,704 sq mi) are in California. The ground water boundaries approximately follow topographic divides.

It is estimated that the total average annual ground water recharge in this sub-basin is about 111,000 ha-m (900,000 acre-ft). This consists of 67,800 ha-m (550,000 acre-ft) of recharge from adjacent highlands, 24,700 ha-m (200,000 acre-ft) of underflow from the Upper Klamath Lake and 18,500 ha-m (150,000 acre-ft) of underflow from the Sprague River sub-basin to the east.

4.4.3 Hydrologic Budget

The outline of the ground water basin is essentially the same as that of the surface water drainage system and has an area of about 14,800 sq km (5,700 sq mi). Precipitation within this area varies from about 380 mm (15 in) on the valley floors to over 1,500 mm (60 in) in the upper parts of the Cascade Range, along the western boundary of the basin. Precipitation is estimated to supply a total inflow of about 826,000 ha-m (6.7 million acre-ft) of water to the basin each year. The complete water budget for the basin is:

Precipitation	$+8.264 \times 10^5$ ha-m	(6.700×10^6 acre-ft)
Evapotranspiration	-6.227×10^5 ha-m	(5.048×10^6 acre-ft)
Pumped Ground Water	-0.428×10^5 ha-m	(0.347×10^6 acre-ft)
Ground Water Outflow	-0.123×10^5 ha-m	(0.100×10^6 acre-ft)
Surface Water Outflow	-1.486×10^5 ha-m	(1.205×10^6 acre-ft)
TOTAL:	0	0

The sum of pumped ground water and ground water outflow represents total withdrawal from the regional system. For purposes of this discussion, it is assumed to be in balance with recharge via infiltration of precipitation. Increases in well pumpage should be matched regionally by decreases in ground water outflow from the system. Local deficits, however, may be significant and may show up as lowered piezometric levels in wells.

4.5 CHEMICAL CHARACTERISTICS OF GROUND WATER

Klamath Basin ground waters fall into two main chemical groups (Table 4.6). Cool wells and springs are of the calcium magnesium bicarbonate type, with low TDS. In these waters, TDS averages about 100 ppm, with bicarbonate concentrations of about 50 ppm. Sodium may be equal to or less abundant than calcium or magnesium in concentration, frequently being less than 10 ppm. Magnesium is more abundant than potassium, with both generally present in concentrations less than 5 ppm. Silica is present in concentrations of about 25 ppm. Chloride and sulfate have very low concentrations (<10 ppm). Relative ion abundances may be given as calcium ≥ sodium ≥ magnesium > potassium and bicarbonate ≥ sulfate ≥ chloride.

TABLE 4.6 CHEMICAL ANALYSES OF WATERS FROM SPRINGS AND WELLS

Name of Spring or Well	Sample Location T, R, Sec.	Date of Sample	Temp., °C	pH	Specific Conductance μ/cm	TDS Evaporation
Eagle Point Spring	36-7-23dca	4-6-75	85	8.3	305	-
Shell Rock Spring	38-8-27	8-6-75	7	6.4	110	-
Cabin Spring	37-8-26	8-5-72	11	5.5	-	-
Hummingbird Spring	37-9-6bcd	4-2-75	11	8.3	135	-
Neubert Spring	37-9-7adc	8-6-75	10	8.2	160	-
Well, 98.6 feet deep	37-9-9dcc	8-6-75	10	6.8	150	158
OIT Well #6	38-9-20adb	3-31-75	79	8.2	1050	-
Mer-Bell-Dairy	38-9-28ccc	1-24-55	81	8.8	1160	-
J. E. Ericson	38-9-28cdc	2-19-55	83	8.7	1230	-
Oregon Water Corp.	38-9-30acb	8-8-75	15	8.0	250	-
Keno Spring	38-12-14	10-16-75	11	7.7	100	72
Alfred Jacobson	39-9-34	5-20-74	30	7.6	290	-
Weyerhaeuser Well #4	39-9-18	10-11-73	22	8.3	200	-
U. S. Air Force	40-7-11ccc	5-27-74	15	8.6	340	-
Dave O'Connor	40-9-23bab	5-7-74	24	7.6	260	-
O. H. Osborn	40-9-27cda	5-31-74	90	9.5	920	-
Anderson Well	40-9-27	11-8-75	27	8.0	450	286
Abe Boehm	40-9-28aca	5-30-74	25	7.1	2700	-
Liskey Well	40-9-34aca	5-9-74	93	8.9	1030	724
Tulana Farms Spring	41-8-5cbb	8-8-75	13	6.9	115	-

TABLE 4.6 (continued)

Name of Spring or Well	Concentrations (milligrams per liter)										
	SiO_2	Na	K	Ca	Mg	HCO_3	CO_3	SO_4	Cl	F	B
Eagle Point Spring	38	62	5.7	0.6	0.1	136	0	<2	16	.75	.14
Shell Rock Spring	32	5.9	1.5	8.1	3.9	50	0	<2	<1	.10	.05
Cabin Spring	29	5.9	1.6	11.2	5.1	94	0	<1	<2	.10	.10
Hummingbird Spring	18	8.0	1.2	9.2	6.5	84	0	<2	1	.10	.07
Neubert Spring	21	7.0	1.2	10.6	8.2	96	0	<2	1	.10	.05
Well, 98.6 feet deep	24	7.6	1.3	12.1	7.2	94	0	<2	1	.11	.05
OIT Well #6	31	195	3.9	24.2	0.1	44	0	400	58	1.45	1.0
Mer-Bell-Dairy	81	213	4.2	23	0	32	8	403	54	1.2	.96
J. E. Ericson	87	221	4.4	25	0	32	8	1.2	56	1.6	.91
Oregon Water Corp.	27	22	-	14.4	0.8	-	-	0.4	4.5	.01	-
Keno Spring	40	4.1	3.0	7	6.2	73	0	13	1.8	.08	.05
Alfred Jacobson	65	69	12	160	2.4	160	0	4	7.9	.10	.50
Weyerhaeuser Well #4	16	32	3.3	10	1.9	115	4.5	2.3	4	.11	.09
U. S. Air Force	31	17	1.6	24	17	200	3	14	2.3	0	0.9
Dave O'Connor	42	32	8.1	12	6.6	130	0	270	9.1	0	0
O. H. Osborn	90	140	4.1	15	0	37	9	36.2	56	1.5	.77
Anderson Well	41	88	2.5	5.0	0.1	165	6.0	300	23	.40	.15
Abe Boehm	100	480	18	180	47	1460	1	360	170	.20	1.4
Liskey Well	90	200	4.0	15	0.1	48	2	2	59	1.5	.65
Tulana Farms Spring	24	5.7	1.2	9.2	4.9	60	0	-	1	.07	.05

TABLE 4.6 (continued)

				Cl:	Ionic Ratios				
			Na+K	Total	Cl	Cl	Cl	HCO_3	Alk
Name of Spring or Well	Na:K	Na:Ca	Ca+Mg	Alk.	SO_4	F	B	B	SO_4
Eagle Point Spring	18.51	180.99	149.60	.40	21.70	11.45	34.87	172.31	53.61
Shell Rock Spring	6.70	12.70	.82	.07	1.36	5.42	6.80	177.38	19.71
Cabin Spring	6.30	0.90	.50	.10	-	-	-	269.60	-
Hummingbird Spring	9.95	1.15	.55	.04	1.35	5.42	7.63	340.56	62.02
Neubert Spring	9.96	1.10	.61	.04	1.35	4.94	7.63	333.47	37.06
Well, 98.6 feet deep	1.70	1.51	1.08	.04	2.72	39.40	-	-	72.39
OIT Well #6	85.1	14.05	14.12	4.53	.39	21.44	17.70	7.80	.09
Mer-Bell-Dairy	86.50	16.20	16.40	4.63	.36	24.10	17.16	7.39	.08
J. E. Ericson	76.80	15.40	15.61	-	.35	18.80	18.78	7.80	.07
Oregon Water Corp.	16.98	2.66	1.33	-	10.0	239.50	-	-	-
Keno Spring	2.32	1.02	.59	.06	12.18	21.85	10.97	259.50	200.10
Alfred Jacobson	9.78	.75	.81	.17	1.64	42.20	4.82	56.76	9.70
Weyerhaeuser Well #4	16.40	5.58	4.51	.12	2.71	19.78	13.56	235.52	23.55
U. S. Air Force	18.07	1.23	.60	.04	2.71	-	.08	400.08	69.54
Dave O'Connor	6.72	4.65	2.80	.24	1.76	-	-	-	7.31
O. H. Osborn	7.88	2.21	2.49	4.19	.56	20.01	22.19	10.06	.13
Anderson Well	59.70	30.80	30.71	.46	1.72	32.80	46.91	194.20	3.72
Abe Boehm	45.35	4.65	3.32	.40	1.53	455.48	37.05	185.11	3.83
Liskey Well	75.00	16.13	14.81	3.64	.52	18.40	28.17	15.40	.14
Tulana Farms Spring	8.10	1.08	.65	.06	.50	7.83	6.10	212.85	9.72

The second type of water, occurring in warm and hot wells and springs, mostly within basins of the Klamath graben, is a sodium bicarbonate chloride sulfate water. TDS in these waters are as high as 4,000 ppm (Sammel, 1976) but average about 700 ppm. The bicarbonate ion is relatively less abundant than in cold water but still may exceed 100 ppm. Sulfate and chloride concentrations characteristically are above 50 ppm. The concentration of boron and fluorine increases with temperature. The relative abundance of cations is sodium > calcium > potassium > magnesium. Sodium concentrations in the hottest wells may be several hundred ppm. The pH of the waters ranges from 8.5 to 9.5. They are more alkaline than the cold waters of the basin, which range from neutral to mildly alkaline. Silica concentrations reach and locally exceed 100 ppm.

4.5.1 Chemistry of Thermal Waters

Water chemistry data is useful in estimating reservoir temperature, fluid state and fluid migration history.

If calcium bicarbonate type waters enter the regional circulation system in recharge areas and descend to depths where temperatures are 80° to 120°C (175° to 250°F) or higher, their composition will change. Characteristically, the change involves an increase in sodium and potassium, derived from the hydration of silicate minerals such as feldspar. Calcium and especially magnesium are likely to decrease in concentration somewhat, due to the decreased solubility of carbonate minerals in water with increasing temperature; in any case, they show depletion relative to sodium.

The magnitude of these changes depends on the validity of a number of assumptions: temperature-dependent reactions actually take place at depth; all of the cation constituents are sufficiently abundant at depth; water-rock equilibration occurs at reservoir temperature; no re-equilibration takes place as the water returns to colder regions; and the hot, mineralized waters do not mix appreciably with cooler meteoric or shallow ground water; also, there are no evaporite beds at shallow depth to yield ions to low temperature solubility reactions.

Most high temperature waters of the Basin and Range and Lava Plateau Provinces exhibit, to varying degree, characteristics of deep circulation. However, most thermal waters of the Klamath Basin show larger amounts of calcium than potassium, and high ratios of sodium to potassium. Therefore, something may retard the solution of potassium in waters of this area; or these waters may be diluted on a large scale by cold meteoric water; or the subsurface temperatures may be lower than the 80° to 120°C (175° to 250°F) range at depths of 2 to 3 km (6,500 to 10,000 ft). Sammel (1976) discussed calcium to magnesium and bicarbonate plus carbonate to chloride ratios in Klamath Basin waters. This and other chemistry indicates that spring and well waters having temperatures greater than 65°C (149°F) are not significantly diluted with cold water but have been cooled mainly by conduction.

Cool meteoric waters generally exhibit the following anion balance: bicarbonate > sulfate ≥ chloride. Heating of this water as it descends into deep aquifers results in a change in the balance as follows: sulfate ≥ chloride > bicarbonate. In thermal waters of the Klamath Basin, sulfate and chloride concentrations increase both absolutely and relative to bicarbonate, but not in proportion to increasing temperature. This supports the idea of relatively low temperature equilibration at depth, as suggested by the cation ratios. The chloride-rich waters of the Klamath Hills area appear to have cooled while retaining chloride concentrations representative of higher temperatues, along a unique dilution trend (Sammel, 1976).

Silica concentrations may be used to determine reservoir temperatures (Fournier and Rowe, 1966). Temperature calculations require designation of either amorphous (chalcedony) or crystalline quartz as the source of silica; usually, this is problematic. Also, siliceous rocks characteristically yield more silica and higher ratios of silica to other species than do basic rocks. These factors affect silica geothermometry in Klamath Basin, where a variety of rock types is present, including diatomite, palagonite and basalt at shallow depths, and acidic ash-flow tuffs at greater depths.

Generally, silica concentrations in Klamath Basin thermal waters are moderate (50 to 118 ppm). With this range of values for silica, and assuming equilibration with chalcedony, temperatures at depth are calculated to be in the range from 120° to 150°C (250° to 300°F), by the method of Fournier and Rowe (1966).

The chloride content of water has been established as a reliable indicator for distinguishing hot water from vapor-dominated systems (White, et al., 1971), as well as for indicating distance and duration of flow. In general, very low chloride concentrations in hot springs and shallow wells characterize vapor-dominated systems at depth, whereas chloride concentrations above 50 ppm in thermal waters tend to characterize hot water systems. Cool water associated with evaporite deposits or connate water in marine formations may contain more than 50 ppm chloride. However, evaporites are not known to occur here, and the only marine formation still likely to contain connate water is the upper Cretaceous sequence of unknown subsurface distribution and depth. Thermal waters in the Klamath Basin tend to have chloride concentrations of 50 ppm or above. Therefore, a hot water rather than a vapor-dominated system is expected here.

Other ions can have significance in the interpretation of geothermal conditions. Among these, ammonia, boron, mercury, carbon dioxide and sulfur compounds in thermal waters may indicate subsurface boiling and consequent enrichment of volatiles in springs and wells. Of these constituents, trace amounts of mercury are present in the altered rocks of both Klamath Hills and Klamath Falls. Boron is nearly absent from cooler waters of the region but is present in higher concentrations in the thermal waters at Klamath Falls. However, the concentration of boron relative to chloride is not high and does not, therefore, suggest vapor transport of boron from an underlying reservoir.

Fluoride in thermal waters may derive from the breakdown of mica and hornblende in igneous rocks, from the presence of primary magmatic gases or from the solubility of fluoride. High fluoride concentrations are common in water from regions of young igneous activity; however, due to the variety of possible sources of the ion, its abundance does not indicate a magmatic source. Relatively high fluoride concentrations characterize thermal waters at Klamath Falls and the Klamath Hills. However, in the absence of other evidence, fluoride abundance is not interpreted to indicate a magmatic source.

Two main water types are present in the area; concentrations of silica, sulfate, sodium and chloride differ systematically between them. Cold waters in upland recharge areas, and in shallow circulation zones below, constitute one type. TDS of these waters is low and the predominant ions are calcium and bicarbonate.

The second water type comprises thermal springs and wells in the area, which are discharge points in the regional circulation pattern and are on or near known or inferred fault zones. Deep circulation has carried these waters through Tertiary tuffs, lavas, and breccias, and they are characterized by relatively high TDS. Composition varies, but the most abundant ions generally are sodium and sulfate, with moderately abundant chloride. Silica, fluoride and boron also are relatively abundant. A tentative conclusion is that the maximum reservoir temperature, based on both the silica and alkali geothermometers, is 120° to 150°C (250° to 300°F) at depths of 1 to 1.5 km (3,300 to 5,000 ft) and 160° to 180°C (320° to 355°F) at depths of 2.5 to 3 km (8,000 to 10,000 ft). A few cool waters of high alkali content may be explained by ion exchange with clay minerals of near-surface rocks and/or selective yielding of sodium and potassium from devitrification of silica and alkali-rich tuffs, such as the surficial Mazama Pumice. Abundant silica also probably results from leaching of low temperature chalcedony in devitrified silicic tuffs and diatomaceous sediments.

The absence of well data from deeper than 600 m (2,000 ft) prevents a definitive statement for the central Lower Klamath Basin. Therefore, the thermal and geochemical anomaly patterns do not conclusively evaluate the potential in the basin, particularly not at depths greater than a few tens of meters. Although a hot water aquifer of mild salinity is likely, the water chemistry does not exclude a saline hot water aquifer or even a steam-bearing deeper horizon that heats the shallow aquifer through upward leakage along faults.

4.6 SEISMICITY

4.6.1 Historical Seismicity

Most of Oregon and adjacent parts of Idaho, Nevada and California form a large region of low seismicity, in comparison with many parts of the western United States. Historically, no major, destructive earthquakes have occurred in Oregon, nor has any instance of surface faulting been reported. Moderate seismicity characterizes the Portland-Willamette Valley area of northwestern Oregon; however, the rest of the state exhibits lower or negligible seismicity (Fig. 4.6). Slight seismicity has been reported near Klamath Falls but not elsewhere in Klamath Basin. Berg and Baker (1963) reported five small shocks, with intensity IV, at Klamath Falls during the years 1947 to 1951.

Throughout the Pacific northwest, including Klamath Basin, very few seismograph stations operated until the year 1962; earthquakes of magnitude smaller than 4.5 to 5 either were not recorded at all or were not recorded at sufficient stations to permit instrumental location of epicenters and determination of Richter magnitude. Thus, nearly all pre-1962 shocks were located using felt-reports, which are highly dependent upon the distribution of population and time of day of occurrence. Also, the "size" of these events was rated on intensity scales, which are crude, graduated ratings of megascopic earthquake effects, such as kind and degree of shaking or of damage to buildings.

Therefore, the earthquake history of this region is poorly known as to the occurrence or non-occurrence, epicenter location, and size of smaller shocks ($M \leq 5$). For this reason, correlation of seismicity with particular faults and determination of magnitude-frequency curves for various areas cannot be done with much confidence.

4.6.2 Seismic Risk

Earthquake risk is poorly known in most of Oregon and northernmost California because of the extremely low seismicity and inadequate reporting of such shocks as have occurred.

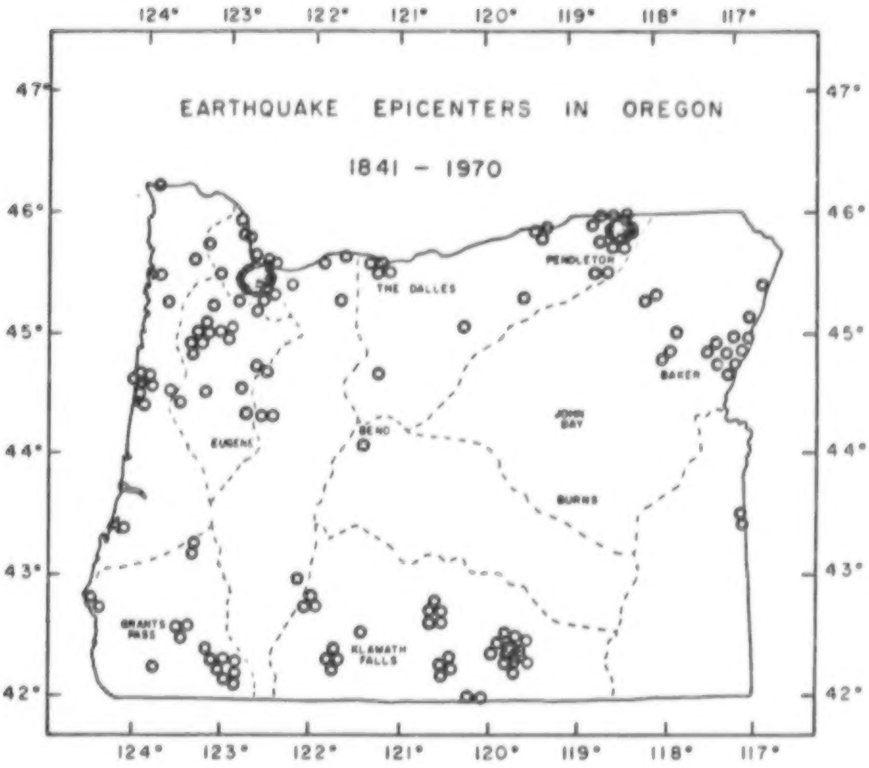
EARTHQUAKE EPICENTERS IN OREGON
1841 - 1970
124°
123°
122°
121°
120°
119°
118°
117°
47°
46°
45°
44°
43°
42°
THE DALLES
PENDLETON
BAKER
JOHN DAY
BEND
EUGENE
BURNS
GRANTS PASS
KLAMATH FALLS

Figure 4.6 Earthquake epicenters in Oregon, 1841-1970. (Couch and Lowell, 1971)

Nevertheless, it may be useful to review the sparse statistics. Couch and Lowell (1971) have analyzed earthquake occurrence in Oregon and described the seismicity of several physiographic provinces. One of the provinces is the Basin and Range, which includes Klamath Basin.

Very limited data suggests a rate of energy release of 8.8×10^{16} ergs/yr for the period 1870 to 1970 (Couch and Lowell, 1971); this figure is probably too low, as the lack of any reported shocks for 1870 to 1906 is highly dubious. In any case, this rate of energy release is equivalent to the occurrence of one magnitude 3.3 earthquake per year per 10,000 sq km; or to one shock of $M \leq 5$ per 50 years per 10^4 sq km. This occurrence rate has been used, along with an assumed "b-slope" of 1.0, to draw the magnitude-frequency curve in Figure 4.7 Clearly, this area has exhibited very low seismicity. Compare the seismicity of central coastal California, which may be expressed as ten $M \leq 5$ shocks per 50 years per 10^4 sq km.

Based upon the above data, the maximum probable earthquake acceleration per 100 years at a given site in the Klamath Basin is expected to be about 0.07 g. Therefore, earthquake risk to well-engineered facilities in this area is quite low in comparison with many other areas, particularly coastal or southern California.

4.6.3 Seismicity and Tectonism

As already noted, earthquake epicenters for most of the period of record (i.e., before 1963) are inaccurately located. Couch and Lowell (1971) estimate that epicenters located from felt-data in the sparsely populated area east of the Cascades have a probable error of 13 km (8 mi); this seems optimistic because the location errors are probably greater. From 1963 to 1971, no instrumentally located shocks occurred in Klamath Basin (Couch and Lowell, 1971). Therefore, available data does not permit correlation of epicenters and faults nor definition of seismically active faults.

Focal mechanism studies by Couch and McFarlane (1970) and Dehlinger, et al. (1963) show a regional stress field that has minimum compressive stress axis oriented east-west, and maximum compressive stress axes in a vertical, north-south plane. This fits a pattern of north-south trending normal faults, and overall east-west extension, as well as right-lateral strike-slip on northwest trending faults.

Therefore, the regional stress field does not fit Klamath Basin, dominated by northwest trending normal faults. This disagreement has two obvious possible explanations:

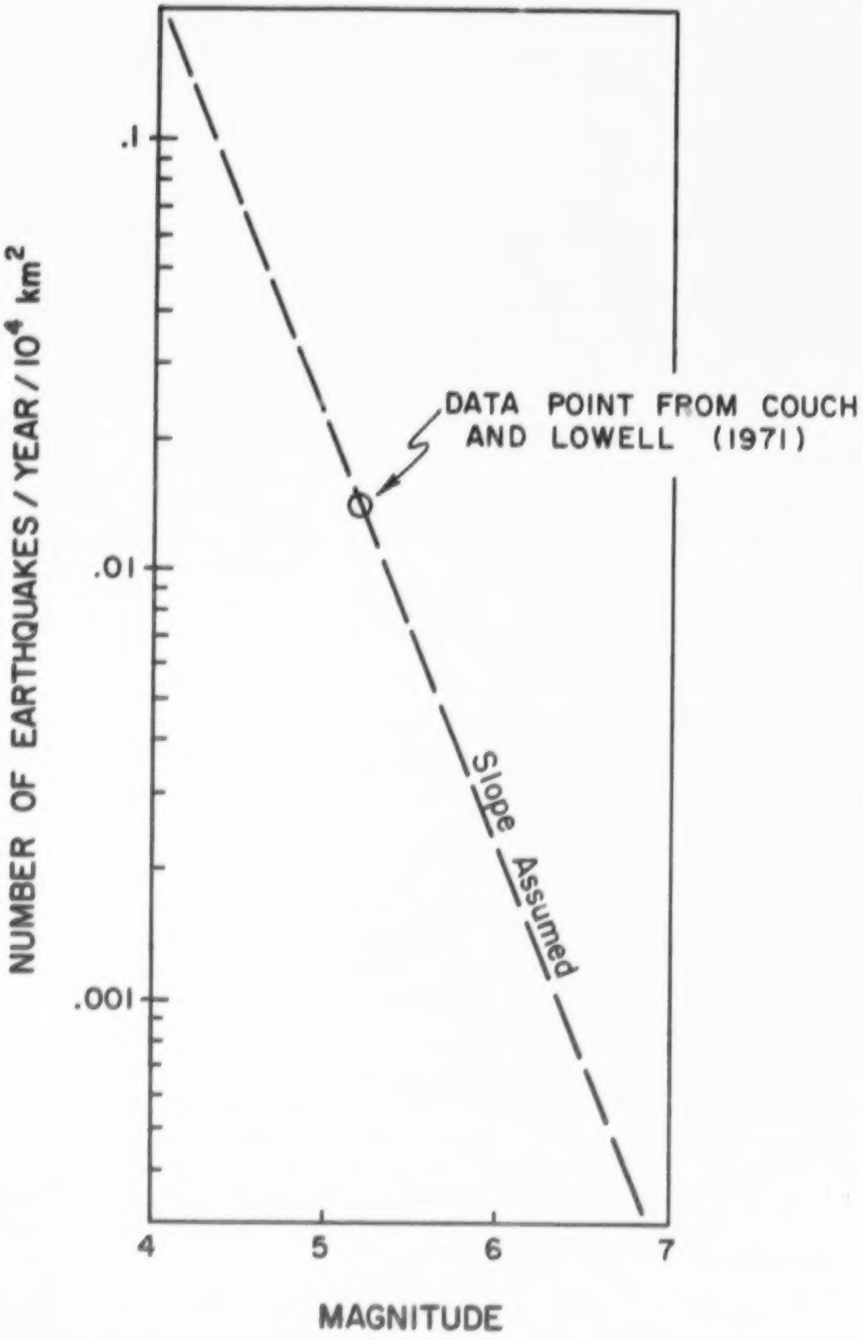

Figure 4.7 Magnitude vs frequency of occurrence for earthquakes in the Basin and Range Physiographic Province of southern Oregon.

(1) The present stress field does not characterize that of late Tertiary and Quaternary time in this region.

2) Young faulting in the Klamath Basin was primarily the result of volcanic subsidence causing reactivation of much older, strike-slip faults.

The second explanation is preferred for two reasons: 1) it does not require a radical change in the stress field, and 2) it fits the observation that late Quaternary fault movements and present-day seismicity are very minor in this region, and that major faulting seems to have been closely associated, in both space and time, with Plio-Quaternary volcanism.

REFERENCES

Berg, J. W., and C. D. Baker. Oregon Earthquakes, 1841 through 1958. Bull. Seism. Soc. Am., v. 53, p. 95-108, 1963.

Callaghan, E., and A. F. Buddington. Metalliferous Mineral Deposits of the Cascade Range in Oregon. USGS Bull. 893, 141 p., 1938.

Couch, R. W., and R. P. Lowell. Earthquakes and Seismic Energy Release in Oregon. Oregon Dept. of Geol. and Min. Ind., The Ore Bin, v. 33, no. 4, p. 61-84, 1971.

Couch, R. W., and W. T. McFarlane. A Fault Plane Solution of the October, 1969 Mount Rainier Earthquake and Tectonic Movements in the Pacific Northwest from Fault Plane and First Motion Studies (abs.). Trans. Am. Geophys. Un., v. 52, 1970.

Dehlinger, P., et al. Investigations of the Earthquake of November 5, 1962, North of Portland. The Ore Bin, v. 25, p. 53-68, 1963.

Fournier, R. O., and J. J. Rowe. Estimation of Underground Temperatures from the Silica Content of Water from Hot Springs and Wet-Steam Wells. Am. J. Sci., v. 264, p. 685-697, 1966.

Hanna, G. D., and G. C. Gester. Pliocene Lake Beds Near Dorris, California. Calif. Acad. Sci. Occ. Papers 42, 1963.

Hardyman, R., J. R. McIntyre and L. K. Richardson. Geologic Map of the Southern Klamath Basin. USGS Open File Map, 1972.

Illian, J. P. Interim Report on the Ground Water in the Klamath Basin, Oregon. Report of the Oregon State Engineer, Salem, Oregon, 1970.

Leonard, A. R., and A. B. Harris. Ground Water in Selected Areas in the Klamath Basin, Oregon. Oregon State Engineering Ground Water Report No. 21, 1974.

Lund, J. W., G. G. Culver and L. S. Svanevik. Utilization of Geothermal Energy. Proc. of the International Conference on Geothermal Energy, Oregon Institute of Technology, Klamath Falls, Oregon, 1974.

Newcomb, R. C. and D. N. Hart. Preliminary Report on the Ground Water Resources of the Klamath River Basin, Oregon. USGS Open File Report, 1958.

Oregon State Sanitary Authority. Quality of Klamath Basin Waters in Oregon, July 1959 to December 1963, 1964.

Pacific Northwest River Basins Commission Meteorological Committee. Climatologic Handbook, Columbia Basin State, 1968-1969.

Peterson, N. V., and E. A. Groh. Geothermal Potential of the Klamath Falls Area, Oregon: A Preliminary Study. Oregon Dept. Geol. and Min. Ind., The Ore Bin, v. 29, no. 11, p. 209-231, 1967.

Peterson, N. V., and J. R. McIntyre. The Reconnaissance Geology and Mineral Resources of Eastern Klamath and Western Lake County, Oregon. Oregon Dept. Geol. and Min. Ind. Bull. 66, 1970

Phillips, K. N. Water Resources and Development; in Mineral and Water Resources of Oregon, A. E. Weissenborn, Principal Investigator, Oregon Dept. Geol. and Min. Ind. Bull. 64, 1969.

Sammel, E. A. Hydrologic Reconnaissance of the Geothermal Area Near Klamath Falls, Oregon. USGS Open File Report 76-127, 1976.

Sass, J. H., and E. A. Sammel. Heat Flow Data and Their Relation to Observed Geothermal Phenomena near Klamath Falls, Oregon. J. Geophys. Res. v. 81, no. 26, p. 4863-4868, 1976.

U. S. Geological Survey. Surface Water Supply of the United States, 1966-1970, Part II, Pacific Slope Basins in California. USGS Water Supply Paper 2129, 1976.

Wells, F. G. Geology of the Medford Quadrange. USGS Map Q 89, 1956.

White, D. E., L. H. P. Muffler and A. H. Truesdell. Vapor-dominated Hydrothermal Systems Compared with Hot Water Systems. Econ. Geol., v. 66, p. 7597, 1971.

Williams, H. Geology of the MacDoel Quadrangle, California. Cal. Div. Mines and Geol. Bull. 151, 78 p., 1949.

SECTION 5

RIO GRANDE RIFT ZONE

5.1 INTRODUCTION

This section presents baseline data on climatology, geology, hydrology and seismology to aid in assessment of environmental impacts of potential geothermal development in the Rio Grande Rift Zone, New Mexico. Aspects of climatology, geothermal characteristics, geology, hydrology and chemical characteristics of ground water are discussed. Seismicity of New Mexico, of the Rio Grande Rift and of the Valles Caldera region is also described.

5.1.1 Summary

For this report, the Rio Grande Rift in New Mexico runs from the Colorado border on the north to the border with Texas and Mexico on the south and has a variable width limited by geologic structures. It includes the valley of the Rio Grande itself and all or part of the closed basins bordering the Rio Grande Valley. Climate and vegetation in the rift vary with altitude and latitude. The low southern river valley is a lower Sonoran desert with 180 mm (7 in) average annual precipitation, 1,780 mm (70 in) average annual evaporation, and a mean annual temperature about 16°C (60°F). The high northern mountains range from Canadian zone forests to arctic tundra, with up to 810 mm (32 in) average annual precipitation, 1,020 mm (40 in) average annual evaporation, and a mean annual temperature about 4°C (40°F).

Surface water and ground water both derive ultimately from precipitation. The Rio Grande is the only large perennial stream in the rift. The ground water surface or water table usually follows the land surface contours. Both surface and ground water are used for domestic, agricultural and industrial purposes in the Rio Grande Rift. Agricultural water usually comes from surface water diversions. Municipal and industrial users mostly rely on ground water.

Geology of the rift is complex. Older rocks, generally Precambrian to Cretaceous in age, occupy the uplifted blocks. Younger sediments, mostly Tertiary and Quaternary in age, fill the downdropped troughs. Complex folding in the mountains and discontinuous faulting throughout the rift make the geologic structure difficult to interpret. A series of subparallel faults bounds the rift. The discontinuous nature of the graben-forming faults allows a great variety of interpretations and leads to major variations in the width of the rift zone.

Seismicity of the rift area may be evaluated from historic earthquake reports, instrumental data from earthquakes and microearthquakes, and faulting of geologically recent geomorphic features. These methods agree in general that the area of greatest seismic activity is near Socorro. The predicted maximum shock in a 100-year period varies widely with the data used to evaluate seismic risk. Historic records show the highest level, a magnitude 6 shock; instrumental data from microseisms show the lowest level, a magnitude 4.6 shock.

5.1.2 Background

This report integrates reports published on the geology, hydrology, climatology, and seismology of the Rio Grande Rift Zone in New Mexico. It provides the background for preparation of an assessment report on the possible environmental impact of geothermal development in the Rio Grande Rift. The environmental impacts that will be considered include ground water pollution, seismic activity and subsidence potential.

Hundreds, perhaps thousands, of publications deal with some aspect of the Rio Grande Rift. Numerous government organizations, schools, groups and individuals have published documents concerning the area. For instance, the New Mexico Geological Society began publishing its annual field conference guidebook in 1950, and of the 27 guidebooks published, 15 contain articles pertinent to the Rio Grande Rift. The New Mexico Bureau of Mines and Mineral Resources lists over a hundred publications that cover parts of the area. Sources have had to be chosen, read and integrated in this report from among the hundreds available, and that choice was often arbitrary. Most sources used are readily available and cover a large area.

Definition of the rift caused another problem in sorting data for use in this report. Most documents deal with the Rio Grande Valley or the Rio Grande drainage basin. Each publication makes its own definition of the area included. The Rio Grande Valley, as we use the term here, refers to the stream valley of the Rio Grande itself and includes the drainage area that contributes direct surface runoff (Fig. 5.1). The Rio Grande drainage basin, as we use the term, includes all the surface area that ultimately contributes to the flow of the Rio Grande. The Rio Grande drainage basin, under this definition, begins in Colorado and ends in Texas and Mexico where the river enters the Gulf of Mexico. Several drainage sub-basins and basins with interior drainage lie within this large Rio Grande

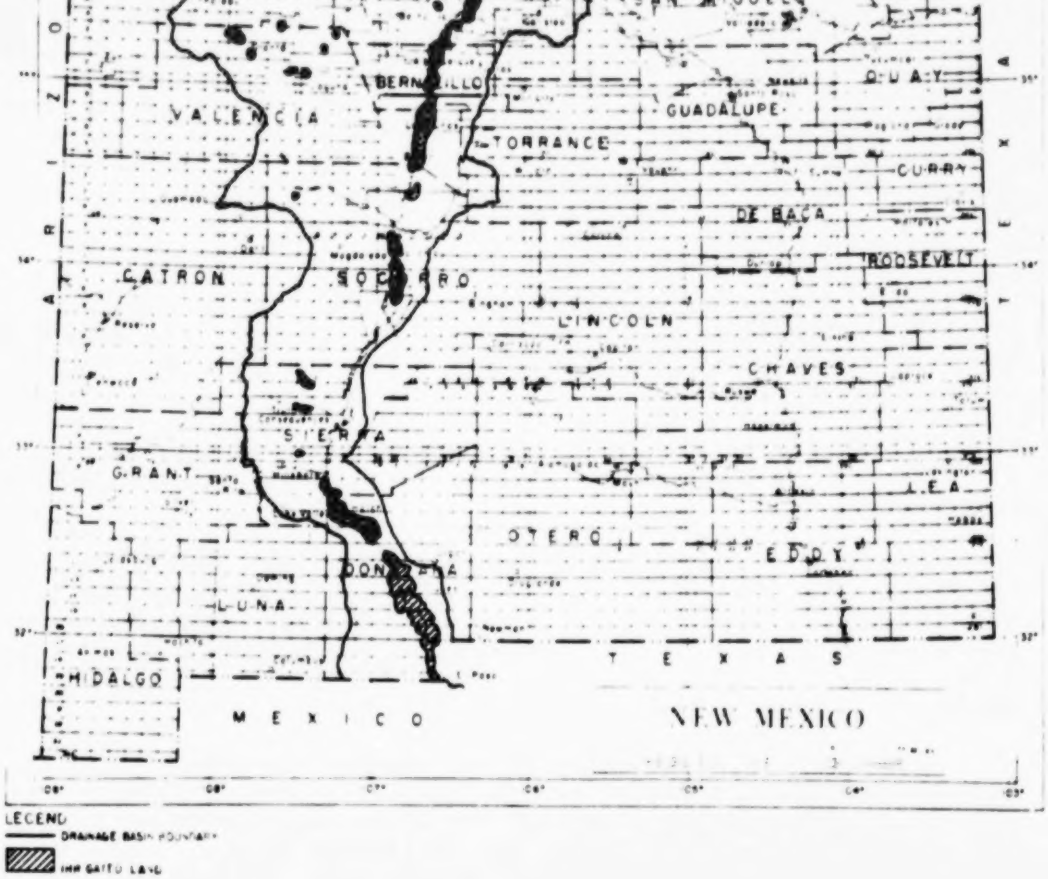
COLORADO
OKLAHOMA
SAN JUAN
RIO ARRIBA
TAOS
COLFAX
UNION
MORA
HARDING
MC KINLEY
SANDOVAL
SANTA FE
SAN MIGUEL
ARIZONA
TEXAS
BERNALILLO
QUAY
VALENCIA
GUADALUPE
TORRANCE
CURRY
DE BACA
ROOSEVELT
CATRON
SOCORRO
LINCOLN
CHAVES
SIERRA
GRANT
LEA
OTERO
EDDY
DONA ANA
LUNA
HIDALGO
MEXICO
NEW MEXICO
LEGEND
DRAINAGE BASIN BOUNDARY
IRRIGATED LAND

Figure 5.1 Map of Rio Grande Valley and area of direct surface runoff. (Anonymous, 1967)

Basin (Figs. 5.2 and 5.3). Some of the basins with interior drainage discharge ground water to the Rio Grande.

Geologic structures bound the Rio Grande Rift area on the east and west sides. The structural geology is complex. The rift may be interpreted as a narrow graben running the length of New Mexico in about the same position as the Rio Grande Valley (Fig. 5.4), or the Rio Grande Rift may be interpreted as a broad series of related and subparallel troughs and horsts.

For this report, the Rio Grande Rift is defined as the part of New Mexico that appears to be physically bounded by a series of related subparallel faults and cross faults that form a structural basin now occupied by the Rio Grande (Plate 5.1). Because this definition is based on geologic structure, it excludes some areas, such as the Pecos River Basin, which lie within the Rio Grande drainage basin. Likewise, it includes some areas west of the Rio Grande that lie outside the area of direct surface runoff, such as the San Augustin Plains. By considering only the area in New Mexico, this report also excludes both the structural and hydrologic extensions of the Rio Grande Rift Valley in Colorado, Texas and Mexico.

5.1.3 Climatology

Spanish colonization of New Mexico began in the sixteenth century and sporadic collection of climatologic data began almost immediately. Although systematic data collection began about 1850, few stations have continuous records.

Table 5.1 and Figures 5.5 and 5.6 show average temperatures and average precipitation values for several places in the Rio Grande Rift.

The Rio Grande Rift extends roughly 645 km (400 mi) in New Mexico, covering 5° of latitude and over 2,750 m (9,000 ft) of altitude. These extremes combine to produce climates ranging from low desert to alpine conditions. Vegetation types vary with altitude, latitude, and precipitation (Figs. 5.7, and 5.8).

Generally, the incised river valley has lower precipitation and higher evaporation than the more mountainous regions bordering it. The northern end of the rift has higher precipitation and lower evaporation than the southern part. Average annual precipitation ranges from 180 mm (7 in) in the far south and incised Rio Grande Valley to about 810 mm (32 in) in the high northern mountains. Water loss by evapotranspiration increases southward along the rift zone. Average annual evaporation ranges from about 1,020 mm (40 in) in the north to about 1,780 mm (70 in) in the southern valley. Table 5.3 shows data from several stations measuring evaporation in the Rio Grande Rift.

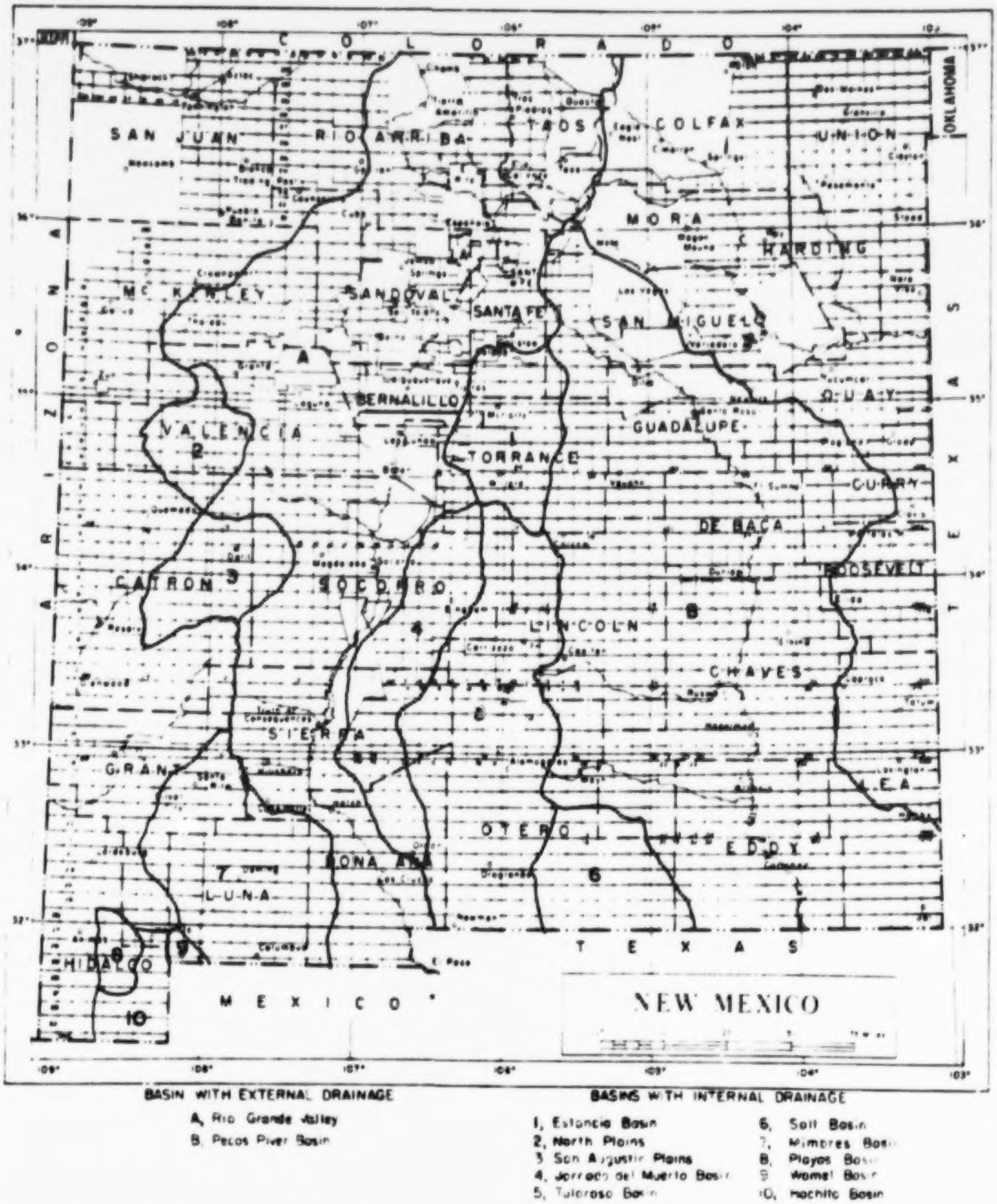
COLORADO
OKLAHOMA
ARIZONA
TEXAS
MEXICO
NEW MEXICO
SAN JUAN
RIO ARRIBA
TAOS
COLFAX
UNION
MORA
HARDING
McKINLEY
SANDOVAL
SANTA FE
SAN MIGUEL
BERNALILLO
VALENCIA
QUAY
GUADALUPE
TORRANCE
CURRY
DE BACA
CATRON
SOCORRO
ROOSEVELT
LINCOLN
CHAVES
SIERRA
GRANT
LEA
OTERO
EDDY
DONA ANA
LUNA
HIDALGO
A
B
1
2
3
4
5
6
7
8
9
10
BASIN WITH EXTERNAL DRAINAGE
A, Rio Grande Valley
B, Pecos River Basin
BASINS WITH INTERNAL DRAINAGE
1, Estancia Basin
2, North Plains
3 San Augustin Plains
4, Jornada del Muerto Basin
5, Tularosa Basin
6, Salt Basin
7, Mimbres Basin
8, Playas Basin
9 Wamel Basin
10, Hachita Basin

Figure 5.2 Rio Grande drainage basin in New Mexico. (Anonymous, 1967)

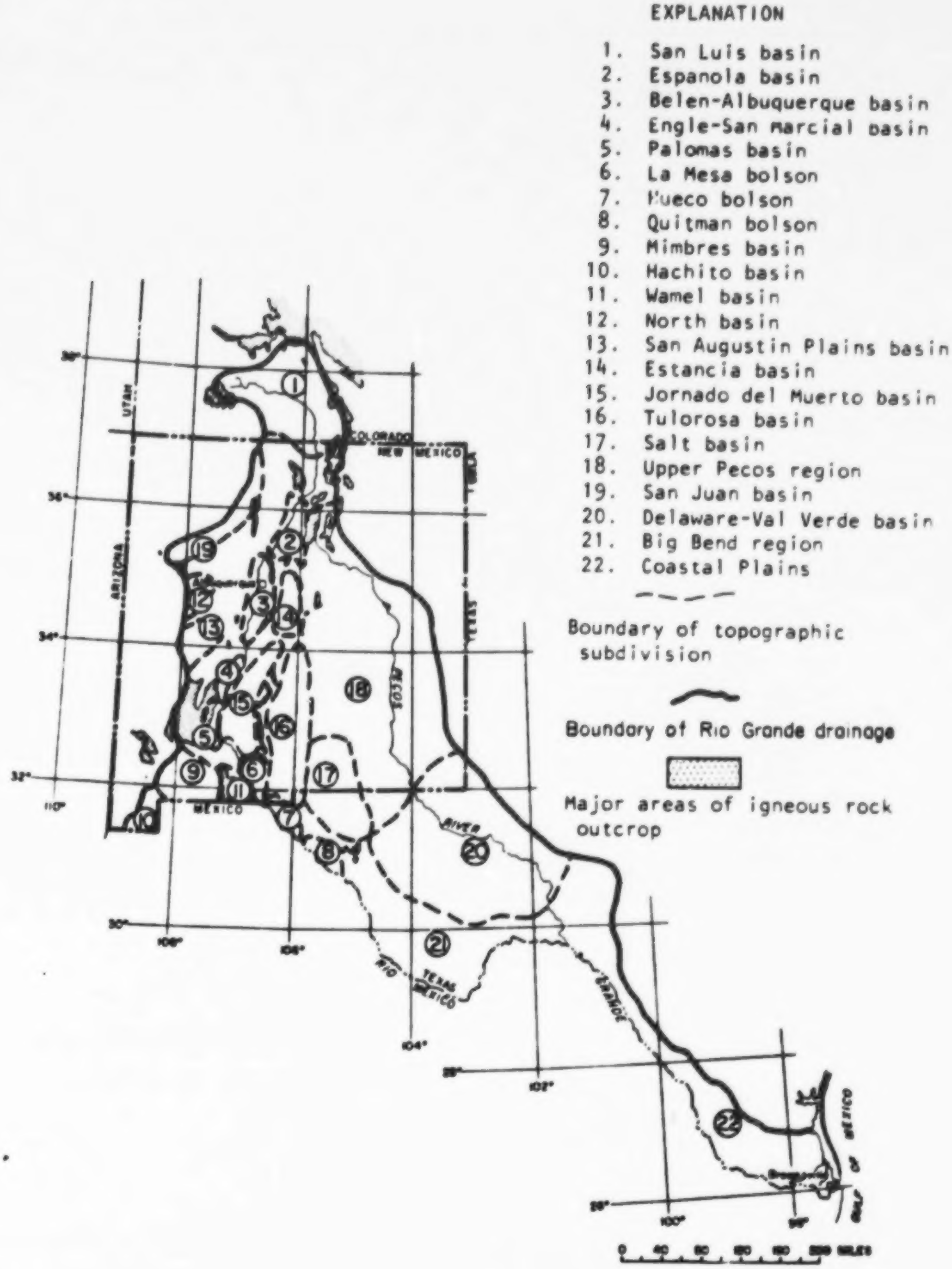
EXPLANATION
1. San Luis basin
2. Espanola basin
3. Belen-Albuquerque basin
4. Engle-San marcial basin
5. Palomas basin
6. La Mesa bolson
7. Hueco bolson
8. Quitman bolson
9. Mimbres basin
10. Hachito basin
11. Wamel basin
12. North basin
13. San Augustin Plains basin
14. Estancia basin
15. Jornado del Muerto basin
16. Tulorosa basin
17. Salt basin
18. Upper Pecos region
19. San Juan basin
20. Delaware-Val Verde basin
21. Big Bend region
22. Coastal Plains
Boundary of topographic subdivision
Boundary of Rio Grande drainage
Major areas of igneous rock outcrop
UTAH
ARIZONA
COLORADO
NEW MEXICO
TEXAS
MEXICO
PECOS
RIVER
RIO
TEXAS
MEXICO
GRANDE
GULF OF MEXICO
38°
36°
34°
32°
30°
28°
26°
110°
108°
106°
104°
102°
100°
98°
0 40 80 120 160 200 MILES

Figure 5.3 Major topographic subdivisions of Rio Grande Rift. (Kelly, et al., 1970)

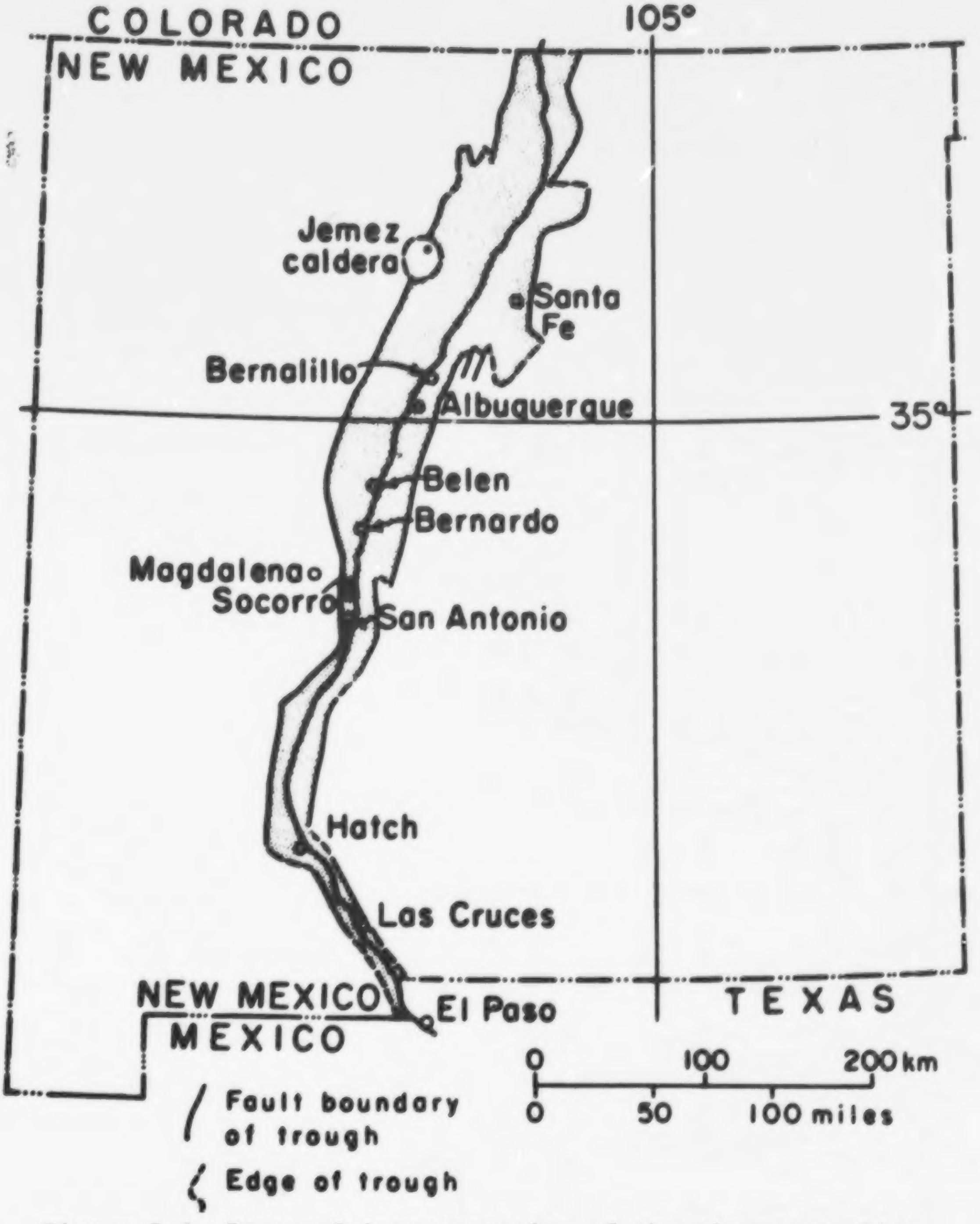
COLORADO
NEW MEXICO
105°
35°
Jemez caldera
Santa Fe
Bernalillo
Albuquerque
Belen
Bernardo
Magdalena
Socorro
San Antonio
Hatch
Las Cruces
NEW MEXICO
MEXICO
El Paso
TEXAS
0
100
200 km
0
50
100 miles
Fault boundary of trough
Edge of trough

Figure 5.4 "Narrow" interpretation of the Rio Grande Rift Zone. (Sanford, et al., 1972)

TABLE 5.1 MEAN TEMPERATURE AND PRECIPITATION AT PLACES IN THE RIO GRANDE BASIN, NEW MEXICO (Anonymous, 1967)

Station		January		February		March		April		May		June		July		August		September		October		November		December		Annual	
		Temp. (°F)	Prec. (inches)	Temp.	Prec.	Temp.	Prec.	Temp.	Prec.	Temp.	Prec.	Temp.	Prec.	Temp.	Prec.	Temp.	Prec.	Temp.	Prec.	Temp.	Prec.	Temp.	Prec.	Temp.	Prec.	Temp.	Prec.
Bandelier NM	Northern Mountains	-	0.78	-	0.80	-	0.92	-	0.87	-	1.40	-	0.83	-	2.47	-	2.40	-	1.84	-	1.17	-	0.80	-	0.90	-	15.47
Bateman Ranch		-	1.78	-	1.90	-	2.14	-	1.47	-	1.80	-	1.23	-	2.37	-	2.98	-	2.30	-	1.70	-	1.16	-	1.73	-	[illegible]
Cerro		-	.59	-	.62	-	.61	-	1.00	-	1.36	-	.86	-	1.60	-	1.98	-	1.56	-	1.09	-	.50	-	.62	-	12.38
Chama		-	1.67	-	1.09	-	1.32	-	1.30	-	1.40	-	.95	-	1.65	-	2.21	-	2.03	-	1.42	-	.93	-	1.77	-	[illegible]
Gavilan		-	1.06	-	1.33	-	1.21	-	1.18	-	1.17	-	.92	-	1.97	-	2.47	-	1.91	-	1.16	-	.90	-	1.33	-	16.60
Jemez Springs		33.3	.86	36.3	.89	41.8	1.06	50.7	1.01	58.0	1.41	66.2	1.44	70.6	2.56	69.2	3.12	63.7	2.28	53.0	1.40	42.0	.81	34.7	.85	51.6	17.69
Los Alamos		-	.78	-	.65	-	.86	-	.95	-	1.43	-	1.31	-	2.82	-	3.85	-	2.09	-	1.36	-	.63	-	.86	-	17.59
Panchuela RS		-	.97	-	1.10	-	1.23	-	1.18	-	1.40	-	.99	-	2.02	-	2.10	-	1.40	-	1.26	-	.83	-	.83	-	15.31
Red River		19.3	1.01	22.2	1.14	28.2	1.42	37.8	1.63	45.2	1.78	53.3	1.28	58.2	2.61	57.4	3.06	51.6	1.63	42.4	1.30	30.3	.97	21.7	.93	38.0	18.76
Regina		24.3	1.02	28.2	1.32	34.8	1.23	44.0	1.36	52.0	1.13	61.0	.79	66.6	2.31	64.9	2.50	58.2	1.60	47.5	1.20	36.7	.83	28.9	1.30	46.3	16.59
Santa Fe		29.8	.66	33.0	.67	39.2	.72	48.3	.83	56.7	1.43	66.1	1.15	70.4	2.26	68.8	2.21	62.8	1.50	52.2	.87	39.2	.62	31.8	.67	49.9	13.79
Taos		-	.74	-	.73	-	.78	-	.94	-	1.18	-	.78	-	1.52	-	1.64	-	1.15	-	1.01	-	.72	-	.58	-	11.77
Tierra Amarilla 4-NNE		-	1.32	-	1.09	-	1.04	-	1.12	-	1.10	-	.99	-	1.87	-	2.26	-	1.84	-	1.07	-	.90	-	1.28	-	[illegible]
Tres Piedras		-	.91	-	.92	-	.80	-	.81	-	1.11	-	.68	-	1.89	-	2.29	-	1.33	-	.89	-	.59	-	.87	-	13.09
Truchas		-	.83	-	1.14	-	.94	-	1.10	-	1.20	-	.81	-	1.93	-	2.32	-	1.67	-	1.14	-	.83	-	.86	-	14.77
Bluewater	(Southwestern Mountains)	27.2	.42	31.2	.35	38.1	.42	46.9	.46	55.3	.50	64.1	.63	69.2	1.73	66.8	2.33	59.6	1.19	48.3	.47	36.1	.46	28.3	.46	47.8	[illegible]
Magdalena		-	.39	-	.41	-	.39	-	.46	-	.55	-	.87	-	2.21	-	2.55	-	2.09	-	.86	-	.33	-	.50	-	11.60
Albuquerque WB-AP	Central Valley	35.7	.30	39.5	.39	46.0	.44	55.5	.53	65.3	.57	74.9	.72	79.0	1.43	76.9	1.30	69.9	1.03	58.2	.84	44.0	.42	36.0	.39	56.6	8.40
Bosque del Apache		-	.41	-	.43	-	.33	-	.27	-	.39	-	.80	-	1.04	-	1.51	-	1.34	-	.76	-	.31	-	.35	-	7.77
Elephant Butte Dam		41.0	.40	46.3	.45	52.3	.30	60.9	.32	69.2	.37	78.1	.73	80.3	1.47	78.6	1.82	73.0	1.36	63.0	.82	49.7	.50	42.7	.43	61.3	9.40
Socorro		37.3	.46	43.0	.47	48.7	.26	58.7	.43	66.7	.77	73.7	.66	79.2	1.33	77.3	1.35	70.7	1.46	59.5	.83	43.9	.34	38.6	.44	58.3	8.76
Mountainair (Central Highlands)		-	.84	-	.60	-	.85	-	.66	-	.83	-	.97	-	2.67	-	2.47	-	1.32	-	.87	-	.38	-	.91	-	13.77
Agricultural College	Southern Desert	40.3	.47	43.3	.44	50.9	.26	59.3	.19	67.1	.32	75.9	.57	79.4	1.31	77.7	1.37	71.3	1.28	61.0	.71	47.6	.31	41.9	.50	59.8	7.93
Hatch		-	.48	-	.42	-	.25	-	.30	-	.31	-	.58	-	1.59	-	1.62	-	1.40	-	.81	-	.23	-	.38	-	8.43
Hillsboro		-	.66	-	.58	-	.44	-	.34	-	.44	-	.72	-	1.80	-	1.89	-	1.93	-	.91	-	.32	-	.66	-	10.73

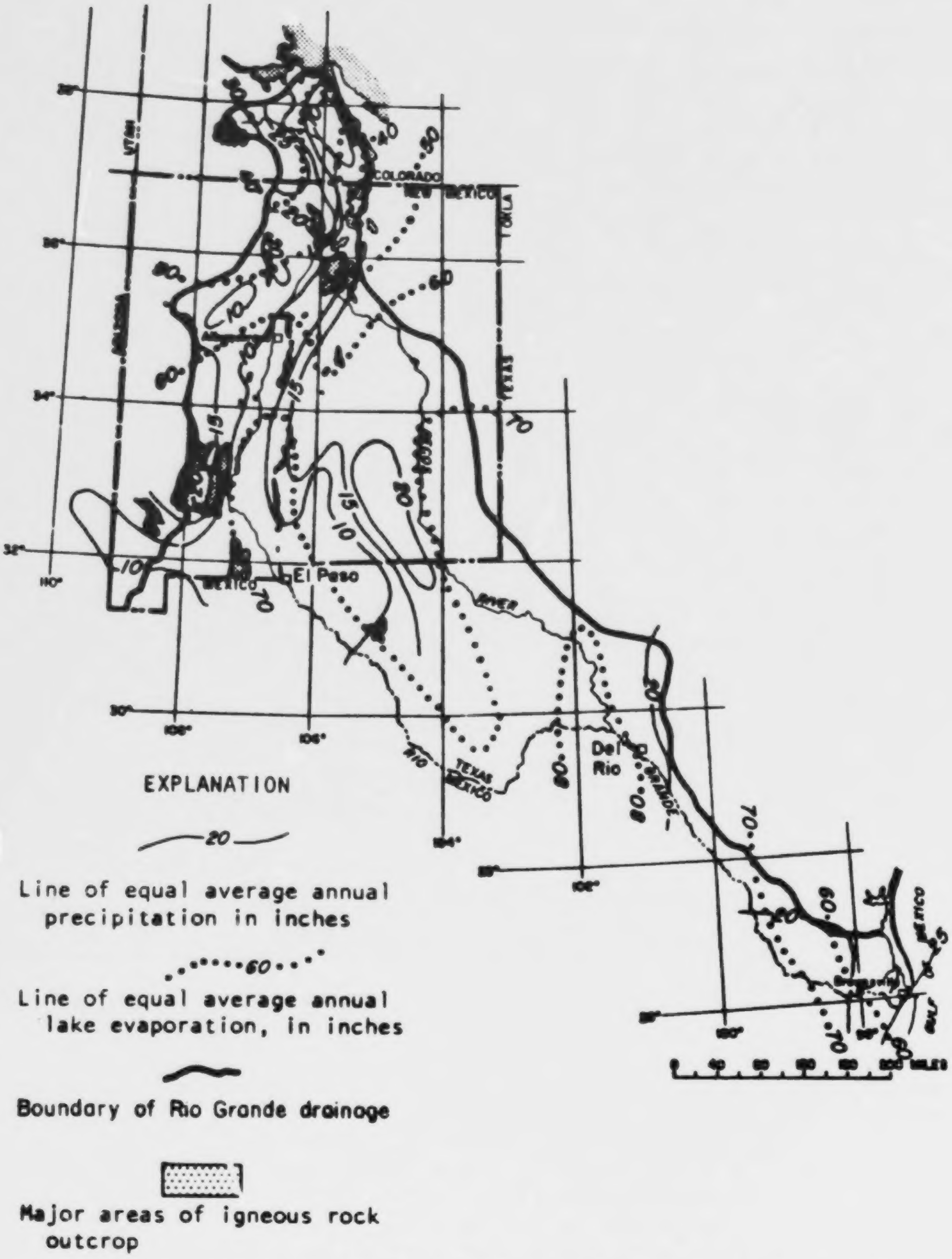
COLORADO
NEW MEXICO
UTAH
ARIZONA
OKLA
TEXAS
El Paso
MEXICO
RIVER
Del Rio
RIO
TEXAS
MEXICO
GULF OF MEXICO
Brownsville
32°
30°
34°
110°
106°
104°
102°
100°
98°
10
15
20
50
60
70
80
0 40 80 120 160 200 MILES
EXPLANATION
20
Line of equal average annual precipitation in inches
60
Line of equal average annual lake evaporation, in inches
Boundary of Rio Grande drainage
Major areas of igneous rock outcrop

Figure 5.5 Average annual precipitation and lake surface evaporation. (Kelly, et al., 1970)

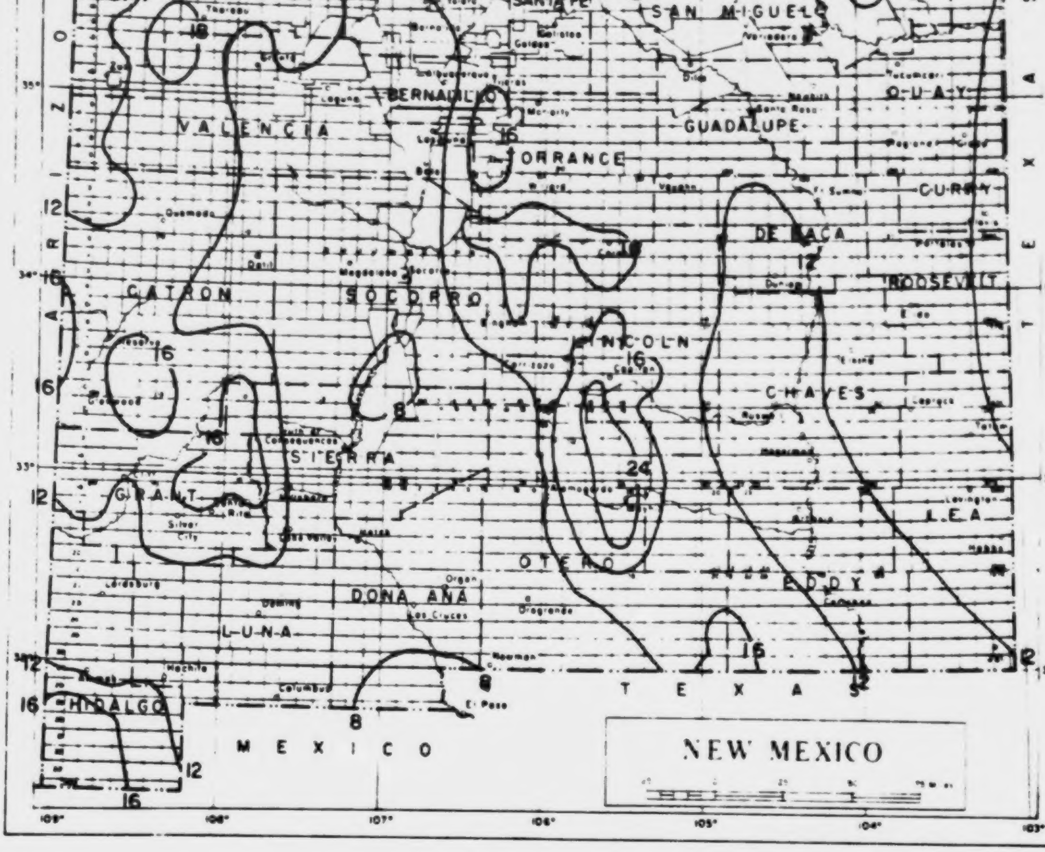
NEW MEXICO
C O L O R A D O
OKLAHOMA
T E X A S
M E X I C O
A R I Z O N A
SAN JUAN
RIO ARRIBA
TAOS
COLFAX
UNION
MORA
HARDING
McKINLEY
SANDOVAL
SANTA FE
SAN MIGUEL
BERNALILLO
VALENCIA
GUADALUPE
QUAY
TORRANCE
CURRY
DE BACA
ROOSEVELT
CATRON
SOCORRO
LINCOLN
CHAVES
SIERRA
GRANT
LEA
OTERO
EDDY
DONA ANA
LUNA
HIDALGO
8
12
16
20
24
30

Figure 5.6 Normal annual precipitation in New Mexico. (Jetton and Kirby, 1970)

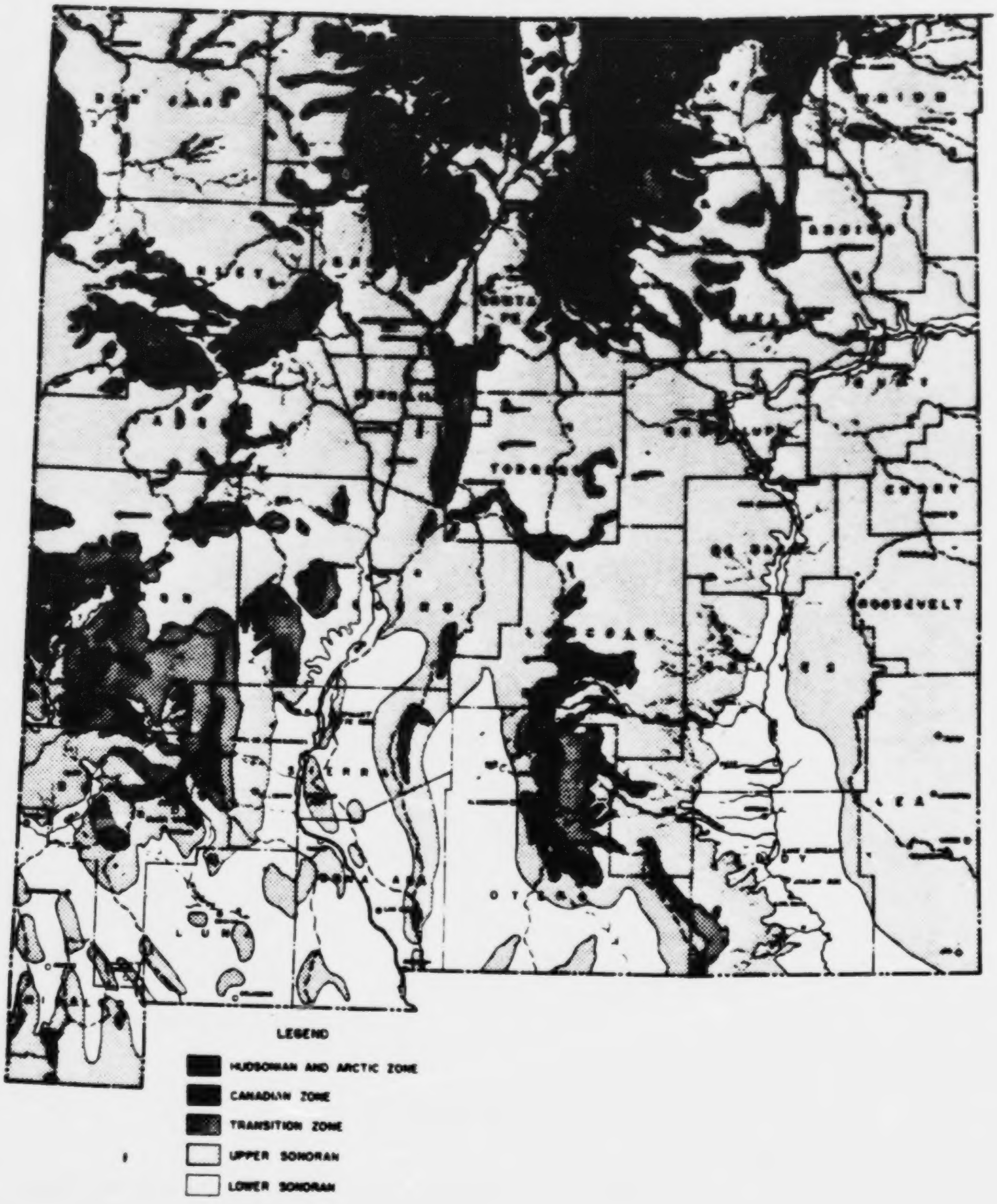
ROOSEVELT
LEGEND
HUDSONIAN AND ARCTIC ZONE
CANADIAN ZONE
TRANSITION ZONE
UPPER SONORAN
LOWER SONORAN

Figure 5.7 Life and crop zones in New Mexico. (Anonymous, 1967)

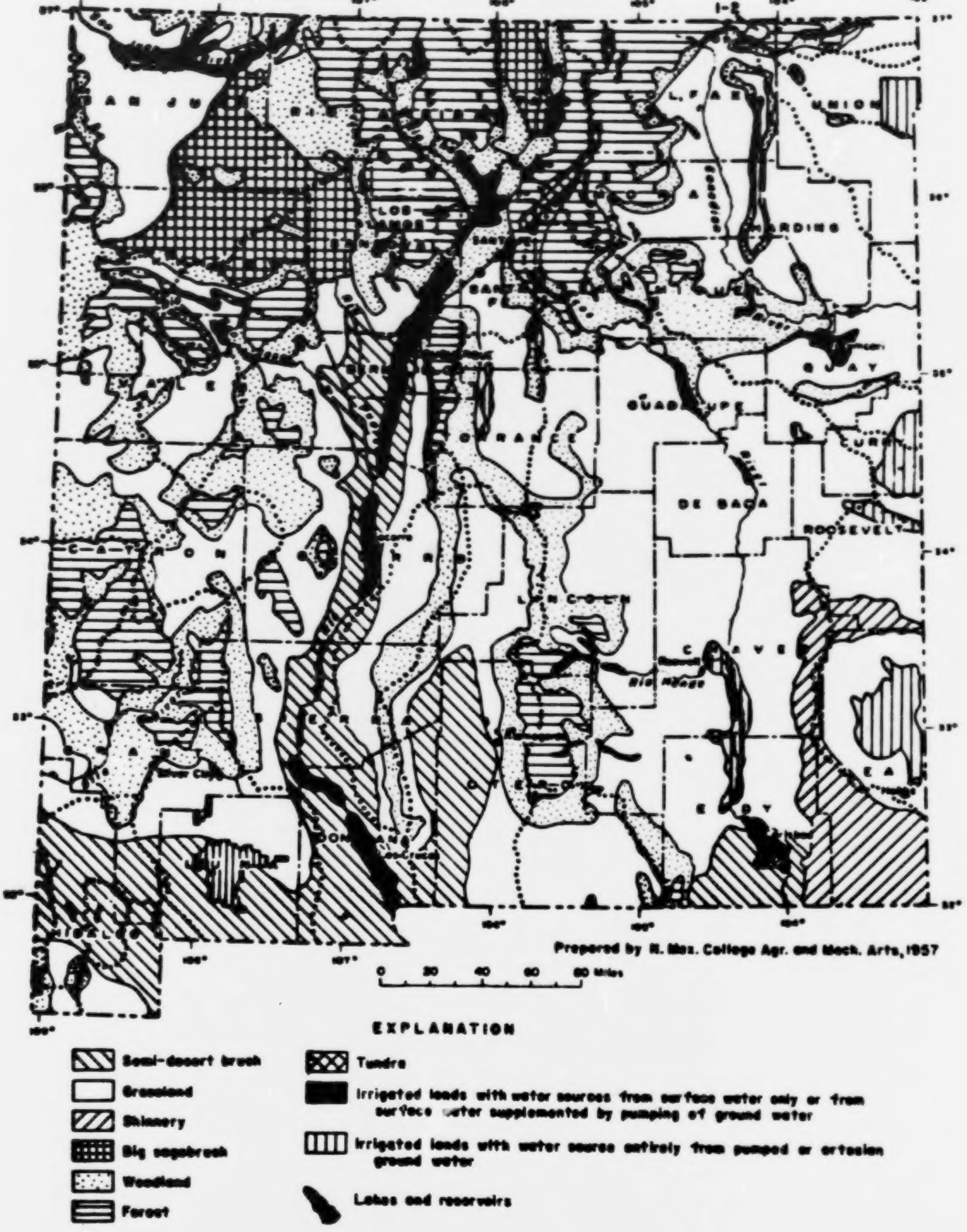
UNION
HARDING
LOS ALAMOS
QUAY
GUADALUPE
TORRANCE
DE BACA
ROOSEVELT
LINCOLN
CHAVES
EDDY
LEA
Rio Hondo
Prepared by N. Mex. College Agr. and Mech. Arts, 1957
0 20 40 60 80 Miles
EXPLANATION
Semi-desert brush
Grassland
Shinnery
Big sagebrush
Woodland
Forest
Tundra
Irrigated lands with water sources from surface water only or from surface water supplemented by pumping of ground water
Irrigated lands with water source entirely from pumped or artesian ground water
Lakes and reservoirs

Figure 5.8 Vegetative-type map of New Mexico. (Anonymous, 1967)

Average annual temperature in rift rises from 4°C (40°F) in the northern mountains to 16°C (60°F) in the southern valleys.

5.2 GEOTHERMAL CHARACTERISTICS

The Rio Grande Rift has attracted attention as a prospective geothermal region, primarily because the Union Oil Company has completed several steam wells in the Valles Caldera.

In addition to the caldera, other geologic phenomena associated with the rift suggest that geothermal resources may be developed elsewhere within it. These phenomena include:

1) a high heat flow,
2) a distribution of warm and hot ground water,
3) a distribution of late Tertiary volcanic rocks,
4) a thin crust, and
5) a possible magma body near Socorro.

The heat flow ranges from 1.5 to more than 2.5 HFU. Perhaps even more important, the heat flow is more than 2.0 HFU over a broad band along the western edge of the rift (Fig. 5.9).

A compilation map (Summers, 1965) showed that thermal water occurrences are concentrated in the rift.

Late Tertiary rocks, including those of the caldera, occur throughout the rift. The associated volcanic activity appears to have begun during Oligocene time and has continued intermittently. Numerous cinder cones mark the landscape. The most recent events are local basalt flows.

Sanford and his associates at the New Mexico Institute of Mining and Technology at Socorro have been monitoring microearthquakes for more than a decade. Recent interpretations of this data suggest that a magma body exists within the rift near Socorro (Sanford, et al., 1976a and b; Shuleski, et al., 1977).

Gravity studies of Reddy (1966), Bridwell (1976) and Cordell (1976) suggest that the crust beneath the rift may be significantly thinner than average. Woodward (1975) has estimated that the crustal extension of the rift near Albuquerque averages about 0.25 mm/yr (0.01 in/yr). He believes that below depths of 10.0 to 15.0 km (6.2 to 9.3 mi) the crust is undergoing plastic deformation.

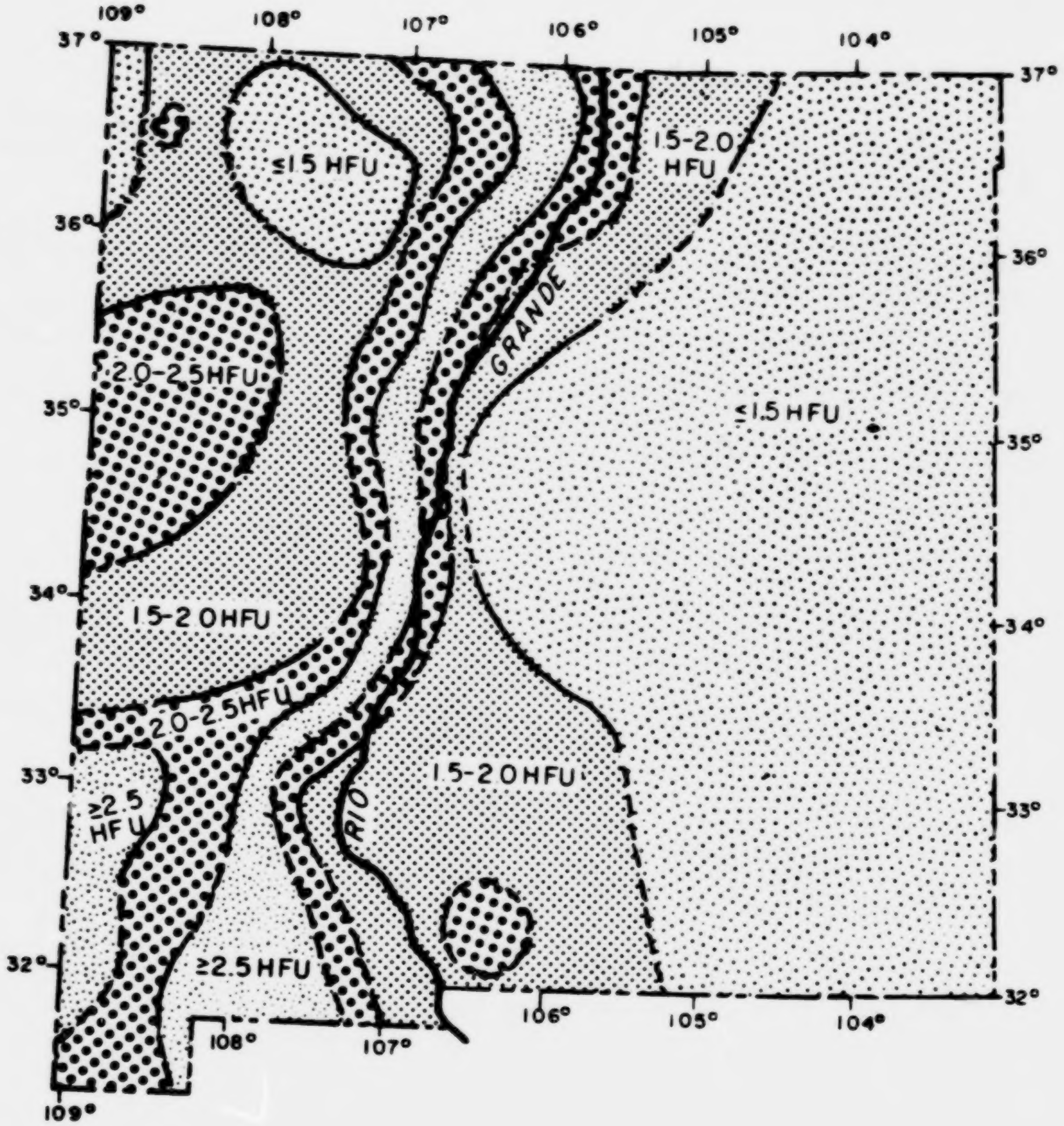
109°
108°
107°
106°
105°
104°
37°
36°
35°
34°
33°
32°
≤1.5 HFU
1.5-2.0 HFU
2.0-2.5 HFU
1.5-2.0 HFU
2.0-2.5 HFU
≥2.5 HFU
≥2.5 HFU
GRANDE
RIO
≤1.5 HFU
1.5-2.0 HFU
108°
107°
106°
105°
104°
109°

Figure 5.9 Heat flow in New Mexico. (Reiter, et al., 1974)

For geothermal purposes Stone and Mizell (1977) subdivided the rift (Fig. 5.10) into the following geothermal regions:

1) San Luis Basin,
2) Jemez Mountains,
3) Albuquerque Basin,
4) Socorro-La Jencia Basin,
5) Truth or Consequences-Rincon Basin
6) Southern Jornada del Muerto-Mesilla Basin and
7) Tularosa Basin.

Detailed discussion of each of these regions is beyond the scope of this report. Therefore, only major items relevant to geothermal development of each area are mentioned below.

San Luis Basin--
The San Luis Basin is actually the New Mexico portion of a larger basin by that name that spans the Colorado-New Mexico border. It consists of a complexly faulted graben located at the northern extremity of the New Mexico portion of the Rio Grande Rift in the Rocky Mountains Province (Fig. 5.10). It covers western Taos County and part of eastern Rio Arriba County. It is bounded on the east by a major fault system at the edge of the Sangre de Cristo Mountains and on the west by the Ojo Caliente Uplift.

Leasing within the San Luis Basin has been confined to state geothermal resource lands north of Ojo Caliente. No drilling is known in this area.

Jemez Mountains--
The Jemez Mountains lie within the Rocky Mountains Province west of the Rio Grande Rift. They cover northern Sandoval County and most of Los Alamos County. Numerous hot springs occur within this target area. Four wells have also yielded thermal waters: the two Los Alamos Scientific Laboratory (LASL), Fenton Hill or Granite Test wells, the site of the LASL Dry-hot-rock experiment and two Kaseman oil wells. Valles Caldera, the remnant of a large volcano which is the dominant feature of the landscape, is also evidence of intense geothermal activity in this area about 40,000 years ago.

Leasing and drilling activity in the Jemez Mountains target area is centered around the Baca Location No. 1 KGRA and the San Ysidro KGRA. Presently, only state geothermal resource lands

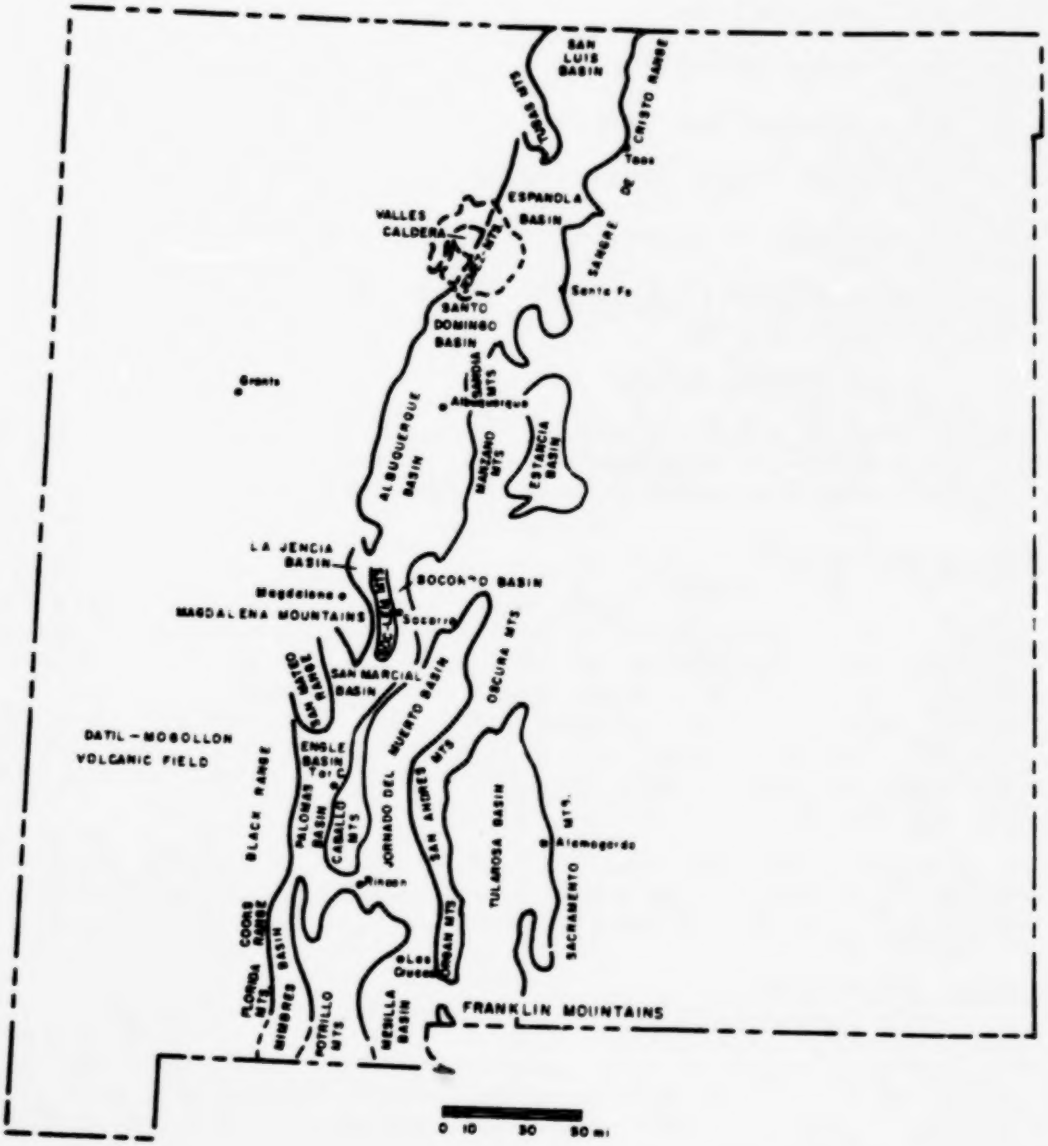
SAN LUIS BASIN
TUSAS MTS
SANGRE DE CRISTO RANGE
Taos
ESPANOLA BASIN
VALLES CALDERA
MTS
Santa Fe
SANTO DOMINGO BASIN
SANDIA MTS
Grants
Albuquerque
ALBUQUERQUE BASIN
MANZANO MTS
ESTANCIA BASIN
LA JENCIA BASIN
SOCORRO BASIN
Magdalena
MAGDALENA MOUNTAINS
Socorro
OSCURA MTS
SAN MATEO RANGE
SAN MARCIAL BASIN
JORNADO DEL MUERTO BASIN
DATIL – MOGOLLON VOLCANIC FIELD
BLACK RANGE
ENGLE BASIN
T or C
PALOMAS BASIN
CABALLO MTS
SAN ANDRES MTS
TULAROSA BASIN
SACRAMENTO MTS.
Alamogordo
Rincon
COOKS RANGE
FLORIDA MTS
MIMBRES BASIN
POTRILLO MTS
MESILLA BASIN
Las Cruces
ORGAN MTS
FRANKLIN MOUNTAINS
0 10 30 50 mi

Figure 5.10 Subdivisions of the Rio Grande Rift.
(Chapin, 1971)

have been leased but Federal lands are available for leasing. Drilling has been confined to private and fee lands. Union Oil Company terminated its recent drilling program in 1975; Sun Oil Company has just begun drilling; Phillips Petroleum Company and Thermal Power Company both have drilled wells in this region.

Albuquerque Basin--

The Albuquerque Basin is the largest structural basin within the Rio Grande Rift. It lies fully within the Basin and Range Province covering parts of Valencia and Bernalillo Counties. Aside from the Quaternary basalt flows capping mesas along the Rio Grande near Albuquerque, the main evidence of geothermal activity in this part of the rift has come from three wells which reportedly yield thermal water.

No Federal or state geothermal resource lands have been leased in the Albuquerque Basin. Drilling activity is associated only with private or fee lands.

Socorro-La Jencia Basin--

This area consists of two semiparallel basins separated by the Socorro-Lemitar-Chupadera Mountains. These basins may actually be remnants of a larger single basin split by a northwest trending intrarlift horst (Chapin, 1971). The Socorro-La Jencia Basin straddles the boundary between the Basin and Range Province and the Colorado Plateau Province. Woodward, et al. (1975) would place the western edge of the Basin and Range Province and the Rio Grande Rift farther west than shown in Figure 5.10.

Thermal waters discharge at three springs in this area; infiltration galleries have been constructed at each. Hot water has also been encountered in a well in Blue Canyon. In addition to these discharges of thermal water, Tertiary volcanic rocks occur in the vicinity.

In anticipation of the designation of the Socorro Peak KGRA, considerable state lands have been leased. No drilling is known in this target area.

Truth or Consequences-Rincon Basin--

This area is situated at the western edge of the Basin and Range Province and includes the portion of the Rio Grande Rift extending southward from Truth or Consequences in the Engle Basin, through the eastern part of the Palomas Basin to Rincon in the central part of the Jornada del Muerto Basin. The area lies within Sierra County.

Thermal springs in the area include those within the town of Truth or Consequences (formerly called Hot Springs) and Derry Warm Springs. Two wells in the area also yield thermal waters (Summers, 1976).

The Truth or Consequences-Rincon Basin has been the focus of considerable leasing of state geothermal resource lands. No drilling for geothermal resources is known for this area.

Southern Jornada Del Muerto-Mesilla Basin--
This area lies within the Basin and Range Province and coincides with the southernmost extension of the Rio Grande Rift. It also lies within Dona Ana County.

Thermal waters at Radium Springs are obtained from one well. Other wells in the area yield thermal waters according to Summers (1976). The area of the Kilbourne Hole KGRA contains basalt cinder cones and extensive basalt flows of late Tertiary age.

Both Federal and state geothermal resource lands have been leased in the northern part of this area near the Radium Spring KGRA.

In the southern part of the area, however, in the vicinity of the Kilbourne Hole KGRA, only Federal lands have been leased to date. No drilling is known in this area.

Tularosa Basin--
The only occurrence of thermal water in the Tularosa Basin is at the Garton Well, south of White Sands National Monument. In addition to this occurrence of thermal water, the young (about 10,000 years old) and extensive lava flow on the basin floor near Carrizozo, together with its volcanic source to the northeast, attest to the considerable geothermal activity here in very recent geologic time.

5.3 GEOLOGY

The Rio Grande flows through a structurally and physiographically low valley that constitutes the Rio Grande Depression. A major continental rift, the depression extends southward over 645 km (400 mi) from southern Colorado, through the length of New Mexico, to near El Paso, Texas (Kelley, 1952). The rift contains the highest mountains and deepest intramontane basins of the territory it traverses. Altitudes in the Rio Grande Rift range from 1,100 m (3,600 ft) in the El Paso Valley to 4,010 m (13,160 ft) on top of Mount Wheeler. Altitudes along the floor of the Rio Grande Valley range from 1,100 m (3,600 ft) in El Paso Valley at the Texas state line to 2,270 m (7,440 ft) in San Luis Valley at the Colorado state line.

In New Mexico, four geological provinces with very different characteristics exist in juxtaposition with the Rio Grande Rift. The northern part of the rift bisects the high ranges of the southern Rocky Mountains and has intermittent contact with the Colorado Plateau to the west. The southern part of the rift is bordered on the west by the Colorado Plateau and the Basin and Range Province. The Great Plains lie to the east of the mountains bordering the rift (Kelley, 1954).

Plate 5.1 shows the surface geology of the Rio Grande Rift area. Countless faults criss-cross the area, and ages of exposed rocks range from Precambrian to Recent. Exposures in the northern mountains show Mississippian and Pennsylvanian sedimentary strata overlying the Precambrian rocks. A few rocks of questionable Devonian age crop out in the Sangre de Cristo Mountains, but no older Paleozoic rocks have been found. In the south, Cambrian, Ordovician, Silurian, Devonian and Mississippian strata all crop out between the Precambrian and Pennsylvanian. Table 5.2 gives a generalized stratigraphic section.

Faulting in the Rio Grande Rift is discontinuous. No single huge fault bounds the Rio Grande Rift on either side. Instead, a series of subparallel faults combine to create linear features that we may regard as bounding the rift area. An individual fault may be traced for miles along its strike until the throw diminishes and that fault dies out. Nearby faults in the system take up the movement and the overriding pattern of blocks and troughs continues even though individual faults do not.

Normal faults commonly bound rift zones, but thrusts and high-angle reverse faults form the apparent limits of some parts of the Rio Grande Rift area. Most of the reverse faults occur along the northeastern rift boundary in the Sangre de Cristo Mountains.

With discontinuous faulting in both uplifted and downdropped parts of the rift system, some areas can be interpreted as horsts within a broad structural trough or as uplifted blocks along the rift boundary. Similarly, some structural depressions may be treated as separate grabens flanking the main rift graben, or as parts of the main rift graben which lie beside horsts in that depression.

The complex structure and wide range of geologic formations found in the Rio Grande Rift prevent any simple, brief characterization of the area from being universally accurate.

The uplifted blocks expose Precambrian rocks in several places. Cambrian to early Miocene sedimentary strata lie above the Precambrian rocks. Tertiary and Quaternary volcanics (notably in the Jemez Mountains), intrusive rocks of various ages (mostly Late Cretaceous and Cenozoic) and alluvial deposits round out the geologic assemblage in the uplifted blocks. Steep reverse faults, normal faults and folds complicate the structural picture. In general, the northern ends of uplifted blocks

TABLE 5.2 GENERALIZED STRATIGRAPHIC SECTION IN THE RIO GRANDE BASIN, NEW MEXICO (Anonymous, 1967)

(*Known or probable aquifer, regardless of areal extent or production potential.)

System	Stratigraphic unit	Thickness (feet)	Distribution	Physical properties	Water-bearing characteristics
Quaternary	*Alluvium	Generally thin; less than 100	Perennial stream channels, flood plains, and locally in dry arroyos.	Unconsolidated silt, sand, and gravel.	Recharged from streamflow; generally yields small to moderate quantities of water to wells, may yield large quantities locally.
	*Pediment, terrace, and bajada deposits	May be as much as 200	Along streams and adjacent to mountains. Terraces are prominent along the Santa Fe River.	Generally unconsolidated silt, sand, gravel, and boulders. Gravel and boulder deposits may be lenticular.	Recharged by surface flow and by direct precipitation. Water generally is less abundant than in stream alluvium; may yield small to large quantities of water to wells.
Quaternary and Tertiary	*Volcanic complex	0 to 2,000±	Caps many mesas and occurs as channel deposits, dikes, sills, and interbedded with sedimentary rocks in most of the Rio Grande basin.	Basalt, andesite, rhyolite, latite, pumice, and tuff.	May yield small to large quantities of water to wells; yield depends primarily on fracture permeability and saturated thickness. Generally is not a principal or reliable aquifer.
Quaternary(?) and Tertiary	*Santa Fe Group	0 to 9,000±	Fills the Rio Grande trough.	Clay, silt, sand, and gravel conglomerate, mostly unconsolidated. Contains volcanic material locally.	Yields large quantities of water (as much as 2,500 gpm locally) to deep wells. This is the most extensive and reliable aquifer in the Rio Grande basin.
Tertiary	Galisteo Formation	900 to 4,500	Exposed in valleys near Cerrillos in Santa Fe County; probably underlies Albuquerque area at great depth.	Sandstone, sand, clay, and shale; also may contain some conglomerate.	Low permeability where tested south of Santa Fe. Formation lies at great depth elsewhere in the basin and uneconomical to tap.
	Sedimentary rocks	0 to 6,000±	Sedimentary rocks are present throughout the Rio Grande basin; however, abundant nomenclature prohibits extensive treatment here.	Sandstone, siltstone, shale and some conglomerate.	Generally yield small quantities of water to wells, locally, beds of sandstone might yield moderate quantities; and cumulative yield from many beds of sandstone could be large.
Cretaceous	*Ojo Alamo Sandstone	70 to 200	San Juan (structural) basin.	Coarse-grained, conglomeratic sandstone.	Known to yield 2 to 30 gpm.
	Kirtland Shale and Fruitland Formation	100± to 600±	do.	Shale, sandy shale, siltstone and interbedded sandstone.	Beds of sandstone of low permeability might yield small quantity of water. Generally not considered as an aquifer.
	*Pictured Cliffs Sandstone	25 to 75	do.	Thin- to thick-bedded sandstone with interbedded siltstone and shale.	Low porosity and low permeability. Generally not considered as an aquifer; however, may yield small quantities of water locally.
	Lewis Shale	600 to 1,400	do.	Fissile clay shale with interbedded siltstone, sandstone, and limestone.	Generally does not yield water; thin beds of sandstone in lower part might yield small amount of water, but it probably is saline.
	*Mesaverde Group	250 to 2,500±	Primarily in the San Juan (structural) basin; underlies most of the Rio Grande basin at great depth.	Shale with interbedded sandstone and coal.	Sandstone may yield small to moderate quantities of water; not tapped in many areas because of great depth.
	*Mancos Shale	350 to 2,300	Crops out at edge of San Juan (structural) basin and underlies most of the Rio Grande basin at great depth.	Dark-gray, marine shale, sandstone interbedded near the base locally.	Beds of sandstone might yield small quantities of water.
	*Dakota Sandstone	25 to 345	San Juan (structural) basin and west of Rio Grande basin.	Sandstone with interbedded carbonaceous shale.	Yields small to moderate quantities of water to wells, not tapped at many places because of great depth. Water quality probably best near outcrops.
Jurassic	*Morrison Formation	210 to 910	San Juan (structural) basin; may underlie other parts of the Rio Grande basin, but probably at great depth.	Variegated shale, claystone, and siltstone with interbedded sandstone.	Yields small to moderate quantities of water to wells, depends on saturated thickness of sandstone.
	*Bluff Sandstone	75 to 150	San Juan (structural) basin; this formation or its equivalent may underlie other parts of the Rio Grande basin.	Sandstone.	May yield small quantities of water to wells where saturated. Generally has low permeability.
	Summerville Formation	60 to 130	do.	Sandstone, siltstone, and sandy shale.	Not known to yield water to wells.
	Todilto Limestone	0 to 100	do.	Gypsum and fissile limestone.	Yields very little water to wells. Water generally has high sulfate content.
	*Entrada Sandstone	130 to 250	do.	Cross-bedded sandstone.	May yield small quantities of poor quality water to wells.
Triassic	*Chinle Formation	600 to 1,400	do.	Mudstone and siltstone with interbedded sandstone.	Sandstone may yield small to moderate quantities of generally poor quality water, quality is best close to the outcrops.
Permian	*San Andres Limestone	50 to 1,000	Probably widespread and crops out in or underlies most of Rio Grande basin.	Limestone, sandstone, siltstone, and gypsum.	Fracture or solution channel permeability. May yield large quantities of water to wells. (Yields as much as 3,000 gpm near Grants.) Water quality is variable and is best close to the outcrops.
	*Glorieta Sandstone	70 to 300	San Juan (structural) basin. This formation or its equivalent may underlie other parts of the Rio Grande basin.	Thick-bedded to massive sandstone.	May yield moderate quantities of water to wells.
	*Yeso Formation	[illegible] to 1,100	Widespread; crops out in or underlies most of Rio Grande basin.	Siltstone, sandstone, and shale.	May yield small to moderate quantities of water to wells.
	*Abo Formation	[illegible] to 1,100	do.	Arkosic sandstone, siltstone, and shale.	Generally low permeability, but yield of water to wells may range from small to large.
Permian and Pennsylvanian	*Sangre de Cristo Formation	250 to 1,000	Sangre de Cristo Mountains; may underlie Santa Fe area.	Arkosic shale, sandstone, and conglomerate.	Generally not an aquifer in the basin because depth to water is too great.
	*Magdalena Group	0 to 4,500	Widespread; crops out in or underlies most of the basin.	Limestone, sandstone, and interbedded shale.	May yield small quantities of water to wells.
Mississippian	Lake Valley Limestone	0 to 60	Mountains in southern part of the basin.	Limestone and some shale.	Unknown.
Devonian	Percha Shale	80 to 185	do.	Shale, claystone, and some sandstone and siltstone.	Do.
Silurian	Fusselman Dolomite	Less than 20 to about 80	do.	Cherty dolomite	Do.
Ordovician	Montoya Dolomite	[illegible] to 400±	do.	Massive dolomite, cherty limestone, claystone, and a basal sandstone.	Do.
	El Paso Limestone	350 to 400±	do.	Thin-bedded limestone; basal unit is laminated, cherty limestone.	Do.
Cambrian	Bliss Formation	0 to 400	do.	Thin- to thick-bedded sandstone with some conglomerate and limestone.	Do.
Precambrian	*Metamorphic and igneous rocks		Underlie all of the Rio Grande basin.	Granite, schist, gneiss, and other metamorphic rocks.	Yield small quantities of water to wells, generally near the outcrops.

are structurally higher, exposing rocks older than those in their southern parts.

Downdropped troughs contain thick sedimentary deposits usually assigned to the Santa Fe Group with an age of Miocene to Recent. Several areas of Miocene and younger volcanics follow the rift. The great thickness of combined Tertiary and Quaternary sediments and volcanics masks older structures in the basins.

Exposed faults in the Santa Fe Group show dips of 70° to 90°. These high angles may not represent the faults at depth since faults cutting the Santa Fe Group are young and the dips probably are measured close to the original surface. They may therefore represent fault refraction near the surface. Most faults in the Rio Grande Valley have a northward trend; those trending eastward tend to be shorter and more widely spaced.

5.4 HYDROLOGY

The Rio Grande Rift includes several drainage basins (Figs. 5.1 and 5.2) which are not always defined in the same way.

Both surface water and ground water are ultimately derived from precipitation. Most water evaporates; plants transpire some of it; and some water runs off so rapidly that it erodes the land and picks up suspended and dissolved solids that make it unfit for most desired uses. A small portion, perhaps as much as 10% in the mountains, infiltrates to become ground water recharge.

The actual amount of water consumed by evaporation (Table 5.3) and transpiration depends on several factors, including temperature, relative humidity of the surrounding air and velocity at which the air passes, and density and type of vegetation. The division of water between surface flow and ground water is affected by these variables and also by other factors such as rate of precipitation and porosity and slope of the surface on which precipitation falls. Gentle rains infiltrate more completely than cloudbursts delivering the same volume of water, irrespective of the vegetation they fall on.

All these factors interact to determine actual water supplies available for use, with no single factor completely overriding the others. For instance, a desert assemblage of brush, sparse grass and cactus transpires less water than the trees, brush and thick grass of mountain forests, but the forest assemblage covers the ground more completely and thereby increases infiltration. The forest vegetation also reduces erosion and thereby reduces sediment load in streams.

TABLE 5.3 AVERAGE CLASS A LAND PAN EVAPORATION IN INCHES, RIO GRANDE BASIN IN NEW MEXICO MEXICO (Anonymous, 1967)

Station	Jan.	Feb.	Mar.	Apr.	May	June	July	Aug.	Sept.	Oct.	Nov.	Dec.	Annual
Bosque del Apache (1947-62)	3.21	4.42	8.18	10.49	12.80	13.79	12.08	11.02	8.68	6.40	3.80	2.74	97.61
Caballo Dam (1942-62)	3.65	5.42	9.34	12.34	15.28	16.80	13.96	12.29	10.36	7.56	4.83	3.22	115.05
El Vado (1936-62)	1.84*	1.85*	3.69*	5.74	7.78	9.73	8.97	7.55	6.39	4.57	2.20	1.23*	61.54*
Elephant Butte Dam (1934-62)	3.49	5.30	8.95	12.58	15.80	17.41	14.75	12.94	10.66	8.17	5.13	3.42	118.60
Jemez Dam (1954-62)	2.96*	2.97*	5.93*	9.76	12.70	14.98	13.97	12.10	10.34	7.12	4.03	1.98*	98.84*
Narrows (1947-62)	2.99	4.68	7.72	11.09	13.67	15.26	13.59	11.81	10.18	7.52	4.36	2.84	105.71
Santa Fe (1948-62)	2.25*	2.26*	4.51*	8.17	9.62	10.94	10.29	8.79	7.90	5.47	3.48	1.50*	75.18*
State University (1918-62)	2.94	4.39	7.61	10.01	12.20	13.20	11.96	10.33	8.37	6.10	3.78	2.64	93.53

* Calculated by percentage distribution.

Water in New Mexico has long been regarded as a public resource that may be appropriated for beneficial use by a private party. This appropriation doctrine contrasts the theory that possession of land carries with it the right to water occurring on or under that land. It protects early water users from ruin by latecomers whose developments interfere with established use. This doctrine serves well in arid environments where water often limits development, and security in water supply is therefore a requisite part of any project.

The State Engineer exercises jurisdiction over appropriation and use of surface water in New Mexico and has similar control over ground water in underground basins that he "declares" by determining and publishing the boundaries of said basins. Most water in the rift also is directly or indirectly affected by interstate and international agreements with Colorado, Texas and Mexico concerning the flow of the Rio Grande System.

Use of surface water in the Rio Grande Rift of New Mexico predates all known records. Indians were irrigating crop land when the Spanish arrived and ruins of even earlier irrigation projects can be found. Surface waters are still diverted and impounded for irrigation and other uses ranging from industry to recreation. Figures 5.11 and 5.12 show surface water measurements for some stations in the rift.

Gaging stations on the Rio Grande record stream flow at several places,but the stream flow they record is not identical with the runoff resulting from precipitation. Reservoirs control their discharge flows, irrigation works remove water from the river at several places, the return flow from irrigation water seldom can be measured, and ground water enters the river in unmeasured amounts. Still, the discharge measured at gaging stations provides the basic data on which surface water apportionments are based.

Various people and government agencies have divided the Rio Grande drainage basin into streams. These sections do not provide for a unit called the Rio Grande Rift in New Mexico.

The major distinction between the Upper Basin and Lower Basin of the Rio Grande follows from the character of the river itself. From its headwaters in Colorado to Fort Quitman, Texas, the Rio Grande flows rapidly downhill along the major rift valley in a series of constrictions and irrigable valleys. Below Fort Quitman the river leaves the main rift valley and meanders slowly southeast down a gentle grade to the Gulf of Mexico. The Rio Grande runs 3,060 km (1,900 mi) from its headwaters to the Gulf of Mexico of which 1,050 km (650 mi) lie in the Upper Basin. The Upper Basin includes all the drainage area above Fort Quitman and contains 82,970 sq km (32,035 sq mi).

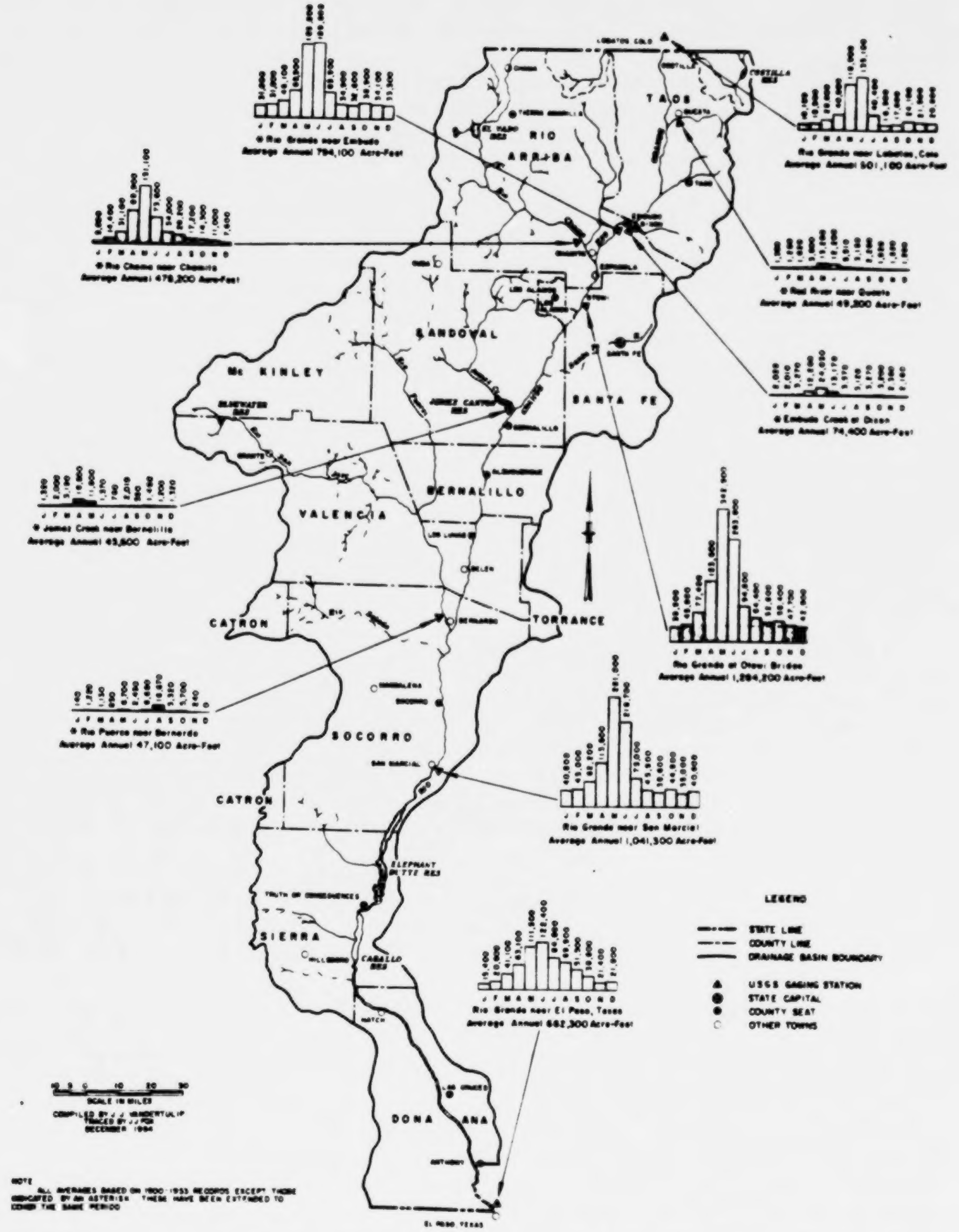
Rio Grande near Embudo
Average Annual 794,100 Acre-Feet
Rio Chama near Chamita
Average Annual 478,200 Acre-Feet
Rio Grande near Lobatos, Colo
Average Annual 501,100 Acre-Feet
Red River near Questa
Average Annual 49,200 Acre-Feet
Embudo Creek at Dixon
Average Annual 74,400 Acre-Feet
Jemez Creek near Bernalillo
Average Annual 43,600 Acre-Feet
Rio Grande at Otowi Bridge
Average Annual 1,284,200 Acre-Feet
Rio Puerco near Bernardo
Average Annual 47,100 Acre-Feet
Rio Grande near San Marcial
Average Annual 1,041,300 Acre-Feet
Rio Grande near El Paso, Texas
Average Annual 682,300 Acre-Feet
J F M A M J J A S O N D
TAOS
RIO ARRIBA
SANDOVAL
Mc KINLEY
SANTA FE
BERNALILLO
VALENCIA
CATRON
TORRANCE
SOCORRO
CATRON
SIERRA
DONA ANA
LOBATOS COLO
COSTILLA RES
EL VADO RES
JEMEZ CANYON RES
BLUEWATER RES
ELEPHANT BUTTE RES
CABALLO RES
TRUTH OR CONSEQUENCES
SANTA FE
BERNALILLO
ALBUQUERQUE
LOS LUNAS
BELEN
BERNARDO
MAGDALENA
SOCORRO
SAN MARCIAL
HILLSBORO
HATCH
LAS CRUCES
ANTHONY
EL PASO TEXAS
LEGEND
STATE LINE
COUNTY LINE
DRAINAGE BASIN BOUNDARY
USGS GAGING STATION
STATE CAPITAL
COUNTY SEAT
OTHER TOWNS
SCALE IN MILES
COMPILED BY J J VANDERTULIP
TRACED BY J J FOX
DECEMBER 1964
NOTE
ALL AVERAGES BASED ON 1900-1953 RECORDS EXCEPT THOSE INDICATED BY AN ASTERISK. THESE HAVE BEEN EXTENDED TO COVER THE SAME PERIOD

Figure 5.11 Average monthly and annual discharges at selected gaging stations, Rio Grande Valley and area of direct surface runoff. (Anonymous, 1967)

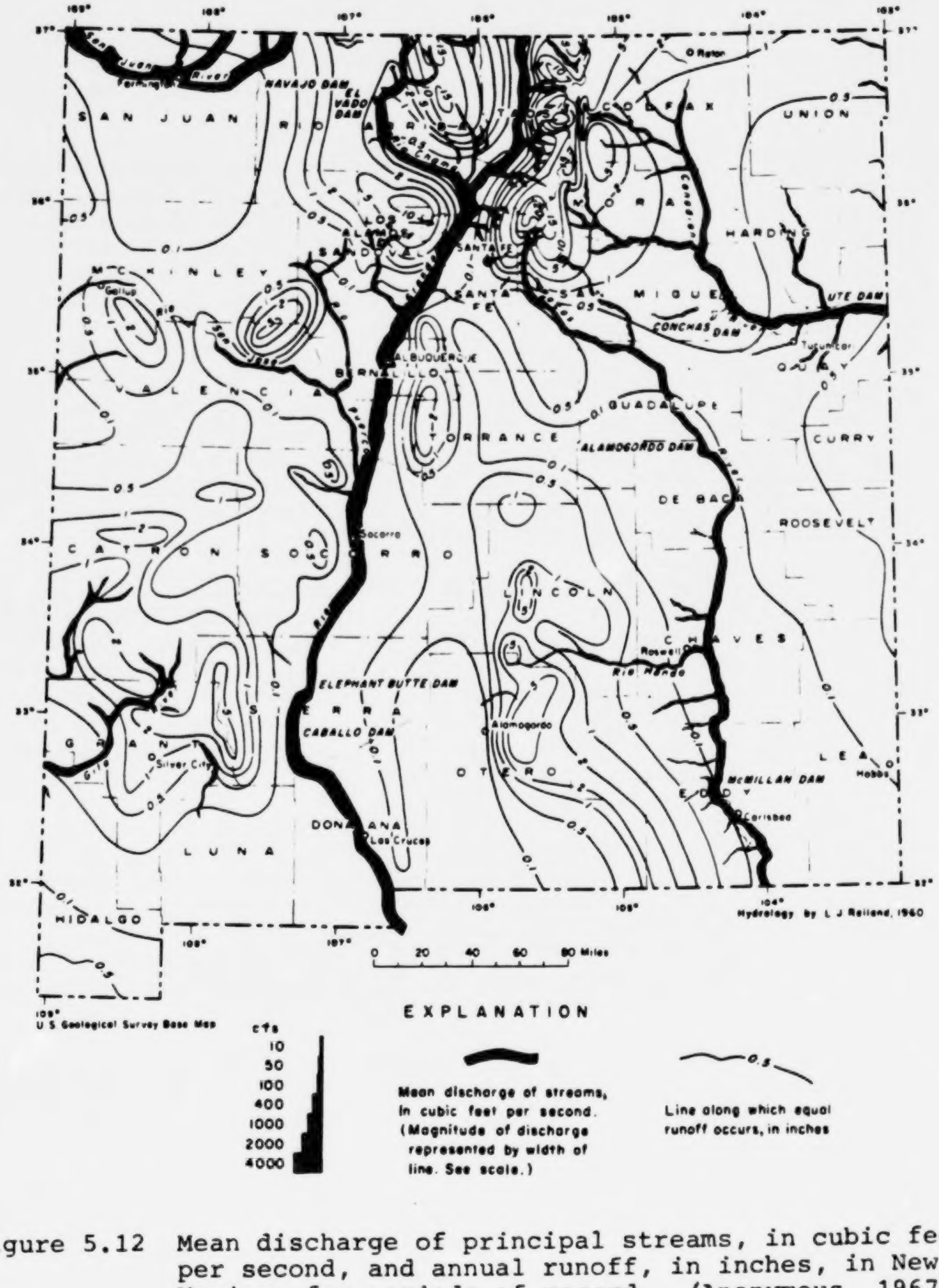
109°
108°
107°
106°
105°
104°
103°
37°
36°
35°
34°
33°
32°
SAN JUAN
RIO ARRIBA
TAOS
COLFAX
UNION
MC KINLEY
SANDOVAL
LOS ALAMOS
SANTA FE
MORA
HARDING
SAN MIGUEL
BERNALILLO
VALENCIA
TORRANCE
GUADALUPE
QUAY
CURRY
DE BACA
ROOSEVELT
CATRON
SOCORRO
LINCOLN
CHAVES
SIERRA
GRANT
OTERO
LEA
EDDY
DONA ANA
LUNA
HIDALGO
Farmington
San Juan River
NAVAJO DAM
EL VADO DAM
O Raton
Santa Fe
Gallup
Albuquerque
CONCHAS DAM
UTE DAM
Tucumcari
ALAMOGORDO DAM
Socorro
Roswell
Rio Hondo
ELEPHANT BUTTE DAM
CABALLO DAM
Alamogordo
Silver City
Las Cruces
McMILLAN DAM
Carlsbad
Hobbs
0.1
0.5
1
2
5
10
0 20 40 60 80 Miles
Hydrology by L J Reiland, 1960
U S Geological Survey Base Map
EXPLANATION
cfs
10
50
100
400
1000
2000
4000
Mean discharge of streams, in cubic feet per second. (Magnitude of discharge represented by width of line. See scale.)
Line along which equal runoff occurs, in inches

Figure 5.12 Mean discharge of principal streams, in cubic feet per second, and annual runoff, in inches, in New Mexico, for periods of record. (Anonymous, 1967)

The Upper Basin of the Rio Grande is further divided into the San Luis Section, the Middle Section, and the San Marcial-Fort Quitman Section. These sections of the Upper Basin hold importance in the division of surface water among the states of Colorado, New Mexico and Texas as prescribed by the Rio Grande Compact.

The San Luis Section includes the Rio Grande drainage in Colorado, which contains 19,900 sq km (7,700 sq mi) above the gaging station at Lobatos, Colorado. The gaging station at Lobatos Bridge measures Colorado's delivery of water to New Mexico under the Rio Grande Compact. The 68-year mean discharge through 1967 was 54,350 ha-m (440,650 acre-ft). Table 5.4 shows discharge data for the Rio Grande at Lobatos.

The Middle Section of the Upper Basin of the Rio Grande includes the river and its tributary valleys from the Colorado-New Mexico border to the San Marcial gaging station at the head of Elephant Butte Reservoir, a river distance of 435 km (270 mi) that contains about 52,000 sq km (20,000 sq mi) of drainage basin. This area contributes most of the water supply to the Rio Grande that originates in New Mexico.

In the language of the Rio Grande Compact, the Rio Grande below San Marcial runs in Texas,and New Mexico's water delivery is measured at the gaging station at San Marcial. That delivery shows a 72-year mean discharge of 114,910 ha-m (931,590 acre-ft) through 1967. Table 5.5 gives discharge data from the San Marcial gaging station. Across the Middle Section of the Upper Basin of the Rio Grande, gaging stations show an increase of 5,540 ha-m (44,940 acre-ft) in average annual discharge.

The San Marcial-Fort Quitman section of the Upper Basin of the Rio Grande contains 400 km (250 mi) of river between San Marcial, New Mexico, and Fort Quitman, Texas, and about 11,140 sq km (4,300 sq mi) of drainage area. Two major storage facilities of the Rio Grande System, Elephant Butte and Caballo reservoirs, lie in this southern reach. The Rio Grande discharges 19,180 ha-m (155,490 acre-ft) at Fort Quitman, according to a 46-year average through 1968 (Table 5.6).

Irrigated acreage varies widely through the years from an estimated 10,342 ha (25,555 acres) in about 1600 to an estimated 103,780 ha (256,445 acres) in 1964. Of the 103,780 ha irrigated in 1964, about 53,657 ha (132,590 acres) relied on surface water, 8,630 ha (21,325 acres) used groundwater and the other 41,492 ha (102,530 acres) used a combination of surface and groundwater.

Surface water in the Rio Grande above Elephant Butte Reservoir has been fully appropriated. Therefore, any new use of surface water would force the abandonment of a previous use.

TABLE 5.4 ANNUAL DISCHARGE OF THE RIO GRANDE NEAR LOBATOS, COLORADO (Jetton and Kirby, 1970)

Calendar year (1)	**Annual discharge in acre-feet** (2)	**Five-year moving average in acre-feet** (3)	**Ten-year moving average in acre-feet** (4)	**Departure from mean in acre-feet** (5)	**Accumulative departure from mean in acre-feet** (6)
1900	304,000	-	-	-136,654	- 136,654
01	284.000	-	-	-156,654	- 293,308
02	98,700	-	-	-341,954	- 635,262
03	627,000	-	-	+186,346	- 448,916
04	188,000	300,340	-	-252,654	- 701,570
05	986,000	436,740	-	+545,346	- 156,224
06	854,000	550.740	-	+413,346	+ 257,122
07	1,440,000	819,000	-	+999,346	+1,256,468
08	362,000	766,000	-	- 78,654	+1,177,814
09	933,000	915,000	607,670	+492,346	+1,670,160
1910	556,000	829,000	632,870	+115,346	+1,785,506
11	1,040,000	866,200	708,470	+599,346	+2,384,852
12	849,000	748,000	783,500	+408,346	+2,793,198
13	295,000	734,600	750,300	-145,654	+2,647,544
14	595,000	667,000	791,000	+154,346	+2,801,890
15	471,000	650,000	739,500	+ 30,346	+2,832,236
16	769,000	595,800	731,000	+328,346	+3,160,582
17	799,000	585,800	666,900	+358,346	+3,518,928
18	260,000	578,800	656,700	-180,654	+3,338,274
19	612,000	582,200	624,600	+171,346	+3,509,620
1920	1,040,000	696,000	673,000	+599,346	+4,108,966
21	863,000	714,800	655,300	+422,346	+4,531,312
22	674,000	689,800	637,800	+233,346	+4,764,658
23	696,000	777,000	677,900	+255,346	+5,020,004
24	753,000	805,200	693,700	+312,346	+5,332,350
25	323,000	661,800	678,900	-117,654	+5,214,696
26	426,000	574,400	644,600	- 14,654	+5,200,042
27	724,000	584,400	637,100	+283,346	+5,483,388
28	325,000	510,200	643,600	-115,654	+5,367,734
29	598,000	479,200	642,200	+157,346	+5,525,080
1930	270,000	468.600	565,200	-170,654	+5,354,426
31	126,000	408,600	491,500	-314,654	+5,039.772
32	596,000	383,000	483,700	+155,346	+5,195,118
33	237,000	365,400	437,800	-203,654	+4,991,464
34	98,880	265,580	372,390	-341,774	+4,649,690
35	360,400	283,660	376,130	- 80,254	+4,569,436
36	281,000	314,660	361,630	-159,654	+4,409,782
37	465,800	288,620	335,810	+ 25,146	+4,434,928
38	570,900	355,400	360,400	+130,246	+4,565.174
39	207,700	377,160	321,370	-232,954	+4,332,220

TABLE 5.4

Calendar year (1)	Annual discharge in acre-feet (2)	Five-year moving average in acre-feet (3)	Ten-year moving average in acre-feet (4)	Departure from mean in acre-feet (5)	Accumulative departure from mean in acre-feet (6)
1940	105,700	326,220	304,940	-334,954	+3,997,266
41	954,300	460,880	387,770	+513,646	+4,510,912
42	681,800	504,080	396,350	+241,146	+4,752,058
43	183,500	426,600	391,000	-257,154	+4,494,904
44	606,300	506,320	441,740	+165,646	+4,660,550
45	276,800	540,540	433,380	-163,854	+4,496,696
46	115,100	372,700	416,790	-325,554	+4,171,142
47	230,300	282,400	393,240	-210,354	+3,960,788
48	664,200	378,540	402,570	+223,546	+4,184,334
49	572,600	371,800	439,060	+131,946	+4,316,280
1950	132,100	342,860	441.700	-308,554	+4,007,726
51	74,320	334,700	353,700	-366,334	+3,641,392
52	468,400	382,320	332,360	+ 27,746	+3,669,138
53	122,100	273,900	326,220	-318,554	+3,350,584
54	59,570	171,300	271,550	-381,084	+2,969,500
55	63,120	157,500	250,180	-377,534	+2,591,966
56	70,130	156,660	245,680	-370.524	+2,221,442
57	444,900	151,960	267,140	+ 4,246	+2,225,688
58	362.500	200,040	236,970	- 78,153	+2,147,535
59	88,420	205,810	188,560	-352,231	+1,795,304
1960	201,000	233.390	195.450	-239,651	+1,555,653
61	169,200	253,200	204,930	-271,451	+1,284,202
62	315.300	227,280	189,620	-125,351	+1.158,851
63	72,570	169,300	184.670	-368,081	+ 790,770
64	57,440	163,100	184,460	-383,211	+ 407,559
65	498,600	222,620	228,010	+ 57,949	+ 465,508
66	255,400	239,860	246,530	-185,254	+ 280,254
67	160,400	208,880	218,080	-280,254	0

68 year mean discharge:440,650 acre-feet.

TABLE 5.5 ANNUAL DISCHARGE OF THE RIO GRANDE AT SAN MARCIAL, NEW MEXICO (Jetton and Kirby, 1970)

Calendar year (1)	Annual discharge in acre-feet (2)	Five-year moving average in acre-feet (3)	Ten-year moving average in acre-feet (4)	Departure from mean in acre-feet (5)	Accumulative departure from mean in acre-feet (6)
1896	581,500	-	-	- 350,090	- 350,090
97	1,781,000	-	-	+ 849,410	+ 499,320
98	865,100	-	-	- 66,490	+ 432,830
99	239,500	-	-	- 692,090	- 259,260
1900	467,900	787,000	-	- 463,690	- 722,950
01	656,200	801,940	-	- 275,390	- 998,340
02	200,700	485,880	-	- 730,890	-1,729,230
03	1,309,000	574,660	-	+ 377,410	-1,351,820
04	654,200	657.600	-	- 277,390	-1,629,210
05	2,422,000	1,048,420	917.710	+1,490,410	- 138,800
06	1,564,000	1,229,980	1,015.960	+ 632,410	+ 493.610
07	2.158,000	1,621,440	1,053,660	+1.226,410	+1,720,020
08	774.100	1,514,460	1,044,560	- 157,490	+1,562,530
09	1,280,000	1,639,620	1.148,610	+ 348,410	+1,910.940
1910	852,700	1,325,760	1.187,090	- 78,890	+1,832,050
11	1,800,000	1,372,960	1,301,470	+ 868,410	+2,700,460
12	1,500,000	1,241,360	1,431,400	+ 568,410	+3,268,870
13	525,400	1,191,620	1.353,040	- 406,190	+2,862.680
14	1,178,000	1,171,220	1,405,420	+ 246,410	+3,109,090
15	1,373,000	1,275,280	1,300.520	+ 441,410	+3,550,500
16	1,649.000	1,245,080	1,309,020	+ 717,410	+4,267,910
17	1,050,000	1,155,080	1,198,220	+ 118,410	+4,386,320
18	411,200	1,132,240	1,161,930	- 520,390	+3,865,930
19	1,579,000	1,212,440	1,191,830	+ 647,410	+4,513,340
1920	1,943,000	1,326,440	1,300,860	+1,011,410	+5,524,750
21	1,488,000	1,294,240	1,269,660	+ 556,410	+6,081,160
22	938,400	1,271,920	1,213,500	+ 6,810	+6,087,970
23	1,224,000	1,434,480	1,283,360	+ 292,410	+6,380,380
24	1,410,000	1,400,680	1,306,560	+ 478,410	+6,858,790
25	419,000	1,095,880	1,211,160	- 512,590	+6,346,200
26	1,050,000	1,008,280	1,151,260	+ 118,410	+6,464,610
27	1,350,000	1,090,600	1,181,260	+ 418,410	+6,883,020
28	591,000	964,000	1,199,240	- 340,590	+6,542,430
29	1,460,000	974,000	1,187,340	+ 528,410	+7,070,840
1930	731,000	1,036,400	1,066.140	- 200,590	+6,870,250
31	490,000	924,400	966.340	- 441,590	+6,428,660
32	1,400,000	934.400	1,012,500	+ 468,410	+6,897,070
33	716,100	959,420	961,710	- 215,490	+6,681,580
34	244,400	716,300	845,150	- 687,190	+5,994,390
35	1,028,000	775,700	906,050	+ 96,410	+6,090,800
36	866,900	851,080	887,740	- 64,690	+6,026,110
37	1,558,000	882,680	908,540	+ 626.410	+6,652,520
38	1,054,000	950,260	954,840	+ 122,410	+6,774,930
39	524,400	1,006,260	861,280	- 407,190	+6,367,740

TABLE 5.5 (continued)

Calendar year (1)	Annual discharge in acre-feet (2)	Five-year moving average in acre-feet (3)	Ten-year moving average in acre-feet (4)	Departure from mean in acre-feet (5)	Accumulative departure from mean in acre-feet (6)
1940	369,000	874,460	825,080	- 562,590	+5,805,150
41	2,831,000	1,2[illegible],280	1,059,180	+1,899,410	+7,704,560
42	1,940,000	1,343,680	1,113,180	+1,008,410	+8,712,970
43	418,200	1,216,520	1,083,390	- 513,390	+8,199,580
44	1,024,000	1,316,440	1,161,350	+ 92,410	+8,291,990
45	814,400	1,405,520	1,139,990	- 117,190	+8,174,800
46	289,300	897,180	1,082,230	- 642,290	+7,532,510
47	433,700	595,920	969,800	- 497,890	+7,034,620
48	933,500	698,980	957,750	+ 1,910	+7,036,530
49	1,054,000	704,980	1,010,710	+ 122,410	+7,158,940
1950	307,000	603,500	1,004,510	- 624,590	+6,534,350
51	114,100	568,460	732,820	- 817,490	+5,716,860
52	1,003,000	682,320	639,120	+ 71,410	+5,788,270
53	260,500	547,720	623,350	- 671,090	+5,117,180
54	215,600	380,040	542,510	- 715,990	+4,401,190
55	264,200	371,480	487,490	- 667,390	+3,733,800
56	136,300	375,920	472,190	- 795,290	+2,938,510
57	1,240,000	423,320	552,820	+ 308,410	+3,246,920
58	1,292,000	629,620	588,670	+ 360,410	+3,607,330
59	247,500	636,000	508,020	- 684,090	+2,923,240
1960	551,600	693,480	532,480	- 379,990	+2,543,250
61	544,500	775,120	575,520	- 387,090	+2,156,160
62	745,900	676,300	549,810	- 185,690	+1,970,470
63	267,000	471,300	550,460	- 664,590	+1,305,880
64	169,000	455,600	545,800	- 762,590	+ 543,290
65	1,036,000	552,480	622,980	+ 104,410	+ 647,680
66	568,800	557,340	666,230	- 362,790	+ 284,910
67	646,700	537,500	606,900	- 284,890	+ 0

72 year mean:931,590

TABLE 5.6 ANNUAL DISCHARGE OF THE RIO GRANDE AT FORT QUITMAN, TEXAS (Jetton and Kirby, 1970)

Calendar year (1)	Annual discharge in acre-feet (2)	Five-year moving average in acre-feet (3)	Ten-year moving average in acre-feet (4)	Departure from mean in acre-feet (5)	Accumulative departure from mean in acre-feet (6)
1923	332.400	-	-	+ 176,910	+ 176,910
24	373,800	-	-	+ 218,310	+ 395,220
25	267,880	-	-	+ 112,390	+ 507,610
26	276,250	-	-	+ 120,760	+ 628,370
27	240,920	298,250	-	+ 85,430	+ 713,800
28	263,810	284.530	-	+ 108,320	+ 822,120
29	211,780	252.130	-	+ 56,290	+ 878,410
1930	188,030	236,160	-	+ 32,540	+ 910,950
31	211,650	223,240	-	+ 56,160	+ 967,110
32	211,120	217.280	257,760	+ 55,630	+1,022,740
33	213,790	207,270	245,900	+ 58,300	+1,081,040
34	102,420	185,400	218,760	- 53.070	+1,027,970
35	145,380	176,870	206,520	- 10,110	+1,017,860
36	149,590	164,460	193,850	- 5,900	+1,011,960
37	178,290	157,890	187.590	+ 22.800	+1,034,760
38	276,240	170,380	188,830	+ 120,750	+1,155,510
39	152.180	180,340	182,870	- 3.310	+1,152,200
1940	124,320	176.120	176,500	- 31.170	+1,121,030
41	330,490	212.300	188,380	+ 175,000	+1,296,030
42	1.270,400	430,730	294.310	+1,114,910	+2,410,940
43	233,290	422,140	296,260	+ 77,800	+2,488,740
44	272,900	446,280	313,310	+ 117,410	+2,606,150
45	207,710	462,960	319,540	+ 52,220	+2,658,370
46	131.380	423,140	317,720	- 24,110	+2,634,260
47	90,780	187,210	308,970	- 64,710	+2,569,550
48	75.340	155,620	288,880	- 80,150	+2,489,400
49	134.030	127,850	287,060	- 21,460	+2,467,940
1950	123,530	111,010	286,980	- 31,960	+2,435,980
51	25,690	89,870	256,500	- 129,800	+2,306,180
52	11,129	73,940	130,580	- 144,360	+2,161,820
53	20,329	62,940	109,280	- 135,160	+2,026,660
54	14,886	39,110	83,480	- 140,600	+1,886,060
55	5,888	15,580	63.300	- 149.600	+1,736,460
56	6,010	11,650	50,760	- 149.480	+1,586,980
57	4,843	10,390	42,170	- 150,650	+1,436,330
58	36,152	13,560	38,250	- 119,340	+1,316,990
59	13.226	13.220	26,170	- 142.260	+1,174,730

TABLE 5.6 (continued)

Calendar year (1)	Annual discharge in acre-feet (2)	Five-year moving average in acre-feet (3)	Ten-year moving average in acre-feet (4)	Departure from mean in acre-feet (5)	Accumulative departure from mean in acre-feet (6)
1960	51,093	22,260	18,920	- 104,400	+1,070,330
61	17,220	24,510	18,080	- 138,270	+ 932,060
62	73,705	38,280	24,340	- 81,780	+ 850,280
63	23,361	35,720	24,640	- 132,130	+ 718,150
64	3,129	33,700	23,460	- 152,360	+ 565,760
65	1,662	23,820	23,040	- 153,830	+ 411,930
66	31,778	26,730	25,620	- 123,710	+ 288,220
67	3,608	12,710	25,490	- 151,880	+ 136,340
68	19,150	11,870	23,790	- 136,340	0

46 Year Average:155,490

Exploitation of groundwater was negligible before about 1900, when expanding population increased demand for all classes of water use. Figure 5.1 shows irrigated areas in the Rio Grande Valley. Groundwater use has expanded until about 90% of the municipal and industrial use in 1969 and 1970 came from groundwater (Lansford, et al., 1973). That use significantly affects water table contours in several local areas. Figure 5.13 shows one area with measured water level changes. Such changes often reverse after pumping ceases.

Figure 5.14 shows the depth to groundwater in New Mexico. Figure 5.15 outlines the major groundwater reservoir in the Rio Grande Basin. In general, the water table contours follow the land surface contours. Water moves from an area of higher head (or potential energy) into an area of lower head, so that the net movement is down the hydraulic gradient, and individual flow paths intersect lines of equal potential at right angles. This generally means that groundwater travels downhill from a mountainous recharge area to a low discharge area such as a river valley or lake.

5.5 CHEMICAL CHARACTERISTICS OF GROUNDWATER

Natural water quality depends on the type of rocks through or over which the water travels. Water running over loose sediments picks up particles and carries them as suspended sediment (Fig. 5.16). Water in contact with soluble rocks carries away part of the rock as dissolved solids (Fig. 5.17).

Dissolved solids are commonly reported in terms of parts per million or milligrams per liter. The U.S. Public Health Service (USPHS) defines saline water as water that contains more than 1,000 mg/l TDS, which equals one gram per liter (gm/l). The Rio Grande Rift contains great volumes of saline water as defined by the USPHS (Fig. 5.18). Kelly, et al. (1970) divided the saline water category into four water quality ranges. Following their scheme, slightly saline water contains 1 to 3 gm/l TDS, moderately saline water contains 3 to 10 gm/l, very saline water contains 10 to 35 gm/l and brine contains more than 35 gm/l. For comparison, average sea water contains more than 35 gm/l, the Salton Sea in California contains 21 gm/l and the Dead Sea in Israel contains 315 gm/l TDS (Krauskopf, 1967). Slightly saline water is commonly used for drinking, irrigation and industrial purposes in New Mexico where better quality water is not available.

Saline groundwater in the rift area usually occurs below potable groundwater, but the thickness of the fresh water zone and the available volume of fresh water vary widely among local areas in the rift. Figure 5.19 shows the thickness of the fresh water unit in the Rio Grande Valley, and Figure 5.20 estimates availability of fresh water.

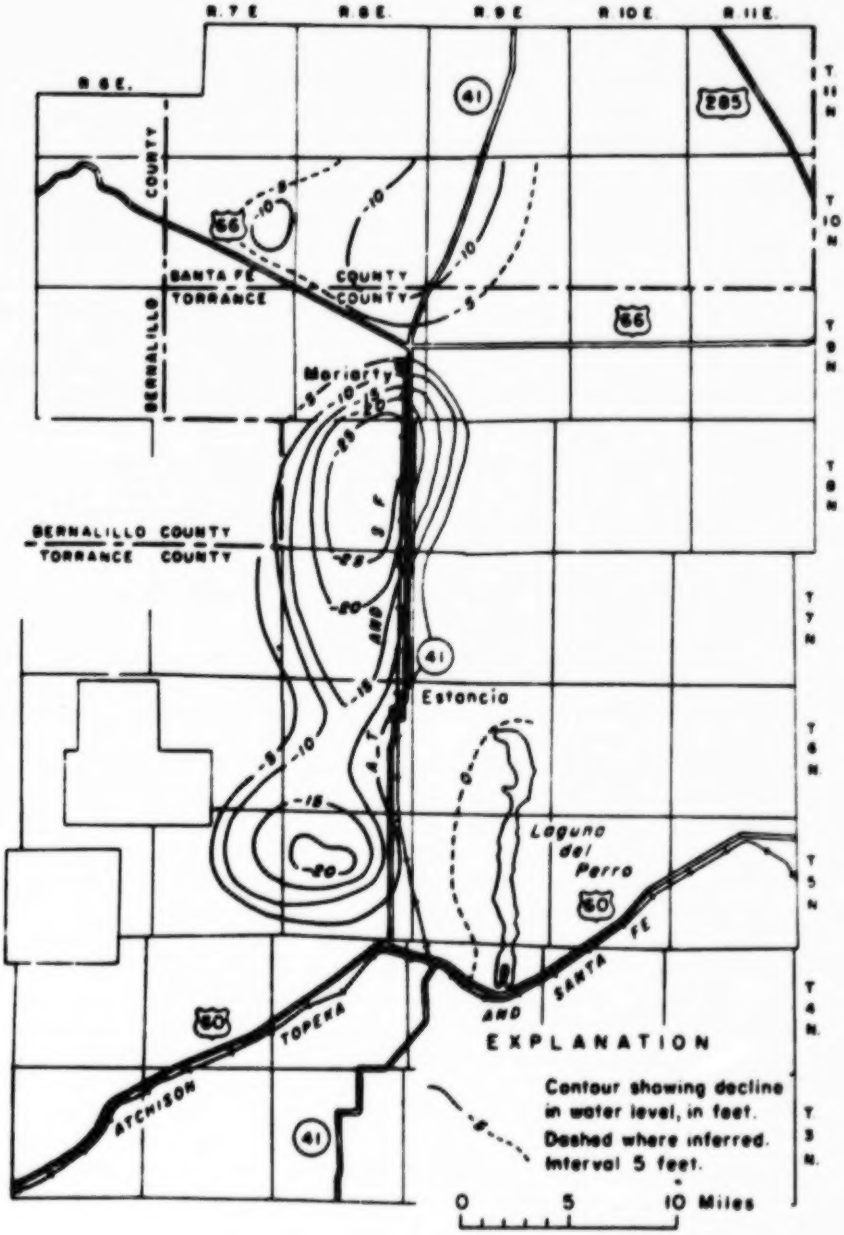
R.7 E.
R.8 E.
R.9 E.
R.10 E.
R.11 E.
R.6 E.
T. 11 N.
T. 10 N.
T. 9 N.
T. 8 N.
T. 7 N.
T. 6 N.
T. 5 N.
T. 4 N.
T. 3 N.
41
285
66
SANTA FE COUNTY
TORRANCE COUNTY
BERNALILLO COUNTY
Moriarty
Estancia
Laguna del Perro
60
ATCHISON TOPEKA AND SANTA FE
A.T. AND S.F.
EXPLANATION
Contour showing decline in water level, in feet. Dashed where inferred. Interval 5 feet.
0
5
10 Miles
-5
-10
-15
-20
-25
0

Figure 5.13 Decline of groundwater level in Estancia Basin, Santa Fe and Torrance Counties, New Mexico, 1948-1960. (Anonymous, 1967)

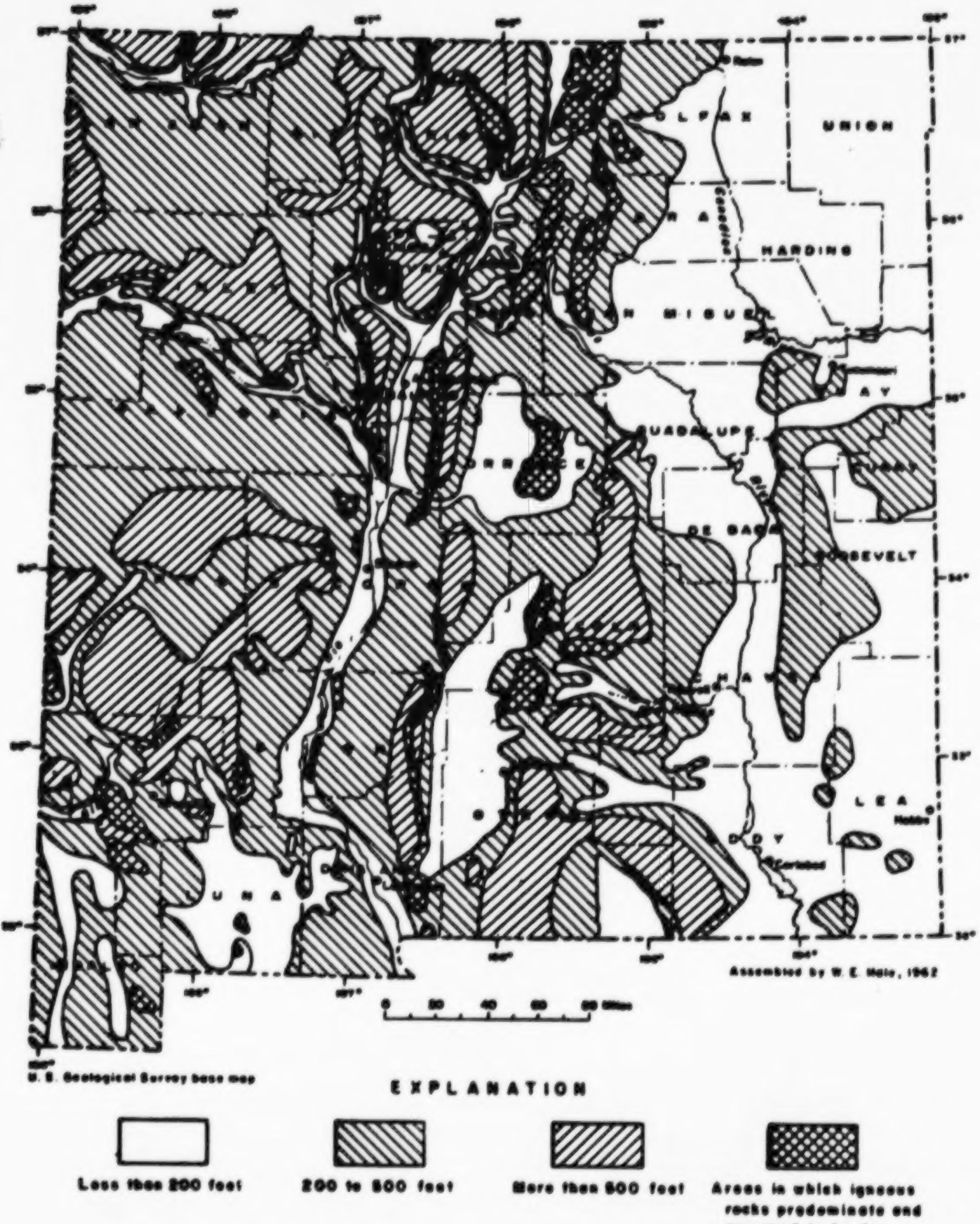
UNION
HARDING
GUADALUPE
DE BACA
ROOSEVELT
LEA
LUNA
37°
36°
35°
34°
33°
32°
104°
103°
0 20 40 60 80 Miles
Assembled by W. E. Hale, 1962
U. S. Geological Survey base map
EXPLANATION
Less than 200 feet
200 to 500 feet
More than 500 feet
Areas in which igneous rocks predominate and assumed to be dry

Figure 5.14 Depth to groundwater in New Mexico. (Anonymous, 1967)

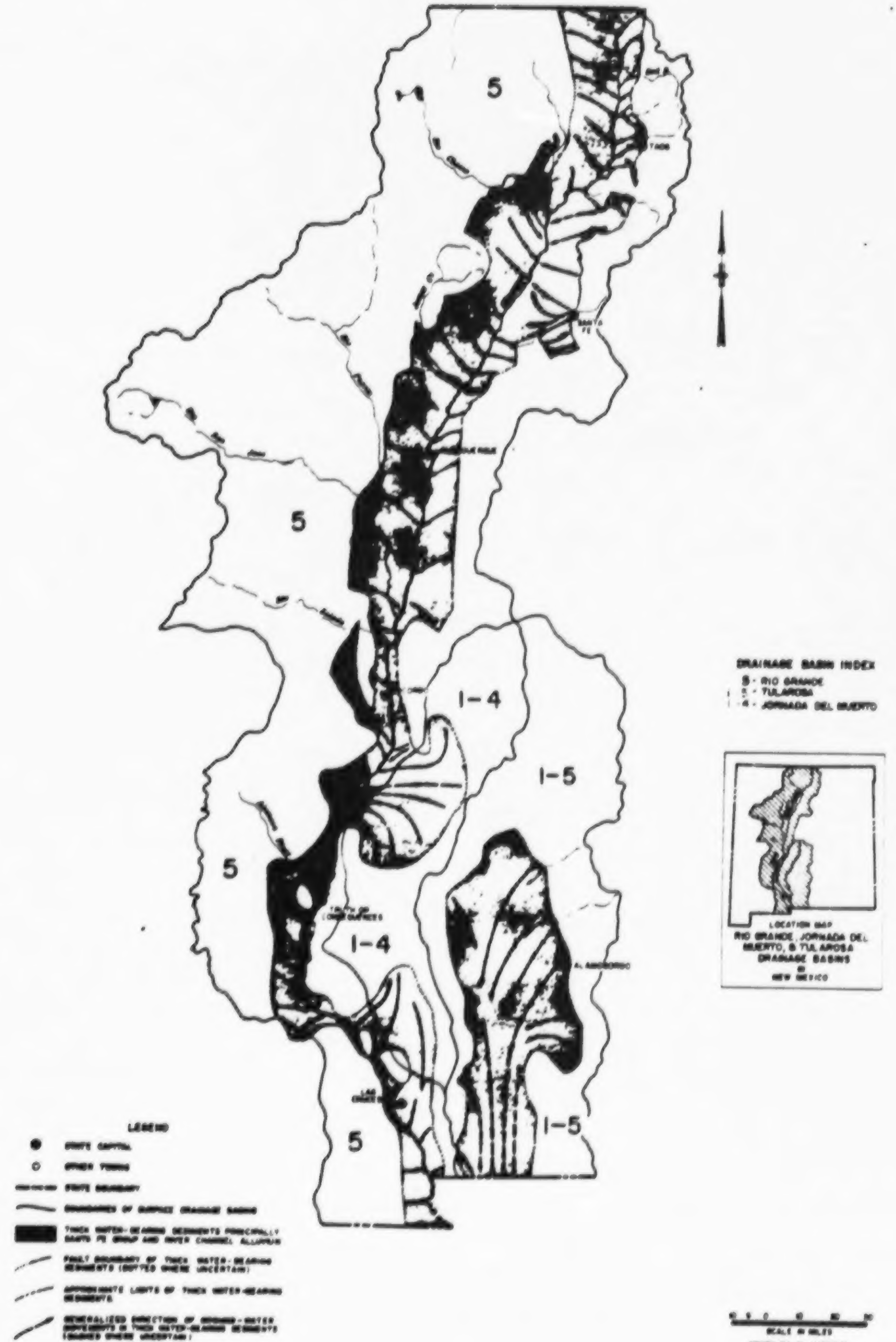
5
5
5
5
1-4
1-4
1-5
1-5
SANTA FE
TAOS
ALAMOGORDO
LAS CRUCES
TRUTH OR CONSEQUENCES
DRAINAGE BASIN INDEX
5 - RIO GRANDE
1-5 - TULAROSA
1-4 - JORNADA DEL MUERTO
LOCATION MAP
RIO GRANDE, JORNADA DEL MUERTO, & TULAROSA DRAINAGE BASINS
IN
NEW MEXICO
LEGEND
STATE CAPITAL
OTHER TOWNS
STATE BOUNDARY
BOUNDARIES OF SURFACE DRAINAGE BASINS
SCALE IN MILES

Figure 5.15 Groundwater reservoir in the Rio Grande Depression, New Mexico. (Anonymous, 1967)

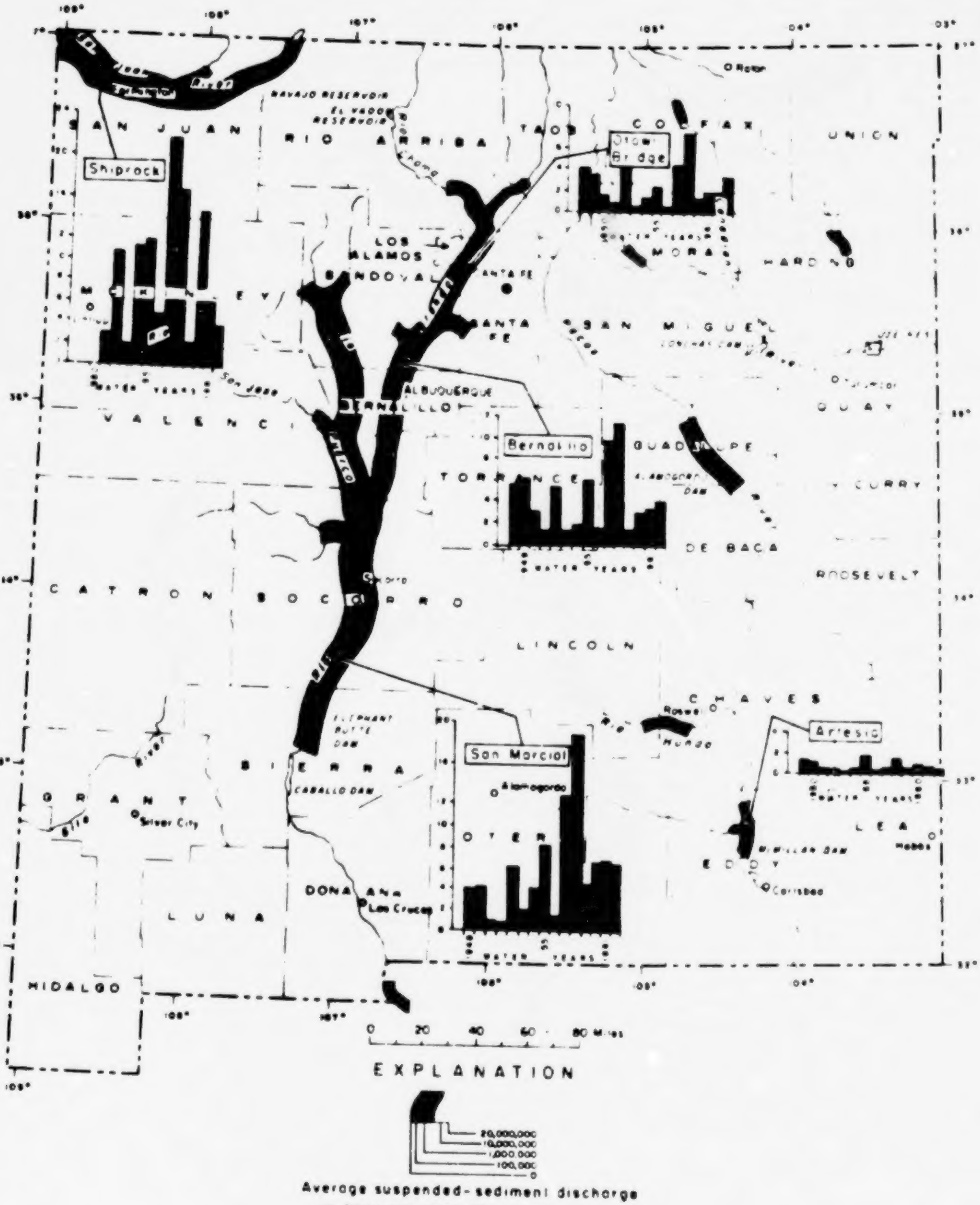
Shiprock
Otowi Bridge
Bernalillo
San Marcial
Artesia
SAN JUAN
RIO ARRIBA
TAOS
COLFAX
UNION
MORA
HARDING
LOS ALAMOS
SANDOVAL
SANTA FE
SAN MIGUEL
McKINLEY
VALENCIA
BERNALILLO
ALBUQUERQUE
TORRANCE
GUADALUPE
QUAY
CURRY
DE BACA
ROOSEVELT
CATRON
SOCORRO
LINCOLN
CHAVES
SIERRA
GRANT
OTERO
EDDY
LEA
DONA ANA
LUNA
HIDALGO
NAVAJO RESERVOIR
EL VADO RESERVOIR
ELEPHANT BUTTE DAM
CABALLO DAM
ALAMOGORDO DAM
McMILLAN DAM
Raton
Santa Fe
Roswell
Alamogordo
Silver City
Las Cruces
Carlsbad
Hobbs
San Juan River
San Jose
Rio Grande
Rio Puerco
Chama
Pecos
Hondo
Gila
WATER YEARS
0 20 40 60 80 Miles
EXPLANATION
20,000,000
10,000,000
1,000,000
100,000
0
Average suspended-sediment discharge in tons per year. Magnitude of discharge represented by width of bar

(Note: Vertical values on inset graphs refer to dissolved solids discharge in millions of tons.)

Figure 5.16 Average annual suspended sediment discharge of streams and suspended sediment discharge by years at selected stations in New Mexico. (Anonymous, 1965)

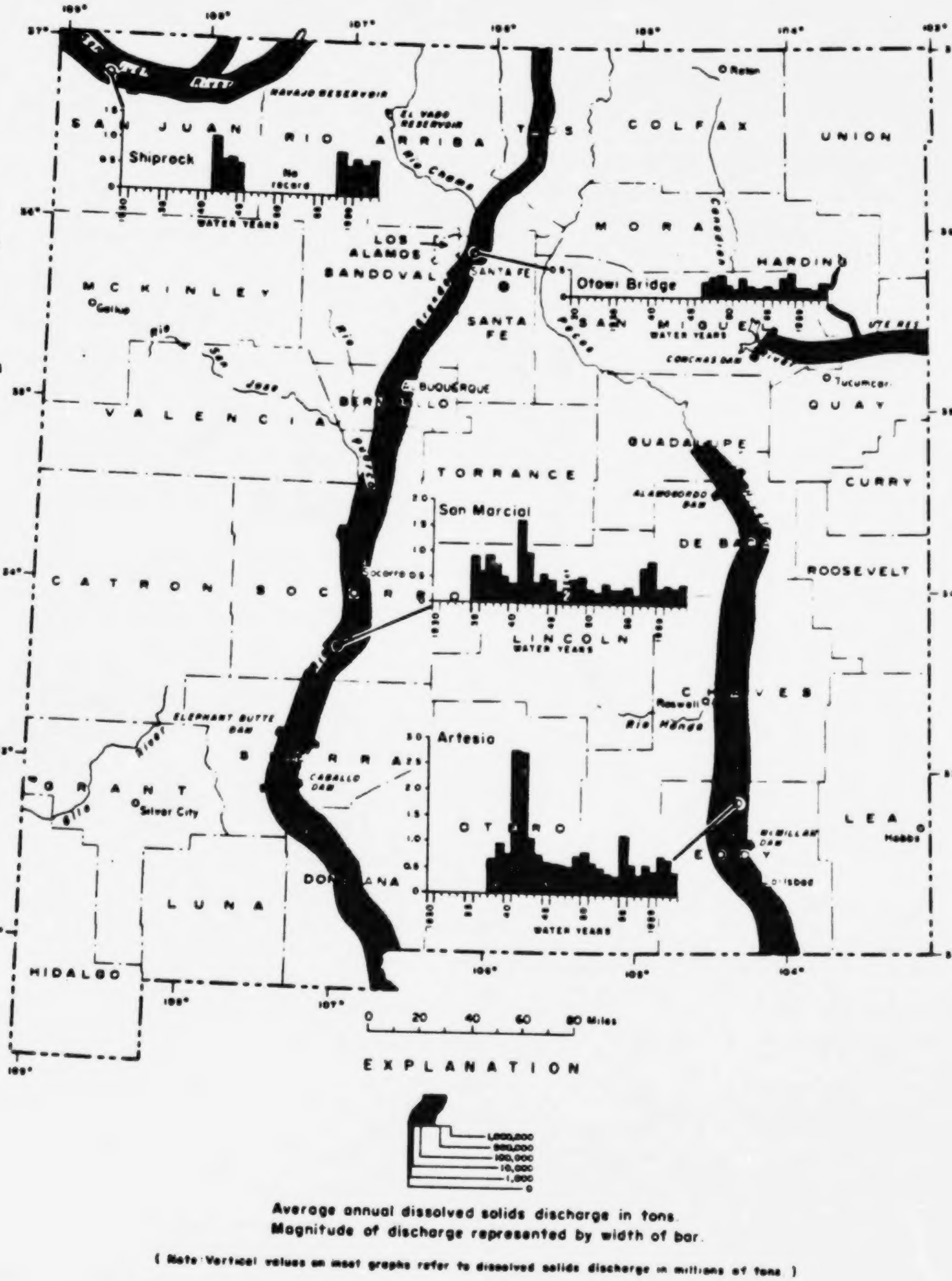
Shiprock
No record
WATER YEARS
Otowi Bridge
WATER YEARS
San Marcial
WATER YEARS
Artesia
WATER YEARS
SAN JUAN
RIO ARRIBA
TAOS
COLFAX
UNION
MORA
HARDING
LOS ALAMOS
SANDOVAL
SANTA FE
MCKINLEY
SAN MIGUEL
QUAY
VALENCIA
BERNALILLO
GUADALUPE
TORRANCE
CURRY
DE BACA
ROOSEVELT
CATRON
SOCORRO
LINCOLN
CHAVES
SIERRA
GRANT
OTERO
LEA
EDDY
LUNA
DONA ANA
HIDALGO
Navajo Reservoir
El Vado Reservoir
Rio Chama
Conchas Dam
Ute Res
Alamogordo Dam
Elephant Butte Dam
Caballo Dam
McMillan Dam
Raton
Gallup
Santa Fe
Albuquerque
Tucumcari
Socorro
Roswell
Rio Hondo
Silver City
Hobbs
Carlsbad
Rio Puerco
Rio San Jose
Pecos River
Gila River
0 20 40 60 80 Miles
EXPLANATION
1,000,000
500,000
100,000
10,000
1,000
0
Average annual dissolved solids discharge in tons.
Magnitude of discharge represented by width of bar.
(Note: Vertical values on inset graphs refer to dissolved solids discharge in millions of tons.)

Figure 5.17 Average annual dissolved solids discharge in years at selected stations in New Mexico (Anonymous, 1965)

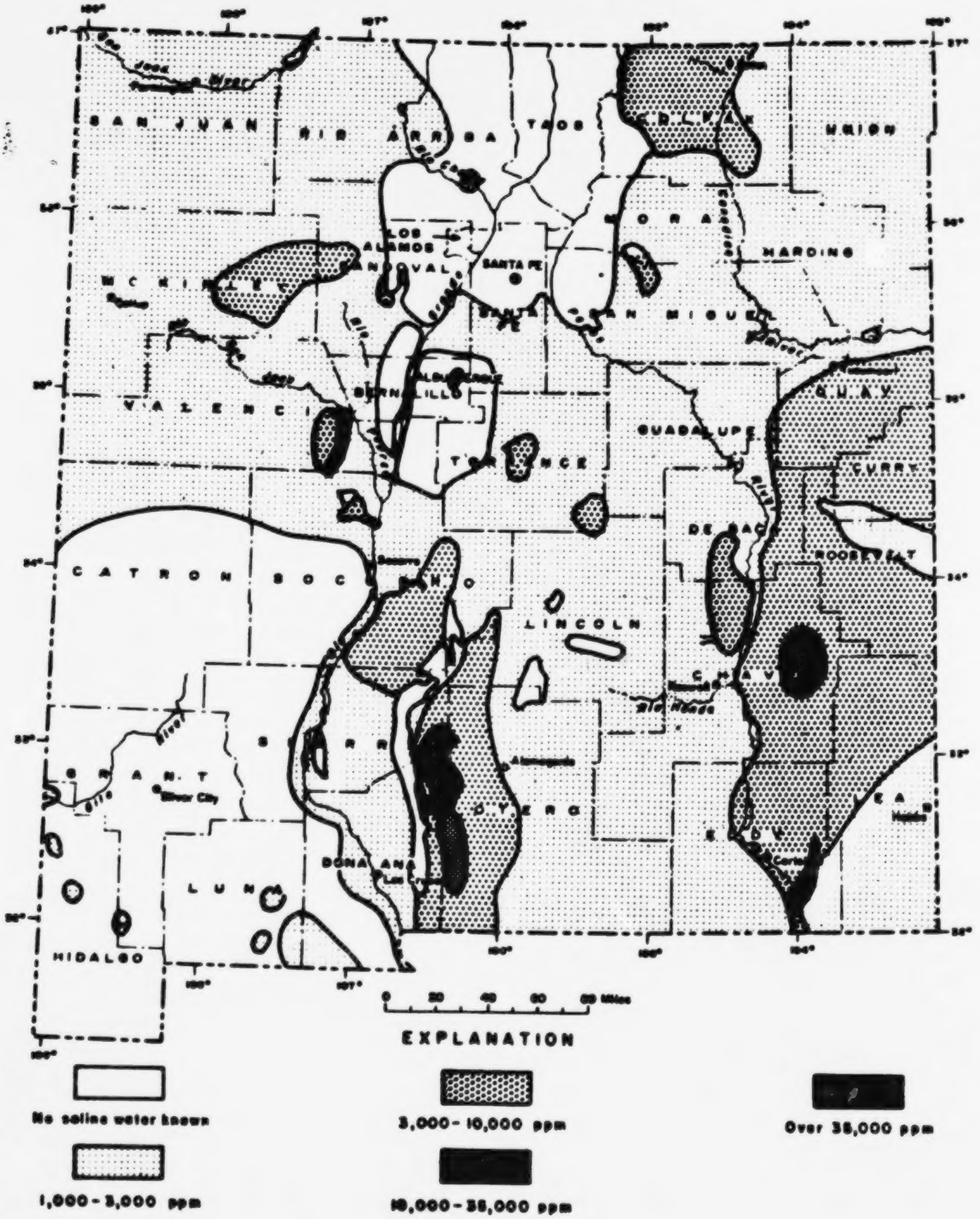
SAN JUAN
RIO ARRIBA
TAOS
COLFAX
UNION
LOS ALAMOS
SANDOVAL
SANTA FE
MORA
HARDING
McKINLEY
SAN MIGUEL
BERNALILLO
VALENCIA
QUAY
GUADALUPE
TORRANCE
CURRY
DE BACA
ROOSEVELT
CATRON
SOCORRO
LINCOLN
CHAVES
GRANT
SIERRA
OTERO
EDDY
LEA
DONA ANA
LUNA
HIDALGO
Silver City
Alamogordo
0 20 40 60 80 Miles
EXPLANATION
No saline water known
1,000-3,000 ppm
3,000-10,000 ppm
10,000-35,000 ppm
Over 35,000 ppm

Figure 5.18 General occurrence of saline groundwater in New Mexico. (Anonymous, 1967)

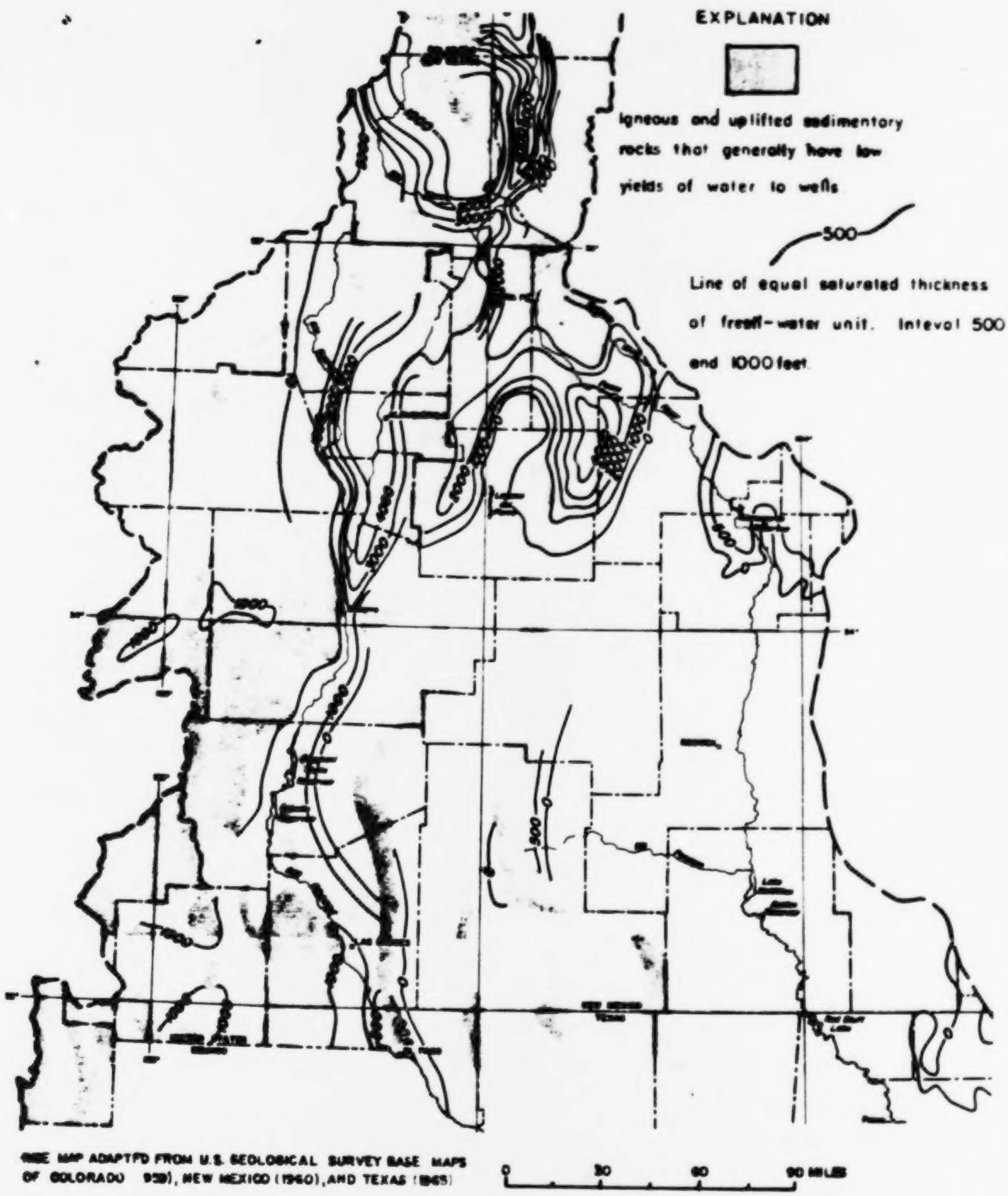
EXPLANATION
Igneous and uplifted sedimentary rocks that generally have low yields of water to wells
500
Line of equal saturated thickness of fresh-water unit. Inteval 500 and 1000 feet
0
30
60
90 MILES

BASE MAP ADAPTED FROM U.S. GEOLOGICAL SURVEY BASE MAPS OF COLORADO 959), NEW MEXICO (1960), AND TEXAS (1965)

Figure 5.19 Thickness of the fresh water unit (less than one gram per liter dissolved solids). (Kelly, et al. 1970)

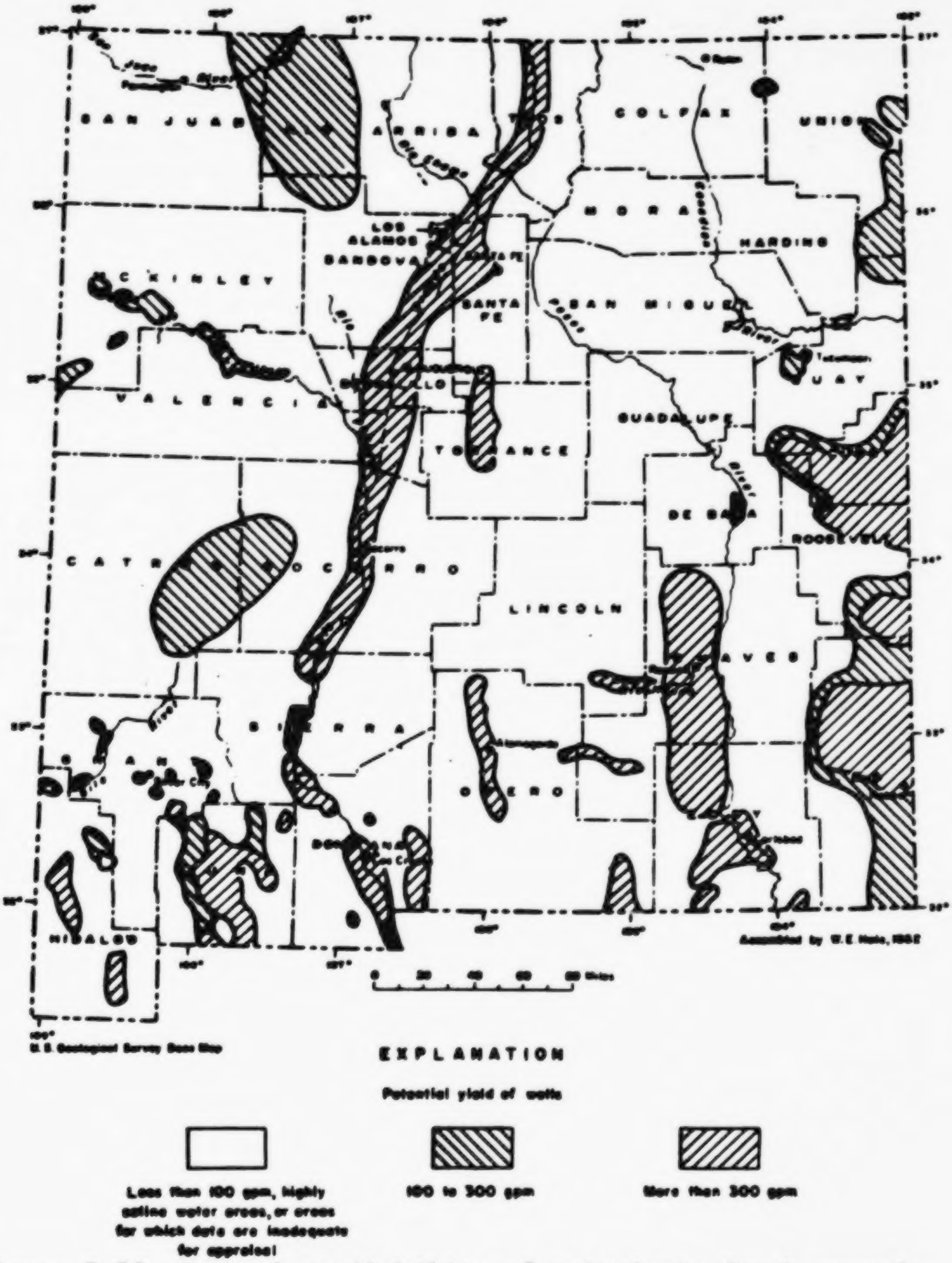

SAN JUAN
ARRIBA
TAOS
COLFAX
UNION
MORA
HARDING
LOS ALAMOS
SANDOVAL
SANTA FE
SAN MIGUEL
McKINLEY
VALENCIA
TORRANCE
GUADALUPE
QUAY
DE BACA
ROOSEVELT
CATRON
SOCORRO
LINCOLN
CHAVES
SIERRA
OTERO
HIDALGO
Assembled by W.E. Hale, 1962
0 20 40 60 80 Miles
U.S. Geological Survey Base Map
EXPLANATION
Potential yield of wells
Less than 100 gpm, highly saline water areas, or areas for which data are inadequate for appraisal
100 to 300 gpm
More than 300 gpm

Figure 5.20 General availability of relatively fresh groundwater in New Mexico. (Anonymous, 1967)

Human activities create wastes that sometimes enter the water and significantly lower water quality. Figure 5.21 locates several sources of waste water in New Mexico.

5.6 SEISMICITY

Seismicity in New Mexico is relatively low, about one-eighteenth that of southern California and about one-tenth that of Nevada (Slemmons, 1975).

Despite the fact that New Mexico was settled by the Spanish in 1542, no earthquakes were reported until 1849 (Northrop, 1976). This is indicative of the poor earthquake history of New Mexico which is due in part to the lack of instrumentation to record even a moderate event and in part to a sparsely distributed population throughout most of New Mexico.

Instrumental studies of New Mexico started in June 1960, when high magnification seismographs were put into operation by the New Mexico Institute of Mining and Technology at Socorro and by the Atomic Energy Commission at Sandia Base near Albuquerque. More high gain stations were placed in operation from 1962 on, and availability of data from several stations, rather than one or two, increased the accuracy of location and magnitude determinations. However, the relatively short period of instrumental records makes it extremely difficult to derive reliable long-term earthquake recurrence statistics.

5.6.1 Seismicity Along the Rio Grande Rift

The Rio Grande Rift has been structurally active for thousands of years, but earthquake activity does not appear to be limited to major faults. Large earthquakes reported in New Mexico during the hundred-odd years for which records have been kept occurred almost exclusively in the Rio Grande Rift. Only one strong shock occurred outside the rift from 1869 to 1960, while nine were reported within the rift (Sanford, et al., 1972).

The distribution of seismic activity in the Rio Grande Rift is fairly well established. Historical reports and recent instrumental studies indicate that most of the shocks have been centered near Socorro. Northrop (1976) reports that, of 523 definitely recorded earthquakes with epicenters in New Mexico from 1849 to 1975, 76% occurred within the rift, and of those, 96% were restricted to the 121 km (75 mi) long segment between Albuquerque and Socorro. Instrumental data from earthquakes with local magnitudes (M_L) (Richter, 1958) greater than 2.7 places the zone of highest activity in the rift south of Socorro to Las Cruces. Instrumental data from microearthquakes ($M_L > 2.7$) places the highest activity in the rift near Socorro (Sanford, et al., 1972). Sanford, et al., (1972) show that on

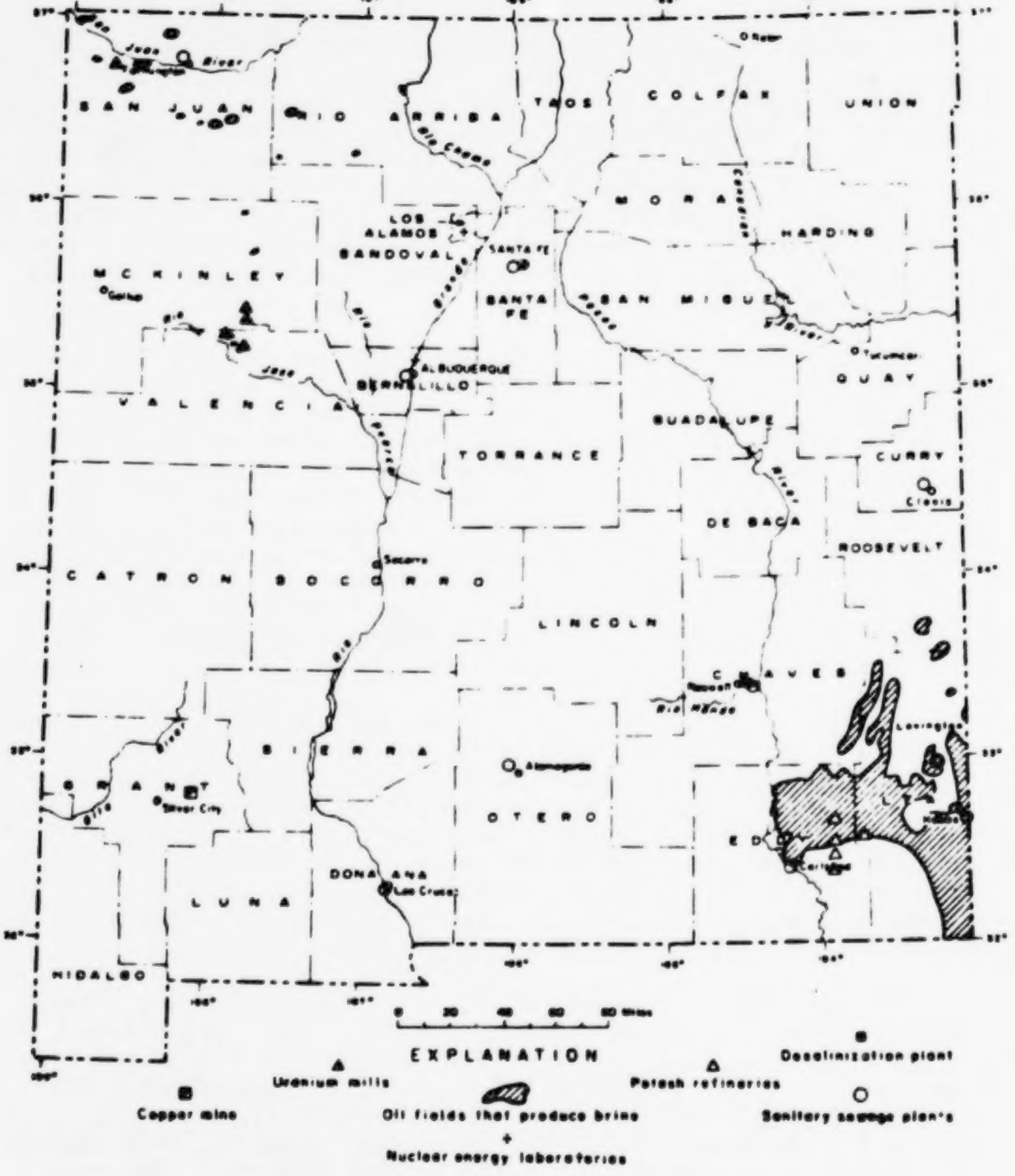

SAN JUAN
RIO ARRIBA
TAOS
COLFAX
UNION
MORA
HARDING
LOS ALAMOS
SANDOVAL
SANTA FE
McKINLEY
SAN MIGUEL
QUAY
VALENCIA
BERNALILLO
GUADALUPE
TORRANCE
CURRY
DE BACA
ROOSEVELT
CATRON
SOCORRO
LINCOLN
CHAVES
SIERRA
GRANT
OTERO
EDDY
DONA ANA
LUNA
HIDALGO
San Juan River
Santa Fe
Albuquerque
Gallup
Tucumcari
Clovis
Socorro
Roswell
Rio Hondo
Alamogordo
Silver City
Las Cruces
Carlsbad
Lovington
Hobbs
0 20 40 60 80 Miles
EXPLANATION
Desalinization plant
Uranium mills
Potash refineries
Copper mine
Oil fields that produce brine
Sanitary sewage plants
Nuclear energy laboratories

Figure 5.21 Principal sources of waste water in New Mexico. (Anonymous, 1965)

the average about 400 earthquakes are recorded each year with magnitudes above 0 and epicenters within 20 km (12.5 mi) of Socorro.

The relatively short record of earthquake activity in New Mexico makes it difficult to accurately appraise the long-term level of activity. Recent instrumental work, including microearthquake surveys, indicates a modest degree of seismicity with a maximum M_L magnitude of 4.2 to 4.9 (Sanford, et al., 1972). On the other hand, historical records show that at least one shock in excess of magnitude 6 has occurred in the rift within the last 100 years (Sanford, et al.,1972). Northrop (1976) predicts a shock of magnitude 6 between Socorro and Albuquerque once every 100 years and a shock of magnitude 5.5 near Los Alamos once every 100 years.

Study of faults cutting and displacing recent geomorphic features such as pediments, alluvial fans and stream drainages can also provide an estimate of the area's seismic activity. The wide variation in ages assigned to these geomorphic features causes a variation in the predicted maximum shock in a 100-year period. Even so, the maximum magnitude earthquake predicted for a 100- year period ranges from 4.6 to 6.6 and thus falls in the range of predictions based on microseismic data or historic reports. Using an intermediate age of less than 40,000 years for the fault scarps cutting recent geomorphic features gives a magnitude of 5.6 for the maximum earthquake in a 100-year period.

Separate data sources agree in general on the area of greatest seismic activity but do not agree in detail. Likewise, the prediction of seismic risk varies among the methods. The highest risk, a maximum earthquake of about magnitude 6 in a 100-year period, comes from historical data; the lowest of about 4.6 comes from microseismic data, with instrumental data from earthquakes giving a maximum magnitude of about 5. Because historical data considers a longer period, it probably produces the best available current estimate of seismic risk.

The New Mexico region of the seismic risk maps prepared by Richter (1958) and Algermissen (1969), are reproduced here as Figures 5.22 and 5.23. Note that Richter's map shows a zone of high seismic risk in central New Mexico, extending along the Rio Grande, in which earthquakes of intensity IX may occasionally be expected. However, Algermissen's map suggests only earthquakes of intensity V and VI in eastern New Mexico. Sanford, et al. (1972) conclude that Richter's estimate of seismic risk for the Rio Grande Rift Zone appears to be too high and Algermissen's too low.

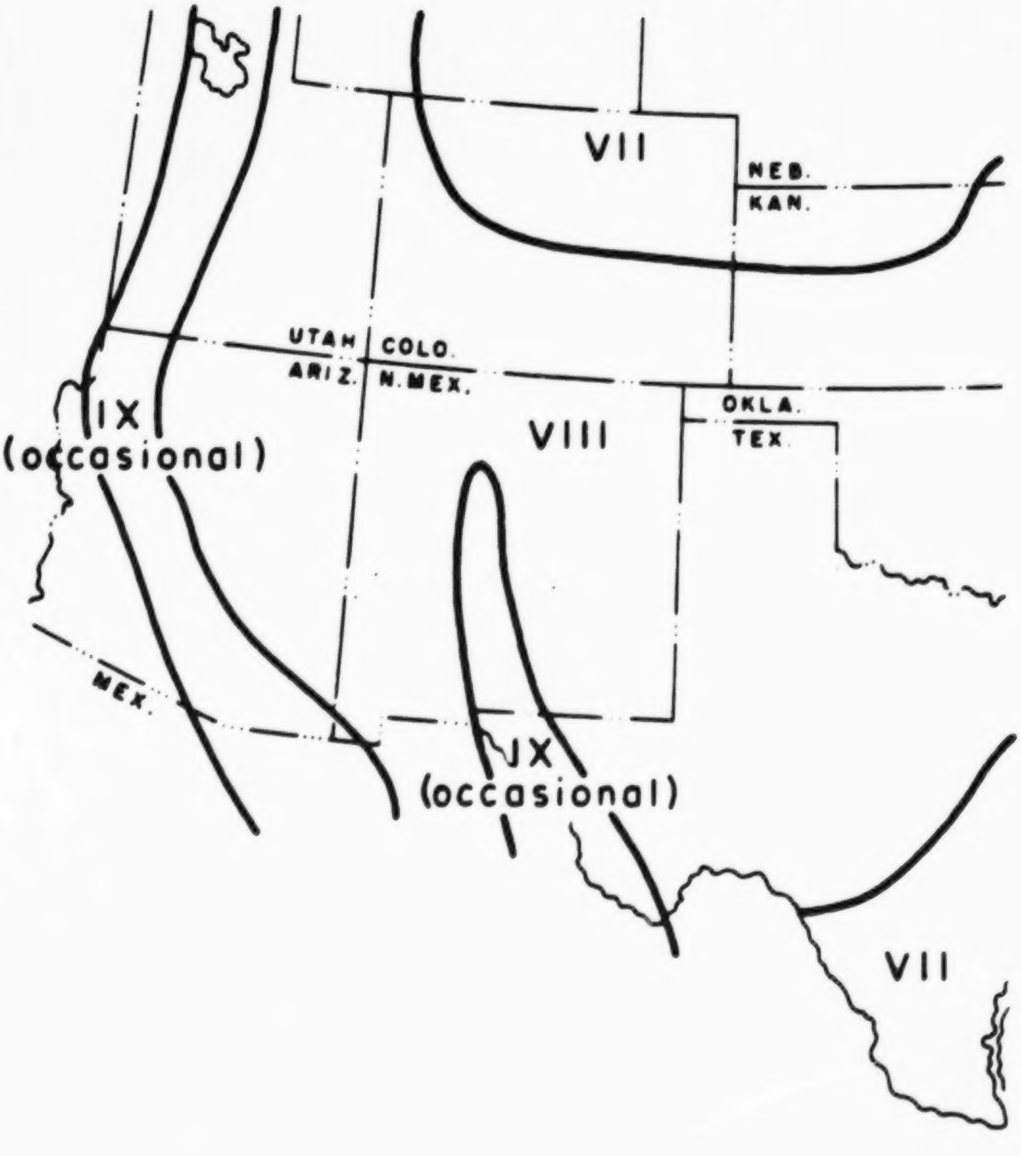
VII
NEB.
KAN.
UTAH
COLO.
ARIZ.
N.MEX.
OKLA.
TEX.
IX
(occasional)
VIII
MEX.
IX
(occasional)
VII

Figure 5.22 Seismic risk map by Richter (1958). (Intensities according to Modified Mercalli Intensity Scale of 1931)

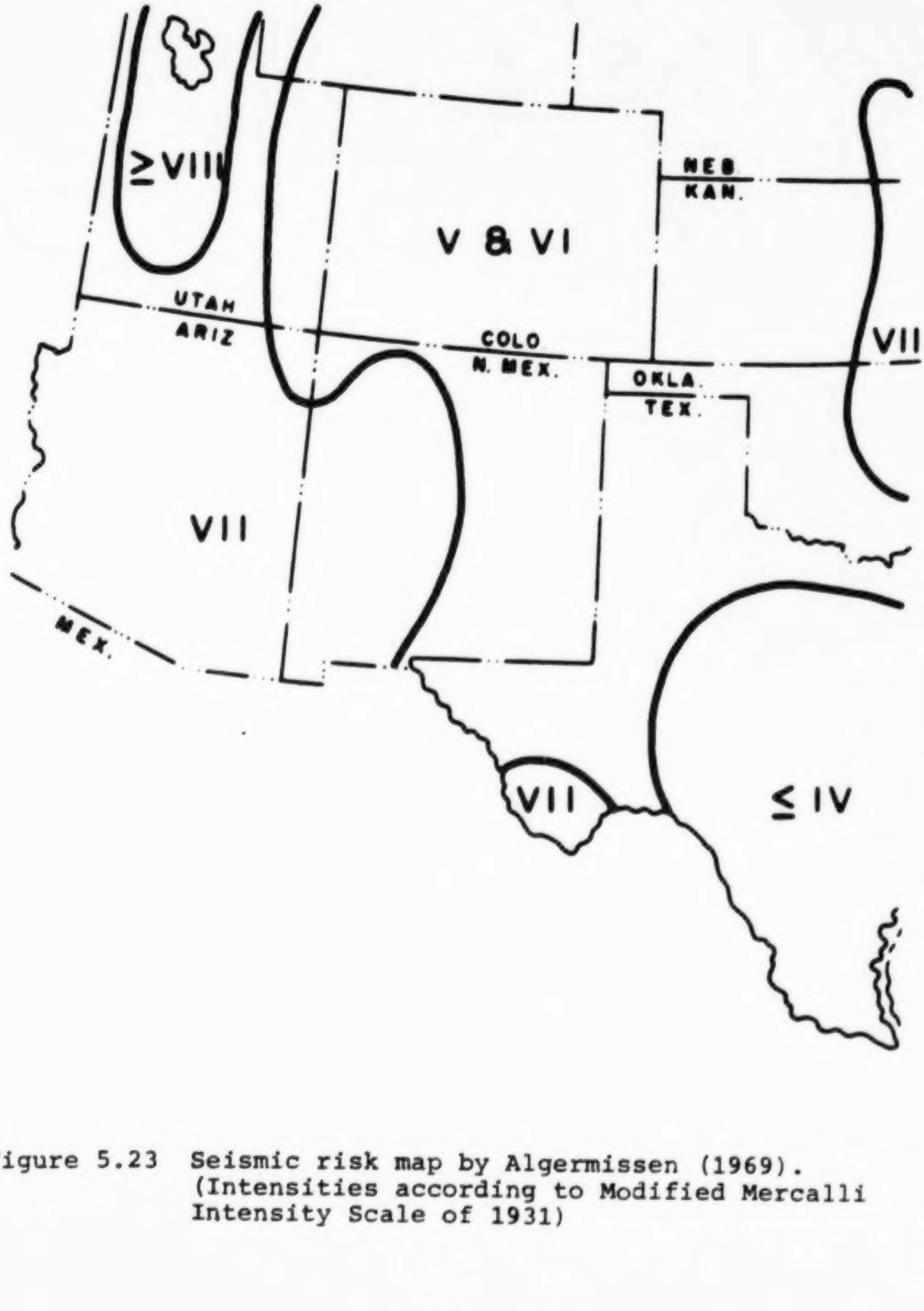
≥ VIII
V & VI
NEB.
KAN.
UTAH
ARIZ
COLO
N. MEX.
OKLA.
TEX.
VII
VII
MEX.
VII
≤ IV

Figure 5.23 Seismic risk map by Algermissen (1969). (Intensities according to Modified Mercalli Intensity Scale of 1931)

5.6.2 Seismicity of the Valles Caldera Region

Valles Caldera lies in the Jemez Mountains along the western margin of the Rio Grande Rift. The Jemez Mountains, a complex of Tertiary and Quaternary volcanics, are genetically associated with the formation of the Rio Grande Rift structure. Purtyman and Jordan (1973) have noted that this geologic regime could produce seismic activity by rupture along faults bounding the rift or by failure of rocks in the Valles Caldera as a result of expansion and movement of magmas along volcanic vents in the Valles Caldera Volcanic Field. However, several authors (Newton, et al., 1976; Slemmons, 1975; Sanford, 1976) have noted the surprisingly low seismicity in the Jemez Mountains. Sanford (1976) reviews the seismicity within a radius of 111 km (69 mi) of Los Alamos for a period of 100 years. Pre-1962 earthquakes are based mainly on historical data. During the 14 years of instrumental observation, 75% of the shocks occurred within the Rio Grande Rift, but the Valles Caldera experienced no seismic activity above the $M_L = 2.5$ level. The largest shock reported in the Jemez Mountains for the 100-year study was a felt earthquake of magnitude 4.0, located directly under Los Alamos on August 17, 1952.

The strongest earthquake within the 111 km (69 mi) radius of Los Alamos was the Cerrillos earthquake of May 28, 1918, located approximately 60 km (37 mi) southeast of Los Alamos. The shock had an energy release of about 14 times the combined energy release of all other shocks within the 111 km (69 mi) radius of Los Alamos during the 100-year period (Sanford, 1976).

Sanford (1976) estimates the recurrence interval for a magnitude 5.5 earthquake once every 100 years for the part of the Rio Grande Rift from Albuquerque to Questra, the limits of the 111 km radius from Los Alamos within the rift. This implies that the seismicity of Los Alamos region is somewhat less than the seismicity of the Albuquerque to Socorro segment of the rift and only one-eighteenth that of the recurrence interval in southern California (Slemmons, 1975).

Sanford (1976) notes a period of relatively high seismic release within the Los Alamos area during the years 1930-31 and 1947-56. Excepting these two periods of high energy release, Sanford's (1976) data appears to indicate a steady decline in seismic energy release for the Los Alamos region since 1918 and a slight increase since 1970. Sanford states that this could be the beginning of a period of relatively accelerated seismic activity similar to that observed during the periods of high seismicity.

Sanford (1976) concludes that his estimate for seismic risk is based upon the assumption that seismic activity will continue at the same level as observed in the past 100 years and estimates the magnitude of the strongest earthquake to occur within a 111 km (69 mi) radius of Los Alamos during a 100-year period as $M_L = 5.5$, producing effects up to intensity VII. He gives a probability of 0.08 for this earthquake to occur within the 111 km (69 mi) radius of Los Alamos, based on the assumption that the shock has equal probability of occurring anywhere within the Rio Grande Rift.

REFERENCES

Algermissen, S. T. Seismic Risk Studies in the United States; in Proc. of the Fourth World Conference on Earthquake Engineering. Asociación Chilena de Sismologiae Ingenieria Antismica, Santiago, Chile, v. 1, p. 14-27, 1969.

Anonymous. Water Resources of New Mexico: Occurrence, Development and Use. State Planning Office, Santa Fe, New Mexico, 321 p., 1967.

Bridwell, R. J. Lithospheric Thinning and Late Cenozoic Thermal and Tectonic Regime of the Northern Rio Grande Rift. New Mex. Geol. Soc., Guidebook 27th Field Conf., p. 283-292, 1976.

Chapin, C. E. The Rio Grande Rift, Part I: Modifications and Additions. New Mex. Geol. Soc., Guidebook 22nd Field Conf., p. 191-201, 1971.

Cordell, L. Aeromagnetic and Gravity Studies in the Rio Grande Graben in New Mexico Between Belen and Pilar. New Mex. Geol. Soc., Spec. Pub. No. 6, p. 62-70, 1976.

Jetton, E. V., and J. W. Kirby. A Study of Precipitation, Streamflow, and Water Usage on the Upper Rio Grande. Atmospheric Science Group, University of Texas at El Paso, Report No. 25, 203 p.,1970.

Kelley, V. C. Tectonics of the Rio Grande Depression of Central New Mexico. New Mex. Geol. Soc., 3rd Field Conference, p. 93-105, 1952.

__________. Tectonic Map of a Part of the Upper Rio Grande Area, New Mexico. Oil and Gas Inv., Map No. OM 157, 1954.

Kelly, T. E., B. N. Myers and L. A. Hershey. Saline Ground Water Resources of the Rio Grande Drainage Basin, a Pilot Study. Office of Saline Water, Research and Development Progress Report, No. 560, Los Angeles, 1970.

Krauskopf, K. B. Introduction to Geochemistry. McGraw-Hill, Inc., 721 p., 1967.

Lansford, R. R., S. Ben-David, T. G. Gebhard, Jr., W. and C. Brutsaert and J. Bobby. An Analytical Interdisciplinary Evaluation of the Utilization of the Water Resources of the Rio Grande in New Mexico: Socorro Region. New Mex. Water Res. Inst. Report No. 023, 1973.

Newton, C. A., D. J. Cash, K. H. Olsen and E. F. Homuth. Los Alamos Scientific Laboratory Seismic Program in the Vicinity of Los Alamos, New Mexico. Los Alamos Scientific Laboratory Informal Report No. LA-6406-MS, 1976.

Northrop, S. A. New Mexico's Earthquake History 1849-1975; in Tectonics and Mineral Resources of Southwest North America. New Mex. Geol. Soc. Spec. Pub. No. 6, p. 77-87, 1976.

Purtyman, W. D., and H. S. Jordan. Seismic Program of the Los Alamos Scientific Laboratory. Los Alamos Scientific Laboratory Pub. No. LA-5595-MS, 1973.

Reddy, R. S. Crustal structure in New Mexico. M.S. thesis, New Mex. Inst. of Mining and Tech., unpub., 1966.

Reiter, M., C. L. Edwards, H. Jartman and C. Weidman. Terrestrial Heat Flow along the Rio Grande Rift, New Mexico and Southern Colorado. Bull. Geol. Soc. Am., v. 86, p. 811-818, June 1974.

Richter, C. F. Elementary Seismology. W. H. Freeman and Company, Inc., 786 p., 1958.

Sanford, A. R. Seismicity of the Los Alamos Region Based on Seismological Data. Los Alamos Scientific Laboratory Information Report No. LA-6416-MS, 1976.

Sanford, A. R., A. J. Buddington, J. P. Hoffman, O. S. Alptekin, L. A. Rush and T. R. Toppozada. Seismicity of the Rio Grande Rift in New Mexico. New Mex. Bur. of Mines and Mineral Res., Circ. 120, 1972.

Sanford, A. R., et al. Microearthquake Investigation of Magma Bodies in the Vicinity of Socorro, New Mexico (abs.). Geol. Soc. Am. Abs. with Program, p. 1085, 1976a.

Sanford, et al. Geophysical Evidence for a Magma Body in the Crust in the Vicinity of Socorro, New Mexico. Paper presented at the ONR-CSM Symposium on "The Nature and Physical Properties of the Earth's Crust," Vail, Colorado, Aug. 2-6, 1976b.

Slemmons, D. B. Fault Activity and Seismicity Near the Los Alamos Scientific Laboratory Geothermal Test Site, Jemez Mountains, New Mexico. Los Alamos Scientific Laboratory Informal Report No. LA-5911-MS, 1975.

Shuleski, P. J., F. J. Caravella, E. J. Rinehart, A. R. Sanford, T. C. Wallace and R. M. Ward. Seismic Studies of Shallow Magma Bodies Beneath the Rio Grande Rift in the Vicinity of Socorro, New Mexico. Geol. Soc. Am. Abs. with Program, v. 9, No. 1, p. 73, 1977.

Stone, W. J., and N. B. Mizell. Geothermal Resources of New Mexico -- a Survey of Work to Date. New Mex. Bur. of Mines and Mineral Res., Open File Report 73, 117 p., 1977.

Summers, W. K. A Preliminary Report on New Mexico's Geothermal Energy Resources. New Mex. Bur. of Mines and Mineral Res., Circ. 80, 41 p., 1965.

__________. Catalog of Thermal Waters in New Mexico. New Mex. Bur. of Mines and Mineral Res. Hydrology Report 4, 80 p., 1976.

Woodward, L.A., J. F. Callender, J. Gries, W. R. Seager, C. E. Chapin, W. L. Shaffer and R. E. Zilinski. Tectonic Map of Rio Grande Region from New Mexico-Colorado Border to Presidio, Texas. New Mex. Geol. Soc., Guidebook 26th Field Conf., p. 239, 1975.

APPENDIX A. GEOLOGIC TIME SCALE (Slemmons, 1975)[c]

MAJOR STRATIGRAPHIC AND TIME DIVISIONS

Subdivisions In Use By The U. S. Geological Survey			Age Estimates Commonly Used For Boundaries (In Million Years)	
Era Or Erathem	System Or Period	Series Or Epoch	(a)	(b)
Cenozoic	Quaternary	Holocene		
		Pleistocene	1.5-2	1.8
	Tertiary	Pliocene	ca. 7	5.0
		Miocene	26	22.5
		Oligocene	37-38	37.5
		Eocene	53-54	53.5
		Paleocene	65	65
Mesozoic	Cretaceous	Upper (Late) Lower (Early)	136	
	Jurassic	Upper (Late) Middle (Middle) Lower (Early)	190-195	
	Triassic	Upper (Late) Middle (Middle) Lower (Early)	225	
Paleozoic	Permian	Upper (Late) Lower (Early)	280	
	Pennsylvanian	Upper (Late) Middle (Middle) Lower (Early)	320	
	Mississippian	Upper (Late) Lower (Early)	345	
	Devonian	Upper (Late) Middle (Middle) Lower (Early)	395	
	Silurian	Upper (Late) Middle (Middle) Lower (Early)	430-440	
	Ordovician	Upper (Late) Middle (Middle) Lower (Early)	ca. 500	
	Cambrian	Upper (Late) Middle (Middle) Lower (Early)	570	
Precambrian	**Time Subdivisions Of The Precambrian** Precambrian Z--base of Cambrian to 800 m.y. Precambrian Y--800 m.y. to 1600 m.y. Precambrian X--1600 m.y. to 2500 m.y. Precambrian W--older than 2500 m.y.			

[a] Geol. Soc. London, The Panerozoic Time-Scale, A Symposium, Geol. Soc. London, Quart. Journ. 120, Suppl., 260-262, 1964 .

[b] W. A. Berggren, A Cenozoic Time Scale -- Some Implications for Regional Geology and Paleobiogeography, Lethaia 5 No. 2, 195-215, 1972 .

[c] Slemmons, D.B. Fault Activity and Seismicity near the Los Alamos Scientific Laboratory Geothermal Test Site, Los Alamos Scientific Laboratory Informal Rept, LA-5911-MS, 1975.

APPENDIX B. U.S.-METRIC CONVERSION TABLE

U.S. CUSTOMARY	U.S. EQUIVALENT	METRIC EQUIVALENT
	Length	
inch (in)	0.082 ft	25.4 millimeters (mm)
inch	0.083 ft	2.54 centimeters (cm)
foot (ft)	0.33 yd, 12 in	0.3048 m3534 (m)
yard (yd)	3 ft, 36 in	0.9144 m
mile (mi)	5,280 ft, 1,760 yd	1.609 kilometer (km)
	Area	
square foot (sq ft)	144 in	0.0929 sq m
square yard (sq yd)	1,294 sq in, 9 sq ft	0.836 sq m
acre	43,560 sq ft, 4,840 sq yd	4,047 sq m
acre	43,560 sq ft, 4,840 sq yd	0.4046 hectare (ha)
square mile (sq mi)	640 acres	2.59 sq km
	Volume	
gallon	4 quarts	3.785 liters (1)
acre-foot (acre-ft)	325,850.28 gallons	0.12335 hectare-meter (ha-m)
acre-foot/acre		0.3048 ha-m
cubic feet (cu ft)		0.02832 cubic meter (cu m)
cubic mile (cu mi)		4.1655 cu km
	Flow Rate	
gallons per second		3.785 liters per second (lps)
gallons per minute (gpm)		3.785 liters per minute (lpm)
gallons per day (gpd)		3.785 liters per day (lpd)
gallons per minute/foot (gpm/ft)		12.418 lpm/m
gallons per day/ft (gpd/ft)		12.418 lpd/m
18.2 gpd/sq ft	Darcy	8.58×10^{-4} cm/sec
pounds per hour		1.262×10^{-4} kg/sec
cu ft per sec (cfs)		28.32 lps

U. S. CUSTOMARY	U. S. EQUIVALENT	METRIC EQUIVALENT
	Miscellaneous	
°F		9/5 (°C) + 32
°C		(°F - 32) 5/9
pounds per square inch (psi)		0.7031 gm/sq cm
pounds per square inch (psi)		0.0689 bar
British Thermal Unit (BTU)		1,055 joules (J)
BTU/lb		2,325.84 J/kg
ounce		28.35 grams
pound		0.4536 kilogram (kg)
ton		0.907 metric ton

APPENDIX C

BASIC CONCEPTS AND SEMANTICS OF HYDROLOGY

The basic premise of groundwater hydrology is that under natural conditions part of the precipitation that falls in an area moves from the land surface down an energy gradient to the water table where it enters the zone of saturation. It then moves through the zone of saturation until it leaves this zone so that it may (1) enter the overlying unsaturated zone, (2) become stream flow, or (3) become vapor and move directly to the atmosphere.

By definition, only the water in the zone of saturation is properly called groundwater. The precipitation that moves to the water table is called recharge and the area over which percolation to the water table occurs is called the recharge area. Water in the groundwater reservoir is said to be in transient storage. The water that leaves the zone of saturation is called discharge, and the area over which discharge occurs is called the discharge area.

Under natural conditions, over a long period of time, a state of dynamic equilibrium exists in which recharge equals discharge and the volume of water in transient storage remains constant (or more precisely fluctuates about a mean).

Because modern hydrologists recognize that under natural hydrodynamic conditions the water moves through the unsaturated zone, they now consider groundwater flow systems to include both saturated and unsaturated flow, so for this report the groundwater flow system shall be used in this larger context.

The water in a natural groundwater flow system has chemical characteristics that depend upon its position in the system and upon the kind of rock through which it flows. The systems are three dimensional, and flow may be across bedding or stratigraphic units as well as parallel to them, so the chemical character of water in a formation does not necessarily reflect chemical changes due exclusively to flow through that formation.

In natural discharge areas, groundwater near or at the surface tends to discharge primarily via evapotranspiration. Local surface buildup of dissolved solids occurs simply because the residual water is enriched in soluble salts.

ENERGY

The energy to drive the water from the recharge area to the discharge area is primarily the potential energy due to gravity acting upon the mass of water.

In general, the energy at a point in a groundwater flow system is expressed as the sum of (1) a quantity that is a function of the mass of water, its altitude, and the gravitational constant at the point, and (2) a quantity that is a function of the pressure exerted by the water at the point. The pressure depends in turn on a number of factors. However, by assuming (1) a gravitational constant, (2) water of uniform density, and (3) no unusual source of pressure (such as electro-osmotic phenomena) one may represent the energy at any point in a groundwater flow system by associating with that point the altitude to which water would rise above the given point. This altitude is generally referred to as the head or potential. For the zone of saturation this altitude would be the altitude of the water level in a piezometer open only at the point. In the unsaturated zone, the determination of the value is much more difficult since capillary pressure must be measured and accounted for. At the boundary between the unsaturated zone and the zone of saturation there exists a capillary fringe. We, therefore, define the water table arbitrarily as the surface through those points where the pressure is equal to local atmospheric pressure. At this surface and below, the effects of capillarity become negligible. Because head consists of an altitude term and a pressure term, groundwater may move from low to high pressure as well as high to low pressure.

HYDRAULIC GRADIENT

The energy gradient, or hydraulic gradient as it is generally called, is a statement of the rate of change of energy along a given flow path. It may be considered to have two components, one horizontal, the other vertical. Where the vertical component is directed downward, the flow is downward; where it is directed upward, the flow is upward.

Recharge occurs where the vertical component of the hydraulic gradient is directed downward. In this region the water table is concave downward.

Discharge occurs where the vertical component of the hydraulic gradient is directed upward. In this area the water table is concave upward. The line along which the vertical component is zero is an inflection line on a water table map and can be used to distinguish the recharge from the discharge areas.

Since flow occurs in response to an energy gradient, horizontal flow through the unsaturated zone is possible and should never be categorically assumed to be negligible. Because vertical hydraulic gradients exist, the shape of the water table should be considered only a guide to the near-surface groundwater flow direction.

DIVIDES

Groundwater flow is three-dimensional. Therefore, in any natural groundwater flow situation under dynamic equililibrium there exists a series of surfaces that extend from the recharge area to the discharge area in such a way that for the flow above the surface, recharge equals discharge. These surfaces are called divides. Between divides recharge equals discharge. At the land surface, the groundwater divide need not follow surface drainage basin divides.

NATURAL GROUNDWATER FLOW SYSTEMS

Natural groundwater flow systems may be classified as simple or complex. They are also classified as local, intermediate or regional. A simple or local flow system involves recharge and discharge over a relatively small area, relatively short flow paths and shallow depth of circulation. Recharge occurs over an essentially continuous area. Discharge derives exclusively from nearby recharge.

A complex or intermediate flow system involves recharge and discharge over a larger area than a local flow system. Flow paths are longer. Circulation extends to greater depths. Recharge areas are not continuous; consequently at least one local flow system is evident.

The most complex flow system is the regional system, which includes recharge and discharge over large areas and contains some very long flow paths that underflow at least one intermediate flow system and one local flow system.

Based on studies of (1) the distribution of head, (2) hydrogen-oxygen isotopes, (3) geochemistry of groundwater, (4) age of groundwater, (5) oceanic discharge of groundwater, and (6) paleohydrologic systems, we know that groundwater flow systems may extend to depths that reach to thousands of feet below sea level.

GROUNDWATER FLOW THROUGH ROCKS

If we examine rocks closely, we find that they are made up of solid mineral grains, interconnected pores and isolated pores. Water flows through the interconnected pores. These pores may be classified as intergranular, fracture or tubular.

Intergranular pores are pores between minerals or other rock-forming particles. The ratio of the shortest to the longest dimension ranges from about 1:1 to 1:5. Usually the pore dimensions of intergranular pores are measured in microns or millimeters.

Fracture pores are all those planar pores such as bedding planes and cracks that develop in response to stresses (e.g., faults, sheetings, columnar joints). These pores have two very long dimensions and one very short dimension. The long dimension is usually measured in meters or tens of meters, whereas the short dimension is usually measured in millimeters or tenths of a millimeter.

Tubular pores include such features as solution cavities and lava tubes as well as a host of trivial near-surface phenomena such as worm tubes. They may also include such items as geyser tubes and man-made wells or bore holes. Tubular pores have two relatively short dimensions and one very long dimension. The short dimensions are usually measured in centimeters or meters, whereas the long dimension is generally measured in hundreds of meters or even kilometers.

TRANSIENT WATER LEVELS

Although a natural groundwater flow system may be in dynamic equilibrium when considered for a long period of time, there may be substantial departures from equilibrium for periods ranging from a few minutes to a few years.

During these transient periods, water is taken into or discharged from storage and associated water level changes occur.

Short-term changes in storage occur because pressure changes cause an elastic response in the rock so that water is taken into or released from storage with no change in the position of the water table. Changes of this sort are brought on by air pressure changes, tidal fluctuations, earthquakes, short term loading or unloading, and pumping from or injecting into wells. These water level changes are here referred to as elastic-storage transients.

When the works of man--such as the installation of a well, construction of a dam or the creation of a sustained synthetic recharge condition--create a long-term change in the flow regime, the elastic-storage transients are noted first and then porosity-storage transients become evident. Finally, if the new condition is sustained for a sufficiently long period a new local flow system is created that is in dynamic equilibrium. The water table shape adjusts to fit the new equilibrium. Energy distribution around the new feature also adjusts until a fixed divide becomes evident and measurable. In those cases where there are many wells or there are many recharge points, the short-term transients associated with individual wells will mask the developing long-term equilibrium of the new flow system.

GROUND WATER MANAGEMENT CONCEPTS

The works of man--wells, irrigation systems, mines and excavations, dams, drains and canals, sewage disposal facilities, etc.--alter natural groundwater systems by changing the location and amount of recharge and/or discharge, and by changing the energy distribution in the groundwater reservoir. Management of a groundwater resource consists of controlling the discharge and recharge rates and durations from or the energy (water level) distribution within the groundwater reservoir, or both, through the use of the works of man.

Management of a groundwater reservoir takes into account the consequence of changes in the discharge-energy relationship as a function of time that are a consequence of the works of man. Management may also take into account the changes in water chemistry and temperature of the water as a function of time due to the works of man.

SAMPLE TYPES

Two types of chemical analyses of groundwater are available.

The most common one is the analysis made to establish the character of the water as it will be used. These are water quality analyses. The other type is rather rare for it reveals (hopefully) the chemical character of the water in the ground. These are hydrogeochemical analyses.

If the water sample represents only a small portion of the flow continuum, and the water sample did not age, it can be considered a hydrogeochemical analysis. Sometimes water quality analyses will meet these criteria.

If we know the chemical character of the water in the ground, we can predict the chemical character of the water as it will be used. The inverse is not necessarily true. A monitoring program should define the chemical character of the water in the rocks as a function of time.

APPENDIX D

GLOSSARY

alluvium: Relatively unconsolidated detrital material (clay, silt, sand, gravel) deposited in comparatively recent geologic time by flowing water.

aquiclude: Relatively impermeable strata that absorbs water slowly and functions as a boundary of an aquifer. It does not transmit ground water quickly enough to supply a well or spring. Clay or shale beds and faults often act as aquicludes.

aquifer: A body of rock or sediment that contains sufficient saturated permeable materials to conduct ground water and yield significant quantities of ground water to wells and springs.

aquitard: Confining strata that retards the flow of water but does not prevent flow to or from an adjacent aquifer.

artesian water: Ground water confined under hydrostatic pressure. Water in an artesian well rises above the level of the water table under artesian pressure, but does not necessarily reach the land surface. The term is sometimes restricted to mean only a flowing artesian well.

Bouguer anomaly: A gravity value calculated by allowing for the attraction effect of topography but not for that of isostatic compensation.

brine: A solution containing more than 3.5% total dissolved solids (35,000 mg/l). This is the approximate TDS of sea water.

caprock (geothermal): A relatively impermeable rock layer overlying a hot water or steam reservoir which prevents the heat or fluid from directly migrating or dissipating upward to the surface.

clast: A rock fragment produced by mechanical weathering of a larger rock mass.

conductive heat flow: Heat transfer from a higher-temperature to a lower-temperature region by molecular impact (vibration) without transfer of matter itself.

convective heat flow: Mass transfer of heat due to temperature-caused density gradients, e.g., circulation of hot water in a convecting geothermal reservoir.

connate water: Water trapped, at the time of deposition, in the interstices of a sedimentary or extrusive igneous rock.

contour line: A line that passes through all consecutive points of equal value for a parameter which is variable, e.g., topographic elevation, ground water level or temperature.

craton: A part of the earth's crust which has attained stability and which has been little deformed for a prolonged period.

deuterium: The hydrogen isotope that occurs in water and has twice the mass of ordinary hydrogen. It is also called heavy hydrogen and its chemical symbol is "D".

diktytaxitic: Rock texture of some olivine basalts in the Pacific Northwest, characterized by numerous jagged, irregular vesicles bounded by crystals.

effluent: Flowing forth or out, emanating: 1) a surface stream that flows out of a lake or larger stream, 2) a liquid discharged as waste.

electrical resistivity survey: A geophysical exploration technique where electric current is artificially introduced into the ground and the distribution of current below the surface is measured by electrodes separated by increasing increments. Depths to geologic interfaces may be determined by plotting apparent resistivity versus electrode separation.

eutrophication: The artificial or natural enrichment of a lake by an influx of nutrients required for the growth of aquatic plants.

fault: A surface or zone of rock fracture along which there has been displacement, from a few centimenters to hundreds of kilometers in scale. Faults are classified according to the relative motion of the rock on each side of the fracture zone, or fault plane. These classifications are illustrated below in the diagrams of fault types.

STRIKE - SLIP

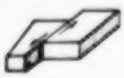

NORMAL

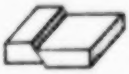

REVERSE

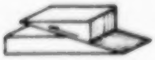

ROTATIONAL

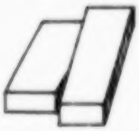

TRANSFORM

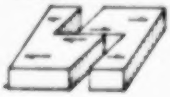

fault scarp: A fairly steep slope or cliff formed directly by movement along one side of a fault and representing the exposed surface of the fault plane before modification by erosion and weathering.

fumarole: A volcanic vent from which gases and vapors are emitted; it is characteristic of a late stage of volcanic activity.

geomorphology: The science of the earth's surface; specifically the classification, description, origin and development of present land forms and their relationships to underlying structures.

geosyncline (variety eugeosyncline, miogeosyncline): An elongate crustal depression or basin, often subsiding, where thousands of meters of sediment accumulate, usually in some phase of a marine environment.

geothermal gradient (temperature gradient): The rate of increase of temperature in the earth with depth. The average gradient is approximately 1°C per 30 m (2°F per 100 ft).

geothermometry (geologic thermometry): 1) The science of the earth's heat; 2) a mineral or mineral assemblage whose characteristics are fixed within known thermal limits thus allowing conclusions about temperatures during process of formation, e.g., sodium, potassium and calcium concentrations in natural waters may be used to predict the last temperature of water-rock equilibration.

graben: A crustal block that is bounded by faults on its long sides, the block being downdropped in relation to the surrounding land.

groundwater: Subsurface water, especially that contained in a saturated zone, or strata, including underground streams.

horst: A crustal block that is bounded by faults on its long sides, the block being uplifted in relation to the surrounding land.

hydraulic gradient: In an aquifer, the rate of change of pressure head (height of a column of water that the pressure can support) per unit of distance of flow at a given point and in a given direction. It is usually expressed in meters per kilometer or feet per mile.

hydrologic budget (variety water budget): An accounting of the inflow to, outflow from, and storage in, a hydrologic unit, e.g., drainage basin, aquifer or reservoir; the relationship between evaporation, precipitation, runoff and change in water storage is implied.

hydrology: The science that deals with all properties of water (liquid and solid) on, under and above the earth's surface.

hydrothermal: Pertaining to heated water (or aqueous solution) or products resulting from heated water, i.e., alteration of rocks or minerals by reaction of hydrothermal water.

igneous rock: A rock that solidified from molten or partly molten material, i.e., from a magma. Intrusive - usually having visible crystal components, and formed deep under the earth's surface, e.g., granite, diorite, gabbro, peridotite. Extrusive - an igneous rock that solidified on or near the surface, e.g., rhyolite, andesite, basalt (lava flows).

inflow: The act or process of flowing in, e.g., the flow of water into a drainage basin.

inlier: An area or group of rocks surrounded by outcrops of younger rocks.

intensity (of an earthquake): A subjective measurement rating the severity of ground motion at a specific site during an earthquake. The Modified Mercalli scale uses Roman numerals from I to XII to describe the motion that was felt and the damage to man-made structures. Intensity at a point depends not only upon the strength of an earthquake (the earthquake magnitude), but also upon the distance to the earthquake epicenter and the geologic and soil conditions at the point.

intrusion: The injection of magma into preexisting rock, resulting in plutons, batholiths and laccoliths (large scale) or stocks, dikes and sills (small scale).

isotherm: A line connecting points of equal temperature.

isotope ratios: Isotope abundances given as a ratio relative to a standard rather than an absolute. Different ratios can indicate changes in environment or origin for a given chemical element. The standard is often Standard Mean Ocean Water (SMOW). Some common ratios are defined as follows:

$$\delta O^{18}(\text{in } {}^{o}/_{oo}) = \left[\frac{(O^{18}/O^{16})_{\text{Sample}}}{(O^{18}/O^{16})_{\text{Standard}}} - 1 \right] 1000$$

Similar definitions exist for ratios of deuterium(D) to hydrogen (H) and for C^{14} to C^{12}

juvenile water: Water derived directly from a magma, reaching the earth's surface for the first time.

KGRA: Known Geothermal Resource Area - a legally defined land area that is considered to have potentially economic geothermal resources.

Langelier-Ludwig diagram: A diagram representing groupings of chemical composition of aqueous solutions.

lithic fragment: A fragment from a preexisting rock mass, usually used in describing a medium-grained sedimentary rock or certain types of volcanic deposits.

mafic: Generally igneous or volcanic rocks, containing iron, magnesium and other dark-colored minerals.

magnetic survey: Measurement of a component or element of the geomagnetic field at different locations. It is usually made to map either the broad patterns of the earth's main field or local anomalies due to variation in rock magnetization. It is often conducted as an aeromagnetic survey.

magnetotelluric survey (MT): An electromagnetic method in which natural electric and magnetic fields are measured; usually two-dimensional horizontal electric field and three-dimensional magnetic field components are recorded.

magnitude (earthquake): A measure of the strength of an earthquake or the strain energy released by it, as determined by seismologist C.F. Richter, who first applied it to southern California earthquakes. For that region he defined local magnitude as the logarithm, to the base 10, of the amplitude in microns of the largest trace deflection that would be observed on a standard torsion seismograph (static magnification = 2,800, period = 0.8 sec, damping constant = 0.8) at a distance of 100 km from the epicenter. Magnitudes determined at teleseismic distances using the logarithm of the amplitude to period ratio of body waves are called body-wave magnitudes and using the logarithm of the amplitude of 20-sec period surface waves are called surface-wave magnitudes. The local body-wave and surface-wave magntidues of an earthquake will have somewhat different numerical values.

mélange: A mixture of rock materials derived from more than one depositional realm, usually sheared and deformed. It is a mappable body, sometimes several kilometers in length.

metamorphic rock: Rock resulting from once solid, preexisting rock subjected to extreme heat, pressure or chemical changes, e.g., slate, schist, greiss, quartzite, marble, serpentine.

meteoric water: Water of atmospheric origin, e.g., rain.

microearthquake: An earthquake having a magnitude of two or less on the Richter scale (cutoff may vary accoridng to user).

Mohorovicić discontinuity (moho): A sharp seismic-velocity discontinuity that separates the earth's crust from the subjacent mantle. Its depth varies from 5 to 10 km (8 to 16 mi) beneath the ocean floor to about 35 km (55 mi) below the continents.

nanoearthquake: An earthquake having a magnitidue of zero or less on the Richter scale (cut off may vary according to user.)

outflow: The act or process of flowing out, e.g., ground water seepage and stream water flowing out of a drainage basin.

pediment: Gently inclined erosion surface carved in bedrock, with a thin veneer of alluvium derived from the upland masses and in transit across the surface. Pediments occur between mountain fronts and valley floors.

percent reactance: The ratio of one anion species to the total anion species, expressed in milliequivalents per liter, and similarly for cation species. For example, if a water contains 0.8 meq/l Ca and the sum of all the cation species is 13.7 meq/l then the percent reactance Ca would be 0.8/13.7 or 6%. This expression provides a method of "normalizing" chemical analyses for data having a wide range of concentrations.

perched water table: Unconfined ground water separated from an underlying main body of ground water by an aquiclude and an unsaturated zone.

permeability: Ability of a rock, sediment or soil to transmit a fluid without impairment of the structure of the medium. A measure of the relative ease of fluid flow under unequal pressure. The customary unit of measurement is the darcy. It is equivalent to the passage of one cubic centimeter of fluid of one centipore viscosity flowing in one second under a pressure differential of one atmosphere through a porous medium having a cross sectional area of one sq cm and a length of 1 cm.

porosity (effective): The ratio of the continuous void space (through which water can move) to total volume, measured at a point in a flow system.

radiometric age-dating: A method of absolute age determination based on nuclear decay of natural elements. Calculating an age, in years, for geologic materials by measuring the presence of short-life radioactive elements, e.g., carbon-12/carbon-14, or by measuring the presence of a long-life radioactive element and its decay product, e.g., potassium-40/argon-40.

recharge: The processes involved in the absorption and addition of water to the zone of saturation.

reinjection well: A well in which fluid is introduced; often used to dispose of waste liquid or possibly to replace ground water removed from strata which might subside if the water were permanently removed.

rift zone: A system of crustal fractures, usually producing a valley or graben-like depression.

sag pond: A small body of water in a depression formed because active or recent fault movement has impounded drainage.

salinity: Total quantity of dissolved salts in water, measured by weight in parts per thousands or parts per million (ppm) with the following qualifications: all carbonate has been converted to oxide. bromide and iodide converted to chloride, and all organic matter completely oxidized.

sedimentary rock: Rock resulting from accumulation of sediment or organic matter, e.g., shale, sandstone, conglomerate, limestone.

seismic survey: A geophysical prospecting technique that utilizes a seismic source, such as a thumper or dynamite, and sensitive detection instruments to record travel times. Interpretation of this data allows the location of geologic structures such as faults and thickness of lithologic units.

sparker survey: A seismic survey in which an electrical discharge in water is the energy source (also called exploding wire).

solfataric activity: A late or decadent type of volcanic activity characterized by the emission of sulfurous gases from the vent.

specific yield: The ratio of the volume of water a given mass of saturated rock or soil will yield by gravity to the volume of that mass.

Stiff diagram: A closed polygon representing the chemical characteristics of a substance. Distinctions between substances can be easily observed by comparison of the different polygonal shapes for each substance.

subduction zone: A region where one crustal block descends beneath another by folding or faulting or both.

temperature gradient: See geothermal gradient.

transmissivity: In an aquifer, the rate at which water of the prevailing viscosity is transmitted through a unit width under a unit hydraulic gradient.

trilateration: A method of surveying where the lengths of the three sides of a series of touching or overlapping triangles are measured (usually by electronic methods) and the angles are computed from the measured lengths.

underflow: The flow of water through the soil or a subsurface stratum, or under a structure.

volcanic rock (extrusive): A rock formed from a magma at or near the earth's surface. Usually fine-grained, sometimes solidifying as ejected from a volcano, e.g. pumice, rhyolite, andesite, basalt (lava flows).

water budget: See hydrologic budget.

APPENDIX E

LIST OF ABBREVIATIONS

acre-ft	--acre-feet
atm	--atmosphere
BTU	--British Thermal Unit
°C	--degrees Celsius (or Centigrade)
cal	--calorie
Cal Tech	--California Institute of Technology
CDWR	--California Department of Water Resources
cfs	--cubic feet per second
cm	--centimeter
cu	--cubic
d	--day
ERDA	--U.S. Energy Research and Development Administration
EPA	--U.S. Environmental Protection Agency
EPRI	--Electric Power Research Institute
°F	--degrees Fahrenheit
ft	--feet
ft/mi	--feet per mile
g	--acceleration of gravity
gm	--grams
gpd	--gallons per day
gpm	--gallons per minute
ha	--hectare
ha-m	--hectare-meter
HFU	--heat flow unit
hr	--hour
in	--inch
J	--joule
KGRA	--known geothermal resource area
kg	--kilogram
kH	--transmissivity
km	--kilometer
kW	--kilowatt
kW.hr	--kilowatt-hour
LASL	--Los Alamos Scientific Laboratory
l	--liter

lb --pound
LBL --Lawrence Berkeley Laboratory
LLL --Lawrence Livermore Laboratory
lpd --liter per day
lpm --liter per minute
lsd --land-surface datum
m --meter
M --earthquake magnitude determined from instrumental data
M_L --earthquake magnitude, local scale
md --millidarcy
md-ft --millidarcy-feet
meq/l --milliequivalence per liter
mg --milligram
mg/l --milligram per liter
mgal --milligal
m/km --meters per kilometer
mm --millimeter
MM --Modified Mercalli Intensity
msl --mean sea level
mv --millivolt
MW --megawatt
NCER --National Center for Earthquake Research
NOAA --National Oceanic and Atmospheric Administration
ohm-m --ohm-meter
OIT --Oregon Institute of Technology
oz --ounce
pCi/l --picocurie per liter
PG&E --Pacific Gas and Electric Company
ppm --parts per million
psi --pounds per square inch
psia --pounds per square inch absolute
psig --pounds per square inch gage
SDG&E --San Diego Gas and Electric
sec --second
sq --square
TDS --total dissolved solids
U.C.B. --University of California, Berkeley
USBR --U. S. Bureau of Reclamation
USGS --U.S. Geological Survey
USPHS --U.S. Public Health Service
U.C.R. --University of California, Riverside
μmho/cm --micro mho per centimeter
ρ --density
ϕch --storage capacity due to compressibility

★ U.S. GOVERNMENT PRINTING OFFICE: 1979—786—265